

Bahman Zohuri

# Compact Heat Exchangers

Selection, Application, Design and  
Evaluation



# Compact Heat Exchangers



Bahman Zohuri

# Compact Heat Exchangers

Selection, Application, Design and Evaluation



Springer

Bahman Zohuri  
Galaxy Advanced Engineering, Inc.  
Albuquerque, NM, USA

ISBN 978-3-319-29834-4      ISBN 978-3-319-29835-1 (eBook)  
DOI 10.1007/978-3-319-29835-1

Library of Congress Control Number: 2016953367

© Springer International Publishing Switzerland 2017

This work is subject to copyright. All rights are reserved by the Publisher, whether the whole or part of the material is concerned, specifically the rights of translation, reprinting, reuse of illustrations, recitation, broadcasting, reproduction on microfilms or in any other physical way, and transmission or information storage and retrieval, electronic adaptation, computer software, or by similar or dissimilar methodology now known or hereafter developed.

The use of general descriptive names, registered names, trademarks, service marks, etc. in this publication does not imply, even in the absence of a specific statement, that such names are exempt from the relevant protective laws and regulations and therefore free for general use.

The publisher, the authors and the editors are safe to assume that the advice and information in this book are believed to be true and accurate at the date of publication. Neither the publisher nor the authors or the editors give a warranty, express or implied, with respect to the material contained herein or for any errors or omissions that may have been made.

Printed on acid-free paper

This Springer imprint is published by Springer Nature  
The registered company is Springer International Publishing AG Switzerland

*This book is dedicated to my daughter  
Dr. Natasha Zohuri MD  
She always encouraged me with my  
publications*

Bahman Zohuri



# Preface

Today's global energy market, places many demands on power generation technology including high thermal efficiency, low cost, rapid installation, reliability, environmental compliance, and operation flexibility.

The demand for clean, non-fossil based electricity is growing; therefore, the world needs to develop new nuclear reactors with higher thermal efficiency in order to increase electricity generation and decrease the detrimental effects on the environment. The current fleet of nuclear power plants is classified as Generation III or less. However, these models are not as energy efficient as they should be because the operating temperatures are relatively low. Currently, groups of countries have initiated an international collaboration to develop the next generation of nuclear reactors called Generation IV. The ultimate goal of developing such reactors is to increase the thermal efficiency from what currently is in the range of 30–35 % to 45–50 %. This increase in thermal efficiency would result in a higher production of electricity compared to current Pressurized Water Reactor (PWR) or Boiling Water Reactor (BWR) technologies.

A number of technologies are being investigated for the Next Generation Nuclear Plant that will produce heated fluids at significantly higher temperatures than current generation power plants. The higher temperatures offer the opportunity to significantly improve the thermodynamic efficiency of the energy conversion cycle. One of the concepts currently under study is the Molten Salt Reactor. The coolant from the Molten Salt Reactor may be available at temperatures as high as 800–1000 °C. At these temperatures, an open Brayton cycle combined with a Rankine bottoming cycle appears to have some strong advantages.

Combined-cycle thermal efficiency increases as gas turbine specific power increases. The gas turbine firing temperature is the primary determinant of specific power.

Gas turbine engines, both aircraft and industrial power generation, represent one of the most aggressive applications for structural materials. With ever growing demands for increasing performance and efficiencies, all classes of materials are being pushed to higher temperature capabilities. These materials must also satisfy

stringent durability and reliability criteria. As materials are developed to meet these demanding requirements, the processing of these materials often becomes very complicated and expensive. As a result, the cost of materials and processes has become a much larger consideration in the design and application of high performance materials. Both the aircraft engine and power generation industries are highly cost competitive, and market advantage today relies on reducing cost as well as increasing performance and efficiency.

The distributed power generation market and renewing attention to renewable source of energy puts some interesting demand on a new aspect of heat exchangers and their compactness going forward with better efficiency of power plant whether it is gas driven, fossil fuel or a new generation of nuclear plant.

For the nuclear power plant, in particular new generation and small modular reactors (SMRs), one of the most economical solutions today is to generate power through small gas turbine systems in the form of Brayton cycle combined with these reactors. These gas turbines arbitrarily can be categorized as micro-turbines with output of (5–200 kW) and mini-turbines with output of (200–500 kW). The thermal efficiency of such micro-turbines is about 20 % or less if no recuperator is used in the system. Using a recuperator (regenerator can also be considered but has a number of problems) operating at 87 % effectiveness, the efficiency of the gas turbine system increases to about 30 %, a substantial performance improvement. However, cost of the recuperator is about 25–30 % of the total power plant, therefore total cost of ownership and return on investments are not very well justified. This necessitates the use of all prime surface heat exchangers with no brazing. Thus the quest for a novel design of new generation compact heat exchangers in support of such combined cycle is there and understanding of such innovative approach among engineers and scientist in the field is rising rapidly.

In order to achieve the above described situation and usage of technology an approach such as combined cycle driven efficiency of power plants either nuclear or otherwise demands a better and more compact heat exchanger utilizing Brayton, Rankine cycle or a combination of them as bottoming or topping configuration.

This book, after providing the necessary concise information on all aspects of this innovative approach such as combined cycle and associated turbines such as micro-turbines combined, moves on to the discussion on various types of compact heat exchanger surfaces and novel designs that can be considered for the cost effective heat exchangers and packaging in the system.

The simple Brayton cycle is modified to include recuperators or compact heat exchangers (which will transfer heat from the turbine exhaust to preheat compressed high pressure air before going to the combustion chamber), it will require less fuel to obtain the desired turbine inlet temperature of compressed air and also the optimum pressure ratio (either for compressor or turbine) is reduced to typically 3–4. This improves the thermal efficiency of the cycle. Alternatively, a regenerator can also be used replacing a recuperator.

Development of high temperature/high strength materials, corrosion resistant coatings, and improved cooling technology have led to increases in gas turbine firing temperatures. This increase in firing temperature is the primary development

that has led to increases in Combined Cycle Gas Turbine (CCGT) thermal efficiencies. The improvements in combined-cycle thermal efficiencies and the commercial development of combined-cycle power plants have proceeded in parallel with advances in gas turbine technologies.

Compact heat-exchangers, filters, turbines, and other components in integrated Next Generation Nuclear Power Plant combined cycle systems must withstand demanding conditions of high temperatures and pressure differentials. Under the highly sulfiding conditions of the high temperature such as inlet hot steam or other related environmental effects, the performance of components degrade significantly with time unless expensive high alloy materials are used. Deposition of a suitable coating on a low cost alloy may improve its resistance to such sulfidation attack and decrease capital and operating costs. A review of the literature indicates that the corrosion reaction is the competition between oxidation and sulfidation reactions. The Fe- and Ni-based high-temperature alloys are susceptible to sulfidation attack unless they are fortified with high levels of Cr, Al, and Si. To impart corrosion resistance, these elements need not be in the bulk of the alloy and need only be present at the surface layers.

Those that practice the art of Nuclear or Mechanical Engineering must have a physical and intuitive understanding of the mechanisms and balances of forces, which control the transport of heat and mass in all physical systems. This understanding starts at the molecular level, with intermolecular forces and the motion of molecules, and continues to the macroscopic level where gradients of velocity, temperature, and concentration drive the diffusion of momentum, heat, and mass, and the forces of pressure, inertia, and buoyancy balance to drive convection of fluids.

This text covers the fundamentals of combined cycle that is required to understand electrical power generation systems and driven efficiency of combined cycle. It then covers the application of these principles to nuclear reactor power systems. It is a general approach to Brayton combined cycle text, and aimed at explaining the fundamentals of combined cycle with these compact heat exchangers in the loop and applying them to the challenges facing actual nuclear power systems. It is written at an undergraduate level, but should also be useful to practicing engineers and scientists as well.

Chapter 1 provides the basic definitions and principles behind the basic and old science of thermodynamics that one needs to understand the study of energy, energy transformations, and its relation to matter, where we need to use the analysis of thermal system or thermal hydraulic through the application of the governing conservation equations, namely Conservation of Mass, Conservation of Energy (first law of thermodynamics), the second law of thermodynamics, and the property relations. Energy can be viewed as the ability to cause changes. This chapter allows us to have a better understanding of Compact Heat Exchangers (CHEs) and their designs for a typical power plant layout and the scope of thermodynamics behind it as part of CHEs applications.

Chapter 2 covers the general aspect of heat exchanges and what types there are as well as general rules of their designs, before we launch to specifics about

compact heat exchangers in the rest of the book. Then we are going to look at, cost, design, performance and their application in appropriate industry, where these CHEs are going to be used.

Chapters 3 and 4 deal with thermal hydraulic and heat transfer of heat exchanger in order for the reader to have a fair idea of how the designed heat exchanger would perform when installed in the power plant and One-Dimensional analysis modeling is presented using MATLAB software while Three-Dimensional modeling study of the heat exchanger is undertaken with the use of the COMSOL Multiphysics software. Specifically speaking Chap. 4 walks the reader through design process and computer modeling, simulation and selection of a Compact Heat Exchanger (CHE) for its application in a Solar Gas Turbine Power Plant and is heavily written around the work that was done by Noah Yakah and his Master of Science thesis under supervision of Dr. James Spelling at KTH School of Industrial Engineering and Managements in Stockholm Sweden and his MATLAB (1-D) and COMSOL (3-D) simulations approach (i.e., Heat Exchanger Design for a Solar Gas-Turbine Power Plant) for the selection of CHE.

Chapter 4 discusses the thermal design compact heat exchanger and it goes through the concept of this selection process both from modeling, physics, and thermal hydraulic criteria and shows what is involved in the selection process, both for fully developed laminar flow and fully developed turbulent and design formulations as well.

Chapter 5 presents analysis of three dimensional modeling of a printed circuit compact heat exchanger using COMSOL Multiphysics functionality and shows different screen shots of this software and how the setup of heat transfer modeling for such exchanger takes place and the work follows as complementary to Chap. 4, where MATLAB software is used to do similar work using one dimensional modeling for a similar type of compact heat exchanger.

Since a lot of concerns in recent years have been raised from the use of fossil fuels such as coal, oil, and natural gas as sources of producing heat energy to generate electricity and the rise of demand on such source energy in order to layout the ground for justification and need for new generation nuclear power plants and other means of renewable energy source, Chaps. 6, 7, and 8 are devoted to different forms of these power plants and how the heat exchangers are improving their overall out efficiencies during off and on grid circumstance, while describing in some more detail how these plants and available options work and goes on to describe heat exchangers in general and then talks about the compact heat exchangers as the most efficient and cost effective for their application in such innovative approaches.

There are also a total of seven appendices added to the book where Appendix A illustrates some table of physical properties and graphs, Appendix B reflects information about gas properties and tabulates them for selected gases and air properties both in SI and British units. Appendix C is a presentation of the thermodynamic properties for water and Appendix D tabulates the thermodynamic properties of Carbon Dioxide ( $\text{CO}_2$ ), while Appendix E shows similar information for Sodium. Finally Appendix F captures some mathematical modeling and

experimental data from work done by Akash Pandey on his work on Performance Analysis of a Compact Heat Exchanger in room temperature. Appendix F shows steps-by-steps of how to use 3-Dimensional analysis using COMSOL Multiphysics to design a gas-to-gas plate fin compact heat exchanger (PFCHX) based on parameters defined for this particular compact heat exchanger as well.

Note that steam tables published in this book were updated by Dr. McDaniel and this author when they published their book with Springer publishing company under the title of Thermodynamics In Nuclear Power Plant Systems in 2015 when they found out some errors in most steam tables recently published by other authors in their related text books.

The book also concentrates on fundamentals of new applications to energy conversion technology in Chap. 4 to cover power conversion systems and their components and how we can take the waste heat from a power plant in order to recover it and put it into use for driving overall output efficiency higher, so the owner of these plants will enjoy better revenue for day-to-day operations.

And finally the last few chapters of the book cover current and projected industrial applications and how the novel design of these compact heat exchangers from a thermal design perspective in principle are applied to their innovative designs, operation, and safety analyses.

Detailed appendices cover metric and English system units and conversions, detailed steam and gas tables, heat transfer properties, and nuclear reactor system descriptions, as well as a holistic approach to understanding of nuclear power plants and each generation in general.

Albuquerque, NM

Bahman Zohuri



# Acknowledgments

I would like to acknowledge all the individuals for their help, encouragement, and support. I have decided not to name them all, but we hope they can at least read this acknowledgment wherever they may be.

Last but not least, special thanks to my parents, wife, children, and friends for providing constant encouragement, without which this book could not have been written. I especially appreciate their patience with pure frequent absence from home and long hours in front of the computer during the preparation of this book.

My sincere appreciation goes to Professors and Instructors of Department of Nuclear Engineering at University of New Mexico Albuquerque, New Mexico, whom provided me the knowledge that I have now and continue teaching me what I need to know to go forward.

I am also indebt to another teacher, mentor and now a true friend, Professor Dimiter N. Petsev of University of New Mexico, Chemical Engineering Department, for whom I have a lot of respect as well.

The other true gentleman for whom I have a lot of respect and helped a lot and pushed me forward is Professor Cassiano R. E de Oliveira of Nuclear Engineering Department at University of New Mexico.



# Contents

<b>1 Definitions and Basic Principles of Thermodynamics . . . . .</b>	<b>1</b>
1.1 Thermodynamics and Energy . . . . .	1
1.2 Scope of Thermodynamics . . . . .	4
1.3 Units and Dimensions . . . . .	6
1.3.1 Fundamental Units . . . . .	6
1.3.2 Thermal Energy Units . . . . .	7
1.3.3 Unit Conversion . . . . .	7
1.4 Classical Thermodynamics . . . . .	8
1.5 Open and Closed Systems . . . . .	9
1.6 System Properties . . . . .	10
1.6.1 Density . . . . .	12
1.6.2 Pressure . . . . .	12
1.6.3 Temperature . . . . .	14
1.7 Properties of the Atmosphere . . . . .	16
1.8 The Laws of Thermodynamics . . . . .	17
References . . . . .	17
<b>2 Heat Exchanger Types and Classifications . . . . .</b>	<b>19</b>
2.1 Heat Exchanger Types . . . . .	19
2.2 Classification According to Transfer Processes . . . . .	22
2.2.1 Indirect Contact Type Heat Exchangers . . . . .	22
2.2.2 Direct Contact Type Heat Exchangers . . . . .	22
2.3 Classification of Heat Exchanger by Construction Type . . . . .	22
2.3.1 Tubular Heat Exchangers . . . . .	23
2.3.2 Plate Heat Exchangers . . . . .	24
2.3.3 Plate Fin Heat Exchangers . . . . .	25
2.3.4 Tube Fin Heat Exchangers . . . . .	26
2.3.5 Printed Circuit Heat Exchanger . . . . .	27
2.3.6 Regenerative Heat Exchangers . . . . .	29

2.4	Condensers . . . . .	29
2.5	Boilers . . . . .	30
2.6	Classification According to Compactness . . . . .	30
2.7	Types of Applications . . . . .	31
2.8	Cooling Towers . . . . .	31
2.9	Regenerators and Recuperators . . . . .	32
2.10	Heat Exchanger Analysis: Use of the LMTD . . . . .	38
2.11	Effectiveness-NTU Method for Heat Exchanger Design . . . . .	45
2.12	Special Operating Conditions . . . . .	50
2.13	Compact Heat Exchangers and Their Classifications . . . . .	51
	References . . . . .	55
<b>3</b>	<b>Compact Heat Exchangers Design for the Process Industry . . . . .</b>	<b>57</b>
3.1	Introduction . . . . .	57
3.2	Compact Heat Exchangers by Their Types . . . . .	58
3.2.1	Description of Plate Fin Heat Transfer Surfaces . . . . .	71
3.2.2	Flow Arrangement and Passage in Compact Heat Exchangers . . . . .	73
3.3	Why Compact Heat Exchangers? . . . . .	80
3.4	Characteristics of Compact Heat Exchangers . . . . .	89
3.5	Classification of Heat Exchangers . . . . .	95
3.6	Design Criteria for Process Heat Exchangers . . . . .	116
3.7	Thermal and Hydraulic Design . . . . .	119
3.7.1	Equations and Parameters . . . . .	121
3.8	The Overall Heat Exchanger Design Process . . . . .	167
3.8.1	Input Information Needed . . . . .	168
3.9	Design Summary . . . . .	170
3.10	Compact Heat Exchangers in Practice . . . . .	179
3.11	Heat Exchanger Materials and Comparisons . . . . .	180
3.12	Guide to Compact Heat Exchangers . . . . .	180
3.12.1	Generic Advantages of Compact Design . . . . .	183
	References . . . . .	183
<b>4</b>	<b>Thermal Design of the Selected Compact Heat Exchanger . . . . .</b>	<b>187</b>
4.1	Introduction . . . . .	187
4.2	Heat Transfer and Pressure Drop Correlations . . . . .	189
4.3	A Short Introduction on Convection Heat Transfer . . . . .	189
4.4	Mathematics of Fluids and Differential Equations with Boundary Conditions . . . . .	190
4.4.1	Free Convection or Natural Heat Transfer Process . . . . .	192
4.4.2	Forced Convection Heat Transfer Process . . . . .	193
4.5	Velocity Problem for Developed and Developing Laminar Flows . . . . .	193
4.5.1	Hydrodynamically Developed Flow . . . . .	196
4.5.2	Hydrodynamically Developing Flow . . . . .	198

4.6	Conventional Convection Problem . . . . .	199
4.6.1	Thermally Developed Flow . . . . .	201
4.6.2	Thermally Developing Flow . . . . .	203
4.7	Thermal Boundary Conditions . . . . .	203
4.7.1	Thermal Boundary Conditions for Singly Connected Ducts . . . . .	204
4.8	Heat Exchanger Variables and Thermal Circuit . . . . .	207
4.9	Solving Convection Heat Transfer Coefficient from Empirical Correlations . . . . .	212
4.10	Internal Flow in a Pipe or Passage . . . . .	218
4.10.1	Fully Developed Turbulent Flow . . . . .	220
4.10.2	Fully Developed Laminar Flow . . . . .	223
4.10.3	Entry Length . . . . .	224
4.11	Thermal Design of the Selected Compact Heat Exchanger . . . . .	226
4.12	Sizing the Compact Heat Exchangers . . . . .	227
4.13	Thermal Design Formulation of Considered Compact Heat Exchangers . . . . .	229
4.14	Assumption Made in the Design of Considered Compact Heat Exchangers . . . . .	232
4.15	Relating Heat Transfer and Pressure Drop . . . . .	233
4.16	Heat Capacity Ratio Analysis for Considered Compact Heat Exchangers . . . . .	235
4.17	Mean Temperature Difference . . . . .	235
4.18	Number of Transfer Units Analysis for Considered Compact Heat Exchangers . . . . .	236
4.19	Fluid Mean Temperature Analysis for Considered Compact Heat Exchangers . . . . .	236
4.20	Thermophysical Properties of the Gases for Considered Heat Exchangers . . . . .	237
4.21	Physical Dimensions and Other Important Geometrical Feature of the PFHE . . . . .	238
4.22	Pressure Drop Analysis of the Exchanger . . . . .	241
4.23	Printed Circuit Compact Heat Exchanger (PCHE) . . . . .	243
4.23.1	Pressure Drop Analysis of the PCHE . . . . .	245
4.23.2	Sensitivity Analysis of the PCHE . . . . .	246
4.23.3	Overall Analysis of the PCHE . . . . .	246
4.23.4	Analysis Performed on the PFHE . . . . .	250
4.23.5	Conclusion for the Selection of a Suitable Heat Exchanger . . . . .	252
	References . . . . .	262
5	<b>Three-Dimensional Modeling of Desired Compact Heat Exchanger . . . . .</b>	267
5.1	Introduction to COMSOL Multiphysics . . . . .	267
5.2	Steps Involved in COMSOL Multiphysics . . . . .	268

5.3	The Conjugate Heat Transfer Interface for Laminar Flow Using COMSOL . . . . .	269
5.3.1	Space Selection . . . . .	269
5.3.2	Adding Physics . . . . .	269
5.3.3	Selecting Study Type . . . . .	270
5.3.4	Geometry . . . . .	271
5.3.5	Boundary Conditions for Conjugate Heat Transfer Interface . . . . .	274
5.3.6	Meshes . . . . .	277
5.3.7	Study . . . . .	277
5.4	Simulation of the 3-D Model . . . . .	279
5.5	Mathematical Theory for Conjugate Heat Transfer Interface . . . . .	280
5.5.1	The Momentum Equation . . . . .	280
5.5.2	The Continuity Equation . . . . .	282
5.5.3	The Energy Equation . . . . .	283
5.6	Results, Discussions, and Conclusion . . . . .	284
5.6.1	Results . . . . .	284
5.6.2	Discussions . . . . .	286
5.6.3	Conclusion . . . . .	287
	References . . . . .	289
<b>6</b>	<b>Thermodynamics of Cycles . . . . .</b>	<b>291</b>
6.1	Introduction . . . . .	291
6.2	Open Cycle . . . . .	298
6.3	Closed Cycle . . . . .	299
6.4	Gas Compressors and Brayton Cycle . . . . .	300
6.5	The Non-ideal Brayton Cycle . . . . .	304
6.6	Open Cycle Gas Turbines . . . . .	306
6.6.1	Aeroderivative Intercooler Gas Turbines . . . . .	308
6.6.2	Operational Issues/Risks . . . . .	309
6.6.3	Opportunities/Business Case . . . . .	309
6.6.4	Industrial Case Studies for Open Cycle Gas Turbine . . . . .	312
	References . . . . .	313
<b>7</b>	<b>Compact Heat Exchangers Application in NGNP . . . . .</b>	<b>315</b>
7.1	Introduction . . . . .	315
7.2	Compact Heat Exchangers Driven Efficiencies in Brayton Cycle . . . . .	321
7.3	Gas Turbine Developments . . . . .	329
7.4	The Brayton Cycle with Recuperator . . . . .	331
7.5	The Brayton Cycle with Intercooling, Reheating, and Regeneration . . . . .	333
7.6	Modeling the Brayton Cycle . . . . .	335
7.7	Conclusion . . . . .	335
	References . . . . .	336

<b>8 Compact Heat Exchangers Application in New Generation of CSP . . . . .</b>	339
8.1 Introduction to Concentrated Solar Power (CSP) . . . . .	339
8.2 New Generation of High Temperature Solar Receivers for CSP . . . . .	344
8.3 Compact Heat Exchangers in High Temperature Solar Receivers of CSP . . . . .	346
8.4 Summary . . . . .	348
References . . . . .	354
<b>9 Compact Heat Exchangers Driven Hydrogen Production Plants . . . . .</b>	355
9.1 Introduction to Hydrogen Production Plants . . . . .	355
9.2 Electrical Energy on Supply and Demand . . . . .	360
9.3 Hydrogen as a Source of Renewable Energy . . . . .	365
9.3.1 Why Hydrogen as a Source of Renewable Energy Now? . . . . .	368
9.3.2 Technical Development for Hydrogen Production . . . . .	369
9.3.3 Technical Development for Hydrogen Production . . . . .	373
9.4 Development of a Hydrogen Combustion Turbine . . . . .	374
9.5 Feasibility Study on Utilization of Hydrogen Energy . . . . .	374
9.6 Hydrogen Production Using Nuclear Energy . . . . .	377
9.7 Constraints Involved for Hydrogen Production Using Nuclear Energy . . . . .	387
9.7.1 Safety: Hydrogen Generation . . . . .	387
9.7.2 Safety: Hydrogen Generation by Facility Location . . . . .	389
9.8 Efficient Generation of Hydrogen Fuels Utilizing Nuclear Power . . . . .	391
9.9 Thermal Characteristics for Coupling a Hydrogen Product Plant to HTR/VHTR . . . . .	396
9.10 Next Generation Nuclear Plant Intermediate Heat Exchanger Acquisition . . . . .	407
9.11 Applicability of Heat Exchanger to Process Heat Applications . . . . .	412
9.12 Applicability of Compact Heat Exchanger to Process Heat Applications . . . . .	415
References . . . . .	417
<b>Appendix A Table and Graphs Compilations . . . . .</b>	421
<b>Appendix B Gas Property Tables for Selected Gases . . . . .</b>	437
<b>Appendix C Thermodynamic Properties for Water . . . . .</b>	465

<b>Appendix D Thermodynamic Property Tables for Carbon Dioxide . . . . .</b>	501
<b>Appendix E Thermodynamic Property Tables for Sodium . . . . .</b>	509
<b>Appendix F Practical Design Steps for Compact Heat Exchangers . . . . .</b>	521
<b>Appendix G Cross-Flow Compact Heat Exchanger Design by Comsol . . . . .</b>	533
<b>Nuclear Systems Acronyms: Glossary of Nuclear Terms (US NRC) . . . . .</b>	553
<b>Index . . . . .</b>	557

## About the Author

**Bahman Zohuri** is currently at Galaxy Advanced Engineering, Inc. a consulting company that he started himself in 1991 when he left both semiconductor and defense industries after many years working as a chief scientist. After graduating from the University of Illinois in the field of Physics and Applied Mathematics, as well as the University of New Mexico from the Nuclear Engineering Department, he joined Westinghouse Electric Corporation where he performed thermal hydraulic analysis and natural circulation for the Inherent Shutdown Heat Removal System (ISHRS) in the core of a Liquid Metal Fast Breeder Reactor (LMFBR) as a secondary fully inherent shut system for secondary loop heat exchange. All these designs were used for Nuclear Safety and Reliability Engineering for Self-Actuated Shutdown System. He designed the Mercury Heat Pipe and Electromagnetic Pumps for Large Pool Concepts of LMFBR for heat rejection purpose for this reactor around 1978 where he received a patent for it. He later on was transferred to the defense division of Westinghouse where he was responsible for the dynamic analysis and method of launch and handling of the MX missile out of canister. The results are applied to MX launch seal performance and muzzle blast phenomena analysis (i.e., missile vibration and hydrodynamic shock formation). He also was involved in analytical calculation and computation in the study of Nonlinear Ion Wave in Rarefying Plasma. The results are applied to the propagation of “Soliton Wave” and the resulting charge collector traces, in the rarefactions characteristic of the corona of a laser irradiated target pellet. As part of his graduate research work at Argonne National Laboratory, he performed computation and programming of multi-exchange integral in surface physics and solid state physics. He holds different patents in areas such as diffusion processes and design of diffusion furnace while he was senior process engineer working for different semiconductor industries such as Intel, Varian, and National Semiconductor corporations. Later on he joined Lockheed Missile and Aerospace Corporation as Senior Chief Scientist and was responsible for the Research and Development (R&D) and the study of vulnerability, survivability and both radiation and laser hardening of different components Strategic Defense Initiative known as Star Wars.

This included of payload (i.e., IR Sensor) for Defense Support Program (DSP), Boost Surveillance and Tracking Satellite (BSTS) and Space Surveillance and Tracking Satellite (SSTS) against laser or nuclear threat. While there, he also studied and performed the analysis of characteristics of laser beam and nuclear radiation interaction with materials, Transient Radiation Effects in Electronics (TREE), Electromagnetic Pulse (EMP), System Generated Electromagnetic Pulse (SGEMP), Single-Event Upset (SEU), Blast and, Thermo-mechanical, hardness assurance, maintenance, device technology.

He did a few years of consulting under his company Galaxy Advanced Engineering with Sandia National Laboratories (SNL), where he was supporting development of operational hazard assessments for the Air Force Safety Center (AFSC) in connection with other interest parties. Intended use of the results was their eventual inclusion in Air Force Instructions (AFIs) specifically issued for Directed Energy Weapons (DEW) operational safety. He completed the first version of a comprehensive library of detailed laser tools for Airborne Laser (ABL), Advanced Tactical Laser (ATL), Tactical High Energy Laser (THEL), Mobile/Tactical High Energy Laser (M-THEL), etc.

He also was responsible for SDI computer programs involved with Battle Management C<sup>3</sup> and artificial Intelligent, and autonomous system. He is author of a few publications and holds various patents such as Laser Activated Radioactive Decay and Results of Thru-Bulkhead Initiation.

Recently he has published five books with CRC and Francis Taylor and Springer on the following subjects:

1. Heat Pipe Design and Technology: A Practical Approach, Published by CRC Publishing Company
2. Dimensional Analysis and Self-Similarity Methods for Engineering and Scientist Published by Springer Publishing Company
3. High Energy Laser (HEL): Tomorrow's Weapon in Directed Energy Weapons Volume I, Published by Trafford Publishing Company
4. Thermodynamics In Nuclear Power Plant Systems, Published by Springer Publishing Company
5. Thermal-Hydraulic Analysis of Nuclear Reactors, Published by Springer Publishing Company
6. Application of Compact Heat Exchangers for Combined Cycle Driven Efficiency in Next Generation Nuclear Power Plants: A Novel Approach, Springer Publishing Company.
7. Next Generation Nuclear Plants Driven Hydrogen Production Plants via Intermediate Heat Exchanger a Renewable Source of Energy, Springer Publishing Company.

# **Chapter 1**

## **Definitions and Basic Principles of Thermodynamics**

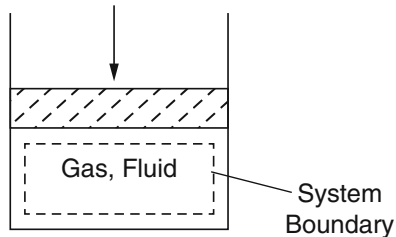
Any subject that deals with energy, or heat in general, requires an understanding of at least the basic principles of thermodynamics and, as in any science we encounter in our life, thermodynamics has its own unique language and vocabulary associated with it. Understanding of such language and vocabulary as well as abbreviations or acronyms and an accurate definition of basic concepts forms a sound foundation for the development of the science of thermodynamics, where it will lead us to have a better understanding of heat, energy, etc. and allow us to have a better grasp of fields and sciences that at least encounter the lateral parameters. In the case of a thermodynamic system, this science can be simply defined as a quantity of matter or a region in a space of consideration for study, and anything external to this system is called the system's surroundings and what separates this region from the rest of the space is defined as the boundary of the system. So, in this chapter we will talk about the basic principles that make up the science of thermodynamics [1–6].

### **1.1 Thermodynamics and Energy**

Thermodynamics can be defined as the study of energy, energy transformations, and its relation to matter. Matter may be described at a molecular (or microscopic) level using the techniques of statistical mechanics and kinetic theory. For engineering purposes, however, we want “averaged” information, i.e., a macroscopic (i.e., bulk energy flow), not a microscopic, description. The reasons behind acquiring such averaged information in a macroscopic form are twofold:

1. Microscopic description of an engineering device may produce too much information to manage.
2. More importantly, microscopic positions and velocities for example are generally not useful and lack enough information to determine how macroscopic systems will act or react unless, for instance, their total effect is integrated.

**Fig. 1.1** Piston (boundary) and Gas (system)



The observation driven macroscopic point of view deals with bulk energy flow which we encounter in Classical Thermodynamics; whereas, the theory driven microscopic point of view is about molecular interactions which we encounter in statistical physics/mechanics or kinetic theory.

We therefore neglect the fact that real substances are composed of discrete molecules and model matter from the start as a smoothed-out continuum. The information we have about a continuum represents the microscopic information averaged over a volume. Classical thermodynamics is concerned only with continua.

A thermodynamic system is a quantity of matter of fixed identity, around which we can draw a boundary (see Fig. 1.1 for an example). The boundaries may be fixed or moveable. Work or heat can be transferred across the system boundary. Everything outside the boundary is the *Surroundings*.

However, restricting ourselves by surroundings requires definition of a boundary that separates the system from the rest of the space of consideration (see Fig. 1.2), which results in defining a control volume.

When working with devices such as engines it is often useful to define the system to be an identifiable volume with flow in and out. This is termed a control volume. An example is shown in Fig. 1.3.

Another definition that we need to know is the concept of a “state” in thermodynamic. The thermodynamic state of a system is defined by specifying values of a set of measurable properties sufficient to determine all other properties. For fluid systems, typical properties are pressure, volume, and temperature. More complex systems may require the specification of more unusual properties. As an example, the state of an electric battery requires the specification of the amount of electric charge it contains.

Properties may be extensive or intensive. Extensive properties are additive. Thus, if the system is divided into a number of sub-systems, the value of the property for the whole system is equal to the sum of the values for the parts. Volume is an extensive property. Intensive properties do not depend on the quantity of matter present. Temperature and pressure are intensive properties.

Specific properties are extensive properties per unit mass and are denoted by lower case letters:

**Fig. 1.2** Boundary around electric motor (system)

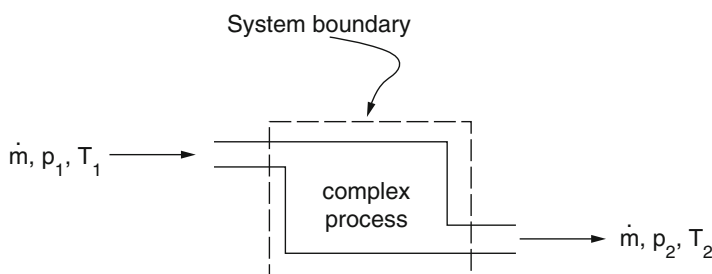
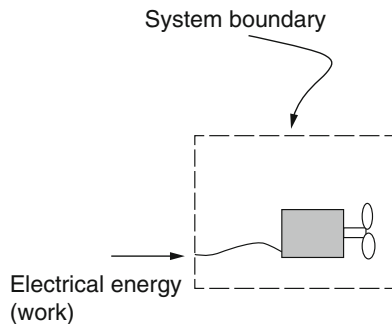


**Fig. 1.3** Sample of control volume

$$\text{Specific Volume} = \frac{V}{m} = v$$

Specific properties are intensive because they do not depend on the mass of the system.

The properties of a simple system are uniform throughout. In general, however, the properties of a system can vary from point to point. We can usually analyze a general system by sub-dividing it (either conceptually or in practice) into a number of simple systems in each of which the properties are assumed to be uniform.

It is important to note that properties describe states *only* when the system is in equilibrium.

In summary, the science of thermodynamics, through its two most important laws, drives the analysis of thermal systems which is achieved through the application of the governing conservation equations, namely Conservation of Mass, Conservation of Energy (first law of thermodynamics), the second law of thermodynamics, and the property relations. While the Energy part can be viewed as the ability to cause changes, as we have learned from our early physics in college, energy is conserved and it transforms from one form into another. For example, a car moving along a straight line on a level road skids to a stop. Its energy was initially kinetic energy (the energy due to motion). What is taking place in this case can be described as:

- The transfer of energy across boundaries, where  
Heat + Gas in piston-cylinder assembly Work Move piston
- The storage of energy in molecules  
Bulk motion Work and Heat Internal energy

The fundamental thing to understand is that a PWR converts nuclear energy to electrical energy and it does this by converting the nuclear energy first to thermal energy and then converting the thermal energy to mechanical energy, which is finally converted to electrical energy. The science of thermodynamics deals with each of these conversion processes. To quantify how each of these processes takes place we must understand and apply the laws of thermodynamics.

## 1.2 Scope of Thermodynamics

Thermodynamics is the science that deals with energy production, storage, transfer, and conversion. It is a very broad subject that affects most fields of science including biology and microelectronics. The primary forms of energy considered in this text will be nuclear, thermal, chemical, mechanical, and electrical. Each of these can be converted to a different form with widely varying efficiencies. Predominantly thermodynamics is most interested in the conversion of energy from one form to another via thermal means. However, before addressing the details of thermal energy conversion, consider a more familiar example. Newtonian mechanics defines work as force acting through a distance on an object. Performing work is a way of generating mechanical energy. Work itself is not a form of energy, but a way of transferring energy to a mass. So when one mass gains energy, another mass, or field, must lose that energy.

Consider a simple example. A 65-kg woman decides to go over Niagara Falls in a 25-kg wooden barrel. (The first person to go over the fall in a barrel was a woman, Annie Taylor.) Niagara Falls has a vertical drop of 50 m and has the highest flow rate of any waterfall in the world. The force acting on the woman and barrel is the force of gravity, which at the surface of the earth produces a force of 9.8 N for every kilogram of matter that it acts on. So we have

$$W = F \times D \quad F = (65 + 25) \times 9.8 = 882.0 \text{ N} \quad D = 50 \text{ m}$$

$$W = 882.0 \times 50.0 = 44,100 \text{ N-m} = 44.1 \text{ kJ}$$

A Newton meter is a Joule and 1000 J is a kilo-Joule. Therefore, when the woman and barrel went over the falls, by the time they had reached the bottom, the force of gravity had performed 44.1 kJ of work on them. The gravitational field had 44.1 kJ of potential energy stored in it, when the woman and the barrel were at the top of the falls. This potential energy was converted to kinetic energy by the time the barrel reached the bottom of the falls. Kinetic energy is also measured in Joules, as with all other forms of energy. However, we are usually most interested in velocities when

we talk about kinetic energies, so let us extract the velocity with which she hit the waters of the inlet to Lake Ontario.

$$\Delta KE = \Delta PE = 44.1 \text{ kJ} = 1/2 mV^2 = (90/2) \text{ kg} \times V^2 \quad V^2 = 44.1 \text{ kJ}/(90/2) \text{ kg}$$

Now it is a matter of converting units. A Joule is a Newton-meter. 1 N is defined as 1 kg accelerated at the rate of 1 m/s/s. So

$$\begin{aligned} 44.1 \text{ kJ} &= 44,100 \text{ N-m} \\ &= 44,100 \text{ kg m/s/s m} \\ &= 44,100 \text{ kg(m/s)}^2 \\ V^2 &= 44,100 \text{ kg(m/s)}^2 / (90/2) \text{ kg} \\ &= 490/(1/2) = 980(\text{m/s})^2 \\ V &= 31.3 \text{ m/s} (\sim 70 \text{ mph}) \end{aligned}$$

Needless to say she recommended that no one ever try that again. Of course, others have, some have made it, and some have drowned.

Before leaving this example, it is worth pointing out that when we went to calculate the velocity, it was unaffected by the mass of the object that had dropped the 50 m. So one-half the velocity squared represents what we will call a specific energy, or energy per kilogram. In addition, the potential energy at the top of the falls could be expressed as a specific potential energy relative to the waters below. The potential energy per pound mass would just be the acceleration of gravity times the height of the falls. Typically, we will use lower case letters to represent specific quantities and upper case letters to represent extensive quantities. Extensive quantities are dependent upon the amount of mass present. Specific quantities are also referred to as intensive variables, though there are some intensive variables that have no extensive counterpart, such as pressure or temperature.

$$\text{p.e.} = mgh / m = gh = 9.8 \times 50 = 0.49 \text{ kJ/kg}$$

It is also worth pointing out that Newton's law of gravity states that

$$F = G \frac{m_1 M_2}{R^2} \quad (\text{Eq. 1.1})$$

where  $m_1$  is the smaller mass and  $M_2$  is the mass of the Earth. We can find the specific force on an object by dividing the gravitational force by the mass of the object. For distances like 50 m on the surface of the Earth ( $R = 6,378,140$  m) we can treat  $R$  as constant, but if the distance the gravitational force acts through is comparable to the radius of the Earth, an integration would be required. Even on the top of Mount Everest, the gravitational potential is within 0.25 % of that at Sea Level, so gravity is essentially constant for all systems operating on the face of the Earth.

## 1.3 Units and Dimensions

Any physical quantity can be characterized by dimensions. The arbitrary magnitudes assigned to the dimensions are called units. There are two types of dimensions, primary or fundamental and secondary or derived dimensions.

Primary dimensions are: mass,  $m$ ; length,  $L$ ; time,  $t$ ; temperature,  $T$

Secondary dimensions can be derived from primary dimensions such as: velocity ( $\text{m/s}^2$ ), pressure ( $\text{Pa} = \text{kg/m s}^2$ ).

There are two unit systems currently available SI (International System) and USCS (United States Customary System) or English (E) system, and they are discussed in this section.

### 1.3.1 Fundamental Units

Before going further it is a very good idea to discuss units for physical quantities and the conversion of units from one system to another. Unfortunately, the field of thermodynamics is beset with two popular systems of units. One is the International System (SI) consisting of the kilogram, meter, and second. The other is the English (E) system consisting of the pound-mass, foot, and second.

Starting with the SI system, the unit of force is the Newton. The unit of work or energy is the Joule, and the unit of pressure is the Pascal. We have,

$$\underline{1 \text{ N} = 1 \text{ kg m/s}^2}$$

$$\underline{1 \text{ J} = 1 \text{ N-m}}$$

$$\underline{1 \text{ Pa} = 1 \text{ N/m}^2}$$

Now the acceleration of gravity at Sea Level on Earth is  $9.8066 \text{ m/s}^2$ , so a  $100 \text{ kg}$  mass will have weight  $980.66 \text{ N}$ . Also when we want to avoid spelling out very large or small quantities we will usually use the standard abbreviations for powers of ten in units of 1000. We have,

$$\underline{\text{kilo} = 10^3}$$

$$\underline{\text{mega} = 10^6}$$

$$\underline{\text{giga} = 10^9}$$

$$\underline{\text{deci} = 10^{-1}}$$

$$\underline{\text{centi} = 10^{-2}}$$

$$\underline{\text{milli} = 10^{-3}}$$

$$\underline{\text{micro} = 10^{-6}}$$

$$\underline{\text{nano} = 10^{-9}}$$

For the English system we have

---

$1\text{bm} \Rightarrow 1\text{lbf}$  (at Sea Level)

---

$1\text{ ft lbf} = 1\text{ lbf} \times 1\text{ ft}$

$1\text{ British Thermal Unit (BTU)} = 778\text{ ft lbf}$

$1\text{ psi} = 1\text{ lbf/in.}^2$

---

Note that the fact that  $1\text{ lbf} = 1\text{ lbm}$  at Sea Level on Earth, means that a mass of  $100\text{ lbm}$  will weigh  $100\text{ lbf}$  at Sea Level on Earth. The acceleration of gravity at Sea Level on Earth is  $32.174\text{ ft/s}^2$ . Thus we have  $1\text{ lbf}/(1\text{ lbm ft/s}^2) = 32.174$ . If we move to another planet where the acceleration of gravity is different, the statement that  $1\text{ lbm} \geq 1\text{ lbf}$  doesn't hold.

Consider comparative weights on Mars. The acceleration of gravity on Mars is 38.5 % of the acceleration of gravity on Earth. So in the SI system we have:

$$W = 0.385 \times 9.8066\text{ m/s}^2 \times 100\text{ kg} = 377.7\text{ N}$$

In the English system we have,

$$W = 0.385 \times 100\text{ lbm} = 38.5\text{ lbf}$$

### 1.3.2 Thermal Energy Units

The British thermal unit (Btu) is defined to be the amount of heat that must be absorbed by a 1 lb-mass to raise its temperature  $1\text{ }^{\circ}\text{F}$ . The calorie is the SI unit that is defined in a similar way. It is the amount of heat that must be absorbed by 1 g of water to raise its temperature  $1\text{ }^{\circ}\text{C}$ . This raises the question as to how a calorie compares with a Joule since both appear to be measures of energy in the SI system. James Prescott Joule spent a major part of his life proving that thermal energy was simply another form of energy like mechanical, kinetic or potential energy. Eventually his hypothesis was accepted and the conversion factor between the calorie and Joule is defined by,

---

$1\text{ cal} = 4.1868\text{ J}$

The constant 4.1868 is called the mechanical equivalent of heat.

### 1.3.3 Unit Conversion

As long as one remains in either the SI system or the English system, calculations and designs are simple. However, that is no longer possible as different organizations and different individuals usually think and work in their favorite system.

In order to communicate with an audience that uses both SI and English systems it is important to be able to convert back and forth between the two systems. The basic conversion factors are,

$$\underline{1 \text{ kg} = 2.20462 \text{ lbm}}$$

$$\underline{1 \text{ lbm} = 0.45359 \text{ kg}}$$

$$\underline{1 \text{ m} = 3.2808 \text{ ft}}$$

$$\underline{1 \text{ ft} = 0.3048 \text{ m}}$$

$$\underline{1 \text{ J} = 0.00094805 \text{ Btu}}$$

$$\underline{1 \text{ Btu} = 1055 \text{ J}}$$

$$\underline{1 \text{ atm} = 14.696 \text{ psi}}$$

$$\underline{1 \text{ atm} = 101,325 \text{ Pa}}$$

$$\underline{1 \text{ psi} = 6894.7 \text{ Pa}}$$

$$\underline{1 \text{ bar} = 100,000.0 \text{ Pa}}$$

$$\underline{1 \text{ bar} = 14.504 \text{ psi}}$$

The bar unit is simply defined by rounding off Sea Level atmospheric pressure to the nearest 100 kPa. There are many more conversion factors defined in the [Appendix](#), but they are all derived from these basic few.

## 1.4 Classical Thermodynamics

Classical thermodynamics was developed long before the atomic theory of matter was accepted. Therefore, it treats all materials as continuous and all derivatives well defined by a limiting process. Steam power and an ability to analyze it and optimize it was one of the main drivers for the development of thermodynamic theory. The fluids involved always looked continuous. A typical example would be the definition of the density of a substance at a point. We have,

$$\rho = \lim_{\Delta V \rightarrow 0} \frac{\Delta m}{\Delta V} \quad (\text{Eq. 1.2})$$

As long as  $\Delta V$  does not reach the size of an atom this works. Since classical thermodynamics was developed, however, we have come to understand that all gases and liquids are composed of very small atoms or molecules and a limiting process that reaches the atomic or molecular level will eventually become discontinuous and chaotic. Nevertheless, the continuous model still works well for the

macroscopic systems discussed in this text and classical thermodynamics is based on it.

At times, we will refer to an atomistic description of materials in order to develop a method of predicting specific thermodynamic variables that classical thermodynamics cannot predict. A typical example is the derivative that is called the constant volume specific heat. This variable is defined as the rate of change of the internal energy stored in a substance as a function of changes in its temperature. Classical thermodynamics demonstrates that this variable has to exist and makes great use of it, but it has no theory for calculating it from first principles. An atomistic view will allow us to make some theoretical estimates of its value. Therefore, at times we will deviate from the classical model and adopt an atomistic view that will improve our understanding of the subject.

Classical thermodynamics is also an equilibrium science. The laws of thermodynamics apply to objects or systems in equilibrium with themselves and their surroundings. By definition, a system in equilibrium is not likely to change. However, we are generally interested in how systems change as thermal energy is converted to and from other forms of energy. This presents a bit of a dilemma in that the fundamental laws are only good for a system in equilibrium and the parameters we want to predict are a result of thermal energy changes in the system. To get around this dilemma, we define what is called a quasi-equilibrium process. A quasi-equilibrium process is one that moves from one system state to another so slowly and so incrementally, that it looks like a series of equilibrium states. This is a concept that classical thermodynamics had a great deal of difficulty clarifying and quantifying. Basically, a process was a quasi-equilibrium process if the laws of equilibrium thermodynamics could characterize it. This is sort of a circular definition, but once again, we will find that the atomistic view allows us to make some predictions and quantifications that identify a quasi-equilibrium process. Quasi-equilibrium processes can occur very rapidly on time scales typical of human observation. For example, the expansion of hot gases out of the nozzle of a rocket engine can be well described as a quasi-equilibrium process with classical thermodynamics.

## 1.5 Open and Closed Systems

In the transfer and conversion of thermal energy, we are interested in separating the *entire universe* into a *system* and its *environment*. We are mainly interested in the energy transfers and conversions that go on within the *system*, but in many cases, we need to consider its interactions with the rest of the world or its *environment*. Systems that consist of a *fixed amount of mass* that is contained within fixed boundaries are called *closed systems*. Systems that *pass the mass back and forth* to the environment are called *open systems*. Both *open* and *closed systems* allow energy to flow across their borders, but the flow of mass determines whether they are *open* or *closed systems*. *Open systems* also carry energy across their borders with

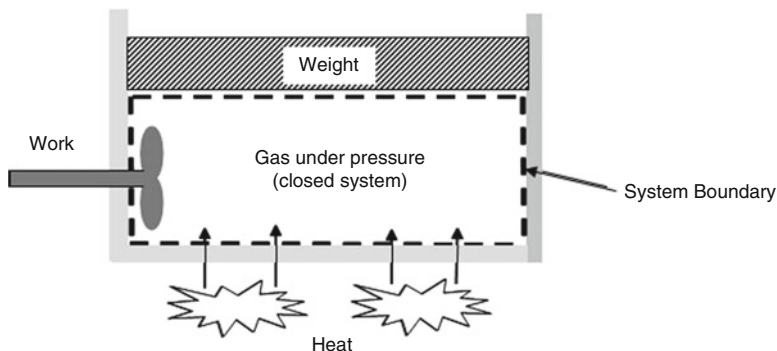


**Fig. 1.4** A closed system

the mass as it moves. Consider the simple compressed gas in the piston below as a *closed system* (Fig. 1.4).

In analyzing the closed system, we are concerned about the changes in the internal energy of the compressed gas as it interacts with its environment and the transfers of mechanical and thermal energies across its boundary.

In analyzing open systems, the concept of a *control volume* comes into play. The *control volume* is the boundary for the open system where the energy changes that we are interested in take place; the thing that separates the open system from its environment. Consider the following open system where we have now allowed mass to flow in and out of the piston of our closed system above (Fig. 1.5).

The *control volume* looks a lot like our system boundary from before, and it is. The only difference is that we now allow mass to flow in and out of our *control volume*. Thermal and mechanical energy can still flow across the boundary, or in and out of the *control volume*. The mass flowing in and out can also carry energy with it either way.

## 1.6 System Properties

In order to characterize a system we have to identify its properties. Initially there are three main properties that we are concerned with—density, pressure, and temperature all of which are *intensive* variables. We use intensive properties to characterize the equilibrium states of a system. Systems are composed of *pure substances* and *mixtures of pure substances*. A *pure substance* is a material that consists of only one type of atom or one type of molecule. A *pure substance* can exist in multiple phases. Normally the phases of concern are gas, liquid, and solid, though for many pure substances there can be several solid phases. Water is an example of a pure substance that can readily be observed in any of its three phases.

A solid phase is typically characterized as having a fixed volume and fixed shape. A solid is rigid and incompressible. A liquid has a fixed volume but no fixed

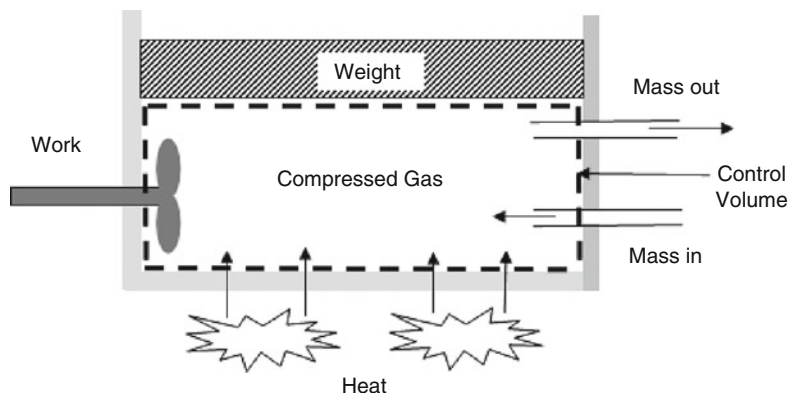


**Fig. 1.5** An open system

shape. It deforms to fit the shape of the container that it is in. It is not rigid but is still relatively incompressible. A gas has no fixed shape and no fixed volume. It expands to fit the container that it is in. To characterize a system composed of one or more pure components and one or more phases we need to specify the correct number of intensive variables required to define a state. Gibbs Phase Rule, named after J. Willard Gibbs who first derived it, gives the correct number of intensive variables required to completely define an equilibrium state in a mixture of pure substances. It is:

$$V = C - P + 2 \quad (\text{Eq. 1.3})$$

$V$  = Number of variables required to define an equilibrium state.

$C$  = The number of pure components (substances) present.

$P$  = The number of phases present.

So for pure steam at Sea Level and above 100 °C, we have 1 component and 1 phase so the number of variables required to specify an equilibrium state is 2, typically temperature and pressure. However, temperature and density would also work. If we have a mixture of steam and liquid water in the system, we have 1 component and 2 phases, so only one variable is required to specify the state, either pressure or temperature would work. If we have a mixture like air that is composed of oxygen, nitrogen, and argon, we have 3 components and 3 phases (the gas phase for each component), and we are back to requiring 2 variables. As we progress, we will introduce additional intensive variables that can be used to characterize the equilibrium states of a system in addition to density, pressure, and temperature.

### 1.6.1 Density

Density is defined as the mass per unit volume. The standard SI unit is kilograms per cubic meter ( $\text{kg}/\text{m}^3$ ). The Standard English unit is pounds mass per cubic foot ( $\text{lbf}/\text{ft}^3$ ). If the mass per unit volume is not constant in a system, it can be defined at a point by a suitable limiting process that converges for engineering purposes long before we reach the atomistic level. The inverse of density is specific volume. Specific volume is an intensive variable, whereas volume is an extensive variable. The standard unit for specific volume in the SI system is cubic meters per kilogram ( $\text{m}^3/\text{kg}$ ). The standard unit in the English system is cubic feet per pound mass ( $\text{ft}^3/\text{lbf}$ ).

### 1.6.2 Pressure

Pressure is defined as force per unit area. The standard unit for pressure in the SI system is the Newton per square meter or Pascal (Pa). This unit is fairly small for most engineering problems so pressures are more commonly expressed in kilo-Pascals (kPa) or mega-Pascals (MPa). The standard unit in the English system really does not exist. The most common unit is pounds force per square inch (psi). However, many other units exist and the appropriate conversion factors are provided in the [Appendix](#).

Pressure as an intensive variable is constant in a closed system. It really is only relevant in liquid or gaseous systems. The force per unit area acts equally in all directions and on all surfaces for these phases. It acts normal to all surfaces that contain or exclude the fluid. (The term fluid includes both gases and liquids.) The same pressure is transmitted throughout the entire volume of liquid or gas at equilibrium (Pascal's law). This allows the amplification of force by a hydraulic piston. Consider the system in the following figure. In Fig. 1.6, the force on the piston at B is greater than the force on the piston at A because the pressure on both is the same and the area of piston B is much larger.

In a gravity field, the pressure in a gas or liquid increases with the height of a column of the fluid. For instance, in a tube containing a liquid held vertically, the weight of all of the liquid above a point in the tube is pressing down on the liquid at that point. Consider Fig. 1.7, then:

$$\begin{aligned} dp &= \rho g dh \\ p(0) &= P(H) + \int_0^H \rho g dh \end{aligned} \tag{Eq. 1.4}$$

**Fig. 1.6** A hydraulic amplifier

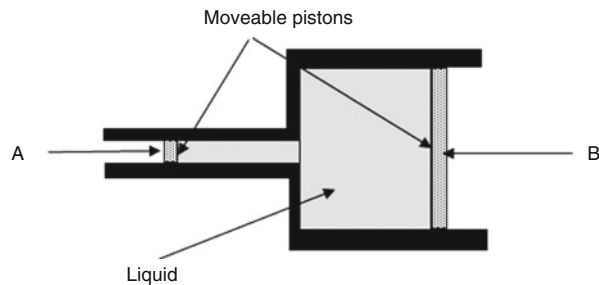
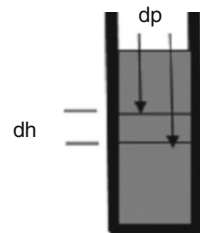


**Fig. 1.7** Pressure in a liquid column



Thus, the pressure at the bottom of the container is equal to the pressure on the top of the fluid in the container plus the integral of the weight of the fluid per unit area in the container.

This raises an interesting concept. Often it is important to distinguish between **absolute pressure** and **gage pressure**. The preceding equation calculates the **absolute pressure**. The **gage pressure** is simply the pressure exerted by the weight of the column without the external pressure on the top surface of the liquid. It is certainly possible to have a negative gage pressure, but not possible to have a negative absolute pressure. A **vacuum pressure** occurs when the absolute pressure in a system is less than the pressure in the environment surrounding the system.

A manometer is a very common way of measuring pressure (setup in Fig. 1.8). A manometer works by measuring the difference in height of a fluid in contact with two different pressures. A manometer can measure absolute pressure by filling a closed end tube with liquid and then inverting it into a reservoir of liquid that is open to the pressure that is to be measured. Manometers can also measure a vacuum gage pressure. Consider Fig. 1.8 below:

The tall tubes on the right in each system are open to the atmosphere. System A is operating at a small negative pressure, or vacuum, relative to the atmosphere. System B is operating at a positive pressure relative to the atmosphere. The magnitude of the pressure in each case can be calculated by measuring the height difference between the fluids in the two sides of the U-tube and calculating its weight per unit area. This is the difference in the pressures inside systems A or B and the atmospheric pressure pushing down on the open columns on the right.

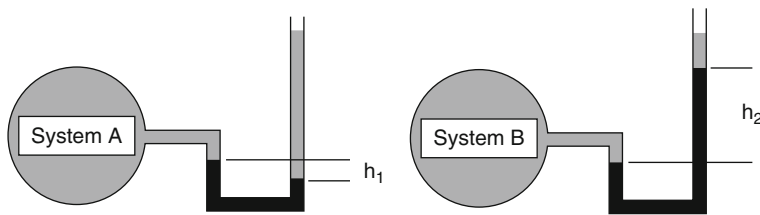


**Fig. 1.8** Pressure measurement with manometers

### 1.6.3 Temperature

The other intensive variable to be considered at this point is the temperature. Most everyone is familiar with temperature as a measure of coldness or hotness of a substance. As we continue our study of thermodynamics, we will greatly refine our concept of temperature but for now it is useful to discuss how a temperature scale is constructed. Traditionally the Fahrenheit scale was established by defining the freezing point of water at Sea Level pressure to be  $32^{\circ}\text{F}$  and the boiling point of water to be  $212^{\circ}\text{F}$  under the same conditions. A thermometer containing a fluid that expands readily as a function of temperature could be placed in contact with a system that contained ice and water vapor saturated air. The height of the fluid in the thermometer would be recorded as the  $32^{\circ}\text{F}$  height. Then the same thermometer would be placed in a water container that was boiling and the height of the fluid in the thermometer marked as the  $212^{\circ}\text{F}$  point. The difference in height between the two points would then be marked off in 180 divisions with each division representing  $1^{\circ}\text{F}$ . The Celsius scale was defined in the same way by setting the freezing point of water at  $0^{\circ}\text{C}$  and the boiling point at  $100^{\circ}\text{C}$ . Water was chosen as the reference material because it was always available in most laboratories around the world.

When it became apparent that absolute temperatures were possibly more important than simple temperatures in the normal range of human experience, absolute temperature scales were defined. The freezing point of water was defined as  $273.15\text{ K}$  and the boiling point was defined as  $373.15\text{ K}$ , to match up with the Celsius scale. Note that the unit on the absolute scale is Kelvin, not degrees Kelvin. It was named in honor of Lord Kelvin who had a great deal to do with the development of temperature measurement and thermodynamics. The freezing point of water was further defined as the equilibrium of pure ice and air saturated water. However, it was difficult to attain this point because as ice melts it forms a layer of pure water around itself, which prevents direct contact of pure ice and air-saturated water. Therefore, in 1954, the two-point method was abandoned and the triple point of water was chosen as a single standard. The triple point of water is  $273.16\text{ K}$ ,  $0.01\text{ K}$  above the ice point for water at Sea Level pressure. A single point can be used to define the temperature scale if temperatures are measured with a constant volume, ideal gas thermometer. Basically, the ideal gas thermometer can measure the pressure exerted by a constant volume of gas in contact with the system

to be measured. It can also measure the pressure exerted by the gas when in contact with a system at the triple point of water. The ratio of the two pressures gives the ratio of the measured absolute temperature to the absolute temperature of the triple point of water.

However, additional secondary standards are defined to simplify calibration over a broad range of temperatures. The International Practical Temperature Scale is defined by:

Triple point of equilibrium hydrogen	13.81 K
Boiling point of hydrogen at 33.33 kPa	17.042 K
Boiling point of hydrogen at 1 atm	20.28 K
Boiling point of neon	27.102 K
Triple point of oxygen	54.361 K
Boiling point of oxygen	90.188 K
Triple point of water	273.16 K
Boiling point of water	373.15 K
Freezing point of zinc	692.73 K
Freezing point of silver	1235.08 K
Freezing point of gold	1337.58 K

Once the absolute temperature scale in Kelvin was defined it became part of the SI system. An absolute scale matching the Fahrenheit scale between the freezing point of water and its boiling point has been defined for the English system. Since there are  $180^{\circ}$  between the freezing and boiling points in the Fahrenheit scale and  $100^{\circ}$  over the same range in the Kelvin scale, the absolute scale for the English system, where the unit of measurement is called a degree Rankine, is simply 1.8 times the number of Kelvin. So the freezing point of water on the Rankine scale is  $491.67^{\circ}\text{R}$  and the boiling point is  $671.67^{\circ}\text{R}$ . Absolute zero on the Rankine scale is  $-459.67^{\circ}\text{F}$ . To convert back and forth the following formulas apply.

$$\begin{aligned} T_{\text{K}} &= T_{\text{C}} + 273 \\ T_{\text{C}} &= T_{\text{K}} - 273 \\ T_{\text{R}} &= T_{\text{F}} + 460 \\ T_{\text{F}} &= T_{\text{R}} - 460 \end{aligned} \quad (\text{Eq. 1.5})$$

$$\begin{aligned} T_{\text{R}} &= 1.8T_{\text{K}} \\ T_{\text{K}} &= \frac{5}{9}T_{\text{R}} \\ T_{\text{F}} &= 1.8T_{\text{C}} + 32 \\ T_{\text{C}} &= \frac{5}{9}(T_{\text{F}} - 32) \end{aligned} \quad (\text{Eq. 1.6})$$

## 1.7 Properties of the Atmosphere

Before going further, it will be useful to have a model for the atmosphere that can be used for calculations. This is important to realize that the atmosphere at Sea Level supports a column of air that extends upwards of 50 miles. Given the equation derived earlier for the pressure in a column of fluid, we have as always to begin at Sea Level.

$$\begin{aligned} dp &= -\rho g dh \\ \text{Let } \rho &= \frac{p}{RT} \\ \text{Then} \\ dp &= -p \frac{g}{RT} dh \end{aligned} \tag{Eq. 1.7a}$$

Or by integration of the last term of Eq. (1.7a), we obtain

$$p = p_{SL} e^{-\frac{g}{RT} h} \tag{Eq. 1.7b}$$

To perform the integration, the above temperature has been assumed constant. This is not quite true as the standard lapse rate for the Troposphere up to about 40,000 ft is approximately 2 °C per 1000 ft or 3.6 °F per 1000 ft. This means that the air is denser than the exponential model predicts. However, it is approximately correct for the Troposphere particularly if only a limited range of elevations is considered and the average temperature is used. The initial values at Sea Level for the standard atmosphere are,

Pressure	14.696 psi	101.325 kPa
Temperature	59 °F (519 °R)	15 °C (288 K)
Density	076,474 lbm/ft³	1.225 kg/m³

Composition	Mole fraction (%)
Nitrogen	78.08
Oxygen	20.95
Argon	0.93
Carbon Dioxide	0.03
Ne, He, CH <sub>4</sub> , etc.	0.01

A more extensive model of the atmosphere as a function of altitude is provided in the [Appendix](#). The relative composition is essentially constant up to the top of the Troposphere.

## 1.8 The Laws of Thermodynamics

It is useful at this time to state the Laws of Thermodynamics. Later chapters will expand on them greatly, but realizing there are four simple laws that all of the analysis is built around will provide some structure to guide the way forward.

**Zeroth Law of Thermodynamics:** *Two bodies in thermal contact with a third body will be at the same temperature.*

This provides a definition and method of defining temperatures, perhaps the most important intensive property of a system when dealing with thermal energy conversion problems.

**First Law of Thermodynamics:** *Energy is always conserved when it is transformed from one form to another.*

This is the most important law for analysis of most systems and the one that quantifies how thermal energy is transformed to other forms of energy.

**Second Law of Thermodynamics:** *It is impossible to construct a device that operates on a cycle and whose sole effect is the transfer of heat from a cooler body to a hotter body.*

Basically, this law states that it is impossible for heat to spontaneously flow from a cold body to a hot body. If heat could spontaneously flow from a cold body to a hot body, we could still conserve energy, so the First Law would hold. But every experiment that has ever been performed indicates that thermal energy always flows the other way. This law seems obvious enough but the implications are very significant, as we will see.

**Third Law of Thermodynamics:** *It is impossible by means of any process, no matter how idealized, to reduce the temperature of a system to absolute zero in a finite number of steps.*

This allows us to define a zero point for the thermal energy of a body be taken under consideration and a subject of this matter is beyond the scope of this book.

## References

1. Zohuri, Bahman, and Patrick McDaniel. 2015. *Thermodynamics in nuclear power plant*. Switzerland: Springer Publishing Company.
2. Cengel, Yunus A., and Michael A. Boles. 2008. *Thermodynamics: An engineering approach*, 6th ed. Boston: McGraw Hill.
3. Elliott, J. Richard, and Carl T. Lira. 1999. *Introductory chemical engineering thermodynamics*. Upper Saddle River, NJ: Prentice Hall.
4. Hsieh, Jui S. 1975. *Principles of thermodynamics*. New York: McGraw Hill.
5. Moran, Michael J., and Howard N. Shapiro. 2008. *Fundamentals of engineering thermodynamics*, 6th ed. New York: John Wiley & Sons.
6. Van Wylen, Gordon J., and Richard E. Sonntag. 1978. *Fundamentals of classical thermodynamics*. SI Version 2e. New York: John Wiley & Sons.

# **Chapter 2**

## **Heat Exchanger Types and Classifications**

A heat exchanger is a heat transfer device that exchanges heat between two or more process fluids. Heat exchangers have widespread industrial and domestic applications. Many types of heat exchangers have been developed for use in steam power plants, chemical processing plants, building heat and air conditioning systems, transportation power systems, and refrigeration units.

The actual design of heat exchangers is a complicated problem. It involves more than heat-transfer analysis alone. Cost of fabrication and installation, weight, and size play important roles in the selection of the final design from a total cost of ownership point of view. In many cases, although cost is an important consideration, size and footprint often tend to be the dominant factors in choosing a design.

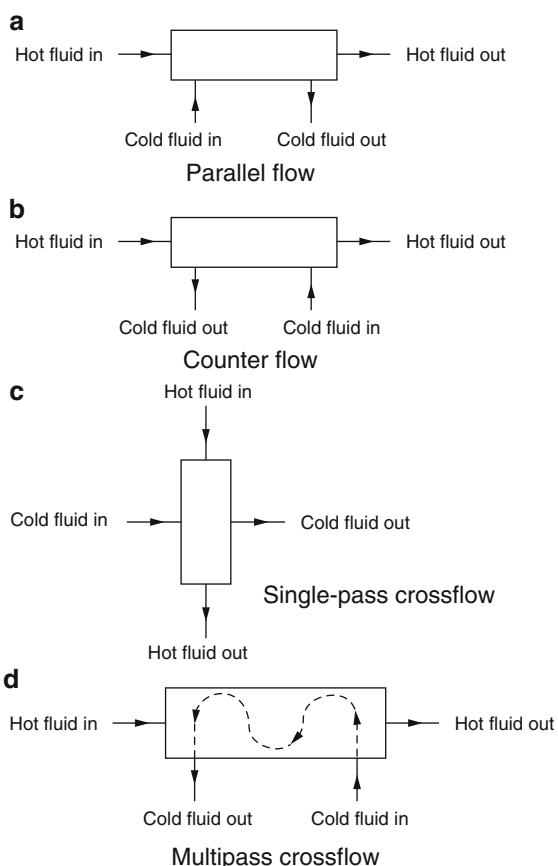
### **2.1 Heat Exchanger Types**

A heat exchanger is a heat transfer device that exchanges heat between two or more process fluids. Heat exchangers have widespread industrial and domestic applications. Many types of heat exchangers have been developed for use in steam power plants, chemical processing plants, building heat and air conditioning systems, transportation power systems, and refrigeration units.

The actual design of heat exchangers is a complicated problem. It involves more than heat-transfer analysis alone. Cost of fabrication and installation, weight, and size play important roles in the selection of the final design from a total cost of ownership point of view. In many cases, although cost is an important consideration, size and footprint often tend to be the dominant factors in choosing a design.

Most heat exchangers may be classified as one of several basic types. The four most common types, based on flow path configuration, are illustrated in Fig. 2.1 below [1].

**Fig. 2.1** Types of flow path configuration through heat exchanger



1. In *concurrent*, or *parallel-flow*, units the two fluid streams enter together at one end, flow through in the same direction, and leave together at the other end.
2. In *countercurrent*, or *counter-flow*, units the two streams move in opposite directions.
3. In *single-pass crossflow* units one fluid moves through the heat transfer matrix at right angles to the flow path of the other fluid.
4. In *multipass crossflow* units one fluid stream shuttles back and forth across the flow path of the other fluid stream, usually giving a crossflow approximation to counterflow.

The most important difference between these four basic types lies in the relative amounts of heat transfer surface area required to transfer the desired amount of heat between the two fluids.

Figure 2.2 below shows the relative area required for each type as a function of the change in temperature of the fluid with the largest temperature change requirement for a typical set of conditions. In the region in which the fluid temperature

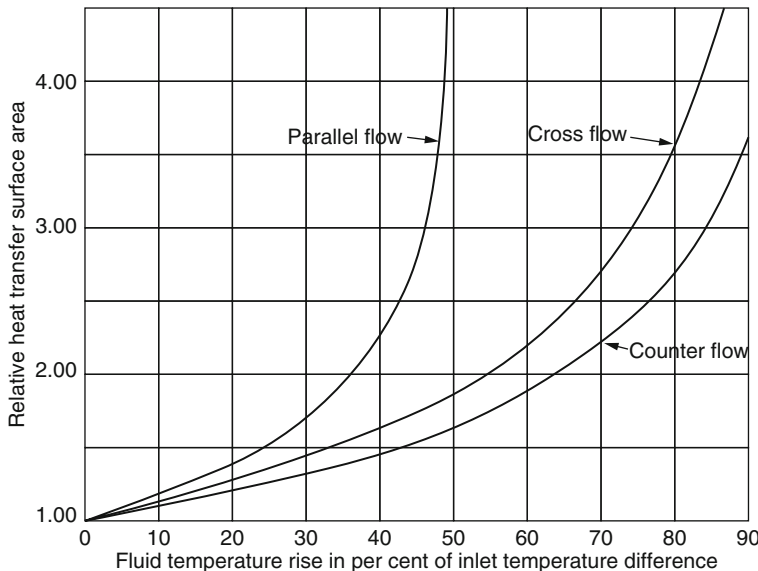


**Fig. 2.2** The required relative heat transfer surface area as a function of the ratio of the temperature rise (or drop) in the fluid stream having the greater change in temperature to the difference in temperature between the inlet streams

change across the heat exchanger is a small percentage of the difference in temperature between the two entering fluid streams, all the units require roughly the same area. The parallel-flow heat exchanger is of interest primarily for applications in this region. Cross-flow units have a somewhat broader range of application, and are peculiarly suited to some types of heat exchanger construction that have special advantages. The counter-flow heat exchanger requires the least area. Furthermore, it is the only type that can be employed in the region in which the temperature change in one or both of the fluid streams closely approaches the temperature difference between the entering fluids streams.

In addition, heat exchangers may be classified as direct contact or indirect contact. In the direct-contact type, heat transfer takes place between two immiscible fluids, such as a gas and a liquid, coming into direct contact. For example, cooling towers, jet condensers for water vapor, and other vapors utilizing water spray are typical examples of direct-contact exchangers.

**Immiscible Fluids are incapable of being mixed or blended together. Immiscible liquids that are shaken together eventually separate into layers. Oil and Water are typical immiscible fluids.**

In the indirect-contact type of heat exchangers, such as automobile radiators, the hot and cold fluids are separated by an impervious surface, and they are referred to as *surface heat exchangers*. There is no mixing of the two fluids.

## 2.2 Classification According to Transfer Processes

Heat exchangers are classified according to transfer processes into indirect and direct contact types.

### 2.2.1 *Indirect Contact Type Heat Exchangers*

In an indirect-contact heat exchanger, the fluid streams remain separate and the heat transfers continuously through an impervious dividing wall or into and out of a wall in a transient manner. Thus, ideally, there is no direct contact between thermally interacting fluids. This type of heat exchanger, also referred to as a surface heat exchanger, can be further classified into direct-transfer type, storage type, and fluidized-bed exchangers.

### 2.2.2 *Direct Contact Type Heat Exchangers*

In this type, heat transfers continuously from the hot fluid to the cold fluid through a dividing wall. Although a simultaneous flow of two (or more) fluids is required in the exchanger, there is no direct mixing of the two (or more) fluids because each fluid flows in separate fluid passages. In general, there are no moving parts in most such heat exchangers. This type of exchanger is designated as a recuperative heat exchanger or simply as a recuperator. (Some examples of direct transfer type heat exchangers are tubular, plate-type, and extended surface exchangers).

Note that the term recuperator is not commonly used in the process industry for shell-and-tube and plate heat exchangers, although they are also considered recuperators. Recuperators are further sub-classified as prime surface exchangers and extended-surface exchangers. Prime surface exchangers do not employ fins or extended surfaces on any fluid side. Plain tubular exchangers, shell-and-tube exchangers with plain tubes, and plate exchangers are good examples of prime surface exchangers. Recuperators constitute a vast majority of all heat exchangers (Fig. 2.3).

## 2.3 Classification of Heat Exchanger by Construction Type

Heat exchangers also can be classified according to their construction features. For example, there are tubular, plate, plate-fin, tube-fin, and regenerative exchangers. An important performance factor for all heat exchangers is the amount of heat

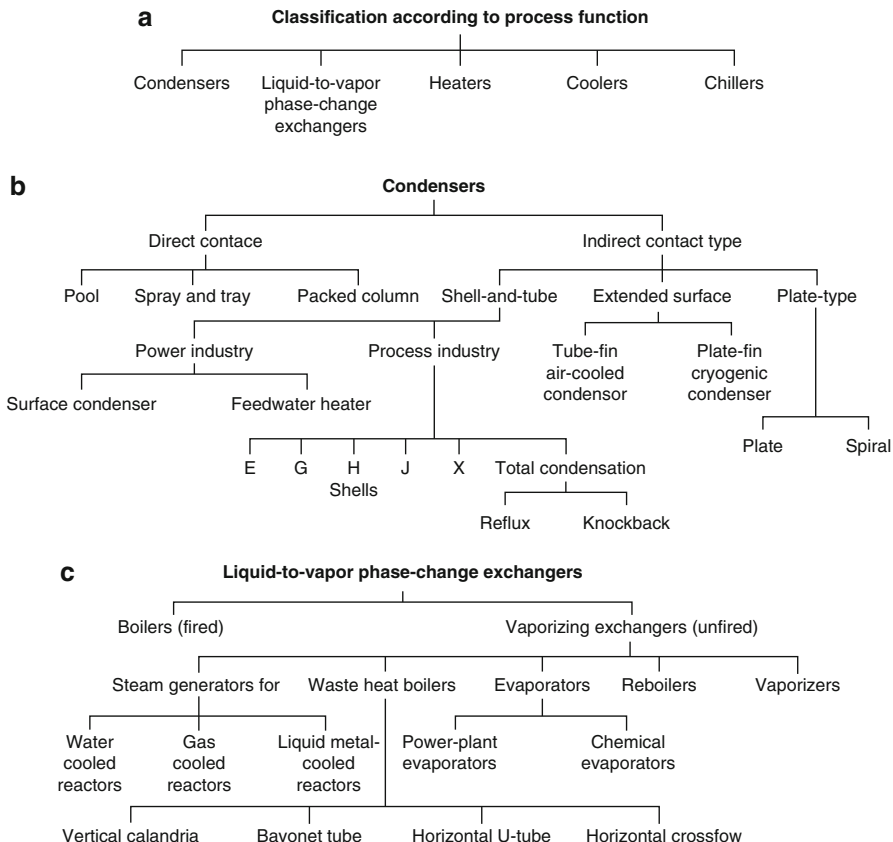


**Fig. 2.3** (a) Classification according to process function; (b) classification of condensers; (c) classification of liquid-to-vapor phase-change exchangers

transfer surface area within the volume of the heat exchanger. This is called its *compactness factor* and is measured in square meters per cubic meter.

### 2.3.1 Tubular Heat Exchangers

Tubular exchangers are widely used, and they are manufactured in many sizes, flow arrangements, and types. They can accommodate a wide range of operating pressures and temperatures. The ease of manufacturing and their relatively low cost have been the principal reason for their widespread use in engineering applications. A commonly used design, called the *shell-and-tube* exchanger, consists of round tubes mounted on a cylindrical shell with their axes parallel to that of the shell.

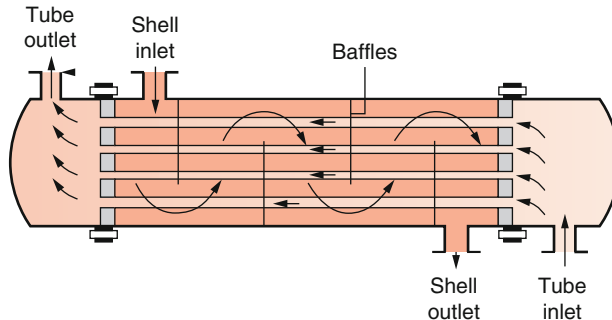


**Fig. 2.4** A shell-and-tube heat exchanger; one shell pass and one tube pass [2]

Figure 2.4 illustrates the main features of a shell-and-tube exchanger having one fluid flowing inside the tubes and the other flowing outside the tubes. The principle components of this type of heat exchanger are the tube bundle, shell, front and rear end headers, and baffles. The baffles are used to support the tubes, to direct the fluid flow approximately normal to the tubes, and to increase the turbulence of the shell fluid. There are various types of baffles, and the choice of baffle type, spacing, and geometry depends on the flow rate allowable shell-side pressure drop, tube support requirement, and the flow-induced vibrations. Many variations of shell-and-tube exchanger are available; the differences lie in the arrangement of flow configurations and in the details of construction.

Baffled heat exchangers with one shell pass and two tube passes and with two shell passes and four tube passes are shown in Fig. 2.5a [3] and b [3], respectively [3].

The character of the fluids may be *liquid-to-liquid*, *liquid-to-gas*, or *gas-to-gas*. Liquid-to-liquid exchangers have the most common applications. Both fluids are pumped through the exchangers; hence, the heat transfer on both the tube side and the shell side is by forced convection. Since the heat transfer coefficient is high with the liquid flow, generally there is no need to use fins [2].

The liquid-to-gas arrangement is also commonly used; in such cases, the fins usually are added on the gas side of the tubes, where the heat transfer coefficient is low.

Gas-to-gas exchangers are used in the exhaust-gas and air preheating recuperators for gas gas-turbine systems, cryogenic gas-liquefaction systems, and steel furnaces. Internal and external fins generally are used in the tubes to enhance heat transfer.

### 2.3.2 Plate Heat Exchangers

As the name implies, plate heat exchangers usually are constructed of thin plates. The plates may be smooth or may have some form of corrugation. Since the plate

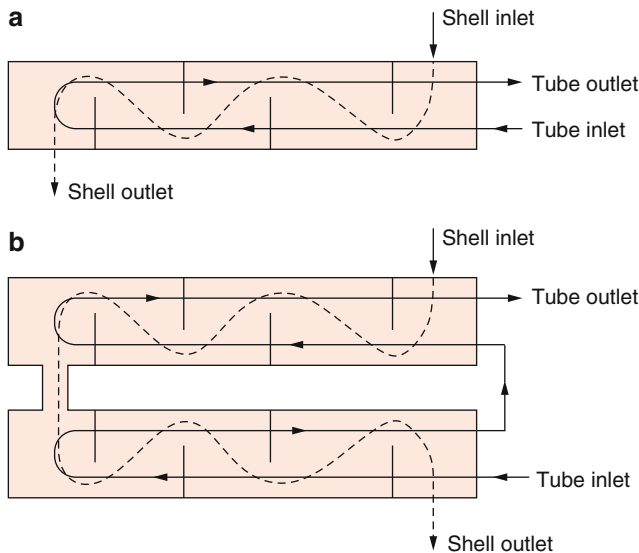


**Fig. 2.5** Shell-and-tube heat exchangers. (a) One shell pass and two tube passes. (b) Two shell passes and four tube passes [3]

geometry cannot accommodate as high pressure and/or temperature differentials as a circular tube, it is generally designated for moderate temperature and/or pressure differentials of the compactness factor for plate exchangers ranges from about 120 to 230 m<sup>2</sup>/m<sup>3</sup>. Further details of these types of heat exchangers can be found in Sect. 3.2.

### 2.3.3 Plate Fin Heat Exchangers

The compactness factor can be significantly improved (i.e., up to about 6000 m<sup>2</sup>/m<sup>3</sup>) by using the plate-fin type of heat exchanger. Figure 2.6 illustrates typical plate-fin configurations. Flat plates separate louvered or corrugated fins. Cross-flow, counterflow, or parallel-flow arrangements can be obtained readily by properly arranging the fins on each side of the plate. Plate-fin exchangers are generally used for gas-to-gas applications, but they are used for low-pressure applications not exceeding about 10 atm (that is, 1000 kPa). The maximum operating temperatures are limited to about 800 °C. Plate-fin heat exchangers have also been used for cryogenic applications.

Further details of these types of heat exchangers can be found in Sect. 3.2.

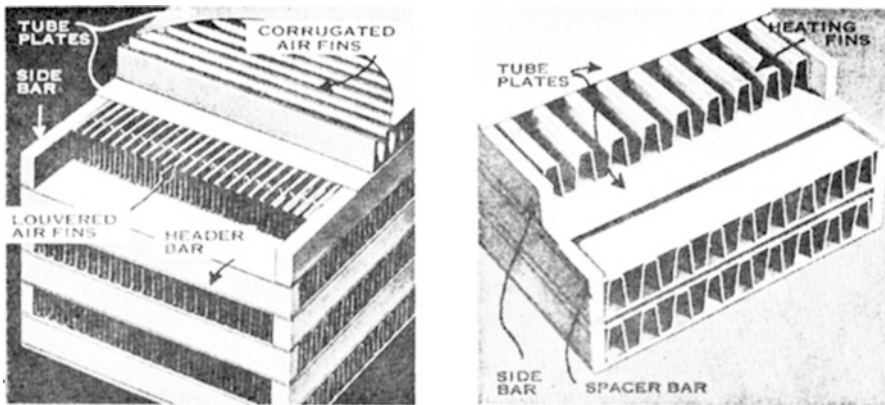


**Fig. 2.6** Plate-fin heat exchangers. (Courtesy of Harrison Radiator Division of General Motors Corporation)

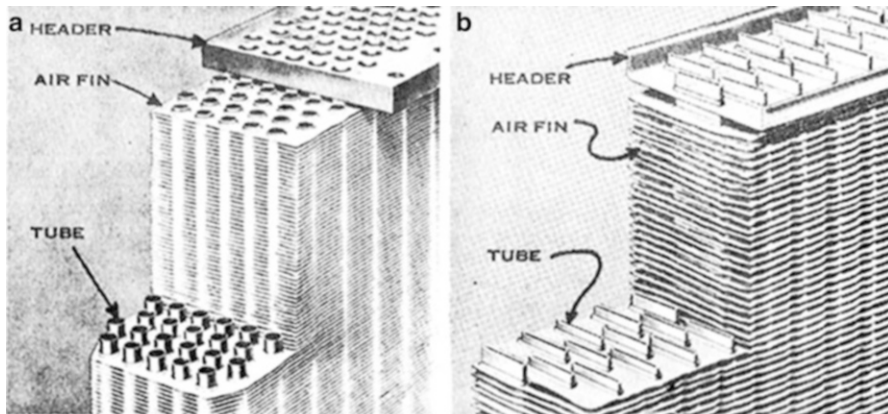


**Fig. 2.7** Tube fin heat exchangers. (a) Round tube and fin. (b) Flat tube and fin. (Courtesy of Harrison Radiator Division of General Motors Corporation)

### 2.3.4 **Tube Fin Heat Exchangers**

When a high operating pressure or an extended surface is needed on one side, tube-fin exchangers are used. Figure 2.7 illustrates two typical configurations, one with round tubes and the other with flat tubes. Tube-fin exchangers can be used for a wide range of tube fluid operating pressures not exceeding about 30 atm and operating temperatures from low cryogenic applications to about 870 °C. The maximum compactness ratio is somewhat less than that obtainable with plate-fin exchangers.

The tube-fin heat exchangers are used in gas turbine, nuclear, fuel cell, automobile, airplane, heat pump, refrigeration, electronics, cryogenics, air conditioning, and many other applications.

### 2.3.5 Printed Circuit Heat Exchanger

The Printed Circuit Heat Exchanger (PCHE) is one of the compact types of heat exchangers available as alternatives to shell and tube heat exchangers. Its name is derived from the procedure used to manufacture the flat metal plates that form the core of the heat exchanger which is done by chemical milling. These plates are then stacked and diffusion bonded, converting the plates into a solid metal block containing precisely engineered fluid flow passages. These channels are typically semicircular in cross section with a depth of 1.5–3 mm. PCHEs are typically built from stainless steels and can operate at temperatures from cryogenic to 800 °C (1500 °F). A typical example of PCHE block is shown below:

#### Advantages of PCHE

- Channels are optimized for counter current flow
- Flexibility of design and high strength offered by techniques of construction
- Materials are stainless steel 316, alloys, nickel, and titanium
- The etch plates are stacked and diffusion bonded together to make the core of the heat exchanger
- High heat transfer surface area per unit volume of the exchanger, resulting in reduced weight, space, and supporting structure
- Used for temperature ranges of –200 to 900 °C
- High pressure drops in excess of 600 bar
- Reduced energy requirement and cost
- Improved process design, plant layout, and processing conditions
- Low fluid inventory compared to conventional designs such as shell-and-tube exchanger
- Four to six times smaller and lighter than conventional designs such as shell-and-tube exchanger
- Extremely high heat transfer coefficients are achievable with small-hydraulic diameter flow passages
- Used for gases, liquids, and two-phase flows (Fig. 2.8)

#### Disadvantages of PCHE

- Expensive when compared to shell and tube units
- Fluid needs to be extremely clean
- Blockages can occur easily due to the fine channels (0.5–2 mm)
- Blockages can be avoided by fine filtration (typically 300 µm), but there will be additional cost
- Filters need to be cleaned regularly

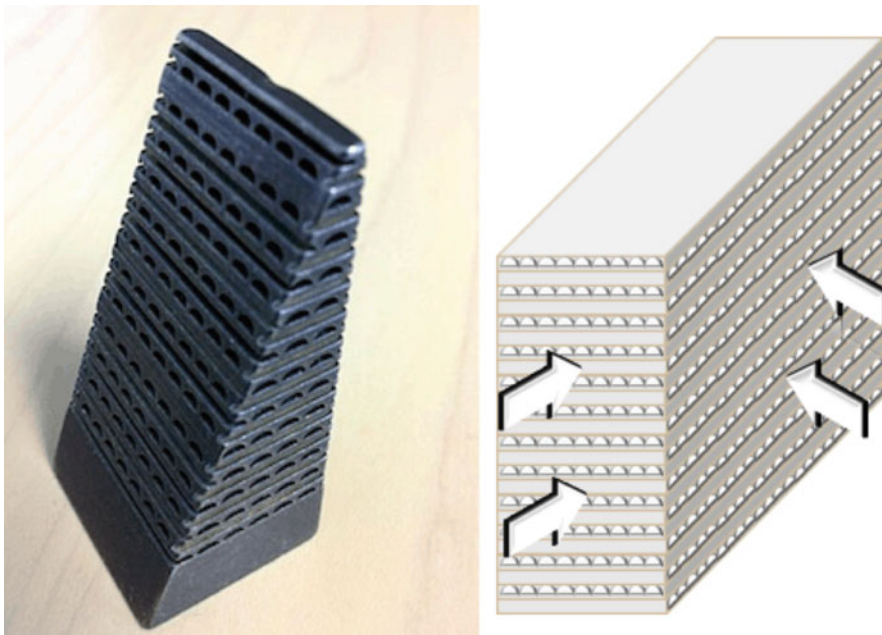


**Fig. 2.8** Heatic heat exchanger products

- Blockages require chemical cleaning which can be difficult in some installations and the system needs to be designed for this
- Galvanic compatibility with the piping material can be an issue. Insulation kit or coated spool piece may be needed

The Printed Circuit Heat Exchanger (PCHE) is a type of Compact Heat Exchanger (CHE) which was originally developed for refrigeration applications and has fluid channels which are etched photo-chemically on one side of each plate with the same technology used for the fabrication of electronic printed circuit boards. The origin of its name “Printed-Circuit” heat exchanger was mentioned in the book by Hesselgreaves [4] and Aquaro and Pieve [5].

The plates forming the exchanger have typical thickness of 1.6 mm, a width of 600 mm, and length of 1200 mm. The channels which are usually of semi-circular profile have diameters of 0.5–2 mm but there are also larger diameters available (up to 5 mm) [5]. The flat plates are then staked after it has been photo-chemically etched and diffusion-bonded together to form strong and compact cores. A plate stake and cross section of a PCHE are shown in Fig. 2.9a and b3, respectively. The PCHE can achieve effectiveness greater than 97 %, with maximum operating temperature and pressures of up to 1000 °C and 500 bars, respectively [6].

Materials which can be used in the manufacture of PCHE include, stainless such as SS 316L, SS 316, SS 304, SS 904L, cupronickel, Monel, nickel and super alloys Inconel 600, Incoloy 800, and 825 [7].

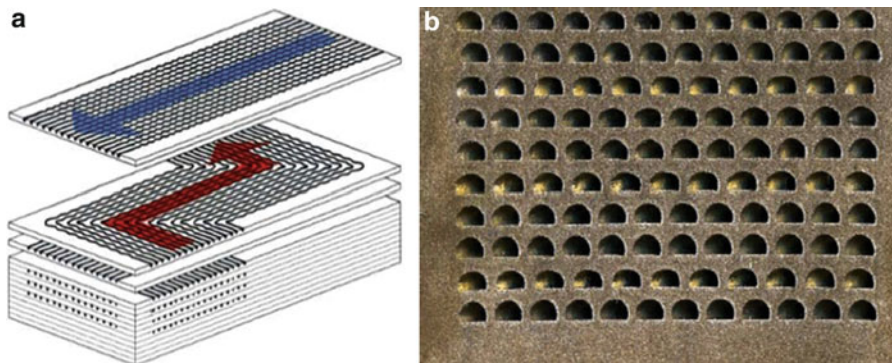


**Fig. 2.9** (a) Plate stake of a PCHE. (b) Cross section of a PCHE

### 2.3.6 Regenerative Heat Exchangers

Regenerative heat exchangers use a heat transfer matrix that is heated by one fluid and then cooled by the second fluid. The flow over the matrix is switched as a function of time with both fluids flowing over the same surfaces of the matrix. They have seen little use in fixed station power plants and will not be emphasized here.

## 2.4 Condensers

Condensers are used for such varied applications as steam power plants, chemical processing plants, and nuclear electric plants for space vehicles. The major types include the *surface condensers*, *jet condensers*, and *evaporative condensers*. The most common type is the surface condenser, which has a feed-water system [8]. Figure 2.10 shows a section through a typical two-pass surface condenser for a large steam turbine in a power plant. Since the steam pressure at the turbine exit is only 1.0–2.0 in Hg absolute, the steam density is very low and the volume rate of flow is extremely large. To minimize the pressure loss in transferring steam from the turbine to the condenser, the condenser is normally mounted beneath and attached to the turbine. Cooling water flows horizontally inside the tubes, while the steam flows vertically downward from the large opening at the top and passes transversely over the tubes. Note that provision is made to aspirate cool air from the regions just above the center of the hot well. This is important because the presence of noncondensable gas in the steam reduces the heat transfer coefficient for condensation.

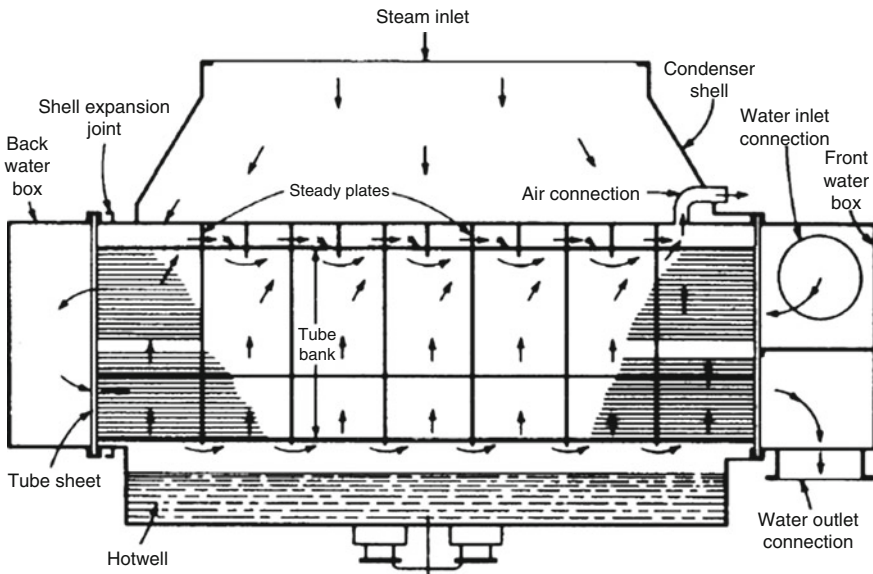


**Fig. 2.10** Section through a typical two-pass surface condenser for a large plant. (Courtesy of Allis-Chalmers Manufacturing Company)

## 2.5 Boilers

Steam boilers are one of the earliest applications of heat exchangers. The term *steam generator* is often applied to a boiler in which the heat source is a hot fluid stream rather than the products of combustion.

An enormous variety of boiler types exist, ranging from small units for house heating applications to huge, complex, expensive units for modern power stations.

## 2.6 Classification According to Compactness

The ratio of the heat transfer, surface area on one side of the heat exchanger to the volume can be used as a measure of the compactness of heat exchangers. A heat exchanger having a surface area density on any one side greater than about  $700 \text{ m}^2/\text{m}^3$  quite arbitrarily is referred to as a compact heat exchanger regardless of its structural design. For example, automobile radiators having an area density approximately  $1100 \text{ m}^2/\text{m}^3$  and the glass ceramic heat exchangers for some vehicular gas-turbine engines having an area density approximately  $6600 \text{ m}^2/\text{m}^3$  are compact heat exchangers. The human lungs, with an area density of about  $20,000 \text{ m}^2/\text{m}^3$  are the most compact heat-and-mass exchanger. The very fine matrix regenerator for the Stirling engine has an area density approaching that of the human lung.

On the other extreme of the compactness scale, plane tubular and shell-and-tube type exchangers, having an area density in the range of 70–500 m<sup>2</sup>/m<sup>3</sup>, are not considered compact [2].

The incentive for using compact heat exchangers lies in the fact that a high value of compactness reduces the volume for a specified heat exchanger performance.

When heat exchangers are to be employed for automobiles, marine uses, aircraft, aerospace vehicles, cryogenic systems, and refrigeration and air conditioning, the weight and size—hence the compactness—become important. To increase the effectiveness or the compactness of heat exchangers, fins are used. In a gas-to-liquid heat exchanger, for example, the heat transfer coefficient on the gas side is an order of magnitude lower than for the liquid side. Therefore, fins are used on the gas side to obtain a balanced design; the heat transfer surface on the gas side becomes much more compact.

## 2.7 Types of Applications

Heat exchangers are often classified based on the application for which they are intended, and special terms are employed for major types. These terms include *boiler, steam generator, condenser, radiator, evaporator, cooling tower, regenerator, recuperator, heater, and cooler*. The specialized requirements of the various applications have led to the development of many types of construction, some of which are unique to particular applications [9].

## 2.8 Cooling Towers

In locations where the supply of water is limited, heat may be rejected to the atmosphere very effectively by means of cooling towers such as those in Figs. 2.11, 2.12, and 2.13. A fraction of the water sprayed into these towers evaporates, thus cooling the balance. Because of the high heat of vaporization of water, the water consumption is only about 1% as much as would be the case if water were taken from a lake or a stream and heated 10 or 20 °F.

Cooling towers may be designed so that the air moves through them by thermal convection, or fans may be employed to provide forced air circulation. To avoid contamination of the process water, shell-and-tube heat exchangers are sometimes employed to transmit heat from the process water to the water recirculated through the cooling tower.

**Fig. 2.11** Vertical induced draft-cooling tower.  
(Courtesy Foster Wheeler Corp.) [1]

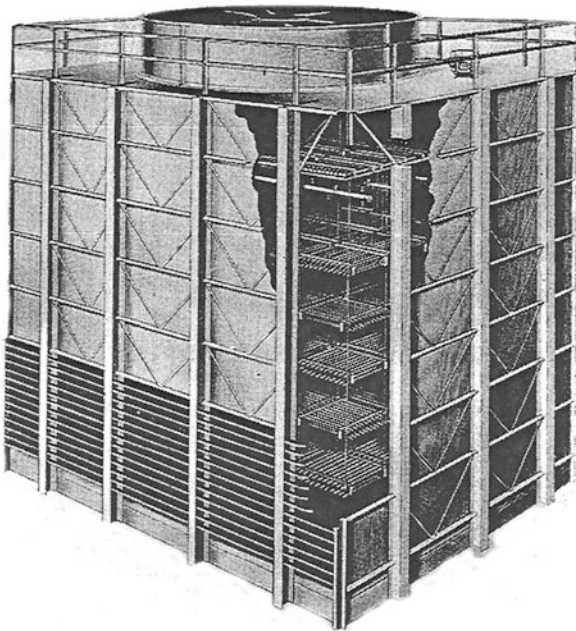


**Fig. 2.12** Schematic of cooling tower



## 2.9 Regenerators and Recuperators

The thermal efficiency of both gas-turbine power plants can be greatly increased if heat can be extracted from the hot gases leaving the gas turbine and added to the air being supplied to the combustion chamber. For a major gain in thermal efficiency, it is necessary to employ a very large amount of heat transfer, surface area. This is

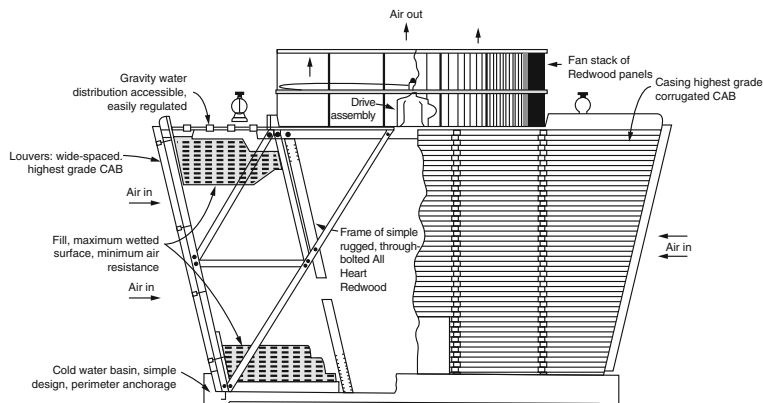
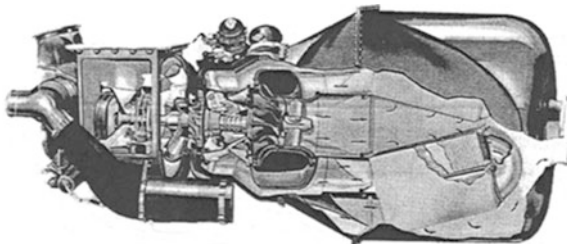


**Fig. 2.13** Forced convection cooling tower with draft induced by a fan [1]

**Fig. 2.14** A small gas-turbine power plant fitted with a recuperator to improve the fuel economy. (Courtesy of AiResearch Manufacturing Company) [9]



particularly noticeable in gas-turbine plants, where even with counterflow the size of the heat exchanger required for good performance is inclined to be large compared to the size of the turbine and compressor. This characteristic can be observed even in the small, portable gas turbine (about 3 ft in diameter) shown in Fig. 2.14. Note that in this device the hot combination gases leave the radial in-flow turbine wheel at the right end of the shaft and enter a set of heat exchanger cores arranged in parallel around the central axis.

Figure 2.15 shows a close-up view of one of these cores. In each core, the hot gases from the turbine flow roughly radially outward through one set of gas passages. Air from the centrifugal compressor wheel, which is at the center of the shaft, flows to the right through the space just inside of the outer casing and axially into the other set of gas passages through the core. The air being heated makes two passes, flowing first to the right in the outer portion of the core and then back to the left through the inner portion, thus giving a two-pass crossflow approximation to counterflow. (The flow passages through the combustion chamber are not shown in this view).

As seen in Fig. 2.15, the heat exchanger core is constructed of alternate layers of flat and corrugated sheets. The flat sheets separate the hot and cold fluid streams, while the corrugated sheets act as fins that roughly triple the heat transfer surface

**Fig. 2.15** A brazed plate-fin recuperator core for the gas turbine of Fig. 2.9.  
(Courtesy of AiResearch Manufacturing) [9]

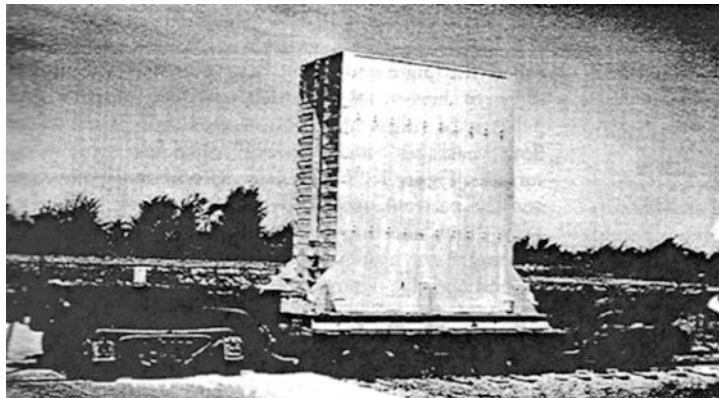
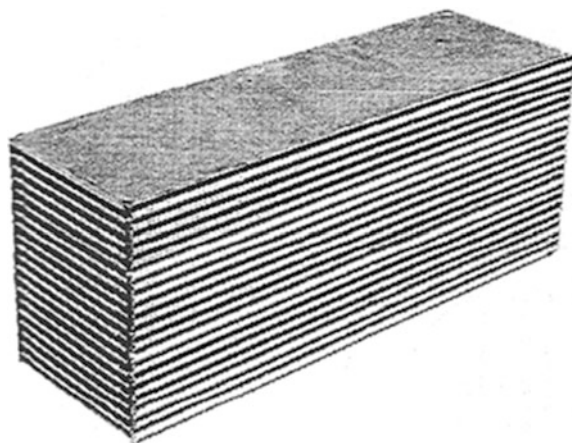


**Fig. 2.16** A welded steel recuperator for a large gas-turbine power plant. (Courtesy Harrison Radiator Division, General Motors Corp) [9]

area per unit of volume. Also note that the axis of the corrugations is at right angles in alternate layers to provide a crossflow pattern for the two fluid streams.

One of several recuperator units to be mounted in parallel in a much larger gas turbine plant is shown in Fig. 2.16. The hot exhaust gas from the turbine enters vertically at the bottom, flows upward through the heat transfer matrix, and discharges vertically from the top. The air from the compressor enters a large circular port at the top at the right end, flows vertically downward in pure counter-flow, and leaves a second circular port at the bottom to flow to the combustion chamber. The hot exhaust gas passages are formed by corrugated sheets sandwiched between flat plates that extend all the way from the bottom to the top of the unit. The air to be heated flows horizontally from the long plenum at the top into the spaces between the walls of the exhaust gas passages. Curved space strips

guide the air through a 90° bend and then downward between the heated walls. A similar header arrangement is used at the bottom. Note that both the flow passage area and the heat transfer surface area for the hot exhaust gas are about three times as great as the corresponding values for the air being heated. This comes about because the two fluid streams differ in density by a factor of about 4.

The air pre-heaters in steam power plants are usually quite different from the units just described for gas turbines. Rotary regenerators are often used. These consist of a cylindrical drum filled with a heat transfer matrix made of alternating flat and corrugated sheets. The drum is mounted so that the hot gas heats a portion of the matrix as it passes from the furnace to the stack. The balance of the matrix gives up its stored heat to the fresh air in route from the forced draft fans to the furnace. The ducts are arranged so that the two gas streams move through the drum in counterflow fashion while it is rotated, so that the temperature of any given element of the metal matrix fluctuates relatively little as it is cycled from the hot to the cold gas streams.

In the steam- and gas-turbine power fields a distinction is sometimes made between air pre-heaters that involve a conventional heat transfer matrix with continuous flow on both sides of a stationary heat transfer surface and those through which the fluids flow periodically. The hot fluid heats one section of the matrix, while the cold fluid removes heat from another section. Where this distinction is made, the term regenerator is applied to the periodic-flow type of heat exchanger, since this term has long been applied to units of this type employed for blast furnaces and steel furnaces, whereas the term recuperator is applied to units through which the flow is continuous.

Recuperators are used for gas turbines, but the gas turbines installed until the mid-1970s suffered from low efficiency and poor reliability. In the past, large coal and nuclear power plants dominated the base-load electric power generation (Point 1 in Fig. 2.17). Base load units are on line at full capacity or near full capacity almost all of the time. They are not easily nor quickly adjusted for varying large

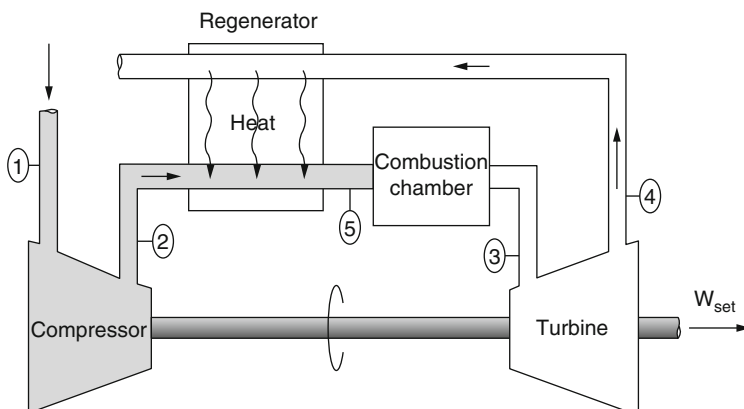
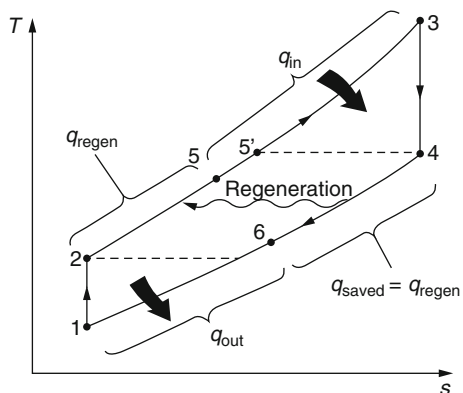


**Fig. 2.17** A gas-turbine engine with recuperator

amounts of load because of their characteristics of operation [10]. However, there has been a historic shift toward natural gas-fired turbines because of their higher efficiencies, lower capital costs, shorter installation times, better emission characteristics, the abundance of natural gas supplies, and shorter start up times (Point 1 in Fig. 2.17). Now electric utilities are using gas turbines for base-load power production as well as for peaking, making capacity at maximum load periods and in emergencies, situations because they are easily brought on line or off line (Point 2 in Fig. 2.17). The construction costs for gas-turbine power plants are roughly half that of comparable conventional fossil fuel steam power plants, which were the primary base-load power plants until the early 1980s, but peaking units are much higher in energy output costs. A recent gas turbine manufactured by General Electric uses a turbine inlet temperature of 1425 °C (2600 °F) and produces up to 282 MW while achieving a thermal efficiency of 39.5 % in the simple-cycle mode. Over half of all power plants to be installed in the near future are forecast to be gas turbine or combined gas-steam turbine types (Fig. 2.17).

In gas turbine engines with the Brayton Cycle that includes a recuperator, the temperature of the exhaust gas leaving the turbine is often considerably higher than the temperature of the air leaving the compressor. Therefore, the high-pressure air leaving the compressor can be heated by transferring heat to it from the hot exhaust gases in a counter-flow heat exchanger, which is also known as a regenerator or recuperator (see Fig. 2.18 on point-1). Gas turbine regenerators are usually constructed as shell-and-tube type heat exchangers using very small diameter tubes, with the high-pressure air inside the tubes and low-pressure exhaust gas in multiple passes outside the tubes [11]. The thermal efficiency of the Brayton cycle increases as a result of regeneration since the portion of energy of the exhaust gases that is normally rejected to the surroundings is now used to preheat the air entering the combustion chamber. This, in turn, decreases the heat input (thus fuel) requirements for the same net work output. Note, however, that the use of a regenerator is recommended only when the turbine exhaust temperature is higher than the compressor exit temperature. Otherwise, heat will flow in the reverse direction (to the

**Fig. 2.18**  $T-s$  diagram of a Brayton cycle with regeneration



exhaust gases), decreasing the efficiency. This situation is encountered in gas turbines operating at very high-pressure ratios (Point 1 on Fig. 2.18).

The highest temperature occurring within the regenerator is the temperature of the exhaust gases leaving the turbine and entering the regenerator (Point 1 on Fig. 2.18). The gas turbine recuperator receives air from the turbine compressor at pressures ranging from 73.5 to 117 psia and temperatures from 350 to 450 °F (Point 3 on Fig. 2.18). Under no conditions can the air be preheated in the regenerator to a temperature above this value. In the limiting (ideal) case, the air will exit the regenerator at the inlet temperature of the exhaust gases. Air normally leaves the regenerator at a lower temperature (Point 1 on Fig. 2.18). Gas turbine exhaust gas passes over the other side of the recuperator at exhaust temperatures ranging from 750 to 1000 °F. Compressor air temperatures are now raised to higher temperatures up to about 750–900 °F as it enters the combustor. Turbine exhaust gases are then reduced to between 500 and 650 °F from the original 750–1000 °F. This heat recovery contributes appreciably to the turbine fuel rate reduction and increase in efficiency (Point 3 on Fig. 2.18). The regenerator is well insulated and any changes in kinetic and potential energies are neglected.

A regenerator with a higher effectiveness saves a greater amount of fuel since it preheats the air to a higher temperature prior to combustion (Point 1 on Fig. 2.18). However, achieving a higher effectiveness requires the use of a larger regenerator, which carries a higher price tag and causes a larger pressure drop because shaft horsepower is reduced. Pressure drop through the regenerator or recuperator is important and should be kept as low as practical on both sides. Generally, the air pressure drop on the high-pressure side should be held below 2 % of the compressor total discharge pressure. The gas pressure drop on the exhaust side (hot side) should be held below 4 in. of water. Therefore, the use of a regenerator with a very high effectiveness cannot be justified economically unless the savings from the fuel costs exceed the additional expenses involved. The effectiveness of most regenerators used in practice is below 0.85. The thermal efficiency of an ideal Brayton cycle with regeneration depends on the ratio of the minimum to maximum temperatures as well as the pressure ratio. Regeneration is most effective at lower pressure ratios and low minimum-to-maximum temperature ratios.

Gas-to-air recuperators (or regenerators) are also used on marine type industrial, and utility open-cycle gas turbine applications. In this application, the recuperator receives air from the turbine compressor at pressure and temperature ranging as above, where gas turbine exhaust gas passes over the other side of the recuperator at exhaust temperature, depending on the turbine. The air side (high pressure side) of the recuperator is in the system between the compressor and the combustor and compressor air is raised to a higher temperature up to what is mentioned above as it enters the combustor. Obviously, pressure drop through the regenerator or recuperator is important and should be kept as low as practical on both sides.

## 2.10 Heat Exchanger Analysis: Use of the LMTD

Utilizing the Logarithmic Mean Temperature Difference (LMTD) method is one way to design or to predict the performance of a heat exchanger, it is essential to relate the total heat transfer rate to measurable quantities such as the inlet and outlet fluid temperatures, the overall heat transfer coefficient, and the total surface area for heat transfer. Two such relations may readily be obtained by applying overall energy balances to the hot and cold fluids, as shown in Fig. 2.19. In particular, if  $q$  is the total rate of heat transfer between the hot and cold fluids and there is negligible heat transfer between the exchanger and its surroundings, as well as negligible potential and kinetic energy changes, application of the steady flow energy equation, gives;

$$q_{\text{total}} = \dot{m}_h (h_{h,i} - h_{h,o}) \quad (\text{Eq. 2.1a})$$

and

$$q_{\text{total}} = \dot{m}_c (h_{c,o} - h_{c,i}) \quad (\text{Eq. 2.1b})$$

where  $h$  is the fluid enthalpy. The subscripts  $h$  and  $c$  refer to the hot and cold fluids, whereas the subscripts  $i$  and  $o$  designate the fluid inlet and outlet conditions. If the fluids are not undergoing a phase change and constant specific heats are assumed, these expressions reduce to

$$q_{\text{total}} = \dot{m}_h c_{p,h} (T_{h,i} - T_{h,o}) \quad (\text{Eq. 2.2a})$$

and

$$q_{\text{total}} = \dot{m}_c c_{p,c} (T_{c,o} - T_{c,i}) \quad (\text{Eq. 2.2b})$$

where the temperatures appearing in the expressions refer to the *mean* fluid temperatures at the designated locations. Note that Eqs. (2.1a), (2.1b), (2.2a), and (2.2b) are independent of the flow arrangement and heat exchanger type.

Now consider the heat transfer at a particular point,  $x$ , on the heat transfer surface. At  $x$  there will be a bulk hot fluid temperature given by  $T_{f,h}(x)$ , a wall

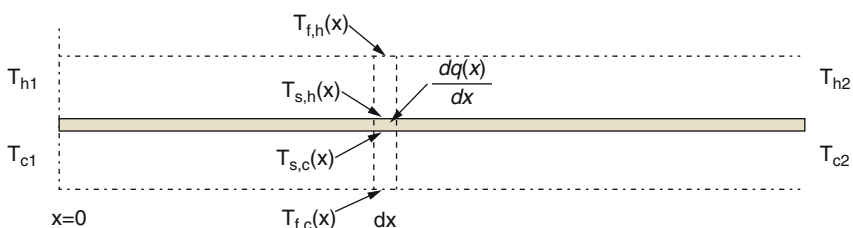


**Fig. 2.19** Heat transfer between two moving fluids separated by a solid boundary

surface temperature on the hot fluid side given by  $T_{s,h}(x)$ , a wall surface temperature on the cold fluid side given by  $T_{s,c}(x)$ , and a cold fluid bulk temperature given by  $T_{f,c}(x)$ . The total temperature drop from the hot fluid at  $x$  to the cold fluid at  $x$  is given by

$$\begin{aligned}\Delta T &= T_{f,h}(x) - T_{f,c}(x) \\ &= T_{f,h}(x) - T_{s,h}(x) + T_{s,h}(x) - T_{s,c}(x) + T_{s,c}(x) - T_{f,c}(x) \\ &= \Delta T_{f,h} + \Delta T_s + \Delta T_{f,c}\end{aligned}$$

Then the heat flux leaving the hot fluid is given by:

$$\frac{dq(x)}{dx} = h_{f,h}A_{f,h}(T_{f,h}(x) - T_{s,h}(x)) = h_{f,h}dA_{f,h}\Delta T_{f,h}(x) \quad \Delta T_{f,h}(x) = \frac{\frac{dq(x)}{dx}}{h_{f,h}dA_{f,h}}$$

The heat flux crossing the wall between the two fluids is given by,

$$\frac{dq(x)}{dx} = \frac{k_s}{\delta_s}dA_s(T_{s,h}(x) - T_{s,c}(x)) = \frac{k_s}{\delta_s}dA_s\Delta T_s(x) \quad \Delta T_s(x) = \frac{\frac{dq(x)}{dx}}{\frac{k_s}{\delta_s}dA_s}$$

And the heat flux into the cold fluid is given by,

$$\frac{dq(x)}{dx} = h_{f,c}dA_{f,c}(T_{s,c}(x) - T_{f,c}(x)) = h_{f,c}dA_{f,c}\Delta T_{f,c}(x) \quad \Delta T_{f,c}(x) = \frac{\frac{dq(x)}{dx}}{h_{f,c}dA_{f,c}}$$

Then the difference in the bulk temperatures of the two fluids can be written as

$$\begin{aligned}T_{f,h}(x) - T_{f,c}(x) &= \frac{\frac{dq(x)}{dx}}{h_{f,h}dA_{f,h}} + \frac{\frac{dq(x)}{dx}}{\frac{k_s}{\delta_s}dA_s} + \frac{\frac{dq(x)}{dx}}{h_{f,c}dA_{f,c}} \\ &= \frac{dq(x)}{dx} \left[ \frac{1}{h_{f,h}dA_{f,h}} + \frac{\delta_s}{k_s dA_s} + \frac{1}{h_{f,c}dA_{f,c}} \right] \quad (\text{Eq. 2.3})\end{aligned}$$

Note that  $\delta_s$  will depend on the geometry. For slab or plate geometry

$$\delta_s = \Delta t \quad \text{the wall thickness}$$

For cylindrical geometry typical of tubes,

$$\delta_s = r_{in} \ln \left( \frac{r_{out}}{r_{in}} \right) \quad r_{out} - r_{in} = \text{the tube wall thickness}$$

Also note that the differential areas do not all have to be equal. There will be a slight difference if the bounding surface is a tube, but the addition of fins to either the hot or the cold side could change the effective area significantly and that is the area that

must be used in Eq. (2.3). Also, note that the areas are areas per unit length. That is why they have been written as  $dA$ .

$$T_{f,h}(x) - T_{f,c}(x) = \frac{dq(x)}{dx} \left( \frac{1}{U \frac{dA}{dx}} \right) \quad \frac{1}{U \frac{dA}{dx}} = \frac{1}{h_{f,h} dA_{f,h}} + \frac{\delta_s}{k_s dA_s} + \frac{1}{h_{f,c} dA_{f,c}}$$

$$\frac{dq(x)}{dx} = U \frac{dA}{dx} (T_{f,h} - T_{f,c})$$

Then the heat lost by the hot fluid is given by

$$\frac{dq(x)}{dx} = -\dot{m}_{f,h} C_{p,h} \frac{dT_{f,h}(x)}{dx} \quad (\text{Eq. 2.4})$$

And the heat gained by the cold fluid is given by

$$\frac{dq(x)}{dx} = \dot{m}_{f,c} C_{p,c} \frac{dT_{f,c}(x)}{dx} \quad (\text{Eq. 2.5})$$

Combining these two equations gives

$$\frac{dT_{f,h}(x)}{dx} - \frac{dT_{f,c}(x)}{dx} = -\frac{dq(x)}{dx} \left( \frac{1}{\dot{m}_h C_{p,h}} + \frac{1}{\dot{m}_c C_{p,c}} \right) = -U \frac{dA}{dx} (T_{f,h} - T_{f,c})$$

$$\Delta T(x) = T_{f,h}(x) - T_{f,c}(x)$$

$$\frac{d\Delta T(x)}{dx} = -U \frac{dA}{dx} \Delta T \left( \frac{1}{\dot{m}_h C_{p,h}} + \frac{1}{\dot{m}_c C_{p,c}} \right)$$

$$\frac{d\Delta T(x)}{\Delta T(x)} = -U \left( \frac{1}{\dot{m}_h C_{p,h}} + \frac{1}{\dot{m}_c C_{p,c}} \right) dA \quad \frac{dA}{dx} dx = dA$$

Integrating gives

$$\ln \left( \frac{\Delta T_2}{\Delta T_1} \right) = -UA \left( \frac{1}{\dot{m}_h C_{p,h}} + \frac{1}{\dot{m}_c C_{p,c}} \right) \quad (\text{Eq. 2.6})$$

Now for the hot fluid flowing from left to right Eq. (2.2a) becomes

$$q_{\text{total}} = \dot{m}_h C_{p,h} (T_{f,h,1} - T_{f,h,2}) \quad \frac{1}{\dot{m}_h C_{p,h}} = \frac{(T_{f,h,1} - T_{f,h,2})}{q_{\text{total}}}$$

In addition, for the cold fluid also flowing from left to right (parallel flow) Eq. (2.2b) becomes

$$q_{\text{total}} = \dot{m}_c c_{p,c} (T_{f,c,2} - T_{f,c,1}) \quad \frac{1}{\dot{m}_c c_{p,c}} = \frac{(T_{f,c,2} - T_{f,c,1})}{q_{\text{total}}}$$

Plugging these into Eq. (2.3) gives

$$\begin{aligned} \ln\left(\frac{\Delta T_2}{\Delta T_1}\right) &= -UA\left(\frac{T_{f,h,1} - T_{f,h,2}}{q_{\text{total}}} + \frac{T_{f,c,2} - T_{f,c,1}}{q_{\text{total}}}\right) = \frac{UA}{q_{\text{total}}} (T_{f,h,2} - T_{f,c,2} - T_{f,h,1} + T_{f,c,1}) \\ \ln\left(\frac{\Delta T_2}{\Delta T_1}\right) &= \frac{UA}{q_{\text{total}}} (\Delta T_2 - \Delta T_1) \quad q_{\text{total}} = UA \frac{(\Delta T_2 - \Delta T_1)}{\ln\left(\frac{\Delta T_2}{\Delta T_1}\right)} \\ q_{\text{total}} &= UA \Delta T_{\text{lm}} \quad \Delta T_{\text{lm}} = \frac{(\Delta T_2 - \Delta T_1)}{\ln\left(\frac{\Delta T_2}{\Delta T_1}\right)} \end{aligned} \quad (\text{Eq. 2.7})$$

This looks a lot like Newton's law of cooling with  $\Delta T_{\text{lm}}$  playing the role of the standard  $\Delta T$ .  $\Delta T_{\text{lm}}$  is called the log-mean temperature difference.

Now consider the counter flow arrangement. In this case Eq. (2.5) becomes,

$$\frac{dq(x)}{dx} = -\dot{m}_{f,c} c_{p,c} \frac{dT_{f,c}(x)}{dx}$$

Moreover, Eq. (2.6) becomes,

$$\ln\left(\frac{\Delta T_2}{\Delta T_1}\right) = -UA\left(\frac{1}{\dot{m}_h C_{p,h}} - \frac{1}{\dot{m}_c c_{p,c}}\right)$$

Then Eq. (2.2b) becomes

$$q_{\text{total}} = \dot{m}_c c_{p,c} (T_{f,c,1} - T_{f,c,2})$$

This gives

$$\begin{aligned} \ln\left(\frac{\Delta T_2}{\Delta T_1}\right) &= -UA\left(\frac{T_{f,h,1} - T_{f,h,2}}{q_{\text{total}}} - \frac{T_{f,c,1} - T_{f,c,2}}{q_{\text{total}}}\right) = \frac{UA}{q_{\text{total}}} (T_{f,h,2} - T_{f,c,2} - T_{f,h,1} + T_{f,c,1}) \\ \ln\left(\frac{\Delta T_2}{\Delta T_1}\right) &= \frac{UA}{q_{\text{total}}} (\Delta T_2 - \Delta T_1) \quad q_{\text{total}} = UA \frac{(\Delta T_2 - \Delta T_1)}{\ln\left(\frac{\Delta T_2}{\Delta T_1}\right)} \end{aligned}$$

which is identical to the equation for the parallel flow heat exchanger. It is important to remember how the  $\Delta T$ 's are defined.

Parallel Flow:  $\Delta T_1 = T_{f,h,\text{in}} - T_{f,c,\text{in}}$     $\Delta T_2 = T_{f,h,\text{out}} - T_{f,c,\text{out}}$

Counter Flow:  $\Delta T_1 = T_{f,h,\text{in}} - T_{f,c,\text{out}}$     $\Delta T_2 = T_{f,h,\text{out}} - T_{f,c,\text{in}}$

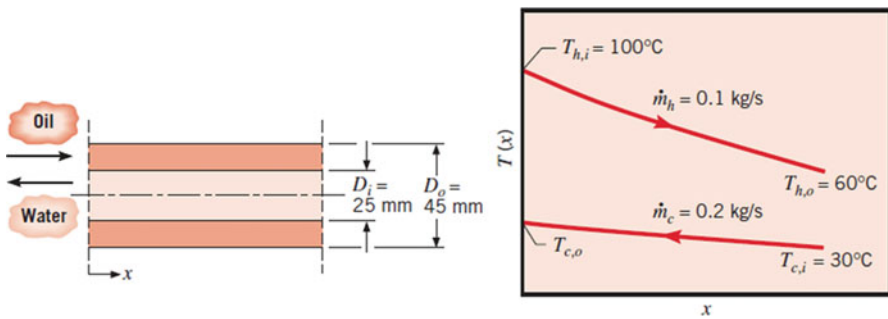


**Fig. 2.20** Schematic of Example 2.1 [9]

**Example 2.1** A counterflow, concentric tube heat exchanger is used to cool the lubricating oil for a large industrial gas turbine engine. The flow rate of cooling water through the inner tube ( $D_i = 25\text{ mm}$ ) is  $0.2 \text{ kg/s}$ , while the flow rate of oil through the outer annulus ( $D_o = 45\text{ mm}$ ) is  $0.1 \text{ kg/s}$ . The oil and water enter at temperatures of  $100$  and  $30^\circ\text{C}$ , respectively. How long must the tube be made if the outlet temperature of the oil is to be  $60^\circ\text{C}$ . (The steel tube that separates the two flows is so thin that the temperature drop across it may be neglected.) See Fig. 2.20.

**Solution Known:** Fluid flow rates and inlet temperature for a counter-flow, concentric tube heat exchanger of prescribed inner and outer diameter.

**Find:** Tube length to achieve a desired hot fluid outlet temperature.

**Assumptions:**

1. Negligible heat loss to the surroundings.
2. Negligible kinetic and potential energy changes.
3. Constant properties.
4. Negligible tube wall thermal resistance and fouling factors  $f$ . Fouling factor is defined in Sect. 3.5.
5. Fully developed conditions for the water and oil ( $U$  independent of  $x$ ).

**Properties:**

Table A.5, unused engine oil ( $\bar{T}_h = 80^\circ\text{C} = 353\text{ K}$ ):

$$c_p = 2131\text{ J/kg K}, \mu = 3.25 \times 10^{-2}\text{ Ns/m}^2, k = 0.138\text{ W/m K}.$$

Table A.6, water ( $\bar{T}_c \approx 35^\circ\text{C} = 308\text{ K}$ ):

$$c_p = 4178\text{ J/kg K}, \mu = 725 \times 10^{-6}\text{ Ns/m}^2, k = 0.625\text{ W/m K}, \text{Pr} = 4.85.$$

**Analysis:**

The required heat transfer rate may be obtained from the overall energy balance for the hot fluid, Eq. (2.1a)

$$q = \dot{m}_h c_{p,h} (T_{h,i} - T_{h,o})$$

$$q = 0.1 \text{ kg/s} \times 2131 \text{ J/kg K} (100 - 60)^\circ\text{C} = 8524 \text{ W}$$

Applying Eq. (2.2b), the water outlet temperature is

$$T_{c,o} = \frac{q}{\dot{m}_c c_{p,c}} + T_{c,i}$$

$$T_{c,o} = \frac{8524 \text{ W}}{0.2 \text{ kg/s} \times 2131 \text{ J/kg K}} + 30^\circ\text{C} = 40.2^\circ\text{C}$$

Accordingly, use of  $\bar{T}_c = 35^\circ\text{C}$  to evaluate the water properties was a good choice. The required heat exchanger length may now be obtained from Eq. (2.7),

$$q = UA\Delta T_{lm}$$

where  $A = \pi D_i L$

$$\Delta T_{lm} = \frac{(T_{h,i} - T_{c,o}) - (T_{h,o} - T_{c,i})}{\ln[(T_{h,i} - T_{c,o})/(T_{h,o} - T_{c,i})]} = \frac{59.8 - 30}{\ln(59.8/30)} = 43.2^\circ\text{C}$$

The overall heat transfer coefficient is

$$U = \frac{1}{(1/h_i) + (1/h_o)}$$

For water flow through the tube,

$$\dot{m} = \rho A V \frac{\dot{m}}{A} = \rho V \text{Re}_D = \frac{\dot{m}_c D_i}{A \mu} = \frac{4 \dot{m}}{\pi D_i \mu} = \frac{4 \times 0.2 \text{ kg/s}}{\pi (0.025 \text{ m}) 725 \times 10^{-6} \text{ N s/m}^2}$$

$$= 14,050$$

Accordingly, the flow is turbulent and the convection coefficient may be computed from the following equation.

$$\text{Nu}_D = 0.023 \text{Re}_D^{4/5} \text{Pr}^{0.4}$$

$$\text{Nu}_D = 0.023 (14,050)^{4/5} (4.85) = 90$$

Hence,

$$h_i = \text{Nu}_D \frac{k}{D_i} = \frac{90 \times 0.625 \text{ W/m K}}{0.025 \text{ m}} = 2250 \text{ W/m}^2 \text{ K}$$

For the flow of oil through the annulus, the hydraulic diameter is as follows. For a more precise definition of the hydraulic diameter, refer to Eqs. (3.3a) and (3.3b) and (3.4a) and (3.4b) of Sect. 3.3.

$$D_h = \frac{4A}{P} = \frac{4(\pi r_o^2 - \pi r_i^2)}{2\pi(r_o - r_i)} = 2(r_o - r_i) = D_o - D_i$$

and the Reynolds number is

$$\text{Re}_D = \frac{\rho u_m D_h}{\mu} = \frac{\dot{m}(D_o - D_i)}{A\mu} = \frac{\dot{m}(D_o - D_i)}{\mu\pi(D_o^2 - D_i^2)/4}$$

$$\text{Re}_D = \frac{4\dot{m}}{\pi(D_o + D_i)\mu} = \frac{4(0.1 \text{ kg/s})}{\pi(0.045 + 0.025)3.25 \times 10^{-2} \text{ kg/sm}} = 56.0$$

The annular flow is therefore laminar. For a constant heat flux the laminar correlation is given as the following relationship.

$$\text{Nu}_i = \frac{h_o D_h}{k} = 4.36$$

and

$$h_o = 4.36 \frac{0.138 \text{ W/mK}}{0.020 \text{ m}} = 30.1 \text{ W/m}^2 \text{ K}$$

The overall convection coefficient is then

$$U = \frac{1}{(1/2250 \text{ W/m}^2 \text{ K}) + (1/30.1 \text{ W/m}^2 \text{ K})} = 29.7 \text{ W/m}^2 \text{ K}$$

and from the rate equation it follows that

$$L = \frac{q}{U\pi D_i \Delta T_{lm}} = \frac{8524 \text{ W}}{29.7 \text{ W/m}^2 \text{ K} \pi(0.025 \text{ m})(43.2^\circ \text{C})} = 84.6 \text{ m}$$

### Comments:

1. The hot side convection coefficient controls the rate of heat transfer between the two fluids, and the low value of  $h_o$  is responsible for the large value of  $L$ .
2. Because  $h_i \gg h_o$ , the tube wall temperature will closely follow that of the coolant water.

Many heat exchangers have been designed based on a log-mean temperature difference. However, there are some problems with proceeding based on the log-mean temperature difference equation. First, it says nothing about cross flow

heat exchangers, which are very common due to the ease of construction of this type of exchanger. Second, it often requires iterative calculations for a design if all of the inlet and exit temperatures are not known a priori. In the example above, we had the outlet temperature of the oil not specified, an iterative solution would have been required. Iterative solutions can certainly be accurate, but they often require more work. Third, the log-mean temperature difference method does not provide a feel for the maximum heat transfer possible given the entering conditions of the fluids. Sometimes this is an important parameter to understand, if the design is to be optimized.

## 2.11 Effectiveness-NTU Method for Heat Exchanger Design

A better method has been developed for heat exchanger design that uses some of the preceding analysis. This method is called the effectiveness-NTU (Number of Transfer Unit) method [8, 9]. It starts by considering the fluid heat transfer capacity rates defined as

$$\begin{aligned} \text{Cold Fluid Capacity Rate } C_c &= \dot{m}_c C_{p,c} \text{ W/K} \\ \text{Hot Fluid Capacity Rate } C_h &= \dot{m}_h C_{p,h} \text{ W/K} \end{aligned} \quad (\text{Eq. 2.8})$$

Then the maximum amount of heat that can be transferred between the two fluids is the Minimum Fluid Capacity Rate times the difference in temperature of the hot fluid entering the exchanger and the cold fluid entering the exchanger. Or

$$\begin{aligned} C_{\min} &= \min(C_c, C_h) \\ q_{\max} &= C_{\min}(T_{h,in} - T_{c,in}) \end{aligned} \quad (\text{Eq. 2.9})$$

Then the heat exchanger effectiveness is defined as

$$\varepsilon = \frac{q_{\text{act}}}{q_{\max}} = \frac{C_h(T_{h,in} - T_{h,out})}{C_{\min}(T_{h,in} - T_{c,in})} = \frac{C_c(T_{c,in} - T_{c,out})}{C_{\min}(T_{h,in} - T_{c,in})} \quad (\text{Eq. 2.10})$$

The number of heat exchanger transfer units is then defined as

$$\text{NTU} = \frac{UA}{C_{\min}} \quad (\text{Eq. 2.11})$$

where  $U$  and  $A$  are defined as above. The heat Capacity-Rate Ratio is defined as,

$$C_r = \frac{C_{\min}}{C_{\max}} \quad (\text{Eq. 2.12})$$

Then in general it is possible to express the effectiveness as

$$\epsilon = \epsilon(\text{NTU}, C_r, \text{Flow Arrangement})$$

Different functions for  $\epsilon$  have been developed for many flow arrangements [8]. The three main flow arrangements of interest are parallel flow, counter flow, and cross flow.

#### Parallel Flow:

For parallel flow the expression is

$$\epsilon = \frac{1 - e^{-\text{NTU}(1+C_r)}}{1 + C_r} \quad (\text{Eq. 2.13})$$

There are two interesting limits,

$$\begin{aligned} C_r \rightarrow 0 & \quad \epsilon = 1 - e^{-\text{NTU}} \\ C_r \rightarrow 1 & \quad \epsilon = \frac{1}{2} \end{aligned} \quad (\text{Eq. 2.14})$$

The  $C_r=0$  limit corresponds to one fluid vaporizing or condensing and the heat capacity rate for this fluid becomes immense. The other limit  $C_r=1.0$  corresponds to both fluids having the same Heat Capacity Rate.

#### Counter Flow:

$$\epsilon = \frac{1 - e^{-\text{NTU}(1-C_r)}}{1 - C_r e^{-\text{NTU}(1-C_r)}} \quad (\text{Eq. 2.15})$$

Addressing the same two limits

$$\begin{aligned} C_r \rightarrow 0 & \quad \epsilon = 1 - e^{-\text{NTU}} \\ C_r \rightarrow 1 & \quad \epsilon = \frac{\text{NTU}}{1 + \text{NTU}} \end{aligned} \quad (\text{Eq. 2.16})$$

The  $C_r = 0$  limit is the same but the  $C_r = 1$  limit is twice as effective for large values of NTU. This essentially is the known performance advantage of counter flow heat exchangers.

Cross Flow: Cross flow has to be broken down into three different types. The performance is different depending on whether or not the fluids are allowed to mix with themselves as they move through the exchanger. A typical tube and shell exchanger would have the fluid moving through the tubes described as unmixed and the fluid moving through the shell would be mixed.

#### Cross Flow—Both Fluids Unmixed

This case requires a series numerical solution and the curves for values of various  $C_r$  values are given in Kays and London [11]. For the case of  $C_r = 0$ , the solution is the same as for counter flow and parallel flow.

$$C_r = 0 \quad \varepsilon = 1 - e^{-\text{NTU}}$$

However, all of the curves for any value of  $C_r$  asymptotically approach 1.0 like the counter flow exchanger. For all  $C_r > 0$  the effectiveness is less than for a counter flow exchanger with the same  $C_r$ .

#### Cross Flow—One Fluid Mixed

For the case of

$$\begin{aligned} C_{\max} &= C_{\text{unmixed}} & C_{\min} &= C_{\text{mixed}} \\ \varepsilon &= 1 - e^{-\Gamma/C_r} & \Gamma &= 1 - e^{-\text{NTUC}_r} \end{aligned} \quad (\text{Eq. 2.17})$$

And for the case of

$$\begin{aligned} C_{\max} &= C_{\text{mixed}} & C_{\min} &= C_{\text{unmixed}} \\ \varepsilon &= \frac{1 - e^{-\Gamma' C_r}}{C_r} & \Gamma' &= 1 - e^{-\text{NTU}} \end{aligned} \quad (\text{Eq. 2.18})$$

Once again for  $C_r = 0$ , this gives the same behavior as the counter flow heat exchanger. For  $C_r = 1.0$ , it gets complicated but it is important to note that if a choice is possible it is better to have the fluid with the smaller heat capacity rate be the mixed fluid (Eq. 2.17).

#### Cross Flow—Both Fluids Mixed

The closed form solution is

$$\varepsilon = \frac{\text{NTU}}{\frac{\text{NTU}}{(1-e^{-\text{NTU}})} + \frac{C_r \text{NTU}}{1-e^{-\text{NTUC}_r}} - 1} \quad (\text{Eq. 2.19})$$

As always, for the case of  $C_r = 0$ , the results are the same as the counter flow exchanger.

For  $C_r = 1.0$  as NTU becomes large, the effectiveness goes to 1/2. However, this is the only case that a better effectiveness can be obtained at a lower NTU. The effectiveness actually decreases after an NTU of about 3–5.

Note that the Number of Transfer Unit (NTU) is also directly related to the overall (total) Stanton number St formulated with the following equation, where  $D_h$  is hydraulic diameter as defined in Sect. 3.3, while  $L$  is fluid flow (core) length on one side of an exchanger in meters (m) or feet (ft).

$$\text{NTU} = \text{St} \frac{4L}{D_h} \quad (\text{Eq. 2.20})$$

There are many other configurations reported by Kays and London [11], but these three are the most important. The availability of solutions for the common cross flow case of one fluid mixed makes this technique very useful.

**Example 2.2** Consider a gas-to-gas recuperator of the shell and tube design.

The tubes are 2 cm diameter tubes spaced on 4 cm centers with a 2 mm thickness made of aluminum. The flow cross section is a 2 m by 2 m square. The pressure ratio for the compressor is 20. Both fluids are air and the cold fluid is in the tubes. The hot fluid enters at 783 K and exits at 670 K and is at atmospheric pressure. The cold fluid enters at 655 K and exits at 768 K and is at 20 atm. The flow rate is 2.5E + 5 kg/h, for a 10 MW power plant.

**Solution** Start with the hot fluid—Calculate Re No.

$$N_{\text{tubes}} = 2401, A_{\text{flow}} = 2^2 - 2401 \times \pi(0.012)^2 = 2.9138 \text{ m}^2$$

$$\dot{m} = \rho AV \quad \rho V = \frac{\dot{m}}{A} = \frac{69.44 \text{ kg/s}}{2.9138} = 23.8 \text{ kg/s/m}^2$$

$$\mu = 3.65E - 5 \quad D = \frac{4(0.04^2 - \pi 0.012^2)}{2\pi 0.012} = 0.0609 \text{ m}$$

$$\text{Re} = \frac{23.8 \times 0.0609}{3.7E - 05} = 39,789.2$$

This is clearly in the turbulent range.

Using the same equations, the cold fluid Re = 56,731.1

$$\text{Pr}_{\text{hot}} = C_p m/k = 1078.8 \times 3.65E - 5 / 0.0564 = 0.697$$

$$\text{Pr}_{\text{cold}} = C_p m/k = 1076.7 \times 3.25E - 5 / 0.050 = 0.700$$

$$\text{Nu}_{\text{hot}} = 0.023 \times 39,789.2^{0.8} \times 0.697^{0.3} = 98.7$$

$$h_{\text{hot}} = 98.7 \times 0.0564 / 0.0609 = 91.5 \text{ W/m}^2/\text{K}$$

$$\text{Nu}_{\text{cold}} = 0.023 \times 56,731.1^{0.8} \times 0.700^{0.4} = 127.0$$

$$h_{\text{cold}} = 127.0 \times 0.0500 / 0.02 = 316.0 \text{ W/m}^2/\text{K}$$

This allows us to calculate  $UA$  as a function of  $L$

$$A_{\text{hot}} = 2\pi(0.012) \times 2401 \times L = 724.8 \times L \text{ m}^2$$

$$A_{\text{cold}} = 2\pi(0.01) \times 2401 \times L = 603.4 \times L \text{ m}^2$$

$$A_{\text{tube}} = 2\pi(0.011) \times 2401 \times L = 663.74 \times L \text{ m}^2$$

$$\begin{aligned} \frac{1}{UA} &= \left( \frac{1}{h_{\text{hot}} A} + \frac{t}{kA} + \frac{1}{h_{\text{cold}} A} \right) \\ &= \frac{1}{91.5(724.8)L} + \frac{0.002}{218(663.74)L} + \frac{1}{316(603.4)L} \\ &= (1.508E - 5 + 1.38E - 8 + 5.25E - 6)/L = \frac{2.03E - 5}{L} \text{ W/K} \end{aligned}$$

$$\dot{Q} = 8.46E + 6 \text{ W} \quad \Delta T_{\text{in}} = 15 \text{ K} \quad \Delta T_{\text{out}} = 15 \text{ K}$$

$$\Delta T_{\text{lmn}} = 15 \text{ K} \quad \dot{Q} = \left( \frac{UA}{L} \right) L \Delta T_{\text{lmn}} \quad L = \frac{\dot{Q}}{(UA/L) \Delta T_{\text{lmn}}}$$

$$L = \frac{8.46E + 6}{4.92E + 4 \times 15} = 11.5 \text{ m}$$

Now try the NTU-Effectiveness method

$$C_{\text{hot}} = 2.5E + 5 / 3600 \times 1078.8 = 7.49E + 04$$

$$C_{\text{cold}} = 2.5E + 5 / 3600 \times 1076.7 = 7.48E + 04 = C_{\text{min}}$$

$$C_r = 0.998 \sim 1.0 \quad \epsilon = \text{NTU}/(\text{NTU} + 1) \quad \text{NTU} = \epsilon/(1 - \epsilon)$$

$$\epsilon = \frac{C_{\text{hot}}(T_{h,\text{in}} - T_{h,\text{out}})}{C_{\text{min}}(T_{h,\text{in}} - T_{c,\text{in}})} = \frac{7.49E + 4 \times (783 - 670)}{7.48E + 4 \times (783 - 655)} = 0.8846$$

$$\text{NTU} = 7.67 \quad \frac{\text{NTU}}{L} = \frac{v_A/L}{C_{\text{min}}} = 0.6576 \quad L = \frac{7.67}{0.6576} = 11.66 \text{ m}$$

Note that the largest resistance to heat transfer was in the hot side convection and the resistance of the tube wall was negligible.

So add fins to the hot side channel by putting a 2 mm thick web between the tubes. See Fig. 2.21

First, recalculate the hydraulic diameter for the hot side

Treating the webs as wetted perimeter gives a new  $D_h = 0.0329 \text{ m}$

This gives a new

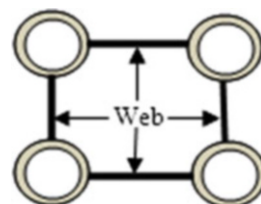
$$\text{Re} = 21,521.3$$

$$\text{Nu} = 60.4$$

$$h = 104.0.$$

Dividing the web in half for a fin for each tube,  
 $w = 0.01$ ,  $t = 0.002$ ,  $P = 0.02$ ,  $A = 0.00002$ ,  $m = 21.79$   $L = 0.008$   
 $mL = 0.1743$   $h_{\text{fin}} = 0.9899$   $h_o = 0.9915$   $A_{\text{tot}} = 0.1394$   
 $h_o \times A_{\text{tot}} = 0.1382$   $A_{\text{hot}}/A_{\text{cold}} = 2.1997$   $A_{\text{hot}}/L = 1327.3$

Fig. 2.21 Web channel



The cold side and tube resistances don't change, so

$$\frac{1}{UA} = \frac{1}{1.25E - 5 \times L} \quad L = \frac{\dot{Q}}{v_A / L \Delta T_{lmn}} = \frac{8.47E + 6}{7.98E + 4 \times 15} = 7.1 \text{ m}$$

Now to get the pressure drops

$$C_{f,hot} = 0.046Re^{-0.2} = 0.046 \times 21,521.3^{-0.2} = 6.25E - 3$$

$$C_{f,cold} = 0.046Re^{-0.2} = 0.046 \times 56,731.1^{-0.2} = 5.15E - 3$$

This gives

$$\tau_{hot} = 6.25E - 3 \times \frac{1}{2} \rho V^2 = \frac{3.13E - 3}{\rho_{hot}} \left( \frac{\dot{m}}{A} \right)_{hot}^2$$

$$\tau_{cold} = 5.15E - 3 \times \frac{1}{2} \rho V^2 = \frac{2.58E - 3}{\rho_{cold}} \left( \frac{\dot{m}}{A} \right)_{cold}^2$$

$$\rho_{hot} = \frac{101,325 \times 28.9669}{8314.4 \times 783} = 0.451 \text{ kg/m}^3 \quad \rho_{cold} = \frac{20 \times 101,325 \times 28.9669}{768 \times 8314.4} = 9.193 \text{ kg/m}^3$$

$$\tau_{hot} = \frac{3.13E - 3}{0.451} (23.83)_{hot}^2 = 3.941 \text{ Pa}$$

$$\tau_{cold} = \frac{2.58E - 3}{9.193} (92.1)_{cold}^2 = 2.38 \text{ Pa}$$

Clearly these pressure drops are negligible compared to atmospheric pressure. This says that the heat exchanger could be made a lot more compact by adding more surface area per unit volume— $\text{m}^2/\text{m}^3$ .

## 2.12 Special Operating Conditions

It is useful to note certain special conditions under which heat exchangers may be operated. Figure 2.20 shows temperature distributions for a heat exchanger in which the hot fluid has a heat capacity rate,  $C_h \equiv \dot{m}_h C_{p,h}$ , which is much larger than that of the cold fluid,  $C_c \equiv \dot{m}_c C_{p,c}$ .

For this case the temperature of the hot fluid remains approximately constant throughout the heat exchanger, while the temperature of the cold fluid increases. The same condition is achieved if the hot fluid is a condensing vapor. Condensation occurs at constant temperature, and, for all practical purposes  $C_h \rightarrow \infty$ . Conversely, in an evaporator or a boiler (Fig. 2.20), it is the cold fluid that experiences a change in phase and remains at a nearly uniform temperature ( $C_c \rightarrow \infty$ ). The same effect is achieved without phase change if  $C_h \ll C_c$ . Note that, with condensation or evaporation, the heat rate is given by Eq. (2.1a) or (2.1b),

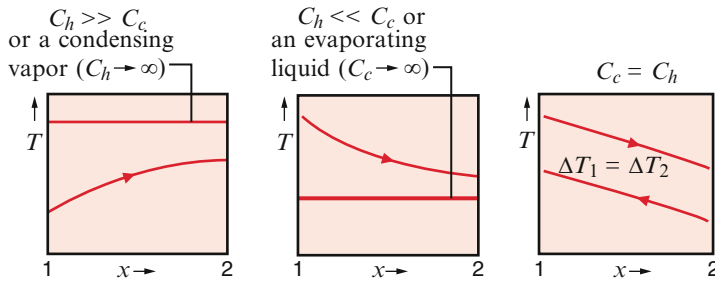


**Fig. 2.22** Special heat exchanger conditions. (a)  $C_h >> C_c$  or a condensing vapor. (b) An evaporating liquid or  $C_h << C_c$ . (c) A counterflow heat exchanger with equivalent fluid heat capacities  $C_h = C_c$  [9]

respectively. Conditions illustrated in Fig. 2.22a or b also characterize an internal tube flow (or *single stream heat exchanger*) exchanging heat with a surface at constant temperature or an external fluid at constant temperature.

The third special case in Fig. 2.22c involves a counterflow heat exchanger for which the heat capacity rates are equal ( $C_h = C_c$ ). The temperature difference  $\Delta T$  must then be constant throughout the exchanger, in which case  $\Delta T_1 = \Delta T_2 = \Delta T_{lm}$ .

## 2.13 Compact Heat Exchangers and Their Classifications

A heat exchanger is quite arbitrarily referred to as a *compact heat exchanger*, providing that it has a surface area density greater than  $700 \text{ m}^2/\text{m}^3$ , which is characterized by the ratio of its surface area per unit volume of the exchanger. A large heat transfer surface area per unit volume of the exchanger, results in reduced space, weight, support structure and footprint, energy requirements and cost, as well as improved process design and plant layout and processing conditions, together with low fluid inventory. This is done by virtue of increasing the heat transfer surface area via fins per unit volume ( $\text{m}^2/\text{m}^3$ ) and there are many variations. See Fig. 2.23a–c.

A special and important class of heat exchangers is used to achieve a very large ( $\geq 400 \text{ m}^2/\text{m}^3$  for liquids such as liquid-to-gas type exchangers and  $\geq 700 \text{ m}^2/\text{m}^3$  for gases such as gas-to-gas type one) heat transfer surface area per unit volume. Termed compact heat exchangers, these devices have dense arrays of finned tubes or plates and are typically used when at least one of the fluids is a gas, and hence is characterized by a small convection coefficient. The tubes may be flat or circular, as in Fig. 2.23a, b, and, c, respectively, and the fins may be plate or circular, as in Fig. 2.23a, b, and c, respectively. Parallel-plate heat exchangers may be finned or corrugated and may be used in single-pass (Fig. 2.23d) or multipass (Fig. 2.23e) modes of operation. Flow passages associated with compact heat exchangers are

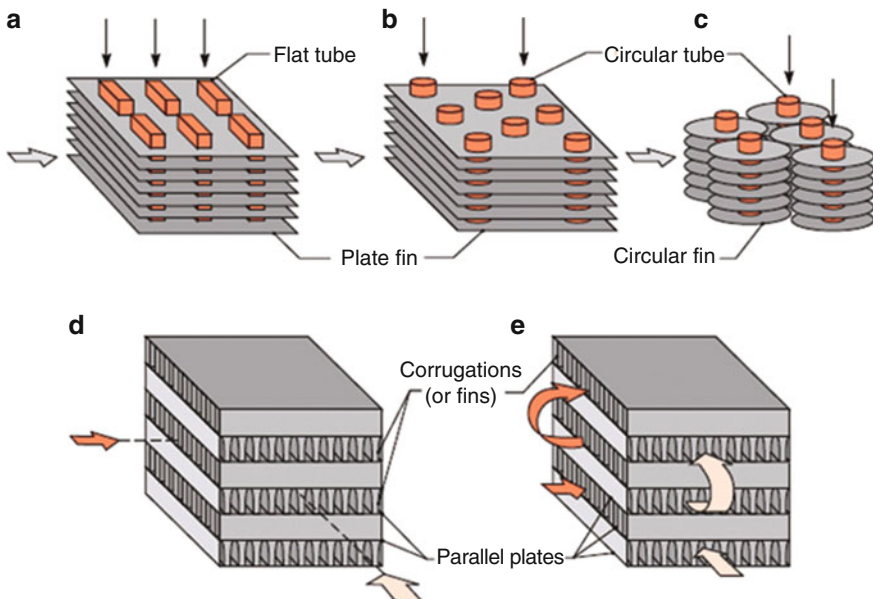


**Fig. 2.23** Compact heat exchanger cores. (a) Fin–tube (flat tubes, continuous plate fins). (b) Fin–tube (circular tubes, continuous plate fins). (c) Fin–tube (circular tubes, circular fins). (d) Plate–fin (single pass). (e) Plate–fin (multipass) [9]

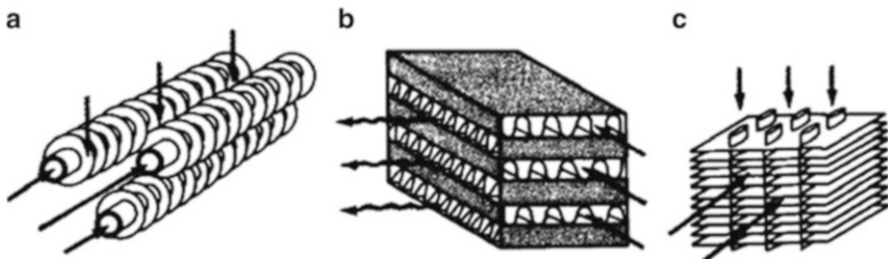


**Fig. 2.24** Typical heat transfer matrices for compact heat exchangers: (a) Circular finned-tube matrix; (b) plain plate-fin matrix; (c) finned flat-tube matrix [9]

typically small ( $D_h \leq 5\text{ mm}$ ),  $D_h$  is the magnitude of the *hydraulic diameter* and the flow is often laminar. Many of the geometries are far too complicated to apply deterministic methods to predict their performance; so many for these compact heat exchangers have had their performance determined experimentally.

Kays and London [11] have studied a wide variety of configurations for heat transfer matrices and catalogued their heat transfer and pressure drop characteristics. Figure 2.24 shows typical heat transfer materials for compact heat exchangers [9]. Figure 2.24a shows a *circular finned-tube array* with fins on individual tubes;

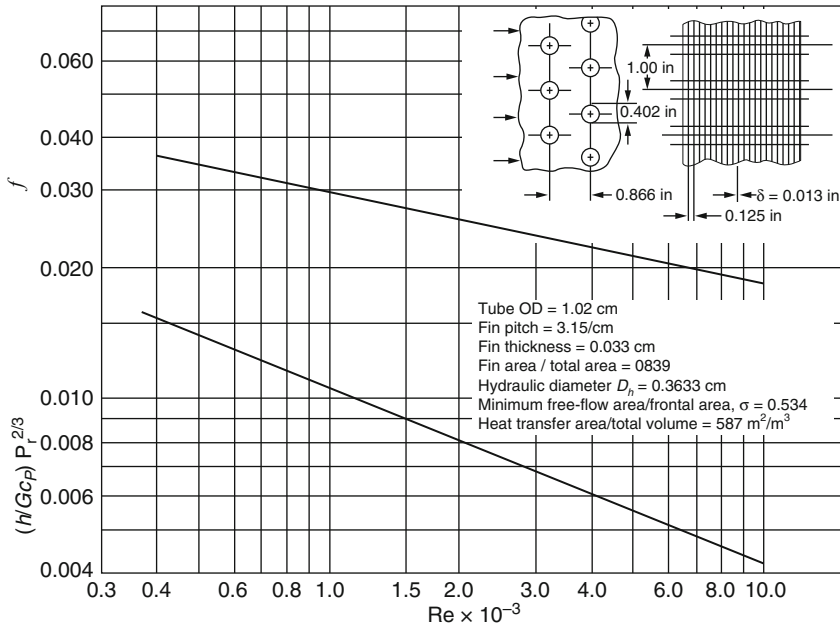


**Fig. 2.25** Heat transfer and friction factor for flow across plate-finned circular tube matrix [8]. (Courtesy of Kays and London [11])

Fig. 2.24b shows a *plain plate-fin matrix* formed by corrugation, and Fig. 2.24c shows a *finned flat-tube matrix* [9].

The heat transfer and pressure drop characteristics of such configurations for use as compact heat exchangers have been determined experimentally as explained above. Figures 2.25, 2.26, and 2.27 show typical heat transfer and friction factor data for three different configurations.

Note that the principal dimensionless groups governing these correlations are the Stanton, Prandtl, and Reynolds numbers [9].

$$St = \frac{h}{Gc_p} \quad Pr = \frac{c_p \mu}{k} \quad Re = \frac{GD_h}{\mu} \quad (\text{Eq. 2.21})$$

Here  $G$  is the *mass velocity* defined as

$$G = \frac{m}{A_{\min}} \text{ kg/(m}^2 \text{s)} \quad (\text{Eq. 2.22})$$

where  $m$  = total mass flow rate of fluid (kg/s) and  $A_{\min}$  = minimum free-flow cross-sectional area ( $\text{m}^2$ ) regardless of where this minimum occurs.

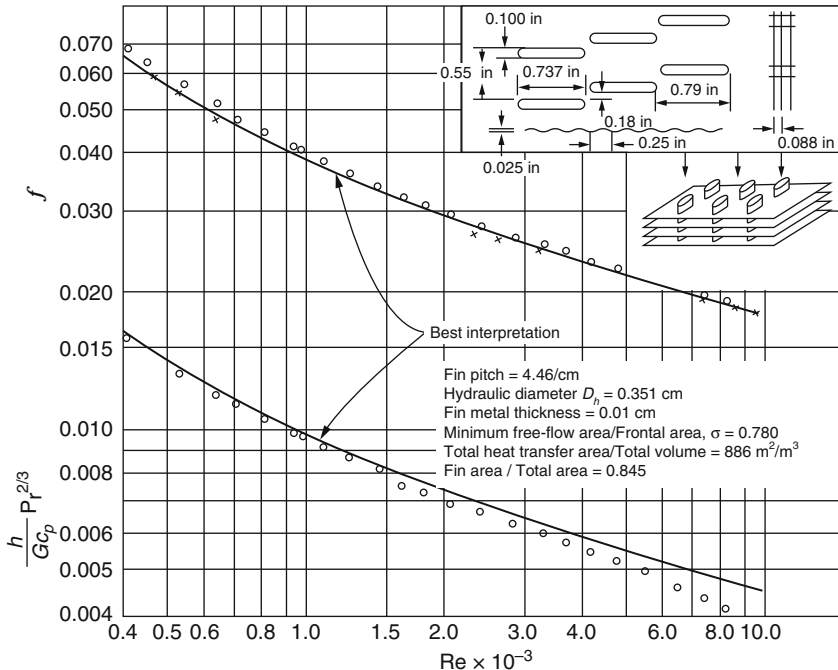


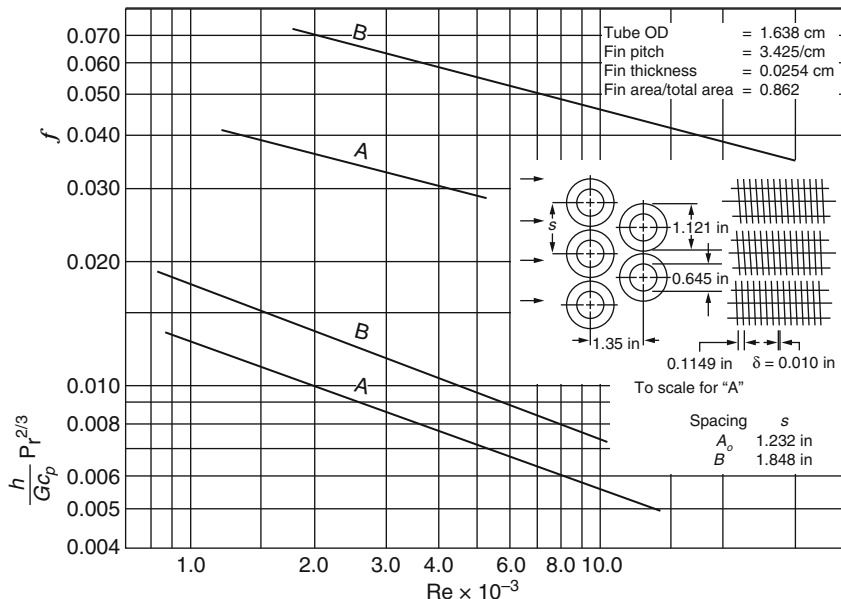
**Fig. 2.26** Heat transfer and friction factor for flow across finned flat-tube matrix [8]. (Courtesy of Kays and London [11])

The magnitude of the *hydraulic diameter*  $D_h$  for each configuration is specified in Figs. 2.25, 2.26, and 2.27. The hydraulic  $D_h$  is defined as;

$$D_h = 4 \frac{LA_{\min}}{A} \quad (\text{Eq. 2.23})$$

where  $A$  is the total heat transfer area and the quantity  $LA_{\min}$  can be regarded as the minimum free-flow passage volume, since  $L$  is the flow length of the heat exchanger matrix.

Thus, once the heat transfer and the friction factor charts, such as those shown in Figs. 2.25, 2.26, and 2.27, are available for a specified matrix and the Reynolds number  $Re$  for the flow is given, the heat transfer coefficient  $h$  and the friction  $f$  for flow across the matrix can be evaluated. Then the rating and sizing problem associated with the heat exchanger matrix can be performed by utilizing either the LMTD or the effectiveness-NTU method of analysis.



	A	B
Hydraulic diameter $D_h$	= 0.5477	1.4674 cm
Minimum free-flow area/frontal area,	= 0.443	0.628
Heat transfer area/total volume	= 323.8	215.6 m <sup>2</sup> /m <sup>3</sup>

**Fig. 2.27** Heat transfer and friction factor for flow across circular finned-tube matrix. (Courtesy of Kays and London [11])

## References

1. Fraas, Arthur P. 1989. *Heat exchangers design*, 2nd ed. Hoboken, NJ: Wiley Interscience.
2. Necati Ozisik, M. 1985. *Heat transfer: A basic approach*. New York: McGraw-Hill.
3. Incropera, F., D. Dewitt, T. Bergman, and A. Lavine. 2007. *Introduction to heat transfer*, 5th ed. Hoboken, NJ: Wiley.
4. Hesselgreaves, J.E. 2001. *Compact heat exchangers, selection, design and operation*. New York: Pergamon Press.
5. Aquaro, D., and M. Pieve. 2007. High temperature heat exchangers for power plants: Performance of advanced metallic recuperators. *Applied Thermal Engineering* 27: 389–409.
6. Jeong, Ji Hwan, Lae Sung Kim, Jae Keun, Man Yeong Ha, Kui Soon Kim, and Young Cheol Ahn. 2007. Review of heat exchanger studies for high-efficiency gas turbines. ASME Turbo Expo 2007: Power for Land, Sea and Air, May 14–17, 2007, Montreal, Canada.
7. Foumeny, E.A., and P.J. Heggs. 1991. *Heat exchange engineering, volume 2, Compact heat exchangers: Techniques of size reduction*. West Sussex, England: Ellis Horwood Limited.
8. Kays, W.M., and A.L. London. 1964. *Compact heat exchangers*, 2nd ed. New York: McGraw-Hill.

9. Incropera, F., D. Dewitt, T. Bergman, and A. Lavine. 2011. *Fundamentals of heat and mass transfer*, 7th ed. New York: Wiley.
10. Pansini, A.J., and K.D. Smalling. 1991. *Guide to electric power generation*. Liburn, GA: The Fairmont Press, Inc.
11. Boyen, J.L. 1975. *Practical heat recovery*. New York: John Wiley & Sons.

# **Chapter 3**

## **Compact Heat Exchangers Design for the Process Industry**

Due to the nature of Compact Heat Exchanges (CHEs)—very light weight, minimum volume and high effectiveness—they have a major technological and innovative role in the advancement of transportation, nuclear and renewable source of energy industries. They also play a similar significant role in the advancement of the process industry such as in oil refinery where hydrogen production is in demand. Here in this chapter, after providing a basic background description and information for the CHEs, we derive thermal hydraulic and heat transfer of heat exchangers in order for the reader to have a fair idea of how the designed heat exchangers would perform when installed in the power plant and One-Dimensional analysis modeling is presented using MATLAB software while the Three-Dimensional modeling study of the heat exchanger is undertaken with the use of the COMSOL Multiphysics software.

### **3.1 Introduction**

A Compact Heat Exchanger (CHE) is a heat transfer device that exchanges heat between two or more processes utilizing an appropriate working fluid or gas. Compact heat exchangers are one of the most important and critical components of many cryogenic systems driving efficiency of modern power plants to a higher degree with the help of either open air or closed loop in conjunction with Brayton cycle when these power plants are operating above 650 °C. Utilizing Brayton cycle in open or closed in any form of bottoming or topping shows very promising higher efficiency for these power plants, i.e., Gas Turbine, Next Generation Nuclear Power Plants or Concentrated Solar Power Farms. The heat exchangers would be considered as compact type when they have surface area density  $\beta$  (surface area to volume ratio) greater than  $700 \text{ m}^2/\text{m}^3$  ( $213 \text{ ft}^2/\text{ft}^3$ ) in either one or more sides of two-stream or multi-stream handling the heat exchanging process between the stream of cold and hot, when one side is gas and the other side is fluid (gas-to-fluid type heat

exchangers). The compact heat exchanger can be referred to as a laminar flow heat exchanger if the surface area density  $\beta$  is above  $3000 \text{ m}^2/\text{m}^3$  ( $914 \text{ ft}^2/\text{ft}^3$ ). And finally, these CHEs are referred to as micro heat exchangers if the surface area density  $\beta$  is above about  $10,000 \text{ m}^2/\text{m}^3$  ( $3050 \text{ ft}^2/\text{ft}^3$ ) [1].

Compact Heat Exchangers (CHEs) technically and historically have played a big role in the industries of aerospace, marine, and automobile transportation systems due to their compact nature and being light weight yet with very high efficiency and effectiveness with a minimum footprint for their size. However they suffer for their certain limitation that is, for maximum operating pressure and temperature, minimum allowed fouling has prevented their widespread adoption and application in the industry, until recent years, where a certain type and class of CHEs offer an excellent efficiency combined with Brayton or combined cycle.

Significant advancement in the design and manufacturing of CHEs have taken place in recent years that now make them very appealing and useful in gas turbine, NGNP, solar energy with concentrated solar power, and wind energy as a new source of renewable energy during off and on grid processing for efficient and cheap electricity productions.

The new generation of Computational Fluid Dynamics (CFD) and Finite Elements Analysis (FEA) computer software with their fast processing platform offer a very smooth and slick approach to the theory of designing these compact heat exchangers resulting in very cost effective manufacturing and reduction of cost of ownership for their operational applications in today's industry. Characteristics of CHEs important to process plants for energy production and cheap electricity along with their pros and cons is part of the design configuration for these CHEs and each approach has its own limitations and advantages or disadvantages. Subsequently, technical and commercial issues that inhibit the broader use of CHEs can be analyzed and studied in each of the following chapters of this book as well.

## 3.2 Compact Heat Exchangers by Their Types

As described in Sect. 2.13 compact heat exchangers and their classification were presented, and for example in the case of gas-to-fluid type CHE, the compactness was defined by its surface area density of greater than  $700 \text{ m}^2/\text{m}^3$  (also see Sect. 3.1).

Compact heat exchangers by types are summarized by their features of various types in Table 3.1 and their principle ones are listed below.

- Plate and Frame Heat Exchangers
- Brazed Plate Heat Exchangers
- Welded Plate Heat Exchangers
- Plate-fin heat exchangers
- Printed Circuit Heat Exchangers
- The Marbond™ Heat Exchanger

**Table 3.1** A summary of different types of compact heat exchangers and their principle features

Feature		Compactness ( $\text{m}^2/\text{m}^3$ )	Stream types <sup>a</sup>	Material <sup>b</sup>	Temperature range ( $^{\circ}\text{C}$ ) <sup>c</sup>	Maximum pressure (bar)	Cleaning methods	Corrosion resistance	Multistream capability	Multipass capability
Type of heat exchanger	Plate -and-frame (gaskets)	$\leq 200$	Liquid-liquid, gas-liquid, two-phase	s/s, Ti, inconel, hastelloy, graphite, polymer	-35 to +200	25	Mechanical <sup>d</sup>	Good <sup>e</sup>	Yes <sup>f</sup>	Yes
Partially welded plate		$\leq 200$	Liquid-liquid, gas-liquid, two-phase	s/s, Ti, inconel, hastelloy	-35 to +200	25	Mechanical <sup>d,g</sup> , Chemical <sup>h</sup>	Good <sup>e</sup>	No	Yes
Fully welded plate (Alfa Rex)		$\leq 200$	Liquid-liquid, gas-liquid, two-phase	s/s, Ti, Ni all OYS	-50 to 350	40	Chemical	Good	No	Yes
Brazed plate		$\leq 200$	Liquid-liquid, two-phase	s/s	-195 to 220	30	Chemical <sup>i</sup>	Good	No	No <sup>k</sup>
Bavex plate		200 up to 300	Gases, liquid, two-phase	s/s, Ni, Cu, H, special steels	-200 to +900	60	Mechanical <sup>d,i</sup> , Chemical	Good <sup>j</sup>	In principle	Yes
Platular plate		200	Gases, liquids, two-phase	s/s, hastelloy, Ni alloys	Up to 700	40	Mechanical <sup>d,m</sup>	Good	Yes <sup>n</sup>	Yes

(continued)

**Table 3.1** (continued)

	Feature	Compactness ( $\text{m}^2/\text{m}^3$ )	Stream types <sup>a</sup>	Material <sup>b</sup>	Temperature range ( $^{\circ}\text{C}$ ) <sup>c</sup>	Maximum pressure (bar)	Cleaning methods	Corrosion resistance	Multistream capability	Multipass capability
Type of heat exchanger	Compabloc plate	$\leq 300$	Liquids	s/s, Ti, inconoly	Up to 300	32	Mechanical <sup>d,o</sup>	Good	Not usually	Yes
Compabloc plate	Packinox plate	$\leq 300$	Gases, liq-uids, two-phase	s/s, Ti, hastelloy, inconel	-200 up to +700	300	Mechanical <sup>d,o</sup>	Good	Yes <sup>f</sup>	Yes
Spiral	$\leq 200$	Liquid-liq-uid, two-phase	c/s, s/s, Ti, inconoly, hastelloy	Up to 400	25	Mechanical <sup>d</sup>	Good	No	No	
Braced plate-fin	800 tip to 1500	Gases, liq-uids, two-phase	Al, s/s, Ni alloy	Cryogenic to +650	90	Chemical	Good	Yes	Yes	
Diffusion-bonded plate-fin	700 up to 800	Gases, liq-uids, two-phase	Ti, s/s	Up to 500	>200	Chemical	Excellent	Yes	Yes	
Primed-circuit	200 up to 5000	Gases, liq-uids, two-phase	s/s, Ni, Ni alloy, Ti	-200 up to +900	>400	Chemical	Excellent	Yes	Yes	
Polymer (e.g. channel plate)	450	Gas-liquid <sup>p</sup>	PVDF <sup>q</sup> , PP <sup>r</sup>	Up to 150	6	Water wash	Excellent	No	Not usually	
Plate-and-shell	-	Liquids	s/s, Ti (shell also in c/s) <sup>t</sup>	Up to 350	70	Mechanical <sup>d,o</sup> , Chemical <sup>u</sup>	Good	No	Yes	

Marbond	$\leq 10,000$	Gases, liquid, two-phase	s/s, Ni, Ni alloy, Ti	-200 up to +900	>900	Chemical	Excellent	Yes	Yes
---------	---------------	-----------------------------	--------------------------	--------------------	------	----------	-----------	-----	-----

Source: Shah and Sekulic [31], Hessegrevs [52], and Reay (2002)

a Boiling and condensing duties are included in the two-phase

b s/s: stainless steel; Ni, nickel; Ti, titanium, Cu, copper and their alloys of these materials and special alloys are also available for use

c The maximum pressure is not likely to occur at the higher operating temperatures, and assumes no pressure/stress-related corrosion

d It can be dismantled

e Functions as a gasket as well as a plate material

f Not common

g On the gasket side

h On the welded side

i Ensures compatibility with die copper braze

j Function of braze as well as plate material

k Not in a single unit

l On the tube side

m Only when flanged access provided; otherwise, chemical cleaning  
n Five fluids maximum  
o On the shell side

p Considering on gas side

q Polyvinylidene difluoride  
r Polypropylene

s PEEK (polyetheretherketone) can go to 250 °C  
t Shell may be composed of polymeric material  
u On the plate side

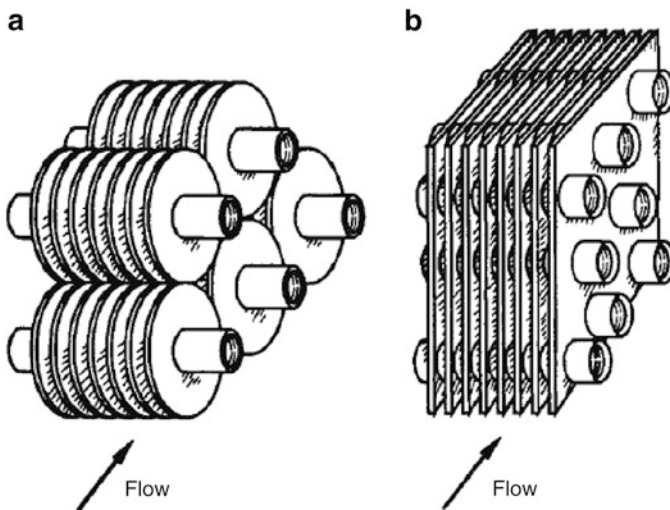
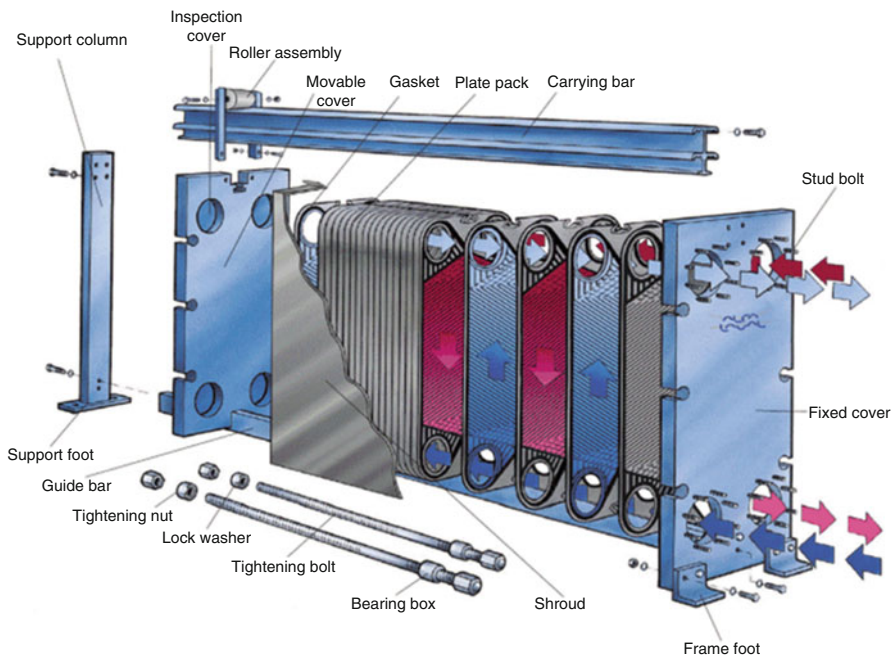


**Fig. 3.1** Tube fin exchanger configuration. (a) Individually finned tubes. (b) Flat fin with continuous form on an array of tubes

Their brief configurations and descriptions are depicted in Figs. 3.1 and 3.2 and so on below and more details are shown in Fig. 2.21.

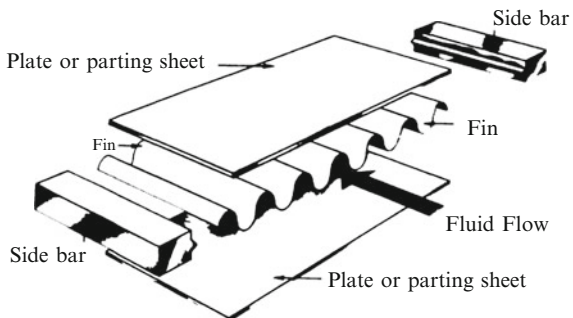
Figure 3.1a shows a tube fin exchanger with continuous formation of an array of tubes where the fin is shown as plain, but can be wavy, louvered, etc. See Figs. 3.4 and 3.46 as well, where various fins arrangements are described and depicted as well. Figure 3.2 is a schematic of a Plate Heat Exchanger (PHE), which is a type of primary surface recuperator and it consists of a number of very thin corrugated metal sheets usually chosen to be stainless steel, although other metals and their alloys can also be employed.

Plate fin heat exchanger is a class of compact heat exchanger where the heat transfer surface area can be enhanced via the extended metal surface interface between the two working fluids and is identified as a fin. Due to uniqueness of the structure of these CHEs, they provide excellent performance and heat transfer efficiency as well as compactness, low weight, and moderate total cost of ownership. As the name suggests, a Plate Fin Heat Exchanger (PFHE) is the class of compact heat exchanger that consists of a stack of alternate flat plates called parting sheets and corrugated fins brazed together as a block. Heat transfer between two working media or fluids takes place along the passage made by the fins between the parting plates or sheets. The separating plate acts as the primary heat transfer and the appendages known as fins as the secondary heat transfer surfaces intimately connected to the primary surface. Fins not only form the extended surfaces for heat transfer, but also work infrastructure support and strength for supporting member against the internal pressure. Figure 3.3 shows the more granular exploded view of two layers of a plate fin heat exchanger (PFHE). Such layers are combined together in a monolithic block to form a complete version of PHEs.



**Fig. 3.2** Diagram of a plate heat exchanger. (Courtesy of Alfa Laval Inc.)

**Fig. 3.3** A plate fin assembly



The most effective class of compact heat exchangers are considered to be plate fin, tube fin for gas-to-gas senraio where all prime surfaces are part of recuperators and compact regenerators with flow arrangements of two fluids are in single-pass crossflow, conterflow or multipass cross-counter flow configurations. All three flow arrangement are described in Sect. 3.2.1.

In the case of the liquid-to-two-phase for compact heat exchangers of plate (PHE) type, their basic construction consists of gasketed and welded plate-and-frame or welded stacked plate without frame and finally printed circuit form of heat exchangers. These entire configurations are schematically presented in Figs. 3.1–3.3 or Fig. 2.21.

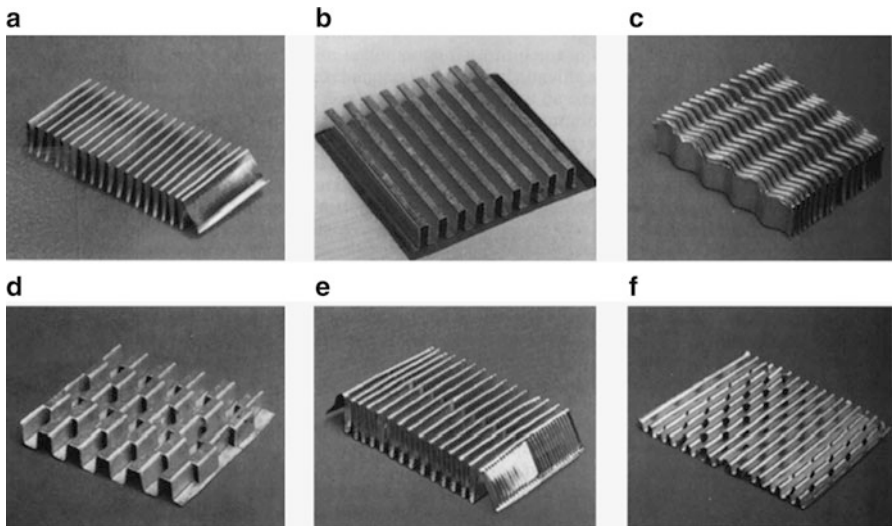


**Fig. 3.4** Corrugated fin geometries for plate fin exchangers: (a) Plain triangle fin. (b) Plain rectangular fin. (c) Wavy fin. (d) Offset strip fin. (e) Multilouver fin. (f) Perforated fin. (Courtesy of Delphi Harrison Systems Lockport, NY)

Out of the various compact heat exchangers, plate fin heat exchangers are (PFHE) unique due to their construction and performance. They are characterized by their high effectiveness, compactness, low weight, and moderate cost of manufacturing. As the name also suggests, a plate fin heat exchanger (PFHE) is a type of compact heat exchanger that is composed of a stack of alternate flat plates as shown in Fig. 3.3 that are called parting sheets and corrugated fins brazed together as a block. Streams or working fluids do the heat exchanging duty by following along the passages made by the fins between the parting sheets. Figure 3.4 presents different categories and the most commonly used of these fins and they are defined as:

1. Uncut plain and straight fins, such as plain triangular and rectangular fins.
2. Plain but wavy fins, where the wavy patterns are in the main fluid flow direction, and
3. Interrupted fins, such as offset strip, louver, perforated, and pin fins.

In the case of category 3 above, louver form of multi-louver fins geometries are shown in Fig. 3.5 and Fig. 3.6 shows automotive condensers and evaporators.

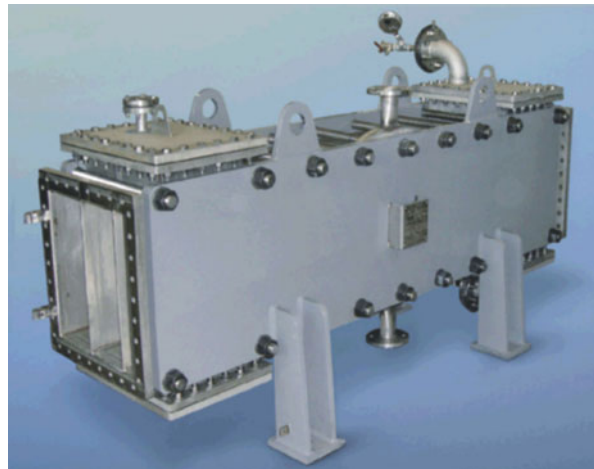
Figure 3.5 is a depiction of fins that are incorporated in a flat tube with round corners, referred to as a formed tube, thus eliminating the need for side bars. If liquid or phase-change fluid flows on the other side, the parting sheet is usually replaced by a flat tube with or without inserts or webs.

As we know a traditional shell-and-tube heat exchanger that is used in typical process industry has a surface area density of less than  $100 \text{ m}^2/\text{m}^3$  on one fluid side with plain tubes, and 2–3 times that with the high fin density low finned tubing.

**Fig. 3.5** Schematic of brazed plate heat exchangers. (Courtesy of SWEP Ltd)



**Fig. 3.6** Diagram of welded plate heat exchanger



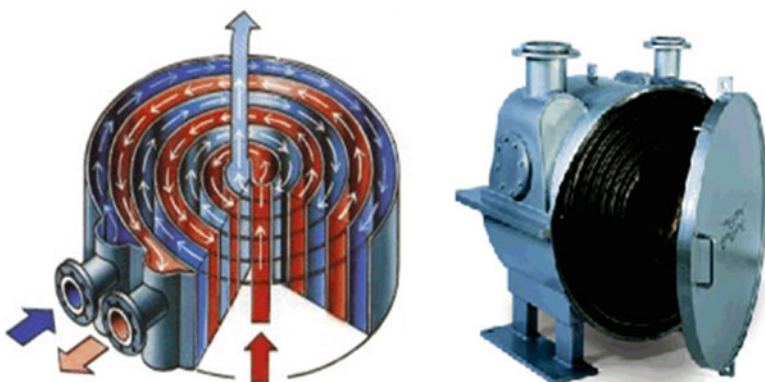
However, the case of extremely high heat transfer coefficients  $h$  are achievable with a small hydraulic diameter flow passage with gases, liquids, and two-phase flows driven by a typical Plate Heat Exchanger (PHE) that has about two times  $h$  or overall heat transfer coefficient  $U$  than that of a shell-and-tube heat exchanger for water-to-water applications type [2].

Plate and Frame Heat Exchanger is the most common type and class of Plate Heat Exchanger (PHE) and consists of plates and gaskets as described above. Materials that are used for manufacturing of this heat exchanger are Stainless Steel (SS), Titanium, and non-metallic, and their operational and functional heat duty is limited to temperatures between  $-35^{\circ}\text{C}$  to  $220^{\circ}\text{C}$  along with pressures up to 25 bar at the flow rate up to  $5000 \text{ m}^3/\text{h}$ .

On the other hand the Brazed Plate Heat Exchangers operates at higher pressure than gasket units with structure materials of Stainless Steel (SS), Copper contained braze with thermal operations limited to  $-195^{\circ}\text{C}$  to  $200^{\circ}\text{C}$  and pressure up to 30 bar. From a preventive maintenance point of view, it is impossible to clean them and the only way is by applying a moderate chemical etching process for clean up. Figure 3.5 is a diagram of a typical brazed plate heat exchanger.

Welded Plate Heat Exchangers are structure-wise configured as plates welded together to increase pressure and temperature to higher limits and the materials that are used are Stainless Steel (SS) and Nickel based alloys and they can be made with Copper, Titanium or Graphite as well. Their thermal operational limits depend on the type of materials used for their structures and can tolerate pressure in excess of 60 bar. Figure 3.6 is a depiction of such heat exchangers.

Another class of Compact Heat Exchanger (CHE) is Spiral Heat Exchanger (SHE), which is configured as two long strips of plate wrapped to form concentric spirals, built out of materials such as Carbon Steel (CS), Stainless Steel (SS), and Titanium with thermal operation of temperature up to  $400^{\circ}\text{C}$  which depends on gasketed materials and pressures up to 25 bar. Figures 3.7 and 3.8 are diagrams of such heat exchanger. Overall, the Spiral Plate Heat Exchanger consists of two relatively long strips of sheet metal, normally provided with welded studs for plate spacing, wrapped helically around a split mandrel to form a pair of spiral channels for two fluids, as shown in Fig. 3.8. Alternate passage edges are closed. Thus, each fluid has a long single passage arranged in a compact package. To complete the exchanger covers are fitted at each end. Any metal that can be cold-formed and welded can be used for this exchanger. Common metals used are carbon steel and stainless steel. Other metals include titanium, Hastelloy, Incoloy, and high-nickel alloys. The basic spiral element is sealed either by welding at each side of the channel or by providing a gasket (non-asbestos based) at each end cover to obtain the following alternative arrangements of the two fluids:



**Fig. 3.7** Diagram of spiral heat exchanger

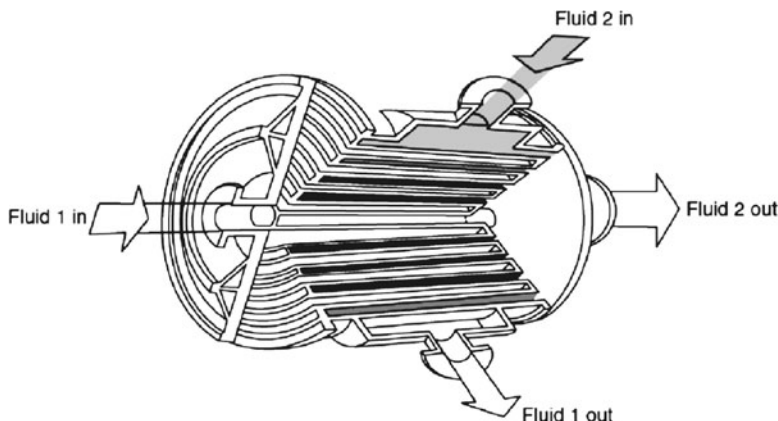


**Fig. 3.8** Spiral plate heat exchanger with both fluids in spiral counter-flow

1. Both fluids in spiral counterflow;
2. One fluid in spiral flow, the other in crossflow across the spiral; or
3. One fluid in spiral flow, the other in a combination of crossflow and spiral flow.

The entire assembly is housed in a cylindrical shell enclosed by two (or only one or no) circular end covers (depending on the flow arrangements above), either flat or conical. Carbon steel and stainless steel are common materials. Other materials used include titanium, Hastelloy, and Incoloy.

A spiral plate exchanger has a relatively large diameter because of the spiral turns. The largest exchanger has a maximum surface area of about  $500 \text{ m}^2$  ( $5400 \text{ ft}^2$ ) for a maximum shell diameter of 1.8 m (72 in.). The typical passage height is 5–25 mm (0.20–1.00 in.) and the sheet metal thickness range is 1.8–4 mm (0.07–0.16 in.).

The heat transfer coefficients are not as high as in a plate exchanger if the plates are not corrugated. However, the heat transfer coefficient is higher than that for a shell-and-tube exchanger because of the curved rectangular passages. Hence, the surface area requirement is about 20 % lower than that for a shell-and-tube unit for the same heat duty.

The counterflow spiral unit is used for liquid–liquid, condensing, or gas cooling applications. When there is a pressure drop constraint on one side, such as with gas flows or with high liquid flows, crossflow (straight flow) is used on that side. For condensation or vaporization applications, the unit is mounted vertically. Horizontal units are used when high concentrations of solids exist in the fluid.

The advantages of this exchanger are as follows: It can handle viscous, fouling liquids and slurries more readily because of a single passage. If the passage starts fouling, the localized velocity in the passage increases. The fouling rate then decreases with increased fluid velocity. The fouling rate is very low compared to that of a shell-and-tube unit. It is more amenable to chemical, flush, and reversing fluid cleaning techniques because of the single passage. Mechanical cleaning is also possible with removal of the end covers. Thus, maintenance is less than with a shell-

and-tube unit. No insulation is used outside the exchanger because of the cold fluid flowing in the outermost passage, resulting in negligible heat loss, if any, due to its inlet temperature being closer to the surrounding temperature.

The internal void volume is lower (less than 60%) than in a shell-and-tube exchanger, and thus it is a relatively compact unit. By adjusting different channel heights, considerable differences in volumetric flow rates of two streams can be accommodated.

The disadvantages of this exchanger are as follows: As noted above, the maximum size is limited. The maximum operating pressure ranges from 0.6 to 2.5 MPa gauge (90 to 370 psig) for large units. The maximum operating temperature is limited to 500 °C (930 °F) with compressed asbestos gaskets, but most are designed to operate at 200 °C (392 °F). Field repair is difficult due to construction features.

This exchanger is well suited as a condenser or reboiler. It is used in the cellulose industry for cleaning relief vapors in sulfate and sulfite mills, and is also used as a thermosyphon or kettle reboiler. It is preferred especially for applications having very viscous liquids, dense slurries, digested sewage sludge, and contaminated industrial effluents. A spiral version free of welded studs for plate spacing on one or both fluid sides but with reduced width is used for sludge and other heavily foul fluids. It is also used in the treatment of bauxite suspensions and mash liquors in the alcohol industry.

Figure 3.9 is a schematic of another type of plate fin geometry that includes drawn-cup and tube-and-center constructions or configurations. In this case the

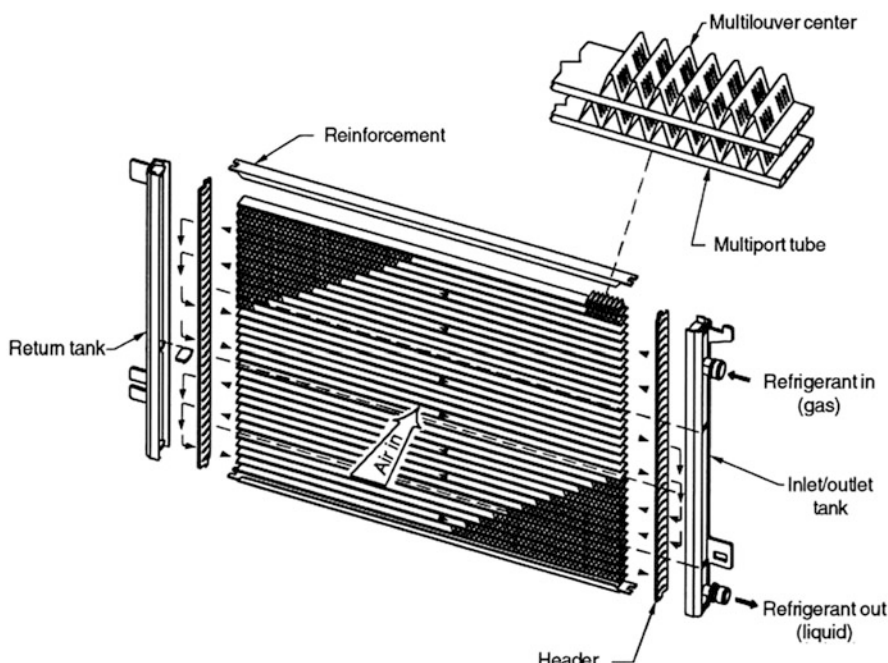


**Fig. 3.9** Flat webbed tube and multilouver fin automotive condenser. (Courtesy of Delphi Harrison Thermal Systems, Lockport, NY)

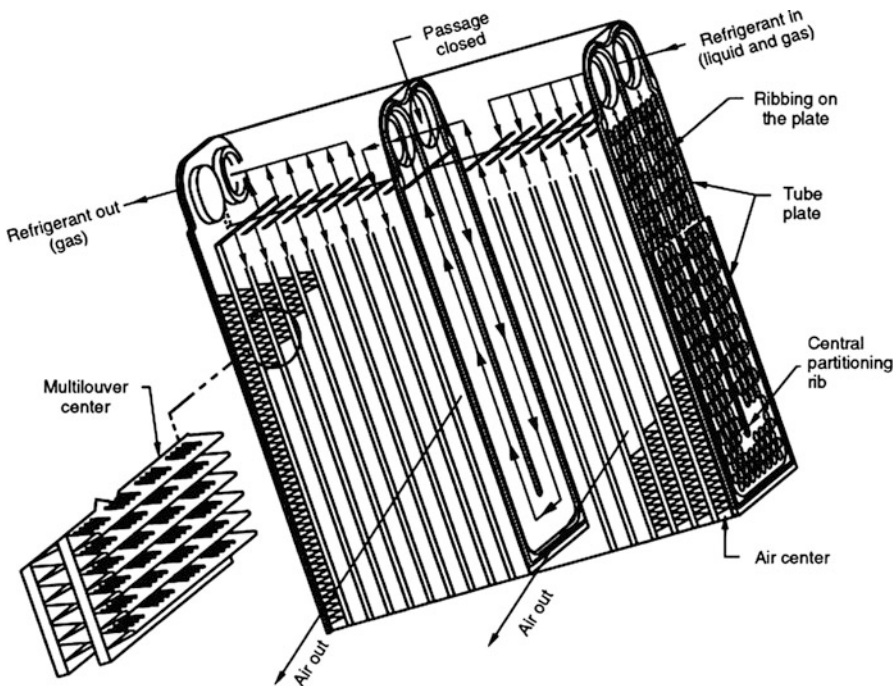


**Fig. 3.10** U-Channel ribbed plates and multilouver fin automotive evaporator. (Courtesy of Delphi Harrison Thermal Systems, Lockport, NY)

plates or flat tubes separate the two fluid streams, and the fins form the individual flow passages. In this configuration the fluid passages are connected in parallel by suitable headers to form one or more fluid sides of the exchanger, and the fins are die or roll shape and they are attached to the plates by brazing, soldering, adhesive bonding, welding, mechanical fit, or extrusion means. Fins may be used on both sides in gas-to-gas heat exchangers and in the case of gas-to-liquid applications, fins are generally used only on the gas side and these fins are installed on the liquid side, where they can be used primarily for structural strength and flow-mixing purposes. Fins in this case are also used for pressure containment and rigidity.

In Europe, a plate-fin exchanger is also referred to as a *matrix heat exchanger*. Louver form of the multi-louver fin is shown in Fig. 3.10, where common usage of fins is depicted.

Another compact heat exchanger class and type is known as Printed Circuit Heat Exchanger (PCHE).

Printed Circuit Heat Exchanger (PCHE) and its plate diagram are presented in Fig. 3.11.

More details of each plate are shown in Fig. 3.12.

This type of exchanger also only has primary heat transfer surface like the Plate Heat Exchanger (PHE). Fine grooves are made in the plate by using the same technology that is employed for printed electrical circuitry. They can achieve very

**Fig. 3.11** Typical Printed Circuit Heat Exchanger (PCHE) diagram

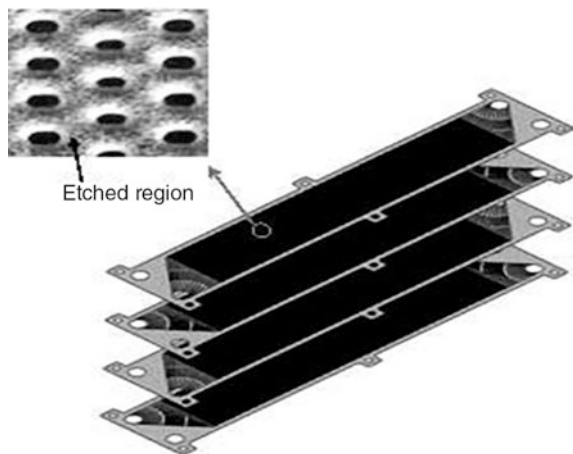
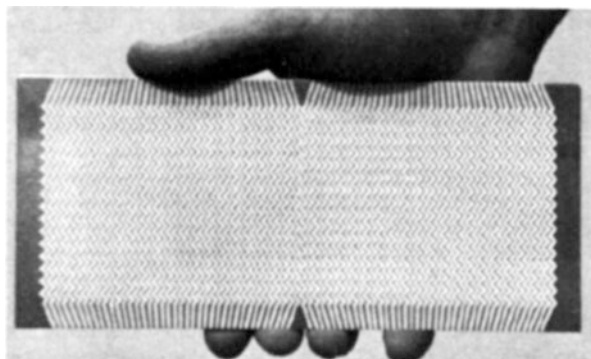


**Fig. 3.12** A chemically milled printed circuit heat exchanger plate [2]



high surface area densities of  $1000\text{--}5000\text{ m}^2/\text{m}^3$  or  $300\text{--}1520\text{ ft}^2/\text{ft}^3$  and a variety of materials such as Stainless Steel (SS) of 316 SS, 316 L SS, 304 SS, 904 L SS, Cupronickel, Monel, Nickel, and super-alloys of inconel 600, inoloy 800 and 825 [3] can be used for the structure. These compact heat exchangers are usually used with relatively clean gases, liquids, and phase-change fluids in chemical processing, fuel processing, waste heat recovery, and refrigeration industries. These types of heat exchangers are new in construction with limited current special applications [4].

The Marbond™ Heat Exchanger is the type that is formed by slotted flat plates, in other words it is formed by plates which have been photo-chemically etched through to form a series of slots. The plates after being chemically etched are then diffusion-bonded together. The manufacturing procedures for the Marbond™ heat exchanger are similar to that of the Printed Circuit Heat Exchanger (PCHE), that is, the chemical etching and the diffusion bonding process, but its construction procedure allows the use of small fluid passageways which significantly increases the

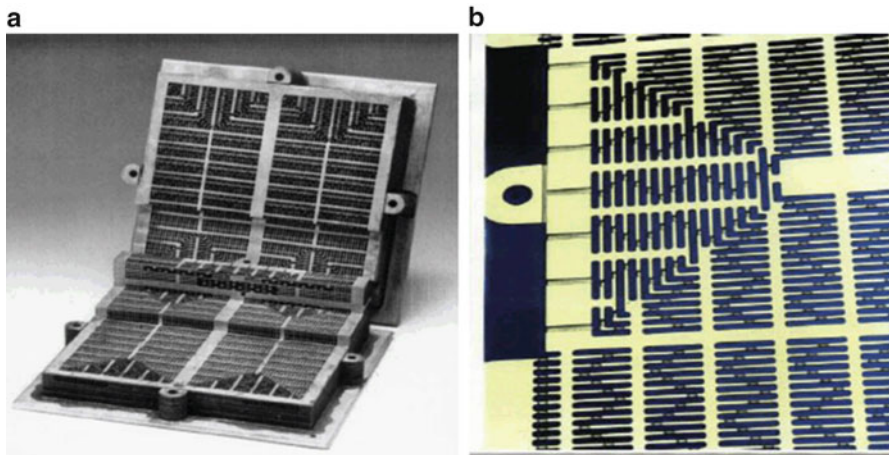


**Fig. 3.13** Marbond™ heat exchanger diagram. (a) An exposed view. (b) Photo-chemically etched plate

compactness of the heat exchanger. Figure 3.13a and b below shows a cutaway view of a Marbond™ and a photo-chemically etched plate of the heat exchanger respectively.

Stacked Plate Heat Exchangers (SPHEs) are another sub-class and type of Plate Heat Exchangers (PHEs) and the only difference between them and the main category of PHE is that they do not have gaskets, and the rectangular plates are stacked and welded at the edges.

The physical size limitations of PHEs (1.2 m wide  $\times$  4 m long max) are considerably extended to 1.5 m wide  $\times$  20 m long. The potential maximum operating temperature is 815 °C (1500 °F) with an operating pressure of 20 MPa (3000 psig) when the stacked plate assembly is placed in a cylindrical pressure vessel and 2 MPa (300 psig) when not contained in a pressure vessel. This exchanger is a new construction with limited current applications. One application of this exchanger is as a feed effluent heat exchanger in manufacturing of unleaded petrol.

More of these heat exchangers along with their pros and cons of operational limits and application with their types and classes as part of the compact heat exchangers series as well as more details are presented in Sect. 3.3.

### 3.2.1 Description of Plate Fin Heat Transfer Surfaces

As we described, the plate fin exchangers are mainly employed for liquid-to-gas and gas-to-gas applications. Due to the low heat transfer coefficients in gas flows, extended surfaces are commonly invoked in plate-fin heat exchangers. Employing special infrastructure and configured extended surfaces, heat transfer coefficients can also be enhanced. As demonstrated by Fig. 3.4 and later by Fig. 3.46 in

Sect. 3.5, these special surfaces through different fin configurations with special geometries provide much higher heat transfer coefficients than the plane extended surface, but at the same time, the pressure drop penalties are also high, though they may not be severe enough to negate the thermal benefits. Both Figs. 3.4 and 3.46 show a variety of these configurations again as extended special surfaces, including the plain plate trapezoidal—a plain rectangular that can perform such function for the demanded thermal duties and application where they are employed.

Surface features are needed in order to improve the gas side coefficients. These features may be divided into two categories:

1. The first, in which the surface remains continuous such as wavy and herringbone fins, and
2. The second in which it is cut such as offset, louvered.

Thermal hydraulic and fluid flow boundary analysis indicates that in a continuous type fin, the corrugations cause the gas to make sudden direction changes so that locally, the velocity and temperature gradients are increased which is depicted in Fig. 3.14. This results in local enhancement of heat transfer coefficient. However, an undesirable consequence of such enhancement in heat coefficient is an increase in the friction factor and pressure drop.

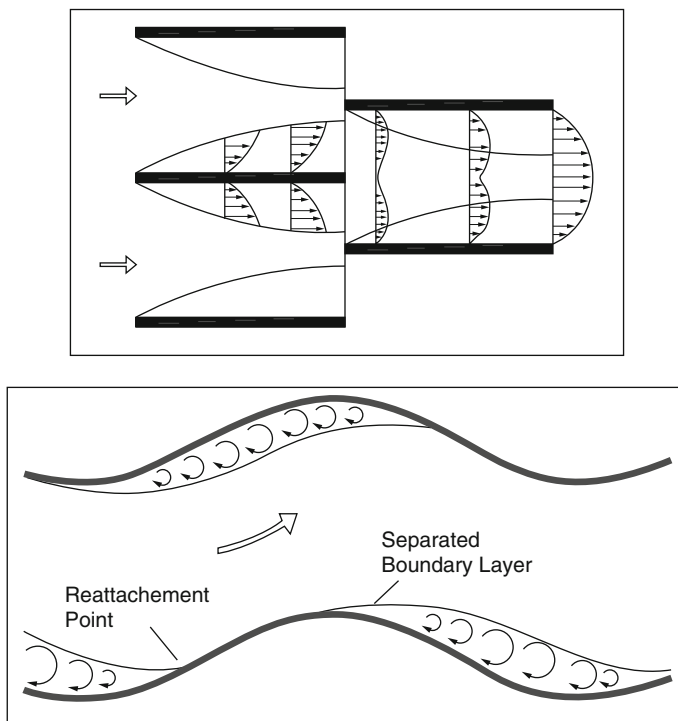


**Fig. 3.14** Details of boundary layer and flow across offset strip and wavy fin

Whereas in a discontinuous type of fin geometry, boundary layers are interrupted, this is not the case on a continuous plate. Adjacent to the leading edge of the fin, both heat transfer coefficients and friction factors are very high due to generation of fresh boundary layers, but in addition to this friction drag, form drag is also formed due to the finite thickness of the fin.

Although the friction drag is associated with high heat transfer coefficient, form drag has no counterpart and represents the form of wasted energy. The form drag could be substantial depending on the quality of the cutting edge. However, machined-formed fins are generally free from this problem. Brief descriptions of applications and associated mechanisms of the extended surfaces or fins are depicted in Fig. 3.4 [5].

### 3.2.2 *Flow Arrangement and Passage in Compact Heat Exchangers*

As part of heat exchanger classification based on flow passages, there are three primary classifications according to their flow arrangement and they are:

1. *Parallel-Flow*: In this class of heat exchanger, the two fluids enter the exchanger at the same end, and travel in parallel to one another to the other side.
2. *Counter-Flow*: In this class of heat exchanger, the fluids enter the heat exchanger from opposite ends; and in the case of a traditional heat exchanger such as shell-and-tube, the counter current configuration is the most efficient for heat duty exchange, in that it can transfer the most heat for the heat transfer medium per unit mass due to the fact that the average temperature difference along any unit length is *higher*.
3. *Cross-Flow*: In this class of heat exchanger, the fluids travel roughly perpendicular to one another through the heat exchangers.

For efficiency, heat exchangers are designed to maximize the surface area of the wall between the two fluids, while minimizing resistance to fluid flow through the exchanger. The exchanger's performance can also be affected by the addition of fins or corrugations in one or both directions, which increase surface area and may channel fluid flow or induce turbulence.

The driving temperature across the heat transfer surface varies with position, but an appropriate mean or average temperature can be defined. In most simple systems this is the Log Mean Temperature Difference (LMTD). Sometimes direct knowledge of the LMTD is not available and the Number of Transfer Units (NTU) method should be used. Both these methods were described in Sects. 2.10 and 2.11.

Figures 3.15a–c are illustrations of the above flow arrangement in a traditional shell-and-tube heat exchanger and heat movement profile for Countercurrent (A) and Parallel (B) flows are presented in Fig. 3.16.

**Fig. 3.15** Traditional shell-and-tube flow arrangements. (a) Shell and tube heat exchanger, single pass (1-1 parallel flow). (b) Shell and tube heat exchanger, 2-pass tube side (1-2 crossflow). (c) Shell and tube heat exchanger, 2-pass shell side, 2-pass tube side (2-2 countercurrent)

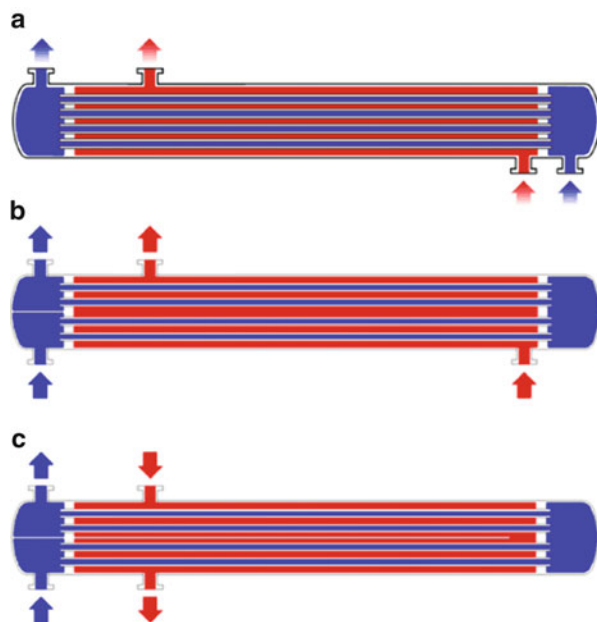
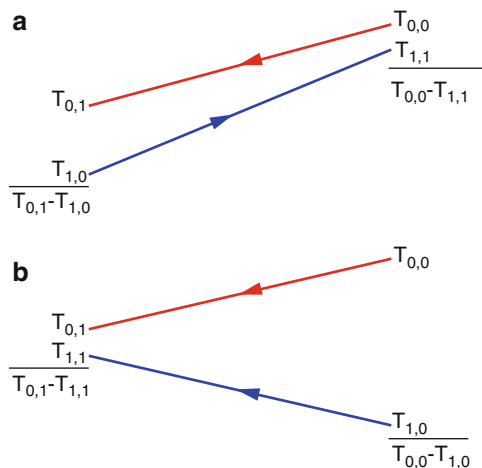


**Fig. 3.16** Countercurrent (a) and parallel (b) flows



For compact heat exchangers (CHEs) the flow arrangement takes different forms and configurations. For an extended-surface compact heat exchanger, crossflow is the most common flow arrangement. This is because it greatly simplifies the header design at the entrance and exit of each fluid.

If the desired heat exchanger effectiveness  $\epsilon$  is high (roughly speaking greater than 75–80 %), the size of a crossflow of such compact type heat exchanger unit

may become excessive, and overall cross-counterflow multipass unit or a pure counterflow unit may be preferred [6].

However, there are manufacturing difficulties associated with a true counterflow arrangement in a compact heat exchanger as it is necessary to separate the fluids at each end. Thus, the header design is more complex for a counterflow heat exchanger. Multipassing retains the header and ducting advantages of a simple crossflow heat exchanger, while it is possible to approach the thermal performance of a counterflow exchanger unit. However, a parallel flow arrangement having the lowest heat exchanger effectiveness  $\varepsilon$  for a given NUT is seldom used as a compact heat exchanger for single-phase fluids [6].

For example a plate stake and cross section of a Printed Circuit Heat Exchanger (PCHE) are shown in Fig. 3.17a and b respectively. The PCHE can achieve effectiveness greater than 97 %, maximum operating temperature and pressures of up to 1000 °C and 500 bars respectively (Jeong et al. [7]).

In this type of compact heat exchanger, there are also various cross sectional channels that can be employed on the plates forming the matrix of the PCHE. Channels employed in the PCHE include the straight or wavy, parallel or offset semicircular cross sections and others. Both Figs. 3.18a and b show the zigzag

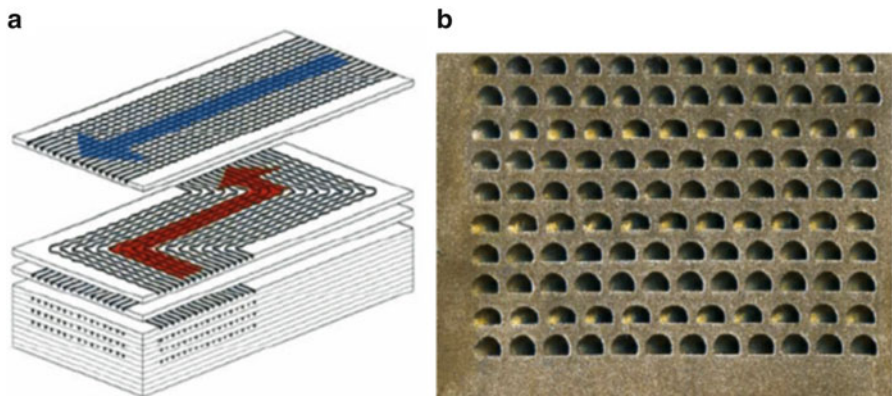


**Fig. 3.17** Illustration of PCHE channels with alternating hot and cold flows with the flow path. (a) Plate stake of a PCHE. (b) Cross section of a PCHE

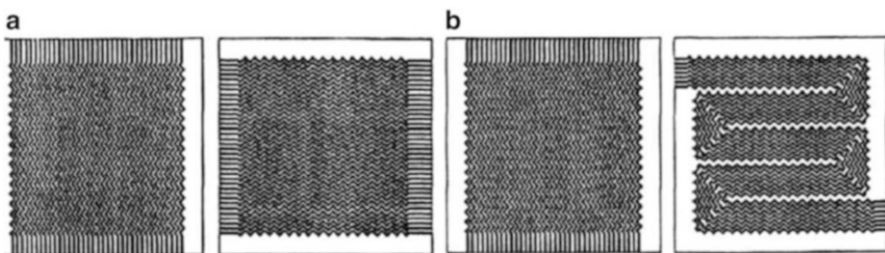


**Fig. 3.18** Schematic showing the flexibility for a simple cross flow and cross-counter flow arrangement in the PCHE [8]. (a) Simple cross flow. (b) Cross-counter flow

shapes of a plate in two different flow arrangements (thus the simple cross flow and cross-counter flow) in the PCHE.

If we want to study the flow arrangement for a plate fin compact heat exchanger, we would be able to summarize it to the fact that, this class of heat exchanger accepts two streams, which may flow in directions parallel or perpendicular to one another. When the flow directions are parallel, the streams may flow in the same or in opposite direction. Thus we can imagine three primary flow arrangements as:

1. Parallel Flow,
2. Counter flow, and
3. Cross flow.

Thermodynamically, the counterflow arrangement provides the highest heat (or cold) recovery, while the parallel flow geometry gives the lowest. The cross flow arrangement, while giving intermediate thermodynamic performance, offers superior heat transfer properties and easier mechanical layout. Under certain circumstances, a hybrid cross-counterflow geometry provides greater heat (or cold) recovery with superior heat transfer performance. Thus, in general engineering design and manufacturing practice, Plate Fine Compact Heat Exchangers (PFCHE) are manufactured in three configurations as:

1. *Cross Flow*: In this arrangement (Fig. 3.19a), usually two streams are handled, thus eliminating the need for distributors. The heater tanks are located on all four

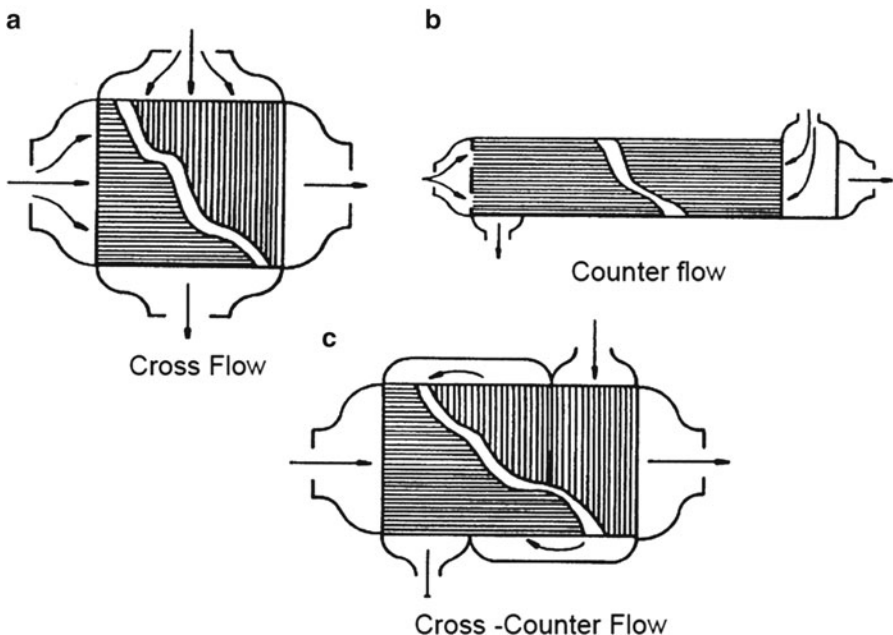


**Fig. 3.19** Illustration of flow arrangements

sides of the heat exchanger core, making this arrangement simple and cheap. If high effectiveness is not necessary and the two streams have widely differing volume flow rate, or if either one or both streams are nearly isothermal, as in single component condensing or boiling, then cross flow arrangement is preferred. Good examples of typical applications include automobile radiators and some aircraft heat exchangers.

2. *Counter Flow*: In this arrangement (Fig. 3.19b), this class of heat exchanger provides the most thermally effective arrangement for recovery of heat or cold from the process stream. Cryogenic refrigeration and liquefaction equipment use this geometry almost exclusively and these days a lot of study around next generation nuclear plant (NGNP) and concentrated solar power (CSP) are taking advantage of such heat exchangers to drive their efficiency to a higher performance stage in the form of combined cycle [9–14]. The geometry of the headers distributor channels is complex and demands proper design.
3. *Cross-Counter Flow*: In this arrangement (Fig. 3.19c), the cross-counter flow geometry is a hybrid of counterflow and cross flow arrangement, delivering the thermal effectiveness of counterflow heat exchanger with the superior heat transfer characteristics of the cross flow configuration as before. In this configuration, one of the streams flows in a straight path, while the second stream follows a zigzag path normal to that of the first stream. Up to six such passes have been employed. While negotiating the zigzag path, the fluid stream covers the length of the heat exchanger in a direction opposite to that of the direct stream. Thus the flow pattern can be seen to be globally counter flow while remaining locally as cross flow. Cross-counter flow PFCHEs are used in applications similar to those of simple cross flow exchangers, but allow more flexibility in design. They are particularly suited to applications where the two streams have considerably different volume flow rate, or permit significantly different pressure drops. The fluid with the larger volume flow rate or that with the smaller value of allowable pressure drop flows through the straight channel, while the other stream takes the zigzag path. For example, in a liquid-to-gas compact heat exchanger, the gas stream with a large volume flow rate and low allowable pressure drop is assigned to the straight path; while the liquid stream with a high allowable pressure drop flows normal to it over a zigzag path. This arrangement optimizes the overall geometry [15].

A conceptual diagram of a Plate Frame Compact Heat Exchanger (PFCHE) along with flow passage is shown in Fig. 3.20a and b. Plate fin compact heat exchangers are compact. In comparison to shell and tube exchangers, they provide a much greater heat transfer area for a given footprint. As they allow for high fluid velocities, they promote high heat transfer rates and reduced fouling. They can be easily opened for cleaning and inspection—particularly important for hygienic service.

Their greatest weakness is the lack of mechanical strength of the gasket. This makes them unsuitable for use at high temperatures and pressures or where leaks must be avoided at all costs (e.g., processing of toxic fluids). In addition, the narrow gap between the plates makes them unsuitable for high viscosity liquids or slurries.

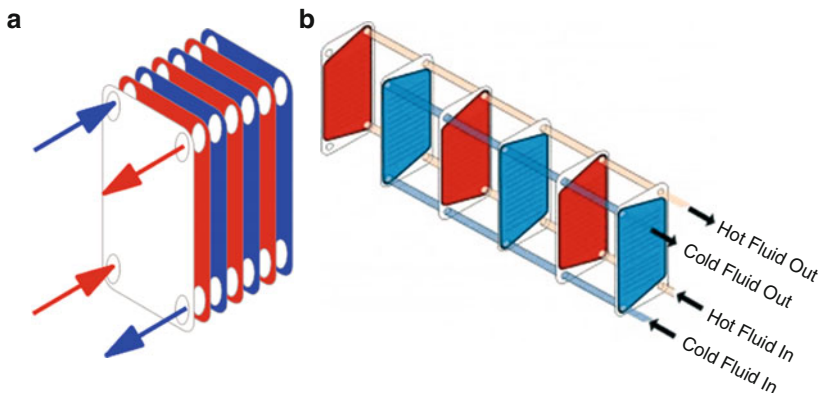


**Fig. 3.20** Conceptual diagram of a Plate and Frame Heat Exchanger (PFCHE) along with its flow passages

**Fig. 3.21** Plate Fin Compact Heat Exchanger with flow (PFCHE) passage depiction

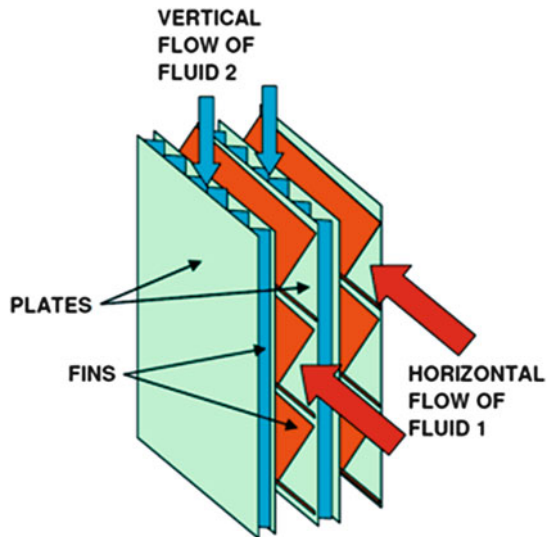
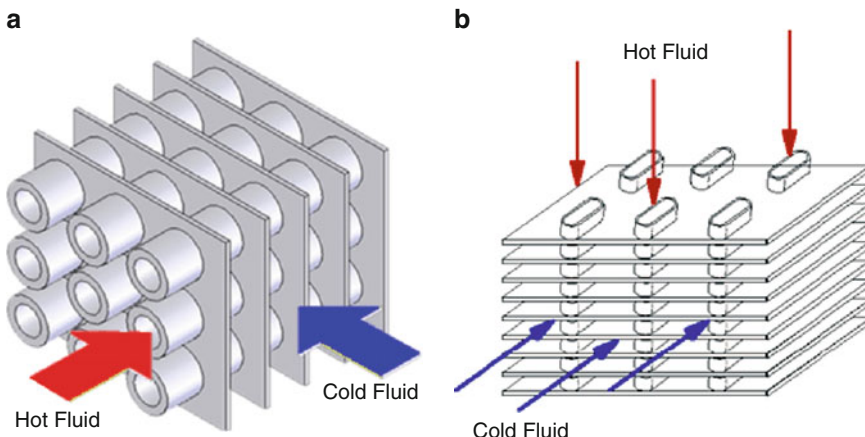


Figure 3.21 depicts the flow passage in a Plate Fin Compact Heat Exchanger (PFCHE), and in these heat exchangers two opposite sides of each chamber are sealed and the other two sides allow the *inflow* and *outflow* of fluid. The sealed sides are rotated at 90° for alternating chambers. So the hot and cold fluid flows are always at 90° to each other. These exchangers can be efficiently used for a wide range of applications and a wide range of temperature and pressure conditions.

The case of Finned Tube configuration and layout of the flow passage is shown in Fig. 3.22a and b.



**Fig. 3.22** Diagram of finned both flat and circular tube compact heat exchanger with flow passage

Welded compact heat exchangers consist of plates that are welded together (Fig. 3.23). Among the many models available on the market today, all have one thing in common: they do not have inter-plate gaskets. This feature is what makes them suitable for processes involving aggressive media or high temperatures where gaskets cannot be used.

Other Compact Heat Exchangers with their flow passage diagrams are shown below, such as Spiral Heat Exchanger (SHE) (Fig. 3.23). Spiral heat exchangers are very basic in their structure. They consist of two separate spiral chambers as shown in the schematic below. These two chambers house hot and cold liquids separated from each other by a spiral metal sheet. Heat transfer coefficients on both sides are high. The hot and cold fluid flows are countercurrent to each other all the way through the exchangers. These factors lead to much lower surface area requirements than shell and tube exchangers. These exchangers can be used for highly viscous fluids at low, medium pressures.

This type of heat exchanger consists of concentric shape flow passages which help create a turbulence flow of a fluid which in turn increases the heat transfer efficiency. Initial installation cost is higher but highly efficient as compared to other types as space saving is greater because of the compact size. Maintenance cost is lowest as compared to other types for the same sized unit.

A spiral heat exchanger has two spiral channels that are concentric, one for each fluid. The curved channels provide great heat transfer and flow conditions for a wide variety of fluids. The overall size of the unit is kept to a minimum. Installation space is optimized because of the efficient size of the unit. The flow of fluid in spiral type is rotary current flow which itself possesses the property of self cleaning of fouling inside the spiral body.

In applications prone to high fouling, consider using a spiral heat exchanger. Its single-channel design minimizes fouling and erosion and helps ensure high flow velocities even with heavy process slurries.

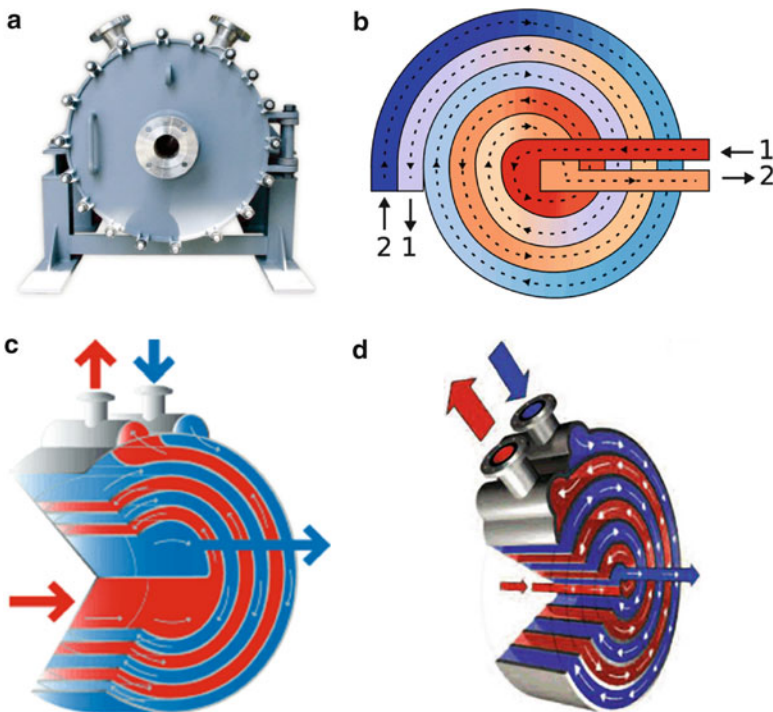


**Fig. 3.23** Schematic drawing of a SHE with flow passage

Figure 3.24 is a diagram of welded compact heat exchangers along with flow passages.

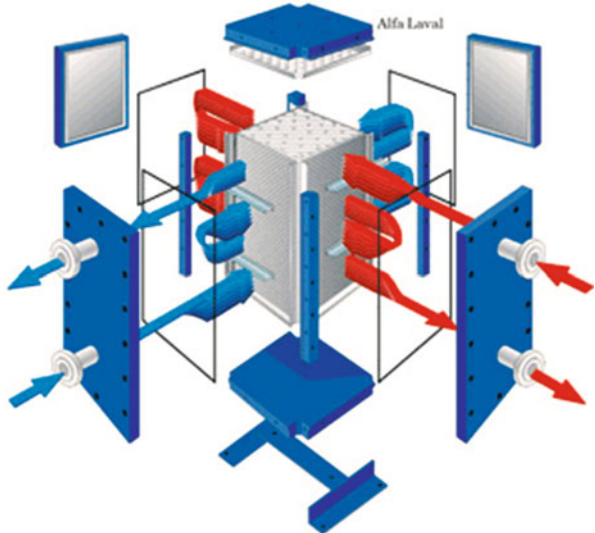
Note that, all-welded compact heat exchangers are very compact compared to shell-and-tube heat exchangers and some of these all-welded heat exchangers are sealed and cannot be opened for inspection and mechanical cleaning. Others can be opened, allowing the entire heat-transfer area and all welds to be reached, cleaned, and repaired if necessary.

In summary, it depends on the application and adoption of the Compact Heat Exchangers; each have their own unique design based on their acquisition for that particular application.

### 3.3 Why Compact Heat Exchangers?

A constraint known as compactness is the most important criteria for these applied heat exchangers wherever they are employed. The demand on these types of heat exchangers and their required compactness to produce high performance heat exchanging duties imposes a constraint on their foot print. They are devices that

**Fig. 3.24** Diagram of welded compact heat exchanger with flow passages



have very small spatial dimensions and there is increasing demand for application in industry—such as aerospace, automobile, nuclear in particular next generation (i.e. GEN-IV), with very high temperature, solar energy such as Concentrated Solar Power (CSP) as a source of renewable energy, hydrogen production power plant in refinery and other related industry, etc. Compact heat exchangers, compared to shell-and-tube exchangers, are characterized by a large heat transfer surface area per unit volume of the exchangers.

We know heat exchangers designs involve handling both the duty of heat transfer rates between the fluids and the mechanical pumping power expanded to overcome fluid friction and move the fluids through the heat exchanger. For these exchangers to be able to operate with high-density fluid conditions, the friction power expenditure is generally small relative to the heat transfer rate, with the conclusion that the friction power expenditure is not that often the controlling influence. On the other hand, for low-density fluids, such as gases, it can be easily seen that it expends as much mechanical energy as allowed to overcome friction power transferred as heat. However it should be noted that in most thermal power systems mechanical energy is worth 4–10 times as much as its equivalent in heat [16].

Thermal hydraulic analysis can easily show that for most flow passages that might be applied as a means of heat transfer surfaces of heat exchanging mechanism and infrastructure, the heat transfer rate per unit of surface area can be increased by increasing fluid-flow velocity accordingly, and this rate of heat transfer varies as somewhat less than the first power of the velocity. By the same idea, the friction power expenditure will also increase with flow velocity, but under this situation, the power varies by as much as the cube of the velocity and certainly not less than square power [16].

These sorts of behaviors give designers of these heat exchangers a challenge to match both heat transfer rate and friction or pressure drop constraint and specifications accordingly, and these behaviors also impose all the characteristics of different types and classes of heat exchangers from a design and manufacturing point of view per their applications and acquisitions. This basically means that when a particular application requires high friction power expenditure, the manufacturer of the heat exchanger can reduce flow velocities by increasing the number of flow passages in it. This also allows a decrease of the heat transfer rate per unit of surface area however, per above relations the reduction in heat transfer rate will be considerably less than the friction power reduction [16].

One can make up for such loss of heat transfer rate by increasing the surface area for example, by lengthening the tubes or fins, which in turn also increases the friction power expenditure proportional to increasing surface area for heat transfer purposes [16].

However, in a heat exchanger where gas is used as flow the friction power limitations generally forces the manufacturer of such exchanger to arrange for moderate low mass velocities of  $G = (W/A_c)$ , where  $W$  is mass flow rate and  $A_c$  is exchanger minimum free-flow area or  $pA_{fr}$  for matrix surface where it is exchanger total frontal area and  $p$  is porosity of a matrix surface, a dimensionless value. These low mass velocities along with low thermal conductivities of gasses compared to liquids, results in low heat transfer rates per unit of surface area. Such constraints force the design of a heat exchanger with a larger surface area for heat transfer duties which are typical characteristics of gas flow in this type of heat exchanger. In the case of gas-to-gas heat exchangers one may require up to ten times the surface area for the condenser side or evaporator side in comparison to liquid-to-liquid heat exchangers in which the total heat transfer rates and pumping power requirements are comparable [16].

An example of such circumstances can be found in regenerators for a gas-turbine plant, and in order to be effective, it requires several times as much heat transfer surface as the combined boiler and condenser in a steam power plant of comparable power capacity.

Compact heat exchangers, compared to shell-and-tube exchangers, are characterized by a large heat transfer surface area per unit volume of the exchangers. A compact heat exchanger reduces space, weight, support structure and foot print, energy requirements, and cost. It improves process design, plant layout and processing conditions, together with low fluid inventory.

All above considerations have guided us to the development of new generations of heat exchangers that are known as Compact Heat Exchangers (CHEs) today. We know that gas-flow exchanger application requires larger heat transfer surfaces for the surface area density, which are known as *compact heat transfer surfaces* and several of them along with their flow arrangements are depicted in Figs. 3.25 and 3.46.

In summary, as we have learned so far, the heat exchanger design balances heat transfer characteristics of the fluids with pumping requirements for fluid transfer through the heat exchanger. For liquids, this power requirement is usually small. In the case of gases, however, it is imperative to consider the pumping power a

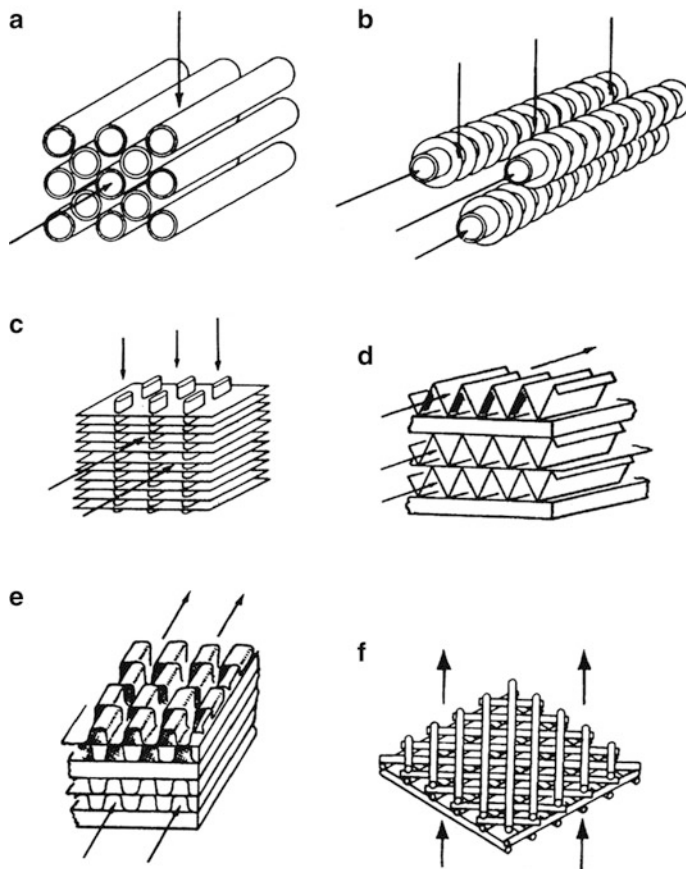


**Fig. 3.25** Some typical examples of compact heat exchanger surfaces. (Courtesy of Kay and London) [17]

suitable design variable because it serves as an indicator for energy requirements in heat exchanger operation. This energy requirement can be high in most thermal power systems, as mechanical energy is significantly higher costs of thermal energy [18].

The velocity of fluid flow is a very important parameter in the design process, as most flow passages would show an increase in the heat transfer per surface area with an increase in fluid velocity. However, the friction-to-power expenditure is also associated with an increase in fluid velocity in the form of a drop in pumping pressure; hence, a heat exchanger design is a function of heat transfer rates and pressure drop specifications [17].

One of the most important and interesting features of the compact heat exchanger surfaces depicted in Figs. 3.25 and 3.46, can be illustrated if the heat transfer rate per unit of surface area is plotted as a function of the mechanical power

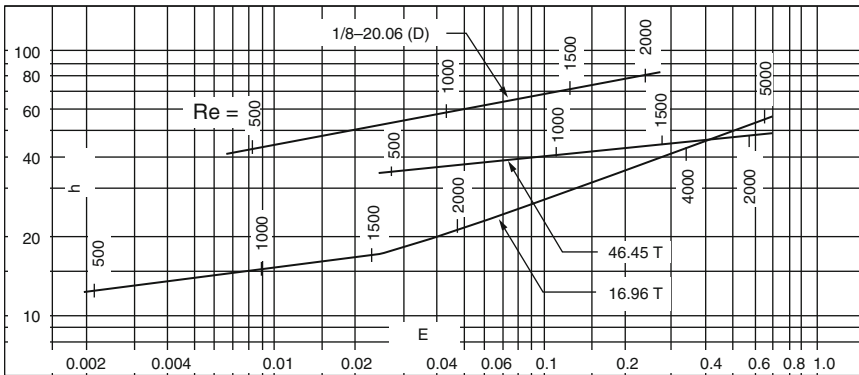


**Fig. 3.26** A comparison of heat transfer and friction power characteristics of three compact surfaces on a unit of surface area basis. Dimensions are  $\text{Btu}/(\text{h ft}^2 \text{ }^\circ\text{F})$  for  $h$  and in  $\text{hp}/\text{ft}^2$  for  $E$ . (Courtesy of Kays and London) [17]

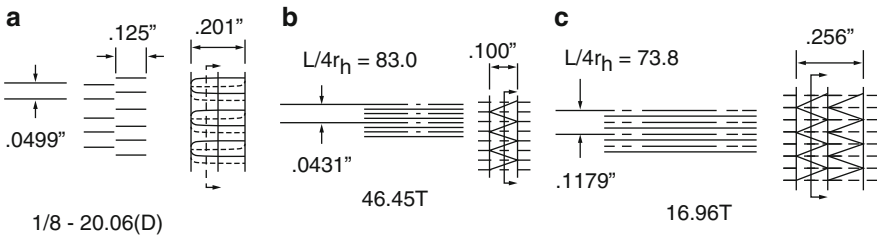


**Fig. 3.27** Illustration extended surface correlating for three plots in Fig. 3.25. (Courtesy of Kays and London) [17]

expended to overcome fluid friction per unit of surface area. A plot of three different surfaces of Fig. 3.25 is depicted in Fig. 3.26, which matches the details shown in Fig. 3.27.

The heat transfer rate for a unit of area and for  $1^\circ$  of temperature difference is merely the heat transfer coefficient  $h$  evaluated for some particular set of fluid properties from Eq. (3.1a) below

$$h = \frac{c_p \mu}{Pr^{2/3}} \frac{1}{4r_h} \left( St Pr^{2/3} \right) Re \quad (\text{Eq. 3.1a})$$

where:

$h$  = Heat transfer coefficient

$c_p$  = Specific heat at constant pressure

$\mu$  = Dynamic viscosity coefficient

$r_h$  = Hydraulic radius

$\text{Pr} = \text{Prandtl number } (\mu c_p/k)$  a fluid properties modulus, where  $k$  is unit thermal conductivity

$\text{St} = \text{Stanton number } (h/Gc_p)$ , a heat transfer modulus, where  $G = (W/A_c)$  is exchanger flow stream mass velocity and it is defined as before

$\text{Re} = \text{Reynolds number } (4R_h G/\mu)$  a flow modulus

The friction power expended per unit of surface area can be readily evaluated per Eq. (3.2) as a function of Reynolds number  $\text{Re}$ , the friction factor  $f$ , and the specified fluid density  $p$ ,  $g_c$  is gravity force and  $\mu$  is dynamic viscosity of fluid as part of its properties.

$$E = \frac{1}{2g_c} \frac{\mu^3}{p^3} \left( \frac{1}{4R_h} \right) f \text{Re}^3 \quad (\text{Eq. 3.2})$$

$E$  versus  $h$  is plotted in Fig. 3.26 and it can be depicted once the basic convection heat transfer and friction characteristics are known as functions of Reynolds number and any particular surface arrangement (see Fig. 3.26) is then represented by a single curve on a plot such as that in Fig. 3.26.

The interesting feature of the plots in Fig. 3.26 is the very wide difference in friction power expenditure for a given heat flux for different surfaces, or conversely, the smaller difference in heat flux for a given friction power expenditure.

Different types of heat exchangers—classified by the type of performance, application, operating environment, physical characteristics, etc.—are available and they are reported by other books written by other authors and given in different literature works as well, and they all can be found on the Internet. Primary interest in compact heat exchangers as the intermediate heat exchanger of the Next Generation Nuclear Power Plant (NGNP) or Concentrated Solar Power (CSP) infrastructure built in a solar energy farm is due to the following specific design characteristics reported by Kuppan [19]:

1. High heat transfer area per unit volume of the core.
2. Small hydraulic diameter of any internal passage ( $D_h = 4r_h = 4A_c L/A$ ) where  $r_h$  is radius,  $A_c$  is exchanger minimum free flow area or  $pA_{fr}$  for matrix surfaces and  $L$  is total heat exchanger flow length while  $A$  is the heat exchanger total heat transfer area on one side.  $A_{fr}$  is frontal or face area on one side of an exchanger in unit of  $\text{m}^2$  or  $\text{ft}^2$  and  $p$  is fluid static pressure in unit of  $\text{Pa} = \text{Pascal} = \text{N/m}^2 = \text{kg/m s}^2$ ,  $\text{lbf/ft}^2$  (psf) or  $\text{lbf/in}^2$  (psi).
3. Pressure drop is an important design consideration.
4. Large frontal area and a short flow length.
5. Little or no chance of fluid contamination.
6. Good for gas-to-gas applications. For preliminary design considerations, the physical dimensions may be assumed, but optimization would be necessary to ensure optimal performance. The output is usually displayed in terms of heat transfer coefficient ( $h$ ), pressure drop across the heat exchanger ( $\Delta p$ ), number of thermal units ( $N$ ), and pumping power ( $W$ ).

The analysis can be performed for primary and secondary sides with different cross-sectional areas as heat transfer media with different volumes and materials. This can be done under the condition of fully turbulent flow regimes for Reynolds number beyond 10,000 by providing high heat transfer coefficients with high pressure drops for desirable applications. This can be developed in particular for pure counter-flow and reasonably can be expended to cross-flow type compact heat exchanger with this kind of flow arrangement. A correlation for different types of surfaces can be established to explain the complete thermal design and result of such analysis for a given class of compact heat exchanger in order to optimize the best possible design practices and approaches [20].

*Note that:* The Hydraulic Diameter is defined as  $4A_o/P$ , where  $A_o$  is the minimum free-flow area on one fluid side of a heat exchanger and  $P$  is the wetted perimeter of flow passages of that side. Note that the wetted perimeter can be different for heat transfer and pressure drop calculations. For example, the hydraulic diameter for an annulus of a double-pipe heat exchanger for  $q$  and  $\Delta p$  calculations is as follows.

$$D_{h,q} = \frac{4(\pi/4)(D_o^2 - D_i^2)}{\pi D_i} = \frac{D_o^2 - D_i^2}{D_i} \quad (\text{Eq. 3.3a})$$

$$D_{h,\Delta p} = \frac{4(\pi/4)(D_o^2 - D_i^2)}{\pi(D_o + D_i)} = D_o - D_i \quad (\text{Eq. 3.3b})$$

where  $D_o$  is the inside diameter of the outer pipe and  $D_i$  is the outside diameter of the inside pipe of a double-pipe exchanger. As Eq. (2.20) indicates, the Number of Transfer Unit (NTU) is also directly related to the overall (total) Stanton number  $St$ , thus NTU can also be interpreted as a modified Stanton number. Note that here the hydraulic diameter  $D_h$  is defined depending on the type of heat exchanger surface geometry involved as follows.

$$D_h = \begin{cases} \frac{4 \times \text{flow area}}{\text{wetted perimeter}} = \frac{4A_o}{P} = \frac{4A_o L}{A} \\ \frac{4 \times \text{core flow area volume}}{\text{fluid contact surface area}} = \frac{4pV}{A} = \frac{4p}{\beta} = \frac{4p}{\alpha} \end{cases} \quad (\text{Eq. 3.4a, b})$$

where  $\alpha$  is the ratio of total heat transfer area  $A$  on one fluid side of an exchanger to the total volume  $V$  of a heat exchanger,  $A = V$ , with unit of  $\text{m}^2/\text{m}^3$  or  $\text{ft}^2/\text{ft}^3$  and  $\beta$  heat transfer surface area density: ratio of total transfer area on one fluid side of a plate-fin heat exchanger to the volume between the plates on that fluid side,  $A = A_{fr}L$ , packing density for a regenerator,  $\text{m}^2 = \text{m}^3$ ,

(continued)

or  $\text{ft}^2 = \text{ft}^3$  and  $A_{\text{fr}}$  is again defined as frontal or face area on one side of an exchanger in unit of  $\text{m}^2$  or  $\text{ft}^2$ .

In Eq. (3.4a,b),  $\mathbf{p}$  is the porosity, a ratio of void volume to total volume of concern. Here the first definition of  $D_h$  is for constant cross-sectional flow passages in a heat exchanger. However, when flow area is expanding/contracting across flow cross sections along the flow length as in three-dimensional flow passages (such as in a corrugated perforated fin geometry of Figs. 3.4f and 3.50), the more general second definition is applicable. In the second definition,  $D_h = 4\mathbf{p}/\beta$  for plate-fin type and regenerative surfaces; for tube bundles and tube-fin surfaces,  $D_h = 4\mathbf{p}/\alpha$ . Note that heat transfer and pressure drop  $D_h$  magnitudes will be different if the heated and flow friction perimeters are different, as illustrated in Eq. (3.3a) and (3.3b).

Given the common understanding and what we know about *turbulent flow* and its characteristics—where the Reynolds number is above 10000, and it provides high heat transfer coefficients even though this turbulent condition imposes high pressure drops—these flows are desirable in heat exchanger applications. On the other hand, *laminar flows* with small hydraulic diameter flow passages in a heat exchanger can provide local high heat transfer coefficient  $h$  ( $\text{W}/\text{m}^2 \text{ K}$ ) along with critical heat flux  $\dot{q}$  and reasonable pressure drops of  $\Delta p$  [2].

If we consider water flow as the working fluid in a circular tube at 310 K and use correlations for laminar flow with Nusselt Number  $\text{Nu} = 3.657$  and turbulent flow known as Gnielinski Correlation 9, then heat transfer coefficient  $h$  ( $\text{W}/\text{m}^2 \text{ K}$ ) can be computed as a function of the inner tube/annulus or of a circular fin diameter  $D_i$  and is shown in Fig. 3.28. Considering Fig. 3.28 one can observe that heat transfer

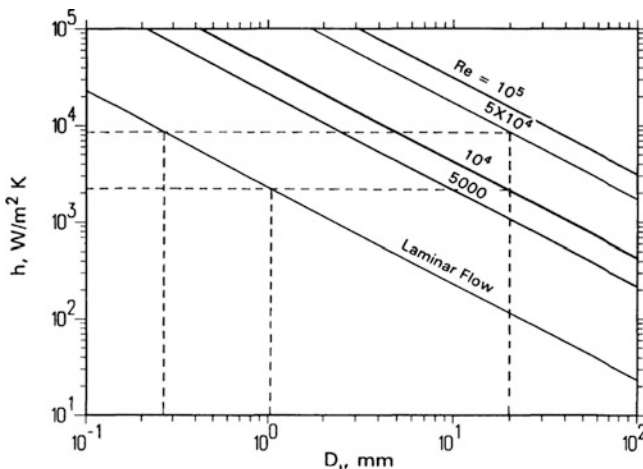


**Fig. 3.28** Heat transfer coefficient as a function of tube diameter for a long circular tube with water flow at 310 K [2]

coefficient  $h$  for a 20 mm diameter tube or circular fin at  $Re = 10^4$  is the same as that for a 1 mm diameter tube in laminar flow! Similarly, the heat transfer coefficients are the same for a 20 mm diameter tube at  $Re = 5 \times 10^4$  and 0.3 mm diameter tube in laminar regime flow region.

The following paragraph is a direct quote from Shah and Robertson's [2] published report.

For a given heat duty, fluid flow rates and mean temperature difference in the exchanger, laminar flow exchangers can offer substantial volume and fluid pumping power reductions over the conventional shell-and-tube exchangers. Consider the case of thermal resistances distributed equally on the hot and cold sides, and where the wall thermal resistance and fouling resistances are negligible. For flow over a tube bank with  $X_T/D_o = 1.25$  and  $X_L/D_o = 2.00$  and  $Re_L = 100$ , the volume ( $V_L/V_T$ ) and fluid pumping power ( $P_L/P_T$ ) ratios as a function of the tube outside diameter ( $D_L/D_T$ ) ratio with  $Re_T$  as a parameter are shown in Fig. 3.30. Here  $X_T$  and  $X_L$  are transverse and longitudinal tube pitches,  $D_o$  is the tube outside diameter,  $Re$  is the Reynolds number and the subscripts  $L$  and  $T$  denote laminar and turbulent flow values for  $Re$ ,  $V$  and  $P$ . This figure shows that a substantial reduction in both volume and pumping power can be achieved with smaller diameter tubes in the range of  $10^{-2} < D_L/D_T < 10^{-1}$ . However, the frontal area requirement and the length of the exchanger are not shown. For a laminar flow exchanger, as  $D_L$  decreases, the frontal area continues to increase very significantly compared with that for the exchanger with turbulent flow and the length continues to decrease significantly. Hence, Fig. 3.29 cannot be used arbitrarily without consideration of the frontal area and flow length requirements. Also, note that Fig. 3.30 is not general; it is specific for the selected geometry of a tube and for selected operating conditions.

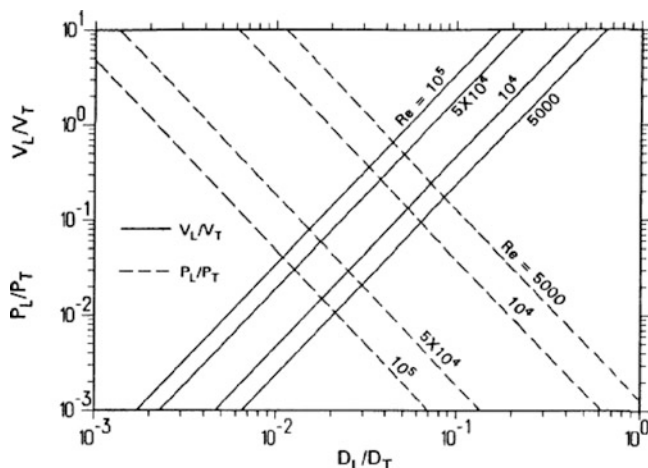


**Fig. 3.29** Ratios of heat exchangers volumes and pumping powers for laminar to turbulent flows as a function of ratio of tube diameter for laminar to turbulent flows [1]

### 3.4 Characteristics of Compact Heat Exchangers

As we have learned so far heat exchangers are a device to transfer energy in terms of heat from one fluid mass (i.e., hot) to another (i.e., cold) or vice versa. In order to do this task a separation wall must exist between these two fluids so they do not mix with each other. See Fig. 3.30 above.

Also, as we have learned compact heat exchangers (CHEs) are a class of heat exchangers that incorporate a large amount of heat transfer surface area per unit volume and in some applications, such as the automotive industry, heat exchangers would be in the compact heat exchanger category since space is an extreme constraint for automotive applications; and then there are applications where these compact heat exchangers are used for micro-turbines as part of the most economical solution of generating power (5–200 kW) in today's market and demand.

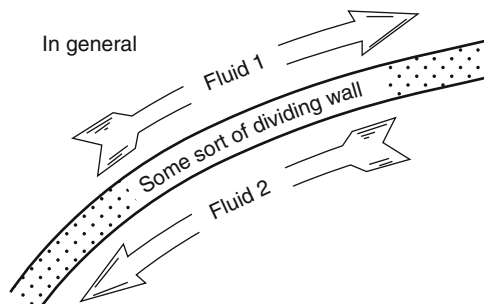
As part of analysis and study of classification of heat exchangers they are presented in detail in Sect. 3.5 of this chapter. However, these exchangers can operate under three circumstances for the two fluids exchange heat energy which allows us to further analyze the pressure drops and heat transfer duties for design and manufacturing proposes, and they are:

1. Gas-to-Liquid Heat Exchangers
2. Gas-to-Gas Heat Exchangers
3. Liquid-to-Liquid Heat Exchangers

We can easily combine the first two categories as one and consider it as a Gas-to-Fluid situation where the fluid could be gas or liquid. One of the uniqueness characteristics of compact heat exchangers are their extended surface exchangers (i.e., Plate-Fin and Tube-Fin compact heat exchangers), as compared with the traditional or conventional shell-and-tube exchangers. These encumbrances will reveal the following differences:

1. Many surfaces available having different orders of magnitude of surface area density as shown in Fig. 3.25;
2. Flexibility in distributing surface area on the hot and cold sides both in single or two passes from flow arrangements (Sect. 3.2.2 and see Fig. 3.31 below as well)

**Fig. 3.30** General concept of heat exchanger schematic



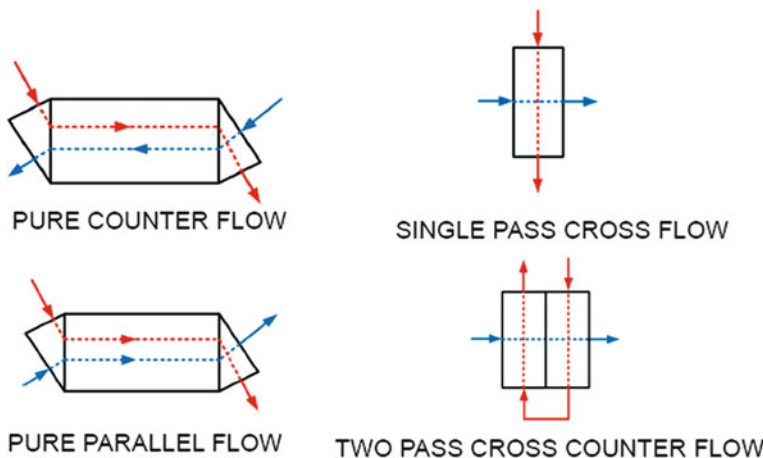


**Fig. 3.31** Flow arrangement determines the order in which the hot fluid and cold fluid interact

point of view (i.e., crossflow condition) as warranted by design considerations, and

3. Generally substantial cost, weight, or volume savings are also considered as part of the characteristics that these classes of exchangers offer.

The important design and operating considerations for compact head exchangers extended surfaces are:

1. Usually at least one of the fluids is a gas to compensate for its low thermal convection heat transfer  $h$ ;
2. Fluids must be clean to avoid any fouling effects and relatively non-corrosive because of small hydraulic diameter  $D_h$  flow passages and no easy techniques for cleaning for the purpose of preventive maintenance;
3. The fluid pumping power and as a result concern for pressure drop from a design constraint point of view and heat transfer rate perspective are very important. See Sect. 3.7 and its sub-sections for further details on pressure drop and thermal analysis;
4. Operating pressures and temperatures are somewhat limited compared to shell-and-tube exchangers due to joining of the fins to plates or tubes such as brazing, mechanical expansion, etc.;
5. With the use of highly compact surfaces, the resultant shape of the exchanger is one having a large frontal area and a short flow length the header design of a compact heat exchanger is thus an important factor for a uniform flow distribution among the very large number of small flow passages;
6. The market potential and demand for this class of CHE should be large enough to guarantee sizable manufacturing from the Return-on-Investment (ROI) point of view and ownership of such a facility for research and tooling costs for new forms to be developed.

In the case of a typical plate-fin class of CHE, some advantages over the conventional shell-and-tube heat exchangers worth mentioning are as follows.

1. Compact heat exchangers are generally fabricated from thin metallic plates thus forming many convoluted and narrow flow passages and giving a large heat transfer surface area per unit volume, typically up to ten times greater than the  $50\text{--}100 \text{ m}^2/\text{m}^3$  provided by a shell-and-tube exchanger for general process application.
2. Compact gas side surfaces have high to ultra high ratios of heat transfer surface area to volume which is known as the compactness ratio ( $\beta$ ) ranging from 1000 to  $6000 \text{ m}^2/\text{m}^3$ .
3. Compact liquid or two-phase side surfaces have a heat transfer surface area to volume ( $\beta$ ) ratio ranging from 400 to  $600 \text{ m}^2/\text{m}^3$ . This high surface area density in turn substantially reduces the heat exchanger volume, mass, and capital cost for the same surface area or the same duty. This will also considerably reduce the structural support requirement and associated installation cost.
4. The heat exchanger can be configured easily for counterflow or multipass cross-counterflow to yield very high exchanger effectiveness ( $e$ ) or designed for very small temperature differences between fluid streams, and for very small pressure drops compared to shell-and-tube exchangers. This saves energy and produces lower thermal pollution thus reducing the impact on the environment.
5. A compact exchanger provides a tighter temperature control, thus it is useful for heat sensitive materials, and improves the product (e.g., refining fats from edible oil) and its quality (such as a catalyst bed). Also, a compact exchanger could provide rapid heating or cooling of a process stream, thus improving the product quality. It requires a low fluid inventory (hold up) in the exchanger; this is important for valuable or hazardous fluids.
6. The plate-fin exchangers can accommodate multiple (up to 12 or more) fluid streams in one exchanger unit [22].

Due to unique compact heat exchanger characteristics including very high heat transfer coefficients and large heat transfer area due to their extended surface exchangers, they show very promising ways of being utilized in applications such as oil refinery, gas processing, petrochemical, solar power, wind mill farms for power generation, next generation nuclear plant, hydrogen production power plant coupled with nuclear power plant via intermediate heat exchangers, chemical and associated process industries etc. The compact heat exchangers which are at present available and the new types which are evolving, offer process flow sheet designers the opportunity and stimulus, not only to save costs by replacing conventional equipment, but also to rethink the approach to process design [2].

A typical gas-to-gas schematic is presented in Fig. 3.32 below, and they are typically used for heat recovery of hot outgoing exhaust air/off gas and ingoing cold fresh air or process gas. Some applications include catalytic processes, industrial drying, and incineration plants (flue gas cooling).

In a gas-to-gas heat exchanger, gases come in contact with the heat exchange surface and transfer via the surface medium to impart heat to the secondary flow.

**Fig. 3.32** Schematic of a gas-to-gas heat compact heat exchanger

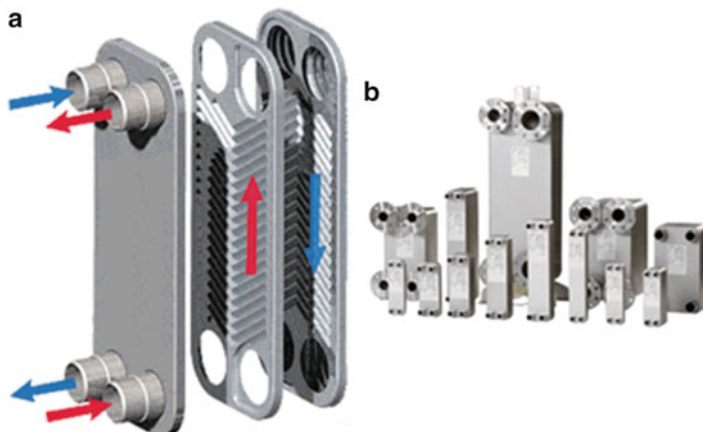
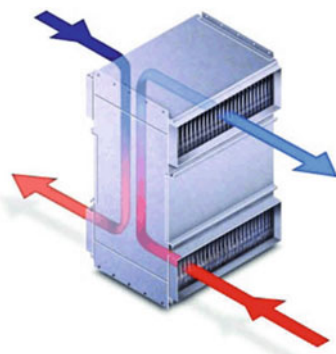


**Fig. 3.33** Schematic of (a) explored brazed plate, (b) assembled photo

Brazed plate heat exchangers are becoming more popular with their compact size and high efficiency design. They are composed of a number of plate elements, each of which comprises two thin nested plates, the elements defining flow spaces between them, with adjacent elements being joined around their periphery by brazing bent edge portions. See Fig. 3.33.

Brazed plate units are up to six times smaller than alternative methods of heat exchange with the same capacity. The significance lies in their unique construction of stainless steel plates brazed together with every plate turned 180° in opposition to each other. This design creates two highly turbulent fluid channels that flow in opposite directions over a massive surface area with significantly higher heat transfer coefficient over less required surface area. As part of their benefits, they offer very low maintenance and their cost of ownership is low while they can be assembled with little investment from a manufacturing point of view from a small number of machine formed parts which results in reduced fabrication time and end

user costs as well. They are light weight and make their maneuvering much easier than the alternative with a very small foot print.

The major limitations of plate-fin and other compact heat exchangers are as follows. Plate-fin and other compact heat exchangers have been and can be designed for high temperature applications (up to about 850 °C), high pressure applications (over 200 bars), and moderate fouling applications. However, applications usually do not involve both high temperature and high pressure simultaneously. Highly viscous liquids can be accommodated in the plate-fin exchangers with a proper fin height; fibrous or heavy fouling fluids are not used in the plate-fin exchangers because mechanical cleaning in general is not possible.

However, these liquids can be readily accommodated in plate heat exchangers. Most of the plate-fin heat exchangers are brazed. At the current state-of-the-art, the largest size exchanger that can be brazed is about  $1.2 \times 1.2 \times 6$  m. While plate-fin exchangers are brazed in a variety of metals including aluminum, copper, stainless steel, nickel and cobalt based super-alloys, the brazing process is generally of a proprietary nature and it is quite expensive to set up and develop specific brazing techniques. Note that due to environmental concerns, dip brazing is being eliminated by the industry, and is replaced by vacuum brazing and neutral environmental atmospheric brazing. Thus, the problem of flux removal (to avoid corrosion) with dip brazing for brazed heat exchangers will no longer be a problem. The plate-fin exchanger is readily repairable, if leaks occur at the external border seams [2].

Fouling is one of the potential major problems in compact heat exchangers (except for plate-and-frame heat exchangers), particularly having a variety of fin geometries or very fine circular or noncircular flow passages that cannot be cleaned mechanically. Hence, extended surface compact heat exchangers may not be applicable in high fouling applications. However, with the understanding of the problem and applying innovative means to prevent/minimize fouling, compact extended surface heat exchangers may be used in at least low to moderate fouling applications. In order to reduce fouling, nonfouling fluids should be used where permissible such as clean air or gases, light hydrocarbons, and refrigerants [2].

Other important limitations of compact heat exchangers are as follows: With a high effectiveness heat exchanger and/or large frontal area, flow malfunctioning distribution becomes important. More accurate thermal design is required and a heat exchanger must be considered as part of a system. Due to short transient times, a careful design of controls is required for startup for compact heat exchangers compared with shell-and-tube exchangers. Flow oscillation could be a problem for compact heat exchangers. No industry standards or recognized practice for compact heat exchangers are yet available, particularly for power and process industry (note that this is not a problem for aircraft, vehicular, and marine transportation industries). Structural integrity should be examined on a case-by-case basis utilizing standard pressure vessel codes [2].

Plate Heat Exchangers (PHEs) are most suitable for liquid-liquid heat transfer duties requiring uniform and rapid heating or cooling as is often the case when treating thermally sensitive fluids. Special plates capable of handling two-phase fluids (e.g., steam condensation) are available. PHEs are not suitable for erosive duties or for fluids containing fibrous materials.

In certain cases, suspensions can be handled but to avoid clogging the largest suspended particle should be at most, one-third the size of the average channel gap. Viscous fluids can be handled but extremely viscous fluids lead to flow malfunction distribution problems, especially on cooling.

Knowing the fact that compact heat exchangers of plate type are mainly used for liquid-to-liquid heat transfer and exchanging duties and related applications, the characteristics of these exchangers are briefly summarized here and they are as follows:

1. The most significant characteristic of a PHE is that it can easily be taken apart into its individual components for cleaning, inspection, and maintenance.
2. The heat transfer surface area can be readily changed or rearranged for a different task or anticipated changing loads, through the flexibility of the number of plates, plate type, and passes arrangements.
3. The high turbulence due to plates reduces fouling to about 10–25 % that of a shell-and-tube exchanger.
4. Because of the high heat transfer coefficients, reduced fouling, absence of bypass and leakage streams, and pure counterflow arrangements, the surface area required for a plate exchanger is 1/2 to 1/3 that of a shell-and-tube exchanger for a given heat duty. This would reduce the cost, overall volume, and maintenance space for the exchanger.
5. Also in this type of PHEs, the gross weight of a plate exchanger is about 1/6 that of an equivalent shell-and-tube exchanger.
6. Leakage from one fluid to the other cannot take place unless a plate develops a hole.
7. Since the gasket is between the plates, any leakage from the gaskets is to the outside of the exchanger. The residence time for fluid particles on a given side is approximately the same for uniformity of heat treatment in applications such as sterilizing, pasteurizing, and cooking.
8. There are no significant hot or cold spots in the exchanger which could lead to the deterioration of heat sensitive fluids. The volumes of fluids held up in the exchanger are small. This is important with expensive fluids, for faster transient response, and for a better process control.
9. Finally and importantly, high thermal performance can be achieved in plate exchangers. The high degree of counterflow in PHEs makes temperature approaches of up to 1 °C possible.
10. The high thermal effectiveness (up to about 93 %) facilitates low grade heat recovery economically.
11. Flow-induced vibration, noise, thermal stresses, and entry impingement problems of shell-and-tube heat exchangers do not exist for plate heat exchangers.

Some other inherent limitations of the plate heat exchangers are due to the plates and gaskets as follows. The plate exchanger is used for a maximum pressure of about 2.5 MPa gage (360 psig), but usually below 1.0 MPa gage (150 psig). The gasket materials (except for the recent Teflon coated type) restrict the use of PHEs in highly corrosive applications; they also limit the maximum operating temperature to 260 °C (500 °F), but usually below 150 °C (300 °F) to avoid the use of

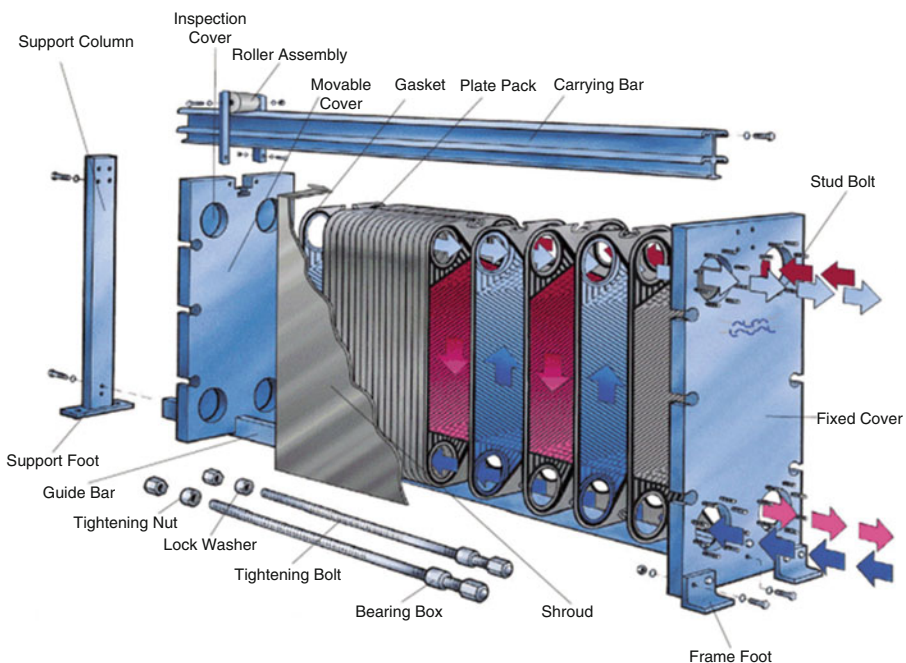


**Fig. 3.34** Schematic gasket plate compact heat exchanger

expensive gasket materials. Gasket life is sometimes limited. Frequent gasket replacement may be needed in some applications. Pin-hole leaks are hard to detect. For equivalent flow velocities, pressure drop in a plate exchanger is very high compared to a shell-and-tube exchanger. However, the flow velocities are usually low and plate lengths are “short”, so the resulting pressure drops are generally acceptable. Some of the largest units have a total surface area of about  $2500\text{ m}^2$  ( $27,000\text{ ft}^2$ ) per frame. Large differences in fluid flow rates of two streams cannot be handled in a PHE.

The Mueller Accu-Therm plate heat exchanger (Fig. 3.34) is a compact heat exchanger consisting of embossed heat transfer plates with perimeter gaskets to contain pressure and control the flow of each medium.

The gasketed plates are assembled in a pack, mounted on upper and lower guide rails, and compressed between two end frames with compression bolts.

### 3.5 Classification of Heat Exchangers

As we have learned so far heat exchangers are devices that are designed for exchanging heat which is a very broad category, so first we need to restrict them to the type of heat exchangers which exchange heat between two fluids. These fluids

can be gasses or liquids. Even with this constraint, it is still difficult to have an overview, and a classification needs to be made. It is possible to classify heat exchangers in a number of ways.

1. The first classification of heat exchangers depends on the basic fluid paths through the heat exchanger. Thus, the differences based on these fluids paths per our previous chapter, are identified as:

- Parallel flow,
- Counter flow, and
- Cross flow.

Each of these categories was described in Chap. 2 of the book and a brief reminder is given here.

Parallel flow are those devices in which the warmed and cooled fluids flow past each other in the same direction, in contrast with the counter flow where these two flow in the opposite direction. In the case of a cross flow, fluids flows pass at right angles to each other.

2. The second classification made, depends on the state of the media in the heat exchanger.

- Liquid-to-liquid exchangers are those in which two liquids interact. Also, gas-to-gas heat exchangers like air preheaters in steam plants and helium-cooled reactor gas turbine plants should be mentioned. These devices operate with heat transfer coefficients that are between 10 and 100 times lower than the coefficients of liquid-to-liquid exchangers.
- Gas-to-gas exchangers are generally much larger and heavier if the same amount of transferred heat is demanded.
- A third type is the liquid-to-gas heat exchanger (or vice versa), usually water and air are used, for instance in automotive radiators. Because of the lower heat transfer coefficients on the gas-side there are usually fins placed on the exchanging surfaces.

3. A third classification method is based on the purpose of heat exchanger. In contrast with the other classifications, this is not a designer's choice but a direct demand to fulfill the need for let's say an evaporator. So any demand based on this classification is generally a starting point, from which the designer needs to make decisions about the other classifications, like the choice between counter flows or cross flow.

Some other examples of purpose classification are briefly: the cooler, which cools liquids or gases by means of water; the chiller, which cools a fluid with a refrigerant such as Freon, to below a temperature that would be obtainable if water was used; and condensers, which condenses a vapor, often in the presence of a non-condensable gas (only shell tube condensers; classification on where condensation occurs: horizontal in-shell, vertical in-shell, horizontal in-tube, and vertical in-tube).

4. The last classification is actually the most important choice of the designer of a heat exchanging system. This is the choice of what kind of construction he is going to use. The two most common options are discussed below: double pipe heat exchangers and shell-and-tube heat exchangers.

In summary all these classifications of heat exchangers are depicted in Figs. 3.35, 3.36, and 3.37.

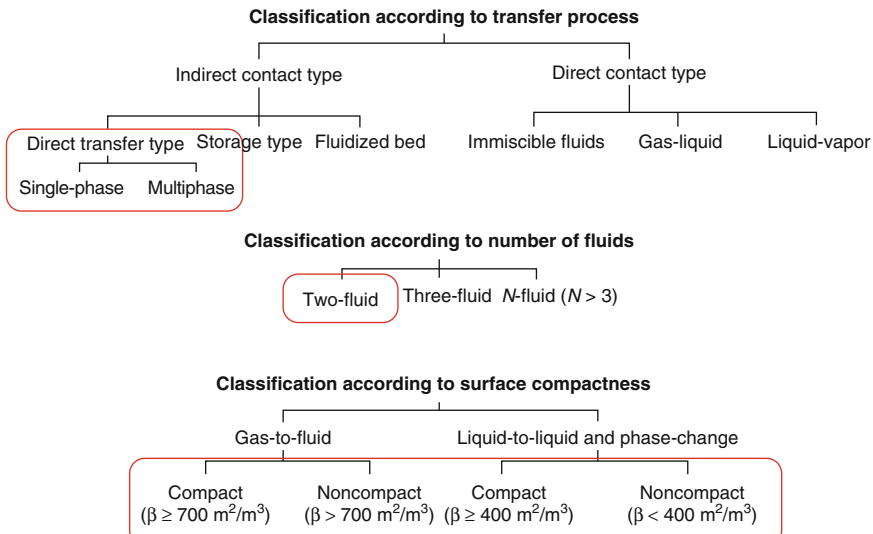


Fig. 3.35 Classification of heat exchangers according to transfer process

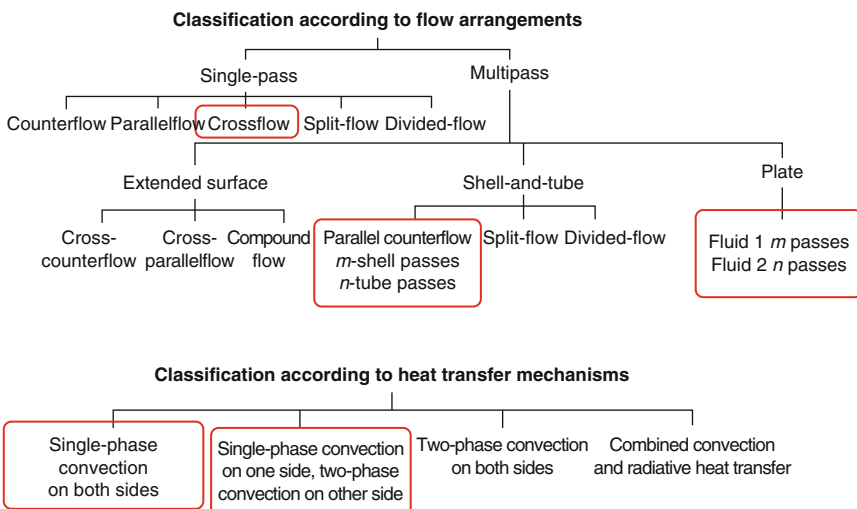
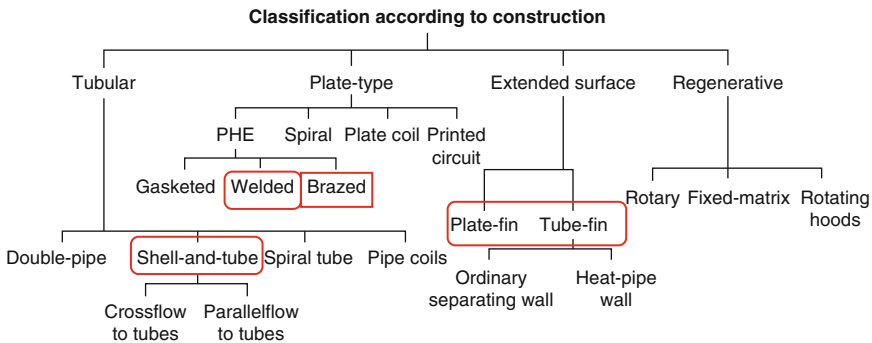


Fig. 3.36 Classification of heat exchangers according to flow arrangement



**Fig. 3.37** Classification of heat exchangers according to construction

Notice that in Fig. 3.35 the parameter  $\beta$  is the designation of compactness or surface area density for heat exchanger. Quantitatively this parameter arbitrarily defines a compact heat exchange surface as one that has an area density greater than  $700 \text{ m}^2/\text{m}^3$  ( $213 \text{ ft}^2/\text{ft}^3$ ). The range of surface area density and hydraulic diameter for various types of compact heat exchanger and heat exchange surfaces can be found in the book by Kay and London [11].

Four types of compact heat exchanger are covered by the ECA Scheme. These are:

1. Plate heat exchangers.
2. Plate-finned heat exchangers.
3. Printed circuit heat exchangers.
4. Compact heat exchangers with precision formed surfaces.

Each of the above compact heat exchangers is briefly described as follows:

### 1. Plate Heat Exchangers

A plate heat exchanger is a type of heat exchanger that uses metal plates to transfer heat between two fluids. This has a major advantage over a conventional heat exchanger in that the fluids are exposed to a much larger surface area because the fluids spread out over the plates. This facilitates the transfer of heat, and greatly increases the speed of the temperature change. It is not as common to see plate heat exchangers because they need well-sealed gaskets to prevent the fluids from escaping, although modern manufacturing processes have made them feasible. See Fig. 3.38.

The concept behind a heat exchanger is the use of pipes or other containment vessels to heat or cool one fluid by transferring heat between it and another fluid. In most cases, the exchanger consists of a coiled pipe containing one fluid that passes through a chamber containing another fluid. The walls of the pipe are usually made of metal or another substance with a high thermal conductivity, to facilitate the interchange, whereas the outer casing of the larger chamber is made of a plastic or coated with thermal insulation, to discourage heat from escaping from the



**Fig. 3.38** Typical schematic of plate heat exchangers. (Courtesy of United Heat Exchanger Company, India) [23]

exchanger. The Plate Heat Exchanger (PHE) was invented by Dr. Richard Seligman in 1923 and revolutionized methods of indirect heating and cooling of fluids.

A plate type heat exchanger is composed of multiple, thin, slightly-separated plates that have very large surface areas and fluid flow passages for heat transfer. This stacked-plate arrangement can be more effective, in a given space, than the shell and tube heat exchanger. Advances in gasket and brazing technology have made the plate-type heat exchanger increasingly practical. In HVAC applications, large heat exchangers of this type are called plate-and-frame; when used in open loops, these heat exchangers are normally of the gasket type to allow periodic disassembly, cleaning, and inspection. There are many types of permanently-bonded plate heat exchangers, such as dip-brazed and vacuum-brazed plate varieties, and they are often specified for closed-loop applications such as refrigeration. Plate heat exchangers also differ in the types of plates that are used, and in the configurations of those plates. Some plates may be stamped with “chevron” or other patterns, where others may have machined fins and/or grooves.

As part of their specifications by manufacturer one can identify, that:

- Liquid foods such as milk, fruit juices, beers, wines, and liquid eggs are pasteurized using plate-type heat exchangers.
- Wine and fruit juices are normally desecrated prior to pasteurization in order to remove oxygen and minimize oxidative deterioration of the products.
- Plate-type heat exchangers consist of a large number of thin, vertical steel plates that are clamped together in a frame.

As part of their applications the following could present:

- The plates produce an extremely large surface area, which allows for the fastest possible transfer.
- Making each chamber thin ensures that the majority of the volume of the liquid contacts the plate, again aiding exchange.
- The troughs also create and maintain a turbulent flow in the liquid to maximize heat transfer in the exchanger.
- A high degree of turbulence can be obtained at low flow rates and a high heat transfer coefficient can then be achieved.

A few advantages worth mentioning for this type of CHE are as follows:

- Easy maintenance and suitable for Clean-In-Place (CIP), plate pack easily accessible
- High heat transfer coefficients
- Flexibility to change plate arrangement and to add or remove plate
- No mixing of product
- Compact constructions
- Optimized heat recovery

Disadvantages of plate type heat exchanger are:

- A bonding material between plates limits operating temperature of the cooler.
- Over tightening of the clamping bolts results in increased pressure drop across the cooler.
- Initial cost is high since Titanium plates are expensive and Titanium is a noble metal, other parts of the cooling system are susceptible to corrosion.
- It can be used, therefore, careful dismantling and assembling need to be done.

## 2. Plate Finned Heat Exchangers

A plate-fin heat exchanger is made of layers of corrugated sheets separated by flat metal plates, typically aluminum, to create a series of finned chambers. Separate hot and cold fluid streams flow through alternating layers of the heat exchanger and are enclosed at the edges by side bars. Heat is transferred from one stream through the fin interface to the separator plate and through the next set of fins into the adjacent fluid.

The fins also serve to increase the structural integrity of the heat exchanger and allow it to withstand high pressures while providing an extended surface area for heat transfer. See Fig. 3.39.

A high degree of flexibility is present in plate-fin heat exchanger design as they can operate with any combination of gas, liquid, and two-phase fluids. Heat transfer between multiple process streams is also accommodated, with a variety of fin heights and types as different entry and exit points available for each stream.

This is a type of heat exchanger design that uses plates and finned chambers to transfer heat between fluids. It is often categorized as a compact heat exchanger to



**Fig. 3.39** Typical schematic of plate finned heat exchangers. (Courtesy of United Heat Exchanger Company, India) [23]

emphasize its relatively high heat transfer surface area to volume ratio. The plate-fin heat exchanger is widely used in many industries, including the aerospace industry for its compact size and lightweight properties, as well as in cryogenics where its ability to facilitate heat transfer with small temperature differences is utilized. Plate-fin heat exchangers are generally applied in industries where the fluids have little chances of fouling.

As part of their specifications by manufacturer one can identify, that:

- The main four types of fins are: plain, which refer to simple straight-finned triangular or rectangular designs; herringbone, where the fins are placed sideways to provide a zig-zag path; and serrated and perforated which refer to cuts and perforations in the fins to augment flow distribution and improve heat transfer.

Some of their applications are as follows:

- Natural gas liquefaction.
- Cryogenic air separation.
- Ammonia production.
- Offshore processing.
- Nuclear engineering.
- Syngas production.

A few advantages that can be expressed for this type of CHE are as follows:

- High thermal effectiveness and close temperature approach. (Temperature approach as low as 3 K between single phase fluid streams and 1 K between boiling and condensing fluids is fairly common.),
- Large heat transfer surface area per unit volume (Typically  $1000 \text{ m}^2/\text{m}^3$ ),
- Low weight,
- Multi-stream operation (Up to ten process streams can exchange heat in a single heat exchanger), and
- True counter-flow operation (Unlike the shell and tube heat exchanger, where the shell side flow is usually a mixture of cross and counter flow).

### 3. Printed Circuit Heat Exchangers (PCHE)

This new type of exchanger was developed by Heatic Pty Ltd over the last 7 years (Johnston (1985) [24], Johnston (1986) [25], Reay (1990) [26]). Flat plates are photo-chemically etched with heat-transfer passages and then diffusion bonded together to form a solid block. The exchanger is illustrated in Fig. 3.35a and b and a schematic cross-section is shown in the figure. It is clear that the heat-transfer surface is effectively all primary. Entry and exit ports may be formed within the block, or alternatively headers may be welded onto the edges as with plate-fin exchangers.

The Printed Circuit Heat Exchanger (PCHE) is one of the compact heat exchangers available as alternatives to shell and tube heat exchangers. Its name is derived from the procedure used to manufacture the flat metal plates that form the

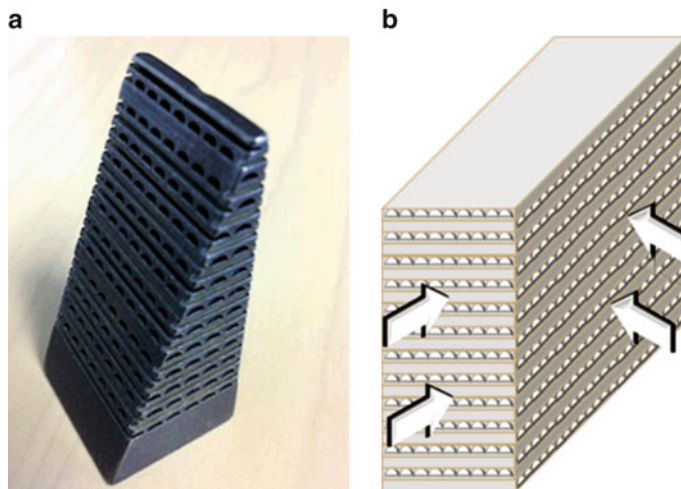


**Fig. 3.40** A typical example of PCHE block

core of the heat exchanger which is done by chemical milling. These plates are then stacked and diffusion bonded, converting the plates into a solid metal block containing precisely engineered fluid flow passages. These channels are typically semicircular in cross section with a depth of 1.5–3 mm. PCHEs are typically built from stainless steels and can operate at temperatures from cryogenic to 800 °C (1500 °F) (Fig. 3.40).

A few advantages of PCHE worth mentioning are given below

- Channels are optimized for counter current flow.
- High heat transfer surface area per unit volume of the exchanger, resulting in reduced weight, space, and supporting structure.
- Used for temperature ranges of –200 to 900 °C.
- High pressure drops in excess of 600 bar.
- Reduced energy requirement and cost.
- Improved process design, plant layout, and processing conditions.
- Low fluid inventory compared to conventional designs such as shell-and-tube exchanger.
- Four to six times smaller and lighter than conventional designs such as shell-and-tube exchanger.
- Extremely high heat transfer coefficients are achievable with small-hydraulic diameter flow passages.
- Used for gases, liquids, and two-phase flows.

Some of the disadvantages are listed below:

- Expensive when compared to shell and tube units.
- Fluid needs to be extremely clean.

- Blockages can occur easily due to the fine channels (0.5–2 mm).
- Blockages can be avoided by fine filtration (typically 300 µm), but there will be additional cost.
- Filters need to be cleaned regularly.
- Blockages require chemical cleaning which can be difficult in some installations and the system needs to be designed for this.
- Galvanic compatibility with the piping material can be an issue. Insulation kit or coated spool piece may be needed.

#### 4. Compact Heat Exchangers with Precision Formed Surfaces

As part of being Compact, Efficient and Economical Heat Exchangers, companies like Tranter [27] heat exchangers share one thing in common—heat transfer through plates instead of tubes. As part of a precision formed surface, their Spiral Heat Exchanger transfers heat through two spirally wound plates. Turbulent flow at low velocity produces high heat transfer efficiency and low fouling. The result is compact units with small heat transfer areas compared to conventional shell-and-tube exchangers. Plate exchangers conserve both materials and labor resources, reducing up-front costs and future operational costs. Their Prime Surface Heat Exchangers configuration is known as PLATECOIL™ and looks like a tank, vessel or reactor unit fabrications, and it is called “IPF”—Infinite PLATECOIL Flexibility™. Among their shapes are tangent bends, pancakes, dished heads, cones, and bends around curves all with precision and dimensional stability unequaled by dimple sheet or pipe fabrications. See Figs. 3.41 and Fig. 3.42 below.

Though compact and light weight, PLATECOIL™ panels can attain surprisingly high jacket operating pressure ratings; and because they deliver higher flow velocities than other technologies, heat transfer is improved—reduced.

**Fig. 3.41** Single-embossed, curved PLATECOIL™ panels are fabricated into pressure reactors offering uniform and controlled heat distribution





Single-embossed, curved PLATECOIL™ panels are fabricated into pressure reactors offering uniform and controlled heat distribution. Though compact and light in weight, PLATECOIL

PLATECOIL™ cone fabrication used to heat a viscous product for economical and efficient handling.

PLATECOIL™ clamp-on panels can be fabricated to bend around corners of rectangular vats.

**Fig. 3.42** Different View Angle of PLATECOIL™. (Courtesy of Tranter Company)

### Fouling Factor:

Fouling is a generic term for the deposition of foreign matter on a heat transfer surface. Deposits accumulating in the small channels of a compact heat exchanger affect both heat transfer and fluid flow. Fouling deposits constricting passages in a compact heat exchanger are likely to increase the pressure drop and therefore reduce the flow rate. Reduced flow rate may be a process constraint; it reduces efficiency and increases the associated energy use and running costs. Maintenance costs will also increase. Fouling remains the area of greatest concern for those considering the installation of compact heat exchangers.

This undesired accumulation of solids on the heat transfer surfaces results in additional resistances to heat transfer of any heat exchangers, thus reducing the exchanger's performance. These deposits, as defined by Somerscales and Knudsen [28] have been identified in terms of six categories that are formed by one or more of the following mechanisms:

1. *Precipitation Fouling*: The precipitation of dissolved substances on the heat transfer surface.
2. *Particular Fouling*: The accumulation of finely divided solids on the heat transfer surface.
3. *Chemical Reaction Fouling*: Deposits formed on the surface by a chemical reaction not involving the surface material.
4. *Corrosion Fouling*: Corrosion of the heat transfer surfaces that produces products fouling the surface and/or roughness on the surface, promoting attachment of the foulants transfer surfaces.
5. *Biological Fouling*: The attachment of macro- and/or microorganisms to the heat transfer surfaces.
6. *Freezing Fouling*: The solidification of a liquid or some of its higher-melting point constituents on the heat transfer surface.

(continued)

Fouling in heat exchangers usually involves several of the processes above, often with synergistic results.

Fouling problems cannot be avoided in many heat exchanger operations, and it is necessary to introduce defensive measures to minimize fouling and the cost of cleaning. The fouling control measures used during either design or operation must be subjected to a thorough economic analysis, taking into consideration all the costs of the fouling control measures and their projected benefits in reducing costs due to fouling. Under some conditions, nearly asymptotic fouling resistances can be obtained, and this suggests a somewhat different approach to the economics.

When a heat exchanger is placed in service, the heat transfer surfaces are, presumably, clean. With time, in some services in the power and process industries, the apparatus may undergo a decline in its ability to transfer heat. This is due to the accumulation of heat insulating substances on either or both of the heat transfer surfaces. The Tubular Exchanger Manufacturers Association (TEMA) undertook the establishment of standards defining design practices not covered by the ASME Code for Unfired Pressure Vessels. Because the ASME code is concerned primarily with safe pressure containment and the means for inspecting it during construction, the contribution of TEMA to sound mechanical construction has been substantial.

In addition, TEMA published a table of fouling factors to assist the designer in preventing the fouling of a single item in a process, including several items of heat transfer equipment. Resistances were tabulated which were to be added to the film resistances ( $1/S_i h_i$  and  $1/S_o h_o$ ) of specific process streams so that the operating period of each would be similar and assure some desired period of continuous operation. The tables of fouling factors were intended as a crude guide toward the equalizations of cumulative fouling in all fouling streams in the assembly.

The fouling factors published by TEMA became entrenched in industrial heat exchanger design. Fouling factors, by the TEMA definition, are time dependent. They are not present when the apparatus is placed in the stream; yet at some definite time in the future, when the apparatus has lost some of its heat transfer capabilities, the fouling factor is deemed to have arrived. TEMA does not delineate the in-between fouling process, and the fouling factor has shed little light on the nature of fouling. The fact that an item of equipment that failed to comply with the TEMA notion of a desired period of continuous operation became a fouling problem is significant. Within the scope of the definition of a fouling factor, the only means for ameliorating fouling was to employ larger fouling factors for repetitive services.

The entire concept of the fouling factor is somewhat indefinite. It is an unsteady state effect that is added indiscriminately to steady-state heat transfer resistances. The difference between a clean and a fouled exchanger is that

(continued)

an intolerable portion of the available temperature difference between fluids must be used to overcome fouling.

Thus, if the outside surface  $S_o$  of a pipe or tube is the reference and  $r_{do}$  is the fouling or *dirt factor*, performance is defined by

$$q = \frac{1}{r_{do}} S \Delta T_{do}$$

where  $\Delta T_{do}$  is the temperature drop across the fouling factor. After solving for the temperature drop,

$$\Delta T_{do} = r_{do} \frac{q}{S}$$

it is observed that the fouling factor only partially controls fouling. The heat flux  $q/S$  is of equal importance. If a fouling factor must be used, it would be more appropriate to specify a fouling factor for a particular process stream along with some range of appropriate temperature differences. TEMA has made some attempt to anticipate temperature differences by classifying fouling factors according to various process services. The result is inexact, as there is much latitude in establishing a process service. In any event, fouling factors which are, in reality, *fouling resistances* are given by TEMA and may be specified by other standards.

Chenoweth [29] provided a summary of the fouling resistances for various gas, vapor, and liquid streams. A partial list of his fouling factors is given in Table 3.2.

The widespread installation of compact heat exchangers has been hindered by the perception that the small passages are more strongly affected by the formation of deposits.

The heat exchanger designer must compensate for exchanger fouling such that a reasonable period of operation can be allowed and maintained between shutdowns for preventive maintenance and cleaning.

For further information refer to the paper by Masoud Asadi and Ramin Haghghi Khoshkho<sup>1</sup> and Handbook of Heat Transfer Applications 2nd Edition by Warren M. Rohsenow, James P. Hartnett, and Ejup N. Ganic.

Vessel sides can be easily designed with two or more zones to efficiently satisfy diverse process requirements. Also, panels can be configured as internal baffles or mixers with heat exchanger surfaces for reduced cycle time. Heavy gauge materials and special reinforcing features effectively withstand agitation forces.

Specially configured curved PLATECOIL™ panels are an economical means of converting existing unjacketed vessels to heated reactors, or of upgrading the thermal capacity of existing reactors. Standard units are available in seven widths and 12 lengths, or in customized variations.

- Jacketed tanks and vessels

---

<sup>1</sup> Investigation into fouling factor in compact heat exchanger, International Journal of Innovation and Applied Studies, Volume 2, Issue 3, March 2013, Pages 238–249.

**Table 3.2** Fouling resistances of various gas, vapor, and liquid streams

Fluid	Fouling resistance ( $10^4 \text{ m}^2 \text{ K/W}$ )	Fluid	Fouling resistance ( $10^4 \text{ m}^2 \text{ K/W}$ )
Liquid water streams		Crude oil refinery streams	
Artificial spray pond water	1.75–3.5	Temperature $\approx 120 \text{ }^\circ\text{C}$	3.5–7
Boiler blowdown water	3.5–5.3	Temperature $\approx 120\text{--}180 \text{ }^\circ\text{C}$	5.25–7
Brackish water	3.5–5.3	Temperature $\approx 180\text{--}230 \text{ }^\circ\text{C}$	7–9
Closed-cycle condensate	0.9–1.75	Temperature $> 230 \text{ }^\circ\text{C}$	9–10.5
Closed-loop treated water	1.75	Petroleum streams	
Distilled water	0.9–1.75	Lean oil	3.5
Engine jacket water	1.75	Liquefied petroleum gases	1.75–3
River water	3.5–5.3	Natural gasoline	1.75–3.5
Seawater	1.75–3.5	Rich oil	1.75–3.5
Treated boiled foodwater	0.9	Process liquid streams	
Treated cooling tower water	1.75–3.5	Bottom products	1.75–3.5
Industrial liquid streams		Caustic solutions	3.5
Ammonia (oil bearing)	5.25	DEA solutions	3.5
Engine lube oil	1.75	DEG solutions	3.5
Ethanol	3.5	MEA solutions	3.5
Ethylene glycol	3.5	TEG solutions	3.5
Hydraulic fluid	1.75	Caustic solutions	3.5
Industrial organic fluids	1.75–3.5	Crude and vacuum liquids	
Methanol	3.5	Atmospheric tower bottoms	12.3
Refrigerants	1.75	Gasoline	3.5
Transformer oil	1.75	Heavy fuel oil	5.3–12.3
No. 2 fuel oil	3.5	Heavy gas oil	5.3–9
No. 6 fuel oil	0.9	Kerosene	3.5–5.3
Cracking and coking unit streams		Light distillates and gas oil	3.5–5.3
Bottom slurry oils	5.3	Naphtha	3.5–5.3
Heavy coker gas oil	7–9	Vacuum tower bottoms	17.6
Heavy cycle oil	5.3–7	Industrial gas or vapor streams	

(continued)

**Table 3.2** (continued)

Fluid	Fouling resistance ( $10^4 \text{ m}^2 \text{ K/W}$ )	Fluid	Fouling resistance ( $10^4 \text{ m}^2 \text{ K/W}$ )
Light coker gas oil	5.3–7	Ammonia	1.75
Light cycle oil	3.5–5.3	Carbon dioxide	3.5
Light liquid products	3.5	Coal flue gas	17.5
Overhead liquid products	3.5	Compressed air	1.75
Light-end processing streams		Exhaust steam (oil bearing)	2.6–3.5
Absorption oils	3.5–5.3	Natural gas flue gas	9
Alkylation trace acid streams	3.5	Refrigerant (oil bearing)	3.5
Overhead gas	1.75	Steam (non-oil bearing)	9
Overhead liquid products	1.75		
Overhead vapors	1.75		
Reboiler streams	3–5.5		
Chemical process streams			
Acid gas	3.5–5.3		
Natural gas	1.75–3.5		
Solvent vapor	1.75		
Stable overhead products	1.75		

Source: Adapted from Chenoweth (1988)

- Clamp-on upgrades
- Cryogenic shrouds
- Drum warmers
- Pipe coolers
- Gas cylinder heaters
- Heavy wall vessels and platens

Compact heat exchangers are employed in many different applications because of their high surface area density. Plate-fin heat exchangers in particular are well suited for gas-to-gas and air-to-air recuperators and heat recovery units, among many other applications. In this thesis, constant property, fully or periodically developed laminar flows of air ( $\text{Pr} = 0.72$ ) inside a variety of different inter-fin channels of plate-fin heat exchangers are studied computationally, with the goal of achieving a better understanding of plate-fin heat exchangers and providing new designs with superior performance to the existing ones.

The majority of plate-fin channels have rectangular, trapezoidal or triangular cross-sectional shapes. Their convective behavior for air flows is investigated and

solutions and polynomial equations to predict the Nusselt number are provided. Besides the limiting cases of a perfectly conducting and insulated fin, the actual conduction in the fin is also considered by applying a conjugate conduction-convection boundary condition at the fin surface between partition plates. For the latter, new sets of solutions and charts to determine the heat transfer coefficient based on the fin materials, channel aspect ratio, and fin density are presented.

Furthermore, while large fin density increases the heat transfer surface area, the convection coefficient can be increased by geometrical modification of the fins. To this end, two different novel plate-fin configurations are proposed (Huzayyin, Omar Ahmed Soliman) [18] and their convective behavior investigated in this thesis. These include:

1. Slotted plate-fins with trapezoidal converging-diverging corrugations, and
2. Offset-strip fins with in-phase sinusoidal corrugations.

The enhanced heat transfer performance of the plate-fin compact core with perforated fin-walls of symmetric, trapezoidally profiled, converging-diverging corrugations is modeled computationally. Air flow rates in the range  $10 \leq Re \leq 1000$  are considered in a two dimensional duct geometry described by the trapezoid inclination angle, the convergent-divergent amplitude ratio, the dimensionless corrugation pitch, and a surface porosity  $\beta$  of 10 %. The fin-wall flow transpiration is seen to promote enhanced heat transfer by inducing cross stream mixing, and periodic disruption and restarting of boundary layers. With uniform heat flux  $H_1$  at the fin walls, an unusual performance is obtained where higher Nusselt number is accompanied with reduction in the corresponding friction factor, relative to a non-slotted geometry of the same dimensions.

In the case of sinusoidal wavy offset-strip channels, he showed that the performance enhancement can be evaluated for air flows in the range of  $10 \leq Re \leq 1000$ , with fins at constant wall temperature  $T$ , and the effect of the wavy-fin amplitude, inter-fin spacing, and fin offset position on the thermal-hydraulic performance is reported. It is generally seen that S-shaped offset channels perform better than C-shaped ones. An average of 400 % reduction in volume of a plate-fin heat exchanger can be achieved with S-shaped offset fins when compared to that with plain parallel fins [18].

In this chapter the benefits of compact heat exchangers, as well as their limitations, will be briefly reviewed; followed by a description of a number of types of compact heat exchangers, some well-established and others relative newcomers to the market.

Table 3.3 presents more details of the various infrastructures of configurations for typical Plate Heat Exchangers (PHEs) compact heat exchangers.

A compact heat exchanger is generally defined as one which incorporates a heat transfer surface having a high “area density”. In other words, it possesses a high ratio of heat transfer surface area to volume. This does not necessarily mean that a compact heat exchanger is of small mass or volume.

**Table 3.3** Typical operating ranges for PHEs

Types of PHE	Plate patterns	Operating temperature (°C)	Maximum pressure (bar)	Flow rate (m <sup>3</sup> /h)	Heat transfer area (m <sup>2</sup> )	Main products in the market
Gasketed conventional	Herringbone	Rubber: -35 to 200	35	0-5768	0.1-3800/unit	GEA-Ecoflex
	Zigzag	Graphite: -20 to 250			0.02-5/plate	APV-ParaFlow
						Tranier-Superchanger-Gc and GL
Wide-gap	Washboard	-35 to 200	16	2000	1472.5/unit	GEA-Ecoflex-Free Flow
	Wide-Gap				0.28-1.56/plate	Tranier-Superchanger-GF
Double-wall	Herringbone	-35 to 200	16	200	400/unit	APV-Easy flow
	Zigzag					Alfa Laval
Brazed	Herringbone	-195 to 225	45	160	75/unit	APV
	Zigzag					Alfa Laval
Semi-welded	Herringbone	-45 to 220	40	970	2500/unit	GEA-EcoBraze
	Zigzag				0.16-1.82/plate	APV-Paraweld
AlfaReX	Herringbone	-50 to 350	40	700	250/unit	Alfa Laval
	Dimpled	-195 to 540 (538 <sup>a</sup> )	115	15	2.056-8.4/plate	Tranier
Maxchanger Compabloc	Herringbone	-195.5 to 350 (170 <sup>a</sup> )	45	4000	4/unit	Tranier-Ultramax
	Dimpled				0.7-840/unit	G EA-Ecoflex Id-Bloc
					0.061-0.989/plate	Alfa Laval-Compabloc

	Hybrid	Hybrid	-200 to 900	80	-	6–8000/unit	GEA-Ecowe Id-Flex
							APV-Hybrid
Shell and Plate	Herringbone	-200 to 950 (230 <sup>a</sup> )	200	1000	0.025–1.55/plate	Alfa Laval-Disc	
							Tranter-Supermax
							GEA-EcoWeld-Shell
							Vaherus
							APV-Parashell
Packinox	Herringbone	550	120 (40 <sup>b</sup> )	-	1000–20,000/unit	Alfa Laval	

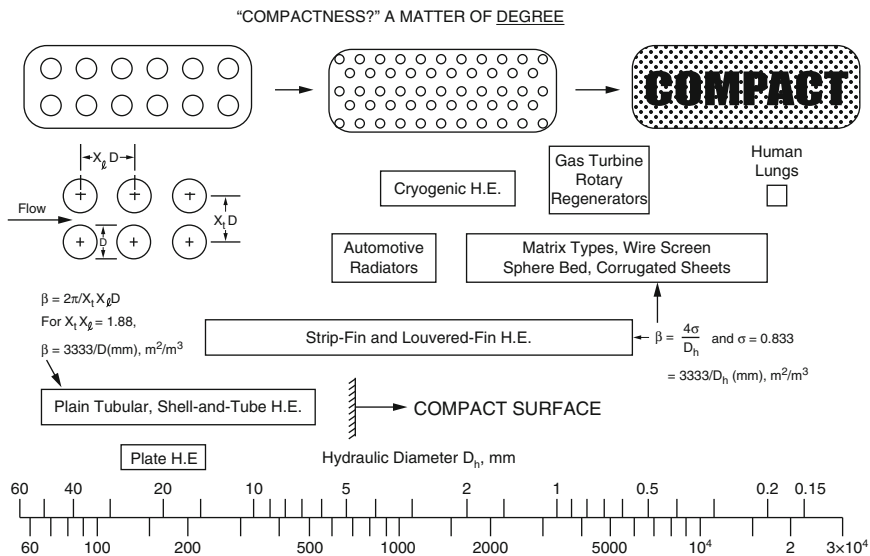


Fig. 3.43 Heat transfer surface area density  $\beta$ ,  $m^2/m^3$

Figure 3.43 shows a spectrum of surface area density for heat exchangers. The range of surface area density and hydraulic diameter is given for various types of heat exchange surfaces, with the dividing line for compactness clearly marked.

To yield a specified heat exchanger performance  $Q/\Delta T_{\text{mean}}$ , within acceptable mass and volume constraints, is calculated by using Eqs. (3.5a) and (3.5b) below

$$\frac{Q}{\Delta T_{\text{mean}}} = U\beta V \quad (\text{Eq. 3.5a})$$

or

$$\frac{Q}{\Delta T_{\text{mean}}\beta} = UV \quad (\text{Eq. 3.5b})$$

Analyzing Eq. (3.5b), it is obvious that a high  $\beta$  decreases volume. Furthermore, compact surfaces generally result in higher overall conductance,  $U$ . And since compact surfaces can achieve structural strength and stability with thinner sections, the reduction in heat exchanger mass is even more pronounced than the reduction in volume [30].

Various techniques can be used to make heat exchangers more compact. Figure 3.44 shows three general types of extended surface geometries which can be used to increase gas-side heat transfer coefficients.

These include:

- A finned-tube heat exchanger with flat fins,
- A finned tube heat exchanger with individually finned tubes, and

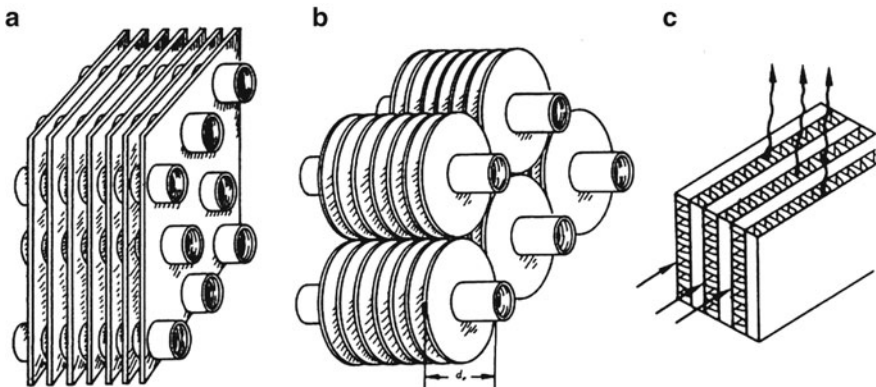


**Fig. 3.44** (a) Finned-tube heat exchanger with flat fins, (b) Individually finned tubes, (c) plate-fin heat exchanger [17]

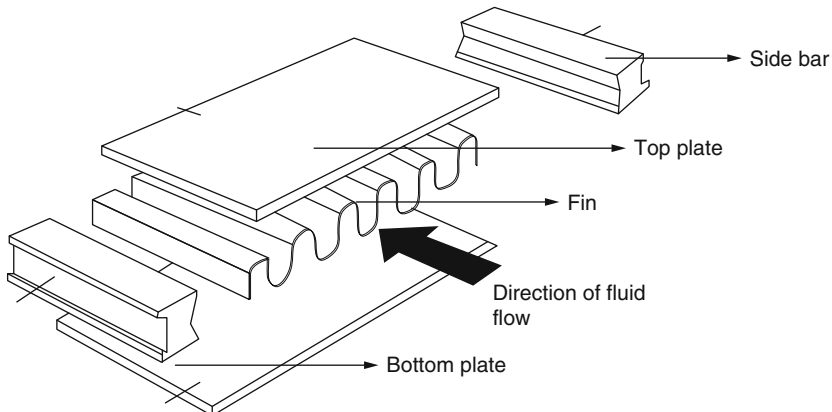


**Fig. 3.45** Construction details of a typical single-element plate-fin heat exchanger

- (c) A plate-fm heat exchanger. This paper focuses on various types of plate-fin geometries.

A typical element of a plate-fin heat exchanger consists of a die-formed **fm** (type of material) plate sandwiched between flat metal separator plates as shown in Fig. 3.45.

These heat exchangers are widely used in cryogenic application because of their low cost, small size, low weight, high thermal capacity and effectiveness relative to other types of heat exchangers. The result of the improved effectiveness is the achievement of true counter current flow where there is an increase in the temperature spread and a closer approach to ideality. This means that the refrigerant cooling curve is closer to the natural gas cooling curve [21].

**Fig. 3.46** Manifold or header. (Courtesy exchanger.com)

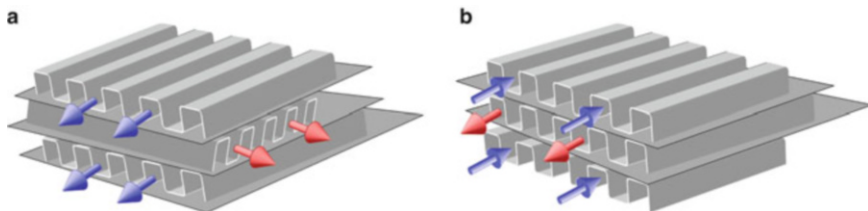
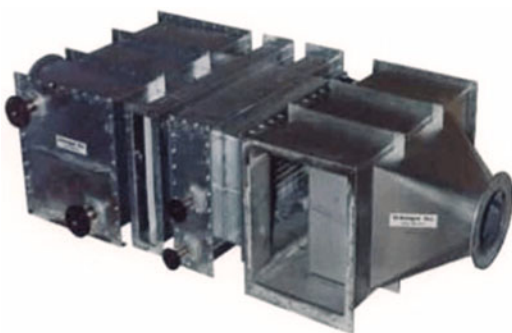


**Fig. 3.47** (a) Cross-flow and (b) Counter-flow arrangements of plate-fin heat exchangers

The exchanger is made up of manifolds or headers which consist of elements. A manifold and an element are shown below, in Figs. 3.46 and 3.47 respectively. An element is made up of a corrugated die-formed fin plate placed between flat metal separator plates. There are side bars along the outside of the fin sections. A stack of the elements is welded to form a rigid matrix and can be designed to meet any configuration and size. The stacks are welded onto the manifolds. Depending on the application, a number of manifolds can be assembled to form the heat exchanger.

The wavy configuration of the fin promotes (Figs. 3.41 and 3.42) turbulence and therefore improves heat transfer. This increase in heat transfer is accompanied by an increase in pressure drop. This is a problem with low density fluids like gases because of the extra work required to surmount the pressure drop.

Figure 3.47a and b shows the side bars are located along the outer edges of the fin sections, while Fig. 3.48 shows the installed stack of these manifold headers.

This work is often much higher than the increase in heat transfer acquired from the fins. For applications where any fin configuration other than the simplest is proposed a thorough analysis of the effect on the system should be conducted.

In designing the plate fin heat exchanger, it is possible for the alternating fin plates to have different heights. There is no requirement to have the same height or spacing of separator plates. This is a useful freedom to have in situations where the difference in density of the hot and cold fluids is large. In cryogenic systems, the refrigerant stream entering the expander has a higher density than the stream coming out of the expander. In such a case as this, it is necessary to use a larger height for the lower density stream so that a common Reynolds number and therefore heat transfer coefficient,  $U$ , can be attained.

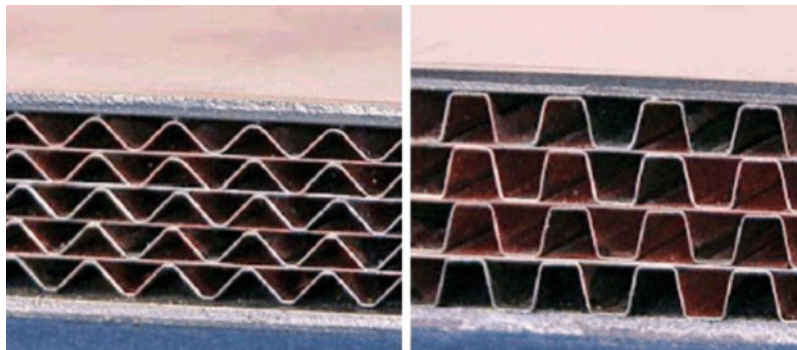
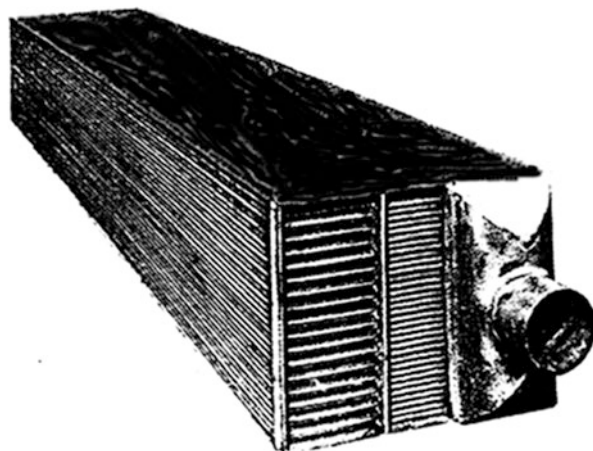


**Fig. 3.48** Fin configurations

**Fig. 3.49** Large matrix of plate-fin heat exchanger elements [21]



Aluminum is the usual material of construction of plate fin heat exchangers for cryogenic applications.

Stacks of such elements are then welded or dip-brazed to form large heat exchange devices like those in Fig. 3.49. A wide variety of plate-fin geometries have been used to obtain enhanced heat transfer, and engineers are constantly working to develop new and more effective enhanced surfaces [21].

Six commonly used plate-fin geometries are shown in Fig. 3.50.

A typical fin spacing is 300–800 fins/m. Due to their small hydraulic diameter and the low density of gases, these surfaces are usually operated in the Reynolds number range  $500 < \text{Re} < 1500$ . As a result, plated-fin enhancement geometries must be effective in the low Reynolds number regime. For example, surface roughness has been shown to promote heat transfer in the turbulent regime, but it does not provide appreciable enhancement in the lower Reynolds number range [21].

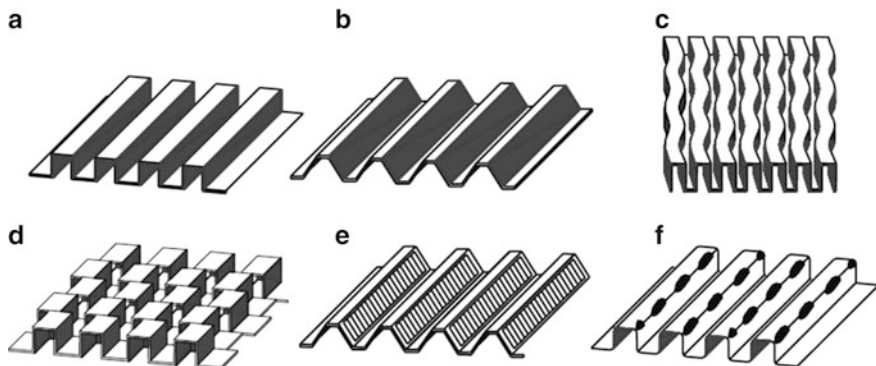


**Fig. 3.50** Type of plate fin surfaces: (a) Plain rectangular fins, (b) Plain trapezoidal fins, (c) Wavy fins, (d) Serrated or offset strip fins, (e) Louvered fins, (f) Perforated fins [15, 21]

### 3.6 Design Criteria for Process Heat Exchangers

There are some criteria that a process heat exchanger must satisfy which are stated easily enough if we confine ourselves to a certain process. The criteria include:

The heat exchanger must meet the process requirements. This means that it must effect the desired change in thermal condition of the process stream within the allowable pressure drops. At the same time, it must continue doing this until the next scheduled shut down for maintenance.

The heat exchanger must withstand the service conditions of the environment of the plant which includes the mechanical stresses of installation, startup, shutdown, normal operation, emergencies, and maintenance. Besides, the heat exchanger must also resist corrosion by the environment, processes, and streams. This is mainly a matter of choosing materials of construction, but mechanical design does have some effect.

The heat exchanger must be maintainable, which usually implies choosing a configuration that permits cleaning and replacement. In order to do this, the limitations are in positioning the exchanger and providing a clear space around it. Replacement usually involves tubes and other components that may be especially vulnerable to corrosion, erosion, or vibration.

The cost of the heat exchanger should be consistent with requirements. Meaning the cost to implement and the cost of installation. Operation cost and cost of lost production due to exchanger malfunction or being unavailable should be considered earlier in the design.

The limitations of the heat exchanger: Limitations are on length, diameter, weight, and tube specifications due to plant requirements and process flow.

As part of the design methodology, we should look at design in terms of an activity that is aimed at providing complete descriptions of an engineering system such as our case of combined cycle of open air Brayton cycle or part of a system, or just of a single system component. By defining a well-defined design methodology,

we can have a very clear path for specification of the system/components and their structure, size, and performance, as well as other characteristics that are important for a manufacturing and utilization purpose such as the next generation of nuclear power plants. This very important departure point for any combined cycle drives efficiency upward either for open or closed cycle [8].

Looking at the scope of these activities one must understand that the design methodology is faced with a very complex structure; and furthermore a design methodology for a heat exchanger as a sub-component of a system must be consistent with the *life-cycle design* of a system, which includes the following stages [31]:

- Problem formulation including interaction with end user.
- Concept development such as selection of preliminary and workable designs.
- Detailed exchanger design that includes design calculations and other important pertinent considerations.
- Manufacturing and cost effectiveness.
- Utilization consideration such as operation, life-cycle, phase-out, and final disposal.

These various quantitative and qualitative design aspects and their interaction and interdependence, would allow us to arrive at an optimum heat exchanger design. Figure 3.47 demonstrates of a methodology for designing a new single heat exchanger from a holistic point of view and may be characterized as a *onetime case study* method—they include [32]:

- Process and design specifications
- Thermal and hydraulic design
- Mechanical design
- Manufacturing considerations and cost both for total cost of ownership and return on investment
- Trade-off factors and system-based optimization

These design considerations are usually not sequential; there could be strong interactions and feedback among the aforementioned considerations, as indicated by double sided arrows in Fig. 3.51, and may require a number of iterations before the design is finalized.

As part of augmentation of the above design methodology, based on the problem of specifications and experience, the heat exchangers construction type and flow arrangement are the front line of selection criteria for such subsystems of bigger systems. For example in the case of Open Air Brayton Cycle as part of enhancing its overall output efficiency—as presented in Chap. 7 of this book—crossflow or counterflow pattern for consideration as a compact heat exchanger of a subsystem were most promising per computer code outputs and related analyses as well as calculations. As we said these analysis were done based on the steady-state case and the codes development were found per this infrastructure.

In summary the selection criteria and construction type depends upon the following parameters as well:

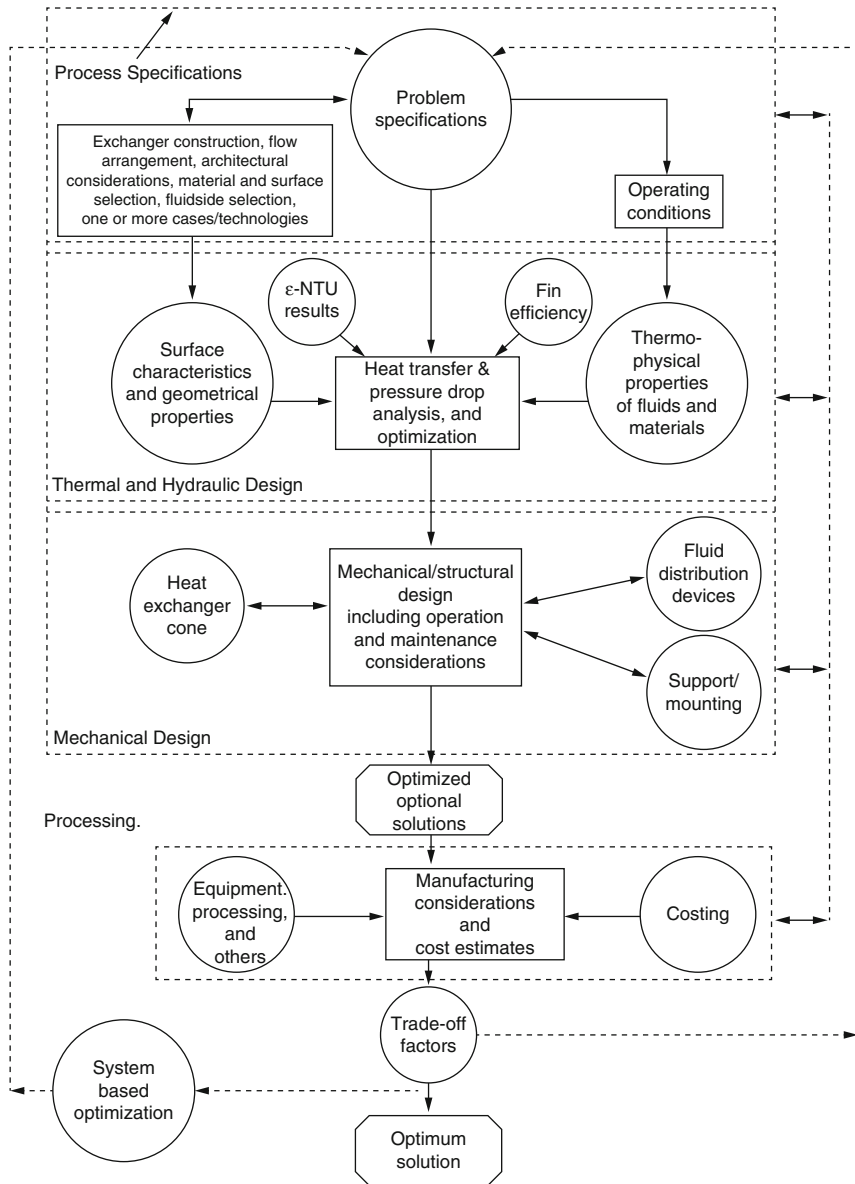


**Fig. 3.51** Heat exchanger design methodology. (Modified from Shah, 1982; Taborek, 1988 [32]; and Kays and London, 1998 [17])

1. Fluids (gas, liquids, or condensing/evaporating) used on each side of a two-fluid heat exchanger.
2. Operating pressure and temperature.
3. Fouling parameter  $f$ .

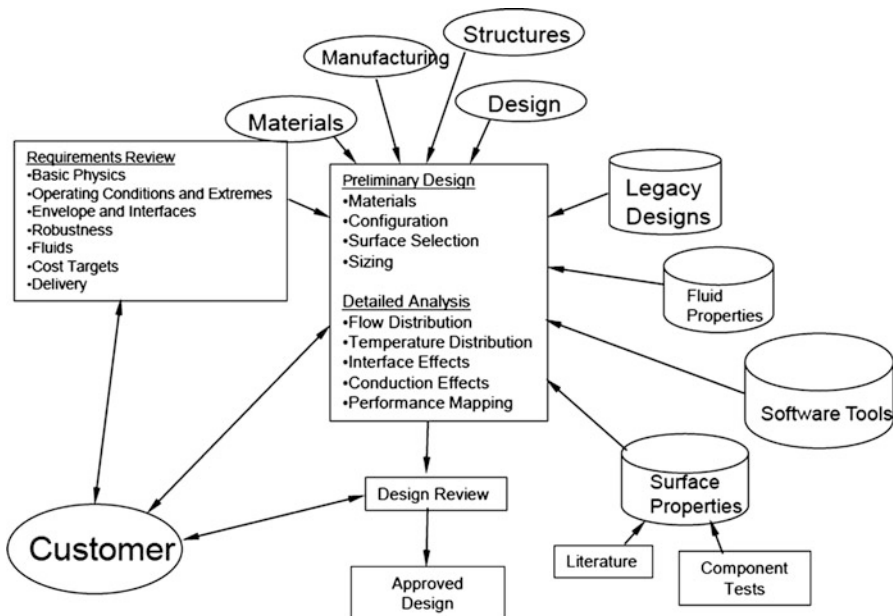


**Fig. 3.52** Compact heat exchanger design methodology steps and process

4. Surface selection for purpose of enhanced mode of heat transfer in an efficient way.
5. Leakage or contamination of one fluid to the other is permitted or not.
6. Cost and available heat exchanger manufacture technology for production and commercial purpose not an R&D prototype.
7. Preventive Maintenance (PM) and intended life-cycle.

As part of the design methodology, one can also use the following chart in particular for design of a compact heat exchanger, so one can go through processes faster. See Fig. 3.52.

Factors that influence the surface selection include the operating pressure, fouling, maintenance requirements, erosion, fabrication, cost, etc.

### 3.7 Thermal and Hydraulic Design

Heat exchanger thermal and hydraulic design and analysis involves a complex analysis and quantitative heat transfer and pressure drop (in case of transient analysis rather than steady-state) or exchanger size. So in today's modern computer capabilities most of the thermodynamics design method and iteration of processes to find the most efficient gain and optimization are done via Computational Fluid

Dynamics (CFD) and design methods and inputs to these analysis are summarized as follows, which depends on the type of exchangers:

- *Basic Thermo-hydraulic Design Methods:*

P-NTU, LMTD,  $\epsilon$ -NTU or  $\psi$ -P methods that can be mentioned.

- *Thermo-physical Properties:*

For any analysis regarding pressure-drop and heat-transfer, the following thermo-physical fluid properties (gas-to-gas or gas-to-fluid as media for heat exchange) are needed and they are defined as:

- $\mu$  = Dynamic viscosity
- $c_p$  = Specific heat at constant pressure
- $k$  = Thermal conductivity
- $\gamma$  = Surface tension

Note that for the conduction wall, thermal conductivity is needed.

- *Surface Geometrical Properties:*

For the purpose of pressure drop and heat transfer analysis, at minimum the following surface geometrical properties are required on each side of a two-fluid heat exchanger, and they are identified as:

- $A$  = Heat transfer area, which includes both primary and secondary surface area if any
- $A_{fr}$  = Core frontal area
- $A_a$  = Minimum free flow area
- $D_h$  = Hydraulic diameter, as defined before
- $L$  = Flow length
- $V$  = Core volume
- $T, W$  = Fine thickness and fin conduction length
- $L_1, L_2, L_3$  = Core dimensions

These quantities are obtained from computation of the basic dimensions layout of the core and heat-transfer surface. In the case of shell-and-tube type heat exchangers, one should take under consideration various leakage and bypass flow areas as well.

- *Surface Characteristics:*

For the purpose of surface characteristic, the heat transfer  $j$  and flow friction  $f$ , are key inputs for the exchanger heat transfer and pressure drop analysis, respectively [13]. Experimental data results for a variety of compact heat exchangers are presented in Kays and London [17]. More references on  $j$  and  $f$  factor are furnished in Shah and Sekulic [32], Chap. 4.

- *Heat Exchanger Specification Sheet:*

The Heat exchanger specification sheet is an important fact sheet to help you choose your design methodology and type of heat exchanger for intended application. There are also Microsoft Excel Sheet Templates that can be found on the web, and they are downloadable free of charge [33]. A simple sample of such a sheet is shown here as Fig. 3.53.

	A	B	C	D	E	F	G	H	I
1	Preliminary Heat Exchanger Design (U.S. units)								
2	Estimation of Heat Transfer Area Needed								
3									
4	<u>Inputs</u>								
5									
6	Fluid <sub>1</sub> mass flow rate, $m_1$ =	25,000	lb/hr						
7									
8	Fluid <sub>1</sub> temp. in, $T_{1in}$ =	190	°F						
9									
10	Fluid <sub>1</sub> temp. out, $T_{1out}$ =	140	°F						
11									
12									
13	Fluid <sub>1</sub> sp. heat, $C_{p1}$ =	0.74	Btu/lb-°F						
14									
15	Fluid <sub>2</sub> temp. in, $T_{2in}$ =	50	°F						
16									
17	Fluid <sub>2</sub> temp. out, $T_{2out}$ =	120	°F						
18									
19	Fluid <sub>2</sub> sp. heat, $C_{p2}$ =	1.0	Btu/lb-°F						
20									
21	Overall heat transf coeff. estim., $U$ =	120.0	Btu/hr-ft <sup>2</sup> -°F						
22									
23									
24	<u>Equations used for calculations:</u>								
25									
26	$Q = \pm (m_1)(C_{p1})(T_{1in} - T_{1out})$								
27									
28	$Q = \pm (m_2)(C_{p2})(T_{2in} - T_{2out})$								
29									
30	$\Delta T_{lm} = [(T_{1in} - T_{2out}) - (T_{1out} - T_{2in})]\ln[(T_{1in} - T_{2out})(T_{1out} + T_{2in})]$								
31									
32	$Q = UA\Delta T_{lm}$								

Fig. 3.53 Heat exchanger specification sample sheet

### 3.7.1 Equations and Parameters

The heat exchanger design equation can be used to calculate the required heat transfer surface area for a variety of specified fluids, inlet and outlet temperatures, and types and configurations of heat exchangers, including counterflow or parallel flow. A value is needed for the overall heat transfer coefficient for the given heat exchanger, fluids, and temperatures. Heat exchanger calculations could be made for the required heat transfer area or the rate of heat transfer for a heat exchanger of area that is given.

Heat exchanger theory leads to the basic heat exchanger design equation:

$$Q = UA\Delta T_{mean} \quad (\text{Eq. 3.6})$$

where  $Q$  is the rate of heat transfer between the two fluids in the heat exchanger in Btu/h,  $U$  is the overall heat transfer coefficient in Btu/h·ft<sup>2</sup>·°F,  $A$  is the heat transfer surface area in ft<sup>2</sup>, and  $\Delta T_{mean}$  is the log mean temperature difference (LMTD) in °F, calculated from the inlet and outlet temperatures of both fluids. Note that the product of  $UA$  is overall heat transfer coefficient and reference surface area [34]. This product is often called the heat transfer conductance.

For design of heat exchangers, the basic heat exchanger design equation can be used to calculate the required heat exchanger area for known or estimated values of

the other three parameters,  $Q$ ,  $U$ , and  $\Delta T_{\text{mean}}$  (sometimes presented as  $\Delta T_m$ ). Each of these parameters will be discussed in the following sections, but before we jump into these parameters we need to have some understanding of how to assess, the basic concept and initial sizing of the intended heat exchanger based on its application within the system, where this exchanger will be used. Thus, next section will describe basic concepts and initial size assessment [35].

### 3.7.1.1 Basic Concept and Initial Size Assessment as Part of Design Process

As part of the design methodology and design process, we have to have a basic concept of the initial sizing of the exchanger per its application and, when pressure drop and thermal (i.e., heat transfer) specification has been fixed, then it is possible to do a quick analysis to determine the most appropriate heat exchanger type based on flow configuration which will be either crossflow or counterflow, or often multipass overall counterflow arrangements (i.e., compact shell and tube exchanger). For this we need first to entertain the effectiveness design or method, Effectiveness method approach, and then the Logarithmic Mean Temperature Difference (LMTD)—the methods were described in Chap. 2 of this book.

Earlier in Chap. 2 of this book we touched upon the effectiveness method also known as NTU, as part of design parameters for heat exchangers; now we are going to evaluate this parameter further as part of our design methodology of a compact heat exchanger as part of our subsystem for the next generation of nuclear power plant (NGNP).

Heat exchangers are usually analyzed using either the Logarithmic Mean Temperature Difference (LMTD) or the Effectiveness-Number of Transfer Units ( $\epsilon$ -NTU) methods. The LMTD method is convenient for determining the overall heat transfer coefficient based on the measured inlet and outlet fluid temperatures. The  $\epsilon$  - NTU method is more convenient for prediction of the outlet fluid temperatures if the heat transfer coefficient and the inlet temperatures are known.

The analysis presented below assumes certain constraints which are:

1. There is no energy loss to the environment.
2. Heat exchanger is at a steady-state.
3. There are no phase changes in the fluids.
4. Heat capacities of the fluids are independent of temperature.
5. Overall heat transfer coefficient is independent of the fluid temperature and position within the heat exchanger.

Since all heat exchangers considered in this experiment have a single pass for both the hot and cold fluids, the discussion below is limited to single-pass heat exchangers. Qualitative dependence of the fluid temperature on the position inside a single-pass heat exchanger is shown in Fig. 3.54. Although Fig. 3.50b shows a situation for parallel flow, our main target for intended compact heat exchanger for driven combined cycle efficiency for next generation of power plant (NGNP) focus

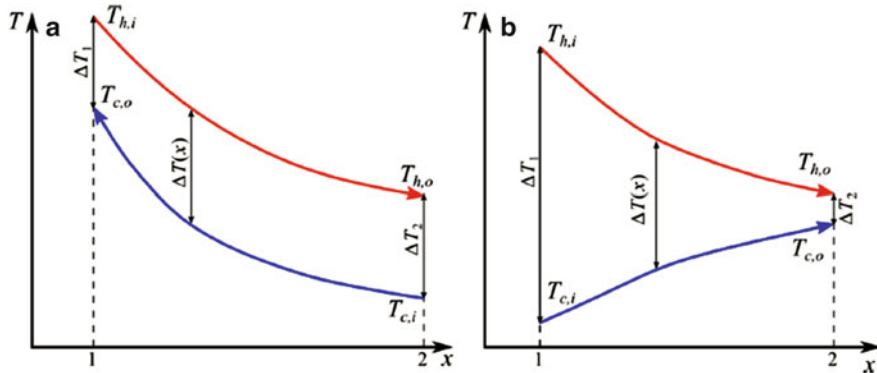
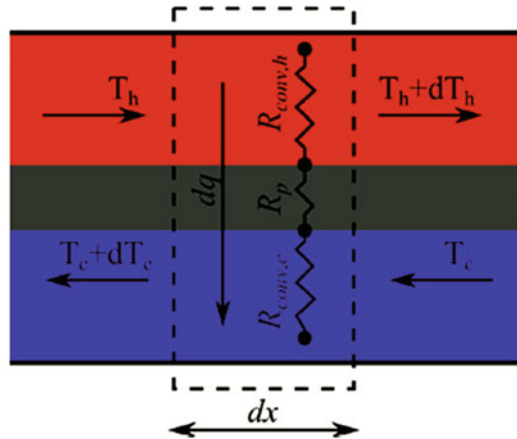


**Fig. 3.54** Temperature profiles in (a) counter-flow and (b) parallel flow single pass heat exchangers. Note that in a counter-flow heat exchanger the outlet temperature of the cold fluid can exceed the outlet temperature of the hot fluid but this cannot happen in a parallel flow system

**Fig. 3.55** Energy balance in a differential element of a single pass heat exchanger operated in the counter-flow regime



either on crossflow or counterflow type of classification of these exchangers. This has been backed-up by computer code and analyses that is presented in Chap. 7 of this book. Presentation of a parallel flow is a matter of compression for the purpose of effectiveness analyses only.

We can analyze the total heat transfer rate  $q$  as follows:

$$q = \int_1^2 dq' \quad (\text{Eq. 3.7})$$

where  $dq$  is some aspect of differential form of Eq. (3.6) for a segment of a single-pass flow heat exchanger from point 1 to point 2 which, is shown schematically in Fig. 3.55, in order to present overall heat transfer coefficient  $U$ . Equation (3.8) is a presentation of overall heat transfer coefficient  $U$  in this segment.

$$dq'(x = U\Delta T(x)dA(x)) \quad (\text{Eq. 3.8})$$

where  $U$  is the overall heat transfer coefficient,  $\Delta T(x)$  is the local temperature difference between the hot and cold fluids within this segment, while  $dA(x)$  is the contact area in the differential segment.

Note that, red, blue, and gray colors represent the hot fluid, cold fluid, and the partition between the fluids, respectively. The dashed rectangle shows a differential segment corresponding to the energy balance Eq. (3.8). Three resistances ( $R_{\text{conv,h}}$ ,  $R_p$ , and  $R_{\text{conv,c}}$ ) contributing to the total resistance of the heat transfer are indicated schematically. Therefore, for overall heat transfer coefficient  $U$  we can write:

$$U = \frac{1}{R_{\text{Total}}} = \frac{1}{R_{\text{conv,h}} + R_p + R_{\text{conv,c}}} \quad (\text{Eq. 3.9})$$

where:

$R_{\text{conv,h}}$  = Convective heat transfer, which means resistance to the convective heat transfer is inversely proportional to the convective heat transfer coefficient,  $h = 1/R_{\text{conv,h}}$ . The convective heat transfer coefficient depends on fluid properties, flow geometry, and the flow rate. It is convenient to describe this dependence using several dimensionless numbers, namely the Reynolds number:

$$\text{Re} = \frac{Lv\rho}{\mu} \quad (\text{Eq. 3.10})$$

The Prandtl number

$$\text{Pr} = \frac{c_p\mu}{k} \quad (\text{Eq. 3.11})$$

And finally the Nusselt number

$$\text{Nu} = \frac{hL}{k} \quad (\text{Eq. 3.12})$$

Here,  $\rho$ ,  $\mu$ ,  $k$ , and  $c_p$  are the density, viscosity, thermal conductivity, and heat capacity of the fluid,  $v$  is the flow velocity, and  $L$  is the characteristic length. The choice of  $L$  depends on the system geometry. For example, for a flow in a circular pipe,  $L$  is the pipe diameter.

The relationship between  $\text{Re}$ ,  $\text{Pr}$ , and  $\text{Nu}$  depends on the system geometry and whether the flow is laminar and turbulent. For example, for a turbulent flow inside a pipe with circular cross-section of diameter  $D$ ,

$$\text{Nu} = 0.027 \text{Re}^{0.8} \text{Pr}^{1/3} \quad (\text{Eq. 3.13})$$

$R_p$  = Conductive heat transfer, which is the resistance  $R_p$  to heat transfer through the partition depends on the system geometry. In the current experiment, you will need to consider heat conduction in the radial direction of a cylindrical tube and heat conduction across a thin plate. Resistances in both of these cases can be obtained analytically by solving the heat diffusion equation.

However, it is possible to obtain  $q$  by combining Eq. (3.8) with energy balance in differential segments of the heat exchanger as:

$$dq = -C_{p,h}dT_k = C_{p,c}dT_c = C_{p,k}dT_k \quad (\text{Eq. 3.14})$$

Here,  $dT_k$  is the temperature change of fluid  $k$  ( $k = c$  or  $h$ ) in the interval under consideration, and  $C_{p,k}$  is the heat capacity rate of fluid  $k$  under constant pressure:

$$C_{p,k} = \dot{m}_k c_k \quad \text{for } k = c \text{ or } h \quad (\text{Eq. 3.15})$$

where  $\dot{m}_k$  and  $c_k$  are the mass flow rate and heat capacity of fluid  $k$ , respectively. This analysis yields:

$$Q = UA\Delta T_{\text{mean}} \quad (\text{Eq. 3.16})$$

This is exactly the equation we introduced previously and is identified as Eq. (3.6), where  $A$  is the total contact area and  $\Delta T_m$  is the logarithmic mean temperature difference (LMTD); and it is the subject of the next section.

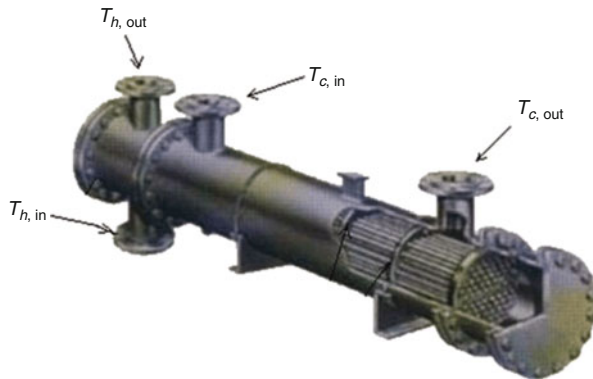
### 3.7.1.2 Logarithmic Mean Temperature Difference (LMTD)

The driving force for any heat transfer process is a temperature difference. For heat exchangers, there are two fluids involved, with the temperatures of both changing as they pass through the heat exchanger, so some type of average temperature difference is needed. Many heat transfer textbooks have a derivation showing that the log mean temperature difference is the right average temperature to use for heat exchanger calculations. In the case of compact shell and tube heat exchanger (Fig. 3.56 below), the mathematical relationship is as follows:

That log mean temperature is defined in terms of the temperature differences as shown in Eq. (3.17).  $T_{h,\text{in}}$  and  $T_{h,\text{out}}$  are the inlet and outlet temperatures of the hot fluid and  $T_{c,\text{in}}$  and  $T_{c,\text{out}}$  are the inlet and outlet temperatures of the cold fluid. Those four temperatures are shown in the diagram at the left for a straight tube, two pass shell and tube heat exchanger with the cold fluid as the shell side fluid and the hot fluid as the tube side fluid.

$$\Delta T_m = \frac{(T_{h,\text{in}} - T_{c,\text{out}}) - (T_{h,\text{out}} - T_{c,\text{in}})}{\ln \frac{(T_{h,\text{in}} - T_{c,\text{out}})}{(T_{h,\text{out}} - T_{c,\text{in}})}} \quad (\text{Eq. 3.17})$$

**Fig. 3.56** Straight tube, two pass compact shell and tube heat exchanger



In a general form Eq. (3.17) can be written as:

$$\Delta T_m = \frac{\Delta T_1 - \Delta T_2}{\ln(\Delta T_1 / \Delta T_2)} \quad (\text{Eq. 3.18})$$

Here, we can define a new term as  $\Delta T_k$ , which, refers to temperature difference of the hot and cold fluids at point k ( $k = c$  or  $h$ ), i.e.,

$$\Delta T_1 = T_{h, in} - T_{c, out} \quad \text{and} \quad \Delta T_2 = T_{h, out} - T_{c, in} \quad (\text{Eq. 3.19})$$

for the counterflow current and for parallel flow it yields to the following form:

$$\Delta T_1 = T_{h, in} - T_{c, in} \quad \text{and} \quad \Delta T_2 = T_{h, out} - T_{c, out} \quad (\text{Eq. 3.20})$$

*Note that:*

1. If heat capacity rates of the cold and hot fluids are the same and the heat exchanger is operated in the counter-flow regime then  $\Delta T$  is independent of position in the heat exchanger. In this case Eqs. (3.16) and (3.18) are not applicable and the total heat transfer rate  $q$  should be obtained by direct integration of Eq. (3.8).
2. This result holds for single pass heat exchangers only. However, the LMTD method can be extended to more complex heat-exchanger designs (e.g., multi-pass and cross-flow systems) using a correction factor (see Ref. [22]).

Now that we have a better understanding of Logarithmic Mean Temperature Difference (LMTD) methodology, we can see that this method is very useful for determining the overall heat transfer coefficient  $U$  based on experimental values of the inlet and outlet temperatures and the fluid flow rates. However, this method is not very convenient for prediction of outlet temperatures if the inlet temperatures and  $U$  are known. In this case, one has to solve a nonlinear system of two equations (see Eq. (3.12) and the overall energy balance) for two unknowns ( $T_{h,out}$  and  $T_{c,out}$ ). This solution requires application of an iterative approach.

A more convenient method for predicting the outlet temperatures is the effectiveness method that is known as Number of Transfer Units (NTU) method sometimes also written as  $\epsilon$ -NTU. This method can be derived from the LMTD method without introducing any additional assumptions. Therefore, the effectiveness-NTU and LMTD methods are equivalent.

An advantage of the effectiveness-NTU method is its ability to predict the outlet temperatures without resorting to a numerical iterative solution of a system of nonlinear equations.

### 3.7.1.3 Effectiveness-Number of Transfer Units (NTU) Method

Now that we have a better understanding of LMTD, we are going to define the heat-exchanger effectiveness  $\epsilon$  as:

$$\epsilon = \frac{q}{q_{\max}} = \frac{C_h(T_{h,in} - T_{h,out})}{C_{\min}(T_{h,in} - T_{c,in})} = \frac{C_h(T_{c,in} - T_{c,out})}{C_{\min}(T_{h,in} - T_{c,in})} \quad (\text{Eq. 3.21})$$

where  $T$  is the actual rate of heat transfer from hot to cold fluid and  $x^* = x/(D_h P_e)$  is the maximum possible rate of heat transfer for given temperatures of the fluids:

$$q_{\max} = C_{\min}(T_{h,in} - T_{c,in}) \quad (\text{Eq. 3.22})$$

In this equation  $C_{\min}$  represents the smaller of the two heat capacity rates between  $C_c$  and  $C_h$ ,

where  $C_c$  and  $C_h$  are cold stream and hot stream heat capacity rates respectively, one of which will be  $C_{\min}$  unless the exchanger is balanced. This allows the effectiveness of the exchanger to be designed and it can be determined directly from the terminal temperatures, if these temperatures and the stream parameters are known. As we said besides this criterion the other major relationship for design that will be needed, is given by Eq. (3.16).

If heat exchanger effectiveness is known, one can readily obtain  $Q$  from Eqs. (3.21) and (3.18) by solving these two equations simultaneously. After that, the outlet temperatures can be obtained from the energy balance.

The efficiency  $\epsilon$  depends on the heat exchanger geometry, flow pattern (i.e., parallel flow, counter-flow, cross-flow, etc.) and the Number of Transfer Units (NTU).

Now we define the Number of Transfer Units (NTU) for the exchanger as:

$$\text{NTU} = \frac{UA}{C_{\min}} \quad (\text{Eq. 3.23})$$

Relationships between the effectiveness and NTU have been established for a large variety of heat exchanger configurations. Most of these relationships involve the ratio of stream capacity rates denoted as  $C_r = C_{\min}/C_{\max}$  of the smaller and the

larger of the heat capacity rates  $C_c$  and  $C_h$ . For example, for a single pass heat exchanger in the parallel flow regime:

$$\epsilon = \frac{1 - \exp[-\text{NTU}(1 + C_r)]}{1 + C_r} \quad (\text{Eq. 3.24})$$

And for a single pass heat exchanger in the counter-flow regime, the effectiveness is expressed as:

$$\begin{cases} \epsilon = \frac{1 - \exp[-\text{NTU}(1 + C_r)]}{1 + C_r \exp[-\text{NTU}(1 - C_r)]} & \rightarrow \text{ if } C_r < 1 \\ \epsilon = \frac{\text{NTU}}{1 + \text{NTU}} & \rightarrow \rightarrow \rightarrow \text{ if } C_r < 1 \end{cases} \quad (\text{Eq. 3.25})$$

Similarly for cross-flow regime, we can define the effectiveness as:

$$\epsilon = \frac{1}{C_r} [1 - \exp\{-C_r[1 - \exp(-\text{NTU})]\}] \quad (\text{Eq. 3.26})$$

Designing a heat exchanger today with the help of tools such as CAD (Computer Aided Design) and CAM (Computer Aided Manufacturing) some mathematical and algebraic relationships between all the above parameters, and consequently the selection of the right heat exchanger for the right application, will be most helpful and makes the design process easier than hand calculations. Table 3.4 below shows the most commonly used configurations proposed by Kays and London [17] and Hesselgreaves [8].

The typical temperature for common arrangements can be depicted as shown in Fig. 3.57.

Eq. (3.26) is a representation of an idealized performance with infinite surface area, and Fig. 3.58 shows the idealized temperature distribution diagram [35].

These acronyms allow us to remember the location of pinch point at either end of the heat exchanger.

Analyzing Fig. 3.59 clearly shows that the maximum heat transferred is obtained when the stream of lowest heat capacity rate has an outlet temperature equal to the inlet temperature (for a counterflow configuration) of the other stream. For the parallel flow arrangement, the state is reached when both streams attain the same temperature at outlet and pinch point is the point of equal temperature. Note that per this idealized situation, the pinch point corresponds to zero temperature difference.

Further analysis of NTU is illustrated graphically in Fig. 3.55, which reveals the product of required area and heat transfer coefficient UA based on Eq. (3.6) or (3.16), which relates these two parameters to the effectiveness, determined by the specified temperatures, and the stream capacity rates ratio  $C_r$ .

From Fig. 3.54 for various heat exchangers types, it is obvious that the configuration causes some differences in the value of effectiveness for low  $C_r$  (i.e.,  $C_r < 0.25$ ), or NTU of less than 1 (i.e.  $\text{NTU} < 1$ ). For this range of  $\text{NTU} < 1$ , we can

**Table 3.4** Effectiveness—NTU relationships [35]

$$\text{Counterflow } \epsilon = \frac{1 - \exp[-\text{NTU}(1 + C_r)]}{1 + C_r \exp[-\text{NTU}(1 + C_r)]}$$

Asymptotic value = 1 as  $\text{NTU} \rightarrow \infty$ , for all  $C_r$

*Unmixed crossflow* (approximation from Kays and Crawford 1993) [36]

$$\epsilon = 1 - \exp \left\{ \frac{(\exp(-\text{NTU}^{0.78} C_r) - 1) \text{NTU}^{0.22}}{C_r} \right\}$$

Asymptotic value = 1 as  $\text{NTU} \rightarrow \infty$ , for all  $C_r$

$$\text{Parallel, or co-current flow } \epsilon = \frac{1 - \exp(-\text{NTU}(1 + C_r))}{1 + C_r}$$

Asymptotic value =  $1/(1 + C_r)$ , for all  $C_r$

$$\text{Crossflow, } C_{\min} \text{ unmixed } \epsilon = \frac{1}{C_r} \{ 1 - \exp[-C_r(1 - \exp(-\text{NTU}))] \}$$

Asymptotic value =  $[1 - \exp(-C_r)]/C_r$  as  $\text{NTU} \rightarrow \infty$

$$\text{Crossflow, } C_{\max} \text{ unmixed } \epsilon = 1 - \exp \left\{ -\frac{1}{C_r} [1 - \exp(-\text{NTU} C_r)] \right\}$$

Asymptotic value =  $[1 - \exp(1/C_r)]$  as  $\text{NTU} \rightarrow \infty$

$$\text{Crossflow, both fluids mixed } \epsilon = \frac{1}{\frac{\text{NTU}}{1 - \exp(-\text{NTU})} + \frac{\text{NTU} C_r}{1 - \exp(-\text{NTU} C_r)} - 1}$$

Asymptotic value =  $1/(1 + C_r)$ , for all  $C_r$

*Multipass overall counterflow, fluid mixed between passes*

$$\epsilon = \frac{\left( \frac{1 - \epsilon_p C_r}{1 - \epsilon_p} \right)^n}{\left( \frac{1 - \epsilon_p C_r}{1 - \epsilon_p} \right) - C_r}$$

with

$\epsilon_p$  = effectiveness of each pass [as a function of  $\text{NTU}_p = (\text{NTU}/n)$ ]

$n$  = number of identical passes (i.e. each pass having the same  $\epsilon_p$ )

and

$$\epsilon_p = \frac{\left( \frac{1 - \epsilon C_r}{1 - \epsilon} \right)^{1/n} - 1}{\left( \frac{1 - \epsilon C_r}{1 - \epsilon} \right)^{1/n} - C_r}$$

Limiting value =  $\epsilon_{\text{counterflow}}$ , as  $n \rightarrow \infty$

*Multipass overall parallel flow, fluids mixed between passes:*

$$\epsilon = \frac{1}{1 + C_r} \left\{ 1 - \left[ 1 - (1 + C_r) \epsilon_p \right]^n \right\}$$

All configurations,  $C_r = 0$  for pure condensation and evaporation:

$$\epsilon = 1 - \exp(-\text{NTU})$$

see that effectiveness is low as well. Now analyzing the given mathematical relationships for effectiveness of heat exchangers of different types that are provided in Table 3.4, it is also clear for the purpose of CAD/CAM design a choice of crossflow type exchanger is most appropriate due to the simplicity of its relationship as shown in this table, which most often applies to liquid/gas compact heat exchangers and their application to enhance overall efficiency of next generation nuclear power plants that are driven by combined cycle such as open air Brayton cycle. This choice in particular applies to the case of exchangers, for which the gas side heat transfer coefficient is low and dominates the overall conductance of UA product. On the other hand if  $C_r$  is higher than 0.25, and particularly if the required effectiveness is higher than 0.80 (i.e.  $\epsilon > 0.80$ ), a counterflow configuration will be a better choice and usually provides the most economical design approach. Figure 3.54c shows that for multipass cross-counterflow the pure counterflow value of effectiveness closely approaches for three or more passes, which is preferred more

**Fig. 3.57** Typical temperature distributions in heat exchangers [35]

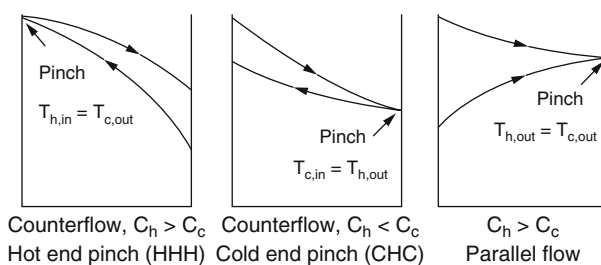
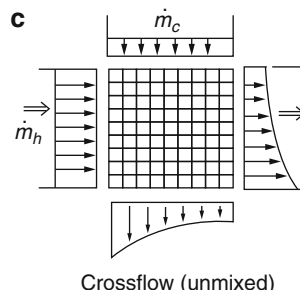
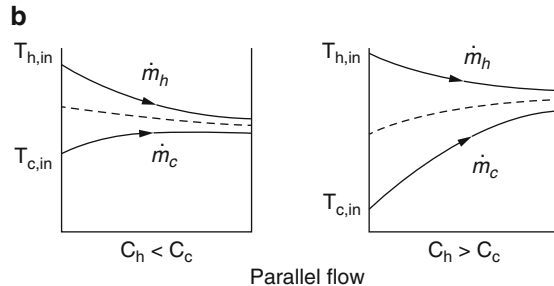
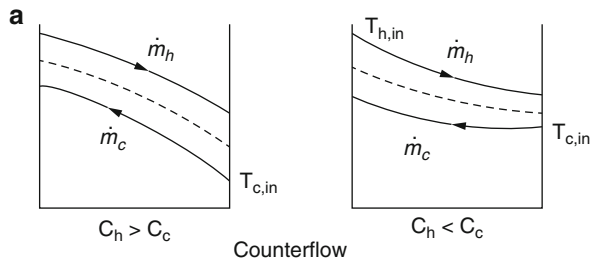


**Fig. 3.58** Idealized temperature distributions showing the pinch point [35]. HHH = Hot fluid has highest heat capacity rate—hot end pinch point. CHC = Cold fluid has highest heat capacity rate—cold end pinch point

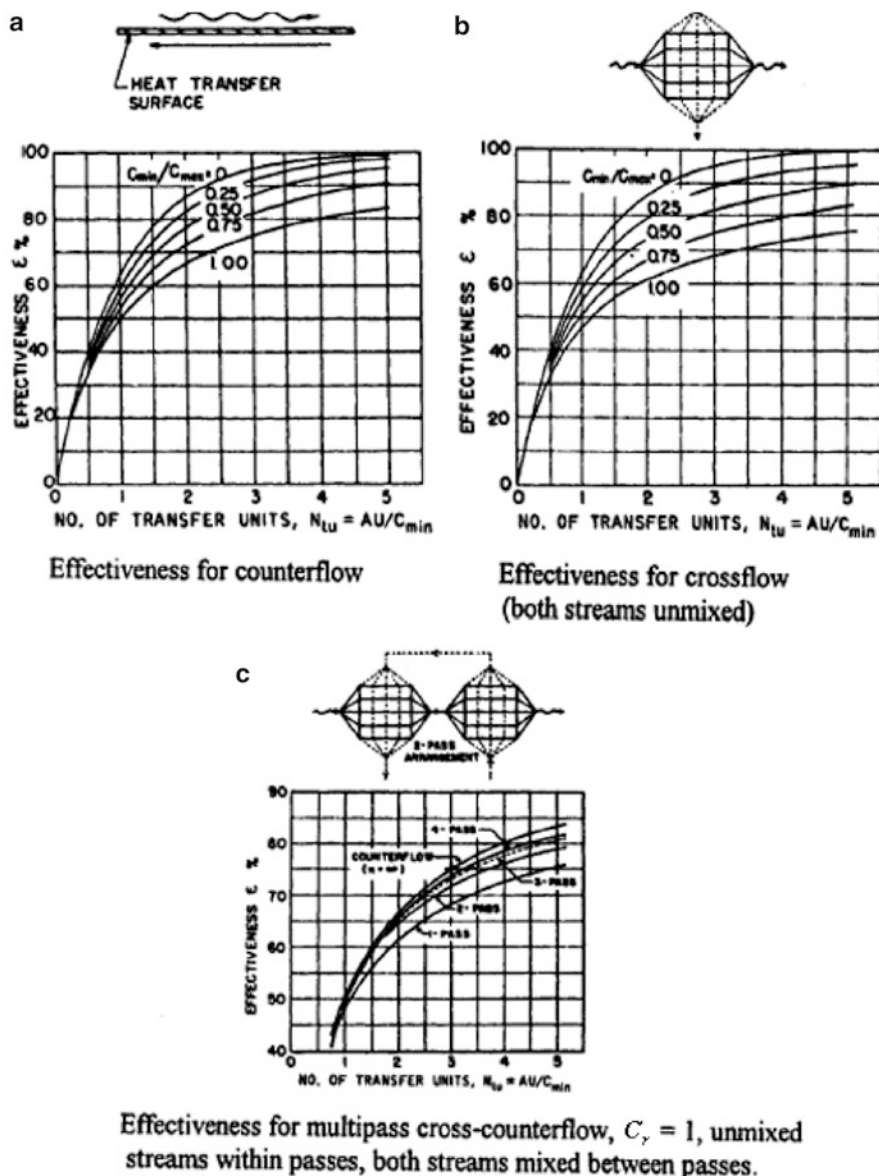


Fig. 3.59 Effectiveness versus NTU curves for simple configurations [11]

often over the pure counterflow configuration because porting is an easier and cheaper design.

For better computer coding utilizing any CAD tool and the scope of calculations where the terminal temperature are often specified, it is better to have NTU as a function of effectiveness  $\epsilon$ , where this parameter can be determined directly.

**Table 3.5** Inverse (NTU -  $\epsilon$ ) relationships

<i>Counterflow:</i>	$NTU = \frac{1}{C_r-1} \ln \left( \frac{\epsilon-1}{C_r(\epsilon-1)} \right)$
<i>Crossflow (<math>C_r = 1</math>):</i>	$NTU = \frac{\epsilon}{1-\epsilon}$
<i>Parallel flow:</i>	$NTU = \frac{-\ln[1-(1+C_r)\epsilon]}{1+C_r}$
<i>Crossflow:</i>	
$C_{\max} \text{ mixed}, C_{\min} \text{ unmixed}$	$NTU = -\ln \left[ 1 + \frac{1}{C_r} \ln(1 - C_r \epsilon) \right]$
$C_{\max} \text{ unmixed}, C_{\min} \text{ mixed}$	$NTU = \frac{-1}{C_r} \ln [1 + \ln(1 - \epsilon)]$
<i>All configurations, <math>C_r = 0</math></i>	$NTU = -\ln(1 - \epsilon)$

Therefore, it is better to create another table (Table 3.5) to explicitly define NTU in terms of  $\epsilon$ . This then gives the overall conductance  $UA$ , and is directly equivalent to the LMTD method as discussed before.

A further aspect strongly affecting counter- versus crossflow choice is that of pressure drop. Before we continue with the mass velocity equation discussion we need to start our discussion on the pressure drop phenomena.

### 3.7.1.4 Pressure Drop

For the application of compact heat exchanger in Next Generation Nuclear Power Plants (NGNPs) or Concentrated Solar Power (CSP) or for that matter any renewable energy system, it is necessary to have accurate design tools for predicting heat transfer and pressure drop. Until recently, these types of heat exchangers were not well studied, and in the scientific literature there were large discrepancies between results reported by different investigators.

Characteristics of compact heat exchangers were defined in Sect. 3.4 and they were divided into three groups of exchangers by their classifications as:

4. Gas-to-Liquid Heat Exchangers
5. Gas-to-Gas Heat Exchangers
6. Liquid-to-Liquid Heat Exchangers

Each type had its own pros and cons per their applications as compared to conventional shell-and-tube heat exchangers. For the purpose of pressure drop analysis, in particular core pressure drop in design of liquid-to-liquid heat exchangers, perfect and accurate knowledge of the friction and its factor characteristic also known as Fanning Friction Factor  $f_F$  of the heat transfer surface is not that important because of the low power requirement for pumping high-density fluids. Since the plate fin heat exchangers are mainly used for gas-to-gas heat transfer—in these cases most of the gases are low density gases—the pumping power requirement in a gas-to-gas heat exchanger is high as compared to that in a liquid-to-liquid heat exchanger. The reality of this matter imposes a constraint to

have an accurate estimation of the friction characteristic of heat exchanger surfaces in gas-to-gas application in contrast to liquid-to-liquid as mentioned above.

The friction factor is defined on the basis of an equivalent shear force in the flow direction per unit friction area. This shear force can be either viscous shear such as *Skin Friction* or pressure force from drag or a combination of both scenarios. Thus, without making an attempt to differentiate between them, it is possible to express them by Fanning Friction Factor  $f_F$  given by Eq. (3.27) below as:

$$f_F = \frac{\tau_s}{\frac{1}{2}(\rho u^2)} \quad (\text{Eq. 3.27})$$

While Eq. (3.27) is the basic definition of friction factor, the pressure drop  $\Delta p$  for internal flow through the ducts can be calculated from Eq. (3.28) as below:

$$\Delta p = \frac{2f_F L G^2}{2D_h} \quad (\text{Eq. 3.28})$$

where:

$G$  = Exchanger flow-stream mass velocity ( $\text{W}/A_c$ )

$L$  = Total heat exchanger flow length

$D_h$  = Hydraulic Diameter of any internal passage and defined as before

$f_F$  = Fanning friction factor as defined in Eq. (3.27)

$u$  = Flow velocity (see more details below) in direction of fluid flow

$\tau_s$  = Shear Stress at the inside pipe wall

The wall shear stress can be related to the pressure loss by multiplying the wall shear stress by the wall area ( $2\pi r_h L$  for a pipe) and dividing by the cross-sectional flow area ( $\pi r_h^2$  for a pipe), where  $r_h$  is Hydraulic radius as defined above (Sect. 3.3). Thus the Fanning Friction Factor can be written as presented in Eq. (3.28).

Note that there is a difference between Fanning Friction Factor  $f_F$  and Darcy Friction Factor  $f_D$  that is explained below and pressure drop  $\Delta p$  in terms of Darcy Friction Factor is shown as Eq. (3.28). Bear in mind that Darcy Friction Factor is four times the Fanning Friction Factor  $f_D = 4f_F$ .

Also note that Darcy Friction Factor is sometimes called as Darcy-Weisbach Friction Factor or Moody Friction Factor as well. Also one should know that, the Darcy-Weisbach equation is a phenomenological formula obtainable by *dimensional analysis*. See the book Dimensional Analysis and Self-Similarity Methods for Engineers and Scientists by Zohuri [32].

The friction factor  $f_D$  or flow coefficient  $\lambda$  is not a constant and depends on the parameters of the pipe and the velocity of the fluid flow, but it is known to high accuracy within certain flow regimes. It may be evaluated for given conditions by the use of various empirical or theoretical relations, or it may be obtained from published charts. These charts are often referred to as Moody diagrams, after L.F. Moody, and hence the factor itself is sometimes called the Moody friction

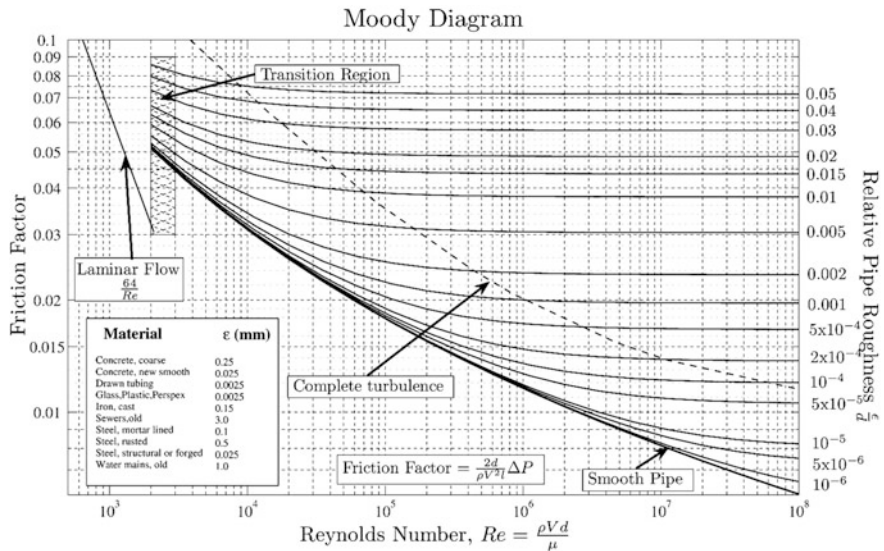


**Fig. 3.60** A typical moody diagram for different materials

factor. It is also sometimes called the Blasius friction factor, after the approximate formula he proposed. A typical Moody diagram is plotted in Fig. 3.60.

So in summary, the Darcy friction factor,  $f_D$ , is usually selected from a chart known as the Moody diagram. The Moody diagram is a family of curves that relate the friction factor,  $f_D$ , to Reynolds number,  $Re$ , and the relative roughness of a pipe,  $\epsilon/D_h$ , where  $\epsilon$  is known as Absolute Pipe Roughness. Table 3.6 taken from Binder (1973) [35] shows some values of this roughness for certain materials where the pipe is made new, and aged pipes typically exhibit a rise in apparent roughness. In some cases this rise can be very significant.

Alternatively, the Darcy Friction Factor is related to Manning's Friction Factor  $n$  through the following relationship:

$$n = \varphi r_h^{1/6} \sqrt{\frac{f_D}{8g}} \quad (\text{Eq. 3.29})$$

where

$n$  = Manning Friction Factor

$\varphi$  = Constant of 1.00 for metric and 1.49 for English units

$r_h$  = Hydraulic Radius

$f_D$  = Darcy Friction Factor

Note that, for laminar (Reynolds number  $Re$  about 1000 and below) flows, it is a consequence of Poiseuille's law that  $f_D = 64/Re$ , where  $Re$  is the Reynolds number calculated by substituting for the characteristic length of the hydraulic diameter of the pipe, which equals the inside diameter for circular pipe geometries.

**Table 3.6** Value of absolute roughness for certain materials that pipe is made of [35]

Pipe material	Absolute roughness, $\epsilon$	
	$\times 10^{-6}$ feet	Micron (unless noted)
Drawn brass	5	1.5
Drawn copper	5	1.5
Commercial steel	150	45
Wrought iron	150	45
Asphalted cast iron	400	120
Galvanized iron	500	150
Cast iron	850	260
Wood stave	600–3000	0.2–0.9 mm
Concrete	1000–10,000	0.3–3 mm
Riveted steel	3000–30,000	0.9–9 mm

For turbulent flow, methods for finding the friction factor  $f$  include using a diagram such as the Moody chart; or solving equations such as the Colebrook–White equation, or the Swamee–Jain equation. While the diagram and Colebrook–White equation are iterative methods, the Swamee–Jain equation allows  $f_D$  to be found directly for full flow in a circular pipe. Details of all these Equations and Laws/Rules are beyond the scope of this book but we encourage folks to refer to the book by (Zohuri and Fathi) [30] or others that can be found in the open and public domain.

Another note can be made here, that most charts or tables indicate the type of friction factor, or at least provide the formula for the friction factor with laminar flow. If the formula for laminar flow is  $f_F = 16/Re$ , it is the Fanning Factor,  $f_F$ , and if the formula for laminar flow is  $f_D = 64/Re$ , it's the Darcy–Weisbach factor,  $f_D$ .

Which friction factor is plotted in a Moody diagram may be determined by inspection if the publisher did not include the formula described above:

1. Observe the value of the friction factor for laminar flow at a Reynolds number of 1000.
2. If the value of the friction factor is 0.064, then the Darcy friction factor is plotted in the Moody diagram. Note that the nonzero digits in 0.064 are the numerator in the formula for the laminar Darcy friction factor:  $f_D = 64/Re$ .
3. If the value of the friction factor is 0.016, then the Fanning friction factor is plotted in the Moody diagram. Note that the nonzero digits in 0.016 are the numerator in the formula for the laminar Fanning friction factor:  $f_F = 16/Re$ .

The procedure above is similar for any available Reynolds number that is an integral power of ten. It is not necessary to remember the value 1000 for this procedure—only that an integral power of ten is of interest for this purpose.

Further analysis of Eq. (3.28) indicates that there is no direct temperature dependency in that equation nor can one be seen in the expression for friction factor Eq. (3.27). Therefore, the  $f_F$  data determined at one temperature/pressure level are directly usable at other circumstances that deal with the temperature/pressure level. On the other hand studies by other researchers show that Colburn

Factor  $j$  (sometimes is shown as  $j_H$ ), defined in Eq. (3.35) further down in this section, and Fanning Friction Factor  $f_F$  are strong functions of fin geometries like fin height, fin spacing, fin thickness etc. See reference by (Zohuri and Fathi) [30].

Since fins are available in varied shapes, it becomes necessary to examine each configuration, as shown in Figs. 3.4, 3.22, 3.25, and finally Fig. 3.45, individually to determine the heat transfer and flow friction characteristic (i.e., Fanning Friction Factor  $f_F$ ) for the specific surface. For a given fine geometry, in general, increase in heat transfer duty performance is associated with increase in flow friction (i.e., friction head) and vice versa.

Generally speaking, the ratio of  $j/f_F$  is taken as a measure of the goodness of the fin surface. Though the preferred fin geometry would have high heat transfer coefficient without correspondingly increased pressure penalty, the selection of particular fin geometry mainly depends on the process requirement; one can sacrifice either heat transfer or pressure loss at the cost of the other.

A fundamental requirement during heat exchanger design is the ability to predict heat transfer coefficients and pressure drop under the conditions of interest. Studies in the literature reporting on single and two phase fluid flow and heat transfer in compact heat exchangers are relatively few. However, extensive applications in process industries exist where the heat is transferred utilizing flows via confined spaces, which can provide more compact design and better performance.

Several features make compact heat exchangers attractive in industrial applications where the energy conservation, space and weight saving, and cost of manufacturing are important considerations. These features include high thermal effectiveness (ratio of actual heat transferred to the theoretical maximum heat which can be transferred), large heat transfer surface to volume ratio (surface area density), low weight per heat-transfer duty, opportunity for true counter flow operation, close temperature approach (as a result of the ability to design for true counter flow), design flexibility, and reduced fluid inventory. Flow mal-distribution and the design of headers to minimize mal-distribution remain inherent problems in the application of such heat exchangers, especially in the case of phase-change heat transfer. The potential for fouling of small flow passages represents a major disadvantage in the use of compact heat exchangers. However, fouling should not be a problem in applications that involve clean fluids.

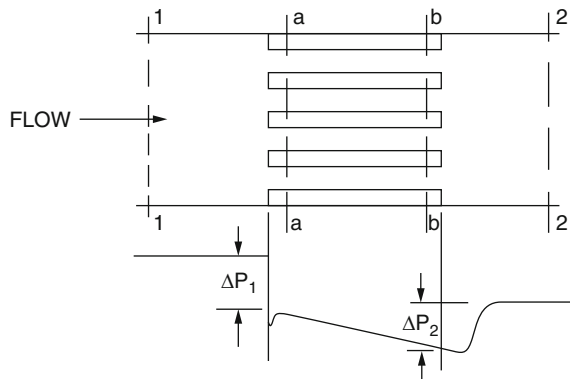
To do further analysis of pressure drop in terms of Darcy Friction Factor, we can start by: given the friction head loss  $h_f$  in a pipe one can relate the pressure loss  $\Delta p$  due to this friction as the height of a column of fluid as Eq. (3.30) below, using Fig. 3.61 as well.

$$\Delta p = \rho g h_f \quad (\text{Eq. 3.30})$$

where  $\rho$  is the density of the fluid in this case.

The pressure drop  $\Delta p$  of fluid through a surface can be calculated as a function of the Darcy-Weisbach friction factor  $f_D$  (some text books show this as  $f_d$  or  $f_D$  so do not be confused by Fanning friction factor  $f_F$ ,  $f_c$  or  $C_f$ ) by Eq. (3.30), neglecting for

**Fig. 3.61** Entrance pressure drop and exit pressure rise in a heat exchanger core. (Courtesy of Kay and London) [17]



practical purpose, the relatively small contributions of entry and exit losses and flow acceleration.

$$\Delta p = \frac{1}{2} \rho u_{\text{mean}}^2 \frac{L}{D_h} f_D = f_F \left( \frac{L}{D_h} \right) 2 \rho u_{\text{mean}}^2 \quad (\text{Eq. 3.31})$$

where

$u_{\text{mean}}$  = the mean flow velocity (m/s), and with mass flow rate  $\dot{m}$ , it is equal to

$$u_{\text{mean}} = \frac{\dot{m}}{\rho A_c} \quad (\text{Eq. 3.32})$$

$\rho$  = flow density ( $\text{kg/m}^3$ )

$D_h$  = the hydraulic diameter of pipe (m)

$L$  = the pipe length (m)

$A_c$  = the flow area that varies with flow length (m)

$f_D$  = Darcy Friction Factor a dimensionless coefficient of either laminar or turbulent flow

$g$  = Acceleration due to gravity ( $\text{m/s}^2$ )

Since the pressure loss equation can be derived from the head loss equation by multiplying each side by  $\rho$  and  $g$ .

Substituting Eq. (3.32) into Eq. (3.31) for velocity  $u$ , we have

$$\frac{2\rho\Delta\rho}{\dot{m}^2} = f_F \frac{4L}{D_h A_c} \quad \text{Constant for given conditions} \quad (\text{Eq. 3.33})$$

And if we consider two surfaces denoted by 1 and 2, with given pressure drop, and we have dropped the subscript F for Fanning Friction of  $f_F$ , we can write:

$$\frac{(A_c^2)_1}{(A_c^2)_2} = \frac{f_1 L_1 (D_h)_2}{f_2 L_2 (D_h)_1} \quad (\text{Eq. 3.34a})$$

Therefore, if the thermal performance is ignored, the flow areas for two surfaces 1 and 2 with similar friction factors are the same if the ratios  $L/D_h$  are the same.

And for given conditions the product  $\text{Pr}^{2/3}N$  is fixed, therefore to compare two surfaces suffixed by 1 and 2, we can write:

$$\frac{L_1}{L_2} = \frac{d_{h,1}j_2}{d_{h,2}j_1} \quad (\text{Eq. 3.34b})$$

Equation (3.34b) shows the flow length is directly proportional to hydraulic diameter while it is inversely proportional to  $j$  factor, which is Reynolds number dependent.

If we consider the dimensionless  $j$ , or Colburn factor in terms of Nusselt number  $\text{Nu} = \frac{\alpha d_h}{\lambda}$ , Reynolds number  $\text{Re}$  and Prandtl number  $\text{Pr}$  as defined in Eq. (3.11) then we can write :

$$j = \frac{\text{Nu}}{\text{Re}\text{Pr}^{1/3}} = \text{St}\text{Pr}^{2/3} \quad (\text{Eq. 3.35})$$

where  $\text{St} = \frac{\alpha}{Gc_p}$  is Stanton number and where  $\alpha$  is non-dimensionalized in terms of mass velocity  $G$ . Note that for a fixed  $G$ ,  $j$  is proportional to  $\alpha$ . Substituting the value of Nusselt number, Eq. (3.35) in terms of  $\alpha$ , reduces to:

$$\begin{cases} \frac{\alpha D_h}{\lambda} = \frac{u D_h}{\nu} j \text{Pr}^{1/3} \\ \text{and} \\ \alpha = \frac{\dot{m}}{\rho \nu} \lambda \text{Pr}^{1/3} \frac{j}{A_c} \end{cases} \quad (\text{Eq. 3.36})$$

Assuming the specified load  $q$  is given by the heat transfer and the rate equation for either side of exchanger analogous to Eq. (3.16) is given as:

$$Q = \alpha A \overline{\Delta T} = \dot{m} c_p (T_2 - T_1) \quad (\text{Eq. 3.37})$$

Manipulation of Eqs. (3.37) and (3.36) and given the value for Nusselt number, we obtain the following relationship:

$$j = \frac{A_c}{A} \text{Pr}^{2/3} N \quad (\text{Eq. 3.38})$$

where  $N = \text{NTU}$  (Number of Thermal Unit).

If we recall the relationship for hydraulic diameter  $D_h$  as:

$$D_h = \frac{4A_c L}{A} \quad (\text{Eq. 3.39})$$

Then we have an alternative equation form for Eq. (3.38) as:

$$j = \frac{D_h}{4L} \Pr^{2/3} N \quad (\text{Eq. 3.40})$$

Now combining Eqs. (3.33) and (3.40), we produce the *core mass velocity equation*, and it can be written as:

$$\left\{ \begin{array}{l} \frac{2\rho\Delta\rho}{\dot{m}^2} = \frac{f_F \Pr^{2/3} N}{jA_c^2} \\ \text{and} \\ \frac{G^2}{2\rho\Delta\rho} = \frac{j/f_F}{\Pr^{2/3} N} \end{array} \right. \quad (\text{Eq. 3.41})$$

$G(\dot{m}/A_c)$  is the mass velocity as per Eq. (2.13)  $\dot{m}/A_c$ . As mentioned,  $G$ , and therefore flow area  $A_c$  can be closely estimated from design specification methodology, and this equation, with the assumption of a typical value  $j/f_F$  ( $f$  is Fanning friction factor) is often used as a starting point for preliminary sizing as we said before [32].

Note that the basic elements of effect of the surface on thermal design, embodied in Eqs. (3.40) and (3.41) above, are as follows:

- that flow length decreases as hydraulic diameter decreases
- that flow area is largely independent of hydraulic diameter

Thus if performance specification includes the pressure drop, as is normally the case, then increasing compactness only implies the reduction of flow length, with a change of shape, or aspect ratio, of the active block. In practice, this reduction in flow length can make longitudinal conduction a problem to be taken into account. In terms of comparing surface 1 and 2, based on Eqs. (3.33) and (3.34b), we can deduce the following equation:

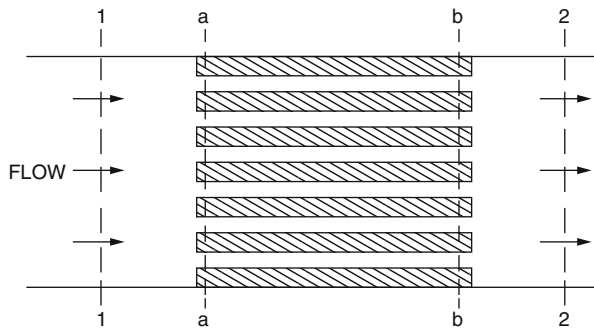
$$\frac{(A_c)_1}{(A_c)_2} = \left[ \frac{f_1}{f_2} \cdot \frac{j_2}{j_1} \right]^{1/2} = \left( \frac{j_2/f_2}{j_1/f_1} \right)^{1/2} \quad (\text{Eq. 3.42})$$

The form of Eq. (3.34a, 3.34b) gives rise to the description of the ratio  $j/f$  as the *Flow Area Goodness Factor* (London) [37].

By now, you are getting a fair idea about one of the design criteria in Sect. 3.6, as part of thermal energy transfer for the process of heat application in enhanced mode, we need information provided by Eq. (3.40) to be able to manufacture the heat transfer surface and testing to collect the correlation data in order to determine the basic performance of an enhanced surface for heat transfer in a compact heat exchanger.

Per our opening argument at the beginning of Sect. 3.7.1.4, we argue that in the design of liquid-to-liquid heat exchangers, accurate knowledge of the friction

**Fig. 3.62** Heat exchanger core model for pressure drop analysis. (Courtesy of Kay and London) [17]



characteristics of the heat transfer surface in not that important due to the low power requirement for pumping of liquids with high-density; however, in the case of gas fluids type media for heat transfer purpose—due to their nature of low density—the friction power per unit mass flow rate plays an important role and it will greatly multiply. Thus, to the designer, the friction characteristic of the surface assumes an importance equal to that of the heat transfer characteristic. So we are going to establish further details of pressure drop equations for core pressure drop based on fluid pumping power, which is a design constraint in many applications of these types of Compact Heat Exchangers (CHEs).

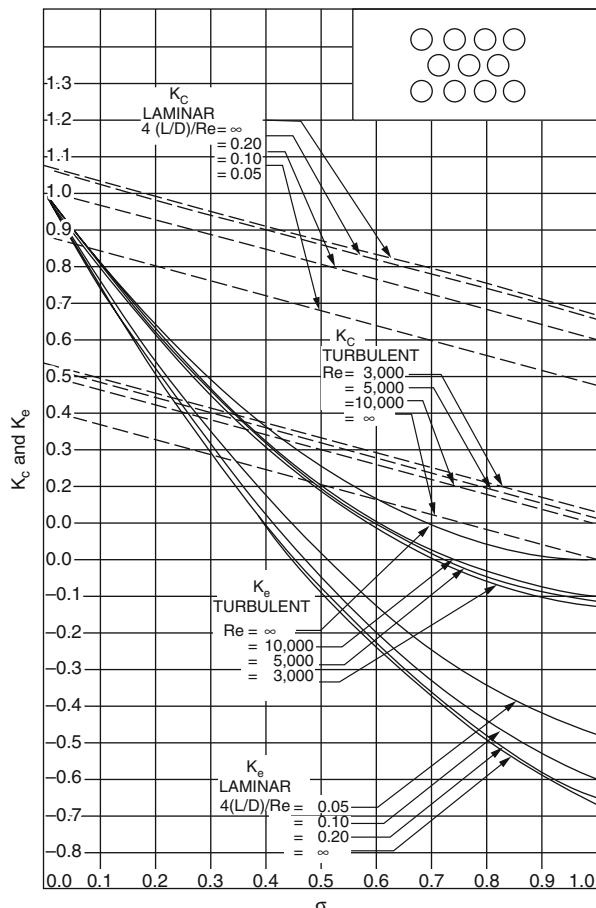
Considering Fig. 3.62, where exchanger flow-stream mass velocity  $G$  ( $\dot{m}/A_c$ ) is based on the minimum free-flow area in the core and per our previous definition  $A_c$  is exchanger minimum free-flow area, or  $pA_{fr}$  for matrix surfaces, for gas flow compact heat exchanger applications we can establish the pressure drop equation for the core pressure drop.

Using Fig. 3.62 again, the pressure changes from section 1 to  $a$  and from  $b$  to 2 are very small relative to the total pressure; thus  $v_a \approx v_1$  and  $v_b \approx v_2$  and  $v$  are specific volume for  $a$  and  $b$  point and section 1 and 2.

As we said the fluid pumping power is a design constraint in many applications and this pumping is proportional to the pressure drop in the exchanger in addition to the pressure drops associated with inlet or outlet headers and their entrance ( $K_c$ ) and exit ( $K_e$ ) loss coefficients, respectively, due to the pressure drop at the entrance and pressure rise at the exit, manifolds, nozzles, or ducting. Now we need to define and derive these two parameters of Entrance Loss  $K_c$  (also known as Contraction Loss) and Exit Loss  $K_e$  (also known as Expansion Loss) coefficients. Both are dimensionless quantities and functions of the contraction and expansion geometry and, in some cases, of the Reynolds number in the tubes of the exchangers. Now with the help of Fig. (3.62) the following discussions can be expressed.

When compact heat exchangers (CHEs) are installed typically they follow a flow contraction at the heat exchanger core entrance and flow expansion rules at the core exit. More often a right angle or abrupt contraction and expansion are used as basic rules, and these introduce additional flow-stream pressure drops that are known as entrance and exit effects. The designers of these exchangers have to be able to predict these additional losses.

**Fig. 3.63** Entrance and exit pressure loss coefficients for multiple-circular-tube compact heat exchanger core with abrupt contraction entrance and abrupt expansion exit [17]

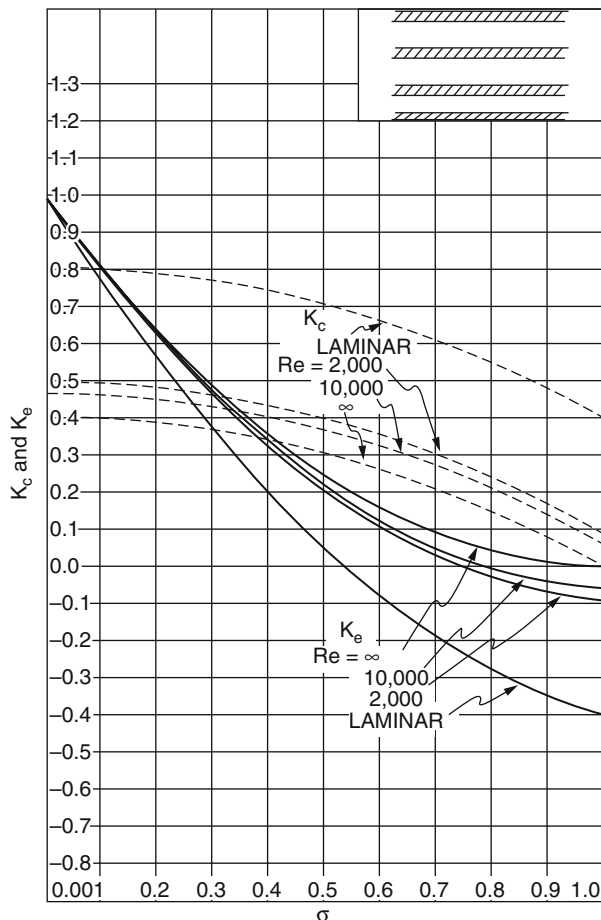


The prediction of such abilities have been investigated both analytically and experimentally by Kays [37] for laminar flows regimes or low Reynolds number and for single and multiple flow arrangement tube systems. The results are plotted by a series of graphs that are presented in the book by Kays and London [17] and regenerated here as Figs. 3.63, 3.64, 3.65, and 3.66 and these figures are found to be very important and useful for the design of a compact heat exchanger of desired application.

Figure 3.62 illustrates the entrance pressure drop and the exit pressure rise characteristics of flow through a heat exchanger core. The pressure drop at the entrance is composed of two parts which have been arbitrary separated as follows:

1. The pressure drop which takes place due to flow-area change alone, without friction.
2. The pressure loss due to the irreversible free expansion that always follows the abrupt contraction, which is due to separation of the boundary layer as

**Fig. 3.64** Entrance and exit pressure loss coefficients for a multiple-tube-flat-duct compact heat exchanger core with abrupt-correction entrance and abrupt-expansion exit [17]



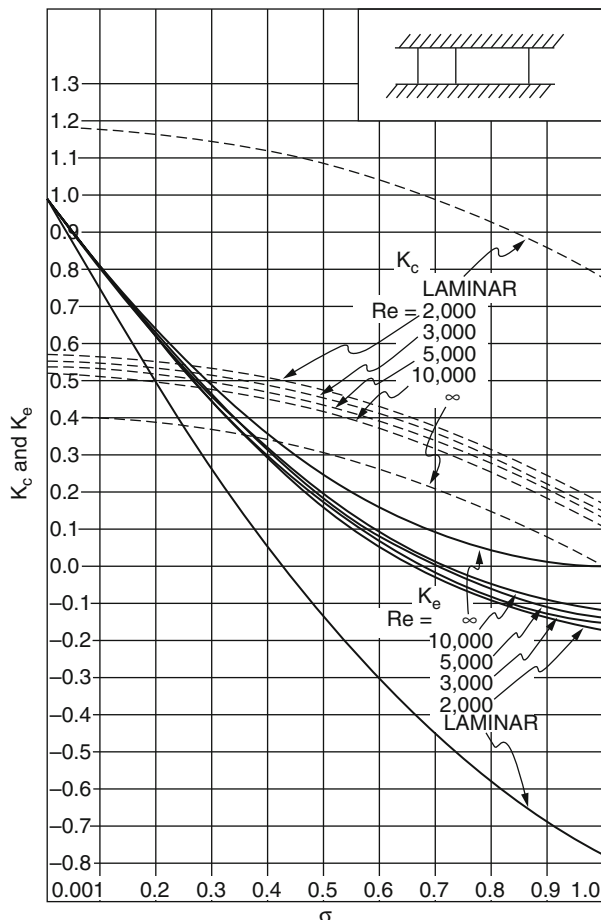
characterized by the Vena Contracta, and the consequent pressure change that arises from the momentum rate associated with changes in the velocity profile downstream from the Vena Contracta.

Although the principle applications under consideration may involve gas flow, density changes in the usual case are sufficiently small that a constant-density treatment is satisfactory [17].

The *Entrance Pressure Drop*  $\Delta p_1$  can then be demonstrated as

$$\frac{\Delta p_1}{\rho} = \frac{u^2}{2g_c} [(1 - \sigma^2) + K_c] \quad (\text{Eq. 3.43})$$

**Fig. 3.65** Entrance and exit pressure loss coefficient for a multiple-square-tube compact heat exchanger core with abrupt-contraction entrance and abrupt-expansion exit [17]



where in this equation:

$u$  = Velocity in the smaller or tubes, i.e., inside the heat exchanger core, and  
 $\sigma$  = Core free-flow to frontal-area ratio or it can account for ratio of minimum free flow area to frontal area

$K_c$  = Contraction loss coefficient for flow at heat exchanger entrance, which is a dimensionless quantity

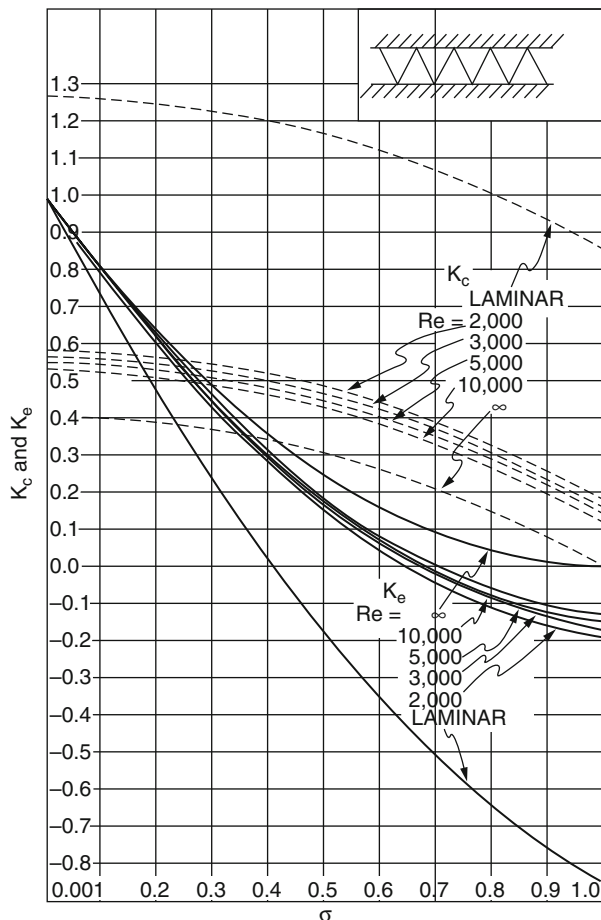
$g_c$  = Gravitational effect or proportionality factor in Newton's second law

$\rho$  = Flow density

The *Exit Pressure Rise*  $\Delta p_2$  is similarly composed of two parts and they are:

1. Pressure rise which takes place due to area change alone, without friction presence, and is identical to the corresponding term in the entrance pressure drop as shown in Eq. (3.43).

**Fig. 3.66** Entrance and exit pressure loss coefficients for a multiple-triangle-tube compact heat exchanger core with abrupt-correction entrance and abrupt-expansion exit [17]



2. Pressure loss associated with the irreversible free expansion and momentum changes following an abrupt expansion, and this term in the pressure case subtracts from the other, thus we can derive the following relationship

$$\frac{\Delta p_2}{\rho} = \frac{u^2}{2g_e} [(1 - \sigma^2) - K_e] \quad (\text{Eq. 3.44})$$

In this equation the variables are defined as above except that  $K_e$  is now the expansion loss coefficient, or abrupt expansion or exit coefficient for flow at compact heat exchanger exit, and it is a dimensionless quantity.

As we mentioned above both  $K_c$  and  $K_e$  are functions of the contraction and expansion geometry of heat exchangers tubes that they are made of and in some cases of Reynolds number in those tubes. On the other hand their dependency on Reynolds number arises from the influence of the velocity profile in the tubes on the momentum rates and from the resulting effect on the change of momentum at the

entrance and exit [17] and sufficient confirmation via experimental procedure has been established by Kays [37] for the validity of the analysis that has taken place to derive both Eqs. (3.43) and (3.44)—at least to a precision adequate for the present application.

The fundamental assumption for deriving these two equations both experimentally and analytically is based upon uniform velocity in the large duct leading to the core, of uniform velocity in the leaving duct, but a fully established velocity profile in the small tubes of the core. This assumption is generally justified by Kays [37] in heat exchanger core analysis because the Reynolds number in the core tubes is invariably many times smaller than that in the entering and leaving ducts. Further discussion of these analyses and their assumption can be found in Kays and London's book [17].

Now establishing the momentum equation for fluid flow based on the conservation of momentum definition using Control Volumes (Zohuri and Fathi) [30] for steady state and using Fig. 3.67 for flow through core of one passage in a heat exchanger and integrating this momentum equation for the flow upstream assuming this upstream flow is idealized as uniform flow, we can derive the total pressure drop on one side of the exchanger thorough the core for most compact heat exchangers as follows (i.e., two different format based on Refs. [9] and [17]):

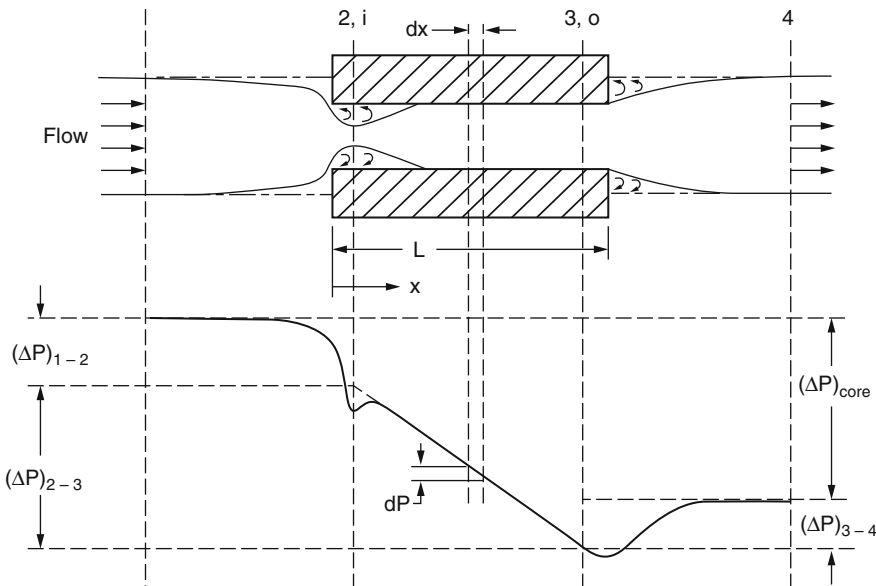


**Fig. 3.67** Pressure drop components associated with one passage of a plate-fin compact heat exchanger [6]

$$\frac{\Delta p}{p_i} = \frac{G^2}{2g_c \rho_i p_i} \left[ \underbrace{(1 - \sigma^2 + K_c)}_{\text{entrance effect}} + \underbrace{f \frac{L}{r_h} \rho_i \left( \frac{1}{\rho} \right)_m}_{\text{core friction}} + \underbrace{2 \left( \frac{\rho_i}{\rho_o} - 1 \right)}_{\text{flow acceleration}} - \underbrace{(1 - \sigma^2 - K_e) \frac{\rho_i}{\rho_o}}_{\text{exit effect}} \right] \text{ Ref. [9]} \\ (\text{Eq. 3.45a})$$

(Reference is Fig. 3.67)

$$\frac{\Delta p}{p_i} = \frac{G^2 v_i}{2g_c p_i} \left[ \underbrace{(1 - \sigma^2 + K_c)}_{\text{entrance effect}} + \underbrace{f \frac{A}{A_c} \frac{v_m}{v_i}}_{\text{core friction}} + \underbrace{2 \left( \frac{v_o}{v_i} - 1 \right)}_{\text{flow acceleration}} - \underbrace{(1 - \sigma^2 - K_e) \frac{v_o}{v_i}}_{\text{exit effect}} \right] \text{ Ref. [29]} \\ (\text{Eq. 3.45b})$$

(Reference is Fig. 3.62)

Note that: porosity  $\mathbf{p}$  replaces  $\sigma$  for matrix surface and volume is presented by  $v$  with related indices for each condition.

In Eq. (3.45a, 3.45b) the parameters are defined as before and  $f$  or as shown as  $f_F$  before is Fanning friction factor for the surface and subscript  $m$  is indication mean value for the parameter that posses it. Again the values of  $K_c$  and  $K_e$  are depicted in Figs. 3.63 through 3.66 for four different entrance flow passage geometries [17].

Further analysis of Eq. (3.45a, 3.45b) indicates that its derivation was based on the assumption of an idealized uniform flow for upstream passage in a Plate-Fin Compact Heat Exchanger as it enters the passage and it contracts due to an area change. In the core, the fluid encounters skin friction and it may also experience form drag at the leading and trailing edges of an interrupted fin surface, while flow separation takes place at the entrance, followed by an irreversible free expansion. The flow may also experience internal contractions and expansion within the core as in a perforated fine core [6]. If heating or cooling is processed in the core, as in any compact heat exchanger, the fluid density and mean velocity change along the flow path length. The flow acceleration or deceleration depends upon the heating or cooling under these processes. Separation of flow at the exit takes place, followed by an expansion due to the area change (see Eq. (3.35b) format) [6].

However, for flow normal to tube banks or through wire matrix surfaces, if it is utilized in periodic-flow-type compact heat exchangers, entrance and exit loss effects are accounted for in the friction factor, and Eqs. (3.45a) and (3.45b) with  $K_c - K_e = 0$  reduces to the following form.

$$\frac{\Delta p}{p_i} = \frac{G^2}{2g_c \rho_i p_i} \left[ \underbrace{(1 + \sigma^2) \left( \frac{\rho_i}{\rho_o} - 1 \right)}_{\text{flow acceleration}} + \underbrace{f \frac{L}{r_h} \rho_i \left( \frac{1}{\rho} \right)_m}_{\text{core friction}} \right] \text{ (Eq. 3.46a)}$$

$$\frac{\Delta p}{p_i} = \frac{G^2}{2g_c p_i} v \left[ \underbrace{(1 + \sigma^2) \left( \frac{v_o}{v_i} - 1 \right)}_{\text{flow acceleration}} + \underbrace{f \frac{A}{A_c} \frac{v_m}{v_i}}_{\text{core friction}} \right] \quad (\text{Eq. 3.46b})$$

If we compare Eq. (3.45a) with Eq. (3.45b), we note that  $(A/A_c) = (L/r_h)$  as per definition of the hydraulic radius as before and specific volume of  $v_i = (1/\rho_i)$  and  $v_o = (1/\rho_o)$  for entrance and exit tube respectively, which similarly can be applied to sets of Eqs. (3.46a) and (3.46b) as well. Furthermore, using Fig. 3.67 as reference, we can write the following relation:

$$\frac{G^2 v_i}{2g_c p_i} = \frac{(V_i/2g_c)}{(p_i/p_i)} = \frac{\text{Dynamic head}}{\text{Static head}} \quad (\text{Eq. 3.47})$$

where  $V_i = G/\rho_i$  is the flow velocity entering the core, based on the minimum free-flow area, which defines  $G$  [17].

The correct mean specific volume  $v_m$  that both Eq. (3.45b) and Eq. (3.45b) require is calculated by the following relationship:

$$v_m = \frac{1}{A} \int_0^A v dA \quad (\text{Eq. 3.48})$$

where  $A$  is heat exchanger total heat transfer area on one side of it.

Now if we consider both Fig. 3.68 where the heat exchanger flow-stream mass velocity  $G$  ( $\dot{m}/A_c$ ) is based on the minimum free flow area in the core and Fig. 3.69 as a reference for the flow temperature conditions that are pictured in them, for a magnitude of unity for  $C_{\min}/C_{\max}$  (see Fig. 3.68 and more details in Sect. 2.11), we see that flow-stream temperatures vary linearly with area in a true counterflow

**Fig. 3.68** Heat exchanger core model for pressure drop analysis. (Courtesy of Kay and London) [17]

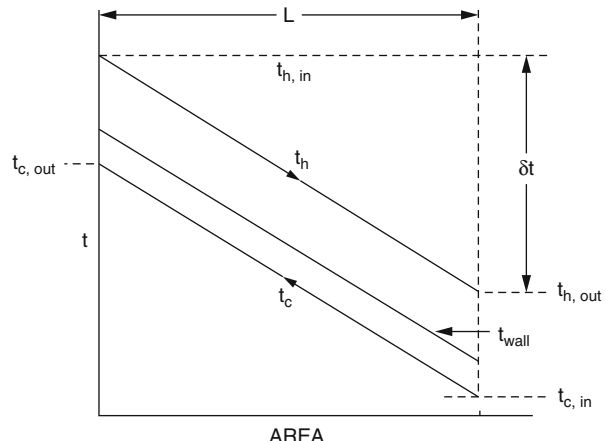
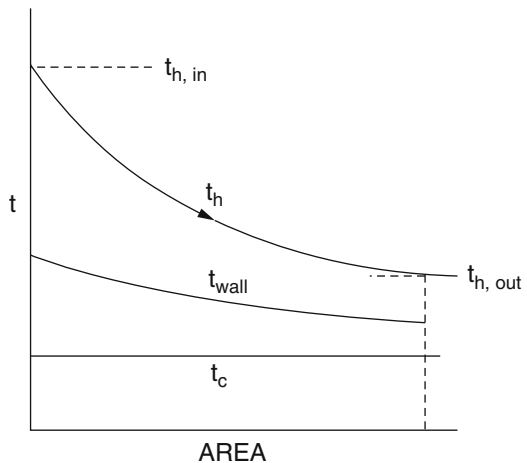


**Fig. 3.69** Temperature distribution in a heat exchanger of any flow arrangement with  $C_c \gg C_h$ . (Courtesy of Kay and London) [17]



arrangement, and also has a good approximation for flow arrangements other than parallel flow, as a result we can write:

$$\frac{v_m}{v_i} = \frac{p_i}{p_{ave}} \frac{T_{ave}}{T_i} \quad (\text{Eq. 3.49})$$

Reference is Fig. 3.67 for this equation  
or

$$v_m \approx \frac{v_i + v_o}{2} \quad (\text{Eq. 3.50})$$

In all these mathematical relationships  $T_{ave}$  and  $p_{ave}$  are arithmetic averages of the terminal magnitudes and in addition the following definitions are expressed

$C$  = Flow-stream capacity rate ( $\dot{m} c_p$ )

$C_{min}$  = Minimum of  $C_c$  or  $C_h$

$C_{max}$  = Maximum of  $C_c$  or  $C_h$

$C_c$  = Flow-stream capacity rate of cold-side fluid

$C_h$  = Flow-stream capacity rate of hot-side fluid

Analyzing Fig. 3.69, if the wall temperature is essentially uniform as in the water cooled intercooler, the condenser, or the evaporator, Eq. (3.50) reduces to the following form:

$$\frac{v_m}{v_i} \approx \frac{p_i}{p_{ave}} \frac{T_m}{T_i} \quad (\text{Eq. 3.51})$$

where  $p_{\text{ave}}$  is the arithmetic average of the terminal magnitudes and  $T_m$  is related to the log-mean-temperature difference between the fluid with the changing temperature and constant fluid temperature  $\Delta T_m$  by:

$$T_m = T_{\text{const}} \pm \Delta T_m \quad (\text{Eq. 3.52})$$

Here, for the conditions shown in Figs. 3.68 and 3.69, the plus sign is used and

$$\text{LMTD} = \Delta t_m = \frac{(t_{h,\text{in}} - t_c) - (t_{h,\text{out}} - t_c)}{(t_{h,\text{in}} - t_c)/(t_{h,\text{out}} - t_c)} = \frac{t_{h,\text{in}} - t_{h,\text{out}}}{N_{tu}} \quad (\text{Eq. 3.53a})$$

or

$$\text{LMTD} = \Delta t_m = \frac{\Delta t_{h,\text{in}} - \Delta t_{h,\text{out}}}{\ln(\Delta t_{h,\text{in}}/\Delta t_{h,\text{out}})} \quad (\text{Eq. 3.53b})$$

Here  $N_{tu}$  is the number of heat transfer units of an exchanger or heat transfer parameter  $\frac{AU_{\text{avg}}}{q_{\text{max}}}$  that is defined by the following equation as:

$$N_{th} = \frac{AU_{\text{avg}}}{Q_{\text{max}}} = \frac{1}{C_{\min}} \int_0^A u dA \quad (\text{Eq. 3.54})$$

In this equation  $U_{\text{avg}}$  is the average unit overall thermal conductance while  $A$  is heat exchanger total heat transfer surface area on one side, and  $Q_{\text{max}}$  is maximum heat transfer rate.

A minus sign will be used out of Eq. (3.52) and a similar expression as Eq. (3.53a, 3.53b) can be generated with  $t_c$  in place of  $t_h$  if  $t_h$  were essentially constant and  $t_c$  varied as  $C_h \gg C_c$ .

Again, the mass velocity  $G$  in Eq. (3.45a, 3.45b) is based on the *minimum free-flow area*, consistent with the definition of Fanning friction factor employed here.

Entrance and exit effects in Eq. (3.45a, 3.45b) normally provide only a small contribution to the overall pressure drop in the usual exchanger design since  $A/A_c$  may be quite large, the core fraction term in Eq. (3.45a, 3.45b) controls the magnitude of  $\Delta p$ . Consequently, high accuracy in the evaluation of  $K_c$  and  $K_e$  is not required. Figures 3.63 through 3.66 illustrates the magnitudes of the entrance and exit loss coefficients as a function of flow geometry and Reynolds number as discussed before.

The Fanning friction factor  $f = f_F$  that is used in Eq. (3.45a, 3.45b) is affected by the variation of fluid properties such as density  $\rho$  and viscosity coefficient  $\mu$  over the flow cross section, as well as variation in the flow direction.

Propping the pressure drop further, we can establish another form of it for a liquid with any type of flow arrangement as discussed before, or for a perfect gas with  $C^* = 1$  and for any flow arrangement, except parallel flow, the mean specific volume  $v_m$  or  $(1/\rho_m)$  using Fig. 3.67 as reference, can be expressed as follows:

$$\left(\frac{1}{\rho}\right)_m = v_m = \frac{v_i - v_o}{2} = \frac{1}{2} \left( \frac{1}{\rho_i} - \frac{1}{\rho_o} \right) \quad (\text{Eq. 3.55})$$

Here  $v$  represents specific volume in  $\text{m}^3/\text{kg}$  or  $\text{ft}^3/\text{lb}_m$ . For a perfect gas with  $C^* = 0$  and any type of flow arrangement, Eq. (3.55) reduces to the new form:

$$\left(\frac{1}{\rho}\right)_m = \frac{\tilde{R}}{p_{ave}} T_m \quad (\text{Eq. 3.56})$$

where  $\tilde{R}$  is the gas constant in  $\text{J}/(\text{kg.K})$  or  $\text{ft}/(\text{lb}_m \cdot \text{R})$ ,  $p_{ave} = (p_i + p_0)/2$  is also known as the arithmetic average of the terminal magnitudes, and  $T_m$  is defined as per Eqs. (3.52), (3.53a), and (3.53b) as well as  $T_{\text{const}}$  again being the arithmetic average temperature of the fluid on the other side of the heat exchanger.

Generally, the core frictional pressure drop in Eqs. (3.45a) and (3.45b) is a dominating term that influences 90 % or more of pressure drop differential  $\Delta p$ , hence Eq. (3.45a, 3.45b) can be approximated to the following form:

$$\Delta p \approx \frac{4fLG^2}{2g_c D_h} \left(\frac{1}{\rho}\right)_m \quad (\text{Eq. 3.57})$$

All the terms in above equations are defined as before.

Note that, the entrance and exit losses in Eq. (3.45a, 3.45b) are important at low values of  $\sigma$  and  $L$  for a short core infrastructure, at high values of  $\text{Re}$ , and for gases; they are negligible for liquids, however bear in mind that the values of  $K_c$  and  $K_e$  that are illustrated in Figs. 3.63 through 3.66 do apply to long tubes for which flow is fully developed at the exit.

As per Shah [6], for partially developed flows,  $K_c$  is lower and  $K_e$  is higher than for fully developed flows and for interrupted surfaces, the flow generally is not fully developed. For highly interrupted fin geometries, the entrance and exit losses are generally small compared to the core pressure drop, and the flow is mixed very well; hence,  $K_c$  and  $K_e$  for  $\text{Re} \rightarrow \infty$  should represent a good approximation.

It is important to note that as part of the flow arrangement for an extended-surface compact heat exchange, where the Plate-Fin Compact Heat Exchangers (PFCHEs) fall into that class and type, cross-flow infrastructure design is the most common flow arrangement configuration. This is due to the fact that such infrastructure greatly simplifies the header design at the entrance and exit of each fluid and dealing with pressure drop analysis becomes more simplified based on the general form of Eqs. (3.45a) and (3.45b).

If the design configuration for this type of heat exchanger is demanding and desires a high heat exchanger effectiveness  $\varepsilon$  presented in Eq. (3.21) greater than 75–80 % as an example, then size of the cross-flow unit may become excessive and over all cross-counterflow multipass as part of the configuration or a pure counterflow unit may be preferred, see Fig. 3.70.

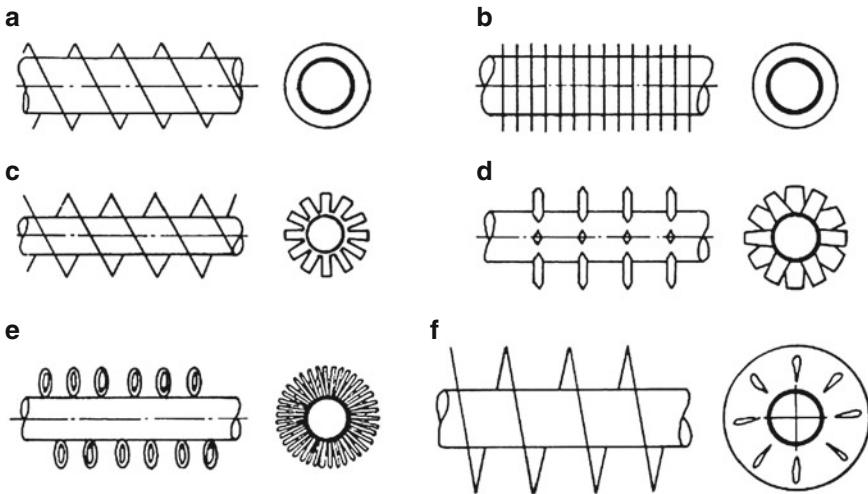


**Fig. 3.70** Individual finned tubes: (a) Helical, (b) annular (disk), (c) segmented, (d) studded, (e) wire loop, (f) slotted helical

However, such configuration imposes manufacturing difficulties associated with a true counterflow infrastructure for flow arrangement in a compact heat exchanger as it requires working fluids to be separated from each other at each end. Therefore, the header design is more complex and we are looking for a more simplified manufacturing of counter flow compact heat exchangers of the type known as PFCH. Bear in mind that multi-passing retains the header and ducting advantages of the simple cross-flow heat exchanger, while it is possible to approach the thermal performance of a counterflow unit. On the contrary, a parallel-flow arrangement having the lowest possible exchanger effectiveness of  $\varepsilon$  for a given Number of Transfer Units (NTU) is seldom used as a compact heat exchanger for single-phase fluids [6].

Consideration of Fig. 3.70 here reveals that each tube row consists of a contraction and an expansion due to the flow area change; thus, the pressure losses associated with a tube row within the core are of the same order of magnitude as those at the entrance with the first tube row and those at the exit with the last tube row. Consequently, the entrance and exit pressure drops are generally lumped into the friction factor  $f = f_F$  for individually finned tubes, and in the case of Eq. (3.45b) it reduces to the following form [6].

$$\frac{\Delta p}{p_i} = \frac{G^2}{2g_c p_i \rho_i} \left[ f \frac{L}{r_h} \rho_i \left( \frac{1}{\rho} \right)_m + 2 \left( \frac{\rho_i}{\rho_o} - 1 \right) \right] \quad (\text{Eq. 3.58})$$

Generalizing the fluid pumping power  $P$  as part of the design constraint in many applications, which is proportional to the pressure drop in the heat exchanger in addition to the pressure drops associated with inlet or outlet headers, manifolds,

nozzles, or ducting, this fluid pumping power with its relation to pressure drop can be written as follows for the heat exchanger:

$$P = \frac{\dot{m} \Delta p}{\rho} \approx \begin{cases} \frac{1}{2g_c} \frac{\mu}{\rho^2} \frac{4L}{D_h} \frac{\dot{m}^2}{A_o} f \text{Re} & \text{for laminar flow} \\ \frac{0.04}{2g_c} \frac{\mu^{0.2}}{\rho^2} \frac{4L}{D_h} \frac{\dot{m}^{2.8}}{A_o^{1.8} D_h^{2.8}} & \text{for turbulent flow} \end{cases} \quad (\text{Eq. 3.59})$$

In this equation the following are the symbols and parameters definitions:

$P$  = Fluid mass power as  $\dot{m} \Delta p / \rho$  (W or hp)

$\dot{m}$  = Fluid mass flow rate =  $\rho V_m A_o$  (kg/s or lb<sub>m</sub>/s)

$V_m$  = Fluid mean axial velocity between plates on one side m<sup>3</sup>, ft<sup>3</sup>

$\Delta p$  = Fluid static pressure drop on the side of a heat exchanger core (Pa, lb<sub>f</sub>/ft<sup>2</sup>)

$g_c$  = Proportionality constant in Newton's second law of motion ( $g_c = 1$  and is dimensionless in SI units;  $g_c = 32.174$  lb<sub>m</sub>·ft/(lb<sub>f</sub>·s<sup>2</sup>)

$A_o$  = Minimum free flow or open area or core free flow area m<sup>2</sup>, ft<sup>2</sup> and sometimes designated as  $A_c$

$D_h$  = Hydraulic diameter of flow passage =  $(4A_o L) / A$  =  $(4\sigma/\alpha)$  (m, ft)

$L$  = Fluid flow core length on one side of the exchanger (m or ft)

$f$  = Fanning friction parameter a dimensionless factor

$\rho$  = Density, for fluid (kg/m<sup>3</sup> or lbm/ft<sup>3</sup>)

$\mu$  = Fluid dynamic viscosity coefficient (Pa s or lb<sub>m</sub>/(h.ft))

Further analysis of both parts of Eq. (3.59) indicates that only the core friction term is considered in the right-hand side approximation for discussion purposes. Now consider the case of specified flow rate and geometry such as  $\dot{m}$ ,  $L$ ,  $D_h$ , and  $A_o$ . As a first approximation,  $f \text{Re}$  in the first term of Eq. (3.59) is constant for fully developed laminar flow, while Fanning friction factor  $f = 0.046 \text{Re}^{-0.2}$  is used to derive the second term in Eq. (3.59) for fully developed turbulent flow. It is obvious that  $P$  is strongly dependent on  $\rho$  in laminar and turbulent flow and on  $h$  in laminar flow and weakly dependent on  $\mu$  in turbulent flow. For high-density moderate-viscosity liquids, the pumping power is generally so small that it has only a minor influence on the design. For laminar flow of highly viscous liquids in large  $L/D_h$  heat exchangers, pumping power is an important constraint; and this is also the case for gases, both in turbulent and laminar flow, because of the great impact of  $1/\rho^2$ . Additionally, it can be mentioned that, when blowers and pumps are used for the fluid flow, they are generally head-limited, and the pressure drop itself can be a major consideration [6].

Additional pressure drop for a liquid flows heat exchangers comes into play as an extra term in case vertical flows passing through such exchanger may not be negligible when this pressure rises or drops and is referred to as "static head" and is given by:

$$\Delta p = \pm \frac{\rho_m g L}{g_c} \quad (\text{Eq. 3.60})$$

where the + sign choice stands for vertical up-flow which is equivalent to pressure drop due to the elevation change and the – sign choice is an indication of vertical down-flow which is equivalent to pressure rise. In this equation  $g$  is gravitation force and  $L$  is the heat exchanger length.

### 3.7.1.5 Compact Heat Exchanger Surface Selection Methodology

Another approach and option to Fig. 3.51 for design of a compact heat exchanger is presented in Fig. 3.71 where surface characteristics are imagined as part of the design process. A methodology of arriving at an optimum compact heat exchanger (CHE) design as a final output process for the application of the CHE is depicted in Fig. 3.72 as well. A final output may be used as an alternative to format a new problem as the input statement for a parametric iteration and study leading to an optimum design envelope for the overall system rather than just an optimum heat exchanger based on some arbitrary infrastructure based on initial specification for the considered application requirements. Figure 3.71 is an elaboration of Fig. 3.72, yet both figures are an alternate version of Figs. 3.51 and 3.52 for any general optimum design approach to compact heat exchanger; and neither of these figures altogether are a comprehensive design procedure and not true and actual steps, and any computer aided design (CAD) requires going through design iteration before converging to an optimum and specification for a true design application. Figure 3.71 is an improved version of 3.72 with two steps replacing the single surface characteristic in Fig. 3.71 compared to Fig. 3.72, and these two steps namely are, surface selection (two or more cases) and surface characteristics including heat transfer, flow friction, and geometrical characteristic of the surface selected [17].

As we know by now a variety of surfaces can be utilized by manufacturers in the design of compact heat exchanger (CHE) applications, where selection of such surface is a function of the quantitative and qualitative considerations. The quantitative consideration may include a performance comparison of heat exchanger surfaces and in the surface selection process make it impossible to fine-tune the selection of a surface from pressure drop and heat transfer consideration alone (Shah) [38].

Quantitative consideration arbitrarily defines a compact heat exchange surface as one that has an area density or heat exchanger compactness  $\beta$  greater than  $700 \text{ m}^2/\text{m}^3$  ( $213 \text{ ft}^2/\text{ft}^3$ ) as before. Figure 3.43 shows a spectrum of surface area density for heat exchangers. The range of surface area density and hydraulic diameter  $D_h$  is given for various types of heat exchanger surfaces, with the dividing line for compactness clearly marked.

Shah [38] summarizes over 30 different methods that have been proposed in the literature to compare the heat transfer and pressure drop characteristics of these surfaces and as he says, “A best performing surface thus selected may not be an optimum heat exchanger surface for a given application as explained by him”, as a result, the selection criteria for such surface should be as meaningful, direct, and simple as possible.

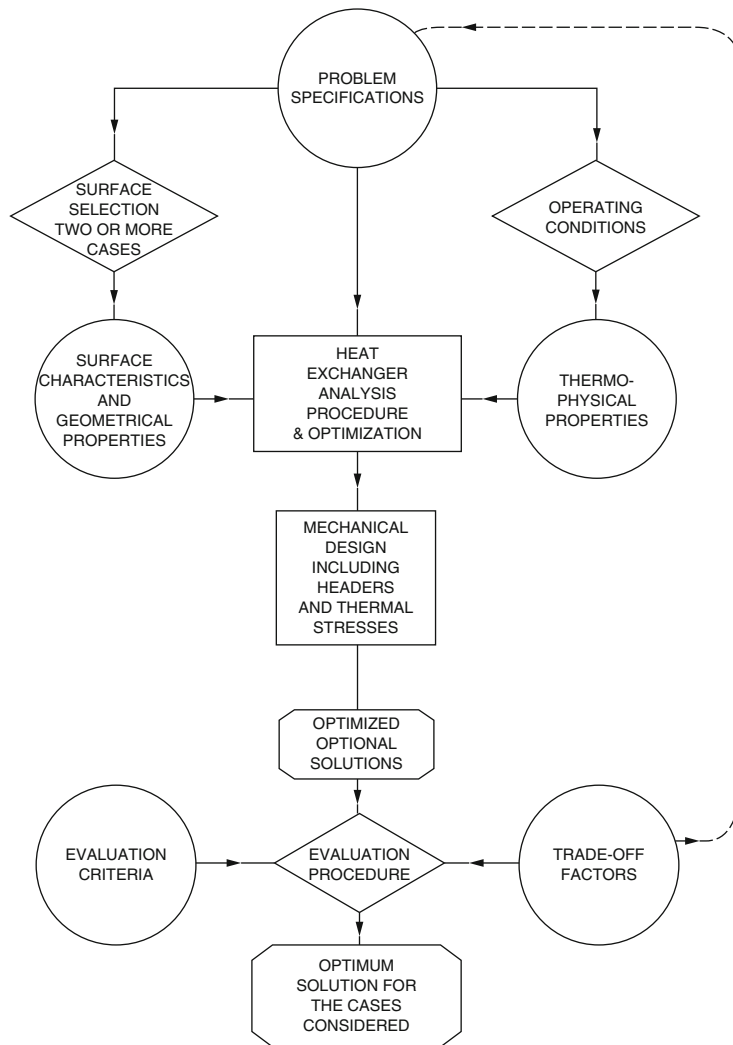


**Fig. 3.71** Methodology of compact heat exchanger design and optimization. (Courtesy of Kay and London) [17]

An appropriate surface selection is one of the most important aspects of compact heat exchanger design and there is no such thing as a surface that is best suited for all applications. Each particular application and objective is a strong variable of surface selection criteria; and as we said this selection should be in quantitative and qualitative steps which are based on designer and manufacture past experience and judgment, which is a function of the ability to build such surfaces, preventive maintenance requirements, performance reliability, safety, cost, and other related

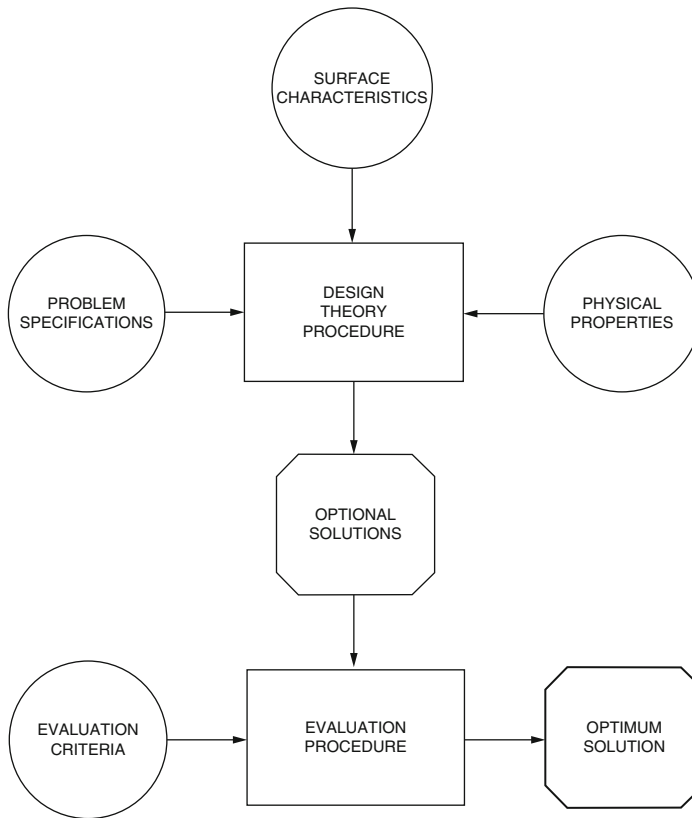


**Fig. 3.72** Methodology of compact heat exchanger design. (Courtesy of Kay and London) [17]

issues that arise from heat transfer duties assigned to the exchanger. Such selection criteria may even be as simple as measuring them by simple “yardsticks”.

Compact surfaces are used to yield a specified heat exchanger performance  $q/\Delta T_{\text{mean}}$  within acceptable mass and volume constraints, where

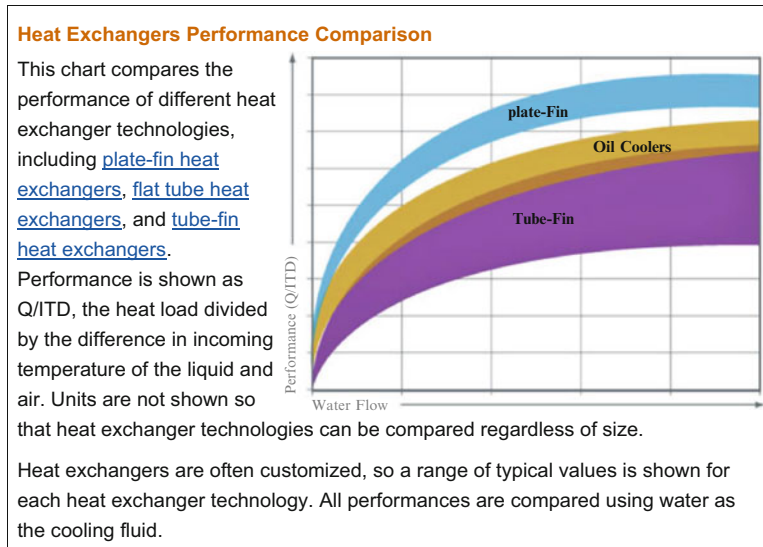
$$\frac{Q}{\Delta T_{\text{mean}}} = U \beta V \quad (\text{Eq. 3.61a})$$

or

$$Q = UA\Delta T_m \quad (\text{Eq. 3.61b})$$

Note sometimes the mean temperature difference  $\Delta T_{\text{mean}}$  is shown with symbol  $\Delta T_m$ , which is what we use in our notation in this text. Also, sometimes mean temperature difference is called the difference in incoming temperature and noted as ITD.

In Eq. (3.61a)  $\beta$  is defined as area density or heat exchanger compactness,  $V$  is the volume of interest for flow in heat exchanger and  $U$  is the overall heat transfer coefficient which is defined per Eq. (3.9) utilizing Fig. 3.55 accordingly.



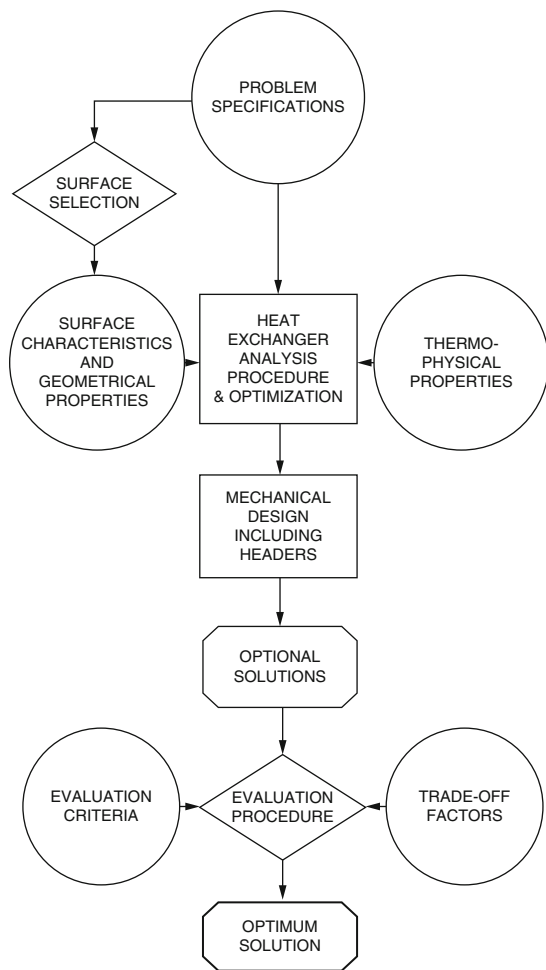
Comparing Eq. (3.61a) and its part (b), namely Eq. (3.61b) reveals that lower heat transfer area  $A$  for specified exchanger effectiveness is  $A = \beta V = (4\sigma/D_h)V$  [23]. In this relation  $\sigma$  is a dimensionless ratio of free flow area to frontal flow rate in a heat exchanger.

From Eq. (3.61a), it is clear that a high area density of  $\beta$  decreases volume. Furthermore, compact surfaces generally result in higher overall heat transfer coefficient  $U$ , and since compact surfaces can achieve structural strength and stability with thinner sections, the reduction in heat exchanger mass is even more pronounced than the reduction in volume  $V$  [21].

Increasing heat exchanger performance usually means transferring more duty or operating the exchanger at a closer temperature approach. This can be accomplished without a dramatic increase in surface area. This constraint directly translates to increasing the overall heat transfer coefficient,  $U$ . The overall heat transfer coefficient is related to the surface area,  $A$ , duty,  $q$ , and driving force mean temperature,  $\Delta T_m$ . See Eq. (3.61b).

As stated in the form of Eq. (3.61b)  $U$  can be calculated from thermodynamic considerations alone. This calculation results in the required  $U$  such that the heat is transferred at the stated driving force and area. Independent of this required  $U$  based on thermodynamics, an available  $U$  can be determined from transport considerations. For this calculation,  $U$  is a function of the heat transfer film coefficients,  $h$  also known as thermal convection heat transfer, the metal thermal conductivity,  $k$ , and any fouling considerations,  $f$ . An exchanger usually operates correctly if the value of  $U$  available exceeds the  $U$  required.

**Fig. 3.73** Methodology of heat exchanger design [38]



Sometimes increasing heat exchanger performance may not result from increases in throughput or higher duties. These issues may arise simply because the exchanger is not working correctly at the present capacity. Solving these problems is usually the first step.

Figure 3.71 by Kays and London [17] and a modified version of Fig. 3.73 by Shah [38] provide a broad perspective approach to a compact heat exchanger design procedure and process as a departure point.

Figure 3.73 suggests four interrelated areas as forwarding steps for heat exchanger thermal design analysis and they are:

1. The surface selection
2. Prediction methods for surface characteristics
3. Theoretical design procedure, and finally

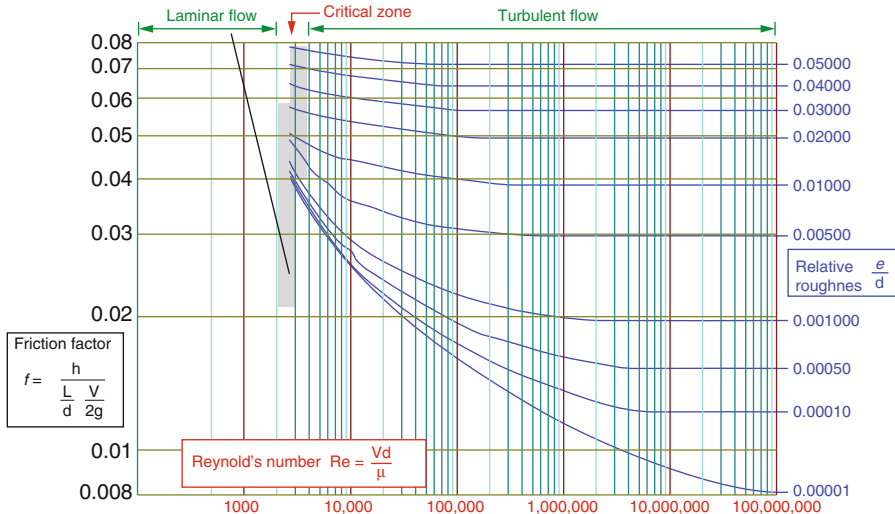


**Fig. 3.74** Moody chart for fully developed turbulent and laminar flow

4. Analytical optimization techniques using tools such as multi-physics software COMSOL or Computational Fluid Dynamics (CFD) ANSYS Fluent for true Three-Dimensional iteration analysis.

Step 1, which is involved with surface selection methodology, utilizes an approach to surface characteristics such as Colburn heat transfer dimensionless modulus  $j = StPr^{2/3}$ , also sometimes denoted as  $j_H$  as shown in Eq. (3.35), and Fanning factor  $f = f_F$  versus Reynolds number plot such as Fig. 3.60 that is known as a Moody plot or Fig. 3.74 where the Darcy-Weisbach equation is used for calculating the friction loss in a pipe, using dimensionless value friction factor also known as the Darcy-Weisbach or the Moody friction factor and it is four time larger than Fanning friction factor. The friction factor or Moody Chart plotted in Fig. 3.74 is based on relative roughness ( $e/D_h$ ) of a pipe/tube against the Reynolds's number. In this figure, the blue color tube lines plot the friction factor for flow in the fully developed turbulent region of the chart, while the straight black line plots the friction factor for the fully developed laminar region of the chart. As you can see the relative roughness depends on  $e$  friction power expended per unit of surface area with dimension of  $\dot{m} \Delta p / \rho A$  or  $W/m^2$  and  $D_h$  is the hydraulic diameter of heat exchanger flow passages in dimension of meter which is equal to four times the hydraulic radius of  $r_h$ .

This chart for the first time enabled the user to obtain a reasonably accurate friction factor for turbulent flow conditions, based on the Reynolds number and the Relative Roughness of the pipe.

Experimental data for a specific compact heat exchanger core (established in the reference by Kays and London, see Fig. 3.75) [17] are typically presented in terms of the dimensionless Colburn heat transfer  $j = j_H$  factor and Fanning friction factor,

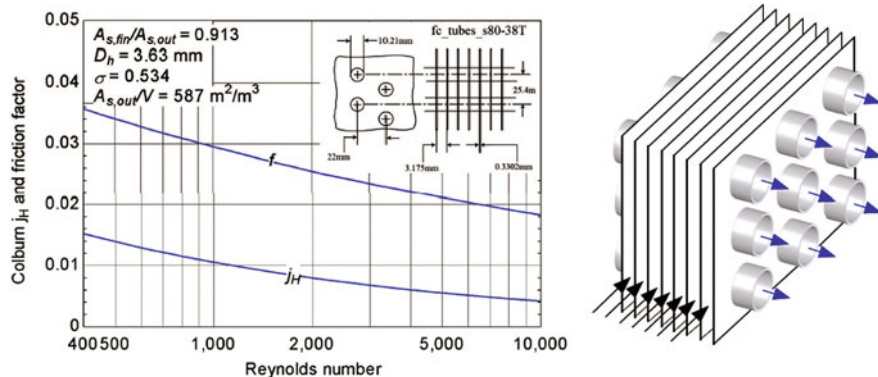


**Fig. 3.75** Plot of relation between Colburn factor and Reynolds number for finned circular tube compact heat exchanger. (Courtesy of F-Chart Software Company)

$f$ , as a function of the Reynolds number,  $\text{Re}$ . The Colburn  $j = j_H$  factor is related to the heat transfer coefficient and the friction factor is related to the pressure drop. The plot below shows the relation for one type of heat exchanger.

Step 2 handles prediction methods for surface characteristics which are used to determine  $f = f_F$  and  $j = j_H$  characteristic of a class of surface geometries when  $f = f_F$  and  $j = j_H$  are available only for a few geometries of the same class. Note that, some of the classes of surface geometries are bare tubes, pin fins, tube with circular fins, louvered fins, strip fins, and wavy fins such is the ones demonstrated in Fig. 3.50.

Step 3 deals with heat transfer analysis of heat exchangers performed based on a theoretical design procedure. The two most recommended common design procedures come from Kays and London's compact heat exchanger book [17] where they suggest for two fluid heat exchangers the  $\epsilon$ -NTU and  $\Delta T_m$  be used. See Sect. 2.12.

Step 4 in above, drives the fact that there are a number of analytical optimization methods that lead to an optimum heat exchanger design [38, 39].

Shah [38] claims that only knowledge of  $f = f_F$  and  $j = j_H$  data is required for the analytical surface selection criteria and prediction methods, which is the second step above as part of the thermal design analysis process, for selection of the surface for the desired compact heat exchanger given the application that uses this exchanger. As part of this prediction method, the knowledge of the other side surface, flow arrangement, design or operating conditions, designer and manufacturer constraints, etc. is not essential, but they are important as part of the design procedure and computer iteration execution as part of the steps for optimizing the final design.

Surface selection could be done by performance enhancement among the various exchangers where they can be compared for their surface selection and the right or best surface for a specified criteria for a given heat exchanger application can be

choosen. A variety of methods have been suggested in many literature works for such comparisons either in compact heat exchanger design or some other heat transfer devices such as heat pipe Bergles et al. [40] offer such reviews from the view point of performance enhancement as a reference and Shah [38] has summarized them.

As part of the performance comparison method, the basic characteristics of compact heat exchanger parameters are in dimensionless form such as Colburn heat transfer factor  $j$  and Fanning friction factor  $f$  as a function of the Reynolds number  $Re$  as we mentioned above and curves can be plotted as direct comparison of factors versus Reynolds number. See Eq. (3.35) and Fig. 3.75.

Therefore, in summary the various methods that are suggested as part of comparing performance enhancement analysis for different heat exchanger surfaces are categorized as follows:

1. Comparison based on Colburn  $j$  and Fanning  $f$  factors.
2. Comparison of heat transfer as a function of fluid pumping power that is described per both parts of Eqs. (3.59) and (3.60).
3. Miscellaneous direct comparison methods, and finally
4. Performance comparison with a reference.

These dimensional or dimensionless comparison methods are reported in various literature and summarized by Shah [38]. Analyzing the summary of the table provided by Shah [38], we find that some comparison methods may have unique advantages to provide a best surface satisfying certain design criteria. It should be emphasized these comparison methods are for the surfaces only as if they would be on one side of the heat exchanger and there is no accounting for overall heat exchanger geometry, flow arrangement, thermal resistance on the other side, wall thermal resistance, overall envelope, and any other design criteria.

When a complete design of a compact heat exchanger is taken under consideration which does not lead to having one side as a strong side where multiplication of dimensionless  $\eta_0 = 1 - (1 - \eta_f)A_f/A$ ,  $A_f$  is the total fin area of heat exchanger on one side in  $m^2$ , convective heat transfer coefficient  $h$  ( $W/m^2 K$ ) and total surface area  $A$  ( $m^2$ ) which includes both primary plus secondary on one side, is high, the best surface selected by the forgoing methods may not be an optimum surface for a given application. This is because the selection of the other side surface and other design criteria, not necessarily related to the surface characteristics, has an effect on the overall performance of the heat exchanger (Shah) [38]. As Shah [38] indicates, there are no simplified methods that would consider the selection of surfaces on both sides within the imposed design constraints and arrive at an optimum design. Heat exchanger optimization procedures which would take into consideration the surfaces on both sides and deal with the constraints associated with them are discussed by Shah et al. [39].

In general, enhanced heat transfer surfaces can be used for three purposes:

- (1) To make heat exchangers more compact in order to reduce their overall volume, and possibly their cost,

- (2) To reduce the pumping power required for a given heat transfer process, or
- (3) To increase the overall heat exchanger conductance  $UA$  value of the heat exchanger.

A higher  $UA$  value can be exploited in either of two ways:

- 1. To obtain an increased heat exchange rate for fixed fluid inlet temperatures, or
- 2. To reduce the mean temperature difference for the heat exchange; this increases the thermodynamic process efficiency, which can result in a saving of operating costs.

In this discussion  $U$  represents the overall heat transfer coefficient of exchanger while  $A$  is the total heat transfer area of primary plus secondary on one side of the desired heat exchanger and as we know by now, compact heat exchangers possess a high ratio of heat transfer surface area to volume, but this does not mean that a compact heat exchanger is of small mass or volume. Hence, it is obvious that “compact” and “small” are not equivalent by their definitions here. However, if compact heat exchangers did not incorporate a surface of such high area density  $\beta$  ( $\text{m}^2/\text{m}^3$ ) (also known as heat exchanger compactness characteristic), the resulting desired units would be much more bulky and massive than their compact heat exchanger (CHE) counterparts [21].

To summarize all this information and knowledge that we have gathered so far with respect to enhanced surfaces for compact heat exchangers we can say that:

Since there are so many different types of heat exchanger enhancements, it is highly unlikely that a commercial simulator could support them all. Furthermore, some propriety data from the manufacturers of the heat transfer enhancement might never be released. However, that does not mean that process and project engineers cannot perform some of the preliminary calculations for new technologies.

The following provides background information on many different types of heat exchanger enhancements. Heat exchanger enhancement must always satisfy the primary goal of providing a cost advantage relative to the use of a conventional heat exchanger [24]. Other factors that should be addressed include fouling potential, reliability, and safety.

Heat exchanger enhancement can be divided into both passive and active methods. Passive methods include extended surfaces, inserts, coiled or twisted tubes, surface treatments, and additives. Active techniques include surface vibration, electrostatic fields, injection, and suction. Hewitt [25] provides numerous examples of the different enhancements. The majority of the current discussion is related to the passive methods involving mechanical modifications to the tubes and baffles. Figure 3.76 shows several different schematics of enhancements to heat exchanger tubes including finning, inserts, and twisting.

Details of each of these enhanced surfaces can be found in the reference by Lunsford [26].

There are a large number of core geometries discussed in the Compact Heat Exchanger book by Kays and London [17] and these data are very useful because the air flow through the finned side of a compact heat exchanger is a complex

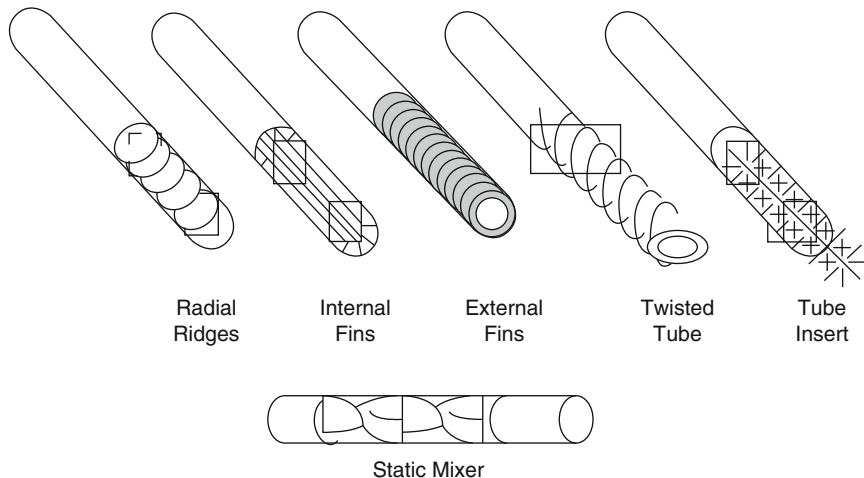


**Fig. 3.76** Examples of tubes with heat transfer enhancement [26]

combination of internal flow in passages and external flow over tubes and other obstructions. The internal and external flow heat transfer correlations that have been developed for simple geometries are not applicable for compact heat exchangers.

However, it is challenging to decipher the dimensionless data presented in the Compact Heat Exchanger book in order to provide useful engineering quantities like heat transfer coefficient and pressure drop.

A software solution exists, namely Engineering Equation Solver (EES) developed by a company named FCHART in Madison Wisconsin, to deal with all the various core geometries defined in Kays and London's [17] Compact Heat Exchanger book as part of their internal library in their EES software package where it simplifies this process.

The Compact Heat Exchanger Library is accessed from the Function Information dialog by selecting the Heat Transfer radio button and then selecting Compact HX from the drop down menu.

### 3.7.1.6 The Goodness Factors

As mentioned only knowledge of Colburn Factor  $j$  and Fanning Factor  $f$  are required and they are necessary and sufficient information for the analytical surface selection criteria and prediction methods and the other knowledge such as other side surface, flow arrangement, design or operating conditions and related designer constraints are not essential and mandatory for surface selections although they help build a complete system of the heat exchanger.

On the other hand the *Goodness Factors* come into play, when the failure of  $j$  and  $f$  curves to portray the relative performance of heat transfer in a satisfactory

manner lead to the development of other performance parameters. And they are divided into two categories namely

1. Area Goodness Comparison [41]
2. Volume Goodness Comparison [41, 42]

Each of these goodness comparisons and methods are defined in more detail below and more details can be found in references by Kays and London [17] or Stone [21].

### Area Goodness Factor

The “area goodness” method actually makes a direct comparison between Colburn heat transfer factor  $j$  and Fanning Factor  $f$  values, and it consists of plotting  $j$  or  $f$  or  $j/f$  versus Reynolds's Number  $Re$  as it is shown in Fig. 3.75 as an example. In the case of the lateral form of  $j/f$  the flow area goodness factor is given by the following relationship:

$$\frac{j}{f} = \frac{\text{Nu} \Pr^{-1/3}}{f \text{Re}} = \frac{1}{A_o^2} \left[ \frac{\Pr^{2/3} \text{NTU} \cdot \dot{m}^2}{2g_c \Delta p} \right] \quad (\text{Eq. 3.62})$$

where NTU is the number of temperature unit which is given by Eq. (2.11) and  $A_o = A_c$  is the core free flow area or minimum free flow or open area defined as before,  $\dot{m} = pV_m A_o$  (kg/s or lb<sub>m</sub>/s) is fluid mass flow rate through the duct, and  $g_c$  is proportionality constant in Newton's second law of motion ( $g_c = 1$  and is dimensionless in SI units;  $g_c = 32.174 \text{ lb}_m \text{ ft}/(\text{lb}_f \text{ s}^2)$ , where  $\rho$  is density for fluid (kg/m<sup>2</sup> or lbm/ft<sup>2</sup>).

For fully developed laminar flow of specified fluid,  $j/f$  is constant for a given surface, regardless of Reynolds number  $Re$ . The right hand of Eq. (3.62) shows that  $j/f$  is inversely proportional to  $A_o^2$  when the bracketed quantities are constant. Therefore, a high  $j/f$  is considered very appealing because it presents a lower flow area, and thus, it means a lower frontal area is required for the heat exchanger. Due to the fact that both Colburn factor  $j$  and Fanning factor  $f$  are dimensionless quantities, they are independent of the hydraulic diameter  $D_h$  based on the fact that  $\text{Nu} = hD_h/k$  (see Chap. 2 of this book). Therefore, when the area goodness factor  $j/f$  is compared for different surfaces, it reveals the influence of the cross-sectional shape regardless of the scale of the geometry [23].

### Volume Goodness Factor

A comparison of surface geometries in terms of core volume is provided by plotting  $h_{\text{std}}$  versus  $E_{\text{std}}$ , where:

$h_{\text{std}}$  = Heat Transfer Coefficient at a standard set of fluid properties [W/(m<sup>2</sup> K), or (h ft<sup>2</sup> °F)]

$E_{\text{std}}$  = Flow-Friction power per unit area for a standard set of fluid properties (W/m<sup>2</sup>, or hp/ft<sup>2</sup>)

$h_{\text{std}}$  is referred to as the “volume goodness factor”. Expressions for  $h_{\text{std}}$  and for  $E_{\text{std}}$  are given in Eqs. (3.63) and (3.64) below:

$$h_{\text{std}} = \frac{k}{D_h} \text{Nu} = \frac{c_p}{Pr^{2/3}} \frac{1}{D_h} j \text{Re} \quad (\text{Eq. 3.63})$$

$$E_{\text{std}} = \frac{\dot{m} \Delta p}{\rho A} = \frac{\mu^3}{2 g_c \rho^2 D_h^3} \frac{1}{f} \text{Re}^3 = V_m r_h \frac{\Delta P}{L} \quad (\text{Eq. 3.64})$$

The dimensionless heat transfer in a heat exchanger is measured by the exchanger effectiveness ( $\epsilon$ ), which is dependent on the Number of Transfer Units (NTU) for fixed flow rates as we defined before.

In a “balanced” heat exchanger, the thermal resistances of both sides of the heat exchanger are of the same order of magnitude. This means that NTU is proportional to  $hA$  (or  $h_{\text{std}}A$ ) for the side of the heat exchanger that is under examination. As a result, a higher  $h_{\text{std}}$  for a given  $E_{\text{std}}$  will yield a lower heat transfer area ( $A$ ) for the specified exchanger effectiveness [23], again as we have defined before. Consequently, a high position on the  $h_{\text{std}}$  vs.  $E_{\text{std}}$  plot signifies a desirable surface geometry. And,  $A = \beta V = (4\sigma/D_h)V$  since, where:  $\sigma$  = dimensionless ratio of free flow area to frontal flow area in a heat exchanger and a high  $h_{\text{std}}$  will yield a smaller heat exchanger volume at a given  $E_{\text{std}}$  for constant  $\sigma$  and  $D_h$ .

### 3.7.1.7 Advantages and Disadvantages of Goodness Factors

Extra difficulties arise in using the goodness factors when comparing surface geometries. For example, the area goodness factor is a useful parameter only when comparing surfaces for a fixed fluid pressure drop. With the volume goodness criterion, it is evident from Eqs. (3.63) and (3.64) that  $h_{\text{std}}$  and  $E_{\text{std}}$  are strongly dependent on hydraulic diameter, unlike the area goodness factor ( $j/f$ ). Thus, hydraulic diameters must be fixed in order to obtain a valid volume goodness comparison. Furthermore, a representative set of fluid properties must be selected for this method and, Cowell [27] points out that neither goodness comparison is fully quantitative.

Even London [43] admits, “These surface goodness factors are not infallible.”

Nevertheless, the goodness factors can provide valuable preliminary information about the relative performance of different heat transfer surfaces. As Shah and London [23] state, “These factors are easy to understand and apply, and may serve a function of screening the selection of surfaces before other design criteria are applied”.

The performance data of a heat exchanger surface geometry are judicially presented as the heat transfer Colburn Factor  $j$  and the Fanning Friction Factor  $f$  as a function of Reynolds number  $Re$ ;  $j$  versus  $f_f$  curves vary over a wide range in magnitude as well as in slope.

Remember that the Colburn  $j$  factor is related to the heat transfer coefficient  $h$  and the Fanning friction factor  $f_f$  is related to the pressure drop.

However, to overcome the problems associated with  $j$  and  $f = f_f$  curves, LaHaye et al. [44] developed two new dimensionless groups. These two parameters are the “Heat Transfer Performance Factor” ( $J = jRe$ ) and the “Pumping Power Factor” ( $F = fRe^3$ ) as defined by Eqs. (3.65) and (3.66), respectively, as follows:

$$J = (\beta h) \frac{Pr^{2/3} D_{eq}}{\beta c_p \mu} = jRe \quad (\text{Eq. 3.65})$$

$$F = \frac{P}{V} \frac{2g_c \rho^2 D_{eq}}{\beta \mu^3} = F = f_f Re^3 \quad (\text{Eq. 3.66})$$

where the following parameters definitions are applied:

$J$  = Transfer performance factor,  $J = jRe$

$F$  = Pumping power factor,  $F = f_f Re^3$

$Re$  = Reynolds number

$A$  = Total heat transfer area in one side of heat exchanger

$A_c$  = Minimum free flow area

$c_p$  = Specific heat at constant pressure

$D_{eq}$  = Equivalent diameter,  $D_{eq} = 4A_c L/A$

$f_f$  = Fanning factor or pressure drop factor

$g_c$  = Proportionally constant in Newton's second law of gravity

$h$  = Surface heat transfer coefficient

$j$  = Colburn factor or heat transfer factor

$L$  = Total flow length

$\ell$  = Flow length between major boundary layer disturbances

$n$  = Slope exponent in the dimensionless performance ( $J$  versus  $F$ ) plot

$Pr$  = Prandtl number

$P$  = Fluid pumping power

$V$  = Core volume between plates

$\beta$  = Ratio of total transfer area on one side of a plate-fin exchanger to the volume between the plates on this side,  $A/V$

$\mu$  = Fluid viscosity

$\rho$  = Fluid density

Plotting the heat transfer performance factor vs. the pumping power factor yields a “dimensionless performance plot,” like the example plot shown in Fig. 3.77. This plot also has the Reynolds number plotted on top of the performance line. Using performance plots like the one in Fig. 3.12 for a number of surfaces, LaHaye

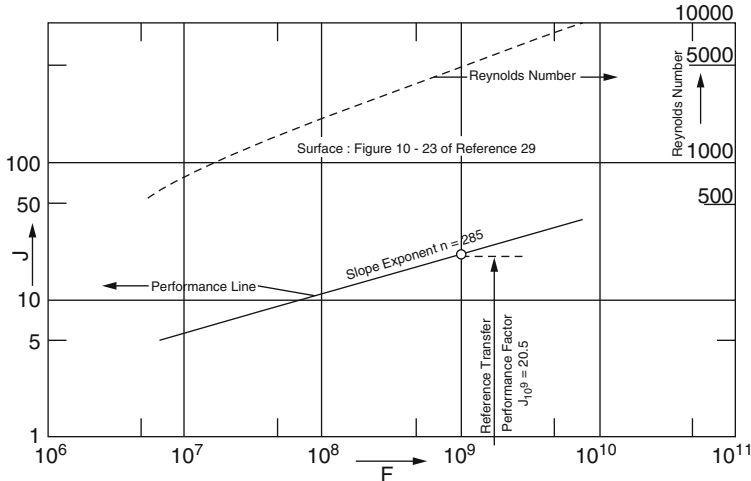


**Fig. 3.77** Example of a dimensionless performance plot based on Fig. 10.23 of Kays and London [17]

et al. [44] then attempted to create a single “idealized” performance plot which could be used to analyze all surface geometries.

Further discussion of this matter can be found in References by Stone [21] and LaHaye et al. [44] and we encourage the readers to refer to them.

### 3.7.1.8 The Core Mass Velocity Equation

The core mass velocity equation, based on what we discussed earlier, can be summarized here, considering the sides are chosen and we drop the suffix *h* for hot side or *c* for cold side, and *N*'s in the following form:

$$\frac{2\rho\Delta p}{\dot{m}^2} = \frac{f\Pr^{2/3}N}{jA_c^2} \quad \text{and} \quad \frac{G^2}{2\rho\Delta p} = \frac{j/f_f}{\Pr^{2/3}N} \quad (\text{Eq. 3.67})$$

All the parameters that are used in these equations are defined as before. For laminar flows, these equations yield to the following form:

$$\frac{2\rho\Delta p}{\dot{m}^2} = \frac{N\Pr}{A_c^2} \frac{k}{\text{Nu}} \quad \text{and} \quad \frac{G^2}{2\rho\Delta p} = \frac{\text{Nu}/k}{\Pr N} \quad (\text{Eq. 3.68})$$

Where the friction factor (Fanning Friction)  $f_f$  is given by  $f_f = k/\text{Re}$ .

Note that, for given conditions of  $\Pr$ ,  $N$ ,  $p$  and  $\Delta p$ , it is clear that  $G$  is only a function of  $j/f_f$ , or  $\text{Nu}/k$ , and most importantly is independent of the hydraulic diameter of the surface. The ratio  $j/f_f$  ( $f_f$  is Fanning friction factor) is only a weak

function of Reynolds number, being of the order of 0.2–0.3 for most compact surfaces. Thus  $G$ , and hence flow area  $A_c$ , can be closely estimated from the design specification [35].

The operating Reynolds number, with which  $j/f_f$  is a weak function and  $j$  is a strong function for most surfaces, in terms of prescribed side NTU and pressure drop:

$$\frac{\text{Re}}{D_h(j/f_f)^{1/2}} = \frac{1}{\eta} \left( \frac{2\rho\Delta p}{\text{Pr}^{2/3}N} \right)^{1/2} \quad (\text{Eq. 3.69})$$

and for laminar flow Eq. (3.69) results as:

$$\frac{\text{Re}}{D_h(\text{Nu}/k)^{1/2}} = \frac{1}{\eta} \left( \frac{2\rho\Delta p}{\text{Pr}N} \right)^{1/2} \quad (\text{Eq. 3.70})$$

If  $G$  has already been calculated and accounted for as above, we can simply write:

$$\text{Re} = \frac{Gd_n}{\mu} \quad (\text{Eq. 3.71})$$

where  $\mu$  is dynamic viscosity of the fluid.

Note that this estimation of  $G$  effectively determines the through-flow velocity, which is also reflected in Eq. (3.70), since this velocity is proportional to  $\text{Re}/d_n$ . The velocity is, in addition, responsible for determining the controllable entropy generation rate, and features in economic optimization (Martin) [45].

## 3.8 The Overall Heat Exchanger Design Process

Design of heat exchangers is an iterative (trial and error) process. Here is a set of steps for the process:

1. Calculate the required heat transfer rate,  $q$ , in Btu/h from specified information about fluid flow rates and temperatures.
2. Make an initial estimate of the overall heat transfer coefficient,  $U$ , based on the fluids involved.
3. Calculate the logarithmic mean temperature difference,  $\Delta T_m$ , from the inlet and outlet temperatures of the two fluids.
4. Calculate the estimated heat transfer area required, using:  $A = q/U\Delta T_m$ .
5. Select a preliminary heat exchanger configuration.
6. Make a more detailed estimate of the overall heat transfer coefficient,  $U$ , based on the preliminary heat exchanger configuration.

### 3.8.1 Input Information Needed

In order to start the heat exchanger design process, several items of information are needed as follows:

1. The two fluids involved need to be identified.
2. The heat capacity of each fluid is needed.
3. The required initial and final temperatures for one of the fluids are needed.
4. The design value of the initial temperature for the other fluid is needed.
5. An initial estimate for the value of the Overall Heat Transfer Coefficient,  $U$ , is needed

Knowing the first four items allows determination of the required heat transfer rate,  $q$ , and the inlet and outlet temperatures of both fluids, thus allowing calculation of the log mean temperature difference,  $\Delta T_m$ . With values now available for  $q$ ,  $U$ , and  $\Delta T_m$ , an initial estimate for the required heat transfer area can be calculated from the equation.

For design of heat exchangers, the basic heat exchanger design equation can be used to calculate the required heat exchanger area for known or estimated values of the other three parameters,  $q$ ,  $U$ , and  $\Delta T_m$ . Each of those parameters will now be discussed briefly.

#### 1. Logarithmic Mean Temperature Difference, $\Delta T_m$

The driving force for any heat transfer process is a temperature difference. For heat exchangers, there are two fluids involved, with the temperatures of both changing as they pass through the heat exchanger, so some type of average temperature difference is needed. Many heat transfer textbooks have a derivation showing that the log mean temperature difference is the right average temperature to use for heat exchanger calculations. That log mean temperature is defined in terms of the temperature differences as shown in Eq. (3.41).  $T_{h_{in}}$  and  $T_{h_{out}}$  are the inlet and outlet temperatures of the hot fluid and  $T_{c_{in}}$  and  $T_{c_{out}}$  are the inlet and outlet temperatures of the cold fluid. Those four temperatures are shown in the diagram at the left for a straight tube, two pass shell and tube heat exchanger with the cold fluid as the shell side fluid and the hot fluid as the tube side fluid. See Fig. 3.23 as well.

$$\Delta T_m = \frac{(T_{h_{in}} - T_{c_{out}}) - (T_{h_{out}} - T_{c_{in}})}{\ln \left\{ \frac{(T_{h_{in}} - T_{c_{out}})}{(T_{h_{out}} - T_{c_{in}})} \right\}} \quad (\text{Eq. 3.72})$$

#### 2. Heat Transfer Rate $q$

Heat Transfer Rate  $q$  can be calculated based on the above design rules. This information can be found by Eq. (3.12) and then an initial estimate for the required heat transfer area can be calculated from the relationship  $A = Q/U\Delta T_m$ .

Heat exchanger calculations with the heat exchanger design equation require a value for the heat transfer rate,  $q$ , which can be calculated from the known flow rate of one of the fluids, its heat capacity, and the required temperature change. The following equation is used:

$$q = \dot{m}_h c_{p,h} (T_{h_{in}} - T_{h_{out}}) \dot{m}_c c_{p,c} (T_{c_{out}} - T_{c_{in}})$$

where (i.e., the units are given in British system and easily can be shown as M.K.S. System as well):

$\dot{m}_h$  = mass flow rate of the hot fluid, slug/h

$c_{p,h}$  = heat capacity of the hot fluid at constant pressure, BTU/slug °F

$\dot{m}_c$  = mass flow rate of cold fluid, slug/h

$c_{p,c}$  = heat capacity of the cold fluid at constant pressure, BTU/slug °F

and the temperatures are as defined in the previous section.

The required heat transfer rate can be determined from known flow rate, heat capacity, and temperature change for either the hot fluid or the cold fluid. Then either the flow rate of the other fluid for a specified temperature change, or the outlet temperature for known flow rate and inlet temperature can be calculated.

### 3. Overall Heat Transfer Coefficient, $U$

The overall heat transfer coefficient,  $U$ , depends on the conductivity through the heat transfer wall separating the two fluids, and the convection coefficients on both sides of the heat transfer wall. For a shell and tube heat exchanger, for example, there would be an inside convective coefficient for the tube side fluid and an outside convective coefficient for the shell side fluid. The heat transfer coefficient for a given heat exchanger is often determined empirically by measuring all of the other parameters in the basic heat exchanger equation and calculating  $U$ . Typical ranges of  $U$  values for various heat exchanger/fluid combinations are available in textbooks, handbooks, and on websites for other types of heat exchangers, such as our intended compact heat exchanger (London and Kays) [17]. A sampling is given in Table 3.7 below for shell and tube heat exchangers:

**Table 3.7** Typical value of heat transfer coefficient

Typical ranges of values of $U$ for shell and tube heat exchangers		
Hot fluid	Cold fluid	$U$ , Btu/h ft <sup>2</sup> °F
Water	Water	140–260
Steam	Water	260–700
Light oils	Water	62–159
Gases	Water	3–50
Water	Light organics	35–53

### 3.9 Design Summary

As part of the design process and methodology for compact heat exchangers, they are generally within the scope of certain constraints which include:

1. Implementation of basic heat exchange equation
2. Flow frontal entrance area
3. Volume, weight, and size
4. Pressure drop

With these constraints in hand, different heat transfer surfaces may be analyzed and plotted on graphs as part of a specification excel sheet for comparison purposes and selection of a final choice for intended application exchanger as a candidate.

#### 1. Basic Heat Transfer or Exchange Equation

Preliminary heat exchanger design to estimate the required heat exchanger surface area can be done using the basic heat exchanger equation,  $Q = UA\Delta T_m$ , (analogues to Eq. (3.16)) if values are known or can be estimated for  $Q$ ,  $A$  and  $\Delta T_m$ . Heat exchanger theory tells us that  $\Delta T_m$  is the right average temperature difference to use. So we need the following basic heat transfer equation:

$$Q = UA\Delta T_m \quad (\text{Eq. 3.73})$$

Where estimated heat transfers area required, using:  $A = Q/U\Delta T_m$  and LMTD is given as Eq. (3.72).

#### 2. Flow Area

Using the mass velocity  $G \propto (St/f_f)^{1/2}$  for a given pressure drop, we can write the following flow area relationship:

$$StPr^{2/3}/f_f \quad \text{Versus} \quad Re \quad (\text{Eq. 3.74})$$

Further investigation of Eq. (3.74), indicates that a higher  $(StPr^{2/3}/f_f)$  surface characteristic implies a smaller flow frontal entrance area ( $A_c$ ) for a given  $\Delta p/p$ . Again  $f$  is Fanning friction factor.

#### 3. Exchanger Volume, Weight, and Size

A useful comparison for the purpose of exchanger volume, weight, and size is provided as:

$$h_{std} \quad \text{Versus} \quad E_{std} \quad (\text{Eq. 3.75})$$

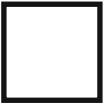
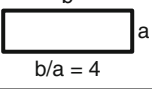
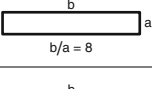
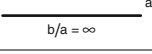
where  $E_{std}$  is the friction power per unfit area in  $\text{hp}/\text{ft}^2$ . Here subscript std is an indication of an evaluation at reference fluid properties (i.e., air at 500 °F and 1 atm) [42].

Equation (3.74) implies the surface with the higher  $h_{\text{std}}$  vs.  $E_{\text{std}}$  characteristic will tend to have the smallest core volume as a result of better compactness. Hence, these surface goodness factors are not infallible and are usually indicative of the relative performance of the surfaces. For the heat exchangers surfaces that operate at Lower Reynolds number near laminar flow, London and Ferguson [42] and Zohuri and Fathi [30] provide good classical analyses for laminar flow solutions for fully developed flow in cylindrical passages. These analyses could be used as a benchmark for several different types of surfaces to be looked at as part of the comparison for final selection of exchangers for all intended purposes and applications in mind (i.e., Open Air Brayton Cycle Driven Efficiency for NGNP), Zohuri [9].

Table 3.8 provides such comparison for different cross-sections of these passages at near laminar flow. Some note worthy points are [9, 46]:

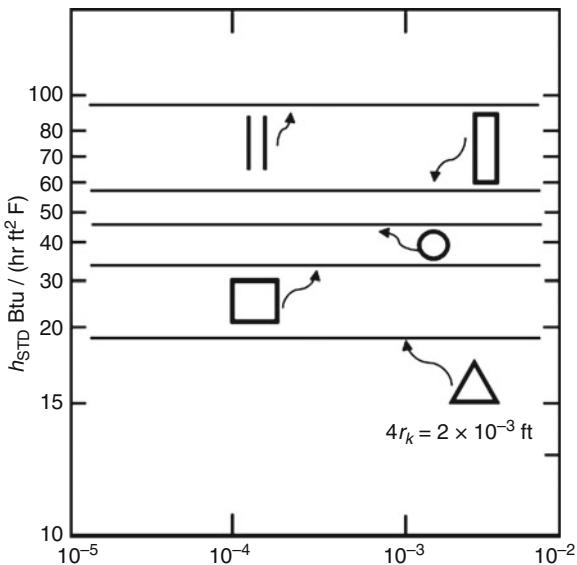
1. The convective heat-transfer coefficient for constant flux conditions  $q$  (BTU/h ft) of flow length is 9–28 % higher than for the constant or uniform wall temperature (i.e., known as *T-boundary condition*) boundary condition. The smallest difference is for the rectangular passage with large aspect ratio and the largest for the

**Table 3.8** Laminar flow solutions. Comparison of laminar-flow solutions for different cross-sections

Cross section	$(\text{Nu})_T$	$\frac{(\text{Nu})_q}{(\text{Nu})_T}$	$f/\text{Re}$	$\left\{ \text{StPr}^{2/3} \right\} / f_f = \frac{1.15(\text{Nu})_T}{f_f \text{Re}}$
	2.35	1.28	13.33	0.203
	3.66	1.19	16.0	0.264
	2.89	1.26	14.2	0.234
 $b/a = 4$	4.65	1.15	18.3	0.292
 $b/a = 8$	5.95	1.09	20.5	0.334
 $b/a = \infty$	7.54	1.09	24.0	0.361

Note: (a) For  $L/4r_h > 100$ ; where  $r_h$  is the hydraulic radius  
 (b) For  $\text{Pr} = 0.66$

**Fig. 3.78** Heat transfer power versus friction power for fully developed lamina flow. Note again, the high-aspect ratio rectangular section shows superiority



triangular passage. See Table 3.6 here and for more detailed information refer to the book by Zohuri and Fathi [9], Chap. 5.

2. The ratio  $St Pr^{2/3}/f_f$  is constant for a given surface irrespective of  $Re$ .
3. Rectangular passages of large aspect ratio tend to have smaller frontal area requirements by about 1/3 relative to the triangular passage.

Note that the rectangular cross-section with high aspect ratio ( $b/a$ ) long and narrow offers the least frontage area.

If we use a given number from Table 3.8 to form  $h_{STD}$  versus  $E_{STD}$ , we produce results for the surfaces all with a common magnitude of  $4r_h = 2 \times 10^{-3}$  ft (for surface density  $\beta$  of  $1200 < \beta < 1800 \text{ ft}^2/\text{ft}^3$ ). Clearly, we can see that there exist large differences between surfaces, with the large-aspect-ratio rectangular passages again being superior to the triangular passages in a rather spectacular fashion as shown in Fig. 3.56—that is a 3.2 to 1.0 higher heat transfer coefficient [41].

Figure 3.78 shows some of these passages that go with data from Table 3.6 and it is interesting to compare these surfaces with each other and to reference them to Fig. 3.54 and Table 3.8.

It is also important to make some preliminary points on the importance of obtaining accurate geometrical dimensions, both for test date reduction purposes and in the comparison of different surface geometries as part of design methodology, and these are the basis for measuring the actual surfaces for the exchanger that is finally selected for its intended application. Bear in mind that there are three parameters of primary interest for the surface geometrical factors:

1. The porosity,  $p$ ,
2. The hydraulic radius  $r_h$ , and
3. The area density  $\beta$ .

Note that only two of these parameters are independent per Eq. (3.76) as shown below:

$$\beta = \frac{p}{r_h} \quad (\text{Eq. 3.76})$$

The definitions of these parameters are mainly important as they specify the geometrical measurements that must be made as:

$$\begin{aligned} p &= \frac{A(\text{flow})}{A_c(\text{frontal})} \\ p &= \frac{A(\text{flow}) \times L}{A(\text{heat transfer})} \\ \beta &= \frac{A(\text{heat transfer})}{A_c(\text{frontal}) \times L} \end{aligned} \quad (\text{Eq. 3.77})$$

Out of any test measurement of different geometry (see Fig. 3.50) of flow passage,  $A_c$ (frontal) and  $L$  of the test core can be measured with good accuracy; however,  $A$  (flow) and  $A$  (heat transfer) are not easily established.

As part of data test reduction processes, it can be shown that:

$$\begin{aligned} \text{Re} &\propto 1/\beta \\ \text{St} &\propto p/\beta \\ f &\propto p^3/\beta \end{aligned} \quad (\text{Eq. 3.78})$$

For surface comparisons that are presented by Eqs. (3.74) and (3.75), it may be shown that

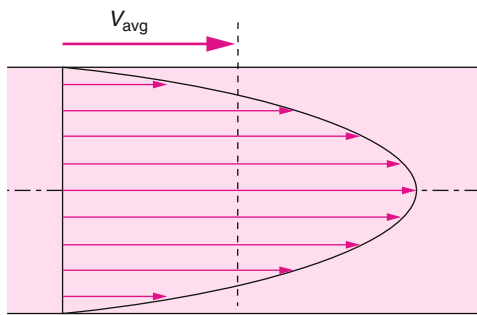
$$\begin{aligned} \text{St Pr}^{2/3}/f &\propto p^2 \\ h_{\text{std}} &\propto p/\beta^2 \\ E_{\text{std}} &\propto p^3/\beta^4 \end{aligned} \quad (\text{Eq. 3.79})$$

#### 4. Pressure Drop for Fully Developed Flow

Although we talked about pressure drop  $\Delta p$  as one of the quantities of interest as part of design methodology for a compact heat exchanger, we will expand upon it from a fully developed laminar flow solution for different cross-section passage point of view. Analysis of pressure drop for flow within a pipe has direct impact on maintaining consistent fluid flow. In order to satisfy this requirement of consistency, we can easily note that  $(dp/dx) = \text{constant}$ , and integrating from  $x = x_1$  where the pressure is  $p_1$  to  $x = x_1 + L$  where pressure is  $p_2$  gives:

$$\frac{dp}{dx} = \frac{p_2 - p_1}{L} \quad (\text{Eq. 3.80})$$

**Fig. 3.79** Average velocity  
 $V_{\text{avg}}$  is defined as the  
 average speed through a  
 cross section



Now taking another value known as average velocity  $V_{\text{avg}}$  into account for a laminar flow profile as shown in Fig. 3.79, we can calculate this value at some stream-wise cross-section determined from the requirement that the *conservation of mass* principle from fluid mechanics must be satisfied and that is:

$$\dot{m} = pV_{\text{avg}}A_c = \int_{A_c} = \rho u(r)dA_c \quad (\text{Eq. 3.81})$$

where:

$\dot{m}$  = Mass flow rate

$\rho$  = fluid density

$A_c$  = cross-sectional area, and

$U(r)$  = velocity profile

Hence, the average velocity for incompressible flow in a circular pipe of radius  $R$  can be expressed as:

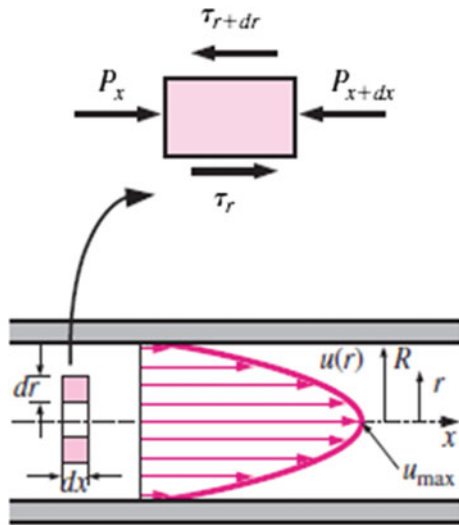
$$V_{\text{avg}} = \frac{\int_{A_c} \rho u(r)dA_c}{\rho A_c} = \frac{\int_{r=0}^{r=R} \rho u(r)2\pi r dr}{\rho \pi R^2} = \frac{2}{R^2} \int_{r=0}^{r=R} u(r)r dr \quad (\text{Eq. 3.82})$$

Note that for fully developed laminar pipe flow  $V_{\text{avg}}$  is half of maximum velocity.

Now consider the steady laminar flow of an incompressible fluid with constant properties in the fully developed region of a straight circular pipe, we can obtain the momentum equation by applying a momentum balance to a differential volume element, as shown in Fig. 3.80.

Figure 3.80 is a depiction of a Free-body diagram of a ring-shaped differential fluid element of radius  $r$ , thickness  $dr$ , and length  $dx$  oriented coaxially with a horizontal pipe in fully developed laminar flow. Under this demonstration, the volume element involves only pressure ( $p$ ) and viscous effects ( $\mu$ ) and therefore the pressure and shear force  $\tau$  must balance each other in given  $x$  and  $r$  directions (i.e., cylindrical coordinate and everything around azimuth angle  $\theta$  is symmetrical.  $x$  is axial direction).

**Fig. 3.80** Free-body diagram of a ring-shaped differential fluid element



$$(2\pi r dr p)_x - (2\pi r dr p)_{x+dx} + (2\pi r dx \tau)_r - (2\pi r dx \tau)_{r+dr} = 0 \quad (\text{Eq. 3.83})$$

Equation (3.51) is established based on the fact that, pressure force acting on a submerged plane surface is the product of the pressure at the centroid of the surface and surface area  $A$  and the force balance is given by this equation on the volume element in flow direction as shown in Fig. 3.80, which is an indication of fully developed flow in horizontal pipe.

Dividing both sides of Eq. (3.83) by  $2\pi r dr dx$  and rearranging algebraically, this equation reduces to the following form as Eq. (3.84):

$$r \frac{p_{x+dx} - p_x}{dx} + \frac{(r\tau)_{r+dr} - (r\tau)_r}{dr} = 0 \quad (\text{Eq. 3.84})$$

Taking the limit as  $dr, dx \rightarrow 0$  yields:

$$r \frac{dp}{dx} + \frac{d(r\tau)}{dr} = 0 \quad (\text{Eq. 3.85})$$

Now substituting  $\tau = -\mu(du/dr)$  and taking  $\mu = \text{constant}$  provides the desired two dimensional linear partial differentials (PDE) Eq. (3.86) as:

$$\frac{\mu}{r} \frac{d}{dr} \left( r \frac{du}{dr} \right) = \frac{dp}{dx} \quad (\text{Eq. 3.86})$$

Note that the quantity  $du/dr$  is negative in pipe flow, and the negative sign is included to obtain positive values for  $\tau$  (i.e.,  $(du/dr) = -(du/dy)$  since  $y = R - r$ ).

Utilizing Fig. 3.81 (which is the free-body diagram of a fluid disk element of radius  $R$  and length  $dx$  in fully developed laminar flow in a horizontal pipe), allows us to justify a solution for partial differential Eq. (3.87) using separation of variable methods, with given boundary conditions below as:

$$\text{Boundary Conditions} \quad \begin{cases} (du/dr) = 0 & \text{at } r = 0 \\ u = 0 & \text{at } r = R \end{cases} \quad (\text{Eq. 3.87})$$

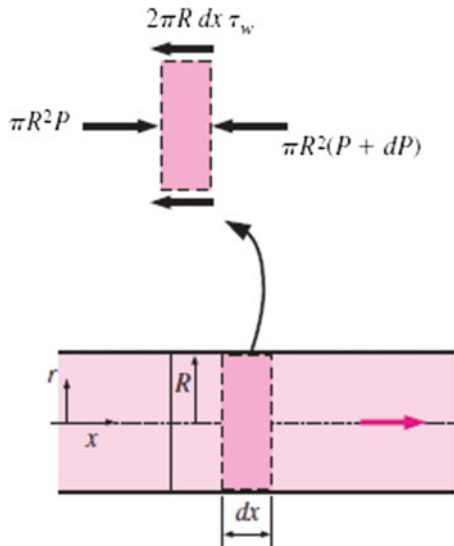
Note that as part of justification, we can claim that, the left side of Eq. (3.86) is a function of  $r$ , and the right side is a function of  $x$ . The equality must hold for any value of  $r$  and  $x$ , and an equality of the form  $f(r) = g(r)$  can be satisfied only if both  $f(r)$  and  $g(r)$  are equal to the same constant. Thus, we conclude that  $(dp/dx) = \text{Constant}$ . This can be verified by writing a force balance on a volume element of radius  $R$  and thickness  $dx$  (a slice of the pipe), which gives (Fig. 3.81).

The general solution of such problem is given as:

$$u(r) = \frac{r^2}{4\mu} \left( \frac{dp}{dx} \right) + C_1 \ln r + C_2 \quad (\text{Eq. 3.88})$$

Applying boundary conditions provided by Eq. (3.87) sets, causes Eq. (3.88) to yield the following form:

**Fig. 3.81** Free-body diagram of a fluid disk element



$$u(r) = -\frac{R_2}{4\mu} \left( \frac{dp}{dx} \right) \left( 1 - \frac{r^2}{R^2} \right) \quad (\text{Eq. 3.89})$$

Now substitution of Eq. (3.89) into Eq. (3.82) and doing the proper calculus, yield the final form for average velocity  $V_{\text{avg}}$  as:

$$\begin{aligned} V_{\text{avg}} &= \frac{2}{R^2} \int_0^R u(r) dr \\ &= -\frac{2}{R^2} \int_0^R \frac{R^2}{4\mu} \left( \frac{dp}{dr} \right) \left( 1 - \frac{r^2}{R^2} \right) r dr \\ &= -\frac{2}{8\mu} \left( \frac{dp}{dr} \right) \end{aligned} \quad (\text{Eq. 3.90})$$

Based on the result of Eq. (3.90), the profile velocity  $u(r)$  as the final form of solution of Eq. (3.89), can also be written as:

$$u(r) = 2V_{\text{avg}} \left( 1 - \frac{r^2}{R^2} \right) \quad (\text{Eq. 3.91})$$

and maximum velocity at centerline of horizontal pipe for a fully developed laminar flow can be derived as  $u(r)|_{\text{max}} = 2V_{\text{avg}}$ , which is an indication of the remark we made earlier that  $V_{\text{avg}} = (1/2)u_{\text{max}}$ .

Now that we have established all the above analysis, we can go back to finalizing the analysis of pressure drop or head loss for a fully developed lamina fluid as part of our compact heat exchangers design methodology by paying attention to Eq. (3.80) and substituting this equation into Eq. (3.90), then the pressure drop can be expressed as:

$$\text{Laminar flow } \Delta p = p_1 - p_2 = \frac{8\mu L V_{\text{avg}}}{R^2} = \frac{32\mu L V_{\text{avg}}}{D^2} \quad (\text{Eq. 3.92})$$

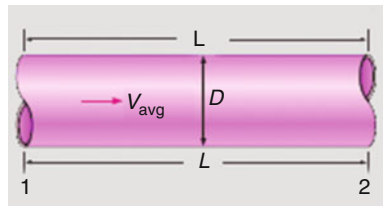
Note that:  $D = D_h = d_h$  is known as hydraulic diameter.

Study of Eq. (3.92) indicates that the pressure drop is proportional to the viscosity  $\mu$  of the fluid, and  $\Delta p$  would be zero if there were no friction. Therefore, the drop of pressure from  $p_1$  to  $p_2$  to  $p_2$  in this case is due entirely to viscous effects, and this equation represents the pressure loss  $\Delta p_L$  when a fluid of viscosity  $m$  flows through a pipe of constant diameter  $D$  and length  $L$  at average velocity  $V_{\text{avg}}$ .

A pressure drop due to viscous effects represents an irreversible pressure loss, and it is called pressure loss  $\Delta p_L$  to emphasize that it is a loss, just like the head loss  $h_L$ , which is proportional to it.

In practice, it is found convenient to express the pressure loss for all types of fully developed internal flows (laminar or turbulent flows, circular or noncircular pipes, smooth or rough surfaces, horizontal or inclined pipes) as shown in Fig. 3.82.

**Fig. 3.82** The relation for pressure and head loss valid for laminar and turbulent flows both circular and noncircular pipes



$$\text{Pressure loss : } \Delta p_L = f_D \frac{L}{D} \frac{\rho V_{\text{avg}}^2}{2}$$

$$\text{Head loss : } h_L = \frac{\Delta p_L}{\rho g} = f_D \frac{L}{D} \frac{\rho V_{\text{avg}}^2}{2}$$

Hence, pressure drop (loss) for such circumstances can be summarized as:

$$\text{Pressure loss : } \Delta p_L = f_D \frac{L}{D} \frac{\rho V_{\text{avg}}^2}{2} \quad (\text{Eq. 3.93})$$

where  $\rho V_{\text{avg}}^2/2$  is the *Dynamic Pressure* and  $f_D$  is the *Darcy friction factor* and can be written as:

**Note that:** the Darcy friction factor  $f_D$  (some textbooks use  $f_d$ ) should not be confused with the *friction coefficient*  $f_c$  (some textbook use  $C_f$ ), which is known as the *Fanning friction factor* and defined as:

$$\text{Fanning friction factor : } C_f = f_c = \frac{2\tau_w}{\rho V_{\text{avg}}^2} = \frac{f}{4}$$

where  $\tau_w$  is internal wall shear stress of the passage or pipe.

$$f_D = \frac{8\tau_w}{\rho V_{\text{avg}}^2} \quad (\text{Eq. 3.94})$$

This friction is also called the Darcy–Weisbach friction factor, named after the Frenchman Henry Darcy (1803–1858) and the German Julius Weisbach (1806–1871).

Setting Eqs. (3.92) and (3.93) equal to each other and solving for  $f_f$  gives the friction factor for fully developed laminar flow in a circular pipe as:

$$\text{Circular pipe, laminar : } f_D = \frac{64\mu}{\rho DV_{\text{avg}}} = \frac{64}{\text{Re}} \quad (\text{Eq. 3.95})$$

Equation (3.64) shows that *in laminar flow, the friction factor is a function of the Reynolds number only and is independent of the roughness of the pipe surface.*

In the analysis of piping or passages on either side of compact heat exchanger systems, pressure losses are commonly expressed in terms of the *equivalent fluid column height*, called the head loss and symbolically shown as  $h_L$ . Noting from fluid statics that  $\Delta p = \rho gh$  and, thus, a pressure difference of  $\Delta p$  corresponds to a fluid height of  $h = \Delta p/\rho g$ , the pipe head loss is obtained by dividing  $\Delta p_L$  by  $\rho g$  to give:

$$\text{Head loss : } h_L = \frac{\Delta p_L}{\rho g} = f_D \frac{L}{D} \frac{V_{\text{avg}}^2}{2g} \quad (\text{Eq. 3.96})$$

Again, note that:  $D = D_h = d_h$  is known as hydraulic diameter.

The head loss  $h_L$  represents the additional height that the fluid needs to be raised by a pump in order to overcome the frictional losses in the pipe. The head loss is caused by viscosity, and it is directly related to the wall shear stress. Equations (3.93) and (3.96) are valid for both laminar and turbulent flows in both circular and noncircular pipes, but Eq. (3.96) is valid only for fully developed laminar flow in circular pipes.

Finally, as part of the design methodology process it is best to have Excel spreadsheet templates that can be downloaded to make preliminary heat exchanger design calculations, see the: “Excel Spreadsheet Templates for Preliminary Heat Exchanger Design” that is given in Fig. 3.53.

## 3.10 Compact Heat Exchangers in Practice

Factors that eventually affect the deployment of compact heat exchangers for their use in open air Brayton combined cycle in support of enhancing the next generation of nuclear power plants overall efficiency in order to make these reactors more cost effective are fairly discussed by Hesselgreaves [8].

The decision that can be made for choosing the right heat exchanger for intended application (i.e., combined cycle, also see Chap. 5) and going through the exercise of design methodology and analysis, fabrication and eventually installation of the unit must be carried out, including all guidelines for future Preventive Maintenance (PM) to increase the life cycle for the heat exchanger as a sub-system of the big picture (i.e., an operational power plant). Reay and Hesselgreaves [8] have a good chapter on this subject and we refer readers to that reference.

### 3.11 Heat Exchanger Materials and Comparisons

Material selection is one of the most important things in high temperature application [47].

There are four main categories of high temperature materials: high temperature nickel-based alloy, high temperature ferritic steels and advanced carbon silicon carbide composite, and ceramics (Sunden 2005) [48].

Ohadi and Buckley (2001) [49] extensively reviewed materials for high temperature applications. High temperature nickel-based material has good potential for helium and molten salts up to 750 °C. High temperature ferrite steels show good performance under fusion and fission neutron irradiation to around 750 °C. Advanced carbon and silicon carbide composite has excellent mechanical strength at temperatures exceeding 1000 °C. It is currently used for high temperature rocket nozzles to eliminate the need for nozzle cooling and for thermal protection of the space shuttle nose and wing leading edges. Many options are available that trade fabrication flexibility and cost, neutron irradiation performance, and coolant compatibility. Table 3.9 compares the properties of the most commonly used high temperature materials (Ohadi and Buckley 2001) [49]. It includes nickel-based alloy, ceramic materials as well as carbon and SiC composites. Figure 3.83 shows the specific strength versus temperature for various composite materials.

Dewson and Li [51] carried out a material selection study of very high temperature reactor (VHTR) intermediate heat exchangers (IHXs) and perhaps the same materials can be looked at and used for a similar practical purpose and intended operation and application of compact heat exchanges for next generation of nuclear power plants (NGNP) ) as well.

Table 3.9 is a presentation of selected properties of the most commonly used high-temperature materials and fabrication technologies.

They selected and compared the following eight candidate materials based on ASME VIII (Boiler and Pressure Vessel Code): Alloy 617, Alloy 556, Alloy 800H, Alloy 880HT, Alloy 330, Alloy 230, Alloy HX, and 253MA.

Table 3.10 lists the allowable design stress (S) at 898 °C, minimum required mechanical properties (ultimate tensile stress [UTS]), 0.2 % proof stress (PS), and elongation (El) at room temperature, together with the nominal compositions of the alloys. They extensively compared the mechanical properties, physical properties, and corrosion resistance for the candidate materials, and finally concluded that Alloy 617 and 230 are the most suitable materials for an IHX.

### 3.12 Guide to Compact Heat Exchangers

As part of our conclusion on the subject of compact heat exchangers, we summarize generic process advantages and limitations of these exchangers designs which is applicable to all technologies; such as general advantages and limitations of

**Table 3.9** Selected properties of most commonly used high-temperature materials and fabrication technologies [49]

High temp. material/ fabrication technology	Metallic Ni alloys (Inconel 718)	Ceramics oxides of Al, Si, Sr, Ti, Y, Be, Zr, B and SiN, AlN, B4C, BN, WC94/C06	Carbon-carbon composite	Carbon fiber-SiC composite
Temperature range	1200–1250 °C	1500–2500 °C	3500 °C (inert environment) 1400–1650 °C (with SiC layer)	1400–1650 °C
Density	8.19 g/cm <sup>3</sup>	1.8–14.95 g/cm <sup>3</sup>	2.25 g/cm <sup>3</sup>	1.7–2.2 %/cm <sup>3</sup>
Hardness	250–410 (Brinell)	400–3000 kg f/mm <sup>2</sup> (V)	0.5–1.0 (MΩ)	2400–3500 (V)
Elongation	<15 %	N/A	N/A	–
Tensile strength	800–1300 MPs	48–2000 MPa	33 (Bulk Mod.)	1400–4500 MPa
Tensile modules	50 GPa	140–600 GPa	4.8 GPa	140–720 GPa
Strength of HE	Strength—adequate, but limited due to creep and thermal exp	Strength—not adequate, low mechanical parameters for stress. Good thermal and electrical parameters	Strength—poor, oxidation starts at 300 °C	Highest due to carbon fiber and SiC
Electrical conductivity	125 μΩ cm	2E–06–1E+18 Ω cm	1275 μΩ cm	1275 μΩ cm
Thermal conductivity	11.2 W/m K	0.05–300 W/m K	80–240 W/m K	1200 W/m K
Thermal expansion	13E–06 K <sup>-1</sup>	0.54–10E–06 K <sup>-1</sup>	0.6–4.5E–06 K <sup>-1</sup>	–
Comments	Metallic expansion joints are the weak link	Often very expensive fabrication cost for conventional applications. Technology is proprietary for the most part. Technologically hard to produce	Life-time is low even protected by SiC (adhesion is poor)	Comparatively less expensive, successful proprietary fabrication technologies available

compact exchangers designs, common applications, fouling, energy efficiency, heat transfer enhancement, exchanger selection and types, specification and operation, process intensification, and last but not least software programs.

In general, a final selection of heat exchanger designs unique for each intended duty and application is needed. In appropriate applications, compact designs offer substantial advantages over more conventional exchanger designs, usually shell and tube heat exchangers.

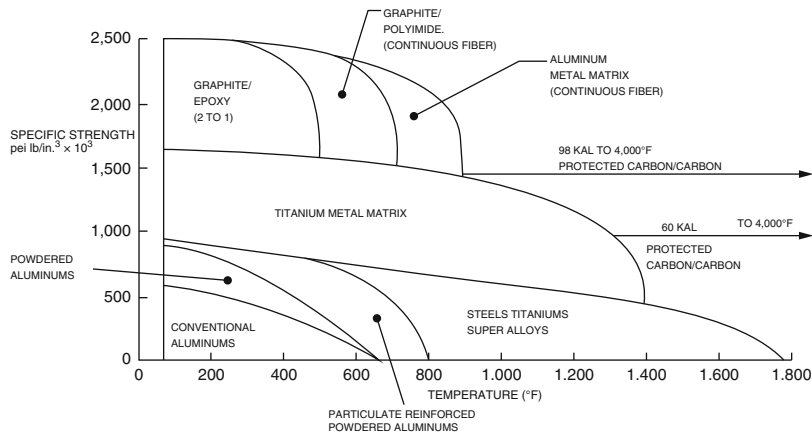


**Fig. 3.83** Specific strength vs. temperature [50]

**Table 3.10** Candidate materials for VHTR IHXs [51]

Alloys	UNS No.	$T_{\max}$ (°C)	S898 °C (MPa)	UTS (MPa)	0.2 % PS (MPa)	EI (%)	Nominal compositions (wt%)
617	N06617	982	12.4	655	240	30	52Ni-22Cr-13Co-9Mo-1.2A1
556	R30556	898	11.0	690	310	40	21Ni-30Fe-22Cr-18Co-3Mo-3W-0.3A1
800HT	N08811	898	6.3	450	170	30	33Ni-42Fe-21Cr
800H	N08810	898	5.9	450	170	30	33Ni-42Fe-21Cr
330	N08330	898	3.3	483	207	30	Fe-35Ni-19Cr-1.25Si
230	N06230	898	10.3	760	310	40	57Ni-22Cr-14W-2Mo-0.3A1-0.05La
HX	N06002	898	8.3	655	240	35	47Ni-22Cr-9Mo-18Fe
253MA	S30815	898	4.9	600	310	40	Fe-21Cr-11Ni-0.2N

Of course in recent years, the benefits of using compact heat exchangers designs are only realized in appropriate applications as part of combined cycle driven efficiency as part of next generation of nuclear power plants (Zohuri) [9, 10] and researchers around universities, national laboratories, and industry are heavily involved in both aspects of these combined cycle approaches (Open or Closed cycle).

The requirement in most heat transfer applications is to maximize the amount of heat transferred, subject to capital cost and pressure drop constraints. Both cost and heat transfer performance generally increase in proportion to exchange surface area as we discussed in detail above.

### 3.12.1 Generic Advantages of Compact Design

The main benefits of using compact heat exchangers are:

- Improved heat exchanger thermal effectiveness.
- Close approach temperatures.
- High heat transfer coefficients and transfer areas per exchanger volume.
- Small size.
- Multi-stream and multi-pass configurations.
- Tighter temperature control.
- Energy savings.
- Reduced inventory volume and hazard risk.
- Process intensification using combined reactor/exchangers.

These technological advantages can be converted into reduced operation and capital costs {Return-On-Investment (ROI) and Total-Cost-of-Ownership (TCO)}, and conserve energy, compared to shell and tube units. The performance characteristics of compact heat exchangers have particular relevance in process integration; for example in composite process heating and cooling curves. Most details of all the above points can be found in different sections of this chapter as well as the publication “Energy Efficiency” [42] and other references that are given at the end of this chapter.

## References

1. Shah, R.K. 1991. Compact heat exchanger technology and applications. In *Heat exchange engineering*, Compact heat exchangers: Techniques for size reduction, vol. 2, ed. E.A. Foumeny and P.J. Heggs, 1–29. London: Ellis Horwood Ltd.
2. Shah, R.K., and J.M. Robertson. 1993. Compact heat exchangers for the process industry. In *Energy efficiency in process technology*, ed. P.A. Pilavachi. Copyright ECSC, EEC, EAEC, Brussels and Luxembourg, AEA Technology and British Crown.
3. Foumeny, E.A., and P.J. Heggs. 1991. *Heat exchange engineering: Vol. 2. Compact heat exchangers: Techniques of size reduction*. West Sussex, England: Ellis Horwood Limited.
4. Johnson, T. 1986. Miniature heat exchangers for chemical processing. *The Chemical Engineer* 431: 36–38.
5. Pandey, Akash. 2011. Performance analysis of a compact heat exchanger. Master of technology thesis in mechanical engineering. Rourkela: National Institute of Technology.
6. Shah, R.K. 1985. Compact heat exchangers. In *Handbook of heat transfer applications*, 2nd ed, ed. W.M. Rohsenow, J.P. Hartnett, and E.N. Ganic, 4-174–4-311. New York: McGraw-Hill. Chapter 4, Part III.
7. Jeong, J.Y., H.K. Hong, S.K. Kim, and Y.T. Kang. 2009. Impact of plate design on the performance of welded type plate heat exchangers for sorption cycles. *International Journal of Refrigeration* 32(4): 705–711.
8. Hesselgreaves, J.E. 2001. *Compact heat exchangers, selection, design and operation*. Oxford: Pergamon Press.
9. Zohuri, B. 2015. *Combined cycle driven efficiency for next generation nuclear power plants: An innovative design approach*. New York: Springer Publishing Company.

10. Zohuri, B. 2014. *Innovative open Air Brayton combined cycle systems for the next generation nuclear power plants*. Albuquerque, NM: University of New Mexico Publications.
11. Zohuri, B., and P. McDaniel. 2015. A comparison of a recuperated open cycle (Air) Brayton power conversion system with the traditional steam Rankine cycle for the next generation nuclear power plant. *Nuclear Science Technology*, October 2015.
12. McDaniel, P.J., B. Zohuri, and C.R.E. de Oliveira. 2014. A combined cycle power conversion system for small modular LMFBRs. *ANS Transactions*, September 2014.
13. Zohuri, B., P. McDaniel, and C.R.E. de Oliveira. 2014. A comparison of a recuperated open cycle (Air) Brayton power conversion system with the traditional steam Rankine Cycle for the next generation nuclear power plant. *ANS Transactions*, June 2014.
14. McDaniel, P.J., C.R.E. de Oliveira, B. Zohuri, and J. Cole. 2012. A combined cycle power conversion system for the next generation nuclear power plant. *ANS Transactions*, November 2012.
15. Mazumdar, Sourav, and Rahul Singh. 2007. CFD studies on flow through compact heat exchangers. A thesis submitted in partial fulfillment of the requirements for the degree of Bachelor of Technology in Mechanical Engineering. Rourkela: Department of Mechanical Engineering, National Institute of Technology.
16. Kays, W.M., and M.E. Crawford. 1993. *Convective heat and mass transfer*, 3rd ed. New York: McGraw-Hill.
17. Kays and London. 1984. *Compact heat exchangers*, 3rd ed. New York: McGraw-Hill.
18. Ravindran, Prashaanth, Piyush Sabharwall, and Nolan A. Anderson. 2010. Modeling a printed circuit heat exchanger with RELAP5-3D for the next generation nuclear plant. INL Report INL/EXT-10-20619, December 2010.
19. Kuppan, T. 2000. *Heat exchanger design handbook*. New York: Marcel Dekker.
20. Ravindran, Prashaanth, Piyush Sabharwall, and Nolan A. Anderson. 2010. Modeling a printed circuit heat exchanger with RELAP5-3D for the next generation nuclear plant. INL/EXT-10-20619, December 2010.
21. Stone, K.M. 1996. Review of literature on heat transfer enhancement in compact heat exchangers. ACRC TR-105, August 1996. Urbana, IL: Air Conditioning and Refrigeration Center, University of Illinois, Mechanical & Industrial Engineering Department.
22. Bell, K.J. 1990. Applications of plate-fin heat exchangers in the process industries. In *Compact heat exchangers*, ed. R.K. Shah, A.D. Kraus, and D.E. Metzger, 591–602. New York: Hemisphere Publishing Corp.
23. Shah, R.K., and A.L. London. 1978. Laminar flow forced convection in ducts. In *Advances in heat transfer*, ed. J. Thomas, F. Irvine, and J.P. Hartnett. New York: Academic Press.
24. Bergles, A.E., A.R. Blumenkrantz, and J. Taborek. 1974. Performance evaluation criteria for enhanced heat transfer surfaces. *Heat Transfer* 2: 239–243. Tokyo: Japan Society of Mechanical Engineers.
25. Hewitt, G.F. 1992. *Handbook of heat exchanger design*. New York: Begell House, Inc.
26. Lunsford, Kevin M. 1998. Increasing heat exchanger performance. In *Hydrocarbon engineering*. Bryan, TX: Bryan Research & Engineering, Inc.
27. Cowell, T.A. 1990. A general method for comparison of compact heat transfer surfaces. *Transaction of the ASME Journal of Heat Transfer* 112: 288–294.
28. Somerscales, E.F.C., and J.G. Knudsen. 1981. *Fouling of heat transfer equipment*. New York: Hemisphere Publishing.
29. Chenoweth, J.M. 1990. Final report of the HTRI/TEMA joint committee to review the fouling section of the TEMA standards. *Heat Transfer Engineering* 11(1): 73–107.
30. Zohuri, B., and N. Fathi. 2015. *Thermal hydraulic analysis of nuclear reactors*. New York: Springer Publishing Company.
31. Shah, R.K., and D.P. Sekulic. 2003. *Fundamentals of heat exchanger design*. New York: John Wiley & Son Publisher.
32. Zohuri, B. 2015. *Dimensional analysis and self-similarity methods for engineers and scientists*. New York: Springer Publishing Company.

33. Forsberg, Charles, Pat McDaniel, and B. Zohuri. 2015. Variable electricity and steam from salt, helium, and sodium cooled base-load reactors with gas turbines and heat storage. In *Proceedings of ICAPP 2015*, May 03–06, 2015—Nice (France) Paper 15115.
34. Nenad Ozošik, M. 1985. *Heat transfer: A basic approach*. New York: McGraw-Hill.
35. Binder, R.C. 1973. *Fluid mechanics*. Englewood Cliffs, NJ: Prentice-Hall, Inc.
36. Kays, W.M., and M.E. Crawford. 1993. *Convective heat and mass transfer*, 3rd ed. New York: McGraw-Hill.
37. Kays, W.M. 1950. Loss coefficient for abrupt changes in flow cross section with low Reynolds number flow in single and multiple tube systems. *Transactions of the ASME* 72: 1067–1074. Tech Report 9, Department of Mechanical Engineering, Stanford University, January 1, 1950.
38. Shah, R.K. 1978. Compact heat exchanger surface selection methods. In *Heat transfer*, 4th ed., 193–199. New York: Hemisphere Publishing Company.
39. Shah, R.K., K.A. Afimiwala, and R.W. Mayne. 1978. In *Proceedings of the sixth international heat transfer conference*, Toronto, August 1978.
40. Bergles, A.E., A.R. Blumenkrantz, and J. Taborek. 1974. In *Proceeding of the fourth international heat transfer conference*, Vol. II, 239–243.
41. London, A.L. 1964. Compact heat exchangers, mechanical engineering. *ASME* 86: 31–34.
42. London, A.L., and C.K. Ferguson. 1949. Test results of high-performance heat exchanger surfaces used in aircraft intercoolers and their significance for gas-turbine regenerator design. *Transactions of the ASME* 71: 17–26.
43. London, A.L. 1964. Compact heat exchangers. *Mechanical Engineering*, *ASME* 86: 31–34.
44. LaHaye, P.G., F.J. Neugebauer, and R.K. Sahuja. 1974. A generalized prediction of heat transfer surfaces. *Transactions of the ASME Journal of Heat Transfer* 96: 511–517.
45. Martin, H. 1999. Economic optimization of compact heat exchangers. In *Proceedings of the international conference on compact heat exchangers and enhancement technology for the process industries*, Banff. New York: Begell House.
46. Compact heat exchangers—module 4.1. Energy Efficiency, GIR, September 2000.
47. Sabharwall, Piyush, and Eung Soo Kim. 2011. *High temperature thermal devices for nuclear process heat transfer applications*. USA: Idaho National Laboratory, September 2011.
48. Sundén, B. 2005. High temperature heat exchangers (HTHE). In *Proceedings of fifth international conference on enhanced, compact and ultra-compact heat exchangers: Science, engineering and technology*, Hoboken, NJ, USA, September 2005.
49. Ohadi, M.M., and S.G. Buckey. 2001. High temperature heat exchangers and microscale combustion systems: Applications to thermal system miniaturization. *Experimental Thermal and Fluid Science* 25: 207–217.
50. Brent, A. 1989. *Fundamentals of Composites manufacturing materials methods and applications*. Dearborn, MI: Society of Manufacturing Engineers.
51. Dewson, S., and X. Li. 2005. Selection criteria for the high temperature reactor intermediate heat exchanger. In *Proceedings of ICAPP'05*, Seoul, Korea, May 15–19, 2005.
52. Hesselgreaves, J.E. 2007. *Compact heat exchangers: Selection, design and operation*. 3rd edition. Pergamon.

# Chapter 4

## Thermal Design of the Selected Compact Heat Exchanger

Interest in a heat exchanger in compact form—and its surfaces with a high ratio of heat transfer area to core volume—is rising at an accelerated pace. The main reasons for the use of such compact surfaces are that smaller, lighter-weight, and lower-cost heat exchangers result. Such approach gains us both the direct geometric advantages of higher area density as well as higher heat transfer coefficient for the smaller flow passage in particular under laminar regime and conditions. Due to the smaller flow passage hydraulic radius, with gas flows particularly, the heat exchanger design range for the Reynolds number usually falls well within that laminar flow regime. Then it follows that theoretically derived laminar flow solutions for fluid friction and heat transfer in ducts of various flow cross-section geometries become important. Toward the end of this chapter two types of compact heat exchangers are selected, namely Printed-Circuit Heat Exchanger (PCHE) and Plate-Fin Heat Exchanger (PFHE), and 1-D and 3-D analysis are presented for their design for a Solar Gas Turbine Power plant based on work done by Yakah [1]; and we have used and presented all the works done in this reference.

### 4.1 Introduction

If we consider a compact heat exchanger, in particular with a gas flow passage with smaller flow passage hydraulic radius  $r_h$ , then this constraint imposes the design of heat exchanger within the range of Reynolds number that falls within the laminar flow regime. This will suggest that one needs to follow heroically derived laminar flow solutions for fluid frictions and heat transfer in ducts of various flow cross-section geometries, and this becomes a very important aspect of design considerations of such compact heat exchangers. In Chap. 3, Table 3.4 provides such comparison for different cross-sections of these passages at near laminar flow and Fig. 3.76 shows some of these passages that go with data from Table 3.5, and it is

interesting to compare these surfaces with each other and to reference them to Fig. 3.52 and Table 3.6.

The solutions related to such fully developed laminar flow, with a passage of cross-section of interest for design purposes and applications in mind, are the subject of interest in this chapter going forward. A direct application of such results may be in the development of new heat exchanger surfaces with improved characteristics [2].

Such critical solutions also become fruitful when they are critically examined and taken under consideration. A wide range for heat transfer coefficient at a given friction power for geometries of different cross-sections of ducts and passages are presented in Table 3.5. Such design consideration for compact heat exchanger that falls under fully developed laminar flow regime has many applications and a few worth mentioning are the aerospace, nuclear, biomedical, hydrogen production power plants, electronics, and instrumentation fields.

Development of heat transfer solutions in fully developed laminar flow and its dependency in duct cross-section of different geometry or passage has long been recognized using thermal hydraulic analysis approaches, where we are interested in flow inlet velocity and temperature profiles, as well as wall temperature and/or flux boundary conditions. In these types of analysis one also needs to take under consideration the fouling factor created in the passage over the life of the heat exchanger as part of design application. Therefore, a theoretical foundation is needed in order to interpret the experimental results in conjunction with a theory to extrapolate them for the design of practical exchanger systems. However, bear in mind in the real world that this kind of theory is structured upon idealizations of geometry and boundaries that are to some degree deviated from the real situation and not necessarily well duplicated either in the application or even modeling of the situation in the laboratory environment.

Thermal design of the heat exchanger problem is either a rating or sizing problem. In the rating problem the heat transfer rate and/or the outlet temperatures, pressure drop performances of an already designed or existing heat exchanger are determined from relevant relations. The thermal design process is an iterative process done by computational analysis to achieve the specified heat transfer rate defined within specification of application for given compact heat exchanger (CHE) while making sure that the pressure and temperature demands are met and correlations between them are fully maintained.

Today the fast paced and modern computer systems, with the help of finite difference and finite elements, have simplified finding the most optimum theoretical solution for mathematicians engaged in the science of heat transfer analysis and thermal hydraulic in order to find a closed solution for such theoretical quest. This computer analysis has exceeded, to some degree, the experimental Verification and Validation (V&V). Since a large number of theoretical solutions are available in the open literature, a compilation and comparison of these solutions, employing a uniform format, should be of value to the designers as well as the researchers that are involved in this field and among such available computer packages in today's market one can name, Multi-Physics COMSOL for three-dimensional analysis,

Matlab for simple one-dimensional calculation of heat transfer, and Fluent software for analysis of thermal hydraulic purposes.

## 4.2 Heat Transfer and Pressure Drop Correlations

Determining the convection heat transfer coefficient  $h$  is, along with fouling estimations, the step that typically produces the greatest inaccuracies in heat exchanger analysis. This is because exact analytical solutions are available only for laminar flow situations, and in actual heat exchangers the flow is almost always turbulent.

The convection heat transfer coefficient must then be solved from empirical correlations, which frequently have margins of error of 10–30 %, sometimes even worse. In general terms, solving the heat transfer coefficient  $h$  can be summarized as [3]:

1. First determining a suitable correlation for one of two dimensionless parameters.
2. Nusselt number  $\text{Nu}$  or the Colburn factor  $j = j_H$ , where we use Colburn factor as  $j$  that we have used throughout the book. Solving a value for  $\text{Nu}$  or  $j = j_H$ .
3. From the value found and the defining equations of  $\text{Nu}$  or, solving  $h$ .

The key is to find what could be considered a “suitable correlation”: this issue is covered in Sect. 4.8. Before that, Sect. 4.3 briefly explains some basic concepts and terminology related to convection heat transfer (this part can be skipped by readers who are familiar with the basics of convection heat transfer), and Sections from 4.9 onward provide a collection of correlations for a variety of flow situations.

## 4.3 A Short Introduction on Convection Heat Transfer

In *convection heat transfer* a combination of mechanisms is active. Pure conduction exists at the wall of heat exchanger, but away from the wall internal thermal energy transport takes place by fluid mass motion as well as conduction. Thus, to understand the convection heat transfer process in short requires a knowledge of both heat conduction and fluid flow under fully developed conditions.

If the motion of the fluid arises only due to external *force fields* such as gravity, centrifugal, or Coriolis body force, the process is referred to as *natural* or *free convection*.

If the fluid motion is induced by some external *means* such as pump, blower, fan, wind, or vehicle motion, the process is referred to as *forced convection*.

For the purpose of our analysis here we consider pure forced convection heat transfer, and laminar flow in a two-dimensional stationary duct is designated as *thermally fully developed* (see Sect. 4.10 and its sub-section as well as Sect. 4.12 of

this chapter) or established as described by Seban and Shimazaki [4] and demonstrated by Eq. (4.1) here.

$$\frac{\partial}{\partial x} \left[ \frac{T_{w,m} - T}{T_{w,m} - T_m} \right] = 0 \quad (\text{Eq. 4.1})$$

where:

$T_{w,m}$  = Perimeter average wall temperature in °F or °C

$T_m$  = Bulk average fluid temperature in °F or °C

$T$  = Temperature of the fluid to a specified arbitrary datum in °F or °C

However, note that  $T$  is a function of  $(y, z)$  as well as  $x$ , unlike fluid velocity component  $u$  in  $x$ -direction (ft/s, m/s), which is a function of  $(y, z)$  only and is independent of  $x$  for fully developed flow. Hydrodynamically and thermally developed flow is designated throughout simply as *fully developed* flow and we define both fully developed laminar and turbulent flow down below as well.

However, the Convection in a heat exchanger takes places almost always by *forced convection* (see Sect. 4.4.2 for definition of forced convection). A significant relative contribution by free convection is rare, and therefore not covered in this guide. If necessary, information on heat transfer by free convection can be found for example from VDI Heat Atlas [5], Incropera et al. [6], or Chap. 9 and we touch upon it here in this chapter.

The differential equations governing both convection heat transfer and friction have similar forms, resulting in *an analogy of friction and heat transfer*. The theoretical backgrounds can be found in heat transfer textbooks; in this guide we limit ourselves to the practical results of this analogy. From the heat exchanger analysis point of view, this analogy manifests itself in the following ways [3]:

1. Similar variables and dimensionless parameters are encountered in both heat transfer and friction analysis.
2. If either heat transfer coefficient or friction factor is known, the analogy can be used to solve at least an approximate value for the other one as well.
3. A surface with a comparatively high heat transfer coefficient is bound to also have a comparatively high friction factor and thus pressure drop, and vice versa.

## 4.4 Mathematics of Fluids and Differential Equations with Boundary Conditions

The linear differential equations and boundary conditions for the velocity and temperature problem both for hydrodynamically developed and developing flows are described and presented separately below, in Sects. 4.5.1 and 4.5.2. These are for steady-state laminar flow through constant cross section ducts and we also define terms such as laminar developed and developing flows, forced convection

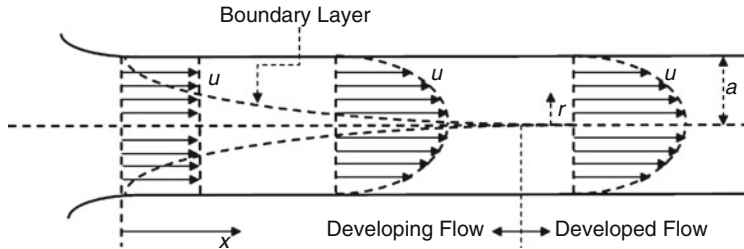


**Fig. 4.1** Developed and developing laminar flow

heat transfer, and thermally developed and developing flows, so one can have a better understanding of these subjects above and going forward.

Flow is *laminar* when the velocity is free of macroscopic fluctuations at any point in the flow field. For steady-state condition of laminar flow, all velocities at a stationary point in the flow field remain constant with respect to “time variable”, but velocities may be different at different points. Laminar flow, also referred to as viscous or stream flow, is characteristic of a viscous fluid flow at low Reynolds number.

The mathematical differential form of laminar flow in a two-dimensional stationary straight duct is depicted in Fig. 4.1 and designated as *hydrodynamically fully developed* (or established) when the fluid velocity distribution at a cross section is of an invariant form, i.e., independent of the axial distance,  $x$ , as shown in Eqs. (4.2a) and (4.2b):

$$\begin{cases} u = u(y, z) & \text{Cartesian Coordinates} \\ \text{or} \\ u(r, \theta) & \text{Cylindrical Coordinate} \end{cases} \quad (\text{Eq. 4.2a})$$

where

$$v, w = 0 \quad (\text{Eq. 4.2b})$$

Streamlines are paths that are established based on definite movement of fluid particles on those paths, and there are no components of fluid velocity normal to the duct axis. Under the assumption of a fully developed laminar flow, the fluid appears to move by sliding laminae of infinitesimal thickness relative to adjacent layers [2].

Depending upon the smoothness of the tube inlet and tube inside wall (i.e., Fanning Friction Factor  $f = f_F$ ), fully developed laminar flow persists up to  $\text{Re} \leq 2300$  for a duct length  $L$  greater than the hydrodynamic entry length  $L_{\text{hy}}$  or  $L_h$  (from now on we use  $L_h$  for the purpose of this book), otherwise for  $f_D$ , the developing flow, as described below, could exist.

First, we can define the hydrodynamic entrance for any duct as a region where the velocity boundary layer develops as depicted in Fig. 4.1, where the this

development takes place from thickness of zero at the entrance to thickness equal to internal radius of pipe  $r = a$  far downstream. Therefore, the flow establishing in this region, due to viscous fluid behavior, can be designated as *hydrodynamically developing* flow. Now that we have defined such region we can assign  $L_{hy} = L_h$  to be hydrodynamic entrance length as the duct length required to achieve a maximum duct section velocity of 90 % of that for fully developed flow when the entering fluid velocity profile is uniform.

Note that going forward we are going to show such length as  $L_h$  to match our definition of  $D_h$  for hydrodynamic diameter of fully developed flow as we have seen in previous sections and chapters of this book.

Now that we established this ground rule, we can say that, the maximum velocity occurs away from the centroid on the axis of symmetry for isosceles triangular, trapezoidal, and sine ducts as seen in Fig. 3.6.

For nonsymmetrical ducts, there are no general rules that can be defined to state the location of fluid maximum axial velocity across the duct cross section for fully developed laminar flow  $u_{max}$  (ft/s or m/s) that is later defined by Eq. (4.6) in Sect. 4.5 and consequent sub-sections of this chapter under velocity problem and solution for fully developed and developing laminar flows. A number of other definitions can be made for the location of  $L_h$  and further information can be found in the reference by Shah and London [2].

However, in a short duct, if we define a dimensionless length  $L_h^+ = L_h / (\text{Re} D_h)$  such that it is less than  $10^{-3}$ , developing laminar flow could exist even up to Reynolds number of  $\text{Re} \simeq 10^5$  which is demonstrated by Shapiro et al. [7] and Sadikov [8]. More information can also be found in the book by Zohuri et al. [9].

Under this condition (i.e., short duct), this laminar boundary layer soon converges to a turbulent situation, and fully developed turbulent flows will exist in this high Reynolds number downstream from the developing region.

#### 4.4.1 Free Convection or Natural Heat Transfer Process

Defining the free convection or natural condition where heat transfer takes place can be described as follows; where in *convection heat transfer*: a combination of mechanisms is active. Pure conduction exists at the wall of the duct, but away from the wall internal thermal energy transport takes place by fluid mass motion as well as conduction at the same time. Thus, the convection heat transfer process requires a good knowledge of both heat conduction and fluid flow. If the motion of the fluid arises solely due to external *force field* such as gravity, centrifugal, or Coriolis body forces, the process is referred to as natural or *free convection*.

### Coriolis Effect

In physics, the Coriolis effect is the apparent deflection of moving objects when the motion is described relative to a rotating reference frame. In a reference frame with clockwise rotation, the deflection is to the left of the motion of the object; in one with counter-clockwise rotation, the deflection is to the right. The mathematical expression for the Coriolis force appeared in an 1835 paper by French scientist Gaspard-Gustave Coriolis, in connection with the theory of water wheels. Early in the twentieth century, the term Coriolis force began to be used in connection with meteorology. For further information use the following link.

[https://en.wikipedia.org/wiki/Coriolis\\_effect](https://en.wikipedia.org/wiki/Coriolis_effect).

#### 4.4.2 *Forced Convection Heat Transfer Process*

In contrast to free convection, if the fluid motion is induced by some external *means* such as pump, blower, fan, wind, or vehicle motion, the process is referred to as *forced convection*.

Note that again laminar flow in a two-dimensional stationary duct is designated as *thermally fully developed* or established when, the dimensionless fluid temperature distribution, as expressed by Eq. (4.1), at a cross section is invariant and independent of variable  $x$  in that direction.

## 4.5 Velocity Problem for Developed and Developing Laminar Flows

An analysis of laminar heat transfer in *Non-newtonian Fluids* requires a thorough understanding of the hydrodynamic behavior of these fluids under the above conditions. The analytical procedure to obtain the velocity profile for *Non-newtonian* fluids with the Power-Law Model using the thermal hydraulic approach is exactly the same as for *Newtonian Fluids* except for the specification of the shear stress in the Momentum equation (Cho and Hartnett [10]).

The assumption of the power-law fluid particularly in the laminar-flow regime is a good approximation for most non-newtonian fluids, including viscoelastic fluids, resulting from the fact that the elastic nature does not play a significant role in laminar pipe flow. Given the above constraints and condition of a fully developed steady-state laminar flow in a straight circular tube, the momentum equation becomes (Bird et al. [11]).

$$\frac{dp}{dx} - \frac{1}{r} \frac{d}{dr} (r\tau_{rx}) = 0 \quad (\text{Eq. 4.3})$$

With the power-law equation for the shear stress in a circular-tube flow,

$$\tau_{rx} = K \left( \frac{du}{dr} \right)^n \quad (\text{Eq. 4.4})$$

and the fully developed velocity profile can be shown as:

$$u = u_{\max} \left[ 1 - \left( \frac{r}{R} \right)^{(n+1)/n} \right] \quad (\text{Eq. 4.5})$$

where

$$u_{\max} = \left( \frac{\tau_w}{K} \right)^{1/n} \frac{R}{1 + 1/n} \quad (\text{Eq. 4.6})$$

where:

$\tau_w$  = Shear Stress or Shear Rate at the wall.

$n$  = Power-Law Index.

$R$  = Tube inside radius  $R = d/2$  with dimension m or ft.

$r$  = Radial Coordinate.

$K$  = Constant in Power-Law Model defined below and has dimension of  $(\text{N S}^n)/\text{m}^2$  or  $(\text{lbf sn}/\text{ft}^2)$ .

Function of fully developed non-newtonian flow velocity profile  $u$  under laminar mode of Eq. (4.4) as a function of  $r/R$  for various power-law index  $n$  is depicted in Fig. 4.2, using Eq. (4.5).

For  $n$  less than 1, this gives a velocity that is flatter than the parabolic profile of *Newtonian* fluids and as  $n$  approaches zero, the velocity profile predicted by this equation approaches a plug flow profile. Figure 4.1 again shows the velocity profile generated by Eq. (4.5) for selected values of the power-law index  $n$ . It should be noted that the velocity profiles given in Fig. 4.1 and later in Figs. 4.4 and 4.5 are valid in the hydrodynamically fully developed region, where the entrance effect can be neglected.

Hence, under this assumption, the Fanning friction factor  $f$  for fully developed laminar flow in circular pipe can again be predicted by Eq. (4.7a) as before:

$$f = \frac{16}{Re} \quad (\text{Eq. 4.7a})$$

Equation (4.7a) is not a good correlation for prediction of Fanning factor in the case of rectangular shaped entrance channel, yet Sadikov [8] suggests the following form of this friction factor as

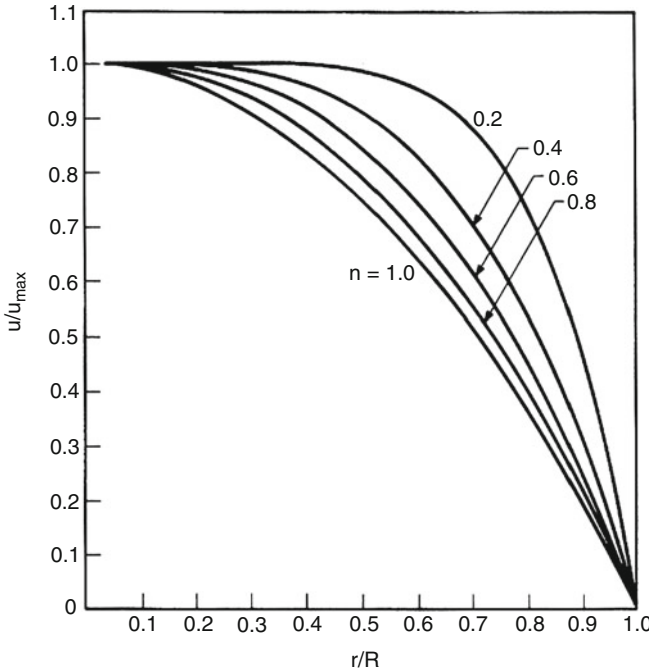


**Fig. 4.2** Velocity profile in fully developed laminar flow for non-newtonian power-law fluid [10]

$$f = \frac{C}{Re} \quad (\text{Eq. 4.7b})$$

where  $C = 14.225$  for a square cross-section channel, and  $C = 24.0$  for a flat channel. This suggestion is corroborated by the data of the reference by Hartnett et al. [12] in which the ratio of the sides of the rectangle is shown to affect the friction coefficient in laminar flow. Based on this information, it is clear that in laminar flow the analogy between heat and momentum transfer is not a basis for adapting data on the Nusselt Number Nu for a circular tube to a rectangular channel. It should be again noted that laminar flow over the initial section of a tube has been observed even at Reynolds numbers greater than critical.

Again, we can note that the experimental measurements of pressure drop along a circular tube in the fully developed laminar-flow region confirm this prediction [13, 14].

Equation (4.7b) is recommended for the prediction of pressure drop for non-newtonian fluids, both purely viscous and visco-elastic, in fully established laminar flow for circular pipe and Eq. (4.8) for rectangular channel given appropriate value of  $C$  accordingly.

### 4.5.1 Hydrodynamically Developed Flow

To develop a mathematical momentum equation for steady flow along a semi-infinite two-dimensional internal surface of a tube of small element as shown in Fig. 4.1 with a free-stream velocity  $u_\infty$  in cylindrical coordinate of  $r$  and  $x$ , we can easily apply momentum theorem in the direction of  $r$  and  $x$  in that coordinate. For application of such theorem for axisymmetric *flow in a circular tube* and for a given boundary layer of interest, we can establish the following form of partial differential equation:

$$\rho u \frac{\partial u}{\partial x} + \rho v \frac{\partial u}{\partial r} + g_c \frac{dp}{dx} = \frac{1}{r} \frac{\partial}{\partial r} \left( r \mu \frac{\partial u}{\partial r} \right) \quad (\text{Eq. 4.8})$$

Note that, this equation is valid for variable properties of  $\rho$  being fluid density (mass per unit of volume) and dynamic viscosity coefficient of  $\mu$  in the same fluid, assuming such fluid is under incompressible conditions. In this equation  $u = u(u, v)$  is fluid velocity in laminar mode with velocity components in  $x$  and  $r$  direction,  $p$  is the pressure, and  $g_c$  is the Newton constant relating force and mass [15].

However, if we consider a fully developed, steady-state laminar flow in a two dimensional singly (as in Fig. 4.3) or multiply connected stationary duct with the boundary  $\Gamma$ , then by such definition a fully developed velocity profile of Eq. (4.8) will reduce to the following form since it appears that  $v = 0$  and  $\partial u / \partial x = 0$ . Thus, we have;

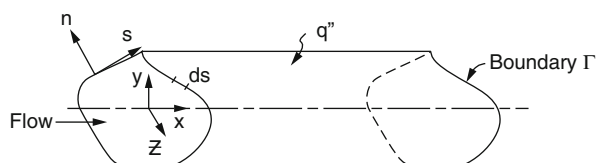
Note that in Fig. 4.3 the wall heat flux is presented as  $q''$ .

$$\frac{\mu}{r} \frac{\partial}{\partial r} \left( r \frac{\partial u}{\partial r} \right) = g_c \frac{dp}{dx} \quad (\text{Eq. 4.9})$$

This is analogous to Eq. (4.3) that we established above. In this equation the pressure  $p$  is independent of  $r$ , thus this equation can be integrated directly twice with respect to  $r$  to yield the desired velocity function and applying the following boundary conditions will result in the radial profile of velocity solution as:

$$\begin{cases} r = 0 & \frac{\partial u}{\partial r} = 0 \\ r = a & u = 0 \end{cases} \quad \text{Boundary Conditions}$$

**Fig. 4.3** A singly connected duct of constant cross-sectional area



The velocity profile solution is given as follows;

$$u = \frac{a^2 g_c}{4\mu} \left( -\frac{dp}{dx} \right) \left( 1 - \frac{r^2}{a^2} \right) \quad (\text{Eq. 4.10})$$

Equation (4.10) is the familiar Parabolic Law. If we assume, the fluid is idealized as liquid or low-speed gas with the fluid properties  $\rho$  (fluid density),  $u$  (fluid velocity),  $c_p$  (specific heat of fluid at constant pressure), and thermal conductivity  $k$  for fluid (Btu/h ft °F or W/m °C) independent of fluid temperature, then the general applicable form of the momentum equation can be established as the following [15].

$$\nabla^2 u = \frac{g_c}{\mu} \frac{dp}{dx} = 0 \quad (\text{Eq. 4.11})$$

where constant  $c$  is a pressure gradient parameter,  $(dp/dx)/(\mu/g_c)$  with dimension of  $(1/\text{ft s})$  in British or  $(1/\text{m s})$  in MKS systems with  $G$  the axial coordinate along the flow length of the duct and  $\nabla^2$  the two-dimensional Laplacian operator.

Here, we have also assumed, there exist no Coriolis Effects or Electromagnetic Forces. Also note that the right-hand side of Eq. (4.11) is independent of  $(x, y)$  or  $(r, \theta)$ , and so it is designated as constant  $c$ .

Equation (4.11) in Cartesian coordinate is represented by;

$$\frac{\partial^2 u}{\partial y^2} + \frac{\partial^2 u}{\partial z^2} = c \quad (\text{Eq. 4.12})$$

In cylindrical coordinates, it is

$$\frac{1}{r} \frac{\partial}{\partial r} \left( r \frac{\partial u}{\partial r} \right) + \frac{1}{r^2} \frac{\partial^2 u}{\partial \theta^2} = c \quad (\text{Eq. 4.13})$$

Assuming no-slip condition, then boundary condition for the velocity problem is given by,

$$u = 0 \quad \text{on } \Gamma \quad \text{evaluated at the duct inside periphery}$$

Given the definition and description of fully developed laminar flow of an incompressible fluid, the solution of the continuity equation or conservation of mass is implicitly provided by the set of Eqs. (4.2a) and (4.2b). Furthermore, the continuity equation is utilized in driven Eq. (4.11), as a result only the solution to the momentum equation is required for the fully developed laminar fluid flow problem described, and further information can be found in the reference by Shah and London [2] and briefly presented here as well.

### 4.5.2 Hydrodynamically Developing Flow

To continue with the subject of this section again we redefine the hydrodynamic entrance region as the place where the velocity boundary layer develops. However, the hydrodynamic entrance flow problem is not strictly a boundary layer problem. This is due to the fact that there is a factor known as the axial molecular momentum transport represented by  $\mu(\partial^2 u / \partial x^2)$ , which is not a negligible quantity, and far from the entrance, the boundary layer thickness is not negligible either when it is compared to the characteristic dimension of the duct.

It is also possible that very close to the entry the transverse pressure gradient across the section may not be negligible, and as a result of all these effects a complete set of Navier-Stokes equations needs to be solved, see Shah and London [2] or Bird, Stewart, and Lightfoot [11]. On the other hand except very close to the entry,  $\mu(\partial^2 u / \partial x^2)$ ,  $(\partial p / \partial y)$ , and/or  $(\partial p / \partial z)$  terms are negligible. A momentum or velocity boundary layer of the Prandtl type is a thin region very close to the body surface or wall where the influence of fluid viscosity is predominant. The remainder of the flow field can to a good approximation be treated as inviscid and can be analyzed by the potential flow theory, even though the physical concept of a boundary layer introduced by Prandtl is not strictly applicable to the entrance flow problem [2].

However, if all the idealizations that are made for the fully developed flow are invoked, the governing boundary layer for the momentum equation in  $x$ ,  $r$ -direction for axially symmetric flow, in cylindrical coordinates is given as [16];

$$u \frac{\partial u}{\partial x} + v \frac{\partial u}{\partial r} = -\frac{g_c}{\rho} \frac{dp}{dx} + \nu \left( \frac{\partial^2 u}{\partial r^2} + \frac{1}{r} \frac{\partial u}{\partial r} \right) \quad (\text{Eq. 4.14})$$

and in Cartesian coordinates, it is given as;

$$u \frac{\partial u}{\partial x} + v \frac{\partial u}{\partial y} + w \frac{\partial u}{\partial z} = -\frac{g_c}{\rho} \frac{dp}{dx} + \nu \left( \frac{\partial^2 u}{\partial y^2} + \frac{\partial^2 u}{\partial z^2} \right) \quad (\text{Eq. 4.15})$$

where  $\nu$  is the kinematic fluid viscosity coefficient which is equal to fluid dynamic viscosity divided by fluid density ( $\mu/\rho$ ) with dimension of  $\text{ft}^2/\text{s}$  or  $\text{m}^2/\text{s}$ , in the case of no-slip the boundary condition can be expressed as;

$$u, v, w = 0 \quad \text{on} \quad \Gamma \quad (\text{Eq. 4.16})$$

And the required initial condition with uniform velocity profile at the entrance is;

$$u = u_e = u_m \quad \text{at} \quad x = 0 \quad (\text{Eq. 4.17})$$

where  $u_e$  and  $u_m$  are fluid entrance velocity and fluid mean axial velocity respectively with dimension of ft/s in British System or m/s in MKS unit, where  $u_m$  with respect to flow area  $A_c$  is defined as;

$$u_m = \frac{1}{A_c} \int_{A_c} u dA_c \quad (\text{Eq. 4.18})$$

Furthermore, we need to solve the continuity equation as well and in Cylindrical coordinate its general form is presented as [16];

$$\frac{\partial u}{\partial x} + \frac{\partial u}{\partial r} + \frac{v}{r} = 0 \quad (\text{Eq. 4.19})$$

While in Cartesian coordinate the same equation can be shown as;

$$\frac{\partial u}{\partial x} + \frac{\partial u}{\partial y} + \frac{\partial u}{\partial z} = 0 \quad (\text{Eq. 4.20})$$

The solution for the hydrodynamic entry length problem can be found by solving Eqs. (4.14) and (4.19) or Eqs. (4.15) and (4.20) simultaneously with the boundary and initial conditions given by Eqs. (4.16) and (4.17).

For axisymmetric ducts, the two unknown variables  $u$  and  $v$  are obtained by solving Eqs. (4.14) and (4.19) in their cylindrical form of them. Since Eq. (4.14) is a nonlinear partial differential equation, various approximation methods can be employed including perturbation theory or some form of asymptotic method may be applied for the solution [17].

The axial pressure distribution consequently can be obtained from another physical constraint such as from solution of the mechanical energy integral equation by multiplying Eq. (4.14) or (4.15) by  $u$  and integrating over the flow cross-sectional area or integral continuity equation. Note that the momentum integral equation is obtained by integrating Eq. (4.14) or (4.15) over the flow cross-sectional area.

For a two-dimensional duct, in which case both  $v$  and  $w$  components exist in the entrance region, a third equation in addition to Eqs. (4.15) and (4.20) is essential for a rigorous solution for  $u$ ,  $v$ , and  $w$ . For further details on equations for square and eccentric annular ducts refer to Shah and London [2, pp. 221 and 333].

## 4.6 Conventional Convection Problem

The formulation of this class of temperature problem involves the specification of the applicable energy equation and the thermal boundary condition at the duct wall. The solution to the temperature problem involves the determination of the fluid and wall temperature distribution and/or the heat transfer rate between the wall and the

fluid. This type of problem presents mathematically complex features, such as heat conduction in normal, peripheral, and axial directions; variable heat transfer coefficient along the peripheral and in the axial direction; invariant or changing dimensionless velocity and temperature profile along the flow length [2, 9].

Solving these types of problems theoretically does provide the quantitative design information on the controlling dimensionless groups and indicates when to ignore certain effects in order to reduce complexity of the problem that such that a theoretical solution can be found. Shah and London [2] provide more details while we briefly touch upon it in the following sections as summary results under Sects. 4.10.1 and 4.10.2.

However, if we focus our attention on the forced convection heat transfer rate from wall to the fluid or from fluid to the wall, the determination of this heat transfer involves the solution of either:

- The conventional convection heat transfer problem or
- The conjugated problem where the combination analyzing the temperature problem for the solid wall along with that for the fluid is involved in order to establish the actual wall-fluid interface heat transfer flux distribution [2].

The simultaneous solutions of the energy equations for the solid and fluid media are obtained by considering temperature and heat flux as continuous functions at the solid wall-fluid interface. In that case, the velocity distribution for the fluid medium must first be found by solving the applicable continuity and momentum equations. Note that dimensionless temperature profile is always variant and never fully developed for this class of problems [2, 9].

The differential energy equations are briefly discussed in the following sections as well as being touched on in the preceding section for two kinds of flows:

- Fully developed flow both hydrodynamically and thermally and they were mathematically established by Eqs. (4.1) and (4.2a), (4.2b) and
- Thermally developing flows with developed or developing velocity profiles as presented by Figs. 4.4 and 4.5 below.

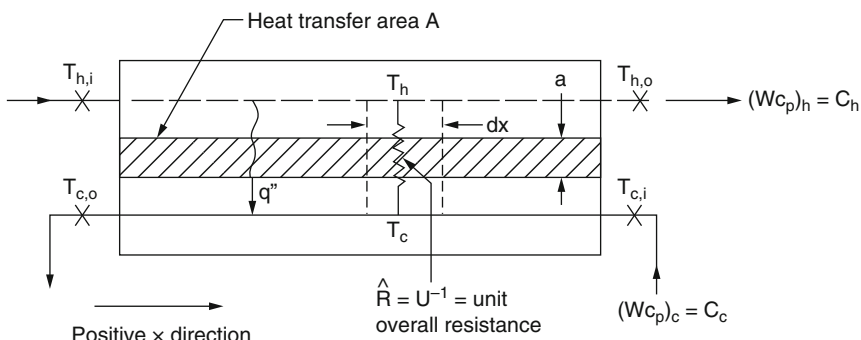


**Fig. 4.4** Nomenclature for heat exchanger variables

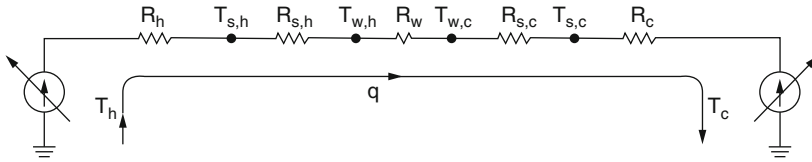


**Fig. 4.5** Thermal circuit for heat transfer in a heat exchanger

On the other hand, note that the flow is always thermally developing for a conjugated problem.

#### 4.6.1 Thermally Developed Flow

The general governing partial differential energy equation for a perfect gas is presented as follows;

$$\begin{aligned} k \nabla^2 T &= k \frac{\partial^2 T}{\partial x^2} + k \left( \frac{\partial^2 T}{\partial y^2} + \frac{\partial^2 T}{\partial z^2} \right) \\ &= \rho c_p u \frac{\partial T}{\partial x} - S - \frac{\mu}{g_c J} \left[ \left( \frac{\partial u}{\partial y} \right)^2 + \left( \frac{\partial u}{\partial z} \right)^2 \right] - \frac{u dp}{J dx} \end{aligned} \quad (\text{Eq. 4.21})$$

This equation is valid under the assumption of fluid being laminar in steady-state with constant properties of specific heat  $c_p$  (Btu/lbm °F, or J/kg °C) at constant pressure, fluid dynamic viscosity coefficient  $\mu$  (lbm/h ft, Pa s), and thermal conductivity  $k$  (Btu/h ft °F, or W/m °C) for fluid. For the governing Eq. (4.21) to be valid, the following assumption also needs to be considered as well and that is the absence of free convection, mass diffusion, chemical reaction of phase, and electromagnetic effects where complement to validation of the above energy equation.

The third term on the right-hand side of Eq. (4.21) is a representation of the work that is done by the fluid on adjacent layers due to action of shear forces and is usually referred to as “viscous dissipation” or “internal friction” both by American or Russian literature respectively.

Sometimes this work also is referred to as “gas compression work”, and this appears in the energy equation when the equations for energy conservation and momentum are manipulated so as to eliminate the kinetic energy term [16]. The corresponding differential energy equation for an *incompressible liquid* is the same as Eq. (4.21) minus the term  $(udp)/(Jdx)$ , due to the fact that this term gets cancelled out with the pressure component of enthalpy for an incompressible liquid [16].

In some cases, depending on the behavior of some liquids and under special circumstances, this flow work term may not be negligible as discussed by Shah and Kay [2, p. 81]. Also, evaluation of Eq. (4.21) indicates that the Laplacian Operand

$\nabla^2$  on the right hand side per its operation on  $u$  contains  $\nabla^2 u$  which is equal to constant  $c$  of Eq. (4.11). The resulting equation mathematically will be a fourth-order partial differential equation for the dependent variable  $T$ . The PDE Eq. (4.21) can be solved using dimensional analysis of the similarity method on all variables and parameters involved in the equation except variable  $T$  [17]. However, a particular of the similarity method can be applied so that when the effects of axial heat conduction, thermal energy sources, and viscous dissipation are negligible, the resulting new form of the energy equation can be introduced as parameter-free [9].

By converting the Energy Equation (4.21) to a non-dimensional form, we introduce the dimensionless  $x^* = x/(D_h P_e)$  where  $P_e$  is Peclet number which is a dimensionless value, and  $y^* = y/D_h$  as well as  $z^* = z/D_h$  and finally  $u^* = u/u_m$ , and substitution of all these new parameters into Eq. (4.21) with a little mathematical manipulation and rearrangement of new terms will reduce Eq. (4.21) to the following dimensionless result;

$$\frac{1}{(P_e)^2} \frac{\partial^2 T}{\partial x^{*2}} + \frac{\partial^2 T}{\partial y^{*2}} + \frac{\partial^2 T}{\partial z^{*2}} = u^* \frac{\partial T}{\partial x^*} - \frac{SD_h^2}{k} - \frac{\mu u_m^2}{g_c J k} \left[ \left( \frac{\partial u^*}{\partial y^*} \right)^2 + \left( \frac{\partial u^*}{\partial z^*} \right)^2 - 2u^* (f \text{Re}) \right] \quad (\text{Eq. 4.22})$$

Where for hydrodynamically developed flow

$$f \text{Re} = -\frac{g_c}{2\mu u_m} \frac{dp}{dx} \quad (\text{Eq. 4.23})$$

is a constant, dependent on the duct geometry. Further analysis of Eq. (4.23) for hydrodynamically developing flow reveals that the right-hand side of the equation is first obtained from the solution of Eq. (4.11) dealing with the velocity problem and then is used in Eq. (4.22) in place of the  $f \text{Re}$  term. Therefore, for *constant axial wall temperature boundary conditions*, the dimensionless temperature  $\theta$  is defined as:

$$\theta = \frac{T_w - T}{T_w - T_e} \quad (\text{Eq. 4.24})$$

Where  $T_w$  is the wall temperature at the inside duct periphery and  $T_e$  the equivalent temperature.

Equation (4.22) can be reduced to the dimensionless form

$$\frac{1}{(P_e)^2} \frac{\partial^2 \theta}{\partial x^{*2}} + \frac{\partial^2 \theta}{\partial y^{*2}} + \frac{\partial^2 \theta}{\partial z^{*2}} = u^* \frac{\partial \theta}{\partial x^*} + S^* + \text{Br}\psi \quad (\text{Eq. 4.25})$$

Where  $\text{Br}$  is dissipation number, which is known as Brinkman number for the constant axial wall temperature and it is a dimensionless parameter  $\psi$  is designated

for the bracketed term in Eq. (4.21) which takes into account the viscous dissipation and flow work, and  $S^*$  is defined as thermal energy source number, a dimensionless value as well [2].

For more details we encourage the reader to look up the book by Shah and London [2].

#### 4.6.2 Thermally Developing Flow

Thermally developing flow also follows all the idealization that is made in the fully developed scenarios, and they all are applicable except that thermal energy sources, viscous dissipation, and flow work within the fluid are neglected. Given the below boundary layer type idealization and the following situations are invoked;

$$\frac{\partial T}{\partial y}, \frac{\partial T}{\partial z} \gg \frac{\partial T}{\partial x} \quad (\text{Eq. 4.26})$$

Then, the governing partial differential equation for the considered boundary layer type energy equation for the developing laminar temperature profile for a perfect gas or an incompressible liquid for cylindrical coordinate is given by Kays as [16];

$$u \frac{\partial T}{\partial x} + v \frac{\partial T}{\partial r} = \alpha \left( \frac{\partial T}{\partial r^2} + \frac{1}{r} \frac{\partial T}{\partial r} + \frac{\partial^2 T}{\partial x^2} \right) \quad (\text{Eq. 4.27})$$

and in Cartesian coordinates defined as;

$$u \frac{\partial T}{\partial x} + v \frac{\partial T}{\partial y} + w \frac{\partial T}{\partial z} = \alpha \left( \frac{\partial^2 T}{\partial x^2} + \frac{\partial^2 T}{\partial y^2} + \frac{\partial^2 T}{\partial z^2} \right) \quad (\text{Eq. 4.28})$$

Equation (4.27) assumes the idealization that the heating is axially symmetrical and the effects of thermal energy source, viscous dissipation, and flow work can be included in the energy equation by adding corresponding terms on the right-hand side of Eqs. (4.26) and (4.27) as well. Readers should again refer themselves to Ref. 1 of this chapter.

## 4.7 Thermal Boundary Conditions

In order to describe the temperature and heat flux conditions at the *inside* wall of the duct, a set of specified thermal boundary conditions are required. The peripheral average heat transfer flux is strongly dependent on the thermal boundary condition

in the laminar flow regime, while very much less dependent in the turbulent flow regime with  $\text{Pr} \geq 1$  [2].

However, the following classification of thermal boundary condition although applicable for laminar flow can also be useful for turbulent flow. Generally speaking, these boundary conditions are not clearly and consistently defined in available literature around this subject when a great deal of variety of thermal boundary conditions can be specified for the temperature; and therefore, these highly sophisticated conclusions are difficult to interpret by a designer, yet a report by Shah and London is summarizes thermal boundary conditions and some solutions for laminar duct forced convection for different duct configurations. Their report summarizes these boundary conditions in series of format for singly, doubly, and finally multiply connected ducts. For a singly connected duct, these thermal boundary conditions are described in a most general form of a set of four different kinds of boundary conditions that are shown in Eq. (4.29) through Eq. (4.32) as described in the next section of this chapter and Table 4.2 is also established.

Presenting all the details of these four sets of boundary conditions is beyond the scope of this book, thus we encourage the reader to use references at the end of this chapter as useful resources to study or research further on the subject of this section.

#### 4.7.1 Thermal Boundary Conditions for Singly Connected Ducts

As mentioned in Sect. 4.3, the Eq. (4.1) is a presentation of a two-dimensional stationary duct is designated as *thermally fully developed* or established when the dimensionless fluid temperature distribution is as expressed by the form in the brackets.

Also note that the thermal entrance region of the duct is that region where the temperature boundary layer is developing. For this region, the dimensionless temperature profile  $(T_{w,m} - T)/(T_{w,m} - T_m)$  of the fluid varies from the initial profile at a point where the heating is started to an invariant form downstream. This is the region that flow is fully developed and treated as *thermally developed* flow and the flow velocity in this region could be either developed or developing. Thermally developed flow with a developing velocity profile is referred to as *simultaneously developing* flow.

The thermal entrance length  $L_{th}$  is defined, somewhat arbitrary, as the duct length required to achieve a value of local  $\text{Nu}_{x,bc}$  equal to 1.05  $\text{Nu}_{bc}$  for fully developed flow, when the entering fluid temperature profile is uniform. In these cases  $\text{Nu}_{x,bc}$  is the peripheral average axially local Nusselt number for the thermal entrance region for the special thermal boundary condition, a dimensionless value, while  $\text{Nu}_{x,bc}$  a dimensionless number is the peripheral average Nusselt number for fully developed flow, the subscript  $bc$  designates the thermal boundary condition of Table 4.1 below for  $x = \infty$  [2].

**Table 4.1** Thermal boundary conditions for developed and developing flows through singly connected ducts [2]

Designation	Description	Equations	Applications
<i>c</i>	Constant wall temperature peripherally as well as axially	$T _F = T_w = \text{constant}$ , independent of $(x, y, z)$	Condensers, evaporators, automotive radiators (at high flows), with negligible wall thermal resistance
<b>T3</b>	Constant axial wall temperature with finite normal wall thermal resistance	$T_{wo}(x, y, z) = T_{wo}(y, z)$ , independent of $x$ $\frac{\partial T}{\partial n^*} _F = \frac{1}{R_w} (T_{wo} - T _F)$	Same as those <b>T</b> with finite wall thermal resistance
<b>T4</b>	Nonlinear radiant-flux boundary condition	$T_a(x, y, z) = T_a(y, z)$ independent of $x$ $\frac{\partial T^*}{\partial n^*} _F = -\gamma [T^* _F^4 - T_a^{*4}]$	Radiators in space power systems, high-temperature liquid-metal facilities, high-temperature gas flow systems
<b>H1</b>	Constant axial wall heat flux with constant peripheral wall temperature	$q'(x) = \text{constant}$ , independent of $x$ $T _F = T_w$ constant, independent of $(y, z)$	Same as those for <b>H4</b> for highly conductive materials
<b>H2</b>	Constant axial wall heat flux with uniform peripheral wall heat	$k \frac{\partial T}{\partial n^*} _F = \text{constant}$ , independent of $(y, z)$	Same as those for <b>H4</b> for very low conductive materials with the duct having uniform wall thickness
<b>H3</b>	Constant axial wall heat flux with finite normal wall thermal resistance	$q'(x) = \text{constant}$ , independent of $x$ $\frac{\partial T}{\partial n^*} _F = \frac{1}{R_w} (T_{wo} - T _F)$	Same as the those for <b>H4</b> with finite normal wall thermal resistance and negligible peripheral wall heat conduction
<b>H4</b>	Constant axial wall heat flux with finite peripheral wall heat conduction	$q'(x) = \text{constant}$ , independent of $x$ $\frac{q'' D_h}{k} - \frac{\partial T}{\partial n^*} _F + K_p \frac{\partial^2 T}{\partial S^2} _F = 0$	Electrical resistance heating, nuclear heating, gas turbine regenerator, counterflow heat exchanger with $C_{\min}/C_{\max} \approx 1$ , all with negligible normal wall thermal resistance
<b>H5</b>	Exponential axial wall heat flux	$q'_x = q'_e e^{mx^*}$ $T _F = T_w = \text{constant}$ , independent of $(y, z)$	Parallel and counterflow heat exchangers with appropriate values of $m$
<b><math>\Delta T^a</math></b>	Constant axial wall to fluid bulk temperature difference	$\Delta T(x) = T_{w,m} - T_m = \text{constant}$ , independent of $x$ $T _F = T_w = \text{constant}$ , independent of $(y, z)$	Gas turbine regenerator

<sup>a</sup>The  $\Delta T$  boundary condition is primarily applied to thermally developing flow. For fully developed flow, it is the same as the **H1** boundary condition. A boundary condition in which the wall temperature varies linearly along the flow direction and remains uniform peripherally is not included in the above list. The local Nusselt numbers in the thermal entrance region for this boundary condition is higher than those for the **T** and **H1** boundary conditions. As  $x^* \rightarrow \infty$ , this boundary condition approaches the **H1** boundary condition. It has been analyzed for a circular tube [18–27] and rectangular and elliptical ducts [28].

**Table 4.2** General classification of thermal boundary conditions [2]

Specified $T_w$ , $q''$ , or $q'' = f(T_w)$ axially and/or Peripherally, as noted in Column (a) and (b)				
General classification	(a) Constant axially, constant peripherally	(b) Constant axially, variable peripherally	(c) Variable axially, constant peripherally	(d) Variable axially, variable peripherally
(1) Specified $T_w$ axially	<b>T</b> ; Applicable to both thermally developed and developing flows	Only <b>T3</b> , <b>T4</b> analyzed; Applicable to both thermally developed and developing flows	Analyzed by superposition methods from the solution of cases suggested by Shah and London [2]; also $\Delta T$ ; applicable to thermally developing flows only	A few solutions; <sup>a</sup> Applicable to thermally developing flows only
(2) Specified $q'$ axially	<b>H1</b> and <b>H2</b> ; applicable to both thermally developed and developing flows	Analyzed by superposition methods from the solution suggested by Shah and London [2], which is applicable to thermally developing flows only also <b>T3</b> and <b>T4</b>	Analyzed by superposition methods from the solution suggested by Shah and London [2], which is applicable to thermally developing flows only, which is applicable to thermally developing flows only also <b>H5</b>	A few solution; <sup>a</sup> applicable to thermally developing flows only
(3) Specified $q' = f(T_w)$ axially	No known solution; applicable to both thermally developed and developing flows	No known solution; applicable to both thermally developed and developing flows	No known solution; applicable to thermally developing flows only	No known solution; applicable to thermally developing flows only

<sup>a</sup>Some specific solutions, using superposition techniques, are available for thermally developing and hydrodynamically developing flows [2]

Note that Table 4.1 is well established by thermal boundary conditions that are presented by Shah and London [2] as a summary of four kinds of conditions that largely covers all varieties of thermal conditions that can be specified for the temperature problem. These four conditions are represented here verbatim from reference 2 and Table 4.2 also shows the general classifications of these thermal boundary conditions. Generally, these boundary conditions are not clearly and consistently defined in most heat transfer and thermal hydraulic literature, thus Shah and London [29] attempt to systemize these thermal boundary conditions, and the results are summarized by them for singly, doubly, and multiply connected ducts. We suggest that readers refer to these references for more detailed information, and we have briefly shown all four kinds of conditions in a most general form here without further details and they are described as:

$$\text{Boundary Condition of First Kind : } T_w = T_w(x, y, z, \tau) \quad (\text{Eq. 4.29})$$

$$\text{Boundary Condition of Second Kind : } q''_w = q''_w(x, y, z, \tau) \quad (\text{Eq. 4.30})$$

$$\text{Boundary Condition of Third Kind : } q''_w = U_w(T_{wo} - T_w) \quad (\text{Eq. 4.31})$$

$$\text{Boundary Condition of Fourth Kind : } \begin{cases} T_w(\tau) = [T_f(\tau)]_w \\ q''_w = [q''_f(\tau)]_w \end{cases} \quad (\text{Eq. 4.32})$$

In all these equations the following variables are defined as:

$T_w$ : Wall or Fluid temperature at the inside duct periphery  $\Gamma$ , ( $^{\circ}\text{F}$ ,  $^{\circ}\text{C}$ ).

$U_w$ : Wall thermal conductance ( $\text{Btu}/\text{h ft}^2 ^{\circ}\text{F}$ ,  $\text{W}/\text{m}^2 ^{\circ}\text{C}$ ).

$\Gamma$ : Inside periphery of the duct wall.

$q''_w$ : Wall heat flux, heat transfer rate per unit heat area  $A$  of the duct; it is an average value with respect to perimeter; for axially constant heat flux cases,  $q'' = q'/P_h$  for fully developed flow if neither axial direction  $x$  and  $m$  are the exponent in Eq. (62) of the reference by Shah and London [2] as  $q'_x = q'_e e^{mx*}$  for exponential axial wall heat flux, which is a dimensionless number.

$\tau$ : Collapsing time.

**Note that:** the boundary conditions of Fourth Kind are widely used for unsteady heat condition problems in a variety of Soviet literature as suggested by Ref. 29 here.

Also note that in Table 4.1, the following nomenclature scheme is suggested by Shah and London [2], which is used for these boundary conditions. Generally, two characters were shown by them and they are presented here in bold letters either  $\text{T}$  or  $\text{H}$  which represents axially constant wall temperature or heat transfer rate, respectively; secondly characters (1, 2, or 3) indicate, the foregoing boundary conditions of the first, second, or third kind in the peripheral direction. For boundary conditions of the first, second, and third kind (1, 2, and 3), the constant temperature, constant heat flux, and a linear condition of heat flux and wall temperature are specified respectively at the duct cross section boundary.

These nomenclature scheme conventions need further clarity, for example  $\text{H1}$  is the presentation of a constant axial heat transfer rate  $q'$  with a constant peripheral surface temperature. The numerals 4 and 5 designed other specialized axial or peripheral boundary conditions. Again bear in mind all these nomenclature conventions are well defined by Shah and London [2, 29], and they are all summarized in both Tables 4.1 and 4.2 combined.

## 4.8 Heat Exchanger Variables and Thermal Circuit

For us to be able to develop relationships between the heat transfer rate  $q$ , surface are  $A$ , fluid terminal temperatures, and finally flow rates in a heat exchanger, we expand upon the basic equations used for analysis—the energy conservation and rate equations touched upon in the previous section. For the purpose of developing

such relationships, we take under consideration a case of compact heat exchanger in the form of counterflow as demonstrated in Fig. 4.4 below in order to introduce the variables associated with this exchanger.

Two energy conservation differential equations for an exchanger that are having an *arbitrary* flow arrangements with certain idealization built into them are established as Eqs. (4.33) and (4.34) in the following forms.

$$dq = q'' dA = -C_h dT_h = \pm C_c dT_c \quad (\text{Eq. 4.33})$$

where  $\pm$  depends upon whether  $dT_c$  is increasing or decreasing with increasing  $dA$ . The overall rate equation on a local basis is

$$dq = q'' dA = U(T_h - T_c)_{\text{local}} dA = U\Delta T dA \quad (\text{Eq. 4.34})$$

Integrating Eqs. (4.33) and (4.34) across the exchanger surface results in

$$q = C_h (T_{h,i} - T_{h,o}) = C_c (T_{c,o} - T_{c,i}) \quad (\text{Eq. 4.35})$$

and

$$q = UA\Delta T_m = \frac{\Delta T_m}{R_o} \quad (\text{Eq. 4.36})$$

In Eq. (4.36), the true mean temperature difference  $\Delta T_m$  is dependent upon the exchanger flow arrangement and the degree of fluid mixing within each fluid stream and  $R_o$  which is also known as the overall thermal resistance and it presents as the inverse of the overall thermal conductance  $UA$  which is made of the following component resistance in series based on Fig. 4.5.

$$R_o = R_h + R_{s,h} + R_w + R_{s,c} + R_c \quad (\text{Eq. 4.37})$$

Where:

$$R_h = \text{hot-side film-convection resistant} = \frac{1}{(\eta_0 h A)_h} \quad (\text{Eq. 4.38})$$

$$R_{s,h} = \text{hot-scale (fouling) resistance} = t_c \frac{1}{(\eta_0 h_s A)_h} \quad (\text{Eq. 4.39})$$

$R_w$  = wall thermal resistance

$$= \begin{cases} \frac{\delta}{A_w k_w} & \text{For a flat wall} \\ \frac{1}{2\pi k_w L N_t} \ln(d_o/d_i) & \text{For a circular tube with single layer wall} \\ \frac{1}{2\pi L N_t} \left[ \sum_j \frac{\ln(d_{j+1}/d_j)}{k_{w,j}} \right] & \text{For a circular tube with muliple-layered wall} \end{cases} \quad (\text{Eq. 4.40})$$

$$R_{s,c} = \text{cold-side scale (fouling) resistance} = \frac{1}{(\eta_0 h_s A)_c} \quad (\text{Eq. 4.41})$$

$$R_c = \text{cold-side film-convection resistance} = \frac{1}{(\eta_0 h A)_c} \quad (\text{Eq. 4.42})$$

In all above equations the following variables are defined as:

$h$  = the heat transfer coefficient

$h_s$  = the scale (fouling) coefficient

$A$  = represents a total of the primary and the secondary (finned) surface area

$\eta_0$  = the total surface temperature effectiveness of an extended (fin) surface where

$\eta_0$  is related to the fin effectiveness  $\eta_f$  and the ratio of the fin surface area  $A_f$  to total surface area  $A$  which is presented as follows;

$$\eta_0 = 1 - \frac{A_f}{A} (1 - \eta_f) \quad (\text{Eq. 4.43})$$

Also note that in all above sets of Eqs. (4.38) to (4.42), subscripts h and c are for the hot and cold fluid sides, respectively. Also note that as part of Eq. (4.40), where we have defined wall thermal resistance  $R_w$ , the  $\eta_{0,h}$  and  $\eta_{0,c}$  are unity for an all prime surface exchangers with no fin involved. If there is going to be any contact or bond resistance present between the fin and the tube or plate on the hot or the cold side it is included as an added thermal resistance on the right-hand side of Eq. (4.37). In the relationship presented by Eq. (4.37), the variable  $\delta$  is the plate thickness,  $A_w$  is the total wall area for heat conduction,  $k_w$  is the thermal conductivity of the wall materials,  $d_o$  is the tube outside diameter, while  $d_i$  is the tube inside diameter and  $L$  is the tube length, and  $N_t$  is the number of tubes. A flat or plain wall is generally associated with a plate-fin or an all prime surface plate of heat exchanger. In any case  $A_w$  is written as

$$A_w = L_1 L_2 N_p \quad (\text{Eq. 4.44})$$

In Eq. (4.44) the following definitions for the involved parameters are:

$L_1$  = Length

$L_2$  = Width, and

$N_p$  = is the total number of separating plates.

Equation (4.37) can be reformed into the following format by substituting Eqs. (4.38), (4.39), (4.41), and (4.42) to present the overall heat coefficient  $UA$  as:

$$\frac{1}{UA} = \frac{1}{(\eta_0 h A)_h} + \frac{1}{(\eta_0 h_s A)_h} + R_w + \frac{1}{(\eta_0 h_s A)_c} + \frac{1}{(\eta_0 h A)_c} \quad (\text{Eq. 4.45})$$

Analyzing Eq. (4.45), the overall heat transfer coefficient  $UA$  may be defined by option in terms of the surface area of either hot fluid surface or cold fluid surface, or wall conduction area, thus we can write the following form of the relationship:

$$UA = U_h A_h = U_c A_c = U_w A_w \quad (\text{Eq. 4.46})$$

However, the option of  $A_h$ ,  $A_c$ , or  $A_w$  *must* be specified in evaluating  $U$  from the product  $UA$ .

For plain tubular heat exchangers,  $U_0$  is based on the tube outside surface area, therefore Eq. (4.45) will be reduced to the following form substituting for the  $R_w$  term associated with a circular tube with single layer wall from Eq. (4.40) as:

$$\frac{1}{U_o} = \frac{1}{h_o} + \frac{1}{h_{o,s}} + \frac{d_o \ln(d_o/d_i)}{2k_w} + \frac{d_o}{h_{i,s} d_i} + \frac{d_o}{h_i d_i} \quad (\text{Eq. 4.47})$$

However, from what we have seen and developed as far as the theory of thermal hydraulic of heat exchanger is concerned, a good knowledge of wall temperature in a heat exchanger is essential to have a good design approach and to determine the localized hot spots, freeze points, thermal stresses, local fouling characteristics, or boiling and condensing coefficients for the given design and specification for the application exchanger in mind.

Based on the thermal circuit of Fig. 4.5, when  $R_w$  is negligible, then  $T_{w,h} = T_{w,c} = T_w$  is computed from the following form of mathematical equation.

$$T_w = \frac{T_h + [(R_h + R_{s,h})/(R_c + R_{s,c})]T_c}{1 + (R_h + R_{s,h})/(R_c + R_{s,c})} \quad (\text{Eq. 4.48})$$

When  $R_{s,h} = R_{s,c} = 0$ , this further simplifies to

$$T_w = \frac{T_h/R_h + T_c/R_c}{1/R_h + 1/R_c} = \frac{(\eta_0 h A)_h T_h + (\eta_0 h A)_c T_c}{(\eta_0 h A)_h + (\eta_0 h A)_c} \quad (\text{Eq. 4.49})$$

Note that  $T_h$ ,  $T_c$ , and  $T_w$  are *local* temperatures in this equation.

Note that the following idealizations that are built into Eqs. (4.33) and (4.34) and their subsequent integration across the surface area for a specified exchanger flow arrangement yields the expressions for the design methods such as effectiveness-NTU (Number of Transfer Unit) and Logarithmic Mean Temperature Difference (LMTD):

Note that these statements are directly quoted from Ref. 31 of this chapter.

1. The heat exchanger operates under steady-state conditions which are first of all constant flow rates, and secondly thermal history of fluid particle is independent of time,
2. All the heat losses to the surroundings are negligible.
3. There are no thermal energy sources in the heat exchanger.
4. In counterflow and parallel-flow exchangers, the temperature of each fluid is uniform over every flow cross section. From the temperature distribution point

of view, in cross-flow exchangers each fluid is considered mixed or unmixed at every cross-section depending upon the specification. For a multipass exchanger, the foregoing statements apply to each pass depending upon the basic flow arrangement of the passes; the fluid is considered mixed or unmixed between passes.

5. Either there are no phase changes (condensation or boiling) in the fluid streams flowing through the exchanger or the phase changes occur under one of the following conditions:
  - (a) Phase change occurs at a constant temperature as for a single component fluid at constant pressure; the effective specific heat for the phase-changing fluid is infinity in this case, and hence the maximum flow stream heat capacity rate of cold fluid or flow-stream capacity rate of hot fluid  $C_{\max}$  approaches to infinity as  $C_{\max} \rightarrow \infty$
  - (b) The temperature of the phase changing fluid varies linearly with heat transfer during the condensation or boiling. In this case, the effective specific heat is constant and finite for the phase-changing fluid.
6. The specific heat of each fluid is constant throughout the exchanger so that the heat capacity rate on each side is treated as constant.
7. The velocity and temperature at the entrance of the heat exchanger on each fluid side are *uniform*.
8. For an extended-surface exchanger, the overall extended-surface temperature effectiveness  $\eta_0$  is considered uniform and constant.
9. The overall heat transfer coefficient between the fluids is *constant* throughout the exchanger, including the case of phase-changing fluid in idealization as step 5 above.
10. The heat transfer area is distributed uniformly on each fluid side. In a multipass unit, heat transfer surface area is equal in each pass.
11. For a plate-baffled shell-and-tube exchanger, the temperature rise per baffle pass is small compared to the overall temperature rise along the exchanger; i.e., the number of baffles is large.
12. The fluid flow rate is uniformly distributed through the exchanger on each fluid side in each pass. No stratification, flow bypassing or flow leakages occur in any stream. The flow condition is characterized by the bulk or mean velocity at any cross-section.
13. Longitudinal heat conduction in the fluid and in the wall is negligible.

Note that idealizations expressed in steps 1 through 4 are necessary in a theoretical analysis of steady-state heat exchangers. Idealization step 5 essentially restricts the analysis to single-phase flow on both sides or many of the foregoing idealizations are not valid, since mass transfer in phase change results in variable properties. Consequently, the heat transfer cannot be analyzed using the theory. The design of a two-phase heat exchanger is beyond the scope of this book and readers should refer to the book by Kakaç, Bergles, and Oliveira Fernandes under the title of “Two-Phase Flow Heat Exchangers: Thermal-Hydraulic Fundamentals and Design (NATO Science Series E)” [30].

Also, in Ref. 31 of this chapter Shah et al. [31], indicate that if idealization 6 is not valid, divide the exchanger into small segments until the specific heats can be treated as constant. Idealization 7 and 8 are primarily important for compact heat exchangers and are discussed in that reference 29.

If for some reason any of these idealizations are not valid for a particular heat exchanger application, the best solution is to work directly with either Eq. (4.33) or (4.34) or their modified form by including a particular effect, and to integrate them over a small exchanger segment in which all of the idealizations are valid.

Note that other design methods such as  $P$ -NTU and  $\psi - P$  and their descriptions as given by Shah and Muller [31] can be found in the book by Rohsenow et al. [31].

## 4.9 Solving Convection Heat Transfer Coefficient from Empirical Correlations

Before we touch this sub-section topic, we need to mention that Nusselt number  $Nu$ , Stanton number  $St$ , and finally Colburn heat transfer factor  $j$  are core parameters in a thermal hydraulic analysis of any convection heat transfer calculation. To summarize all these parameters as part of convection heat transfer analysis, we can express that the physical significance of Nusselt number  $Nu$  is a dimensionless temperature gradient of the fluid at surface, and it is described as;

$$Nu = \frac{hL}{k} \quad (\text{Eq. 4.50})$$

where  $L$  is the characteristic length and  $k$  is the thermal conductivity of the fluid with units of  $\text{W}/\text{m K}$   $h$  is convection heat transfer coefficient [ $\text{W}/\text{m}^2 \text{K}$ ], and Stanton number in turn is defined as a modified Nusselt number as;

$$St = \frac{Nu}{Re \cdot Pr} \frac{h}{u\rho c_p} \quad (\text{Eq. 4.51})$$

where  $u$  is the flow velocity [ $\text{m}/\text{s}$ ],  $\rho$  is fluid density with dimension of  $\text{kg}/\text{m}^3$ ,  $c_p$  is specific heat with units [ $\text{J}/\text{kg K}$ ] while  $Pr$  is the Prandtl number and  $Re$  is Reynolds number and both are dimensionless parameters.

Finally, the Colburn factor  $j$  is defined from the Stanton number as;

$$j = St Pr^{2/3} = \frac{Nu \cdot Pr^{-1/3}}{Re} \quad (\text{Eq. 4.52})$$

All the parameters in Eq. (4.52) are defined as before and careful consideration should be taken into account when we use velocity  $v$  in Stanton number in Eq. (4.51). Different correlation may call upon usage of mean, maximum, or in certain circumstances some other value of velocity may be used.

Taking into consideration both Eqs. (4.51) and (4.52) simultaneously, we notice that the Prandtl number is a fluid property that represents the ratio of Kinematic Viscosity  $\nu$  also known as momentum diffusivity of the fluid to the thermal diffusivity  $\alpha$  of the fluid. With definitions of fluid kinematics viscosity  $\nu$  and thermal diffusivity  $\alpha$ , the new form of Prandtl number  $\text{Pr}$  can be defined as;

$$\text{Pr} = \frac{\nu}{\alpha} = \frac{(\mu/\rho)}{(k/\rho c_p)} = \frac{\mu c_p}{k} \quad (\text{Eq. 4.53})$$

Where all the parameters used in Eq. (4.53) are defined as follows;

$\nu$  = Kinematic viscosity of fluid [ $\text{m}^2/\text{s}$ ]

$\alpha$  = Thermal diffusivity of fluid which is defined as  $\alpha = k/\rho c_p$  with units of [ $\text{m}^2/\text{s}$ ]

$k$  = Thermal conductivity of fluid [ $\text{W}/\text{m}^2 \text{ K}$ ]

$\rho$  = Density of fluid [ $\text{kg}/\text{m}^3$ ]

$c_p$  = Specific heat of fluid at constant pressure [ $\text{kg}/\text{m}^3$ ]

$\mu$  = Dynamic viscosity of fluid which is defined as  $\mu = \nu\rho$  with units of [ $\text{Pa s}$ ]

As a matter of interest, in addition to the core dimensionless parameters described above, there are numerous other ones sometimes used in other aspects of thermal hydraulic analysis and some of these are briefly listed without further explanation for reference purposes in Table 4.3.

Now that we have briefly introduced all these dimensionless parameters above, we can go back to our first goal when solving the convection heat transfer coefficient and find the correct value of Nusselt number  $\text{Nu}$  or Colburn number  $j$ . Once that goal is achieved as the second step we can simply determine the fluid convection heat transfer coefficient  $h$ , by utilizing Eq. (4.50) or Colburn factor  $j$  by solving Eq. (3.35) in the form of Reynolds analogy as;

$$\frac{1}{2} f_D = \frac{f_D}{8} = \frac{\text{Nu}}{\text{Re}} = \text{St} \quad (\text{Eq. 4.54})$$

Where:

$f_D$  = Darcy or Moody friction

**Table 4.3** Dimensionless parameters

Parameter	Equation	Explanation
Euler number $\text{Eu}$	$\text{Eu} = \frac{\Delta p}{1/2(\rho u)}$	Pressure drop non-dimensionalized with dynamic pressure
Graetz number $\text{Gz}$	$\text{Gz} = \frac{d}{x} \text{Re Pr}$	Used in entrance region calculations; $x$ = distance from pipe entry, $d$ = diameter of circular tube
Peclet number $\text{Pe}$	$\text{Pe} = \text{Re Pr}$	Ratio of thermal energy transported to the fluid to axially conducted heat in the flow
Grashof number $\text{Gr}$	$\text{Gr} = \frac{g\beta\Delta T L^3}{\mu^2}$	Ratio of buoyancy to viscous forces in free convection
Rayleigh number $\text{Ra}$	$\text{Ra} = \text{Gr Pr}$	A modified Grashof number in free convection

Thus we can write:

$$h = \text{Nu} \frac{k}{L} \quad \text{or} \quad C_{\min}/C_{\max} h = \frac{u\rho c_p}{\text{Pr}^{2/3}} \quad (\text{Eq. 4.55})$$

Correlations for Nu and or  $j$  are provided in heat transfer and heat exchanger design of many textbooks and for some limited values here in this book. In choosing a suitable correlation, for proper application of heat exchanger, the following factors need to be taken under consideration and they are [3]:

1. The correlation must be for the correct surface geometry and flow direction.
2. Is the flow laminar or turbulent?
3. Does the range of validity of the correlation cover the case at hand? (check at least Reynolds and Prandtl numbers)
4. In the case of a flow in a tube, does the entry length make up a significant portion of the tube length?
5. Is the correlation for local or average heat transfer coefficient?
6. Are there particular characteristics such as surface roughness or highly variable fluid properties in the flow case that the correlation should take into account?
7. Are there different correlations for constant surface temperature  $T_s$  or constant surface heat flux  $q''$ , and if so, which is the better approximation for the case?
8. At what temperature should the fluid properties be evaluated?

The first point is obvious; empirical correlations for Nusselt number Nu and Colburn heat transfer factor  $j$  for the wrong flow geometry cannot yield correct results.

Finding whether the flow is laminar or turbulent is done by calculating the Reynolds number and comparing it to the Critical Reynolds number  $\text{Re}_{\text{critical}} = \text{Re}_{\text{cr}}$  of the flow geometry. If  $\text{Re} < \text{Re}_{\text{cr}}$  the flow is laminar, if it is much greater than  $\text{Re}_{\text{cr}}$ , it is turbulent. For a flow in a pipe  $\text{Re}_{\text{cr}} = 2300$ , for parallel flow across a flat plate  $\text{Re}_{\text{cr}} = 5 \cdot 10^5$ .

The region where  $\text{Re}$  is only slightly greater than critical Reynolds number is problematic, as the transition to turbulence is neither an abrupt nor always predictable change: instead, turbulence begins to increase gradually as the  $\text{Re}$  increases above  $\text{Re}_{\text{cr}}$ , and this transition regime may cover a wide range of  $\text{Re}$ .

Furthermore, under favorable circumstance the flow may sometimes even remain completely laminar even if Reynolds number is noticeably above  $\text{Re}_{\text{cr}}$ . For pipe flows this unpredictable transition regime ranges from 2300 to approximately  $10^4$ . Results for convection heat transfer coefficient in the transition regime must be considered to have a large margin of uncertainty.

Flows in channels normally have a certain part of entry length, typically in the range of 10...60 times diameter, where the flow is not yet fully developed, and the convection heat transfer coefficient has not reduced to its fully developed value. If this thermal entry length makes up a significant proportion of the total flow length, the initially higher values of  $h$  must be taken into account [3].

In the context of this guide, we limit ourselves to the assumption of constant values of overall heat transfer coefficient, and therefore, also in solving the convection heat transfer coefficient, the goal is to find the average value  $\bar{h}$ .

Solving the average  $\bar{h}$  from a correlation for local Nusselt number correlation is relatively straightforward. If location in the flow direction is denoted with  $x$  and there is a function that gives the Local Nusselt number  $\text{Nu}_x$  as a function of some parameters, for example distance  $x$  from the beginning of the flow,  $\text{Re}$ , and  $\text{Pr}$ ,

$$\text{Nu}_x = \text{Nu}_x(x, \text{Re}, \text{Pr}) \quad (\text{Eq. 4.56})$$

Then using the definition of  $\text{Nu}$ , the local heat transfer coefficient must be

$$h_x = \text{Nu}_x \frac{k}{L}(x, \text{Re}, \text{Pr}) \quad (\text{Eq. 4.57})$$

Finding  $\bar{h}$  over any given range from  $x_1$  to  $x_2$  can then be done easily by integrating from  $x_1$  to  $x_2$  and dividing with distance between those points (see Fig. 4.6):

$$\bar{h} = \frac{1}{x_2 - x_1} k \int_{x_1}^{x_2} \frac{1}{L} \text{Nu}_x(x, \text{Re}, \text{Pr}) dx \quad (\text{Eq. 4.58})$$

If characteristic length is not the distance  $x$  in flow direction, which it depends on the case, the correlation of  $\text{Nu}$  may or may not be,

$$\bar{h} = \frac{k}{(x_2 - x_1)L} \int_{x_1}^{x_2} \text{Nu}_x(x, \text{Re}, \text{Pr}) dx \quad (\text{Eq. 4.59})$$

However, several correlations may exist for the same flow situation, some being simple but ignoring the minor effects such as surface roughness or fluid properties, while for some assuming constant  $T_s$  approximation and some for constant surface  $q''$ . Under these circumstances a judgment must be made on which is the best approximation for the case and application at hand, and which assumptions such as smooth surface or constant fluid properties are reasonable for that case and related applications where we need to use the exchanger.

In various empirical correlations of  $\text{Nu}$  or  $j$  the characteristic length can be different, even in correlations developed for the same geometry. However, separate friction factor as seen above are often encountered and involved as well and by now

**Fig. 4.6** Average and local convection heat transfer coefficients

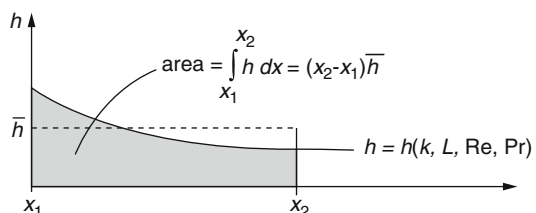
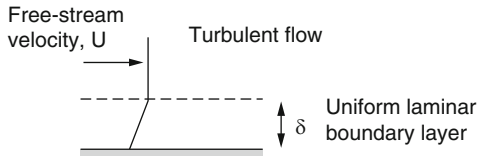


**Fig. 4.7** Representation of the uniform boundary layer model



we know that they are Fanning friction  $f_f$  or in some text books and literature it is called the coefficient of friction, and the other one is Darcy friction  $f_D$  also known as Moody friction. Naturally, a care should be taken in order not to confuse these two frictions. In some textbooks Fanning friction is denoted as  $f$  or  $C_f$  which can lead to great confusion, but throughout this book we denote this friction as  $f_f$  as we have done so far.

As we have established in Eqs. (3.27), (3.28), and (3.93), and again here we can re-emphasize that the Fanning friction factor is defined as the ratio of fluid wall shear stress  $\tau$  to the dynamic pressure of the fluid flow as:

$$f_f = \frac{\tau}{\frac{1}{2} \rho u^2} \quad (\text{Eq. 4.60})$$

Equation (4.60) leads to derivation of Reynolds analogy if we take Fig. 4.7 into account.

Based on the configuration in Fig. 4.7, we consider flow over a flat plate. If we assume a simple shear flow in a uniform laminar boundary layer, we can approximate the wall stress  $\tau$  as:

$$\tau \approx \mu \frac{u}{\delta} \quad (\text{Eq. 4.61})$$

where  $u$  is the free-stream velocity and  $\delta$  is fictitious uniform boundary layer thickness. So,

$$\delta \approx \mu \frac{u}{\tau} = \frac{\mu u}{\frac{1}{2} \rho u^2 f_f} = \frac{v}{\frac{1}{2} u f_f} \quad (\text{Eq. 4.62})$$

and dividing by the length of the flat plate,  $L$ :

$$\frac{\delta}{L} \approx \frac{v}{\frac{1}{2} u L f_f} = \frac{1}{\frac{1}{2} \text{Re}_L f_f} \quad (\text{Eq. 4.63})$$

where  $\text{Re}_L = \frac{uL}{v}$

Next, we define the Sherwood number;

$$\text{Sh}_L = \frac{\bar{k}L}{D_{AB}} \quad (\text{Eq. 4.64})$$

which is based on the length scale  $L$ . The average mass transfer coefficient  $\bar{k}$  is based on the film model and some concentration boundary layer thickness  $\delta_c$ :

$$\bar{k} = \frac{D_{AB}}{\delta_c} \quad (\text{Eq. 4.65})$$

Thus,

$$\text{Sh}_L = \frac{D_{AB}}{\delta_c} \frac{L}{D_{AB}} = \frac{L}{\delta_c} = \frac{L}{\delta} \frac{\delta}{\delta_c} \quad (\text{Eq. 4.66})$$

Finally, we know from scaling analysis that when  $\text{Sc} = 1$ ,  $\delta = \delta_c$ , and thus, the Sherwood number can be evaluated as;

$$\frac{\bar{k}L}{D_{AB}} = \frac{L}{\delta} = \frac{\frac{1}{2} u L f_f}{v} \quad (\text{Eq. 4.67})$$

If we equate the very first and last terms,

$$\frac{1}{2} f_f = \frac{\bar{k}}{u} \quad (\text{Eq. 4.68})$$

since  $v/D_{AB} = 1$ . This is the *Reynolds analogy* which relates the friction factor to the mass transfer coefficient.

Therefore, Darcy friction factor on the other hand can be defined simply on the basis of the Darcy-Weisbach equation for friction pressure drop in a pipe flow as;

$$\Delta p = \frac{\rho u^2}{2} \left( f_D \frac{L}{D} \right) \Leftrightarrow f_D = \frac{2\Delta p}{\rho u^2} \frac{D}{L} \quad (\text{Eq. 4.69})$$

where:

$L$  = Pipe Length

$D$  = Pipe Diameter

$\frac{1}{2} \rho u^2$  = Dynamic pressure

As we also mentioned in Chap. 3, in terms of Fanning friction factor, the Darcy friction factor is simply equal to  $4f_f$  or  $f_D = 4f_f$ .

Also, it is worth mentioning that one can expand Eq. (3.35) to a range of  $0.6 < \text{Pr} < 60$  with the Chilton-Colburn analogy to the form:

$$\frac{1}{2} f_f = \text{St} \text{Pr}^{2/3} = \frac{\text{Nu}}{\text{Re}} \text{Pr}^{-1/3} = j \quad (\text{Eq. 4.70})$$

These analogies can be used for flows in circular tubes or unobstructed parallel flow across a flat plate, and under these simple flow geometries they provide accurate

results. However, they should not be used for more than rough estimates for more complex flow geometries.

A close observation of Eqs. (4.54) and (4.60) combined with Eqs. (4.69) and (4.70) reveals that both convection heat transfer coefficient which is directly proportional to Nusselt number  $\text{Nu}$ , Stanton number  $\text{St}$  or Colburn number  $j$  and friction pressure drop directly proportional to  $f_f$  or  $f_D$  are to some extent proportional to flow velocity. More exactly, practical experience has shown that this dependency is usually for drop in turbulent flow approximately as shown here;

$$\Delta p \propto u^{1.6 \dots 1.8} \quad (\text{Eq. 4.71})$$

Together from these it follows, that the proportionality of  $\Delta p$  and in turbulent flow is typically approximate to the following format as:

$$h \propto \Delta p^{0.4} \quad (\text{Eq. 4.72})$$

If the flow were laminar, then the proportionality would be  $h \sim \Delta p^{0.3}$  as demonstrated by Sarkomaa [32].

## 4.10 Internal Flow in a Pipe or Passage

The two key factors defining the behavior of a flow in a tube are:

1. Whether the flow is laminar or turbulent, and
2. Whether entry length constitutes a significant portion of the whole tube length.

In heat exchangers the flow is almost always turbulent and the portion of entry length is rarely significant, but entry length and laminar flow are also briefly considered at the end of the following text in this section. An extensive discussion on this matter is provided by Zohuri and Fathi [9] as well as others that can be found in open literature or textbooks.

When the flow is fully developed in an internal channel, its velocity profile will be a parabola for laminar flow (assuming constant viscosity), and a somewhat blunter shape if the flow is turbulent. Typically it will take up from approximately 10–60 channel diameters or hydraulic diameter  $D_h = D$  for this profile to develop in Fig. 4.8. The development of the velocity profile in the entry length is demonstrated

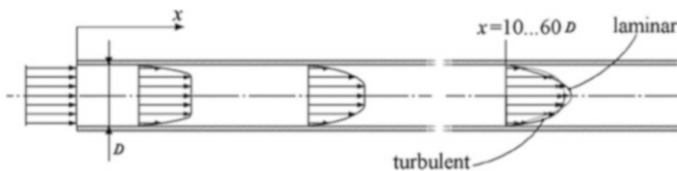


**Fig. 4.8** Forming of the velocity profile inside of a tube

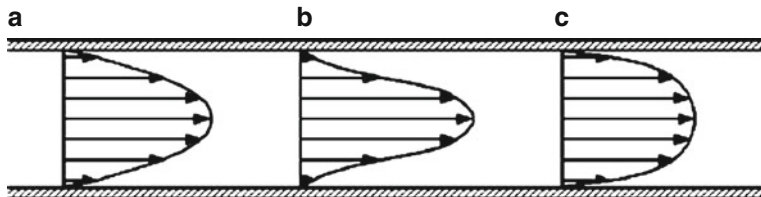


**Fig. 4.9** Velocity profiles in a laminar flow in a pipe: (a) constant viscosity, (b) cooling liquid or heating gas, (c) cooling gas or heating liquid

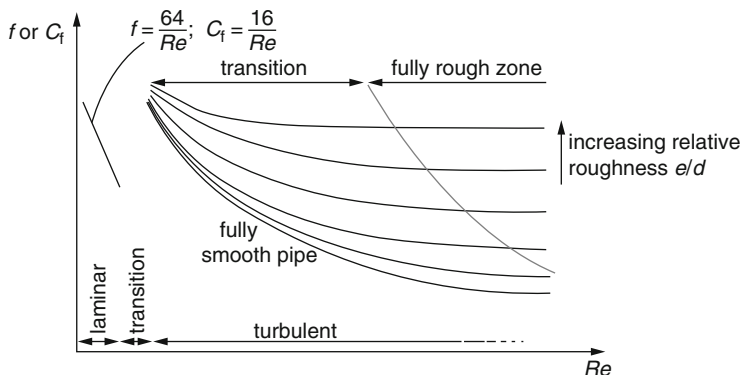


**Fig. 4.10** Illustration of a Moody's chart;  $f = f_f = C_f$  is the Fanning Friction Factor,  $f = f_D$  the Darcy Friction Factor, and  $e$  the absolute surface roughness

in Fig. 4.8. If the fluid is heated or cooled by the tube walls and fluid viscosity varies as a function of temperature, the actual velocity profile will be different (Fig. 4.9).

For a turbulent flow in a tube, surface condition approximation of constant  $T_s$  or constant surface temperature with heat flux  $q''$  has negligible effect as long as  $Pr > 0.7$ . This covers most but not all fluids; liquid metals in particular have much smaller Prandtl numbers [3].

Whether surface roughness has an effect depends not only on the absolute roughness of the tube itself, but also the flow. As can be seen in the illustration of Moody's chart in Fig. 4.10, which is a modified version of Fig. 3.72, the effect of surface roughness on Fanning friction factor  $f = f_F = f_f$  or  $C_f$  becomes less at low Reynolds numbers. At low enough Reynolds number and small relative roughness the friction factor of the flow becomes almost independent of the roughness, and therefore, the tube can be considered smooth.

The characteristic length  $L$  depends on geometry of the pipe and for flows inside circular tubes it is the tube inner diameter  $D_i$ , used in both Reynolds number and Nusselt numbers. Although most heat transfer correlations are for tubes of circular cross-section, these can be easily adapted to other cross-sectional shapes with little loss in accuracy by simply replacing the inner diameter  $D_i$  with the hydraulic diameter  $D_h$ , Eq. (3.4a), i.e.,  $D_h = 4A_o/P$ . As we defined in Chap. 3 of this book,

the Hydraulic Diameter is defined as  $4A_o/P$ , in non-circular channel, where  $A_o$  is the minimum free-flow area on one fluid side of a heat exchanger and  $P$  is the wetted perimeter of flow passages of that side.

Correlations for different cases of flow in a tube are to be evaluated at ***mean bulk temperature***  $T_b$ , or just bulk temperature,

$$T_b = \frac{1}{2}[T_i - T_o] \quad (\text{Eq. 4.73})$$

where  $T_i$  and  $T_o$  are inlet and outlet temperature respectively.

#### 4.10.1 Fully Developed Turbulent Flow

So far we have established enough ground in order to be able to deal with this section under the topic of *fully developed turbulent flow* and go forward with a simple correlation for such flow circumstances in a circular tube, and it can be obtained by simply solving Nusselt number  $\text{Nu}$  or Colburn factor  $j$  from the Chilton-Colburn analogy, Eq. (4.70), and substituting an equation for  $f_f$  in the case of a smooth tube as a function of Reynolds number as below:

$$\begin{aligned} j &= 0.023 \text{Re}^{-0.2} \\ \text{Nu} &= 0.023 \text{Re}^{0.8} \text{Pr}^{1/3} \end{aligned} \quad (\text{Eq. 4.74})$$

where all fluid properties are to be evaluated at mean bulk temperature  $T_b$  which is presented by Eq. (4.73). For a smooth tube within a range of  $0.5 < \text{Pr} < 3$  and  $10^4 < \text{Re} < 10^5$  the correlation seems to be accurate to within  $-20 \dots +28\%$  (Shah and Sekulic 2003, p. 483) [33]. Dittus-Boelter correlation is a slightly improved correlation for fully developed turbulent flows in smooth pipes, for heating

$$\text{Nu} = \begin{cases} 0.024 \text{Re}^{0.8} \text{Pr}^{0.4} & \text{for heating case} \\ 0.026 \text{Re}^{0.8} \text{Pr}^{0.3} & \text{for cooling case} \end{cases} \quad (\text{Eq. 4.75})$$

Equation (4.75) is valid within  $10^4 < \text{Re} < 1.2 \times 10^5$  and  $0.7 < \text{Pr} < 120$ . Within this range errors are approximately  $-26 \dots +7\%$  for water, expanding to  $+10 \dots +33\%$  for air at Prandtl Number  $\text{Pr} = 0.7$  and  $-39 \dots +21\%$  for oils for  $\text{Pr} = 120$ . Below  $\text{Re} = 10^4$  the results are much worse (Shah and Sekulic 2003, p. 484) [33]. It is evident that the Dittus-Boelter correlation is also suitable only for rough initial estimates but not accurate sizing calculations.

The largest errors of Dittus-Boelter correlation occur when the temperature difference between bulk temperature  $T_b$  and tube surface temperature  $T_s$  is greater than approximately  $6^\circ\text{C}$  for liquids, or  $60^\circ\text{C}$  for gases (Chapman, p. 281) [34]. A further improved version for cases where greater temperature differences are

present has been proposed by Sieder and Tate [35] taking into account the effect of fluid properties varying as a function of temperature with a correction factor  $\phi$  as follows;

$$\text{Nu} = a \text{Re}^{0.8} \text{Pr}^{0.33} \phi \quad (\text{Eq. 4.76})$$

where the constant  $a$  is in various sources given values ranging from 0.019 to 0.027.

The function  $f$  taking into account variable fluid properties also has different forms in different textbooks; according to (Perry 1988, p. 894) [36] it depends on the type of flow:

$$\phi = \begin{cases} \left(\frac{\mu}{\mu_s}\right)^{0.14} & \text{for liquid, all cases} \\ 1 & \text{for gases, cooling} \\ \left(\frac{T_b}{T_s}\right)^{0.50} & \text{for gases, heating} \end{cases} \quad (\text{Eq. 4.77})$$

where  $T_s$  is surface temperature.

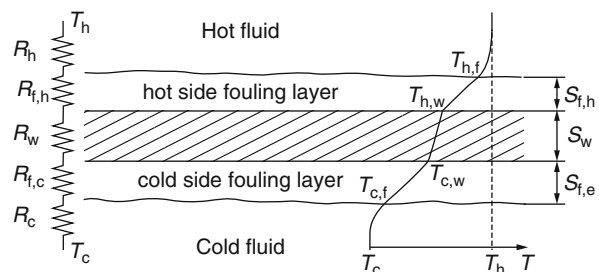
As with the Colburn and Dittus-Boelter correlations, also in Sieder-Tate correlation, all properties should be evaluated at bulk temperature  $T_b$ , except those with subscript  $s$ , which are to be evaluated at the estimated average surface temperature.

The following Eq. (4.78) can be used to estimate the surface temperatures of heat exchanger tubing. Eq. (4.78) can be established from the basics of heat transfer rate, which if determined in terms of total thermal resistance  $R_{\text{Total}}$  [K/W] as a sum of surface convection resistances and the conduction resistances through the heat exchanger wall material and layers of fouling materials on both sides of the surface as per Fig. 4.11, instead of  $U$  the heat transfer rate through any wall:

$$q = (T_h - T_c)/R_{\text{Total}} \quad (\text{Eq. 4.78})$$

Although Eq. (4.76) improves the accuracy over the Dittus-Boelter correlation, errors as large as  $\pm 20\%$  are still possible (Chapman 2002, p. 282) [34]. More accurate correlations also exist, but they inevitably lose the simplicity of the aforementioned three correlations which are easy to use, but are also too inaccurate to be used in final sizing calculations.

**Fig. 4.11** Thermal circuit for a fouled heat transfer surface



A correlation by Petukhov and Popov for fully developed rough tubes gives results accurate to within  $\pm 5\%$  (Shah and Sekulic 2003, p. 482) [33]:

$$\text{Nu} = \frac{\frac{1}{2}f_f \text{Re} \cdot \text{Pr}}{a + 12.7 \sqrt{\frac{f_f}{2} (\text{Pr}^{2/3} - 1)}} \quad (\text{Eq. 4.79})$$

where all properties are evaluated at bulk temperature  $T_b$  given by Eq. (4.73) and the parameter  $a$  is calculated from Reynolds number  $\text{Re}$  and Prandtl number  $\text{Pr}$  as;

$$a = 1.07 + \frac{900}{\text{Re}} + \frac{0.63}{1 + 10\text{Pr}} \quad (\text{Eq. 4.80})$$

The correlation is valid within  $400 < \text{Re} < 5 \times 10^6$  and  $0.5 < \text{Pr} < 2000$ . Gnielinski has proposed a slightly simpler version accurate to within  $\pm 10\%$  for an otherwise similar range of parameters, but down to  $\text{Re} = 3000$ , and with properties evaluated at  $T_b$ :

$$\text{Nu} = \frac{\frac{1}{2}f_f \text{Re} - 1000\text{Pr}}{1 + 12.7 \sqrt{\frac{f_f}{2} \text{Pr}^{2/3} - 1}} \quad (\text{Eq. 4.81})$$

Although the Gnielinski correlation is useful down to smaller Reynolds numbers  $\text{Re}$  than most turbulent flow correlations, it still tends to over-predict  $j = \text{St}\text{Pr}^{2/3}$  at the transition regime. An improvement to transition regime can be achieved by simply taking a weighed mean value between the laminar and fully turbulent values of  $j_H$  (Shah and Sekulic 2003, p. 481) [33].

$$\begin{aligned} \text{Nu} &= \gamma \text{Nu}_{\text{Laminar}} + (\gamma + 1) \text{Nu}_{\text{Turbulent}} \\ \gamma &= 1.33 - \left( \frac{\text{Re}}{6000} \right) \end{aligned} \quad (\text{Eq. 4.82})$$

All the physical properties appearing in the dimensionless groups in the Gnielinski correlation should be evaluated at the arithmetic average of the bulk average temperatures of the fluid at the inlet and the exit. The Gnielinski correlation also applies only to fully developed heat transfer conditions, so that we can use the same approximate criterion  $L/D > 60$  that is recommended for the other correlations by Welty et al. [37] for long circular tube based on average Nusselt number for turbulent flow in the tube as below.

$$\overline{\text{Nu}}_D \approx \text{Nu}_{D,f_D} \quad (\text{Eq. 4.83})$$

Effects of entry and surface thermal conditions are less pronounced for turbulent flow and can be neglected. In Eq. (4.83),  $f_D$  represents the Darcy (or Moody) friction factor.

Similar correlation, that is,  $L/D < 60$  for short circular tube also provided;

$$\frac{\overline{\text{Nu}}_D}{\text{Nu}_{D,f_D}} \approx 1 + \frac{C}{L/D^m} \quad \text{for } C \approx 1 \quad m \approx 2/3 \quad (\text{Eq. 4.84})$$

### 4.10.2 Fully Developed Laminar Flow

In contrast to fully developed turbulence flow, we are now in a position to describe a fully developed laminar flow in circular tube as well. Laminar flow is rarely experienced in heat exchangers due to the very poor convection heat transfer coefficients that are an inevitable result of the flow remaining laminar.

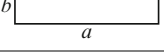
If the flow is laminar, it can be shown that Nusselt number Nu has a constant value that is independent of the friction factor  $f_f$ , Reynolds number Re, Prandtl number Pr and axial location along the pipe (provided that location is outside of the entry length into the tube). For circular tube Nu is then

$$\text{Nu} = \begin{cases} 4.36 & \text{if } q'' \text{ is constant} \\ 3.66 & \text{if } T_s \text{ is constant} \end{cases} \quad (\text{Eq. 4.85})$$

Values of Nu for some non-circular tube geometries are listed in Table 4.4 below.

In association with fully developed laminar flow, we previously showed fully developed laminar heat transfer for the involved flow as well, which resulted from non-newtonian fluids flowing through a circular tube with a fully-developed velocity profile and constant heat flux boundary condition at the wall and could be solved with given energy equations such as Eq. (4.21), or Eq. (4.27) with proper boundary

**Table 4.4** Nusselt number for fully developed laminar flow in some non-circular tube geometries

Geometry	$a/b$	Nu (constant $T_s$ )	Nu (constant $q''$ )	$f_f \text{Re}$
	1	3.09	3.00	14.2
	2	3.01	3.39	15.6
	8	2.90	5.60	20.6
	1.1	2.93	4.44	18.2
	$2/\sqrt{3}$	1.89	2.47	13.3

conditions assigned to such partial differential equations (PDEs). Note that in order to solve these PDEs we need to have precise information about the fully developed velocity profile  $u$  along with Eq. (4.5) for the power-law fluid Rohsenow et al. pp. 2–13 [31].

### 4.10.3 Entry Length

When a fluid passes into a pipe from a reservoir source, it undergoes a development of its velocity profile in the course of its flow through the pipe. The length of pipe required to attain fully developed conditions is called the hydrodynamic entrance length, which is proportional to the Reynolds number for the laminar flow case. For Newtonian fluids, the hydrodynamic entrance length  $L_e$  in circular and square-shaped channels is given by the following equation [31]:

$$\frac{L_e}{D_h} = (0.035 \sim 0.0575) \text{Re} \quad (\text{Eq. 4.86})$$

Note that for square-shaped channels the hydraulic diameter  $D_h$  is taken as the characteristic length.

For Non-newtonian fluids Burger [38] calculated the entrance length theoretically using the von Karman integral method under the assumption of power-law fluid. Table 4.5 provides the results for hydrodynamic entrance length in laminar pipe flow for four values of  $n$  based on Burger [38] theoretical solution.

Experimental studies generally reveal that Non-newtonian additives including high-molecular-weight polymers do not affect the entrance length in the laminar region [39–41]. Therefore, it is recommended that Eq. (4.86) be used to estimate the hydrodynamic length of purely viscous and visco-elastic fluids in laminar flow.

In turbulent flow in a channel, particularly in circular tubes, the thermal entry length where the convection heat transfer coefficient is higher than the fully developed value is generally quite short, and can frequently be neglected without significant loss of accuracy in predicting  $u$ . In non-circular, angular tubes the entry length can be noticeably longer due to areas of laminar flow in the corner regions (Shah and Sekulic 2003, p. 502) [33]. The smaller the values of Re and Pr, the longer the thermal entry length will be. Regardless of the boundary conditions (constant heat flux or constant surface temperature), the ratio of average Nusselt

**Table 4.5** Hydrodynamic entrance length in laminar pipe flow [38]

$n$	$L_e/(D_h \text{Re})$
1.00	0.0575
0.75	0.0480
0.50	0.0340
0.25	0.0170

number up to a distance  $x$  from tube entry,  $\text{Nu}_{\text{avg}}$ , to the fully developed Nusselt number  $\text{Nu}_{\infty}$ , can be calculated from

$$\frac{\text{Nu}_{\text{avg}}}{\text{Nu}_{\infty}} = 1 + \frac{\text{Pr}^{1.8} (0.68 + \frac{3000}{\text{Re}^{0.81}})}{(x/D_h)^{0.9}} \quad (\text{Eq. 4.87})$$

The correlation is valid within  $3500 < \text{Re} < 10^5$ ,  $0.7 < \text{Pr} < 75$ , and  $(x/D_h) < 3$ . With  $\text{Pr} = 0.7$ , the results agree within  $\pm 12\%$  of data from experimental measurements (Shah and Sekulic 2003, pp. 505–506) [33].

In laminar flow the entry length is frequently longer than in turbulent flow. Correlations for Nusselt number or Colburn factor  $j$  are typically expressed as a function of a dimensionless group Graetz number  $\text{Gz}$ ,

$$\text{Gz} = \frac{x}{D_h} \text{Re} \cdot \text{Pr} \quad (\text{Eq. 4.88})$$

Where the characteristic length in  $\text{Re}$  is the hydraulic diameter  $D_h$ . For constant surface temperature Sieder and Tate [35] have presented a correlation for local Nusselt number  $\text{Nu}_x$  (Incropera et al. 2002, p. 490) [42] as;

$$\text{Nu}_x = 1.86 \cdot \text{Gz}^{1/3} \cdot \left( \frac{\mu}{\mu_s} \right)^{0.14} \quad (\text{Eq. 4.89})$$

In the above equation  $\mu_s$  is dynamic viscosity at the internal wall of the duct and all properties are evaluated at the mean bulk temperature  $T_b$ , except  $\mu_s$ , which is evaluated at the surface temperature  $T_s$ .

For cases where the Fanning friction factor  $f_f$  of the fully developed flow is known, a correlation by Bhatti and Shah exists for Nu as (Shah and Sekulic 2003, p. 503) [33]:

$$\text{Nu} = C(f_f \text{Re})^{1/3} \text{Gz}^{1/3} \quad (\text{Eq. 4.90})$$

where  $C$  is a constant, depending on the surface condition (constant heat flux or constant surface temperature), and whether the correlation is to provide the local value of  $h$  at distance  $x$  from entry, or the average between distance  $x$  and entry. Values for  $C$  can be read from Table 4.6 below.

**Table 4.6** Values of constant  $C$  for Eq. (4.91) [33]

	Constant $T_s$ at all locations along the tube surface	Constant $q'$ , with a constant $T_s$ throughout perimeter at any $x$
For local $\text{Nu}_x$	0.427	0.517
For average $\text{Nu}_{\text{avg}}$	0.517	0.775

## 4.11 Thermal Design of the Selected Compact Heat Exchanger

The Printed Circuit Heat Exchanger (PCHE) is the heat exchanger that was selected to be used for the proposed power plant. The PCHE was selected after a literature review on available gas-to-gas heat exchangers revealed that the PCHE meets all the modalities (that is an exchanger that can withstand higher temperature fluids, achieve higher effectiveness, and has a lower pressure drop) set for the heat exchanger to be employed in the proposed power plant. Therefore, this chapter focuses on the design of the PCHE, and a quick description of Plate Fin Heat Exchanger (PFHE). The design of the PFHE was also considered so as to be able to compare the performance of the PCHE to that of the PFHE size to deliver the same output, with the same input parameters and constraints imposed.

As part of the selection criteria a review of various compact heat exchangers for high temperature, high effective, and low pressure drop involved with applications in the case of concentrated solar power or combined cycle application for driving efficiency of advanced high temperature reactors as part of NGNP for our purpose did identify three promising possibilities among available compact heat exchangers for high temperature applications. They are the:

1. Plate Fin compact heat exchangers;
2. Printed-Circuit compact heat exchangers, and finally;
3. The Marborn™ type compact heat exchangers.

The choice of these three compact heat exchangers is elaborated further on in Sect. 4.23.5 of this chapter.

The thermal design aspects and problems associated with these heat exchangers is either referred to as a rating or sizing problem. In the rating problem the heat transfer rate and/or the outlet temperatures, pressure drop performances of an already designed or existing heat exchanger are determined from relevant relations.

The sizing problem on the other hand entails determining or selecting of exchanger constructional type, the type of flow arrangement, selecting the tubes and fin or channel type and materials to be used, and the physical size of heat exchanger that would meet the defined heat transfer and pressure drops performances for given limitations.

The thermal design process to be carried out in the following sections is therefore a sizing problem from the definitions above. The thermal design process is an iterative process done to achieve the specified heat transfer rate while making sure that the pressure and temperature demands are maintained. The design process from here on is based on Yakah's Master of Science Thesis work [1].

## 4.12 Sizing the Compact Heat Exchangers

There are some basic design aspects which would be design constraints and they need to be taken under consideration as part of sizing requirements for the desired heat exchanger, depending on its applications. For us to be more precise in order to go forward with this subject we will narrow down our choice of compact heat exchanger to the one that we know as Printed Circuit Heat Exchanger (PCHE) where we use this exchanger for the purpose of using heat from Concentrated Solar Power (CSP) as part of the design component for a Solar Gas Power Plant (SGPP). The compact heat exchangers in this case will be used in the power plant for the purposes of waste heat recovery, recuperation, and intercooling.

The choice for compact heat exchanger for the best optimum heat exchange for application in SGPP was narrowed down to PCHE type of exchanger as the best candidate for waste heat recovery and recuperation. In order to ascertain the viability of this assertion the PCHE was designated and One-Dimensional (1-D) modeling and heat transfer analysis was done based on MATLAB software capability utilizing the conditions that a heat exchanger for waste heat recovery would be subjected to. The option and choice of using the conditions of the waste recovery that this heat exchanger would encounter was due to the fact that, it is the heat exchanger that would be subject to many harsh conditions as a result of higher temperature of up to 650 °C being used. For the purpose of Small Modular Reactors (SMRs) as part of new generation power plants or for that matter a high temperature advanced reactor of IV-GEN and in combination with combined cycles the same temperature will be applied and these types of compact heat exchangers are an excellent choice and similar analysis will apply here [43, 44].

As part of 1-D modeling using MATLAB capability and functionality the Plate Fin Heat Exchanger (PFHE) family of compact heat exchanger was chosen as well to demonstrate similar performance in order to compare and make a decision between the two compact heat exchangers, i.e., PCHE and PFHE, which one has a better and stronger basis for deciding on whether to stick to the choice of PCHE or not.

The results obtained from MATLAB and the 1-D modeling of the design of the heat exchangers indicate that the PCHE performed better with regard to pressure drops across the heat exchangers with values of 1.17 % and 2.47 % for the cold and hot sides respectively and with a compactness value of  $1300 \text{ m}^2/\text{m}^3$  for the PCHE compared to the compactness value of  $855 \text{ m}^2/\text{m}^3$  recorded from the PFHE. However, the PFHE recorded higher heat transfer coefficients, and a subsequent higher overall transfer coefficient [1].

The results obtained from the simulation of the Three-Dimensional (3-D) model using COMSOL Multi-Physics software buttress the decision to employ the PCHE as heat exchangers to be used for waste heat recovery and recuperation as a wise one, with an effectiveness of 0.94 against the design value of 0.90, and with pressure drops as desired of the optimum heat exchanger [1].

As part of sizing the compact heat exchanger, we will discuss the selection of the heat exchanger construction type, flow arrangement, surface geometries, and so on in the following sections of this chapter as part of all knowledge we have gathered from previous chapters and sections throughout the book.

There are some basic design aspects which would have to be decided right from the onset of the design process, and these includes;

- The flow arrangement, the type of fins to be employed in the case of the PFHE,
- The cross section of channels to be employed in the case of the PCHE, and
- The type of material that would be used in the manufacturing of the selected heat exchanger.

Flow arrangements employed in heat exchangers includes;

1. Counter-flow,
2. Parallel-flow,
3. Cross-flow,
4. Cross counter-flow, and
5. A combination of any of these flow configurations.

The decision to select a particular flow arrangement to be employed on a heat exchanger depends on a lot of astute factors as mentioned earlier and these include; the desirable effectiveness, expected pressure drop across the heat exchanger, workable pressure limits, the maximum velocities allowed, fluid flow paths of the fluids to be used in the exchanger, permissible thermal stresses, anticipated temperature levels, and other important design criteria (Shah and Sekulic 2003) [33].

One of the requirements of the heat exchanger for the proposed Solar Gas-Turbine power plant is to be able to provide a higher effectiveness. It is in this regard that the counter-flow arrangement is selected to be employed in both the PFHE and PCHE to be designed. The counter-flow arrangement has been found to be the most efficient flow arrangement, producing the highest temperature change in each fluid with given overall thermal conductance (the product of the overall heat transfer coefficient,  $U$ , and the heat transfer area,  $A$ ), fluid flow rates (or the mass flow rate), and fluid inlet temperatures relative to other flow arrangements employed in heat exchanger designs (Shah and Sekulic 2003) [33].

Per our discussion in the previous chapter various fins arrangements are available for use in the design of the PFHE, and Fig. 3.4a–f shows different types of fin shapes employed in the design of PFHEs.

The offset strip fins (also known as serrated fins) were selected to be employed in the PFHE, this is because it has been found to be the most widely used fins and also the one with the highest heat transfer performance compared to its frictional factor (Shah and Sekulic 2003) [33] and (Foumeny and Heggs 1991) [45].

There are also various cross sectional channels that can be employed on the plates forming the matrix of the PCHE. Channels employed in the PCHE include the straight or wavy, parallel or offset semicircular cross sections and others. Figure 3.17 shows the zigzag shapes of a plate in two different flow arrangements (thus the simple cross flow and cross-counter flow) in the PCHE.

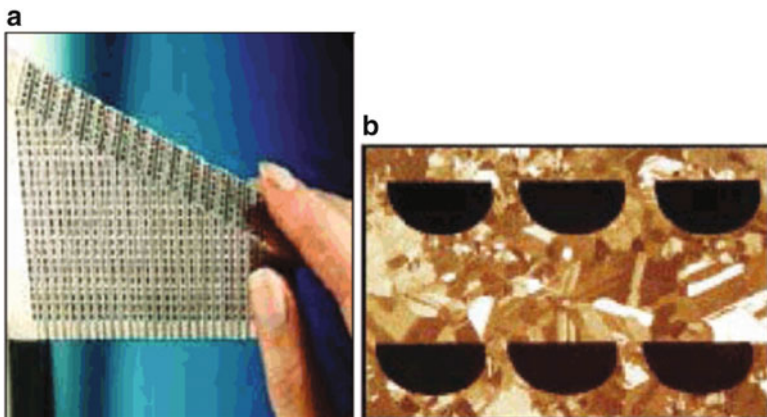


**Fig. 4.12** Printed Circuit Heat Exchanger (Heatic™ Homepage 2011). **(a)** Photo of PCHE. **(b)** Cross-sectional view of PHCE



**Fig. 4.13** A photo-micrograph of semicircular passage as depicted in the PCHE

The semi-circular cross section was chosen for the design of the PCHE because, although there is generally meager information available on the design of PCHEs, there are quite a number of design processes on PCHE where the semicircular channels are employed. Figure 4.12a and b shows a photomicrograph of the semicircular passages in the PCHE (Fig. 4.13).

Various fins arrangements are available for these compact heat exchangers and they are adequately defined in Chap. 3 of this book along with depiction of their images.

## 4.13 Thermal Design Formulation of Considered Compact Heat Exchangers

Rating and sizing problems in compact heat exchangers are usually characterized by two major important equations and they are as flows:

$$q = q_j = \dot{m}_j \Delta h_j \quad j = \begin{cases} 1 & \text{Cold side of the fluid} \\ 2 & \text{Hot side of the fluid} \end{cases} \quad (\text{Eq. 4.91})$$

Where:

$q$  = the rate of heat transfer, in W

$\dot{m}$  = the mass flow rate, in kg/s

$h$  = the enthalpy of the fluid at the given temperature, in kJ/kg

Equation (4.91) is a presentation of both cold and hot fluids in the heat exchanger where  $j = 1$  or  $2$  is designated to either the cold or hot side of fluid flowing within the heat exchanger depending on the criteria defined for the application where this exchanger will be used. Eq. (4.91) is presented in most literature as the enthalpy rate equation as well.

This first equation relates the heat transfer rate,  $q$  with the enthalpy rate change for an open non-adiabatic system with a solitary bulk flow stream which enters and leaves the system under consideration in isobaric conditions, and this has been shown with either  $j = 1$  or  $2$  as stated earlier.

The first equation can also be defined taking into consideration the mass flow rate, the specific heat capacity, and the change in temperature on both fluid streams (that is either the cold and hot sides or the one and two fluid streams sides) of the heat exchanger and it is expressed as;

$$\Delta h_j = (c_p)_j \Delta T_j = (c_p)_j (|T_{j,i} - T_{j,o}|) \quad (\text{Eq. 4.92})$$

Where i and o denote the inlet and outlet sides of the heat exchanger respectively.

With known mass flow rates, inlet temperatures, and specific heat capacity which are determined from tables using mean temperatures (can be assumed to be the same as the inlet temperature in the first iteration) on the fluid side, the output temperatures for each flow side can then be determined from the relations;

$$T_{h,o} = T_{h,i} - \frac{q}{c_{p_h}} \quad (\text{Eq. 4.93})$$

$$T_{c,o} = T_{c,i} - \frac{q}{c_{p_c}} \quad (\text{Eq. 4.94})$$

The outlet temperatures can be refined if we take into account the heat capacity ratio and effectiveness as part of our analysis and consider the following relations as:

$$T_{h,o} = T_{h,i} - \varepsilon \frac{C_{\min}}{C_c} (T_{h,i} - T_{c,o}) \quad (\text{Eq. 4.95})$$

$$T_{c,o} = T_{c,i} - \varepsilon \frac{C_{\min}}{C_c} (T_{h,i} - T_{c,o}) \quad (\text{Eq. 4.96})$$

The heat exchanger effectiveness,  $\epsilon$  is the means by which the thermal performance of heat exchangers can be assessed, and it is defined as the ratio of the actual heat transfer transferred from the hotter fluid to the maximum possible heat transfer rate that could have transferred as derived in Sect. 2.11 and briefly is shown here in terms of Eq. (4.97).

$$\epsilon = \frac{T_{c,o} - T_{c,i}}{T_{h,o} - T_{h,i}} \quad (\text{Eq. 4.97})$$

This parameter is usually a function of the flow arrangement that is chosen and employed for a particular application, for example in terms of compact heat exchanger drive efficiency of combined cycle in advanced high temperature nuclear power plant, cross-flow or parallel is preferred [43].

The effectiveness is sometimes referred to as the thermal efficiency of the heat exchanger as well, and the above equation is valid when using the same fluids on both sides (i.e., Liquid-to-Liquid or Gas-to-Gas type exchanger); however, in situations where different fluids are employed the heat capacities are required to be under consideration too. As we have elaborated in Chap. 2 of this book, the heat exchanger effectiveness can also be calculated using the Number of Transfer Unit (NTU). As we have demonstrated in Chap. 2, utilization of the method (i.e., NTU) to calculate the effectiveness of the exchanger requires certain parameters to be known or have been considered as part of the calculation. However, bear in mind that at the early stage of any preliminary heat exchanger design procedure and process, these parameters are not known yet or cannot be calculated, therefore for the purpose of quick back envelope analysis the effectiveness can be calculated explicitly using Eq. (4.97).

The heat capacities ( $C_{\min}$ ,  $C_h$  and  $C_c$ ) are also were defined in Chap. 2 of this book and can be expressed again as Eq. (4.98) here, which is the second major equation to be considered in sizing and rating heat exchangers, and it replicates a convection-conduction heat transfer phenomenon in a two-fluid heat transfer exchanger.

$$Q = UA\Delta T_m \quad (\text{Eq. 4.98})$$

where:

$Q$  = the rate of heat transfer, W

$A$  = the total heat transfer area,  $\text{m}^2$

$\Delta T_{\text{mean}}$  = the Logarithmic Mean Temperature difference, K

$U$  = the overall heat transfer coefficient,  $\text{W}/\text{m}^2 \text{K}$

The relation in Eq. (4.98) states that the heat transfer rate,  $q$  varies directly to the heat transfer area  $A$ , and the mean temperature difference,  $\Delta T_{\text{mean}}$  between the fluids, where  $U$  (overall heat transfer coefficient) is the constant of proportionality.

The  $\Delta T_{\text{mean}}$  can also be related in such a way that takes into consideration the terminal differences between the fluids such as  $(T_{h,i} - T_{c,o})$  and  $(T_{c,o} - T_{c,i})$  and its

definition depends on the flow arrangement (orientation of flow in the heat exchanger) employed.

The design process would determine the physical size to deliver the expected heat transfer rate and also determine the pressure drop across the heat exchanger.

The thermal analysis that is applied in order to optimize the Compact Heat Exchanger (CHE) under consideration here is based on satisfying in general three objectives in a cost effective manner and these objectives are:

1. Transfer of required heat duty;
2. Cold-side pressure drop below a maximum allowable value, and finally;
3. Hot-side pressure drop below a maximum allowed value.

Generally speaking the allowable pressure drops that are specified for any CHE can be in a somewhat objective manner. However, during the design process and iteration of optimization, further subjective points can be introduced for proper choice of the surface geometry that will be used and if the process streams should be contacted in a configuration such as counter-flow or cross-flow type compact heat exchangers that are most effective for driving overall efficiencies in cases such as combined cycle in Next Generation Nuclear Plant (NGNP) (Chap. 7 of the book) or Concentrated Solar Power (CSP) farms (see Chap. 8 of the book).

Stream pressure drops can be set through total cost optimization involving a trade-off between exchanger capital cost and pumping power cost of both fluids on either side of the exchanger [45].

The new algorithm and method for this task, presented by Polley [45], can be used for both configuration of cross-flow and counter-flow exchangers therefore, the exchanger designers can easily determine which flow configuration and arrangement can be utilized given particular application and heat duty assigned to that particular heat exchanger.

This procedure could be applied to any surfaces in which both friction factor  $f_F$  (i.e., Fanning Friction Factor) and heat transfer  $j$  factor (i.e., Colburn heat transfer factor) can be expressed as simple power functions of Reynolds Number as shown in previous chapters and sections of this book, and since this is a true circumstances for most compact surfaces used in heat exchangers, the methodology is quite general.

The problem of surface selection is overcome through the use of ‘Performance Indices’ based on the  $j$ -factor and friction factor data as for example presented in Kays and London’s book “Compact Heat Exchangers” [46]. This methodology can also be extended to cover thermal duties involving two-phase flow scenarios [45].

#### **4.14 Assumption Made in the Design of Considered Compact Heat Exchangers**

A lot of assumptions are made in this chapter for the problem and analysis for a particular type of compact heat exchanger that is selected for the purpose of our analysis. The chosen compact heat exchanger, as mentioned at the beginning of this

chapter, is Printed Circuit Compact Heat Exchanger (PCHE) and this choice is based on application of this class of heat exchanger for a proposed power plant, in our case Concentrated Solar Power Plant.

A lot of assumptions need to be made for the exchanger heat transfer problem formulations notably in the area of energy balances, rate equations, boundary conditions, and other useful analysis that are required to be considered. An assumption is usually invoked in the design process whenever it becomes necessary. Those that are useful in almost all heat exchanger designs and this application in particular are;

1. The heat exchanger would operate under steady-state condition, i.e., operate with constant flow rates and fluid temperatures (both at the inlet and within the heat exchanger) independent of time.
2. Heat losses to and from the surroundings are neglected.
3. Non existence of thermal energy sources or sinks in the heat exchanger.
4. Uniform distribution of fluid temperature over every cross section of the exchanger.
5. The wall thermal resistance is assumed as a constant and uniform in the entire heat exchanger.
6. No phase change, since we are only dealing with flue gases on one side and air on the other side of the exchanger.
7. The individual and the overall heat transfer coefficients of both fluids are assumed constant (thus independent of temperature, time, and position) throughout its flow in the heat exchanger matrix.
8. Both fluids employed in the heat exchanger are assumed to be of constant specific heat capacities.
9. The flow velocity and temperature of both fluids at the inlet of the heat exchanger on each fluid side is considered uniform over the flow cross section.
10. The fluid flow rate is uniformly distributed through the exchanger on each fluid side in each pass.

Other assumptions throughout this chapter are quoted whenever it becomes necessary.

## 4.15 Relating Heat Transfer and Pressure Drop

In Chap. 3, Sect. 3.7.1.4, we extensively elaborated on pressure drop and showed all the analysis related to such drop with Eqs. 3.31 through 3.3 and showed that the knowledge of the friction characteristic of the heat transfer surface relatively speaking, does not have an influence on design of *Liquid-To-Liquid* heat exchanger as much as it does over a *Gas-To-Gas* one. The reason is simply because of the low power requirement for pumping high-density fluid (Kays and London) [46].

However, in the case of a gas-to-gas heat exchanger, because of their lower density, the friction power per unit mass flow rate is greatly multiplied, therefore,

the friction characteristic of the surface plays an important part equal to the heat transfer characteristic, thus, the friction characteristic that is required to be considered, is the flow-friction factor  $f$ , which is discussed in Chap. 3 as a function of flow geometry and Reynolds number as well as in tables of data provided by Kays and London [46].

As part of analyzing the related heat transfer and pressure drop in order to optimize the compact heat exchangers of our choice and their applications in CSP and NGNP applications, the following formulations were considered as part of the pressure drop associated with the flow of a fluid through the core of a compact heat exchanger that is given by Kays and London [46] as:

$$\Delta p = \frac{1}{2\rho} f \frac{A}{A_c} \cdot \frac{(\dot{m})^2}{A_c} \quad (\text{Eq. 4.99})$$

In this equation the following parameter is defined as:

$$f = x \text{Re}^{-y} \quad (\text{Eq. 4.100})$$

And  $A_c$  is the exchanger minimum free-flow area while,  $A$  is the exchanger total heat transfer area on one side or defined as you can see in Eq. (4.101) below.

The heat exchanger volume and surface area are related through the definition of the surface hydraulic diameter as:

$$A = 4V_t (D_h/\sigma) \quad (\text{Eq. 4.101})$$

A combination of Eqs. (4.99), (4.100), and (4.101) will produce the following conclusion as:

$$\Delta p = k_p V_t (D_h/\sigma) \quad (\text{Eq. 4.102})$$

where:

$$k_p = (2x/\rho) (\mu/D_h)^y \dot{m}^{2-y} (\sigma/D_h) \quad (\text{Eq. 4.103})$$

Relation between the film heat transfer coefficient and exchanger minimum free flow area  $A_c$  is written as:

$$h = k_h (1/A_c)^{1-b} \quad (\text{Eq. 4.104})$$

where:

$$k_h = a(\lambda/D_h) \text{Pr}^{1/3} (\dot{m} D_h / \mu)^{1-b} \quad (\text{Eq. 4.105})$$

with  $a$  the constant and  $b$  the exponent in the  $j$ -factor relationship. Combination of Eqs. (4.101) and (4.103) yields

$$\Delta p = (k_p/k_h)zV_t h^z \quad (\text{Eq. 4.106})$$

where:

$$z = (3 - y)/(1 - b) \quad (\text{Eq. 4.107})$$

Also, bear in mind that two-phase heat transfer in compact heat exchangers tends to be dominated by convective effects. In the case of vaporization nucleate boiling is very soon suppressed and the dominant process is thin film evaporation, whilst with condensation vapor shear is significant. Further information can be found in the paper by G.T. Polly in the reference by Foumeny and Heggs [45].

## 4.16 Heat Capacity Ratio Analysis for Considered Compact Heat Exchangers

In order to determine the heat capacity ratio,  $C^*$ , the product of the mass flow rates and the specific heat capacity for both sides of the heat exchanger are calculated. The minimum of the two products is assigned to 1 (which is also referred to as  $C_{\min}$ ) and considered to be the “weaker” side of the exchanger and the maximum assigned to 2 and considered the “stronger” side and  $C_c = (\dot{m} C_p)_c$  and  $C_b = (\dot{m} C_p)_b$ , when  $C_c = C_b$  and  $C_b = C_2$  but if  $C_c < C_b$  then  $C_b = C_1$  and  $C_c = C_2$

Therefore, we can write

$$C^* = \frac{C_1}{C_2} \quad (\text{Eq. 4.108})$$

## 4.17 Mean Temperature Difference

As defined from the relation for the calculation of heat transfer rate in Eq. (4.98), the heat transfer rate,  $q$ , varies directly to the heat transfer surface area,  $A$ , and the mean temperature difference,  $\Delta T_{\text{mean}}$ , where  $U$  is the constant of proportionality referred to as the overall heat transfer coefficient. The value of  $\Delta T_{\text{mean}}$  is dissimilar for different heat exchangers employing different flow arrangements with the same inlet and outlet temperatures. The mean temperature difference as defined is not just the arithmetic mean but the logarithmic mean value which is defined for counter flow arrangements as;

$$\Delta T_{\text{mean}} = \frac{\Delta T_1 - \Delta T_2}{\ln\left(\frac{\Delta T_1}{\Delta T_2}\right)} \quad (\text{Eq. 4.109})$$

with

$$\Delta T_1 = T_{h,in} - T_{c,out}, \quad (\text{Eq. 4.110})$$

and

$$\Delta T_2 = T_{h,out} - T_{c,in} \quad (\text{Eq. 4.111})$$

## 4.18 Number of Transfer Units Analysis for Considered Compact Heat Exchangers

The Number of Transfer Units (NTU) can be defined as the ratio of the overall thermal conductance (thus the product of the overall heat transfer coefficient,  $U$  and the heat transfer area,  $A$ ) to the minimum heat capacity rate. The NTU is expressed mathematically as;

$$\text{NTU} = \frac{UA}{C_{\min}} \quad (\text{Eq. 4.112})$$

The NTU of the heat exchanger can also be defined as a function of the effectiveness, heat capacity ratio, and the flow arrangement. It is determined in this design process from the relation;

$$\text{NTU} = \frac{1}{(1-C)} \ln \frac{(1-C^*)}{(1-\varepsilon)} \quad \text{for } 0 < C^* < 1 \quad (\text{Eq. 4.113})$$

## 4.19 Fluid Mean Temperature Analysis for Considered Compact Heat Exchangers

The following fluid properties density,  $\rho$ , dynamic viscosity,  $\mu$ , thermal conductivity,  $k$ , and Prandtl number,  $\text{Pr}$ , would have to be determined to be able to calculate the physical size (area) of the heat exchanger that would be required to deliver the expected heat transfer rate, determine pressure drops on both sides of the exchanger, and analyze other performance characteristics of the exchanger. The above mentioned fluid properties would be determined using the mean fluid temperatures  $T_{\text{ref}}$  for both fluid sides at specified pressures, and;

$$T_{c,\text{ref}} = \frac{T_{c,i} + T_{c,o}}{2} \quad (\text{Eq. 4.114})$$

and

$$T_{h,\text{ref}} = \frac{T_{h,i} + T_{h,o}}{2} \quad (\text{Eq. 4.115})$$

## 4.20 Thermophysical Properties of the Gases for Considered Heat Exchangers

The Thermophysical properties of the gases for side 1 and side 2 are listed in Table 4.7. Side 1 is air from the turbine of the bottoming cycle of the proposed power plant at a pressure of 5 bars. For side 2 the gas is flue gas at a pressure of 1 bar and consists of 79 % Nitrogen, 15 % Carbon dioxide, and 6 % Oxygen. The flue gas enters the heat exchanger at a pressure of 1 bar, pressure drop is assumed to be 3 % on both sides of the exchanger.

The Thermophysical properties listed in Table 4.7 are obtained from the National Institute of Standards and Technology (NIST) [47] at the given temperatures and pressures. All the values are obtained from the online NIST book and its software, except the mean density which is calculated from;

$$\frac{1}{\rho_{\text{mean}}} = \left[ \frac{1}{2} \left( \frac{1}{\rho_{\text{in}}} + \frac{1}{\rho_{\text{out}}} \right) \right] \quad (\text{Eq. 4.116})$$

**Table 4.7** Thermophysical properties of the gases used in the compact heat exchanger at the specified temperature and pressure

Properties	Symbols	Side 1	Side 2	Unit
Reference temperature	$T_{\text{ref}}$	714.9939	740.6448	K
Inlet pressure	$p_{\text{in}}$	5	1	Bar
Outlet pressure	$p_{\text{out}}$	4.85	0.97	Bar
Specific heat capacity	$c_p$	1079.7	1109.4	J/kg K
Viscosity	$\mu$	0.000034784	0.000034658	Pa s
Thermal conduction	$k$	0.051732	0.052733	W/m K
Prandtl number	Pr	0.72595	0.72917	—
Densities (inlet)	$\rho_{\text{in}}$	2.4312	0.48479	kg/m <sup>3</sup>
Densities (outlet)	$\rho_{\text{out}}$	1.9678	0.58713	Kg/m <sup>3</sup>
Mean densities	$\rho_{\text{mean}}$	2.1751	0.5311	kg/m <sup>3</sup>

#### **4.21 Physical Dimensions and Other Important Geometrical Feature of the PFHE**

In order to determine the total surface area of the Plate-Fin Heat Exchanger (PFHE) lets us first look at the arrangement of fins, the parts involved, and some important parameters of this type of exchanger that would be needed. Figure 4.14 shows the matrix of the PFHE core, the arrangements of fins (offset strip fin), and a small section of an idealized offset strip fin geometry.

From Fig. 4.14, the following parameter definitions are applied:

$\delta_3$  = Plate thickness

$\delta$  = Fin thickness

$s$  = Spacing between a surface of a fin

$\ell_s$  = Fin offset length

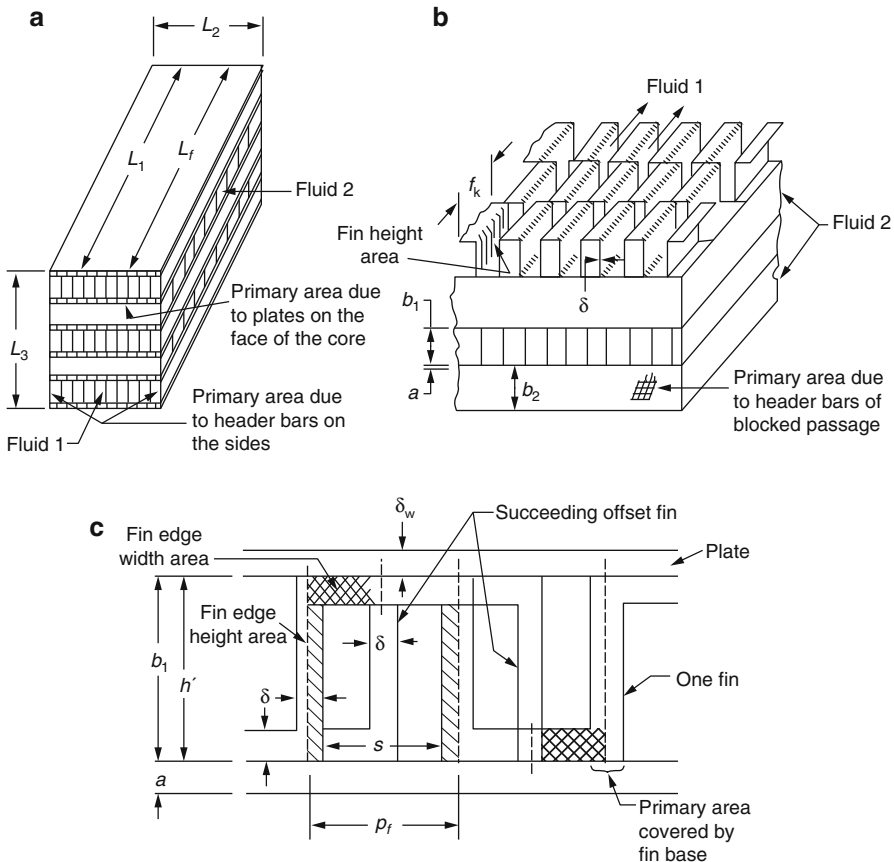


**Fig. 4.14** (a) Plate-fin heat exchanger. (b) Offset strip fin geometry. (c) A small section of offset strip fin geometry [33]

- $L_f$  = Flow length in the L1 direction  
 $L_1$  = Length of a plate  
 $L_2$  = Width of a plate  
 $L_3$  = Height or stack of the exchanger  
 $b_1$  = Plate spacing for fluid side 1  
 $b_2$  = Plate spacing for fluid side 2  
 $n_f$  = Total number of fins  
 $n_{off}$  = Number of fin offsets  
 $P_f$  = Fin pitch  
 $\eta_f$  = Fin efficiency  
 $N_p$  = Number of passages  
 $h$  = Heat transfer coefficient

The surface area of the PFHE consists of a primary and secondary surface area (also the fin area). For fluid side 1 the primary surface area is calculated from the relation;

$$A_{-P1} = 2L_1L_2N_p - 2\delta L_f n_f + 2b_1L_1N_p + 2(b_2 + \delta_w)(N_p + 1)L_2 \quad (\text{Eq. 4.117})$$

The secondary surface area for fluid side 1 can be determined on the other hand from the relation;

$$A_{-f1} = 2(b_1 - \delta)L_f n_f + 2(b_1 - \delta)\delta n_{off} n_f + (P_f - \delta)\delta(n_{off} - 1)n_f + 2P_f\delta n_f \quad (\text{Eq. 4.118})$$

The total surface area for fluid side 1 would therefore be the addition of the primary surface area and the secondary area of fluid side 1, which is given by;

$$A_{-1} = A_{-P1} + A_{-f1} \quad (\text{Eq. 4.119})$$

The overall heat transfer area of the heat exchanger is the addition of the total heat transfer surface area of fluid side 1 and that of fluid side 2. However, It has to be noted that, since fluid side 2 is the “stronger” side, the number of passages is one more than that of fluid side 1. In this design all dimensions for fluid side 2 are assumed to be the same as that of fluid side 1.

The volume occupied by the plates or parting sheets in the total volume of the plate-fin heat exchanger is given by

$$V = [b_1N_p + b_2(N_p + 1) + 2\delta_w(N_p + 1)] L_1L_2 \quad (\text{Eq. 4.120})$$

Other definitions which are of immense importance are defined as follows;

Minimum free-flow area;

$$A_{-0} = b_1L_2N_p - [(b_1 - \delta) + P_f]\delta n_f \quad (\text{Eq. 4.121})$$

Surface area density or compactness of heat exchanger  $\beta$  is given by:

$$\beta = \frac{\text{Total Surface Area, } A}{\text{Total Heat Exchanger Volume, } Vol} \quad (\text{Eq. 4.122})$$

Mass flux velocity,  $G$  in  $\text{kg/m}^2 \text{ s}$  is given by:

$$G = \sqrt{\left[ \left( \frac{j}{f_F} \right) \left( \frac{\Delta p}{p_{in}} \right) \frac{2p_{in}\eta_0\rho_{min}}{\text{NYUPr}^{\frac{2}{3}}} \right]} = \left[ \left( \frac{j}{f_F} \right) \left( \frac{\Delta p}{p_{in}} \right) \frac{2p_{in}\eta_0\rho_{min}}{\text{NYUPr}^{\frac{2}{3}}} \right] \quad (\text{Eq. 4.123})$$

The Colburn and Fanning friction factors ( $j$  and  $f_F$ ) are defined respectively for the offset strip fin in the PFHE as;

$$j = 0.6522 \text{Re}^{-0.5403} \left( \frac{s}{h'} \right)^{-0.1541} \left( \frac{\delta}{\ell_s} \right) \left( \frac{\delta}{s} \right)^{-0.0678} \times \left\{ 1 + 5.269e^{-5} \text{Re}^{1.340} \left( \frac{s}{h'} \right)^{0.504} \left( \frac{\delta}{\ell_s} \right)^{0.456} \left( \frac{\delta}{s} \right)^{-1.055} \right\}^{0.1} \quad (\text{Eq. 4.124})$$

$$f_F = 0.6522 \text{Re}^{-0.7422} \left( \frac{s}{h'} \right)^{-0.1856} \left( \frac{\delta}{\ell_s} \right)^{0.3035} \left( \frac{\delta}{s} \right)^{-0.2659} \times \left\{ 1 + 7.669e^{-8} \text{Re}^{4.429} \left( \frac{s}{h'} \right)^{0.920} \left( \frac{\delta}{\ell_s} \right)^{3.767} \left( \frac{\delta}{s} \right)^{0.236} \right\}^{0.1} \quad (\text{Eq. 4.125})$$

The hydraulic diameter for PFHE can also be calculated from;

$$D_h = \frac{4sh'\ell_s}{2(s\ell_s + h'\ell_s + h'\delta) + s\delta} \quad (\text{Eq. 4.126})$$

In Eqs. (4.123), (4.124), (4.125), and (4.126), parameters  $s$  and  $h'$  are defined as:

$$s = P_f - \delta \quad \text{and} \quad h' = b - \delta$$

Where  $P_f$  is fin pitch  $\delta$  is plate thickness and  $b$  is plate spacing for fluid side 1 or side 2.

The ratio  $j/f_F$  is assumed to be 0.25 in the first iteration since the Reynolds number is not known at this point, and it was found to be a good approximation for the ratio (Shah et al. 2003) [33].

The Reynolds number  $\text{Re}$  is then calculated from

$$\text{Re} = \frac{Gc_p}{\mu} \quad (\text{Eq. 4.127})$$

The heat transfer coefficient,  $h$  is calculated from the relation of the following format:

$$h = j \frac{G c_p}{Pr^{2/3}} \quad (\text{Eq. 4.128})$$

For the first iteration the total extended surface efficiency  $\eta_0$  is assumed to be 0.9 but it is finally determined from the relation;

$$\eta_0 = 1 - (1 - \eta_f) \frac{A_f}{A} \quad (\text{Eq. 4.129})$$

The fin efficiency,  $\eta_f$ , is calculated from the relationship below as;

$$\eta_f = \frac{\tanh(ml)}{ml} \quad \text{Where} \quad l = \frac{h}{2} - \delta \quad \text{and} \quad m = \left( \frac{2h}{k_f \delta} \right)^{1/2} \quad (\text{Eq. 4.130})$$

Where  $m$  is mean value.

The overall heat transfer coefficient,  $U$ , can now be calculated assuming that, there is no fouling and the ratio of the surface area for fluid side 1 and 2 is approximately equal to unity. The overall heat transfer coefficient is then determined from;

$$U = \left[ \frac{1}{\eta_0 h_h} + \frac{1}{\eta_0 h_c} \right]^{-1} \quad (\text{Eq. 4.131})$$

In Eq. (4.131)  $\eta_0$  is the total extended fin surface efficiency, and  $h$  is the heat transfer coefficient and subscripts  $h$  and  $c$  are indications of the hot and cold side of the exchanger respectively.

## 4.22 Pressure Drop Analysis of the Exchanger

The relative pressure drop across the heat exchanger for both fluid sides can be determined from the relation;

$$\left( \frac{\Delta p}{p_{in}} \right) = \frac{G^2}{2p_{in}\rho_{in}} \left[ (1 - \sigma^2 - k_{\text{entrance}}) + f \frac{L\rho_{in}}{r\rho_{out}} + 2 \left( \frac{\rho_{in}}{\rho_{out}} - 1 \right) - (1 + \sigma^2 + k_{\text{exit}}) \frac{\rho_{in}}{\rho_{out}} \right] \quad (\text{Eq. 4.132})$$

Where:

$G$  = Mass flux velocity ( $\text{kg}/\text{m}^2 \text{ K}$ )

$p_{in}$  = Inlet pressure of the heat exchanger (Pa)

$\rho_{in}$  = Inlet fluid density ( $\text{kg}/\text{m}^3$ )

$\rho_{out}$  = Outlet fluid density ( $\text{kg}/\text{m}^3$ )

$k_{\text{entrance}}$  = Fluid entrance pressure loss coefficient

$k_{\text{exit}}$  = Fluid exit pressure loss coefficient

$\sigma$  = Frontal ratio defined in Eq. (4.137) and defined as ration of free-flow area to frontal area  $A_c/A_{\text{frontal}}$  and it is a dimensionless value

Where the  $f$  used in Eq. (4.132) is a corrected  $f_F$  value of the one determined in Eq. (4.125), and is determined from the relation;

$$f = \left[ f_0 \left( \frac{T_w}{T_{\min}} \right)^m \right] \quad (\text{Eq. 4.133})$$

With the assumption that there is no fouling, and only thermal resistance on both sides of the exchanger,  $T_w$  is determine from the relation;

$$T_w = \frac{(T_h/R_h) + (T_c/R_c)}{(1/R_h) + (1/R_c)} = \frac{(\eta_0 h A)_h T_h + (\eta_0 h A)_c T_c}{(\eta_0 h A)_h + (\eta_0 h A)_c} \quad (\text{Eq. 4.134})$$

Where  $R_h$  is the thermal resistance on the hot side of the exchanger in (K/W), while  $R_c$  is the thermal resistance on the cold side of the heat exchanger.

Where;

$$R_h = \frac{1}{(\eta_0 h A)_h} \quad (\text{Eq. 4.135})$$

and

$$R_c = \frac{1}{(\eta_0 h A)_c} \quad (\text{Eq. 4.136})$$

As we said  $k_{\text{entrance}}$  and  $k_{\text{exit}}$  are the entrance and exit pressure loss coefficients respectively, which are determined from charts and are dependent on the Reynolds number, surface geometry, and the frontal area ratio,  $\sigma$ , which is defined as;

$$\sigma = \frac{b\beta D_h}{4(2b + 2\delta)} \quad (\text{Eq. 4.137})$$

All of the parameters used in this Eq. (4.137) are defined as before, and in the equation, it is assumed that plate spacing for both fluid sides are the same ( $b = b_1 = b_2$ ). The hydraulic radius in terms of hydraulic diameter for the cold and hot side of the heat exchanger is calculated from;

$$r_c = (D_{hc}/4) \quad \text{For cold side} \quad (\text{Eq. 4.138})$$

and

$$r_h = (D_{hh}/4) \quad \text{For hot side} \quad (\text{Eq. 4.139})$$

## 4.23 Printed Circuit Compact Heat Exchanger (PCHE)

For the Printed Circuit Compact Heat Exchanger also known and called Printed Circuit Heat Exchanger (PCHE), it is assumed that the channels forming the plates have a semicircular cross section running through the length of the plates in the exchanger. Figure 4.15 shows an illustration of channels employed in the PCHE with its alternating hot and cold flow. The arrangement of the flow paths are also shown in the second diagram of the same figure.

The cross sectional area,  $A_{ch}$ , and perimeter,  $P$ , of a semicircular channel can be calculated from the relations;

$$A_{ch} = \frac{\pi d^2}{8} \quad (\text{Eq. 4.140})$$

$$P = \frac{\pi d}{2} + d \quad (\text{Eq. 4.141})$$

Where  $d$  is the diameter of a cross section of a flow channel forming the compact heat exchanger and Fig. 4.15 is the presentation of another flow arrangement of semicircle flow channels in PCHE with its alternating hot and cold flows with their paths.

The free flow area  $A_f$  and the heat transfer area  $A_h$  of the primary or secondary side can be determined from the relations;

$$A_f = N_{ch} \times A_{ch} \quad (\text{Eq. 4.142})$$

and

$$A_h = N_{ch} \times L \times P \quad (\text{Eq. 4.143})$$

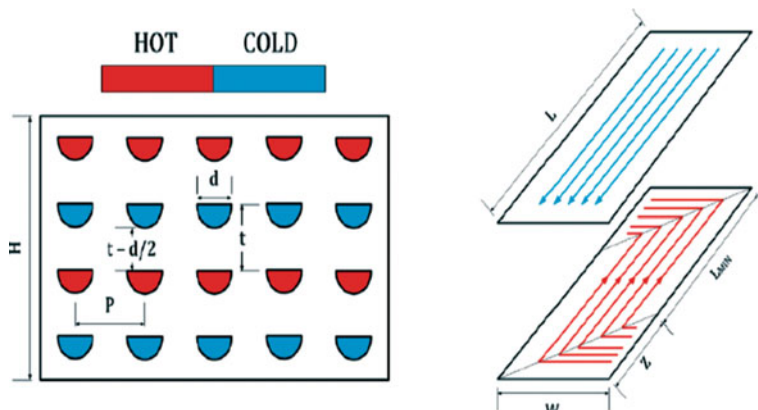
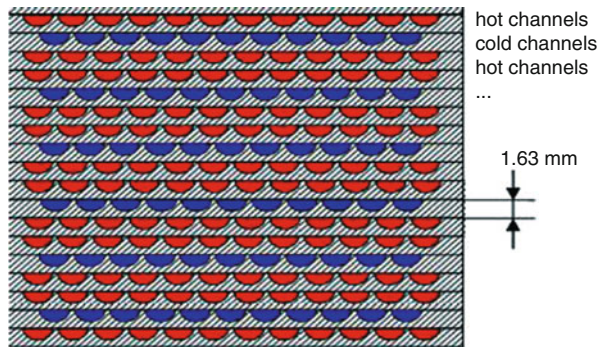


**Fig. 4.15** Printed Circuit Heat Exchanger (PCHE) cross-section

**Fig. 4.16** Sketch of another flow channel arrangement for Printed Circuit Heat Exchanger (PCHE) [48]



Where  $P$  is the perimeter of a channel,  $N_{ch}$  is the total number of channels used in the primary and secondary sides of the heat exchanger, and  $L$  is the flow length.

In the sizing of the PCHE, more channels are usually employed on the hot fluid side; this is done in order to facilitate maximum heat transfer. In other cases a cold plate is sandwiched between double hot plates and this also enhances heat transfer between the two fluids used in the exchanger. An example of this flow arrangement is shown in Fig. 4.16 (Nikitin et al. 2006) [48].

The hydraulic diameter  $D_h$  is calculated from the relationship of the following form as;

$$D_h = \frac{4A_0}{P} \quad (\text{Eq. 4.144})$$

Assuming that the PCHE has the following dimensions; flow length,  $L$ , width,  $W$ , and the stack of the exchanger,  $H$ :

The volume,  $V$ , of the PCHE can then be calculated from;

$$V = L \times W \times H \quad (\text{Eq. 4.145})$$

The surface area density or compactness,  $\beta$  can be calculated just as in the case of the PFHE from;

$$\beta = \frac{A_h}{V} \quad (\text{Eq. 4.146})$$

From Eq. (4.98), the heat transfer rate,  $q$  can also be defined for the PCHE as;

$$q = hA_h\Delta T_m \quad (\text{Eq. 4.147})$$

Where  $h$  is the heat transfer coefficient.

The Colburn factor,  $j$  can be expressed in terms of the Number of Transfer Units (NTU) and taking either Eq. (4.135) or (4.136) into consideration as;

$$j = \text{NTU} \frac{r_h}{L} \text{Pr}^{2/3} - \text{NTU} \frac{D_h}{4L} \text{Pr}^{2/3} \quad (\text{Eq. 4.148})$$

The Colburn factor,  $j$  can also be expressed in terms of heat transfer coefficients

$$j = \frac{\text{Nu}}{\text{RePr}^{2/3}} \quad (\text{Eq. 4.149})$$

With the Nusselt number (Nu) defined as;

$$\text{Nu} = \frac{hD_h}{k} \quad (\text{Eq. 4.150})$$

Where  $k$  is the thermal conductivity of the fluids used in the exchanger.

However, It has to be noted that the Nusselt number is assumed to be constant for the PCHE for constant wall temperatures, and in situations where the Reynolds number is greater than 2000 ( $\text{Re} > 2000$ ) then a relation is used to calculate the Nusselt number rather than assuming it to be a constant value as was the case in this design.

### 4.23.1 Pressure Drop Analysis of the PCHE

We have extensively talked about pressure drop as part of the process for compact heat exchanger design and now for our particular case of PCHE here we put our knowledge of this subject into use and briefly indicate the pressure drop for this heat exchanger.

The frictional pressure drop across the exchanger is worth considering, since we seek to find a lower pressure drop heat exchanger. The frictional pressure drop over the PCHE is calculated from;

$$\Delta p_{\text{friction}} = f_F \frac{4L}{D_h} \frac{1}{2} \rho V^2 \quad (\text{Eq. 4.151})$$

The Fanning friction factor,  $f_F$  is determined for conditions where  $0.5 < \text{Re} < 2000$  and Reynolds number less than 2000 as;

$$f_F = \frac{64}{\text{Re}} \quad (\text{Eq. 4.152})$$

Note that  $V$  represents the volume of concern in the exchanger.

However, for situations where  $\text{Re}$  is greater than 2000 the Fanning friction  $f_F$  is defined as;

$$f_F = \{0.79 * [\log(\text{Re}) - 1.64]\}^{-2} \quad (\text{Eq. 4.153})$$

### 4.23.2 *Sensitivity Analysis of the PCHE*

In selecting particular dimensions for both heat exchangers (PCHE and PFHE) a sensitivity analysis was carried out to assess how it affects the whole exchanger with respect to pressure drop across both sides of the heat exchanger and also the volume of the exchanger.

### 4.23.3 *Overall Analysis of the PCHE*

In selecting dimensions for the width, height, and diameter for the heat exchanger matrix a sensitivity analysis was carried out to assess how pressure drops across the heat exchanger when certain important parameters for the PCHE are varied. This was done by keeping all other parameters but the parameter under consideration constant, and noting the pressure drop across the heat exchanger. The graphs of the parameters considered are plotted against the pressure drop across both sides of the heat exchanger.

In a similar fashion, in selecting dimensions for the PFHE a sensitivity analysis was carried out by (Noah Yakah) [1] by varying the length of plate and other dimensions as well.

#### 4.23.3.1 **Width of the PCHE**

To analyze how varying the width of the exchanger affects the performance of the PCHE with respect to pressure drop, the width of the exchanger was varied while other parameters were kept constant. Figure 4.17 shows graphs of the width of the heat exchanger in meters against the pressure drop across the heat exchanger expressed as a percent.

Increasing the width of the exchanger decreases the pressure drop on both sides of the heat exchanger as illustrated in Fig. 4.17; this is because increasing the width increases the number of channels on a given plate and subsequently increases the free flow area. Since the flow velocity varies inversely as the free flow area, the flow velocity decreases as a result. The pressure drop across the heat exchanger varies directly proportional to the square of the flow velocity, and as such increasing the flow velocity may increase the flow regime but will adversely increase the pressure drop.

Therefore, increasing the flow area reduces the flow velocity which lowers the Reynolds number of the fluid flow which decreases the heat transfer magnitude but helps to decrease the pressure drop across the heat exchanger.

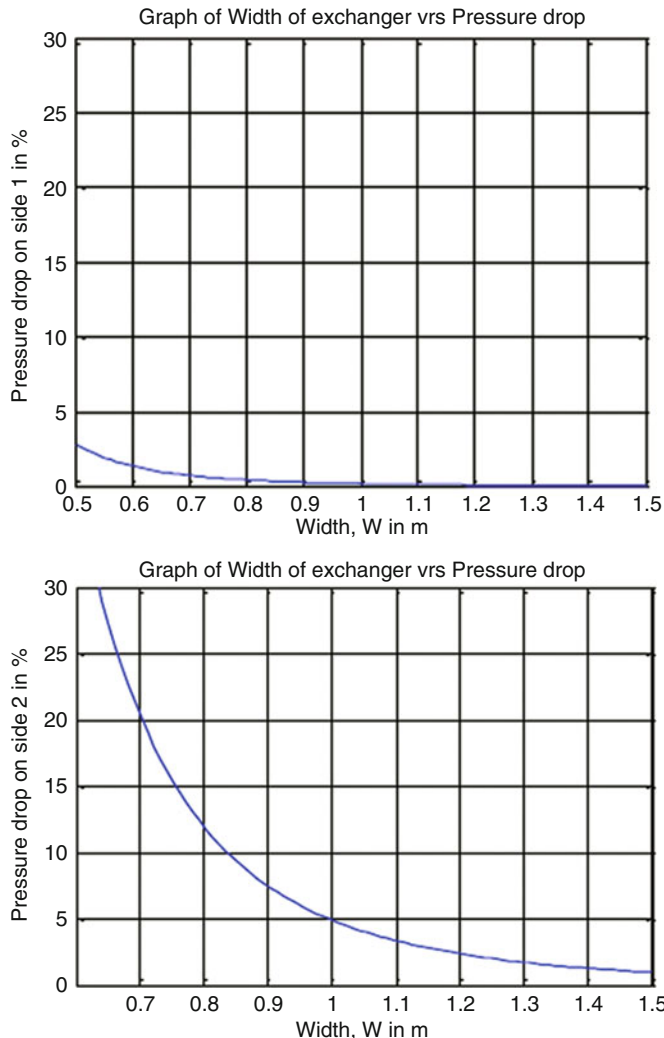


**Fig. 4.17** Graphs of width of heat exchanger against the pressure drop across the exchanger [1]

#### 4.23.3.2 The Height and Stack of the PCHE

Similarly, to assess how the change in the height/stack of the heat exchanger affects the pressure drop the height was varied while other parameters were kept constant.

Figure 4.18 shows graphs of how varying the height/stack of the heat exchanger affects the pressure drop.

Increasing the height and stack of the heat exchanger increases the flow area of the exchanger, since that increases the number of plates that would form the exchanger which would consequently increase the flow area and reduce the flow velocity. Pressure drop across the heat exchanger will inherently decrease with increasing height/stack of exchanger.

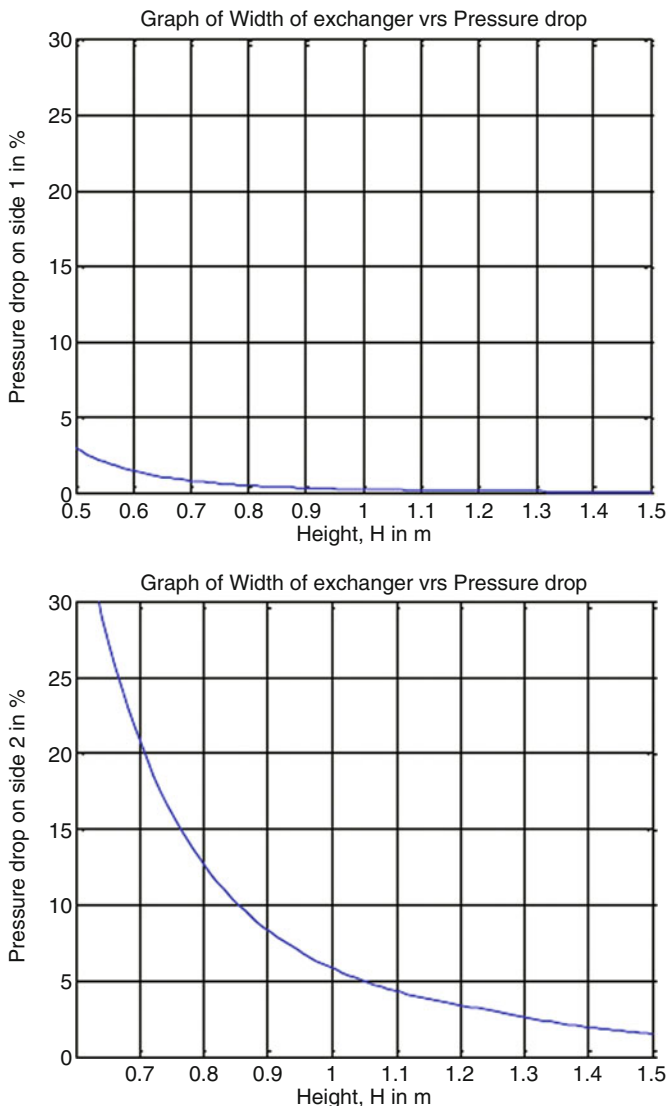


**Fig. 4.18** Graphs of height and stack of heat exchanger against pressure drop across the exchanger [1]

#### 4.23.3.3 Diameter of Channels Forming the PCHE

In order to analyze how changing the diameter of the channels forming the heat exchanger affects change in pressure drop, we have to ensure that dimensions for the pitch and thickness of the plates are appropriate. That is the diameter of the channels should be less than the pitch, and also two times the thickness of the plates

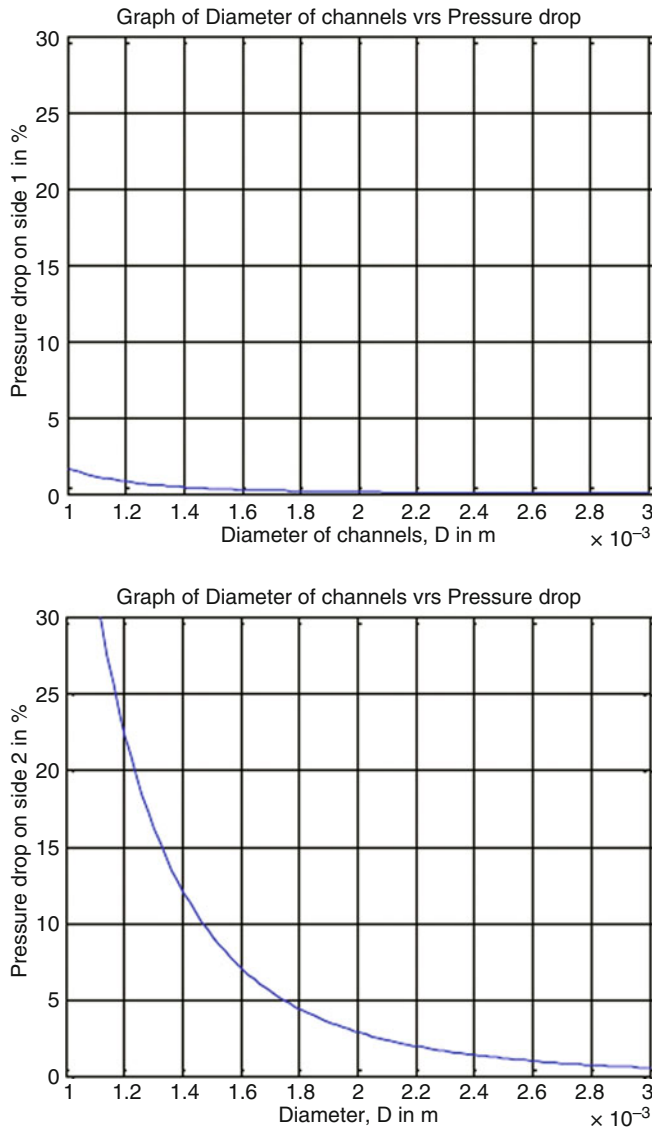


Fig. 4.19 Graphs of diameter of channels against pressure drop across exchanger [1]

should be greater than the diameter of channels. Figure 4.19 shows graphs of the diameter of the channels forming the heat exchanger against the pressure drop across the heat exchanger.

Increasing the diameter of channels in the plates of the heat exchanger will increase the free flow area which decreases the flow-velocity, and as a result the pressure drop across the exchanger decreases.

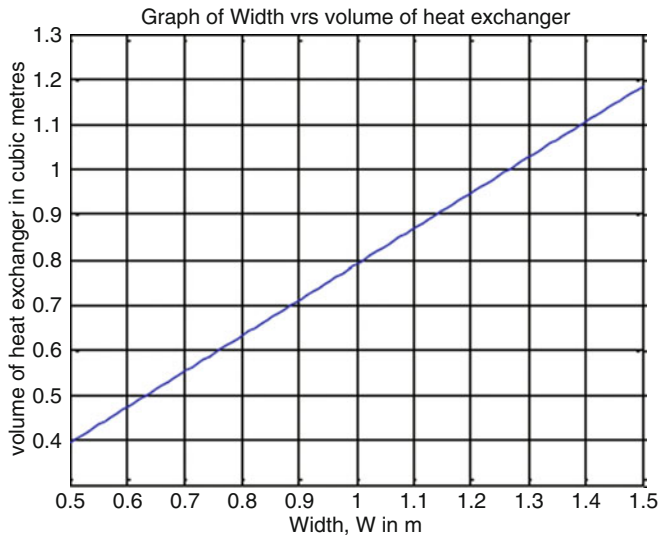


Fig. 4.20 A graph of the width versus volume of heat exchanger [1]

#### 4.23.3.4 Effect of Varying Parameters on the Volume of the PCHE

When the length, width, and height of the PCHE are varied the total volume of the heat exchanger increases, this is simply because the volume varies directly proportional to those parameters. Figure 4.20 shows a graph of width of the PCHE versus the volume of the exchanger. It has to be noted, however, that the volume calculated here would be slightly different from the total volume of the heat exchanger.

Varying the diameter for fixed length, width, and height of the PCHE would, however, not alter the volume of the heat exchanger.

#### 4.23.4 Analysis Performed on the PFHE

In selecting dimensions for the PFHE, a sensitivity analysis was carried out to ascertain how performance criterion such as pressure drop across heat exchangers is affected and also the effect on the physical outlook of the exchanger. Figure 4.21a-c shows graphs of length of the exchanger against pressure drops across the exchanger and the volume of the heat exchanger. On the other hand increasing width of the PFHE decreases the pressure drop across the heat exchanger, but the increase in width increases the volume of the exchanger.

Selection of appropriate dimensions for the PCHE and the PFHE was arrived at after the sensitivity analysis was performed and Tables 4.8 and 4.9 below show the parameters and results from the 1-D modeling of the PCHE and PFHE respectively.

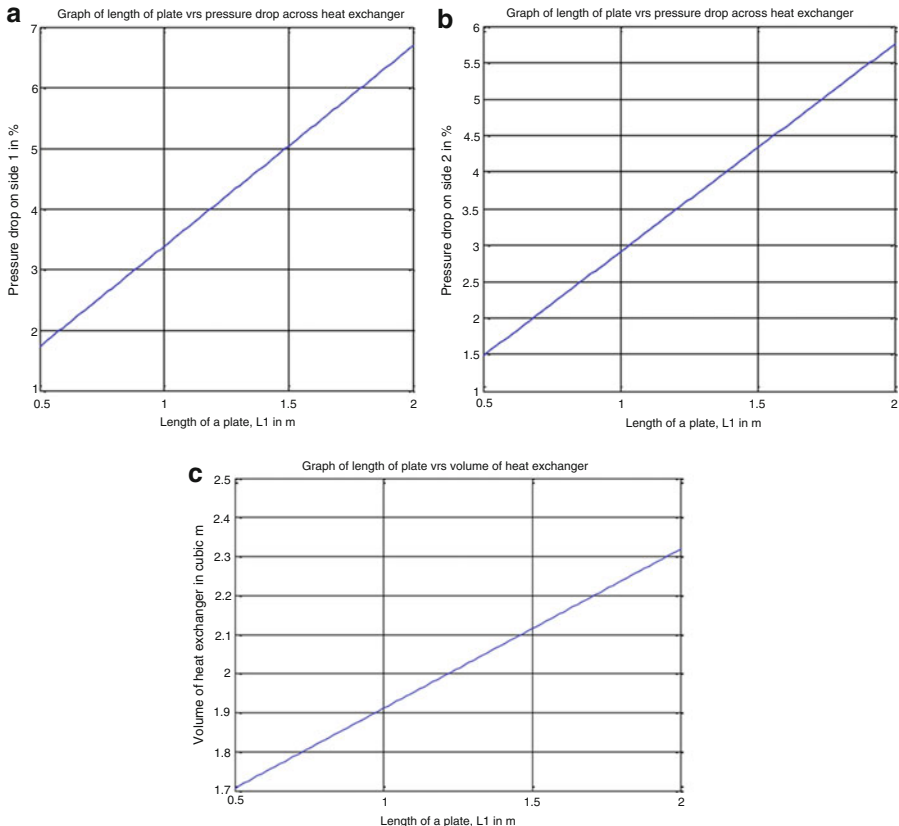


**Fig. 4.21** Graphs of length of the exchanger against pressure drops across the exchanger. (a) A graph of length of a plate versus pressure drop across side 1. (b) A graph of length a plate versus pressure drop across side 2. (c) A graph of length of a plate versus the volume of heat exchanger [1]

**Table 4.8** Parameter and results of the 1-D of the PCHE [1]

Parameter	Value
Length of exchanger, $L$ (m)	1.1
Diameter of channels, $D$ (mm)	2.0
Plate thickness, $th$ (mm)	1.5
Total number of plates, $N_{tCH}(-)$	1,373,760
Pressure drop-side 1, (%)	1.17
Pressure drop-side 2, (%)	3.29
Total heat transfer area, $A_{tot}$ ( $m^2$ )	5095
Heat transfer coefficient-side 1, ( $W/m^2 K$ )	174
Heat transfer coefficient-side 2, ( $W/m^2 K$ )	201
Overall heat transfer coefficient, $U$ ( $W/m^2 K$ )	92
Thermal power, $q$ (MW)	12.15

**Table 4.9** Parameter and results from the 1-D modeling of the PFHE [1]

Parameter	Value
Plate thickness, $\delta_w$ (mm)	1.5
Fin thickness, $\delta$ (mm)	0.15
Spacing between surfaces of a fin, $s$ (mm)	0.0015
Fin offset length, $\ell_s$ (mm)	6
Length of a plate, $L_1$ (m)	2.0
Width of a plate, $L_2$ (m)	1.6
Flow length in the $L_1$ direction, $L_f$ (m)	$L_1 \cdot 0.025$
Plate spacing for fluid side 1, $b_1$ (mm)	5.545
Plate spacing for fluid side 2, $b_2$ (mm)	5.545
Hydraulic diameter, $D_h$ (mm)	3.8
Total number of fins, $n_f$ (-)	81,000
Number of passages, $N_p$	133
Total surface area, $A$ ( $m^2$ )	4554
Pressure drop on the primary side, $\Delta P$ (%)	4.59
Pressure drop on the secondary side, $\Delta P$ (%)	4.84
Heat transfer coefficient-Primary side, $h_c$ ( $W/m^2 K$ )	163.90
Heat transfer coefficient-secondary side, $h_h$ ( $W/m^2 K$ )	378.48
Overall heat transfer coefficient, $U$ ( $W/m^2 K$ )	104.91

#### 4.23.5 Conclusion for the Selection of a Suitable Heat Exchanger

A review of various heat exchangers for high temperature, highly effective, and low pressure drop applications identify three promising heat exchangers for high temperature applications. These are the Plate-Fin, Printed-circuit, and the Marbond™ heat exchangers. The features of the Marbond™ heat exchangers as listed in Table 4.10, makes it attractive for high temperature applications like the proposed power plants and even higher temperature applications, but since it is a new heat exchanger much research and work needs to be carried out if it is to be considered for use in the proposed power plant or for other similar applications. The PFHE has been used for quite some time now, but its high capital cost and other limitations mentioned earlier does not make it the best option for this application, nevertheless it can be considered as an alternative. The PCHE which has been deemed promising is no doubt the exchanger that should be considered for this project, considering its compactness of up to  $5000\ m^2/m^3$ , effectiveness as much as 98.7 %, maximum operating of up to  $1000\ ^\circ C$ , and pressure up to 500 bars.

As part of our conclusion the following chart in Fig. 4.22 shows a depiction of the Pressure in the range  $0 < p < 600$  Bar versus Temperature in the range  $-200 < T < 800\ ^\circ C$  plot for Printed Circuit Heat Exchanger (PCHE), Formed Plate Heat Exchanger (FPHE), and others as well courtesy of Heatric™.

**Table 4.10** A summary of different type of heat exchangers and their principle features

Feature						
Type of heat exchanger	Compactness ( $\text{m}^2/\text{m}^3$ )	Stream types <sup>a</sup>	Material <sup>b</sup>	Temperature range ( $^{\circ}\text{C}$ ) <sup>c</sup>	Maximum pressure (bar)	Cleaning methods
Plate-and-frame (gaskets)	$\leq 200$	Liquid-liquid, gas-liquid, two-phase	s/s, Ti, Incoloy, Hastelloy, graphite, polymer	-35 to +200	25	Mechanical <sup>d</sup>
Partially welded plate	$\leq 200$	Liquid-liquid, gas-liquid, two-phase	s/s, Ti, Incoloy, Hastelloy,	-35 to +200	25	Mechanical <sup>d,g</sup> , Chemical <sup>h</sup>
Fully welded plate (Alfa Res)	$\leq 200$	Liquid-liquid, gas-liquid, two-phase	s/s, Ti, Ni alloys	-50 to 350	40	Chemical
Brazed plate	$\leq 200$	Liquid-liquid, two-phase	s/s	-195 to 220	30	Chemical <sup>i</sup>
Bavex plate	200 up to 300	Gases, liquids, two-phase	s/s, Ni, Cu, Ti, special steels	-200 to +900	60	Mechanical <sup>d,i</sup> , Chemical
Platular plate	200	Gases, liquids, two-phase	s/s, hastelloy, Ni alloys	Up to 700	40	Mechanical <sup>d,m</sup>

(continued)

Table 4.10 (continued)

	Feature							
Type of heat exchanger	Compactness ( $\text{m}^2/\text{m}^3$ )	Stream type <sup>a</sup>	Material <sup>b</sup>	Temperature range ( $^{\circ}\text{C}$ ) <sup>c</sup>	Maximum pressure (bar)	Cleaning methods	Corrosion resistance	Multistream capability
Compabloc plate	$\leq 300$	Liquids	s/s, Ti, Incoloy	Up to 300	32	Mechanical <sup>d</sup>	Good	Not usually Yes
Packinox plate	$\leq 300$	Gases, liquids, two-phase	s/s, Ti, Hastelloy, Inconel	-200 up to +700	300	Mechanical <sup>d,o</sup>	Good	Yes <sup>f</sup> Yes
Spiral	$\leq 200$	Liquid-liquid, two-phase	c/s, s/s, Ti, Incoloy, Hastelloy	Up to 400	25	Mechanical <sup>d</sup>	Good	No No
Brazed plate-fin	800 up to 1500	Gases, liquids, two-phase	Al, s/s, Ni alloy	Cryogenic to +650	90	Chemical	Good	Yes Yes
Diffusion-bonded plate-fin	700 up to 800	Gases, liquids, two-phase	Ti, s/s	Up to 500	>200	Chemical	Excellent	Yes Yes
Printed-circuit	200 up to 5000	Gases, liquids, two-phase	s/s, Ni, Ni alloy, Ti	-200 up to +900	>400	Chemical	Excellent	Yes Yes
Polymer (e.g., channel plate)	450	Gas-liquid <sup>p</sup>	PYDF <sup>q</sup> , pp <sup>r</sup>	Up to 150	6	Water wash	Excellent	No Not usually

Plate-and-shell	—	Liquids	s/s, Ti, (shell also in c/s) <sup>a</sup>	up to 350	70	Mechanical <sup>d,o</sup> , Chemical <sup>c,l</sup>	Good	No	Yes
Marbond	≤10,000	Gases, liquids, two-phase	s/s, Ni alloy, Ti	-200 up to +900	>900	Chemical	Excellent	Yes	Yes

Source: Shah et al. [33], Hesselgreaves [49], and Reay [50]

<sup>a</sup>Boiling and condensing duties are included in the two-phase

<sup>b</sup>s/s: Stainless Steel; Ni: Nickel; Ti: Titanium; Cu: Copper and their alloys of these materials and special alloys are also available for use

<sup>c</sup>The maximum pressure is not likely to occur at the higher operating temperatures, and assume no pressure/stress-related corrosion

<sup>d</sup>It can be dismantled

<sup>e</sup>Functions as a gasket as well as a plate material

<sup>f</sup>Not common

<sup>g</sup>On the gasket side

<sup>h</sup>On the welded side

<sup>i</sup>Ensures compatibility with the copper braze

<sup>j</sup>Function of braze as well as plate material

<sup>k</sup>Not in a single unit

<sup>l</sup>On the tube side

<sup>m</sup>Only when flanged access provided; otherwise, chemical cleaning  
Five fluids maximum

<sup>n</sup>On the shell side

<sup>o</sup>Considering on gas side

<sup>p</sup>Polyvinylidene difluoride

<sup>q</sup>Polypropylene

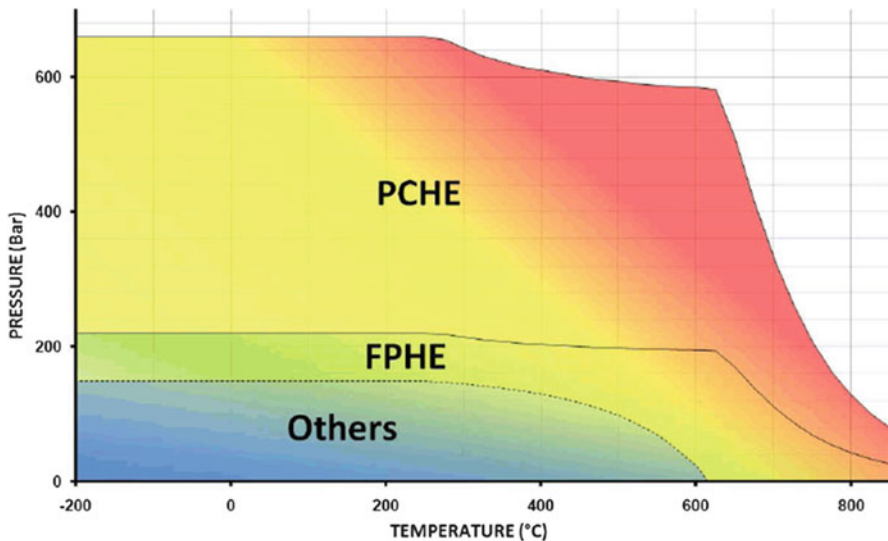


**Fig. 4.22** Plot of pressure vs. temperature for PCHE, FPHE and others

**Table 4.11** Current PCHE and FPHE heat exchangers manufactured by Heatic Company

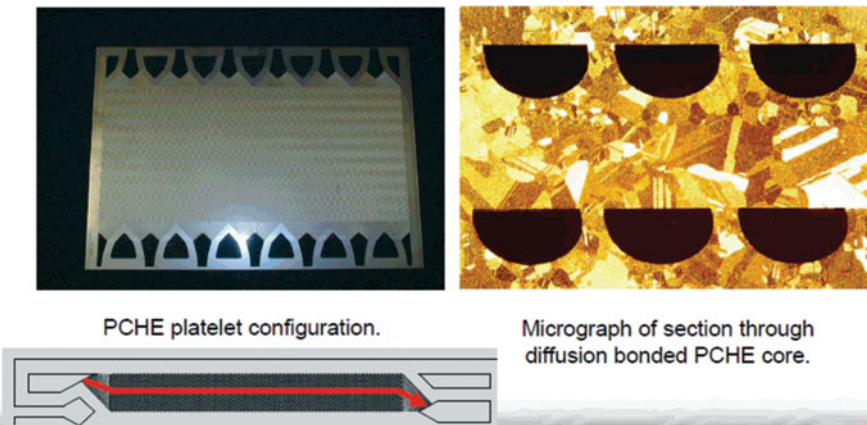
Requirements	PCHE	FPHE
High temperatures	800 °C + (Limited by material)	800 °C + (Limited by material)
High pressures	600 bar + (Max typical)	200 bar + (Max typical)
High effectiveness	98 % +	98 % +
Low pressure drop	Based on design	Bigger channels
High compactness	Highly compact	
Erosion resistance	Limited by material	
Corrosion resistance	Limited by material	
Longer life	Limited by material	

The following Table 4.11 is a demonstration of currently available PCHE and FPHE with their specifications that are manufactured by the Heatic™ manufacturing company as of 2012.

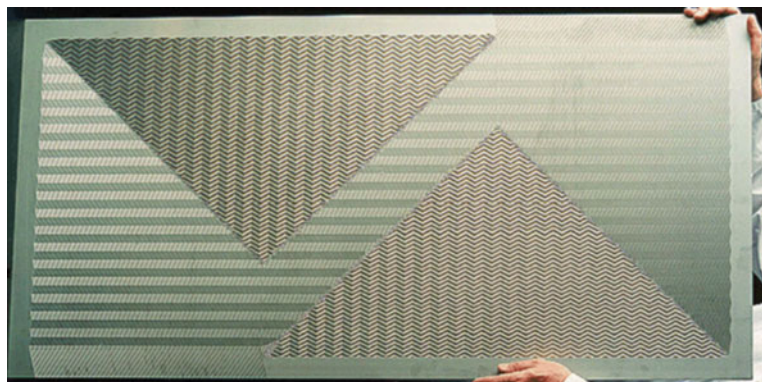
Figures 4.23 and 4.24 are presentations of both a PCHE and a single core plate with size up to  $1.5 \times 0.6 \times 0.6$  m respectively developed by Heatic™ Manufacturer.

Figure 4.25 is a presentation of a Formed Plate Heat Exchanger (FPCH) with plate-fin style construction, pressure capability to 200 bar, temperature capability the same as PCHE, and Channel cross section up to  $3 \text{ mm} \times 3 \text{ mm}$ .

Materials that are used by Heatic™ to manufacture these Compact Heat Exchangers (CHPs) are as follows:



**Fig. 4.23** Printed Circuit Heat Exchanger (PCHE). (Courtesy of Heatic Manufacturer)



**Fig. 4.24** PCHE plate size—up to 1.5 m long by 0.6 m wide. (Courtesy of Heatic Manufacturer)

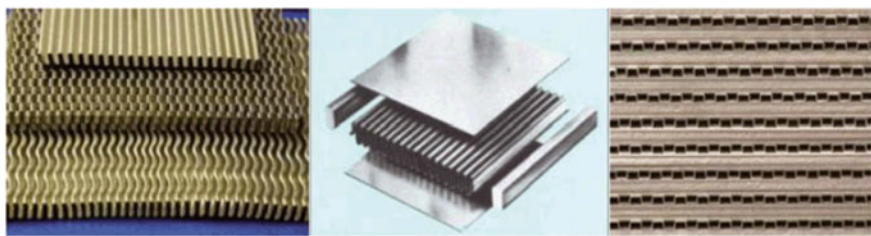


**Fig. 4.25** Depiction of FPCH. (Courtesy of Heatic Manufacturer)

- *Available:*

- Stainless steels 316L/316, 304L/304
- Duplex 2205 (S 31803)
- Titanium grade 2
- Moly (NO 8367)

- *Development:*

- Alloy 59 (NO 6059)
- SS 310 (S 31008)
- 800H (NO 8810)
- Alloy 617
- Dual material (copper to stainless)

A summary of the various important attributes of the three short list heat exchangers shown in Figs. 4.26 and 4.27, attests to the fact that the PCHE is the best option for this application. Although we briefly described this type of heat exchanger in Chap. 2, we explain more details here and show some advantages of this exchanger at the temperature we are interested in such as utilization of it in combined cycle driven efficiency of new generation of power plants as well as our case of solar gas turbine power plant.

The plate bundle of a plate-fin heat exchanger is composed of a fin, division plate, and seal packing. A fin and a seal packing, which are placed in between two adjacent division plates, form an interlayer called a passage. The inter-layers are

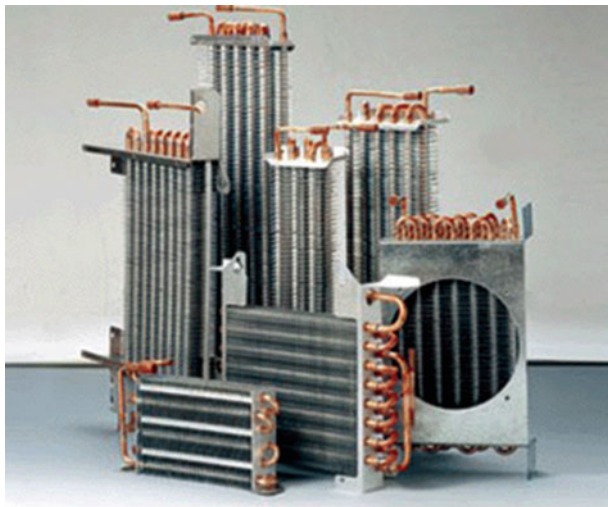
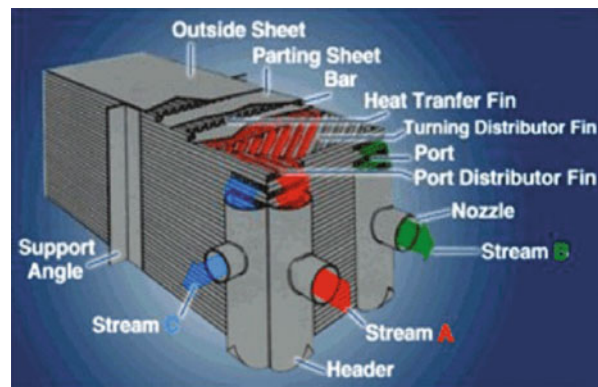


**Plate-fin heat exchanger**

**Fig. 4.26** Plate Fin Heat Exchanger

**Fig. 4.27** Structure of Plate-Fin Heat Exchanger



superposed into a whole by brazing, according to the different ways of fluid flow, forming the bundle of the plate (or called the core body).

Generally, there are one or two strength layers where fluid does not flow on both sides of the plate bundle, and the strength layers are known as false passage. Besides, the distributing section (flow guidance) and fluid-collecting box (shell cover) for the fluid inlet and outlet are mounted on the plate bundle. In this way, a complete plate-fin heat exchanger is formed.

The materials adopted by the plate-fin heat exchanger include pure aluminum, aluminum alloy, copper, brass, nickel, titanium, stainless steel, and inconel alloy. Aluminum is applicable to dip brazing with salt solution, so at present nearly all the plate-fin heat exchangers are made of the manganese-aluminum alloy, which is corrosion-resistant.

Figure 4.27 shows a structure of the PFHE. Various fins designs have been developed and used over the years and this includes plain, slit, offset spin, louver, and perforated fins [51].

The PFHE has an estimated [52] effectiveness greater than 90 % maximum operating temperature and pressure of 650 °C and 120 bar respectively. Materials employed in the manufacturing of the PFHE include aluminum which is usually for low temperature applications, stainless steel, titanium, nickel, and alloys of these materials.

#### 4.23.5.1 Features of Plate Fin Heat Exchanger

The main features of the plate-fin heat exchanger are as follows:

1. *High heat transfer efficiency*

The reason why the heat transfer efficiency is high is that the fin can cause the disturbance for the fluid to make the thermal boundary layer rupture and renew continuously. The heat transfer coefficient of forced convective gas is 35–350 W/ (m<sup>2</sup> °C), the overall heat transfer coefficient of forced convective

oil is  $120\text{--}1740 \text{ W}/(\text{m}^2 \text{ }^\circ\text{C})$ , while the overall heat transfer coefficient of gas-gas in the shell-and-tube heat exchanger is only  $10\text{--}35 \text{ W}/(\text{m}^2 \text{ }^\circ\text{C})$ .

## 2. Compact structure and light weight

For aluminum plate-fin heat exchanger, its heat transfer area per unit volume generally  $1500\text{--}2500 \text{ m}^2/\text{m}^3$ , also defines the compactness, which is 8–20 times that of the shell-and-tube heat exchanger. The weight of aluminum plate-fin heat exchanger is one tenth that of the shell-and-tube heat exchanger with the same heat transfer area, but its metal consumption per unit heat transfer area can be dozens of times smaller than the shell-and-tube heat exchanger.

## 3. Wide range of application

The plate-fin heat exchanger can be applicable to the heat transfer of various different fluids such as gas to gas, gas to liquid, and liquid to liquid. Depending on the arrangement and combination of various flow passages, the plate-fin heat exchanger can adapt to the heat transfer in different working conditions such as countercurrent, cross flow, multi-flow, and multi-pass flow. The plate-fin heat exchanger can be shaped and produced in batches to meet different requirements, so the cost can be reduced and the interchangeability is enlarged.

## 4. Manufacturing process

The manufacturing process is complicated and the requirements for manufacture are strict.

## 5. Preventive maintenance

The plate-fin heat exchanger blocks easily and the cleaning and maintenance are difficult. If inner leakage occurs owing to corrosion, it is hard to maintain the exchanger. In practical production, the plate-fin heat exchangers made of aluminum are used as air separation devices, petrochemical devices, and mechanical power equipment.

## 6. Service range

The service ranges are as follows:

The design temperature is from  $-200$  to  $150 \text{ }^\circ\text{C}$ , and the design pressure is from 0 to 0.6 MPa.

### 4.23.5.2 Fin Types of Plate Fin Heat Exchanger

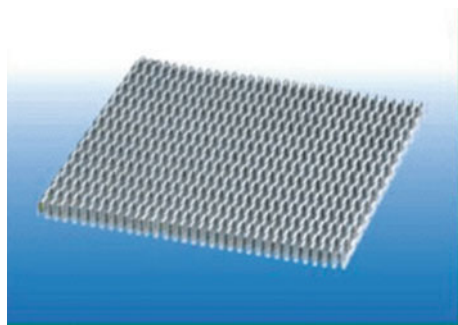
The function of the fin is to enlarge the heat transfer area and improve the compactness and heat transfer efficiency of the heat exchanger. Besides, the fin doubles as a division plate, which can improve the strength and loading capacity of the exchanger.

The common fins mainly include the plain type, the serrated type, the porous type, and the herringbone corrugated type.

#### 1. Plain type fin

The feature of plain type fin is that it has a linear passage, which only plays a role in supporting and enlarging the heat transfer area but has little effect on promoting the fluid turbulence. Its heat transfer and fluid dynamic properties are similar to those of the fluid flowing inside the circular tube. The length of the

**Fig. 4.28** Typical serrated fin



passage has an obvious effect on the heat transfer result. Compared with other fins, the heat transfer coefficient and resistance of the plain type fin are smaller. The plain type fin is mostly used in services where the requirement for resistance is stricter and the heat transfer coefficient is larger.

#### 2. Serrated type fin

The feature of serrated type fin is that there are some micro-grooves along the fin length, forming the serrated-shaped passage. The serrated type fin is so helpful in promoting the fluid turbulence and damaging the boundary with thermal resistance that properties similar to those during turbulence appear within the range of low  $Re$  number. Therefore, the serrated type fin is one of the efficient fins. With the same pressure drop, its heat transfer coefficient is 30 % higher than the flat fin, but its resistance is larger. The serrated type fin is mainly used as the gas passage and the oil passage with smaller temperature difference between high-temperature and low-temperature fluids and higher viscosity. See Fig. 4.28.

#### 3. Porous fin

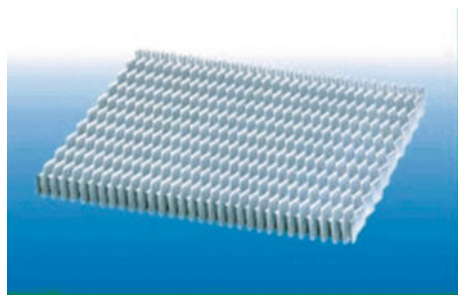
Some holes are distributed on the fin to make the thermal resistance boundary layer rupture continuously, to improve the heat transfer efficiency and make the fluid distribute more uniformly on the fin, and finally it is beneficial to scour and remove impurities in the fluid. With the range of larger  $Re$  ( $Re = 103\text{--}104$ ), the heat transfer coefficient of the porous fin is higher than that of the plain fin. The porous fin is mainly used for the heat transfer with phase change and as the flow guidance on the distributing section at the inlet and outlet of the heat exchanger.

#### 4. Corrugated fin

The corrugated fin is corrugated in the longitudinal direction to make the flow direction of the fluid change continuously, to promote the turbulence. Micro rupture may exist in the thermal resistance boundary layer at the bending positions, so the heat transfer efficiency can be improved. The heat transfer performance of the corrugated fin is in between the plain type and the serrated type. See Fig. 4.29.

The compressive strength of the fin is higher, so the corrugated fin can be used for gas heat transfer with higher pressure.

**Fig. 4.29** Typical corrugated fin



#### 5. Venetian-blind fin

The venetian-blind fin is cut off repeatedly at a certain distance to make the passage of the fin appear like venetian blinds. The grids of the venetian blinds can continuously damage the thermal resistance boundary layer, so the heat transfer process can be reinforced. The smaller the spacing at the broken place is, the more the heat transfer is reinforced, but the pressure drop will increase. The performance of the venetian-blind fin is in between the serrated type fin and the corrugated-shape fin. Therefore, the venetian-blind fin is also one of the efficient fins.

#### 6. Strip type fin

The strip type fin is formed by cutting the plain fin into short discontinuous strips and then arranging the strips irregularly at a certain distance from each other. In principle, the strip type fin is similar to the venetian-blind fin. The difference between it and the venetian-blind fin is that their manufacturing methods and relative positions are different. The fin length along the flow direction is short and discontinuous, which makes the thermal boundary layer on the fin rupture without enough time to grow, so the heat transfer performance of the strip type fin is good.

#### 7. Pin-shaped fin

The pin-shaped fin is a special fin among the fins. The movement of the fluid on the pin-shaped fin is similar to that of the fluid vertical to the tube bundle. The length along the flow direction is very small to make the thermal boundary layer damaged frequently and make the thickness of the thermal boundary layer remain the thinnest, so its heat transfer performance is very high, but the friction loss is also large.

## References

- Yakah, Noah. 2014. Heat exchanger design for a solar gas-turbine power plant. Master of Science Thesis, KTH School of Industrial Engineering and Management, Energy Technology EGI-2012-110MSG EKV925, Division of Heat and Power, SE-100 44 Stockholm.
- Shah, R.K., and A.L. London. 1978. Laminar flow forced convection in ducts. In *Advances in heat transfer*, ed. J. Thomas, F. Irvine, and J.P. Harnett. New York: Academic Press.

3. Saari, Jussi. *Heat exchanger dimensioning*. Lappeenranta University of Technology, Faculty of Technology LUT Energy.
4. Seban, R.A., and T.T. Shimazaki. 1951. Heat transfer to a fluid flowing turbulently in a smooth pipe with walls at constant temperature. *Transactions of the ASME* 73: 803–809.
5. VDI Heat Atlas. 1988. VDI-Gesellschaft Verfahrenstechnik und Chemieingenieurwesen, ed. Edited by specialists, engineers and researchers of the German Engineers Society (VDI).
6. Incropera, Frank P., David P. Dewitt, Theodore L. Bergman, and Adrienne S. Lavine. 2007. *Introduction to heat transfer*. Danvers, MA: Wiley.
7. Shapiro, A.H., R. Siegel, and S.J. Kline. 1954. Friction factor in the laminar entry region of a smooth tube. In *Proc. U.S. Natl. Congr. Appl. Mech.*, 2nd., 773–741. New York: Am. Soc. Mech. Eng.
8. Sadikov, I.N. 1965. Laminar heat transfer over the initial section of a rectangular channel". *Journal of Engineering Physics (USSR)* 8: 287–291.
9. Zohuri, B., and N. Fathi. 2015. *Thermal hydraulic analysis of nuclear reactors*. New York: Springer.
10. Cho, Y.I., and J.P. Hartnett. 1985. Nonnewtonian fluids. In *Handbook of heat transfer applications*, 2nd ed, ed. W.M. Rohsenow, J.P. Hartnett, and E.N. Ganic, 2-1-2-50. New York: McGraw-Hill. Chapter 4, Part III.
11. Bird, R.B., W.E. Stewart, and E.N. Lightfoot. 1960. *Transport phenomena*. New York: Wiley.
12. Hartnett, Koch, and McCornas. *Teploperpredacha* 84, no. 1, 1962.
13. Tung, T.T., K.S. Ng, and J.P. Hartnett. 1978. Pipe friction factor for concentrated aqueous solutions of polyacrylamide. *Letters in Heat Mass Transfer* 5: 59.
14. Ng, K.S., Y.I. Cho, and J.P. Hartnett. 1980. Heat transfer performance of concentrated polyethylene oxide and polyacrylamide solutions. *AICHE Symposium Series* 76(199): 250.
15. Kays, W.M. 1966. *Convective heat and mass transfer*. New York: McGraw-Hill.
16. Kays, W.M. 1966. *Convective heat and mass transfer*. New York: McGraw-Hill.
17. Zohuri, B. 2015. *Dimensional analysis and self-similarity methods for engineers and scientists*. New York: Springer.
18. Sellers, J.R., M. Tribus, and J.S. Klein. 1956. Heat transfer to laminar flow in a round tube or flat conduit—the Graetz problem extended. *Transactions of the ASME* 78: 441–448.
19. Mitchell, J.W. 1969. An expression for internal flow heat transfer for polynomial wall temperature distributions. *Journal of Heat Transfer* 91: 175–177.
20. Eckert, E.R.G., T.F. Irvine Jr., and J.T. Yen. 1958. Local laminar heat transfer in wedgeshaped passages. *Transactions of the ASME* 80: 1433–1438.
21. Reynolds, W.C. 1963. Effect of wall heat conduction on convection in a circular tube with arbitrary circumferential heat input. *International Journal of Heat Mass Transfer* 6: 925.
22. Siegel, R., E.M. Sparrow, and T.M. Hallman. 1958. Steady laminar heat transfer in a circular tube with prescribed wall heat flux. *Applied Scientific Research, Section A* 7: 386–392.
23. Noyes, R.N. 1961. A fully integrated solution of the problem of laminar or turbulent flow in a tube with arbitrary wall heat flux. *Journal of Heat Transfer* 83: 96–98.
24. Hasegawa, S., and Y. Fujita. 1968. Turbulent heat transfer in a tube with prescribed heat flux. *International Journal of Heat Mass Transfer* 11: 943–962.
25. Bankston, C.A., and D.M. McEligot. 1969. Prediction of tube wall temperatures with axial variation of heating rate and gas property variation. *Nuclear Science and Engineering* 37: 157–162.
26. Zabrodskiy, S.S. 1972. Several specific terms and concepts in Russian heat transfer notation. *Heat Transfer-Soviet Research* 4(2): i–iv.
27. Grigull, U., and H. Tratz. 1965. Thermischer einlauf in ausgebildeter laminarer Rohrstromung. *International Journal of Heat Mass Transfer* 8: 669–678.
28. Javeri, V. 1976. Analysis of laminar thermal entrance region of elliptical and rectangular channels with Kantorowich method. *Waerme-Stoffuebertrag* 9: 85–98.

29. Shah, R.K., and A.L. London. 1974. Thermal boundary conditions and some solution for laminar duct forced convection. *Journal of Heat Transfer* 96:159–165; condensed from *Am. Soc. Mech. Eng., Pap.* 72-WA/HT-54 (1972).
30. Kakaç, Sadik, Arthur E. Bergles, and E. Oliveira Fernandes (eds.). 1988. *Two-phase flow heat exchangers: thermal-hydraulic fundamentals and design (NATO Science Series E)*, 1988th ed, 1988. New York: Springer.
31. Shah, R.K., and A.C. Muller. 1985. Heat exchangers. In *Handbook of heat transfer applications*, 2nd ed, ed. W.M. Rohsenow, J.P. Hartnett, and E.N. Ganic, 4-1. New York: McGraw-Hill. Chapter 4, Part III.
32. Sarkomaa, Pertti. 1994. Lammonsiirtimien Suunnittelumenetelmat ja lampotekninen Mitoitus. LTKK, Opetusmoniste C-65, Lappeenranta, May 1994.
33. Shah, R.K., and D.P. Sekulic. 2003. *Fundamentals of heat exchanger design*. New York: Wiley.
34. Chapman, Alan J. 2002. *Heat transfer*, 4th ed. New York: Macmillan Publishers.
35. Sieder, E.N., and G.E. Tate. 1936. Heat transfer and pressure drop of liquids in tubes. *Industrial Engineering Chemistry* 28: 1429.
36. Perry, R.E. 1988. *Perry's chemical engineering's handbook*, 4th ed. New York: McGraw-Hill. International Edition.
37. Welty, J.R., C.E. Wicks, and R.E. Wilson. 1976. *Fundamentals of momentum, heat and mass transport*. Hoboken, NJ: Wiley.
38. Bogue, D.C. 1959. Entrance effects and prediction of turbulent in non-newtonian flow. *Industrial Engineering Chemistry* 51: 874.
39. Dodge, D.W., and A.B. Metzner. 1959. Turbulent flow of non-newtonian system. *AICHE Journal* 5: 189.
40. Tung, S.S., and T.F. Irvine Jr. 1979. Experimental study of the flow of a viscoelastic fluid in a narrow isosceles triangular duct. In *Studies in heat transfer*, ed. T.F. Irvine Jr. et al. New York: McGraw-Hill.
41. Lee, H.S., and T.F. Irvine, Jr. 1981. Degradation effects and entrance length studies for a drag reduction fluid in a square duct. State Univ. of New York at Stony Brook TR-382.
42. Frank P. Incropera, and DeWitt David. 2002. *Fundamentals of heat and mass transfer*, 5th ed. United States: John Wiley & Sons, Inc.
43. Zohuri, B. 2015. *Combined cycle driven efficiency for next generation nuclear power plants: an innovative design approach*. New York: Springer.
44. Zohuri, B. 2015. *Application of compact heat exchangers for combined cycle driven efficiency in next generation nuclear power plants*. New York: Springer.
45. Foumeny, E.A., and P.J. Heggs. 1991. *Heat exchange engineering, vol. 2: Compact heat exchangers: techniques of size reduction*. West Sussex: Ellis Horwood Limited.
46. Kays, W.M., and A.L. London. 1964. *Compact heat exchangers*, 2nd ed. New York: McGraw-Hill.
47. Linstrom, P., and W. Mallard. NIST chemistry Web-Book, NIST standard Reference Database Number 69, National Institute of Standards and Technology. Available at: <http://webbook.nist.gov/chemistry/fluid/>.
48. Nikitin, K., Y. Kato, and L. Ngo. 2006. Printed Circuit Heat Exchanger thermal-hydraulic performance in supercritical CO<sub>2</sub> experimental loop. *International Journal of Refrigeration* 29: 807–814.
49. Hesselgreaves, J.E. 2001. *Compact heat exchangers, selection, design and operation*. Oxford: Pergamon.
50. Reay, D.A. 2002. Compact heat exchangers, enhancement and heat pumps. *International Journal of Refrigeration* 25: 460–470.
51. McDonald, Collins F. 1990. Gas turbine recuperator renaissance. *Heat Recovery Systems & CHP* 10(1): 1–30.

52. Jeong, Ji Hwan, Lae Sung Kim, Jae Keun, Man Yeong Ha, Kui Soon Kim, and Young Cheol Ahn. 2007. Review of heat exchanger studies for high-efficiency gas turbines. ASME Turbo Expo 2007: Power for Land, Sea and Air, May 14–17, 2007, Montreal, Canada.
53. Gnielinski, V. 1975. Neue Gleichungen für den Wärme- und den Stoffübergang in turbulent durchströmten Rohren und Kanälen. *Forschung im Ingenieurwesen* 41: 8–16.

# **Chapter 5**

## **Three-Dimensional Modeling of Desired Compact Heat Exchanger**

In order to have a fairly accurate idea of how the desired or designated compact heat exchanger would perform when installed and used for the given application, in our case a Concentrated Solar Power (CSP) Plant, a 3-Dimensional Modeling study and analysis was done using the COMSOL™ Multiphysics Version 5.2 Computer Software. This chapter discusses the 3D model and the results obtained when the model was simulated. The chapter starts by introducing COMSOL Multiphysics, followed by a brief description of the theory for conjugate heat transfer interface, steps that are followed in modeling when using the COMSOL™ software, and the various stages involved in building and simulating a model in COMSOL™ Multiphysics with great focus on the designed heat exchanger that is described in the previous chapter.

### **5.1 Introduction to COMSOL Multiphysics**

COMSOL Multiphysics (formerly known as FEMLAB) is a finite element analysis, solver and simulation software/FEA software package used for various physics and engineering applications. It is usually used when a coupled phenomenon or Multiphysics is to be simulated. In addition COMSOL Multiphysics also offers a broader interface to MATLAB and its toolboxes, and can be used for a large variety of programming, preprocessing, and post processing possibilities (Source: [www.comsol.com](http://www.comsol.com) and [www.wikipedia.org](http://www.wikipedia.org)) (see Fig. 5.1).

COMSOL Multiphysics™ is also described as an Engineering simulation software that offers an environment which facilitates all steps involved in modeling processes, that is defining the geometry, meshing, specifying the physics to be studied, solving the problem, and allowing the results to be visualized (Source: [www.comsol.com](http://www.comsol.com)).

COMSOL Multiphysics is a finite element analysis, solver, and Simulation software/Finite Elements Analysis (FEA) Software package for various physics

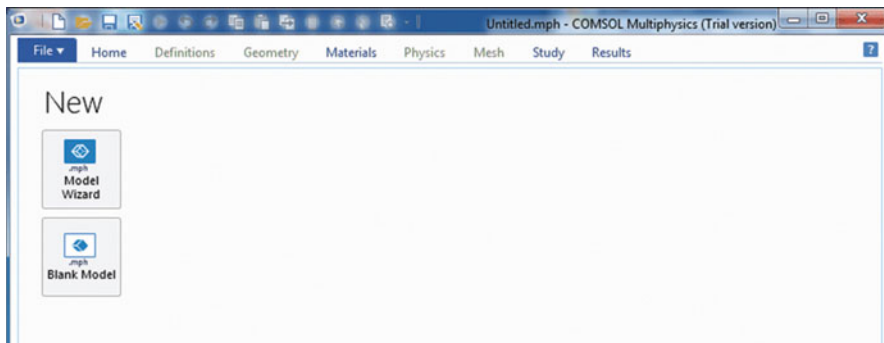


**Fig. 5.1** Screen shot of COMSOL™ version 5.2 home page

and engineering applications, especially coupled phenomena or multiphysics. The package is cross-platform (Windows, Mac, and Linux). In addition to conventional physics-based user interfaces, COMSOL Multiphysics also allows for entering coupled systems of Partial Differential Equations (PDEs). The PDEs can be entered directly or using the so-called weak form.

COMSOL Multiphysics® is a simulation environment designed with real-world applications in mind. The idea is to mimic as closely as possible effects that are observed in reality. To do this, there is the need to consider multiphysics process capabilities.

The PDEs can be entered directly or using the so-called weak form (see finite element method for a description of weak formulation). Since version 5.0 (2014), COMSOL Multiphysics is also used for creating physics-based apps. These apps can be run with a regular COMSOL Multiphysics license but also with a COMSOL Server license. An early version (before 2005) of COMSOL Multiphysics was called FEMLAB.

## 5.2 Steps Involved in COMSOL Multiphysics

As mentioned earlier, COMSOL Multiphysics facilitates all the steps involved in modeling from defining the geometry to meshing.

The tasks involved in the use of COMSOL Multiphysics to model the heat exchanger are enumerated in the following steps;

- Selecting space dimension to be used for modeling after starting COMSOL Multiphysics either One-Dimensional (1-D), Two-Dimensional (2-D) or Three-Dimensional (3-D) space
- Adding physics to the model to be studied
- Selecting the study type to be undertaken
- Defining the geometry of component or part to be modeled
- Adding of materials to be used for the various parts of the model

- Entering the necessary boundary conditions for the model
- Meshing, computing, and post-processing

## 5.3 The Conjugate Heat Transfer Interface for Laminar Flow Using COMSOL

Using COMSOL Multiphysics to model designing the compact heat exchanger (CHE) one starts the space selection in the home page of the software.

### 5.3.1 Space Selection

To model in COMSOL Multiphysics a space needs to be selected first, and this can be either in 1D, 2D or 3D depending on what one wants to study. The 3D space was selected for this study since we desire to study the performance of the heat exchanger in 3D. Figure 5.2 displays the various options available for modeling as it appears in the software.

### 5.3.2 Adding Physics

After selecting the space of interest, the next step is to add the physics that we wish to study. A lot of modules can be studied with the COMSOL Multiphysics software as stated earlier. Some of these modules include; AC/DC module, Acoustic module, Batteries and Fuel cells module, CFD module, Corrosion module, Electrodeposition module, Heat Transfer module, etc.

The **Heat Transfer module > Conjugate Heat Transfer > Laminar flow** is the physics added for this study. This interface is selected for modeling the heat exchanger because; the calculated Reynolds number of flow in the heat exchanger depicted a laminar flow regime (see Figs. 5.3 and 5.4).



**Fig. 5.2** A window showing the select space dimension in COMSOL™ Multiphysics model wizard

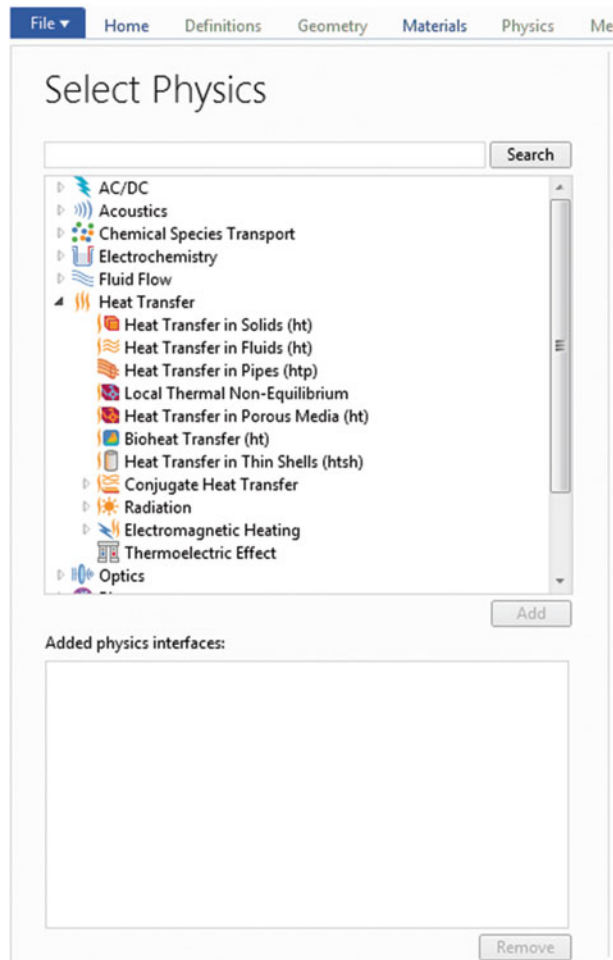


**Fig. 5.3** A window showing the add physics model wizard in COMSOL™ Multiphysics

Then in the next step, when choosing the **Laminar Flow** by default, where the initial values are added by default one gets the following window screen shot of COMSOL™ for this particular condition as in Fig. 5.5.

### 5.3.3 Selecting Study Type

The type of study that one wishes to study is selected after adding the desired physics one wishes to study. There are two main types of studies that can be studied, and the study can be either preset studies for selected physics (e.g., Stationary or

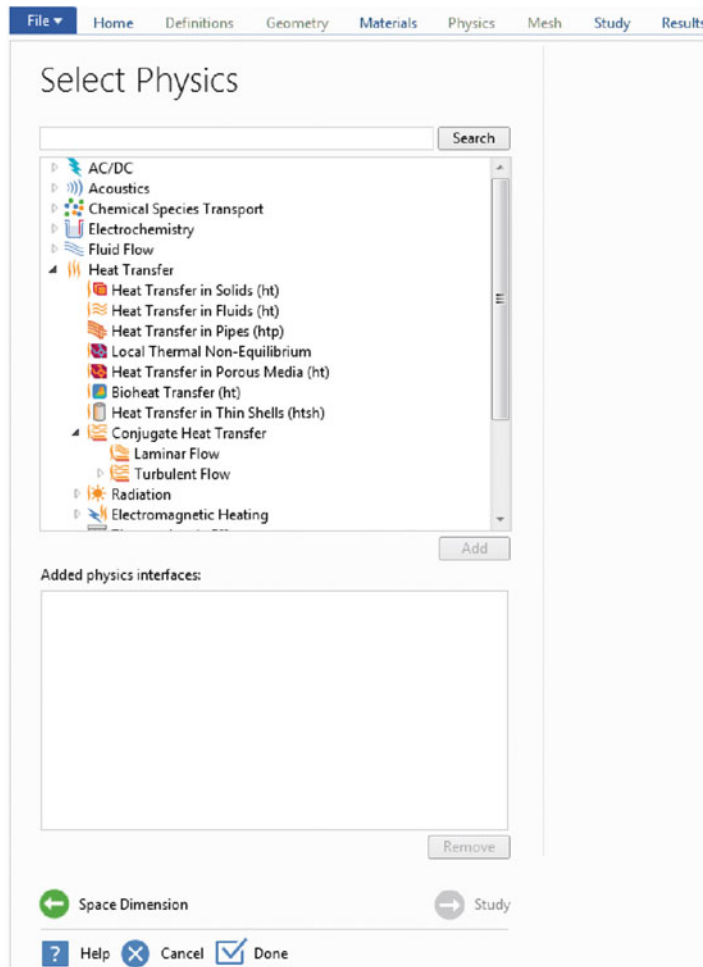


**Fig. 5.4** A window showing the add physics model wizard in COMSOL<sup>TM</sup> Multiphysics for laminar flow

time dependent) or custom studies (e.g., Empty study, eigenfrequency, etc.). Figure 5.6 shows the model wizard select study type window as displayed in COMSOL<sup>TM</sup> Multiphysics.

### 5.3.4 Geometry

In order to be able to model any component or part, the first thing to do is to draw the geometry of the model either in 1-D, 2-D or 3-D depending on what physics one

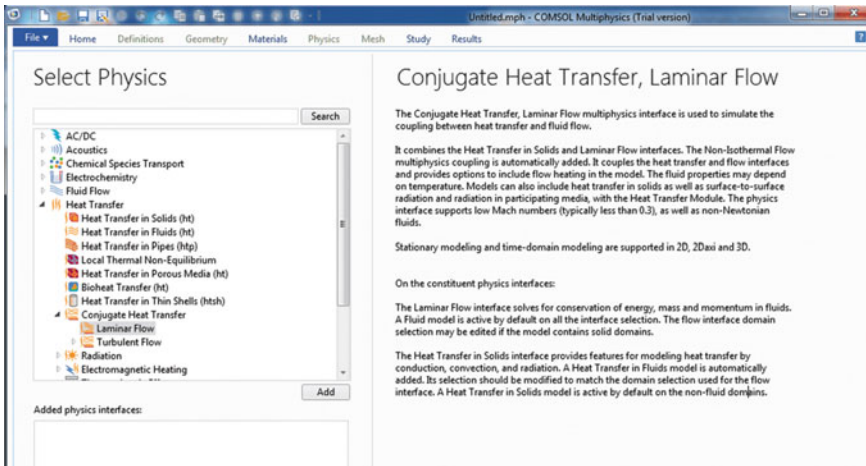


Fig. 5.5 COMSOL screen shot for conjugate heat transfer, laminar flow

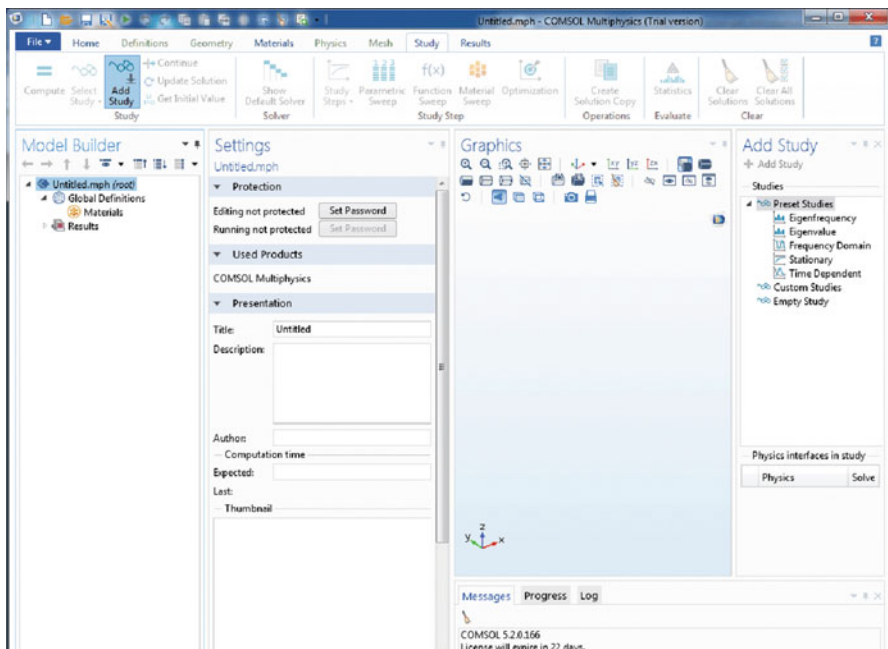
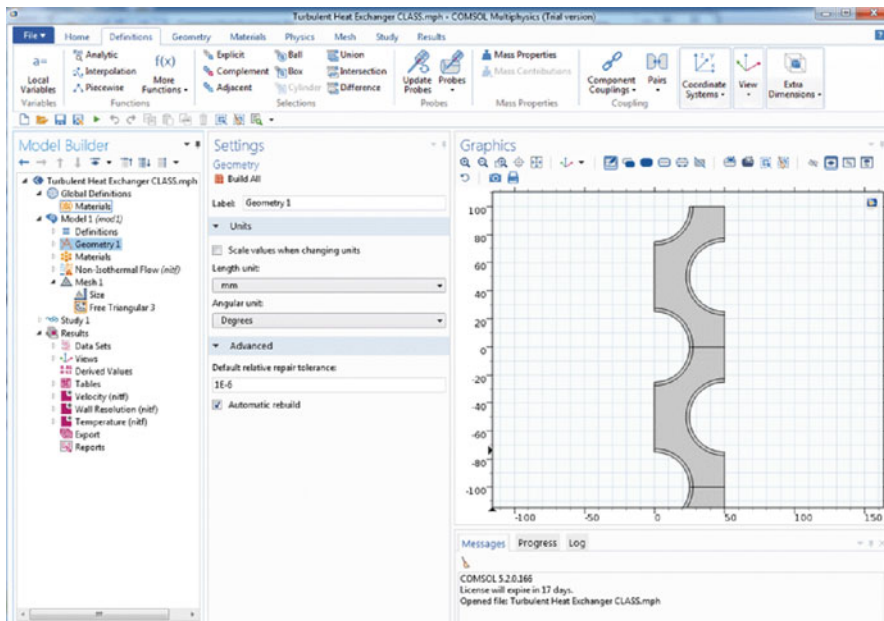


Fig. 5.6 A window showing select study type in COMSOL™ Multiphysics

wishes to study. COMSOL™ Multiphysics has a platform where the geometry can be built as desired.

A 3-D geometry of a piece of the heat exchanger was drawn to perform the modeling in this assignment, it consists of two channels both for the hot and cold



**Fig. 5.7** A COMSOL window is illustrating various tools used in constructing model geometry and Model Builder Mode<sup>®</sup>

sides of the heat exchanger, with dimensions realized from the MATLAB design. Only a small part of the heat exchanger is to be simulated, and this is to reduce the computational time and memory usage in the simulation and computation platform (Fig. 5.7).

### 5.3.4.1 Interface Identifier

The interface identifier is a text string that can be used to reference the respective physics interface if the need arises. This is usually the case when coupling the interface to another physics interface or in cases when we attempt to identify and use variables defined by this physics interface. This can however be changed when we desire to. The default for **Conjugate Heat transfer** is “nif”.

### 5.3.4.2 Domain Selection

The domain settings under the **Conjugate Heat Transfer** enable you to select the domains where you want to define the dependent variables and their respective governing equations (see Fig. 5.8).

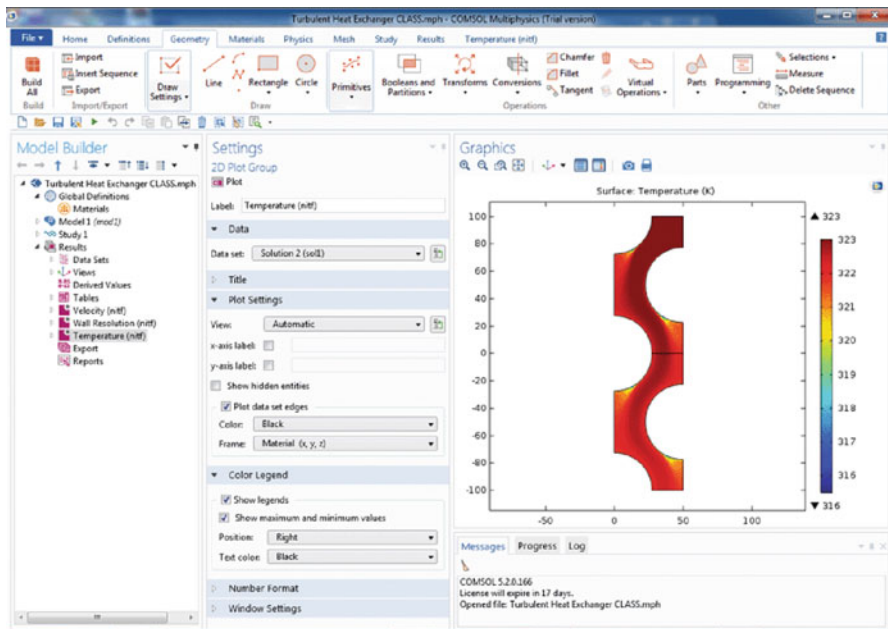


**Fig. 5.8** A screenshot of window showing setting in the conjugate heat transfer in COMSOL Multiphysics®

### 5.3.4.3 Physics Model

This is where the interface properties controlling the type of model are specified, but since we are modeling a laminar flow as has been selected from the beginning, **Turbulence model type** would be selected by default as **None**. In cases where we need to model flows at very low Reynolds numbers there is a box that can be checked to ensure that inertial terms in the Navier-Stokes equations are neglected and rather the linear version of the Stokes equations are invoked. The box to check is labeled as **Neglect inertial term (Stokes flow)** (Fig. 5.9).

### 5.3.4.4 Dependent Variables

This interface is where the dependent variables are defined, and in the conjugate heat transfer the dependent variables are temperature, velocity, and pressure.

### 5.3.5 Boundary Conditions for Conjugate Heat Transfer Interface

The following are some boundary conditions for the **Conjugate Heat Transfer** interfaces (only those that are used in this work are discussed, and these conditions are also available for all heat transfer modules).

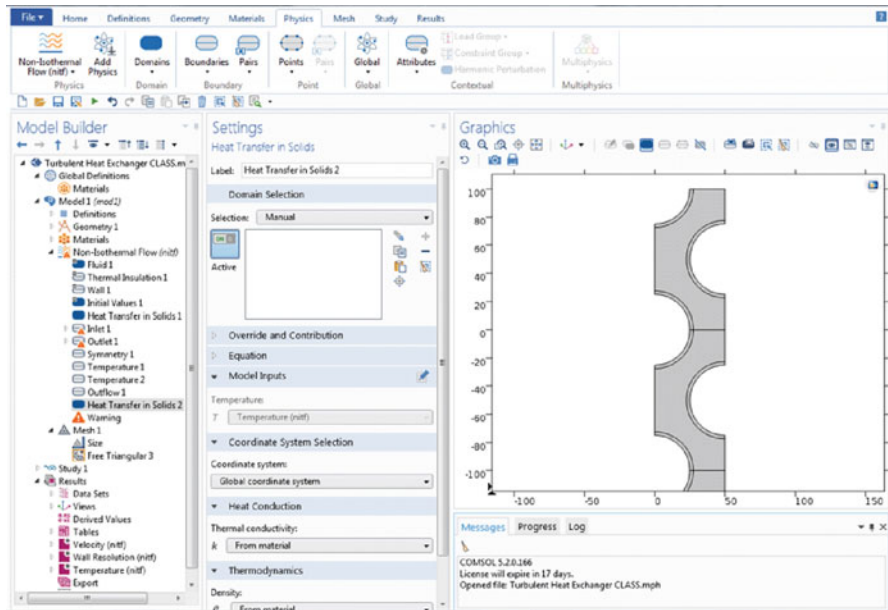


Fig. 5.9 Show screen shot

### 5.3.5.1 Heat Transfer in Solids

The **heat transfer in solids** node is selected as default in the **Conjugate Heat Transfer** interface and the equation used here is the heat equation (energy conservation equation), the same as the one described for the theory for the conjugate heat transfer interface. That is

$$\rho c_p u \Delta T = \Delta \cdot (k \Delta T) + Q \quad (\text{Eq. 5.1})$$

Where the symbols are the same as those stated under the heat equation as quoted earlier.

### 5.3.5.2 Thermal Insulation

The thermal insulation boundary condition is added to all heat transfer interfaces by default and this boundary condition ensures that there is no heat flux across the boundaries and this is expressed as

$$-n \cdot (-kk\Delta T) = 0 \quad (\text{Eq. 5.2})$$

The above equation implies that the temperature gradient across the boundary must be zero, and the relation to hold the temperature on one side of the boundary must equal the temperature on the other side.

#### **5.3.5.3 Initial Values**

This node is used to initialize the values of the dependent values to zero and is added to the model by default; as such its selection cannot be altered whatsoever.

#### **5.3.5.4 Inlet**

The inlet node includes a set of boundary conditions which describes the fluid flow at the entry point. These boundary conditions are;

- (a) Velocity
- (b) Pressure, No viscous stress
- (c) Normal stress

The inlet node is used to specify the type of flow regime at the entry of the model, also the inlet velocity, mass flow rate, length of the flow, pressure, and average velocity need to be specified using this node.

#### **5.3.5.5 Temperature**

The temperature node is used to specify the temperature somewhere in the geometry; this can be on the boundaries and surfaces in most cases. The boundaries the temperature is subjected to are selected either as all boundaries or by manually selecting the appropriate boundaries or surfaces. They are usually selected manually since the temperature acts only at some points in the model.

The equation for the temperature is  $T = T_0$ , where  $T_0$  is the temperature being subjected to the particular boundary or boundaries selected. It is prescribed in the SI unit (K) and the default is given as 293.15 K.

#### **5.3.5.6 Outflow**

This node provides an appropriate boundary condition where convection-dominated heat transfer exists at the outlet boundaries. In models with convective heat transfer, the conditions relating to the heat transfer states that convection is the only heat transfer that exists at the boundaries and as a result the temperature gradient in the normal direction equals zero with no existence of radiation.

There are usually no user inputs for these nodes, but if it becomes necessary the boundaries that are convection-dominated boundaries are selected as the outflow.

### 5.3.5.7 Symmetry

The symmetry node is similar to the insulation condition in that there is no heat flux across the boundary. This boundary condition usually does not require any user input, however the symmetry boundaries need to be defined or selected.

### 5.3.5.8 Heat Flux

The heat flux node is used to add heat flux across boundaries. The boundaries for heat flux addition are selected and the heat flux magnitudes are entered. In this work since we want to ensure there is no heat flux across certain boundaries we select and use the default value of heat flux which is zero (in other words there is no heat flux across the boundaries selected).

## 5.3.6 *Meshes*

The discretization of the geometry model into smaller units of simple shapes is referred to as mesh elements. The mesh generator in COMSOL Multiphysics discretizes the domains of the geometry into tetrahedral, hexahedral, prism or pyramid meshes.

The boundaries in the geometry are on the other hand discretized into either triangular or quadrilateral boundary elements.

Meshes and sizes for boundaries geometries can be defined by the user or chosen from ones already defined. Figure 5.10 shows a window displaying selected meshes in COMSOL Multiphysics®.

## 5.3.7 *Study*

After building the model, the model can be simulated by right clicking on study and clicking on compute. Modeling can sometimes take longer since simulation time depends on the many factors considered when building the model. Examples of factors that can affect simulation time include boundary conditions employed and the type of mesh and size used among others. After ensuring that the necessary boundary conditions are entered, including selecting appropriate meshes and sizes, the model is then run. The model can be visualized after simulation and the results obtained analyzed after which the necessary deductions are made.

In cases where only a part of the component is modeled, the results on the part obtained can be extrapolated to obtain results for the whole component. Figure 5.11

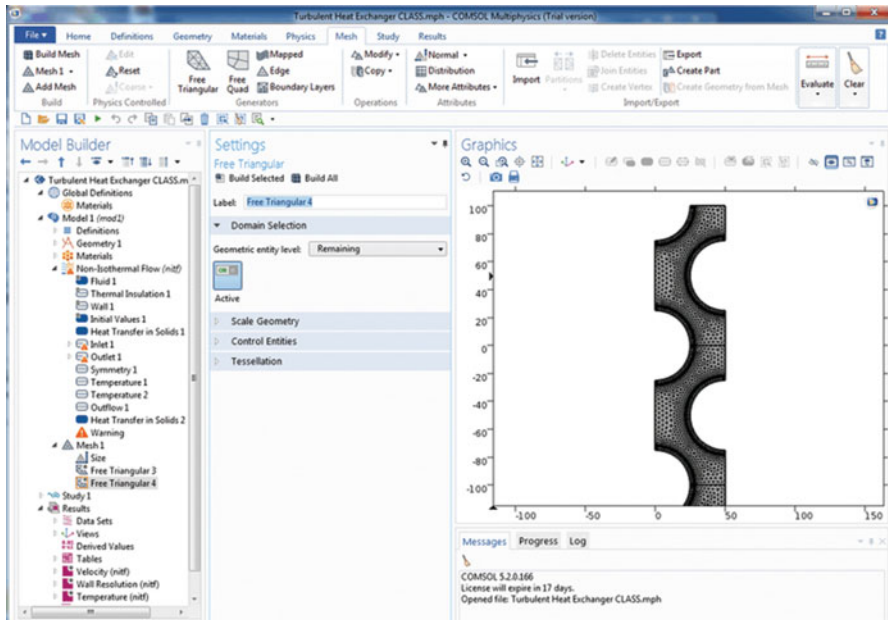


**Fig. 5.10** A section of how meshes are displayed in the Model Builder in COMSOL Multiphysics®

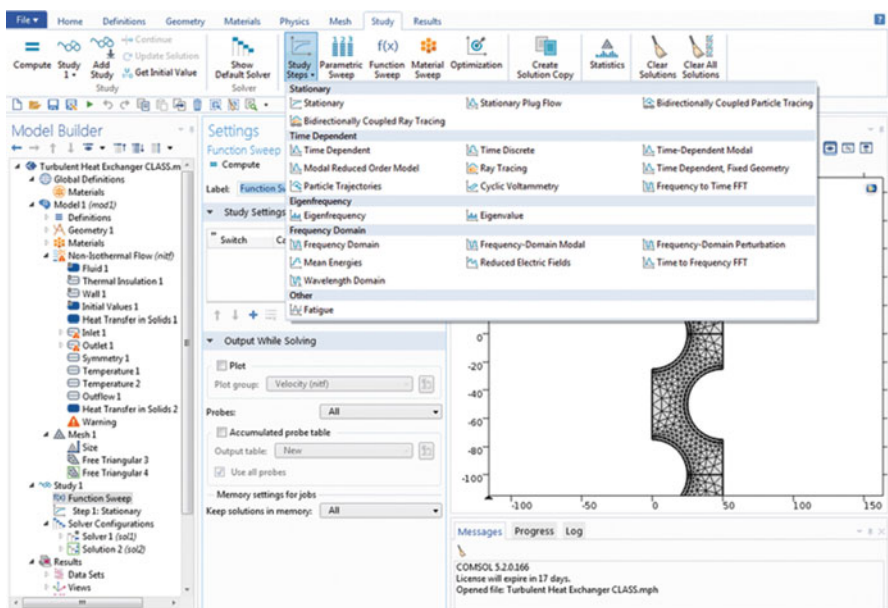


**Fig. 5.11** A window of a tree showing arrangement of nodes in COMSOL Multiphysics®

shows an example of a window showing a tree arrangement of nodes in a model wizard in COMSOL Multiphysics.

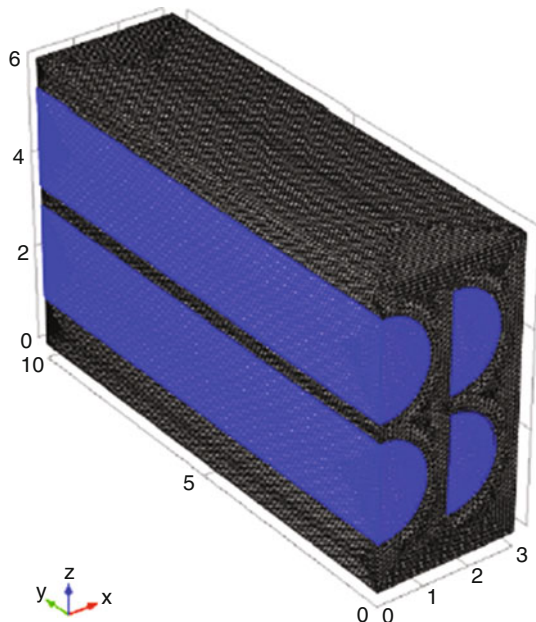
## 5.4 Simulation of the 3-D Model

The 3D model simulated consists of a cube of metal which has four semi-circular (two for the cold fluid and two for the hot fluid) channels running through the length of the block, Fig. 5.12 shows a diagram of the 3-D model with the semi-circular channels. The model consists of three materials—material for the heat exchanger matrix and the two different fluids flowing on both sides (hot and cold) of the exchanger.

The material for heat exchanger matrix (Inconel 617) and air used as fluid for the cold side of the exchanger were selected and added from the built in library materials. The third material (flue gases) was added by entering the necessary properties that would be needed in the simulations since it was not found in the built in materials or material library.

Selection of meshes and specifying the sizes is the final step before a model is simulated in COMSOL Multiphysics. It is worth noting that the choice of meshes for a model has great influence on the accuracy of results to be obtained from the simulation process. In this regard various meshes were tried for the simulation of the model. Some of these meshes employed resulted in the simulations running for hours without converging to find a solution. The combination of meshes that return

**Fig. 5.12** A diagram of the 3-D model simulated



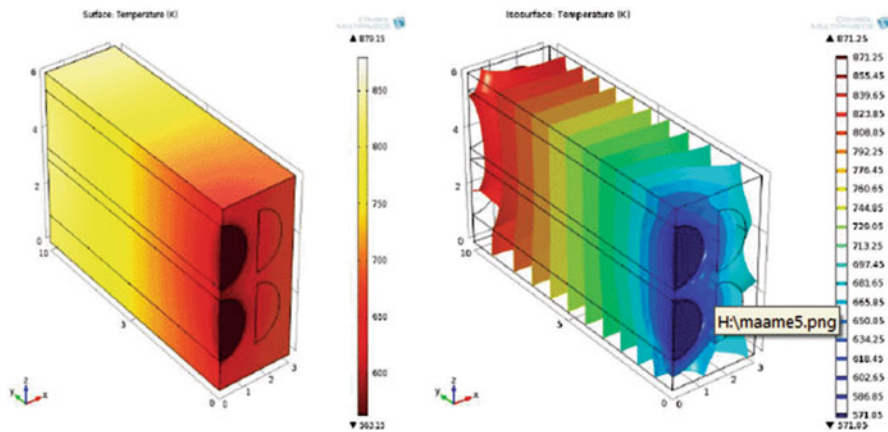


**Fig. 5.13** Diagrams of the model showing the temperature variations after simulations

some good results after simulation is the case of combining quadrilateral for domains of the geometry and using triangular for the boundaries.

After simulations, the model was visualized after which important output parameters were calculated. Figure 5.13 shows the variations of temperature along the length of the model.

## 5.5 Mathematical Theory for Conjugate Heat Transfer Interface

The mathematical formulation used and solved for in COMSOL Multiphysics for **Conjugate Heat Transfer** (also used for almost all simulations in the heat transfer interface) for steady-state, laminar flow interface is the incompressible (is also applicable to compressible flows) Navier-Stokes equation and an energy conservation equation. The Navier-Stokes formulation basically consists of a momentum and continuity equation. The Navier-Stokes equations and the energy conservation equation are derived from the principle of conservation of mass, momentum, and energy [1].

### 5.5.1 The Momentum Equation

It can be shown by resolution of forces acting on a particle of a cube of fluid that;

$$\rho \frac{D\vec{V}}{Dt} = \Delta \cdot \sigma + F \quad (\text{Eq. 5.3})$$

Here  $\sigma$  is the stress tensor and  $F$  represents the sum of the various gravitational forces acting on the cube and  $\vec{V} = u\hat{i} + v\hat{j} + w\hat{k}$  fluid vector velocity. The stress tensor  $\sigma$  is however a rank two symmetric tensor which is expressed mathematically by its covariant components consisting of normal stresses,  $\sigma$  and shear stresses,  $\tau$  as;

$$\sigma_{ij} = \begin{pmatrix} \sigma_{xx} & \tau_{xy} & \tau_{xz} \\ \tau_{yx} & \sigma_{yy} & \tau_{yz} \\ \tau_{zx} & \tau_{zy} & \sigma_{zz} \end{pmatrix} \quad (\text{Eq. 5.4})$$

The stress tensor above can further be divided into two distinct terms as;

$$\begin{aligned} \sigma_{ij} &= \begin{pmatrix} \sigma_{xx} & \tau_{xy} & \tau_{xz} \\ \tau_{yx} & \sigma_{yy} & \tau_{yz} \\ \tau_{zx} & \tau_{zy} & \sigma_{zz} \end{pmatrix} \\ &= - \begin{pmatrix} p & 0 & 0 \\ 0 & p & 0 \\ 0 & 0 & p \end{pmatrix} + \begin{pmatrix} \sigma_{xx} + p & \tau_{xy} & \tau_{xz} \\ \tau_{yx} & \sigma_{yy} + p & \tau_{yz} \\ \tau_{zx} & \tau_{zy} & \sigma_{zz} + p \end{pmatrix} \end{aligned} \quad (\text{Eq. 5.5})$$

And it can be expressed as:

$$- \begin{pmatrix} p & 0 & 0 \\ 0 & p & 0 \\ 0 & 0 & p \end{pmatrix} + \begin{pmatrix} \sigma_{xx} + p & \tau_{xy} & \tau_{xz} \\ \tau_{yx} & \sigma_{yy} + p & \tau_{yz} \\ \tau_{zx} & \tau_{zy} & \sigma_{zz} + p \end{pmatrix} = -pI + \mathbb{T} \quad (\text{Eq. 5.6})$$

In Eqs. (5.5) and (5.6)  $p$  is the pressure and is given by negative of the mean of the normal stresses presented by;

$$p = -\frac{1}{2}(\sigma_{xx} + \sigma_{yy} + \sigma_{zz}) \quad (\text{Eq. 5.7a})$$

and  $I$  is the  $3 \times 3$  identity matrix, presented as:

$$I = \begin{pmatrix} 1 & 0 & 0 \\ 0 & 1 & 0 \\ 0 & 0 & 1 \end{pmatrix} \quad (\text{Eq. 5.7b})$$

Finally  $\mathbb{T}$  is the deviatoric stress tensor, presented as:

$$\mathbb{T} = \begin{pmatrix} \sigma_{xx} + p & \tau_{xy} & \tau_{xz} \\ \tau_{yx} & \sigma_{yy} + p & \tau_{yz} \\ \tau_{zx} & \tau_{zy} & \sigma_{zz} + p \end{pmatrix} \quad (\text{Eq. 5.7c})$$

The Navier-Stokes equation can at this point be expressed in its general form as;

$$\rho \frac{D\vec{V}}{Dt} = -\nabla p + \vec{\nabla} \cdot \mathbb{T} + F \quad (\text{Eq. 5.8})$$

Manipulation of Eq. (5.8), shows that the deviatoric stress tensor  $\mathbf{T}$  can be expressed as;

$$\mathbf{T} = \mu \left[ \nabla \vec{V} + (\nabla \vec{V})^T \right] - \frac{2}{3} \mu (\vec{\nabla} \cdot \vec{v}) I \quad (\text{Eq. 5.9})$$

Note that Del Operator is  $\vec{\nabla} = \frac{\partial}{\partial x} \hat{i} + \frac{\partial}{\partial y} \hat{j} + \frac{\partial}{\partial z} \hat{k}$ .

The Momentum equation for the fluid flow can therefore be simplified for steady state analysis as;

$$\rho (\vec{V} \cdot \vec{\nabla}) \vec{V} = \nabla \cdot \left\{ -pI + \mu \left[ \nabla \vec{V} + (\nabla \vec{V})^T \right] - \frac{2}{3} \mu (\nabla \cdot \vec{V}) I \right\} F \quad (\text{Eq. 5.10})$$

In Eq. (5.9) symbol  $\mu$  is fluid dynamic viscosity.

### 5.5.2 The Continuity Equation

In order to be able to derive the equation, a differential control volume of sizes  $dx$ ,  $dy$ , and  $dz$  is considered. The flux of mass per second for all three directions, assuming that the density and velocity are functions of space and time, is expressed as;

$$-\frac{\partial}{\partial x}(\rho u) dy dz \quad -\frac{\partial}{\partial y}(\rho v) dx dz \quad -\frac{\partial}{\partial z}(\rho w) dy dz \quad (\text{Eq. 5.11})$$

For the  $x$ ,  $y$  and  $z$  direction respectively.

From the principle of conservation of matter, the summation of all three must be equal to the time rate of change of mass,  $\frac{\partial}{\partial t}(\rho dx dy dz)$ .

Considering that a control volume is independent of time, the  $dx dy dz$  terms can be neglected or cancelled from the various terms and as such the resulting equation simplified as;

$$\frac{\partial \rho}{\partial t} + \frac{\partial}{\partial x}(\rho u) + \frac{\partial}{\partial y}(\rho v) + \frac{\partial}{\partial z}(\rho w) = 0 \quad (\text{Eq. 5.12})$$

The above equation can further be simplified by introducing the gradient vector notation and the equation further simplified as;

$$\frac{\partial \rho}{\partial t} + \vec{\nabla} \cdot \rho \vec{V} = 0 \quad (\text{Eq. 5.13})$$

For steady state analysis case, we have;

$$\frac{\partial \rho}{\partial t} = 0 \quad (\text{Eq. 5.14})$$

Therefore, the continuity equation is simplified to the following form as;

$$\vec{\nabla} \cdot \rho \vec{V} = 0 \quad (\text{Eq. 5.15})$$

Where  $\vec{V} = u\hat{i} + v\hat{j} + w\hat{k}$  refers to velocity field (m/s),  $p$  the pressure acting on the surfaces (Pa),  $F$  the summation of forces again acting on the volume (N/m),  $\rho$  the fluid density,  $\mu$  dynamic viscosity (Pa S), and  $\vec{\nabla}$  (Del) the vector differential operator, and as we said before  $I$  is a  $3 \times 3$  identity matrix defined by Eq. (5.7b).

### 5.5.3 The Energy Equation

For non-isothermal fluid flow, the fluid temperature is considered to be a function of the directions (thus  $x$ ,  $y$ , and  $z$ ) and time ( $t$ ). The energy equation is the law of conservation of energy which basically gives the distribution of temperature in space. Just as was the case in the derivation of the continuity equation, we consider a similar differential control volume of the same size. After which an energy balance equation is written as;

**Energy input = energy output + energy accumulation**

The energy input is the summation of internal energy, kinetic energy, pressure-work volume, heat conduction, and heat generated,  $Q$  in the volume of the fluid. The energy output is almost the same as that for the energy input except the heat generated is zero in this case. The accumulated energy however is only the summation of internal and kinetic energy.

The energy equation can be expressed explicitly after some manipulations (Rao) [2] as;

$$\rho c_p u \nabla T = \vec{\nabla} \cdot (k \vec{\nabla} T) + Q \quad (\text{Eq. 5.16})$$

Here  $T$  denotes temperature (K),  $k$  is the fluid thermal conductivity ( $\text{W}/\text{m}^2$ ),  $Q$  is the heat source or sink, and  $c_p$  is the specific heat capacity at constant pressure. In the energy equation the temperature gradient,  $\nabla T$  is what is responsible for heat conduction (invokes heat flow).

## 5.6 Results, Discussions, and Conclusion

This section presents results for the MATLAB models for both the PCHE and PFHE. Computed results obtained from the 3D simulations using the COMSOL Multiphysics software including discussions made on the presented results as well as conclusions drawn are also included in this chapter. The conclusion in this chapter ends with two recommendations for future work and consideration.

### 5.6.1 Results

The results obtained from the MATLAB model for the PCHE are presented in Table 5.1, while those for the PFHE are presented in Table 5.2. A comparison of some results obtained from the PCHE MATLAB model to that of its 3D model simulated using the COMSOL Multiphysics software is also tabulated in Table 5.3.

The parameters and some results obtained from the design of the PCHE using MATLAB are tabulated in Table 5.1. The pressure drops across sides 1 and 2 were determined to be 1.17 % and 3.29 % respectively, heat transfer coefficients for sides 1 and 2 were determined to be  $174 \text{ W/m}^2 \text{ K}$  and  $201 \text{ W/m}^2 \text{ K}$  respectively, with an overall heat transfer coefficient of  $92 \text{ W/m}^2 \text{ K}$ . The thermal power output is as expected across the exchanger, a value which was determined earlier in the proposed power plant.

Parameters used for the design of the PFHE and some results recorded for the MATLAB model of the PFHE are tabulated in Table 5.2. The inlet and outlet temperatures, the thermal output required of the PFHE, are the same as those determined in the design of the PCHE. Heat transfer coefficients of 163.90 and  $378.48 \text{ W/m}^2 \text{ K}$  were obtained for sides 1 and 2 of the PFHE respectively, with an overall heat transfer coefficient of  $104.91 \text{ W/m}^2 \text{ K}$ . Pressure drops across sides 1 and 2 of the PFHE were determined to be 4.59 % and 4.84 % respectively.

**Table 5.1** PCHE design parameters and results

Parameter	Value
Length of exchanger, $L$ (m)	1.1
Diameter of channels, $D$ (mm)	2.0
Plate thickness, $th$ (mm)	1.5
Total number of plates, $N-tCH$	1,373,760
Pressure drop-side 1 (%)	1.17
Pressure drop-side 2 (%)	3.29
Total heat transfer area, $A_{tot}$ ( $\text{m}^2$ )	5095
Heat transfer coefficient-side 1 ( $\text{W/m}^2 \text{ K}$ )	174
Heat transfer coefficient-side 2 ( $\text{W/m}^2 \text{ K}$ )	201
Overall heat transfer coefficient, $U$ ( $\text{W/m}^2 \text{ K}$ )	92
Thermal Power, $Q$ (MW)	12.15

**Table 5.2** PFHE design parameters and results

Parameter	Dimension
Plate thickness, $\delta_w$ (mm)	1.5
Fin thickness, $\delta$ (mm)	0.15
Spacing between surfaces of a fin, $s$ (mm)	0.0015
Fin offset length, $\ell_s$ (mm)	6
Length of a plate, $L_1$ (m)	2.0
Length of a plate, $L_2$ (m)	1.6
Flow length in the $L_1$ direction, $L$ (m)	$L_1 \cdot 0.025$
Plate spacing for fluid side 1, $b_1$ (mm)	5.545
Plate spacing for fluid side 2, $b_2$ (mm)	5.545
Hydraulic diameter, $D_h$ (mm)	3.8
Total number of fins $n_t$	81,000
Number of passage, $N_p$	13.3
Total surface area, $A$ ( $m^2$ )	4554
Pressure drop on the primary side, $\Delta p$ (%)	4.59
Pressure drop on the secondary side, $\Delta p$ (%)	4.84
Heat transfer coefficient-Primary side, $h_c$ ( $W/m^2 K$ )	163.90
Heat transfer coefficient-Primary side, $h_h$ ( $W/m^2 K$ )	378.48
Overall heat transfer coefficient, $U$ ( $W/m^2 K$ )	104.91

**Table 5.3** A comparison of results for the PCHE MATLAB® model and 3-D COMSOL®

Parameter	MATLAB	3-D Model COMSOL
Length of exchanger, $L$ (m)	1.1	563.2
Diameter of channels, $D$ (mm)	2.0	858.75
Plate thickness, $th$ (mm)	1.5	879.2
Total number of plates, $N_{tCH}$	1,373,760	591.37
Pressure drop-side 1 (%)	1.17	205.19
Pressure drop-side 2 (%)	3.29	220.93
Total heat transfer area, $A_{tot}$ ( $m^2$ )	5095	106
Heat transfer coefficient-side 1 ( $W/m^2 K$ )	174	1.06
Heat transfer coefficient-side 2 ( $W/m^2 K$ )	201	2.47
Overall heat transfer coefficient, $U$ ( $W/m^2 K$ )	92	93.59
Thermal Power, $Q$ (MW)	12.15	12.23

A comparison of results obtained from the designed PCHE using MATLAB and that of the 3-D model simulated are tabulated in Table 5.3. The inlet temperatures of both sides of the exchanger are the same for both the MATLAB and 3-D models since they are initial conditions imposed, but the outlet temperatures for the 3D model recorded are slightly lower than those of the MATLAB model. However, there is an improvement in the heat transfer coefficients obtained in the 3-D model with values of 205.19 and 220.93  $W/m^2 K$  against 174  $W/m^2 K$  and 201  $W/m^2 K$  for the MATLAB model for sides 1 and 2 respectively, with an overall heat transfer

coefficients of  $92 \text{ W/m}^2 \text{ K}$  for the MATLAB against  $106 \text{ W/m}^2 \text{ K}$  for the 3D model. Pressure drops recorded for the 3D model also showed a slight decrease for side 1 and a significant decrease for side 2 of the exchanger.

### 5.6.2 Discussions

The result obtained from the PCHE MATLAB model compared to that obtained from the 3-D model simulation looks quite good although there are some small variations. The variations in values obtained for the design process compared to that of the simulation of the 3-D model can be attributed to the various assumptions made in the design process. In the calculation of the heat transfer coefficient in the design process the Nusselt number was assumed to be a constant, this accounted for the difference in the values obtained. From Eq. (4.151) it can be deduced that the heat transfer coefficient varies directly as the Nusselt number and as such its value has great influence on the maximum value of the heat transfer coefficient that can be attained. Nonetheless in this situation (in laminar flows, i.e., flows with  $\text{Re} < 2000$ ) we can only use this assumed constant value.

Another important parameter that was assumed and has great influence on the temperature and pressure obtained is the specific heat capacities of the fluids employed in the heat exchanger. It was assumed that the specific heat capacities for both fluids are to be constant across the cross section of the channels, an assumption which does not hold entirely for conditions where the fluid's temperature and pressure are changing. This is because, in actuality, the specific heat capacities of the fluids flowing changes with changes in temperature and pressure. Therefore enforcing this assumption would have an effect on outlet temperature and pressure as well as the heat transfer coefficient, it is what accounted for the change in outlet temperatures for both models.

From Eq. (4.152) it can be seen that the pressure drop across the PCHE varies directly as the product of the fanning friction factor, the density of the fluid, the square of the flow velocity, and the length of the heat exchanger (inversely as the hydraulic diameter). Therefore the pressure drop across the heat exchanger increases with increasing length, flow velocity, and density of the fluid being employed. One advantage of using the PCHE is that the heat transfer area can be increased by reducing the diameter thereby employing a lot of channels on each plate: however, decreasing the diameter of the channels in the exchanger is limited by the pressure drop. Since the pressure drop across the exchanger varies inversely as the hydraulic diameter, decreasing the diameter of channels will decrease the hydraulic diameter which increases the pressure drop across the exchanger.

All other results obtained from the MATLAB model compared to the 3-D model simulation exhibit quite a small margin of difference which looks good considering the various assumptions made in the design process (this is because some of these assumptions may not necessarily be entirely true when the heat exchanger is working in its real environment).

The calculated value of effectiveness expected of the designed heat exchanger was 0.90, but results obtained from the 3-D model simulations using the NTU effectiveness method gave an impressive effectiveness of 0.94.

Pressure drop performance was also impressive for the cold as well as the hot side of the heat exchanger, although the cold side of the exchanger is the most critical point since that side of the heat exchanger is in the loop for the bottom cycle of the power plant compared to the hot side which exits to the atmosphere. The surface area density of the PCHE with a compactness value of almost  $1300 \text{ m}^2/\text{m}^3$  is better than that of the PFHE with a surface area density or compactness value of  $855 \text{ m}^2/\text{m}^3$ . It should however be noted that the volume calculated and used in this report might be less compared to the actual heat exchanger size, but at least this gives a fair idea of heat exchanger size to be employed since in the design process only the core of the exchanger is considered and this excludes the piping and housing for the exchanger.

The conditions imposed for the design of the PFHE is the same as that of the PCHE, but the calculation of certain parameters such as the heat transfer coefficients, hydraulic diameter, and pressure drops across the exchanger was obtained using relations different from that which were used for the calculation of the same parameters for the design of the PCHE. The results from the PFHE model also look quite impressive in the sense that the heat transfer coefficients obtained are good compared to that of the PCHE model. The pressure drops although are quite a bit higher compared to that of the PCHE, but as stated in the last paragraph the layout of the proposed power plant shows that the pressure drop across the heat exchanger in the bottoming cycle side of the proposed power plant is the side which is more critical and the PFHE did not perform bad in that regard since the model can be optimized to reduce the pressure drop across it (with a pressure drop of less than 5 % not far from the desired required pressure drop of less than 3 %).

### 5.6.3 Conclusion

The results obtained from the simulations of the 3-D model compared to the MATLAB model of the PCHE gave a clear indication that it is a good heat exchanger that can be used to meet the desired requirements of a heat exchanger to be employed in the proposed power plant. The performance of the PCHE I would say looks more promising compared to the PFHE; this can be seen from the results obtained from both the MATLAB and 3-D model of the PCHE. The PFHE however, did not perform badly with some good values recorded for the heat transfer coefficients and subsequently a higher overall heat transfer coefficient.

The heat exchanger to be employed in the proposed power plant is to be of high effectiveness, have a lower pressure drop across, and also be as compact as possible so as to obtain benefits that are associated with the use of compact heat exchangers. The performance of the PCHE models with respect to the desired characteristics of the expected heat exchanger was good.

The choice of using the PCHE as the exchanger for the proposed power plant is therefore a wise one, and this has been affirmed by the results obtained from both the MATLAB model and 3D models. However, I would like to add that considering the results of the PFHE, it can be taken as an alternative heat exchanger to the PCHE.

The PCHE can therefore be used as a heat exchanger for heat recovery and as a recuperator. As stated earlier, a heat exchanger is recommended for use as an intercooler based on experience from the design of a heat exchanger for waste heat recovery and recuperation. In considering the intercooler, which would operate under mild conditions with respect to temperatures and pressures (much lower values compared to that of the waste heat recovery and recuperation), a much simpler heat exchanger can be employed for this purpose, and Noah Yakah [1] in this regard recommends the use of the Plate Heat Exchanger.

He also suggests the two following recommendations for further work in future or any related considerations.

1. The pressures of operations for the proposed power plant are very low and that has great effect on the performance of the entire power plant most especially that of the heat exchanger. His first suggestion or recommendation is therefore that the working pressures of the proposed power plant be increased not forgetting that increasing the working operation pressures should be guided by the type of materials that are being employed. Increasing the working pressures of operations of the power plant has many benefits notwithstanding also the fact that there may be some associated drawbacks. An increase in working pressures of operations in the power plant means an increase in pressures of operations in the heat exchanger, and increasing pressures in the heat exchanger (keeping all other parameters constant) would mean an increase in the density of fluids employed in the exchanger and subsequently a decrease in fluid flow velocity. This would mean an increase in Reynolds number and subsequently heat transfer coefficients while keeping the pressure drop at the minimum, since the heat transfer coefficient varies directly as the Reynolds number and the pressure drop varies directly as the square of the flow velocity.
2. Second, he recommends that a different fluid should be tried and tested for use in the proposed power plant most especially in the bottoming cycle (where there is no combustion taking place), since its operations depend heavily on the quantum of waste heat recovered from the topping cycle. The fluid to be used should be one of higher density so that the Reynolds number of the fluid flow can be increased (for the heat exchangers to operate in turbulent flows mode) so as to increase the heat transfer coefficients, the power output of the power plant, and thermal power output of the heat exchanger while not necessarily increasing the pressure drop across it.

## References

1. Yakah, Noah. Heat exchanger design for a solar gas-turbine power plant. Master of Science Thesis, KTH School of Industrial Engineering and Management, Energy Technology EGI-2012-110MSG EKV925, Division of Heat and Power, SE-100 44 Stockholm.
2. Rao, S.S. 1988. *The finite element method in engineering*. Oxford: Pergamon Press.

# **Chapter 6**

## **Thermodynamics of Cycles**

An important application of thermodynamics is the analysis of power cycles through which the energy absorbed as heat can be continuously converted into mechanical work. A thermodynamic analysis of the heat engine cycles provides valuable information regarding the design of new cycles or a combined cycle for improving the existing cycles, or pushing efficiency gas turbine output with Brayton or combined with topping or bottoming Rankine cycle via heat exchangers/recuperators respectively. Application of combined cycle driven power plants, either steam or nuclear, plays a very important role in industry these days in order to make existence of these power plants more cost effective. In this chapter we briefly touch upon thermodynamic cycles so readers can have a general idea both on gas power cycles and vapor power cycles and how heat exchangers are important components to be considered when these cycles are combined.

### **6.1 Introduction**

A thermodynamic cycle is a series of processes where the properties of the system are the same after the cycle as they were prior. Three main properties are tracked when a system undergoes a set of processes and they are:

- Temperature,
- Pressure, and
- Specific volume

To be considered a cycle, all three properties need to be the same at their initial state and at the end. One property could remain the same throughout any of the processes; the cycle is considered isothermal if temperature is constant, isobaric if pressure is constant, and isochoric or isometric if specific volume is constant. The

most efficient type of cycle is one that has only reversible processes, such as the Carnot cycle, which is made up of four reversible processes.

As far as the thermodynamic cycle definition in general is concerned, there are two classes of cycles and they are:

1. Power Cycles and
2. Heat Pump Cycles.

Each of these cycles is defined based on the thermodynamic tasks assigned to them and briefly can be described as follows:

Power cycles are used when there exists some way of converging some heat energy input into mechanical work output, while heat pump cycles transfer heat from low to high temperature stages by using mechanical work as the input source respectively. Cycles are composed of the quasi-static processes going through the entire cycle and can operate as power or heat pump cycles by controlling them in the direction of the cycle process. This direction can be defined as either clockwise or counter-clockwise which can be indicated using the Pressure-volume (*P-V*) diagram or Temperature-entropy (*T-s*) diagram respectively.

A thermodynamic cycle in respect to net mechanical work by input from heat energy in a closed loop on the *P-V* diagram mathematically can be presented as:

$$W = \oint P dV \quad (\text{Eq. 6.1})$$

Equation (6.1) is the indication of net work that is equal to the area inside the closed loop of the *P-V* diagram as depicted in Fig. 6.1, and this is because of the following argument:

- (a) The Riemann sum of work done on the substance due to expansion, minus
- (b) The work done to re-compress.

The net work presented by Eq. (6.1) is equal to the balance of heat *Q* transferred into the system and mathematically is presented by Eq. (6.2) in the following form:

$$W = Q = Q_{\text{in}} - Q_{\text{out}} \quad (\text{Eq. 6.2})$$

Equation (6.2) makes a cyclic process into an isothermal process, even though the internal energy changes during the course of the cyclic process, and this means the

**Fig. 6.1** Depiction of net work in closed loop of *P-V* diagram

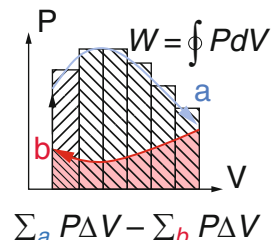
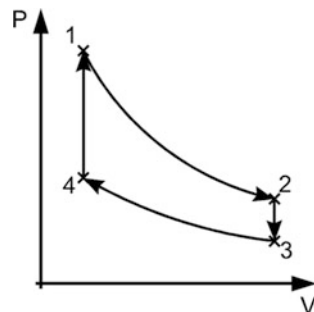


**Fig. 6.2** Illustration of Otto cycle in  $P$ - $V$  diagram



cyclic process finishes with the system's energy in a closed loop on the  $P$ - $V$  diagram with the same amount of energy as when the process began. If the cyclic process moves clockwise around the loop, then the net work  $W$  will be positive, and it represents a heat engine. If it moves counterclockwise, then the net work  $W$  will be negative, and it represents a heat pump.

In the  $P$ - $V$  diagram each point of the cycle process can be presented as shown in Fig. 6.2 of an Otto Cycle, and the definitions of each process for this cycle are written as follows:

#### Otto Cycle Loop and description of each point in the thermodynamic cycles

- 1 → 2: Isentropic Expansion: Constant Entropy ( $s$ ), Decrease in Pressure ( $P$ ), Increase in Volume ( $V$ ), Decrease in Temperature ( $T$ ).
- 2 → 3: Isochoric Cooling: Constant Volume ( $V$ ), Decrease in Pressure ( $P$ ), Decrease in Entropy ( $s$ ), Decrease in Temperature ( $T$ ).
- 3 → 4: Isentropic Compression: Constant entropy ( $s$ ), Increase in pressure ( $P$ ), Decrease in volume ( $V$ ), Increase in temperature ( $T$ )
- 4 → 1: Isochoric Heating: Constant volume ( $V$ ), Increase in pressure ( $P$ ), Increase in entropy ( $s$ ), Increase in temperature ( $T$ ).

Some of the most important thermodynamics processes that we need to know in order to deal with any thermodynamic cycle are as follows:

- **Adiabatic:** No energy transfer as heat ( $Q$ ) during that part of the cycle would amount to  $dQ = 0$ . This does not exclude energy transfer as work.
- **Isothermal:** The process is at a constant temperature during that part of the cycle ( $T = \text{constant}$ ,  $dT = 0$ ). This does not exclude energy transfer as heat or work.
- **Isobaric:** Pressure in that part of the cycle will remain constant. ( $P = \text{constant}$ ,  $dP = 0$ ). This does not exclude energy transfer as heat or work.
- **Isochoric:** The process is at constant volume ( $V = \text{constant}$ ,  $dV = 0$ ). This does not exclude energy transfer as heat or work.
- **Isentropic:** The process is one of constant entropy ( $s = \text{constant}$ ,  $ds = 0$ ). This excludes the transfer of heat but not work.

Making certain sequences of assumption as part of modeling a real system using thermodynamic cycles, which is often necessary to reduce the number of degrees of

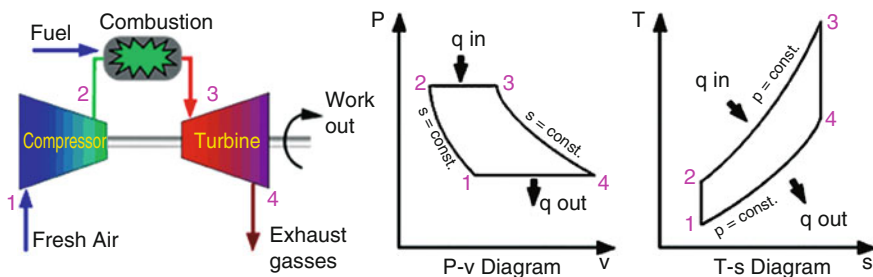


**Fig. 6.3** Presentation an idealized process in  $P$ - $V$  and  $T$ - $s$  diagrams of a Brayton cycle mapped to actual processes of a gas turbine engine

freedom associated to the problems at hand, will reduce the problem to a very manageable form. Such simplified modeling is depicted in Fig. 6.3, which is a presentation of a real system modeled by an idealized process in  $P$ - $V$  and  $T$ - $s$  diagrams of a Brayton cycle mapped to actual processes of a gas turbine engine.

The actual device can be made up of a series of stages, each of which is itself modeled as an idealized thermodynamic process. Although each stage which acts on the working fluid is a complex real device, they may be modeled as idealized processes which approximate their real behavior. If energy is added by means other than combustion, then a further assumption is that the exhaust gases would be passed from the exhaust to a heat exchanger that would sink the waste heat to the environment and the working gas would be reused at the inlet stage.

In summary, an important application of thermodynamics is the analysis of power cycles through which the energy absorbed as heat can be continuously converted into mechanical work. A thermodynamic analysis of the heat engine cycles provides valuable information regarding the design of new cycles or for improving the existing cycles. In this chapter, various gas power cycles are analyzed under some simplifying assumptions.

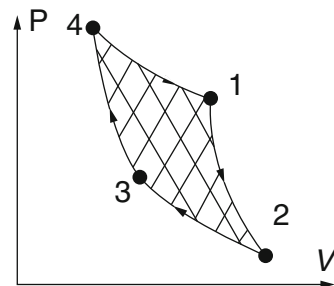
Two of the most important areas of application of thermodynamics are power generation and refrigeration, and they both are usually accomplished by a system that operates on a thermodynamic cycle.

Thermodynamically, the word “cycle” is used in a procedure or arrangement in which some material goes through a cyclic process and one form of energy, such as heat at an elevated temperature from combustion of a fuel, is in part converted to another form, such as mechanical energy of a shaft, the remainder being rejected to a lower temperature sink that is also known as a heat cycle.

A thermodynamic cycle is defined as a process in which a working fluid undergoes a series of state changes and finally returns to its initial state. A cycle plotted on any diagram of properties forms a closed curve (see Fig. 6.4).

Note that a reversible cycle consists only of reversible processes. The area enclosed by the curve plotted for a reversible cycle on a  $P$ - $V$  diagram represents the net work of the cycle as we explained in the preceding chapters:

**Fig. 6.4** Schematic of a closed cycle



- The work is done on the system, if the state changes happen in an anticlockwise manner.
- The work is done by the system, if the state changes happen in a clockwise manner.

The purpose of a thermodynamic cycle is either to produce power, or to produce refrigeration/pumping of heat. Therefore, the cycles are broadly classified as follows:

- (a) Heat engine or power cycles.
- (b) Refrigeration/heat pump cycles.

A thermodynamic cycle requires, in addition to the supply of incoming energy:

1. A working substance, usually a gas or vapor;
2. A mechanism in which the processes or phases can be carried through sequentially; and
3. A thermodynamic sink to which the *residual heat* can be rejected.

The cycle itself is a repetitive series of operations.

Any thermodynamic cycle is essentially a *closed cycle* in which the working substance undergoes a series of processes and is always brought back to the initial state.

However, some of the power cycles operate on an *open cycle*. This means that the working substance is taken into the unit from the atmosphere at one end and is discharged into the atmosphere after undergoing a series of processes at the other end. The following are illustrations of heat engines operating on an open cycle:

- Petrol and diesel engines in which the air and fuel are taken into the engine from a fuel tank and products of combustion are exhausted into the atmosphere.
- Steam locomotives in which the water is taken in the boiler from a tank and steam is exhausted into the atmosphere.

The basic processes of the cycle, either in open or closed, are heat addition, heat rejection, expansion, and compression. These processes are always present in a cycle even though there may be differences in working substance, the individual processes, pressure ranges, temperature ranges, mechanisms, and heat transfer arrangements.

Many cyclic arrangements, using various combinations of phases but all seeking to convert heat into work, were proposed by many investigators whose names are attached to their proposals; for example, the *Diesel*, *Otto*, *Rankine*, *Brayton*, *Stirling*, *Ericsson*, and *Atkinson* cycles. Not all proposals are equally efficient in the conversion of heat into work. However, they may offer other advantages, which have led to their practical development for various applications. See also *Brayton cycle*; *Carnot cycle*; *Diesel cycle*; *Otto cycle*; *Stirling engine*; *Thermodynamic processes*.

Essentially, such devices do not form a cycle. However, they can be analyzed by adding imaginary processes to bring about the state of the working substance, thus completing a cycle. Note that the terms *closed* and *open* cycles that are used here do not mean closed system cycle and open system cycle. In fact, the processes both in closed and open cycles could either be closed or open system processes.

There is a basic pattern of processes common to power-producing cycles. There is a compression process wherein the working substance undergoes an increase in pressure and therefore density. There is an addition of thermal energy from a source such as a *fossil fuel*, a *fissile fuel* (a fissile material is one that is capable of sustaining a *chain reaction* of nuclear fission), or solar radiation. Work is done by the system on the surroundings during an expansion process. There is a rejection process where thermal energy is transferred to the surroundings. The algebraic sum of the energy additions and abstractions is such that some of the thermal energy is converted into mechanical work.

Different types of working fluids are employed in power plants. The nature of the working fluids can be classified into two groups:

- (a) Vapors.
- (b) Gases.

The power cycles are accordingly classified into two groups:

1. Vapor power cycles in which the working fluid undergoes a phase change during the cyclic process.
2. Gas power cycles in which the working fluid does not undergo any phase change.

In the thermodynamic analysis of power cycles, our main interest lies in estimating the energy conversion efficiency or the thermal efficiency. The thermal efficiency of a heat engine is defined as the ratio of the network output  $W$  delivered to the energy absorbed as heat  $Q$  and mathematically is presented by symbol  $\eta$  and can be written as:

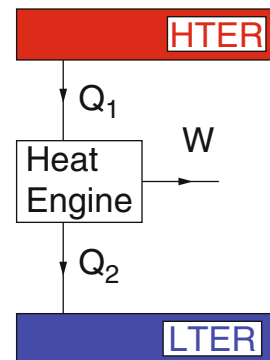
$$\eta = \frac{W}{Q} \quad (\text{Eq. 6.3})$$

and it can be illustrated as Fig. 6.5 below;

In this depiction, we identify the following:

**LTER** = Low Temperature Energy Reservoir

**Fig. 6.5** Graphic illustration of thermal efficiency



**HTER** = High Temperature Energy Reservoir

Using these definitions and referring to Fig. 6.4, Eq. (6.5) can be written more precisely as follows;

$$\eta = \frac{W}{Q_1} \quad (\text{Eq. 6.4})$$

where  $Q_1$  is the heat supplied at high temperature.

There is a procedure or arrangement in which one form of energy, such as heat at an elevated temperature from combustion of a fuel, is in part converted to another form, such as mechanical energy on a shaft, and the remainder is rejected to a lower-temperature sink as low-grade heat.

Heat engines, depending on how the heat is supplied to the working fluid, are categorized in two types:

- (a) *External combustion.*
- (b) *Internal combustion.*

In external combustion engines, such as steam power plants, heat is supplied to the working fluid from an external source such as a furnace, a geothermal well, a nuclear reactor, or even the sun [1].

In internal combustion engines, such as automobile engines, this is done by burning the fuel within the system boundaries [1].

Our study of gas power cycles will involve the study of those heat engines in which the working fluid remains in the gaseous state throughout the cycle. We often study the ideal cycle in which internal irreversibility and complexities (the actual intake of air and fuel, the actual combustion process, and the exhaust of products of combustion among others) are removed. We will be concerned with how the major parameters of the cycle affect the performance of heat engines. The performance is often measured in terms of the cycle efficiency of  $\eta_{th}$  as the ratio of network  $W_{net}$  and energy as heat of  $Q_{in}$ . In Fig. 6.6 one can observe an *Actual Cycle* versus an

**Fig. 6.6** Illustration of actual vs. ideal cycle in a  $P-v$  diagram

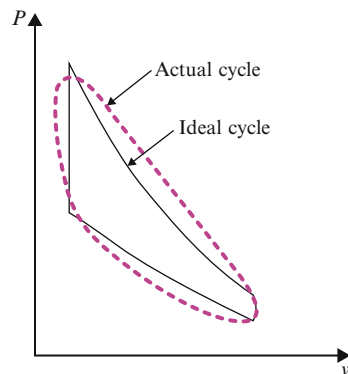
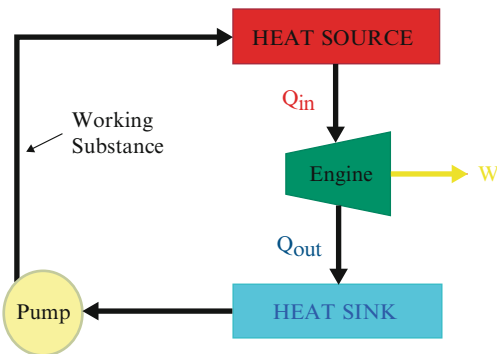


**Fig. 6.7** Basic thermodynamic cycle



*Ideal Cycle* in a  $P-v$  diagram, and using Eq. (6.3) and referring to Fig. 6.7 below mathematically we can show that;

$$\eta_{th} = \frac{W_{net}}{Q_{in}} \quad (\text{Eq. 6.5})$$

Several cycles utilize a gas as the working substance, the most common being the Otto cycle and the diesel cycle used in internal combustion engines. We touch upon some of these cycles in this chapter such as Otto, Brayton, Carnot, etc., and we will expand on them among other cycles for further evaluation as well.

## 6.2 Open Cycle

When internal combustion engine operation is examined, it is seen to differ in the process of heat supply for a typical heat engine cycle because there is a permanent change in the working fluid during combustion. Therefore, the fluid does not pass

through a cycle so the internal combustion engine is often referred to as an “open cycle” device, not a cyclic thermodynamic heat engine.

The term “open cycle”, while meaningless from a thermodynamic perspective, refers to the fact that energy is supplied to the engine from outside in the form of petroleum fuel and the unconverted portion of energy remaining in the spent combustion mixture is exhausted to the environment. “Closing the cycle”, i.e., returning the rejected products to the starting point where they can be reused, is left for nature to accomplish—hence the term “open cycle” comes into play.

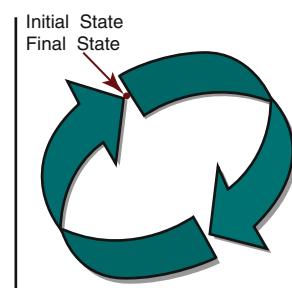
An internal combustion engine is therefore a device for releasing mechanical energy from petroleum fuel using air as the working medium rather than a heat engine for processing air in a thermodynamic cycle. Heat, as such, is not supplied to the internal combustion engine, so it cannot be a heat engine in the sense described in most thermodynamic references.

A simulated heat engine cycle can be constructed to correspond approximately to the operation of an internal combustion engine by substitution of analogous heat transfer processes for some of the actual engine processes. The specific mechanism of such heat transfer is neglected because the simulation is only a theoretical model of the engine, not an actual device. Such cycles, called *air standard cycles*, are a subject of study in thermodynamic cycles and are useful in the elementary study of internal combustion engines.

### 6.3 Closed Cycle

Thermodynamic cycles can be categorized yet another way as closed and open cycles. In closed cycles, the working fluid returns to the initial state at the end of the cycle and is recirculated. By the same thinking, in open cycles, the working fluid is renewed at the end of each cycle instead of being recirculated. For example, in automobile engines, the combustion gases are exhausted and replaced by a fresh air-fuel mixture at the end of each cycle. The engine operates on a mechanical cycle, but the working fluid does not go through a complete thermodynamic cycle [1, 2] (Fig. 6.8).

**Fig. 6.8** Illustration of a thermodynamic closed cycle



As we said before, any thermodynamic cycle is essentially a *closed cycle* in which, the working substance undergoes a series of processes and is always brought back to the initial state.

## 6.4 Gas Compressors and Brayton Cycle

The work in a gas compressor is calculated by,

$$\dot{W}_{\text{comp}} = \dot{m} (h_e - h_i) \quad (\text{Eq. 6.6})$$

If we assume that the gas in the compressor is calorically perfect, then we have,

$$\dot{W}_{\text{comp}} = \dot{m} c_p (T_e - T_i) \quad (\text{Eq. 6.7})$$

In many cases, this is a reasonable approximation. For noble gases, it is very accurate because they are calorically perfect. For air and similar working fluids, it is reasonable because the temperature rise is not that great and an average value of  $c_p$  is usually adequate. However, the average value of  $c_p$  should be chosen based on a temperature between  $T_e$  and  $T_i$ , not one at 300 K.

If then we assume that a compressor operates isentropically (adiabatic and reversible), the exit temperature can be related to the pressure rise in the compressor as shown below in Eq. (6.8);

$$T_e = T_i \left( \frac{p_e}{p_i} \right)^{\frac{\gamma-1}{\gamma}}$$

$$\dot{W} = \dot{m} c_p [T_e - T_i] = \dot{m} c_p T_i \left[ \frac{T_e}{T_i} - 1 \right] = \dot{m} \frac{\gamma R}{\gamma - 1} T_i \left[ \left( \frac{p_e}{p_i} \right)^{\frac{\gamma-1}{\gamma}} - 1 \right] \quad (\text{Eq. 6.8})$$

There are basically three types of compressors—reciprocating, centrifugal flow, and axial flow. In a reciprocating or positive displacement compressor, a piston slides in a cylinder and valves open and close to admit low-pressure fluid and exhaust high-pressure fluid. In centrifugal flow and axial flow compressors, the fluid enters at one end and is compressed by rotating blades and exits at the opposite end of the compressor. In the centrifugal flow compressor, the flow is in a radially outward direction and the compression is achieved by forcing the flow against the outer annulus of the compressor. In an axial flow compressor, a set of rotating blades move the flow through the compressor, acting as airfoils. They force the flow through an increasingly narrower channel, thus increasing the density and pressure. Gasoline and diesel engines are examples of reciprocating compressors, as are positive displacement pumps. Water pumps are examples of centrifugal flow compressors, similar to the rotor in a washing machine. Jet engine compressors are typically axial flow compressors. Reciprocating compressors require no priming

### Ideal Brayton Cycle

*T - s diagram*

---

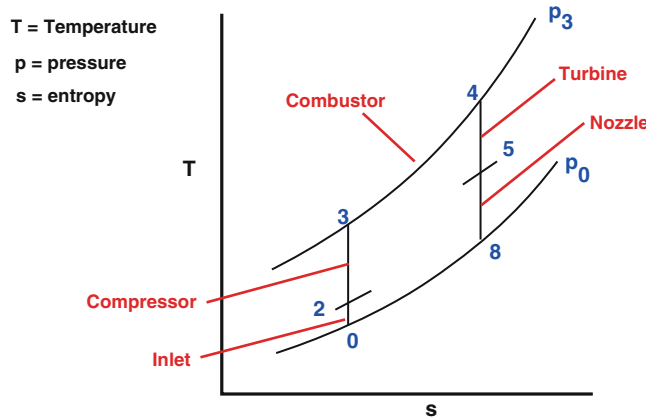


**Fig. 6.9** Illustration of Brayton cycle. (Courtesy of NASA)

and can reach very high pressures, but only moderate flow rates. Centrifugal flow and axial flow compressors usually require priming and can reach very high flow rates, but moderate pressures.

In this section we discuss the **Brayton Thermodynamic Cycle** which is used in all gas turbine engines. Figure 6.9 shows a *T-s* diagram of the Brayton Cycle. Using the turbine engine station numbering system, we begin with free stream conditions at station **0**. In cruising flight, the inlet slows the air stream as it is brought to the compressor face at **station2**. As the flow slows, some of the energy associated with the aircraft velocity increases the static pressure of the air and the flow is compressed. Ideally, the compression is isentropic and the static temperature is also increased as shown in the plot. The compressor does work on the gas and increases the pressure and temperature isentropically to **station3**, the compressor exit. Since the compression is ideally isentropic, a vertical line on the *T-s* diagram describes the process. *In reality, the compression is not isentropic and the compression process line leans to the right because of the increase in entropy of the flow.* The combustion process in the burner occurs at constant pressure from **station3** to **station4**. The temperature increase depends on the type of fuel used and the fuel-air ratio. The hot exhaust is then passed through the power turbine in which work is done by the flow from **station4** to **station5**. Because the turbine and compressor are on the same shaft, the work done on the turbine is exactly equal to the work done by the compressor and, ideally, the temperature change is the same. The nozzle then brings the flow isentropically (adiabatic and reversible) back to free stream pressure from **station5** to **station8**. Externally, the flow conditions return to free stream conditions, which completes the cycle. The area under the *T-s* diagram is

proportional to the useful work and thrust generated by the engine. The  $T$ - $s$  diagram for the ideal Brayton Cycle is shown here:

The Brayton cycle analysis is used to predict the thermodynamic performance of gas turbine engines.

As we know the gas turbine is another mechanical system that produces power, and it may operate on a cycle when used as an automobile or truck engine, or on a closed cycle when used in a nuclear power plant [3].

Usage of the Brayton process in a simple gas turbine cycle can be described as an open cycle operation where air first enters the compressor, and passes through a constant-pressure combustion chamber, then goes through the turbine, and then exits as a product of combustion to the atmosphere, as shown in Fig. 6.10a. A similar situation can be studied when the combustion chamber of a heat exchanger gets added onto the loop of Fig. 6.10a in order to organize a closed cycle as can be seen in Fig. 6.10b. Energy from some external source enters the cycle and the additional heat exchanger that has been added onto the loop transfers heat from the cycle so that the air can be returned to its initial state, as clearly seen in Fig. 6.10b.

The Brayton cycle is a theoretical cycle for a simple gas turbine. This cycle consists of two isentropic and two constant pressure processes. Figure 6.11 shows

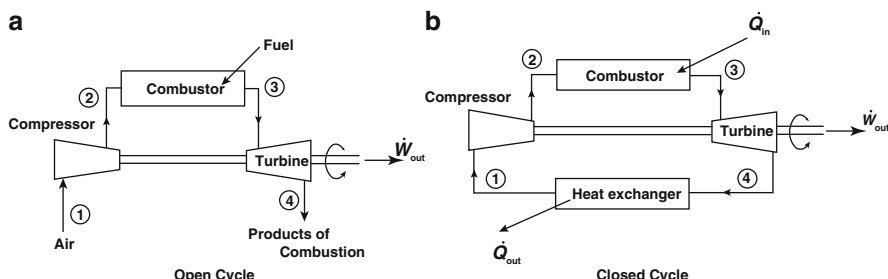


**Fig. 6.10** Illustration of Brayton components for open and closed cycles

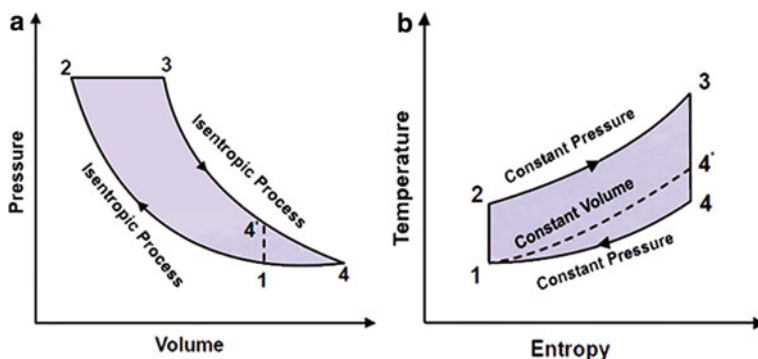


**Fig. 6.11** Illustration of the Brayton cycle on  $P$ - $V$  and  $T$ - $s$  diagram

the Brayton cycle on  $P$ - $V$  and  $T$ - $s$  coordinates. The cycle is similar to the Diesel cycle in compression and heat addition. The isentropic expansion of the Diesel cycle is further extended followed by constant pressure heat rejection.

The following notation gives the thermal efficiency in mathematical format for the ideal cycle used to model the gas turbine, which utilizes isentropic compression and expansion in the Brayton process:

$$\eta_{\text{th}} = \frac{\text{Heat added} - \text{Heat rejected}}{\text{Heat added}} = \frac{\dot{Q}_{\text{out}}}{\dot{Q}_{\text{in}}} \quad (\text{Eq. 6.9a})$$

$$\begin{aligned} \eta_{\text{th}} &= \frac{mC_p(T_3 - T_1) - mC_p(T_4 - T_1)}{mC_p(T_3 - T_2)} \\ &= 1 - \frac{T_4 - T_1}{T_3 - T_2} \\ &= 1 - \frac{T_1(T_4/T_1) - 1}{T_2(T_3/T_2) - 1} \end{aligned} \quad (\text{Eq. 6.9b})$$

Using the following isentropic process and relations we have;

$$\frac{T_2}{T_1} = \left(\frac{P_2}{P_1}\right)^{\frac{1}{\gamma}} \quad \text{and} \quad \frac{T_3}{T_4} = \left(\frac{P_3}{P_4}\right)^{\frac{1}{\gamma}} \quad (\text{Eq. 6.9c})$$

For ideal gas and observation the  $P$ - $V$  diagram of Fig. 6.11a obviously shows that we can state  $P_2 = P_3$  and  $P_1 = P_4$  as a result, using Eq. (6.10c), will induce the following;

$$\frac{T_2}{T_1} = \frac{T_3}{T_4} \quad \text{or} \quad \frac{T_4}{T_1} = \frac{T_3}{T_2} \quad (\text{Eq. 6.9d})$$

Then the Thermal efficiency  $\eta_{\text{th}}$  from Eq. (6.9a) can be reduced to the following form;

$$\eta_{\text{th}} = 1 - \frac{T_4}{T_3} = 1 - \frac{T_1}{T_2} \quad (\text{Eq. 6.9e})$$

Now if we introduce a term of the pressure ration  $r_p = P_2/P_1$  the thermal efficiency from Eq. (6.9e) will take a form of the following;

$$\frac{T_4}{T_3} = \frac{T_4}{T_3} = \frac{V_2}{V_1} = \frac{1}{r_p^{\gamma-1}} \quad (\text{Eq. 6.9f})$$

$$\frac{1}{r_p^{\gamma-1}} = \left(\frac{V_2}{V_1}\right)^{\gamma-1} \left\{ \left(\frac{P_1}{P_2}\right) \right\}^{(\gamma-1)} = (r_p)^{\frac{\gamma-1}{\gamma}} \quad (\text{Eq. 6.9g})$$

$$\eta_{\text{th}} = 1 - \frac{T_1}{T_2} = 1 - \left(\frac{P_1}{P_2}\right)^{(1-\gamma)/\gamma} \quad (\text{Eq. 6.9h})$$

or

$$\eta_{\text{th}} = 1 - r_p^{(1-\gamma)/\gamma} \quad (\text{Eq. 6.9i})$$

Note that the above final expression for thermal efficiency  $\eta_{\text{th}}$  in both forms of Eqs. (6.9h) and (6.9i) were obtained based on the assumption of using constant specific heats. For more accurate calculations the gas tables should be utilized.

In an actual gas turbine the compressor and the turbine are not isentropic and some losses take place. These losses, usually in the neighborhood of 85 %, significantly reduce the efficiency of the gas turbine engine [2].

Considering all the above we can see that the back work ratio is defined for a Brayton system as  $W_{\text{comp}}/W_{\text{turb}}$ . This is an important feature of the gas turbine that limits the thermal efficiency that is required for the compressor to have high work and is measured by this ratio. This can actually be fairly large approaching 1.0. If the compressor is too inefficient, the Brayton Cycle will not work. Only after efficient air compressors were developed was the jet engine feasible.

## 6.5 The Non-ideal Brayton Cycle

The Ideal Air Standard Brayton Cycle assumes isentropic compression and expansion processes. So far this has not been achieved in any real device. The isentropic efficiency for these processes is defined as

$$\text{Isentropic efficiency (compression)} = \frac{\Delta h_{\text{isentropic}}}{\Delta h_{\text{actual}}} \quad (\text{Eq. 6.10})$$

$$\text{Isentropic efficiency (expansion)} = \frac{\Delta h_{\text{actual}}}{\Delta h_{\text{isentropic}}} \quad (\text{Eq. 6.11})$$

Unfortunately the isentropic efficiency of a compressor or turbine will depend on the pressure ratio for the device. In doing parametric or design studies it is more useful to define an efficiency that does not depend on the pressure ratio, but only on the manufacturing tolerances and efficiencies of individual stages. This small stage, or infinitesimal stage, efficiency is called the polytropic efficiency.

Consider the combined First and Second Law for an infinitesimal process.

$$dh = vdp + Tds \quad (\text{Eq. 6.12})$$

The term  $Tds$  represents a heat flow for the process. During a compression, the inefficiency of the process represents a heat flow into the system. For an expansion

the inefficiency represents a heat flow out of the system. So on an infinitesimal basis we can write,

$$\begin{aligned} dh &= vdp + (Tds) = {}^v dp / e_{c,poly} \quad \text{for a compressor} \\ dh &= vdp + (-Tds) = e_{t,poly} \times vdp \quad \text{for a turbine} \end{aligned} \quad (\text{Eq. 6.13})$$

Then these two equations can be integrated similar to the way the isentropic relation was integrated. For an isentropic expansion of a calorically perfect ideal gas we have,

$$\begin{aligned} vdp &= \frac{RT}{p} dp \\ dh &= c_p dT = \frac{RT}{p} dp \\ \frac{dT}{T} &= \frac{R}{C_p} \frac{dp}{p} = \frac{\gamma - 1}{\gamma} \frac{dp}{p} \\ \left(\frac{T_2}{T_1}\right) &= \left(\frac{p_2}{p_1}\right)^{\frac{\gamma-1}{\gamma}} \end{aligned} \quad (\text{Eq. 6.14})$$

For a polytropic compression we have,

$$\begin{aligned} vdp &= \frac{RT}{e_{c,poly} p} dp \\ dh &= c_p dT = \frac{RT}{e_{c,poly} p} dp \\ \frac{dT}{T} &= \frac{R}{C_p} \frac{dp}{p} = \frac{\gamma - 1}{e_{c,poly} \gamma} \frac{dp}{p} \\ \left(\frac{T_2}{T_1}\right) &= \left(\frac{p_2}{p_1}\right)^{\frac{\gamma-1}{e_{c,poly} \gamma}} \end{aligned} \quad (\text{Eq. 6.15})$$

And for a polytropic expansion we have,

$$\begin{aligned} vdp &= \frac{e_{t,poly} RT}{p} dp \\ dh &= c_p dT = \frac{e_{t,poly} RT}{p} dp \\ \frac{dT}{T} &= \frac{R}{C_p} \frac{dp}{p} = \frac{e_{t,poly} (\gamma - 1)}{\gamma} \frac{dp}{p} \\ \left(\frac{T_2}{T_1}\right) &= \left(\frac{p_2}{p_1}\right)^{\frac{e_{t,poly} \gamma - 1}{\gamma}} \end{aligned} \quad (\text{Eq. 6.16})$$

Now for a calorically perfect gas, the isentropic efficiency of a compressor is given by,

$$\eta_{c, \text{isen}} = \frac{C_p(T_{\text{out,isen}} - T_{\text{in}})}{C_p(T_{\text{out,actual}} - T_{\text{in}})} = \frac{\frac{T_{\text{out,isen}}}{T_{\text{in}}} - 1}{\frac{T_{\text{out,actual}}}{T_{\text{in}}} - 1} = \frac{\left(\frac{P_{\text{out}}}{P_{\text{in}}}\right)^{\frac{\gamma-1}{\gamma}} - 1}{\left(\frac{P_{\text{out}}}{P_{\text{in}}}\right)^{\frac{\gamma-1}{\gamma e_{c,\text{poly}}}}} \quad (\text{Eq. 6.17})$$

And the isentropic efficiency of a turbine is given by,

$$\eta_{t, \text{isen}} = \frac{C_p(T_{\text{out,actual}} - T_{\text{in}})}{C_p(T_{\text{out,isen}} - T_{\text{in}})} = \frac{\frac{T_{\text{out,actual}}}{T_{\text{in}}} - 1}{\frac{T_{\text{out,isen}}}{T_{\text{in}}} - 1} = \frac{\left(\frac{P_{\text{out}}}{P_{\text{in}}}\right)^{\frac{e_{t,\text{poly}}(\gamma-1)}{\gamma}} - 1}{\left(\frac{P_{\text{out}}}{P_{\text{in}}}\right)^{\frac{\gamma-1}{\gamma e_{c,\text{poly}}}}} \quad (\text{Eq. 6.18})$$

There are more thermodynamic cycles than what it is described here and explaining every one of them is beyond the scope of this book, so we encourage all readers to take a look at the reference by Zohuri and McDaniel [2] and Chap. 14 of that reference for more details.

## 6.6 Open Cycle Gas Turbines

A gas turbine is an internal combustion engine that operates with rotary rather than reciprocating motion. Gas turbines are composed of three main components: compressor, combustor, and power turbine. In the compressor section, air is drawn in and compressed up to 30 times ambient pressure and directed to the combustor section where fuel is introduced, ignited, and burned. Combustors can be either annular, can-annular, or silo. An annular combustor is a doughnut-shaped, single, continuous chamber that encircles the turbine in a plane perpendicular to the air flow. Can-annular combustors are similar to annular combustors, however they incorporate several can shaped combustion chambers rather than a single combustion chamber. Annular and can-annular combustors are based on aircraft turbine technology and are typically used for smaller scale applications. A silo combustor has one or more combustion chambers mounted external to the gas turbine body. Silo combustors are typically larger than annular or can-annular combustors and are used for larger scale operations.

The compressor, combustor, and turbine are connected by one or more shafts and are collectively called the gas generator or gas turbine. Figures 6.12 and 6.13 below illustrate the typical gas turbine generator configuration and schematic [4].

Hot gases from the combustion section are diluted with additional air from the compressor section and directed to the power turbine section at temperatures up to 2600 °F. Energy from the hot exhaust gases, which expand in the power turbine section, is recovered in the form of shaft horsepower. More than 50 % of the shaft horsepower is needed to drive the internal compressor and the balance of recovered shaft horsepower is available to drive an external load. In the open cycle gas

**Fig. 6.12** Open cycle gas turbine configuration

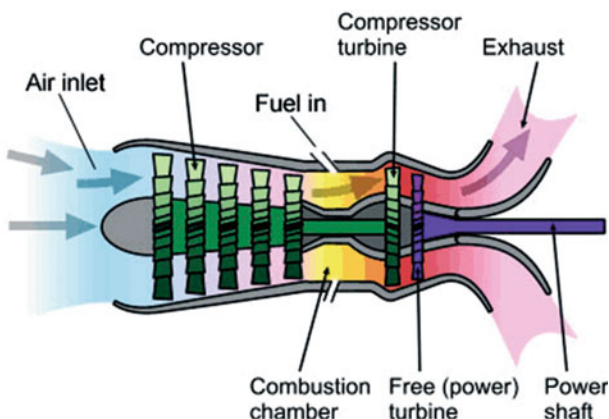
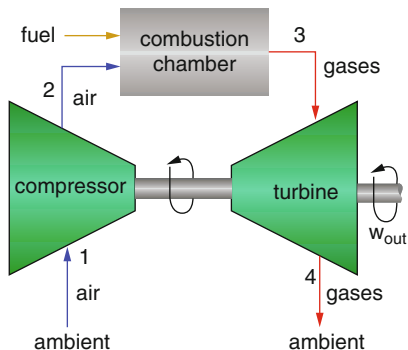


**Fig. 6.13** Open cycle gas turbine schematic of JR1 engine [4]

turbine, the heat content of the exhaust gases exiting the turbine is discarded as opposed to using a heat exchanger to preheat the combustion air entering the combustor (regenerative cycle) or recovered in a heat recovery steam generator to raise process steam, with or without supplemental firing (cogeneration) or recovered, with or without supplementary firing to raise steam for a steam turbine (combined cycle or repowering). The open or simple cycle is the most basic operating cycle of a gas turbine with a thermal efficiency ranging from 15 to 42 %. Open cycle gas turbines are available in a wide range of power outputs ranging from 300 hp to over 200,000 hp (0.22–149.14 MW).

As alternatives to the use of gas turbine cycles have already been explored (in the combined cycle section), this section focuses on alternative technologies to the standard turbine unit itself that render the open cycle turbine more efficient. Relatively few manufacturers build large machines; among them are Alstom, General Electric, Mitsubishi Heavy Industries, and Siemens. The high efficiency gas turbines (H class) and aero-derivative intercooler gas turbines, developed by

**Table 6.1** High efficiency gas turbine models

Manufacture	Model	Simple cycle efficiency	Combined cycle efficiency	Power produced (simple) (MW)
Alstom	GT24	40	58.4	230.7
Mitsubishi	M501J	41	61.5	327
General Electric	7FA	38.5	58.5	216
General Electric	LMS100	44	53.8	103
Siemens	SGT6-8000H	40	60.75	274
Siemens	SGT6-2000E	33.9	51.3	112
Hitachi	H-25	34.8	50.3	32

these manufacturers and considered as possible alternatives to the typical gas turbine in the open cycle system, are discussed in great detail below.

Five to three hundred and seventy-five megawatt typical sized turbines are sold by various manufacturers with higher efficiencies for larger models. Smaller sized turbines are typically used for offshore applications due to lower weight. Gas turbines are produced in a range of efficiencies, with larger and newer models being the most efficient. More efficient models, however, cost more due to the additional advanced components and less per delivered energy; therefore, a complete economic analysis (net present value, discounted payback) should back-up investment decisions. A major cause of the increased efficiency is a higher operating temperature in the turbines, which is permitted due to the use of advanced materials and coatings that can handle more heat. Upgraded cooling systems are essential to handle this heat, and new sealing systems are used to reduce the cooling air loss. These upgrades, combined with new advanced compressors, result in expensive but highly efficient gas turbines that may be considered as alternatives to the traditional turbines. Table 6.1 provides a summary of the high efficiency gas turbines on the market today.

### 6.6.1 Aeroderivative Intercooler Gas Turbines

Intercooler systems work to increase efficiency by allowing for higher pressure ratios in the combustion zone. This is achieved by splitting the compression unit into two sections: the Low Pressure Compressor (LPC) and the High Pressure Compressor (HPC). The intake air is first compressed by the LPC, and then sent to the intercooler where the pressure is held constant but the temperature is decreased. The air then goes through the HPC and is sent to the combustor. Since the air in the engine cannot exceed a given temperature due to the material used in the turbine, there is traditionally a limit on the pressure ratio; since compressing gas

increases its temperature. By cooling the air part way through but not losing any of the pressure gain, the intercooler allows for a second compression to occur, allowing air in the combustor to be within the temperature limits but with a much higher pressure ratio. The higher ratio causes the turbine to generate more power with the same fuel input, increasing the overall efficiency of the turbine.

An example of new innovations to the aero-derivative gas turbine is the 35–65 MW high pressure turbine (HPT) developed by GE [5]. The LM6000 PG offers a 25 % simple cycle power increase compared to its predecessor. The applications of these turbines include oil and gas platforms, university cogeneration systems, and industrial park combined cycle installations. These turbines are designed to operate on partial power, withstand voltage swings, and be capable of faster dispatching.

### ***6.6.2 Operational Issues/Risks***

Gas turbines are complex high speed components, with tight dimensional tolerances, operating at very high temperatures. Components are subject to a variety of potential issues. These include creep, fatigue, erosion, and oxidation with impact damage an issue if components fail or following maintenance. Creep may eventually lead to failure but is of most concern because of the dimensional changes it produces in components subject to load and temperature. A major part of maintenance is checking of dimensions and tolerances. Fatigue is of particular concern at areas of stress concentration such as the turbine blade roots. Therefore, regular inspection and maintenance is a requirement, particularly for gas turbines operating in harsh environments such as offshore applications [6]. This would include electrical and control systems in addition to the gas turbine itself.

### ***6.6.3 Opportunities/Business Case***

The general trend in gas turbine advancement has been toward a combination of higher temperatures and pressures. While such advancements increase the manufacturing cost of the machine, the higher value in terms of greater power output and higher efficiency provides net economic benefits. The industrial gas turbine is a balance between performances and cost which results in the most economic machine for both the user and manufacturer. Applications in the oil and gas industry include pipeline natural gas compression stations in the range of 800–1200 psi (5516–8274 kPa) and compression is required as well as oil pipeline pumping of crude and refined oil. Turbines up to about 50 MW may be either industrial or modified aeroderivative engines while larger units up to about 330 MW are designed for specific purposes. For electric power applications, such as large industrial facilities, simple-cycle gas turbines without heat recovery can

provide peaking power in capacity constrained areas, and utilities often place gas turbines in the 5–40 MW size range at substations to provide incremental capacity and grid support. A significant number of simple-cycle gas turbine based Combined Heat and Power (CHP) systems are in operation at a variety of applications including oil recovery, chemicals, paper production, food processing, and universities. Note that CHP is also known as cogeneration, which is the simultaneous production of electricity and heat from a single fuel source, such as: natural gas, biomass, biogas, coal, waste heat, or oil.

CHP is not a single technology, but an integrated energy system that can be modified depending upon the needs of the energy end user [7].

CHP provides:

- Onsite generation of electrical and/or mechanical power.
- Waste-heat recovery for heating, cooling, dehumidification, or process applications.
- Seamless system integration for a variety of technologies, thermal applications, and fuel types into existing building infrastructure.

The two most common CHP system configurations are:

- Gas turbine or engine with heat recovery unit.
- Steam boiler with steam turbine.

The system configuration is shown in Figs. 6.14 and 6.15.

In order to achieve the two above processes for the most common CHP, design and application of an appropriate heat exchanger, in particular in the form of Compact Heat Exchanger (CHE), is required.

Gas turbine or reciprocating engine CHP systems generate electricity by burning fuel (natural gas or biogas) to generate electricity and then use a heat recovery unit to capture heat from the combustion system's exhaust stream. This heat is converted into useful thermal energy, usually in the form of steam or hot water.

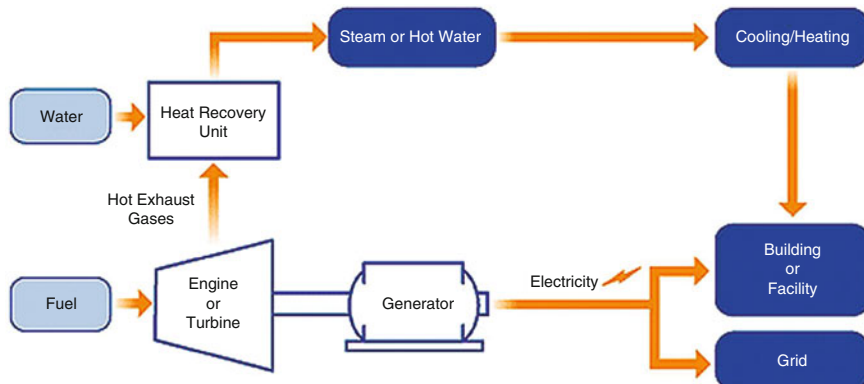


**Fig. 6.14** Gas turbine or engine with heat recovery unit

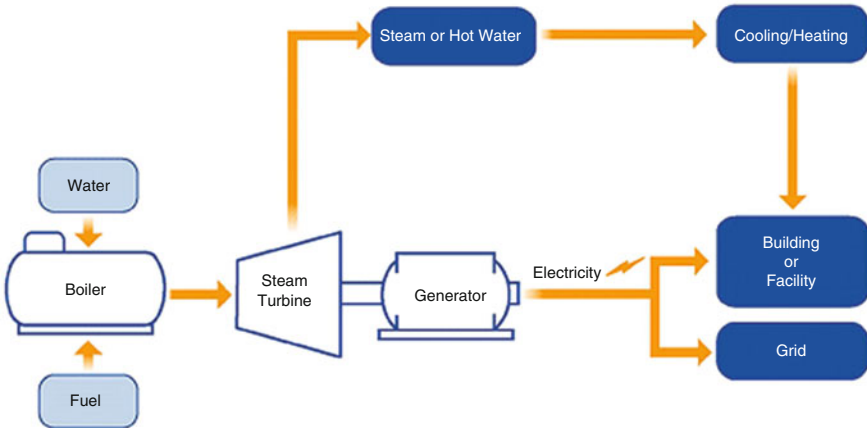
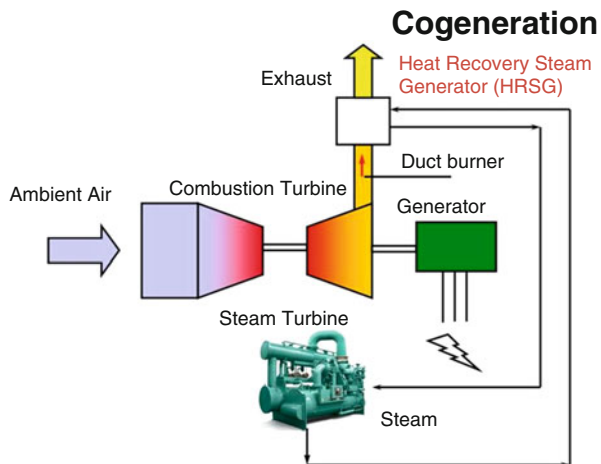


**Fig. 6.15** Steam boiler with steam turbine

**Fig. 6.16** Overall schematic of CHP with HRSG. (Courtesy of Energy Solutions Center)



Gas turbines/engines are ideally suited for large industrial or commercial CHP applications requiring ample amounts of electricity and heat.

Steam turbines normally generate electricity as a byproduct of heat (steam) generation, unlike gas turbine and reciprocating engine CHP systems, where heat is a byproduct of power generation. Steam turbine-based CHP systems are typically used in industrial processes, where solid fuels (biomass or coal) or waste products are readily available to fuel the boiler unit.

To function CHP imposes the integration of a power system such as an engine or turbine and a Heat Recovery Steam Generator (HRSG) usually a boiler, which is located on or nearby the user's facility. Figure 6.16 is an overall schematic of such configuration.

CHP application can be found throughout literature as well as in Ref. [7] of this chapter.

#### **6.6.4 Industrial Case Studies for Open Cycle Gas Turbine**

The following is a presentation of industrial case studies for open cycle gas turbines:

##### **1. High Efficiency Gas Turbine**

The new line of high efficiency gas turbines has been designated the H class, and are currently built by few manufacturers. After an extensive validation process, GE installed their model, the 9H, at Baglan Bay in 2003. This new model increased efficiency by allowing the firing temperatures to increase 200 °F (93.3 °C) higher than previous models, potentially reaching 2600 °F (1426.7 °C). The plant has been reliably providing up to 530 MW to the UK national grid since then, operating at over 60 % efficiency (as part of a combined cycle system) [8].

Another manufacturer, Siemens, tested their H class model, the SGT5-8000H, at full load in Ingolstadt, Germany in 2008. The gas turbine unit's efficiency was shown to be 40 %, and was part of a combined cycle system reaching a world record of 60.75 % efficiency [9]. This plant has been providing power to the German grid since the testing period finished, all at this same efficiency.

Only these H class turbines truly showcase all of the new adjustments that can be made to increase efficiency, and they have very large footprints and have specified outputs of 375 MW and higher. However, the technologies behind the H class turbines (advanced materials, improved cooling, etc.) are available on smaller systems. These cases were chosen to illustrate that they are all effective and operational.

##### **2. Aeroderivative Intercooler Gas Turbines**

GE has produced the LMS 100, an extremely high efficiency Aeroderivative engine. Operating at up to 44 % efficiency at full base load, it generates over 100 MW after a 10 min start-up. The Groton Generating Station in South Dakota was the first plant to begin using the LMS100, and it has been successfully operational since 2006 [8]. This technology, while currently available from GE, is the newest and least tested technology identified here. However, due to its successful initial testing and extremely high efficiency for a simple cycle, it is an important alternative to consider.

For further information on combined cycle and application of compact heat exchanger (CHE) driven efficiency of these combines refer to books by Zohuri [9, 10].

## References

1. Cengel, Yunus A., and Michael A. Boles. 2011. *Thermodynamics: An engineering approach*, 7th ed. New York: McGraw Hill.
2. Zohuri, B., and Patrick McDaniel. 2015. *Thermodynamics in nuclear power plant systems*. New York: Springer Publisher.
3. Potter, Merle C., and Craig W. Somerton. 2006. *Thermodynamics for engineers*, McGraw-Hill Schaum's outlines series, 2nd ed. New York: McGraw-Hill.
4. <http://www.ipieca.org/energyefficiency/solutions/77801>
5. Aeroderivative Technology: A more efficient use of gas turbine Technology, Wacke, A, General Electric, DRAFT – 2010 – Jan-15.
6. Wall, Martin, Lee Richard, and Simon Frost. Offshore gas turbines (and major driven equipment) integrity and inspection guidance notes. Research Report, 430, ESR Technology Ltd for the Health and Safety Executive 2006.
7. <http://www.epa.gov/chp/basic/>
8. Reale, Michael J., and James K. Prochaska. 2005. New high efficiency simple cycle gas turbine—GE's LMS100. Industrial Application of Gas Turbines Committee, 14 Oct 2005. Web. 29 Jul 2013.
9. Zohuri, B. 2015. *Combined cycle driven efficiency for next generation nuclear power plants: An innovative design approach*. New York: Springer Publishing Company.
10. Zohuri, B. 2015. *Application of compact heat exchangers for combined cycle driven efficiency in next generation nuclear power plants*. New York: Springer Publishing Company.

# **Chapter 7**

## **Compact Heat Exchangers Application in NGNP**

A number of technologies are being investigated for the Next Generation Nuclear Plant (NGNP) that will produce heated fluids at significantly higher temperatures than current generation power plants. The higher temperatures offer the opportunity to significantly improve the thermodynamic efficiency of the energy conversion cycle. Selection of the technology and design configuration for the NGNP must consider both the cost and risk profiles to ensure that the demonstration plant establishes a sound foundation for future commercial deployments. The NGNP challenge is to achieve a significant advancement in nuclear technology while at the same time setting the stage for an economically viable deployment of the new technology in the commercial sector soon after 2020. Energy is the elixir of life for the world's economy and for individual prosperity. Efforts being made for greater energy efficiency—especially in industrial countries—have indeed proved effective: as evidenced by the fact that energy consumption throughout the world is growing slower than gross domestic products. At the same time, however, the hunger for energy in quickly growing economies is leading to shifts in energy mix—which drives undesired CO<sub>2</sub> emissions upward. In conversion of primary energy to final and useful energy, technology from universities and national laboratories plus industry toward design of NGP has made key contributions to efficient handling of the resources of our planet.

### **7.1 Introduction**

A nuclear reactor produces and controls the release of energy from splitting the atoms of uranium. Uranium-fuelled nuclear power is a clean and efficient way of boiling water to make steam which drives turbine generators. Except for the reactor itself, a nuclear power station works like most coal or gas-fired power stations. Recent studies by national laboratories and researchers in the United States and around the world on combined cycle driven efficiency using either open air or

closed CO<sub>2</sub> using Brayton with bottoming or topping Rankine cycle show a lot of promise, in particular for development of small modular reactors as part of Next Generation Nuclear Plant (NGNP) that will produce heated fluids at significantly higher temperatures than current generation power plants. To take advantage of excessive heat generated by nuclear energy of next generation requires a proper acquisition strategy for either Intermediate Heat Exchanger (IHX) or Compact Heat Exchanger (CHE) and possibly Reheater or Recuperator as part of a Heat Exchanger (HX) subsystem, which is a very important process [1].

Combined cycle driven efficiency for a nuclear system takes advantage of this innovative technology and shows a very promising result. Numerous publications are presented by Zohuri [2–6], McDaniel, Zohuri et al. [7, 8], and Forsberg et al. [9] where readers can refer for further information. There are a number of changes to the plant components that have to be made. The most significant of course is that the combustion chamber has to be replaced by a **Heat Exchanger** in which the working fluid from the nuclear reactor secondary loop is used to heat the air (Fig. 7.1). The normal Brayton cycle is an internal combustion where the working fluid is heated by the combustion of the fuel with the air in the combustion chamber. The walls of the combustion chamber can be cooled and peak temperatures in the working fluid can be significantly above the temperature that the walls of the chamber can tolerate for any length of time.

For the nuclear reactor system the heat transfer is in the opposite direction. All reactor components and fluids in the primary and secondary loops must be at a higher temperature than the peak temperature of the gas exiting the heat exchanger. This severely restricts the peak temperature that can be achieved for the air entering the turbine.

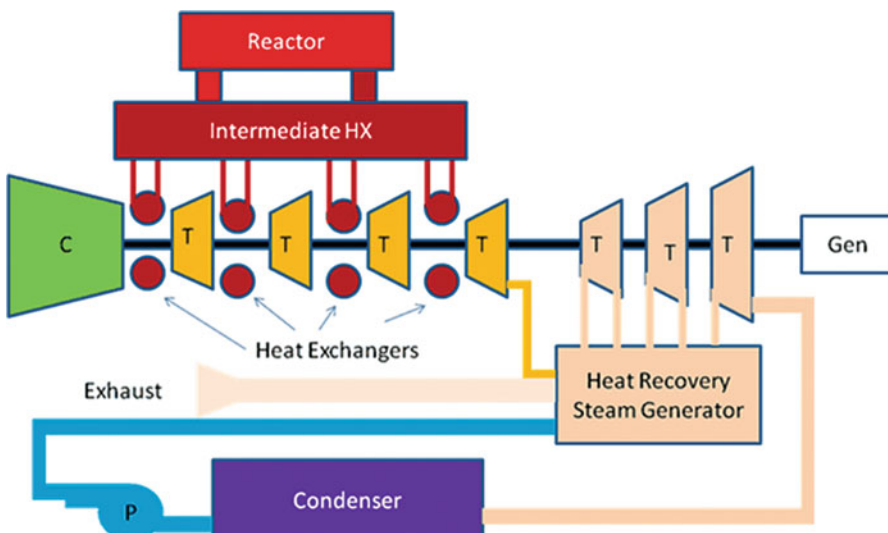


**Fig. 7.1** Layout for four turbine combined cycle with intermediate heat exchanger

Out of six GEN-IV configurations that the Department of Energy (DOE) has selected, the High Temperature Gas-cooled Reactor (HTGR) design for the Next Generation Nuclear Plant (NGNP) Project is a front runner for such an innovative approach. The NGNP will demonstrate the use of nuclear power for electricity and hydrogen production. It will have an outlet gas temperature in the range of 850–950 °C and a plant design service life of 60 years. As part of our studies, we also showed the air Brayton Combined Cycle (BCC) power system [10–15] and Nuclear air-Brayton Combined Cycle (NACC) power systems; the higher temperature for outlet gas the better opportunity exists to increase our overall thermal efficiency of the power plant in order to make it cost effective and be more compatible with natural gas plant cost wise both from Total Cost of Ownership (TCO) and Return On Investment (ROI) for the owner of such nuclear plants. The reactor design will be a graphite moderated, helium-cooled, prismatic or pebble-bed reactor, and use low-enriched uranium, TRISO-coated fuel. The plant size, reactor thermal power, and core configuration will ensure passive decay heat removal without fuel damage or radioactive material releases during accidents. The NGNP Materials Research and Development (R&D) Program is responsible for performing R&D on likely NGNP materials in support of the NGNP design, licensing, and construction activities.

As part of Intermediate Heat Exchanger (IHX) acquisition and its application in NGNP, the compact designs are attractive to minimize the capital investment in materials by driving overall capital savings in footprint, volume, and structural support costs; however, they represent a significant technical risk at this stage of their development. Qualification of diffusion bonding methods and development of in-service inspection methods represent significant schedule risk.

Looking at the compact heat exchanger as an alternative solution will drive overall capital savings in footprint, volume, and structural support costs. A reduction in overall unit footprint, volume, and weight by up to 85 % when compared to traditional technologies such as shell and tube, generates significant cost savings in the following areas:

- Reduced deck and skid volume required for implementation and installation.
- Reduced structure support requirements.
- Reduced pipe-work runs and sizing.
- Improved access for maintenance.
- Reduced relief and flare systems.
- Topside craneage for installation and maintenance.

Compact heat exchangers would allow the exceptionally high heat transfer efficiency-to-volume ration using methods such as printed circuit heat exchangers. Also, the plate heat exchangers improve thermal management and economy in both fossil-fired and nuclear stations. Compact size, trusted-quality products, and ease of maintenance makes them an attractive choice for new construction, retrofits or capacity expansions. The compact heat exchangers are a perfect fit in heating/condensing, liquid, gas or two-phase operations where reliability, safety, and uptime are important considerations.

The definition of compactness is quite an arbitrary matter. The ratio of the heat transfer surface area on one side of the heat exchanger to the volume can be used as a measure of the compactness of heat exchangers. A heat exchanger having a surface area density on any one side greater than about  $700 \text{ m}^2/\text{m}^3$  quite arbitrarily is referred to as a compact heat exchanger regardless of its structural design. For example, automobile radiators having an area density on the order of  $1100 \text{ m}^2/\text{m}^3$  and the glass ceramic heat exchangers for some vehicular gas-turbine engines having an area density on the order of  $6600 \text{ m}^2/\text{m}^3$  are compact heat exchangers. The human lungs, with an area density of about  $20,000 \text{ m}^2/\text{m}^3$ , are the most compact heat-and-mass exchanger. The very fine matrix regenerator for the Stirling engine has an area density approaching that of the human lung.

On the other extreme of the compactness scale, plane tubular and shell-and-tube type exchangers, having an area density in the range of  $70\text{--}500 \text{ m}^2/\text{m}^3$ , are not considered compact [10]. The incentive for using compact heat exchangers lies in the fact that a high value of compactness reduces the volume for a specified heat exchanger performance.

When heat exchangers are to be employed for automobiles, marine uses, aircraft, aerospace vehicles, nuclear power plants or any other generating elasticity power plants such as gas or fossil fueled systems, cryogenic systems, refrigeration and air conditioning, the weight and size—hence the compactness—become important. To increase the effectiveness or the compactness of heat exchangers, fins are used. In a gas-to-liquid heat exchanger, for example, the heat transfer coefficient on the gas side is an order of magnitude lower than for the liquid side. Therefore, fins are used on the gas side to obtain a balanced design; the heat transfer surface on the gas side becomes much more compact.

In order to obtain such a balanced design for heat transfer between two sides, we have to be concerned about pinch point. The pinch point is defined as the point where the temperature difference is a minimum. The temperature difference at the pinch depends on the decision of heat exchanger; in general, the smaller the temperature difference the more expensive the heat exchanger.

A number of technologies are being investigated for the Next Generation Nuclear Plant that will produce heated fluids at significantly higher temperatures than current generation power plants. The higher temperatures offer the opportunity to significantly improve the thermodynamic efficiency of the energy conversion cycle. One of the concepts currently under study is the Molten Salt Reactor. The coolant from the Molten Salt Reactor may be available at temperatures as high as  $800\text{--}1000^\circ\text{C}$ . At these temperatures, an open Brayton cycle combined with a Rankine bottoming cycle appears to have some strong advantages. Thermodynamic efficiencies approaching 50% appear possible. Requirements for circulating cooling water will be significantly reduced. However, to realistically estimate the efficiencies achievable it is essential to have good models for the heat exchangers involved as well as the appropriate turbo-machinery. This study has concentrated on modeling all power conversion equipment from the fluid exiting the reactor to the energy releases to the environment.

Waste heat is heat generated in a process by way of fuel combustion or chemical reaction, which is then “dumped” into the environment and not reused for useful and economic purposes. The essential fact is not the amount of heat, but rather its “value”. The mechanism to recover the unused heat depends on the temperature of the waste heat gases and the economics involved.

Large quantities of hot flue gases are generated from boilers, kilns, ovens, and furnaces. If some of the waste heat could be recovered then a considerable amount of primary fuel could be saved. The energy lost in waste gases cannot be fully recovered. However, much of the heat could be recovered and adopting the following measures as outlined in this chapter can minimize losses.

To achieve what is required, acquisition of the right heat exchanger or recuperator with the right classification by flow arrangements is needed. In this case the most commonly used type is the recuperative heat exchanger and they can be classified by flow arrangement, where numerous possibilities exist for flow arrangement in heat exchangers. In this type the two fluids can flow in *parallel-flow*, in *cross-flow*, in *counter-flow*, or in a combination of these.

The temperature variations of each type are shown in Fig. 7.2a–c. It can also be shown that for all three cases of Fig. 7.2 the true temperature difference is the Logarithmic Mean Temperature Difference, **LMTD**, as given by Eq. (7.1) and was thoroughly defined in Chap. 3:

$$\text{LMTD} = \frac{(\Delta T(z)_B - \Delta T(z)_A)}{\ln\left(\frac{\Delta T(z)_B}{\Delta T(z)_A}\right)} \quad (\text{Eq. 7.1})$$

In Eq. (7.1), where  $\Delta t_A$  is the temperature difference between the two streams at end point A and  $\Delta t_B$  is the temperature difference between the two streams at end B.

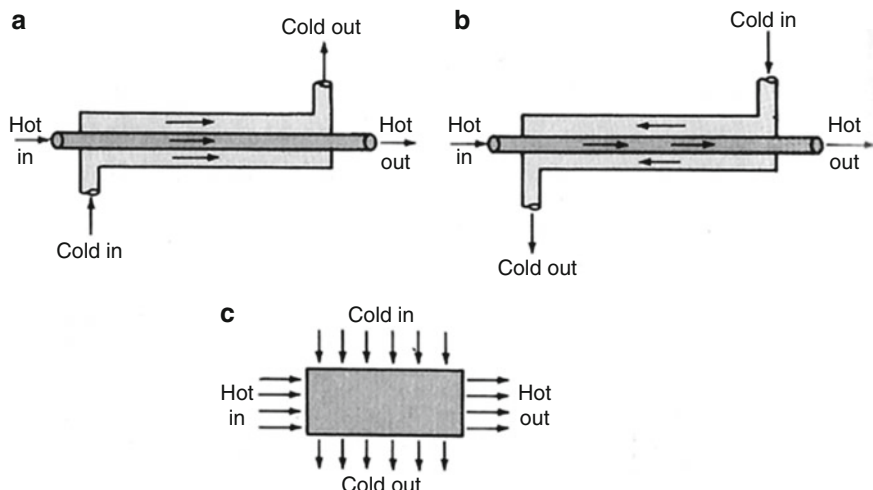


**Fig. 7.2** (a) Parallel-flow, (b) counter-flow, and (c) cross-flow [16]

With this definition, the LMTD can be used to find the exchanged heat in a heat exchanger.

$$Q = U \times A_r \times \text{LMTD} \quad (\text{Eq. 7.2})$$

where  $Q$  is the exchanged heat duty and KMS system has unit of Watts,  $U$  is the heat transfer coefficient in Watts per Kelvin per square meter, and  $A_r$  is the exchange area. Note that estimating the heat transfer coefficient may be quite complicated.

Equation (7.2) can be easily derived using basic heat transfer, taking it in a heat exchanger along let's say the  $z$ -direction from point  $A$  to point  $B$  between two fluids as fluid 1 and 2, so the analysis can be done in one-dimensional space.

The analysis is as follows assuming the local exchanged heat flux at  $z$  is proportional to the temperature difference:

$$q(z) = U\{T_2(z) - T_1(z)\}/D = U\{\Delta T(z)\}/D \quad (\text{Eq. 7.3})$$

where  $D$  is the distance between the two fluids

$$\begin{aligned} \frac{dT_1(z)}{dz} &= k_A\{T_1(z) - T_2(z)\} = -k_A\Delta T(z) \\ \frac{dT_2(z)}{dz} &= k_B\{T_2(z) - T_1(z)\} = -k_B\Delta T(z) \end{aligned} \quad (\text{Eq. 7.4})$$

Summed from the two above equations, we get

$$\frac{d(\Delta T)}{dz} = \frac{d\{T_2(z) - T_1(z)\}}{dz} = \frac{dT_2(z)}{dz} - \frac{dT_1(z)}{dz} = k\Delta T(z) \quad (\text{Eq. 7.5})$$

where  $k = k_A + k_B$ , and  $k$  is the sum of thermal conductivity of two working fluids at point  $A$  and  $B$  where the heat is exchanging between them, while  $k_A$  and  $k_B$  are thermal fluid 1 and 2 respectively and MKS unit dimensions are W/m K.

Now analyzing the total exchanged energy  $Q$  is found by integrating the local heat transfer  $q$  from  $A$  to  $B$ .

$$Q = \int_A^B q(z)dz = \frac{U}{D} \int_A^B \Delta T(z)dz = \frac{U}{D} \int_A^B \Delta T(z)dz \quad (\text{Eq. 7.6})$$

Use the fact that the heat exchanger area  $A_r$  is the pipe length  $B - A$  multiplied by the inter-pipe distance  $D$ :

$$Q = \frac{UA_r}{B - A} \int_A^B \Delta T(z)dz = \frac{UA_r \int_A^B \Delta T(z)dz}{\int_A^B dz} \quad (\text{Eq. 7.7})$$

In both integrals make a change of variables from  $z$  to  $\Delta T(z)$ :

$$Q = \frac{UA_r \int_{\Delta T(z)_A}^{\Delta T(z)_B} \left(\frac{1}{k}\right) d[\Delta T(z)]}{\int_{\Delta T(z)_A}^{\Delta T(z)_B} \left(\frac{1}{k \Delta T(z)}\right) d[\Delta T(z)]} \quad (\text{Eq. 7.8})$$

Integrating at this point is a very trivial process, and finally results in:

$$Q = U \times A_r \times \frac{\Delta T(z)_B - \Delta T(z)_A}{\ln[\Delta T(z)_B / \Delta T(z)_A]} \quad (\text{Eq. 7.9})$$

From which the definition of Logarithmic Mean Temperature Difference (LMTD) follows and Eq. (7.1) with help from Eq. (7.2) is proven.

To prove the relationship of Eq. (7.1) between two fluids of 1 and 2 at point  $A$  and  $B$  certain assumptions along with their limitations have been made and they are as follows.

1. It has been assumed that the rate of change for the temperature of both fluids is proportional to the temperature difference; this assumption is valid for fluids with a constant specific heat, which is a good description of fluids changing temperature over a relatively small range. However, if the specific heat changes, the LMTD approach will no longer be accurate.
2. A particular case where the LMTD is not applicable are condensers and reboilers, where the latent heat associated to phase change makes the hypothesis invalid.
3. It has also been assumed that the heat transfer coefficient ( $U$ ) is constant, and not a function of temperature. If this is not the case, the LMTD approach will again be less valid.
4. The LMTD is a steady-state concept, and cannot be used in dynamic analyses. In particular, if the LMTD were to be applied on a transient in whom for a brief time, the temperature differential had different signs on the two sides of the exchanger, the argument to the logarithm function would be negative, which is not allowable.

## 7.2 Compact Heat Exchangers Driven Efficiencies in Brayton Cycle

As analyzed and demonstrated, the modeling of a computer code in Steady-State approach (i.e., Transient-Analysis) should be considered for better accuracy sooner than later [2–6]. If the simple Brayton cycle is modified to include a recuperator (which will transfer heat from the turbine exhaust to preheat compressed high

pressure air before going to the combustion chamber), it will require less fuel to obtain the desired turbine inlet temperature of compressed air and also the optimum pressure ratio (either for compressor or turbine) is typically reduced to 3–4. This improves the thermal efficiency of the cycle. Alternatively, a regenerator can also be used replacing a recuperator.

With the distributed power generation market, and renewing attention to nuclear power plants, in particular new generation and small modular reactors (SMRs), one of the most economical solutions today is to generate power through small gas turbine systems in the form of Brayton cycle combined with these reactors. These gas turbines arbitrarily can be categorized as microturbines with output of 5–200 kW and mini-turbines with output of 200–500 kW. The thermal efficiency of such microturbines is about 20 % or less if no recuperator is used in the system. Using a recuperator (regenerator can also be considered but has a number of problems) operating at 87 % effectiveness, the efficiency of the gas turbine system increases to about 30 %, a substantial performance improvement. However, cost of the recuperator is about 25–30 % of the total power plant, therefore total cost of ownership and return on investments are not very well justified.

This means that the heat exchanger or recuperator (McDonald and Wilson) [10] must be designed to achieve high performance with minimum cost. While the offset strip fins geometry is one of the highest performing surfaces it is also quite expensive to manufacture. This necessitates the use of all prime surface heat exchangers with no brazing as part of the heat exchanger design and acquisition process.

As presented in Chap. 3, Compact Heat Exchangers (CHEs) transfer more energy in a cost-effective manner than other heat exchangers and save more energy when compared with standard technology such as shell and tube. It was further demonstrated that compact heat exchangers transfer heat from one fluid, either gas or liquid, to another. Compact Heat Exchangers (CHEs) have a significantly greater surface area per unit volume than conventional types of heat exchangers [17]. For the purposes of the Energy Efficiency performance and Capacity Scheme, also known as the Enhanced Capital Allowance (ECA) scheme, a CHE is defined as a heat exchanger with a surface to volume ratio of  $>200 \text{ m}^2/\text{m}^3$ .

#### **Energy Efficiency Performance and Capacity Scheme Also Known as the Enhanced Capital Allowance (ECA) Scheme**

The Scheme calls for manufacturers and importers of refrigeration equipment to establish that their products conform to certain requirements on energy efficiency, performance, and capacity. Such equipment is then “ECA Registered” and appears on what is known as the “Energy Technology List”. Anyone purchasing equipment from the list will be entitled to 100 % tax relief on their investment in the first year.

The Scheme has been developed by the Inland Revenue and DEFRA (the Department for Environment, Food & Rural Affairs) and is managed by the Carbon Trust.

(continued)

In order to meet the requirements of the new ECA Scheme, manufacturers must have their refrigeration equipment tested to prove that it conforms to various requirements on energy efficiency, performance, and capacity.

Compact heat exchangers are characterized by a high surface area per unit volume, which can result in a higher efficiency than conventional heat exchangers; in a significantly smaller volume (typically compact heat exchangers can achieve efficiencies of over 95 % CF (Cubic Foot); eighty percent for non-compact heat exchangers).

Compact heat exchangers transfer more energy in a cost-effective manner than other heat exchangers and save more energy when compared to standard technology. Investments in CHEs can only qualify for Enhanced Capital Allowances (ECA) if the specific product is named on the Energy Technology Product List.

The use of compact heat exchangers for both single- and two-phase applications in the process industries is being actively encouraged. Thermal Energy Transfer for Process Heat Application in Enhanced Mode.

Recent technological developments in next generation nuclear reactors have created renewed interest in nuclear process heat for industrial applications. The Next Generation Nuclear Plant (NGNP) will most likely produce electricity and process heat for hydrogen production. Process heat is not restricted to hydrogen production, but is also envisioned for various other technologies such as the extraction of iron ore, coal gasification, and enhanced oil recovery. To utilize process heat, a thermal device is needed to transfer the thermal energy from NGNP to the hydrogen plant in the most efficient way possible. There are several options for transferring multi-megawatt thermal power over such a distance.

One option is simply to produce only electricity, transfer it by wire to the hydrogen plant, and then reconvert the electric energy to heat via Joule or induction heating. Electrical transport, however, suffers energy losses of 60–70 % because of the thermal-to-electric conversion inherent in the Brayton cycle. A second option is to transport thermal energy via a single phase forced convection loop where a fluid is mechanically pumped between heat exchangers at the nuclear and hydrogen plants. High temperatures, however, present unique challenges for materials and pumping. Single phase, low pressure helium is an attractive option for NGNP, but is not suitable for a single-purpose facility dictated to hydrogen production because low pressure helium requires higher pumping power and makes the process very inefficient. A third option is two-phase heat transfer utilizing a high temperature *Thermosyphon*. Heat transport occurs via evaporation and condensation, and the heat transport fluid is recirculated by gravitational force. Thermosyphons have the ability to transport heat at high rates over appreciable distances, virtually isothermally, and without any requirement for external pumping devices [18].

Heat pipes and thermosyphons have the ability to transport very large quantities of heat over relatively long distances with small temperature loss (Zohuri). The applications of heat pipes and thermosyphons require heat sources for heating and

heat sinks for cooling. The development of the heat pipe and thermosyphon was originally directed toward space applications. However, the recent emphasis on energy conservation has promoted the use of heat pipes and thermosyphons as components in terrestrial heat recovery units and solar energy systems. Thermosyphons have less thermal resistance, wider operating limits (the integrity of the wick material might not hold in heat pipes at very high temperatures), and lower fabrication costs than capillary heat pipes, which makes a thermosyphon a better heat recovery thermal device. Recent study and analysis by Mahdavi et al. [19], based on numerical investigation of hydrodynamics and thermal performance of a specially configured heat pipe for high-temperature thermal energy storage systems, where the compressibility of the working fluid and viscous dissipation were taken into account, is a promising way of showing better heat transfer between working fluids where results showed that the thermal resistance decreases with the increase of the operating temperature and vapor radius while it increases with the increase of the heat input.

Perhaps the most important aspect of thermosyphon technology is that it can easily be turned off when required, whereas a heat pipe cannot be turned off. This safety feature makes the licensing of NGNP process heat transfer systems comparatively easier, and it can easily be shown that the thermosyphon systems have the potential and benefits of being used in order to transfer process heat from the nuclear plant to the hydrogen production plant.

The other advantages of the thermosyphon devices are their capabilities and abilities to transport very large amounts of heat in virtually isothermal conditions with minimum loss of heat at high rates over considerable distances in a passive mode, without any requirement for external pumping devices. As we have discussed before as part of licensing constraint for safety demands there must be a proper distance between the nuclear power plant and hydrogen production plant, therefore making use of heat pipe and thermosyphon devices easily satisfies this requirement in a very cost effective and efficient way.

For a hot fluid inlet temperature of less than about 675 °C, stainless steel material can be used for the heat exchanger, which has reasonable cost. However, for higher inlet temperatures in heat exchangers associated with higher turbine inlet temperatures, super alloys are essential, which increases the material cost of the exchanger alone by a factor of 4–5.

Power generation is generally in Megawatts. There is a need for small power generation for remote areas that do not have enough grid power availability, emergency power, uninterrupted power requirement, and other reasons. With the decontrol on centralized power generation monopoly, more and more use of distributed power generation is taking place. The common mode is to generate the power by a Diesel engine. This is a costly power generation. The alternative way is to generate electricity using a gas turbine in a simple Brayton cycle. Gas turbine technology has advanced considerably over the last 60 years and power generation on a large scale (in Megawatts) is common particularly in hydro and thermal power plants. While gas turbine technology with smaller power range (to produce power in 5–500 kW range) has been developed, it is very costly.

Compact heat exchangers can also be seen in gas turbines using the combined cycle approach. The gas turbines developing power in the 5–200 kW range are referred to as microturbines and those in the 200–500 kW range as miniturbines (McDonald). We will now briefly summarize microturbine technology.

### Definition of Microturbine

A “microturbine” implies a small compact gas turbine based power system and includes a turbo-compressor (a turbine and compressor on a single shaft), a combustion chamber and a generator, with a recuperator as an optional component. However, almost all microturbines require recuperators to achieve desirable system thermodynamic efficiency.

If the simple Brayton cycle is employed and modified to include a recuperator (which will transfer heat from the turbine exhaust to preheat compressed high pressure air before going to the combustion chamber), it will require less fuel to obtain the desired turbine inlet temperature of compressed air and also the optimum pressure ratio (either for compressor or turbine) is reduced to typically 3–4. This improves the thermal efficiency of the cycle Zohuri [2–4].

Alternatively, a regenerator can also be used replacing a recuperator. A number of regenerative cycles are presented by McDonald and Wilson [17]. However, the durability and air-to-gas leakage problems are serious enough that the recuperator is not being considered after over 50 years of development. The regenerator development also started after the Second World War. Very high performance brazed plate-fin type recuperators have been developed and are being used in large systems today. With cost pressures, the modern recuperator designs for microturbine systems use prime surfaces on both fluid sides with no brazing, just stacking, and are welded at the side edges to form air flow passage, to prevent the leaks and mixing of the fluids. This allows high heat transfer performance with low pressure drop, an essential design requirement today. Since both fluids are gases (compressed air and turbine exhaust gas) in the heat exchanger, the design of inlet and outlet manifolds is challenging to ensure good flow distribution through the core on both fluid sides [12].

### Brazing Process

Brazing is a metal-joining process whereby a filler metal is heated above melting point and distributed between two or more close-fitting parts by capillary action. The filler metal is brought slightly above its melting (liquids) temperature while protected by a suitable atmosphere, usually a flux. It then flows over the base metal (known as wetting) and is then cooled to join the workpieces together. It is similar to soldering, except the temperatures used to melt the filler metal are higher for brazing.

When using a recuperator in a microturbine, the recuperator cost is about 25–30 % of the microturbine system. When a significant cost reduction is necessary, the brazed plate-fin type costly recuperator is not acceptable.

The alternative is to use a high performance prime surface recuperator without any brazing. This avoids the costly fin manufacturing and brazing thus reducing the cost of the recuperator without performance reduction [11].

As part of design criteria for such recuperator one should follow the major steps toward design and development of a gas-to-gas recuperator of compact heat exchanger in this case (R. K. Shah) [12]:

- Find out approximate core size using prior empirical data and finite difference tools.
- Manufacture heat transfer surface and test to determine  $j$  (Colburn factor  $j = St Pr^{2/3}$ ) and  $f$  (Fanning friction factor, some text book show that as  $f_c$ ) nodes versus Reynolds (Re) number design data. The basic performance data for an enhanced surface are shown as curves of the Colburn factor  $j$ , and the Fanning friction factor  $f_f$ , plotted versus Reynolds number Re. Kays and London [13] present  $j$  and  $f$  vs. Re for a large number of compact surfaces, in one of the first comprehensive collections of data on enhanced surfaces for compact heat exchangers.
- Determine core size and tool sample plates for manufacturing development and test scores.
- Analyze flow and temperature in the core using Computational Fluid Dynamics (CFD) to predict flow and temperature distribution, as well as verify performance.
- Compute thermal stresses using transient temperature distribution models input into the finite element analysis program. If thermal stresses are not acceptable, modify appropriately the heat transfer surface design.
- Build cores, instrument, and test to verify thermal models.
- Refine the design to mitigate risks brought to light by analysis and test results.

Some of the materials used for the compact heat exchangers (recuperator) are: 300 series stainless steel (AISI 347 SS) for temperatures below about 675 °C, Inconel 625, Inconel 803, Haynes 120, Haynes 214, and PM2000 materials up to about 900 °C. For a 50 kW microturbine, the recuperator would weigh about 40 kg and the thin foil stainless steel would cost about \$12/kg. Thus the rounded off recuperator material cost would be about \$500 (Refer to McDonald).

The plate-fin recuperator technology and manufacturing processes are known, there is good design flexibility, and the recuperator would be light weight. There are some important limitations for the plate-fin design: high material and capital cost, long braze cycle, potential for high repair rate, limited material flexibility, complicated assembly, and difficult automated manufacturing. Thus the current emphasis is on the development of a recuperator using primary surface only with the following attributes (R. K. Shah):

- Basic core construction consists of a Laser welded stack of stamped plates (one or two parts).
- Simple construction leads to highly robust design.
- Fully automated Laser welding process is possible to seal side edges and form flow passages on one fluid side. Laser welding eliminates the high cost of nickel braze materials that are traditionally used in high temperature heat exchangers.

In order for combined cycle in the form of Brayton cycle configuration to be economically viable, the recuperator or heat exchanger implemented in it, as one of the components of the system, must be cost effective and compact for applications that require compact packaging. One such application is a hybrid engine with a microturbine generating electricity at the maximum efficiency and the hybrid or direct-drive vehicles then running on the electricity. For an automotive application with an engine power rating of 65–100 kW and cost \$25/kW, the recuperator should be manufactured for about \$150. Such an exchanger should be operating at high temperatures, have low-cost manufacturing methods, and be easy to replace or maintain (McDonald and Wilson) [10].

In summary, when one is looking for a special surface geometry to enhance heat transfer in an industrial heat exchanger application, in particular for next generation of nuclear plants (NGNP), we have a large number of options to choose from. Now the question is:

**How can one compare the performance improvement given by various enhanced surfaces?**

Certainly, one can judge the relative heat transfer enhancement for selected geometries by comparing the heat transfer coefficients or dimensionless heat transfer parameters (i.e., Nusselt number, Stanton number, etc.) yielded by each enhanced surface. However, this will only give a partial indication of performance [10, 15].

Enhanced surfaces do provide a greater heat transfer coefficient, but they also lead to increased fluid flow friction and pressure drop. Sometimes, the benefits gained from heat transfer enhancement are not great enough to offset the increased friction losses. Clearly, then, the performance goal is to gain maximum enhancement of heat transfer with minimum penalty on pumping power. However, this balance is difficult to quantify in a manner that allows straightforward comparisons between various enhanced surface geometries.

Generally speaking, heat transfer surfaces can be used for three purposes:

1. To make heat exchangers more compact in order to reduce their overall volume, and possibly their cost,
2. To reduce the pumping power required for a given heat transfer process, or
3. To increase the overall  $UA$  value of the heat exchanger.

### **Heat Exchanger Value of $UA$**

Nearly all heat transfer equipment can be analyzed from the following basic design equation

$$q = UA\Delta T \quad (1)$$

which relates the heat flow rate or duty ( $q$ ) to the driving force or temperature difference ( $\Delta T$ ) by a proportionality constant ( $UA$ ), where  $U$  is a coefficient and  $A$  is the heat transfer area. Heat exchanger analyses usually involve the process of determining the  $UA$  required for the process to operate and comparing that to the  $UA$  available.

The  $UA$  required is normally determined based only on thermodynamics. The  $UA$  available is calculated from the heat exchanger geometry and the transport properties of the fluid.

A higher  $UA$  value can be exploited in either of two ways:

4. To obtain an increased heat exchange rate for fixed fluid inlet temperatures, or
5. To reduce the mean temperature difference for the heat exchange; this increases the thermodynamic process efficiency, which can result in a saving of operating costs.

Enhancement techniques can be separated into two categories [20]:

**1. Passive:**

Passive methods require no direct application of external power. Instead, passive techniques employ special surface geometries or fluid additives which cause heat transfer enhancement

**2. Active:**

On the other hand, active schemes such as electromagnetic fields and surface vibration do require external power for operation.

The majority of commercially interesting enhancement techniques are passive ones. Active techniques have attracted little commercial interest because of the costs involved, and the problems that are associated with vibration or acoustic noise [21].

Special surface geometries provide enhancement by establishing a higher  $hA$  per unit base surface area. Where  $h$  is the heat transfer coefficient and  $A$  is the heat transfer surface area on the same fluid side for which the value of  $h$  is mentioned.

Clearly, there are three basic ways of accomplishing this [21]:

1. Increase the effective heat transfer surface area ( $A$ ) per unit volume without appreciably changing the heat transfer coefficient ( $A$ ). Plain fin surfaces enhance heat transfer in this manner.
2. Increase  $h$  without appreciably changing  $A$ . This is accomplished by using a special channel shape, such as a wavy or corrugated channel, which provides

mixing due to secondary flows and boundary-layer separation within the channel. Vortex generators also increase  $h$  without a significant area increase by creating longitudinally spiraling vortices that exchange fluid between the wall and core regions of the flow, resulting in increased heat transfer.

3. Increase both  $h$  and  $A$ . Interrupted fins (i.e., offset strip and louvered fins) act in this way. These surfaces increase the effective surface area and enhance heat transfer through repeated growth and destruction of the boundary layers.

In forced-convection heat transfer between a gas and a liquid, the heat transfer coefficient of the gas may be 10–50 times smaller than that of the liquid. The use of specially configured surfaces can be used to reduce the gas-side thermal resistance. For heat transfer between two gases, the difficulty in inducing the desired heat exchange is even more pronounced. In this case especially, the use of enhanced surfaces can substantially reduce heat exchanger size. This is the motivation behind the design of a category of heat exchangers with reduced size and greatly enhanced gas-side heat transfer, which are referred to as “compact”.

### 7.3 Gas Turbine Developments

Brayton cycle drive efficiency started having an impact when the gas turbines experienced phenomenal progress and growth since their first successful development in the 1930s. The early gas turbines built in the 1940s and even 1950s had simple-cycle efficiencies of about 17 % because of the low compressor and turbine efficiencies and low turbine inlet temperatures due to metallurgical limitations of those times. Therefore, gas turbines found only limited use despite their versatility and their ability to burn a variety of fuels. The efforts to improve the cycle efficiency concentrated in three areas:

1. Increasing the turbine inlet (or firing) temperatures.
2. Increasing the efficiencies of turbo-machinery components.
3. Add modifications to the basic cycle.

The simple-cycle efficiencies of early gas turbines were practically doubled by incorporating intercooling, regeneration (or recuperation), and reheating. The back work ratio of a gas-turbine cycle improves as a result of intercooling and reheating. However, this does not mean that the thermal efficiency will also improve. Intercooling and reheating will always decrease the thermal efficiency unless they are accompanied by regeneration. This is because intercooling decreases the average temperature at which heat is added, and reheating increases the average temperature at which heat is rejected.

Therefore, in gas-turbine power plants, intercooling and reheating are always used in conjunction with regeneration. These improvements, of course, come at the expense of increased initial and operation costs, and they cannot be justified unless the decrease in fuel costs offsets the increase in other costs. In the past, the relatively

low fuel prices, the general desire in the industry to minimize installation costs, and the tremendous increase in the simple-cycle efficiency due to the first 2 (Fig. 7.4 *T-s* Diagram) increased efficiency options to approximately 40 % which left little desire for incorporating these modifications. With continued expected rise in demand and cost of producing electricity, these options will play an important role in the future of gas-turbine power plants. The purpose of this paper is to explore this third option of increasing cycle efficiency via intercooling, regeneration, and reheating [16]. - Figure 7.3 is an illustration of a recuperator with different configurations.

Gas turbines installed until the mid-1970s suffered from low efficiency and poor reliability. In the past, large coal and nuclear power plants dominated the base-load electric power generation (Point 1 in Fig. 7.4). Base load units are on line at full capacity or near full capacity almost all of the time. They are not easily nor quickly adjusted for varying large amounts of load because of their characteristics of operation [22]. However, there has been a historic shift toward natural gas-fired

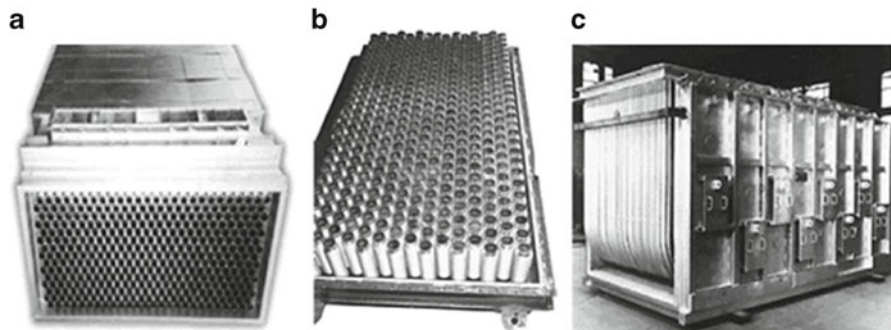


**Fig. 7.3** Presentation of different recuperator configurations (a) vertical recuperator, (b) recuperator inside, and (c) horizontal recuperator

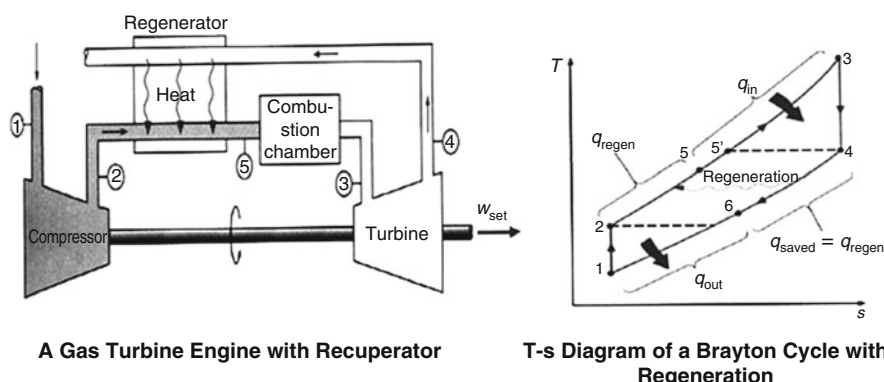


**Fig. 7.4** Illustration of a gas turbine engine along with its *T-s* diagram

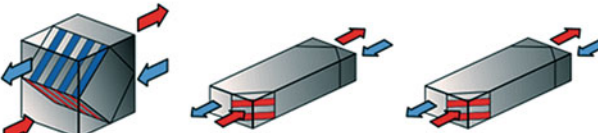
turbines because of their higher efficiencies, lower capital costs, shorter installation times, better emission characteristics, the abundance of natural gas supplies, and shorter start up times (Point 1 in Fig. 7.4). Now electric utilities are using gas turbines for base-load power production as well as for peaking, making capacity at maximum load periods, and in emergency situations because they are easily brought on line or off line (Point 2 in Fig. 7.4). The construction costs for gas-turbine power plants are roughly half that of comparable conventional fossil fuel steam power plants, which were the primary base-load power plants until the early 1980s, but peaking units are much higher in energy output costs. A recent gas turbine manufactured by General Electric uses a turbine inlet temperature of 1425 °C (2600 °F) and produces up to 282 MW while achieving a thermal efficiency of 39.5 % in the simple-cycle mode. Over half of all power plants to be installed in the foreseeable future are forecast to be gas turbine or combined gas-steam turbine types (see Fig. 7.3).

If the simple Brayton cycle is modified to include a recuperator (which will transfer heat from the turbine exhaust to preheat compressed high pressure air before going to the combustion chamber), it will require less fuel to obtain the desired turbine inlet temperature of compressed air and also the optimum pressure ratio (either for compressor or turbine) is typically reduced to 3–4. This improves the thermal efficiency of the cycle. Alternatively, a regenerator can also be used replacing a recuperator. A number of regenerative cycles are presented by McDonald and Wilson [17].

## 7.4 The Brayton Cycle with Recuperator

A recuperator is a special purpose counter-flow energy recovery heat exchanger positioned within the supply and exhaust air streams of an air handling system, or in the exhaust gases of an industrial process, in order to recover the waste heat. Figure 7.5, below, shows the three major configurations of a recuperator.

In gas-turbine engines, the temperature of the exhaust gas leaving the turbine is often considerably higher than the temperature of the air leaving the compressor. Therefore, the high-pressure air leaving the compressor can be heated by transferring heat to it from the hot exhaust gases in a counter-flow heat exchanger, which is also known as a regenerator or recuperator (see Fig. 7.4 on point-1). Gas turbine regenerators are usually constructed as shell-and-tube type heat exchangers using very small diameter tubes, with the high pressure air inside the tubes and low pressure exhaust gas in multiple passes outside the tubes [22]. The thermal efficiency of the Brayton cycle increases as a result of regeneration since the portion of energy of the exhaust gases that is normally rejected to the surroundings is now used to preheat the air entering the combustion chamber. This, in turn, decreases the heat input (thus fuel) requirements for the same net work output. Note, however, that the use of a regenerator is recommended only when the turbine exhaust temperature is higher than the compressor exit temperature. Otherwise, heat will

Principle	
Profile	
Counter current Heat exchanger	Vertical flat panel
Efficiency	50 – 70 %
	Horizontal flat panel
	Cellular
	70 – 80 %
	85 – 99 %

**Fig. 7.5** Types of recuperator, or cross plate heat exchanger

flow in the reverse direction (to the exhaust gases), decreasing the efficiency. This situation is encountered in gas turbines operating at very high-pressure ratios (Point 1 on Fig. 7.4).

The highest temperature occurring within the regenerator is the temperature of the exhaust gases leaving the turbine and entering the regenerator (Point 1 in Fig. 7.4). The gas turbine recuperator receives air from the turbine compressor at pressures ranging from 73.5 to 117 psi and temperatures from 350 to 450 °F (Point 3 in Fig. 7.4). Under no conditions can the air be preheated in the regenerator to a temperature above this value. In the limiting (ideal) case, the air will exit the regenerator at the inlet temperature of the exhaust gases. Air normally leaves the regenerator at a lower temperature (Point 1 in Fig. 7.4). Gas turbine exhaust gas passes over the other side of the recuperator at exhaust temperatures ranging from 750 to 1000 °F. Compressor air temperatures are now raised to higher temperatures up to about 750–900 °F as the air enters the combustor. Turbine exhaust gases are then reduced to between 500 and 650 °F from the original 750 to 1000 °F. This heat recovery contributes appreciably to the turbine fuel rate reduction and increase in efficiency (Point 3 in Fig. 7.4). The regenerator is well insulated and any changes in kinetic and potential energies are neglected.

A regenerator with a higher effectiveness will save a greater amount of fuel since it will preheat the air to a higher temperature prior to combustion (Point 1 in Fig. 7.4). However, achieving a higher effectiveness requires the use of a larger regenerator, which carries a higher price tag and causes a larger pressure drop thus reducing shaft horsepower. Pressure drop through the regenerator or recuperator is important and should be kept as low as practical on both sides. Generally, the air pressure drop on the high-pressure side should be held below 2 % of the compressor total discharge pressure. The gas pressure drop on the exhaust side (hot side) should

be held below 4 in. of water. Therefore, the use of a regenerator with a very high effectiveness cannot be justified economically unless the savings from the fuel costs exceed the additional expenses involved. The effectiveness of most regenerators used in practice is below 0.85. The thermal efficiency of an ideal Brayton cycle with regeneration depends on the ratio of the minimum to maximum temperatures as well as the pressure ratio. Regeneration is most effective at lower pressure ratios and low minimum-to-maximum temperature ratios.

## 7.5 The Brayton Cycle with Intercooling, Reheating, and Regeneration

The net work of a gas-turbine cycle is the difference between the turbine work output and the compressor work input, and decreasing the compressor work, increasing the turbine work or both can increase it. Carrying out the compression process in stages and cooling the gas in between the lower and higher-pressure stages will decrease the work required to compress a gas between two specified pressures. This is called multistage compression with intercooling. As the number of stages is increased, the compression process becomes nearly isothermal at the compressor inlet temperature, and the compression work decreases (Point 1 Fig. 7.7). However, a source of a cooling fluid is required.

Likewise, the work output of a turbine operating between two pressure levels can be increased by expanding the gas in stages and reheating it in between—utilizing multistage expansion with reheating. This process involves dividing the turbine into two parts, a high-pressure and a low-pressure turbine. After the gas passes through the high-pressure turbine it is extracted from the turbine and admitted to a second combustor. Reheated gas flows into the low-pressure turbine, which may be on a separate shaft, or both turbines and the compressor, which may be connected to a common shaft. In either case, the reheat process is thermodynamically the same [22]. This is accomplished without raising the maximum temperature in the cycle. As the number of stages is increased, the expansion process becomes nearly isothermal.

This is based on a simple principle:

- The steady-flow compression or expansion work is proportional to the specific volume of the fluid. Therefore, the specific volume of the working fluid should be as low as possible during a compression process and as high as possible during an expansion process. This is precisely what intercooling and reheating accomplish.

Combustion in gas turbines typically burns 1/4 the amount of oxygen available to avoid excessive temperatures. Therefore, the exhaust gases are rich in oxygen, and reheating can be accomplished by simply spraying additional fuel into the

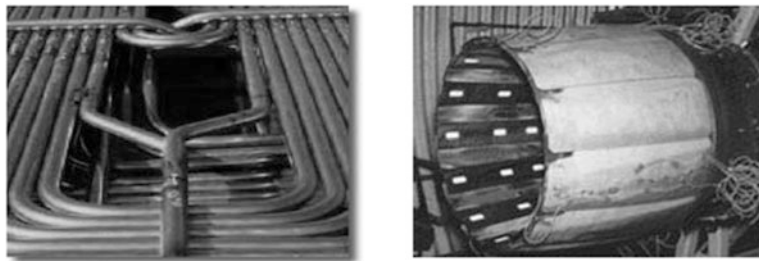


**Fig. 7.6** Illustration of jet engine with reheat principle

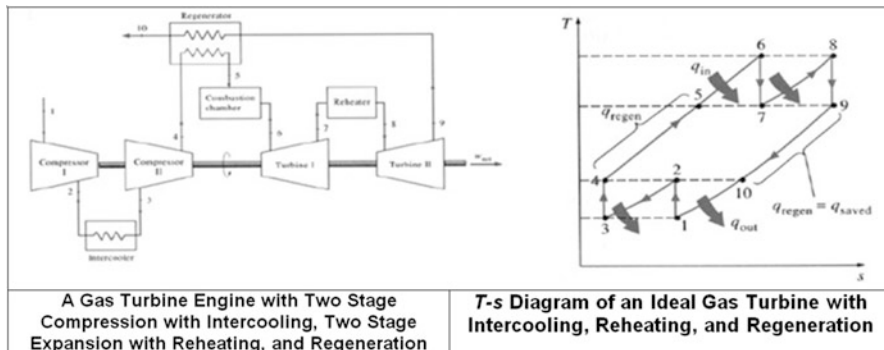


**Fig. 7.7** Illustration of two stage gas turbine along with its *T-s* diagram

exhaust gases between two expansion states. This is how an afterburner works in a jet engine as well (see Fig. 7.6).

The working fluid leaves the compressor at a lower temperature and the turbine at a higher temperature, when intercooling and reheating are utilized. This makes regeneration more attractive since a greater potential for regeneration exists. Also, the gases leaving the compressor can be heated to a higher temperature before they enter the combustion chamber because of the higher temperature of the turbine exhaust.

The gas enters the first stage of the compressor and is compressed isentropically to an intermediate pressure and cooled at constant pressure. It is then compressed in the second stage isentropically to the final pressure. The combustion chamber must then heat to the inlet temperature for the first turbine. The gas now enters the regenerator, where it is heated at a constant pressure. In an ideal regenerator, the gas will leave the regenerator at the temperature of the turbine exhaust. The gas enters the first stage of the turbine and expands isentropically where it enters the reheater. It is reheated at constant pressure, where it enters the second stage of the turbine. The gas exits the turbine and enters the regenerator, where it is cooled at a constant pressure. The cycle is completed by cooling the gas to the initial state (or purging the exhaust gases) (Fig. 7.7).

In the analysis of the actual gas-turbine cycles, the irreversibility present within the compressor, the turbine, and the regenerator as well as the pressure drops in the heat exchangers must be taken into consideration.

## 7.6 Modeling the Brayton Cycle

Any external combustion or heat engine system is always at a disadvantage to an internal combustion system. The internal combustion systems used in current jet engine and gas turbine power systems can operate at very high temperatures in the fluid, and cool the structures containing the fluid to achieve high thermodynamic efficiencies. In an external energy generation system, like a reactor powered one, all of the components from the core to the heat exchangers heating the working fluid must operate at a higher temperature than the fluid. This severely limits the peak cycle temperature compared to an internal combustion system. This liability can be overcome to a certain extent by using multiple expansion turbines and designing highly efficient heat exchangers to heat the working fluid between expansion processes. Typically the combustion chamber in a gas turbine involves a pressure drop of 3–5 % of the total pressure. Efficient liquid salt to air heat exchangers can theoretically be designed with a pressure drop of less than 1 %. This allows three to five expansion cycles to achieve a pressure drop comparable to a combustion system. Multiple turbines operating at different pressures have been common in steam power plants for a number of years. In this study two to five gas turbines operating on a common shaft were considered. Multiple expansion turbines allow a larger fraction of the heat input to be provided near the peak temperature of the cycle significantly improving the thermodynamic efficiency. The exhaust from the last turbine is provided to the Heat Recovery Steam Generator (HRSG) to produce the steam used in the Rankine bottoming cycle. After the hot air passes through the HRSG it is exhausted to the atmosphere. A detailed comparison of this system was made with a recuperated stand alone Brayton cycle and the dual cycle appears to be more efficient for open systems. Further information can be found in references by Zohuri [2–6] and McDaniel et al. [7, 8].

## 7.7 Conclusion

The Next Generation Nuclear Plant (NGNP), a Very High Temperature Gas-Cooled Reactor (VHTR) concept of Generation IV, will provide the first demonstration of a CO<sub>2</sub> closed-loop and an open air loop Brayton cycle at a commercial scale, producing a few hundred megawatts of power in the form of electricity and hydrogen (Mizia [1], Zohuri [2, 4]). The power conversion unit (PCU) for the NGNP will take advantage of the significantly higher reactor outlet temperatures of the VHTRs to provide higher efficiencies than can be achieved with the current

generation of light water reactors. Besides demonstrating a system design that can be used directly for subsequent commercial deployment, the NGNP will demonstrate key technology elements that can be used in subsequent advanced power conversion systems for other Generation IV reactors. In anticipation of the design, development and procurement of an advanced power conversion system for the NGNP, the system integration of the NGNP, and hydrogen plant was initiated to identify the important design and technology options that must be considered in evaluating the performance of the proposed NGNP.

As part of renewable energy and the system integration of the VHTRs and the hydrogen production plant, Intermediate Heat Exchangers (IHXs) are used to transfer the process heat from VHTRs to the hydrogen production plants (Zohuri [23]). Therefore, the design and acquisition of the right configuration of the ultimate Intermediate Heat Exchanger (IHX) is very important. An IHX is one of the essential components in the VHTR systems since it transfers reactor core heat to the other systems for the application of electricity generation or hydrogen production. Therefore, its effectiveness is directly related to the overall system efficiency and economics. Generally, the VHTR systems use gas coolant having poor heat transfer capability that requires a very large size and heat transfer area. For this reason, a Compact Heat Exchanger (CHE) with a large surface area density such as Printed Circuit Heat Exchanger (PCHE) is being considered as a potential candidate for an IHX, replacing the classical shell and tube design. This type of heat exchanger is widely used in industry, especially for gas-to-gas or gas-to-liquid heat exchange [24].

If the number of compression and expansion stages is increased, the ideal gas-turbine cycle with intercooling, reheating, and regeneration will approach the Ericsson cycle and the thermal efficiency will approach the theoretical limit (the Carnot efficiency). That is, the thermal efficiency almost doubles as a result of regeneration, intercooling, and reheating. However, the contribution of each additional stage to the thermal efficiency is less and less, and the use of more than two or three stages usually cannot be justified economically.

## References

1. Mizia, R.E. 2008. Next generation nuclear plant intermediate heat exchanger acquisition strategy. INL/EXT-08-14054, April 2008.
2. Zohuri, B. 2015. *Combined cycle driven efficiency for next generation nuclear power plants: An innovative design approach*. New York: Springer Publishing Company.
3. Zohuri, B., and Patrick McDaniel. 2015. *Thermodynamics in nuclear power plant*. New York: Springer Publishing Company.
4. Zohuri, B. 2014. *Innovative open air Brayton combined cycle systems for the next generation nuclear power plants*. Albuquerque, NM: University of New Mexico Publications.
5. Zohuri, B., and P. McDaniel. 2015. A comparison of a recuperated open cycle (air) Brayton power conversion system with the traditional steam Rankine cycle for the next generation nuclear power plant. Will be published in Nuclear Technology, October 2015.

6. Zohuri, B., P. McDaniel, and C.R.E. de Oliveira. 2014. A comparison of a recuperated open cycle (air) Brayton power conversion system with the traditional steam Rankine cycle for the next generation nuclear power plant. *ANS Transactions*, June 2014.
7. McDaniel, P.J., B. Zohuri, and C.R.E. de Oliveira. 2014. A combined cycle power conversion system for small modular LMFBRs. *ANS Transactions*, September 2014.
8. McDaniel, P.J., C.R.E. de Oliveira, B. Zohuri, and J. Cole. 2012. A combined cycle power conversion system for the next generation nuclear power plant. *ANS Transactions*, November 2012.
9. Forsberg, Charles, Pat McDaniel, and B. Zohuri 2015. Variable electricity and steam from salt, helium, and sodium cooled base-load reactors with gas turbines and heat storage. *Proceedings of ICAPP 2015*, May 03-06, 2015—Nice (France) Paper 15115.
10. McDonald, C.F., and D.G. Wilson. 1996. The utilization of recuperated and regenerated engine cycles for high-efficiency gas turbines in the 21st century. *Applied Thermal Engineering* 16: 635–653.
11. Huzayyin, Omar Ahmed Soliman. 2011. Computational modeling of convective heat transfer in compact and enhanced heat exchangers. University of Cincinnati, 193 pages; 3475151.
12. Shah, R.K. Compact heat exchangers for microturbines. Rochester Institute of Technology Dept. of Mechanical Engineering 76 Lomb Memorial Drive Rochester NY 14623-5604 USA.
13. McDonald, C.F. 2000. Low cost recuperator concept for microturbine applications. ASME Paper No. 2000-GT-167, ASME, New York, NY.
14. McDonald, C.F. 2000. Low-cost compact primary surface recuperator concept for microturbines. *Applied Thermal Engineering* 20: 471–497.
15. Kays, W.M., and A.L. London. 1984. *Compact heat exchangers*, 3rd ed. New York: McGraw-Hill.
16. Cengel, Y.A., and M.A. Boles. 2001. *Thermodynamics: An engineering approach*, 4th ed. Boston, MA: McGraw-Hill College.
17. Necati Ozisik, M. 1985. *Heat transfer a basic approach*. New York: McGraw-Hill.
18. [www.intechopen.com](http://www.intechopen.com)
19. Mahdavi, Mahboobe, Songgang Qiu, and Saeed Tiari. 2015. Numerical investigation of hydrodynamics and thermal performance of a specially configured heat pipe for high-temperature thermal energy storage systems. *Applied Thermal Engineering* 81: 325–337.
20. Bergles, A.E., R.L. Webb, and G.H. Junkan. 1979. Energy conservation via heat transfer enhancement. *Energy* 4: 193–200.
21. Stone, K. 1996. Review of literature on heat transfer enhancement in compact heat exchangers. Air Conditioning & Refrigeration Center Mechanical & Industrial Engineering Dept., University of Illinois, 1206 West Green Street Urbana IL 61801.
22. Boyen, J.L. 1975. *Practical heat recovery*. New York: John Wiley & Sons Inc.
23. Zohuri, B. 2015. *Next generation nuclear plants driven hydrogen production plants via intermediate heat exchanger a renewable source of energy*. New York: Springer Publishing Company.
24. Oh, C.H., and Eung S. Kim. Design option of heat exchanger for the next generation nuclear plant. 4th International Topical Meeting on High Temperature Reactor, September 2008, Idaho National Laboratory Report INL/CON-08-14278.

# **Chapter 8**

## **Compact Heat Exchangers Application in New Generation of CSP**

Recent studies by researchers and engineers around the globe show another promising aspect of Compact Heat Exchangers (CHEs) driving an efficient Concentrated Solar Power (CSP) system and how CHEs can be reviewed as a device for future applications for a new generation of high temperature solar receivers. In a case like this a combined cycle can also be introduced into the CSP system as part of another overall renewable source of energy to produce additional electricity to impact the national electrical grid system during off peak and on peak demand on electricity; an example is the recent Department of Energy efforts for such a renewable source of energy spear headed by Idaho National Laboratory (INL).

### **8.1 Introduction to Concentrated Solar Power (CSP)**

Concentrated Solar Power has been known to human being for centuries and heat aspects have been applied to early generations of mankind. It is no surprise to know from history the myths of concentrated solar power as the very first generation of directed energy weapons by the famous Greek mathematician, physicist, engineer, inventor, and astronomer, Archimedes of Syracuse, where he used different mirrors to collect sun beams and focus them on the Roman's fleet in order to destroy enemy ships with fire. This is known as The Archimedes Heat Ray.

In recent years the same concentrated solar power is far from destroying the Roman's fleet with its energy and has found a peaceful way of delivering its energy as a renewable source of energy both on and off peak by converting it to electricity. Although CSP with its solar farm panels (see Fig. 8.1) as part of a renewable energy source system is not delivering the same output of electricity as traditional fossil fuel, gas power, and nuclear plants, it shows a very promising path toward such a system considering what the green environment imposes on production of electricity and also could be part of hydrogen production plants where usage of compact heat exchangers come into play.



**Fig. 8.1** Illustration of a Solar Farm in Southern California. *Source:* U.S. Department of Energy—Energy Efficiency and Renewable Energy. Published by: U.S. Energy Information Administration

Usage of Photo-Voltaic (PV) cells technology at individual homes around urban areas that use solar power to generate more efficient electricity is becoming more and more popular and many consumers think of them as solar power systems. CSP technologies that concentrate sunlight to create heat that can be used to generate electricity are also becoming more popular. Some PV cells utilize CSP and most CSP application is on technologies where concentrated solar energy heats a fluid, gas, or solid which is then used to generate electricity using steam generated by the source of heat.

Concentrating solar power (CSP) is a utility-scale renewable energy option for generating electricity that is receiving considerable attention in the southwestern United States and other sunbelts worldwide.

CSP technologies use mirrors to reflect and concentrate sunlight onto receivers that collect the solar energy and convert it to heat. The thermal energy can then be used to produce electricity via a steam turbine or heat engine driving a generator. CSP systems can be classified by how they collect solar energy: power tower systems, linear concentrator systems, and dish/engine systems (see Fig. 8.2).

Power tower systems consist of numerous large, flat, sun-tracking mirrors, known as heliostats that focus sunlight onto a receiver at the top of a tower. The heated fluid in the receiver (see Fig. 8.3) is used to generate steam, which powers a turbine and a generator to produce electricity. Some power towers use water/steam as the heat-transfer fluid. Individual commercial plants can be sized to produce up to 200 MW of electricity [1].

Linear concentrator systems capture the sun's energy with large mirrors that reflect and focus the sunlight onto a linear receiver tube. The receiver contains a fluid that is heated by the sunlight and then used to create steam that spins a turbine generator to produce electricity. Alternatively, steam can be generated directly in the solar field, eliminating the need for costly heat exchangers. Currently, individual systems can generate about 80 MW of electricity.

Dish-Engine systems use parabolic dishes of mirrors to direct and concentrate sunlight onto a central engine that produces electricity. The dish/engine system

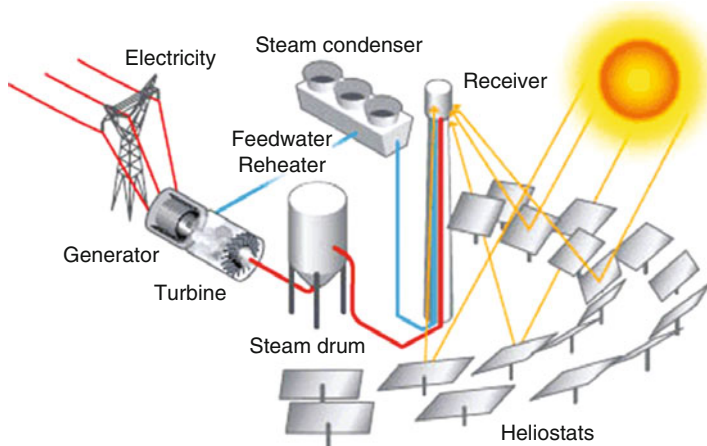


**Fig. 8.2** Depiction of CSP concept [1]

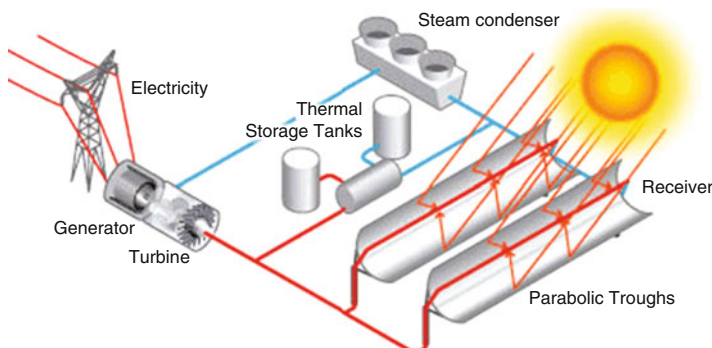


**Fig. 8.3** Depiction of CSP using parabolic trough concept with receiver [1]

produces relatively small amounts of electricity compared to other CSP technologies—typically in the range of 3–25 kW (see Fig. 8.4).

In Dish-Engine systems design concept mirrors are distributed over a parabolic dish surface to concentrate sunlight on a receiver fixed at the focal point. In contrast to other CSP technologies that employ steam to create electricity via a turbine, a dish-engine system uses a working fluid such as hydrogen that is heated up to 1200 °F in the receiver to drive an engine such as the Stirling engine. Each dish rotates along two axes to track the sun (see Fig. 8.5).

Under these conditions, power tower systems use a central receiver system, which allows for higher operating temperatures and thus greater efficiencies. Computer-controlled flat mirrors (called heliostats) track the sun along two axes and focus solar energy on a receiver at the top of a high tower. The focused energy is used to heat a transfer fluid (over 1000 °F) to produce steam and run a central power generator.

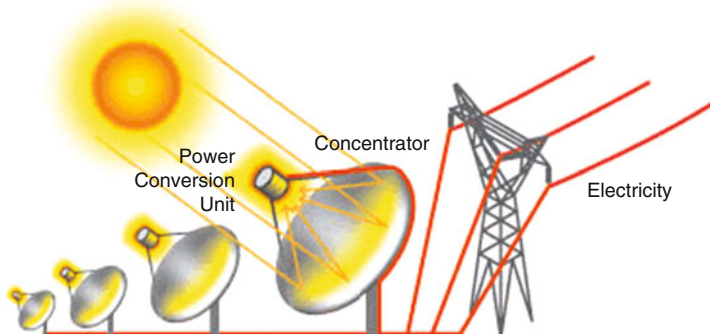


**Fig. 8.4** CSP dish engine systems



**Fig. 8.5** Depiction of dish-engine for CSP. (Courtesy of Sandia National Laboratories/Randy Montoya)

As part of the requirement for such a system to work properly, areas of high direct normal solar radiation should be taken into consideration in order to concentrate the sun's energy; it must not be too diffuse. This feature is captured by measuring the direct normal intensity (DNI) of the sun's energy. Production potential in the U.S. Southwest stands apart from the rest of the U.S.

Like other thermal power plants, such as natural gas, coal, and nuclear, some systems require access to water for cooling. In the case of concentrated solar power (CSP), it only requires small amounts of water to wash collection and mirror surfaces. CSP plants can utilize wet, dry, and hybrid cooling techniques to maximize efficiency in electricity generation and water conservation.

There are other key requirements for concentrating solar power plants that are beyond the scope of this book, and we encourage readers to refer to various literature and books available on the internet written on the subject of solar power.

Solar Powering America was formed by the U.S. Department of Energy (DOE), U.S. Department of Agriculture (USDA), Housing and Urban Development (HUD), and the Environmental Protection Agency (EPA) to coordinate their efforts in support of meeting the goals in the President's Climate Action Plan. These goals include doubling U.S. renewable energy deployment between 2012 and 2020 and installing 100 MW of solar on federally-assisted housing.

Solar power is more affordable, accessible, and prevalent in the United States than ever before. Since 2008, U.S. installations have grown 17-fold from 1.2 gigawatts (GW) to an estimated 20 GW today (see Fig. 8.6).

One obvious fact about CSP is the cost of electricity generation, where thermal energy can be used as a heat source via CSP to turn turbines or heat engine driving generators, is dropping drastically due to better design and reduction on cost of manufacturing solar panels and other associated components (see Fig. 8.7).

CSP technologies are deployed primarily in four system configurations: parabolic trough and linear Fresnel focus sunlight in a linear fashion whereas dish engines and power towers (also known as central receivers) focus sunlight to a point. Overall they can be listed as:

1. Parabolic trough.
2. Linear Fresnel also known as Compact Linear Fresnel Reflector (CLFR).
3. Power tower (Central receiver).
4. Dish engine.



**Fig. 8.6** Solar powering America [1]

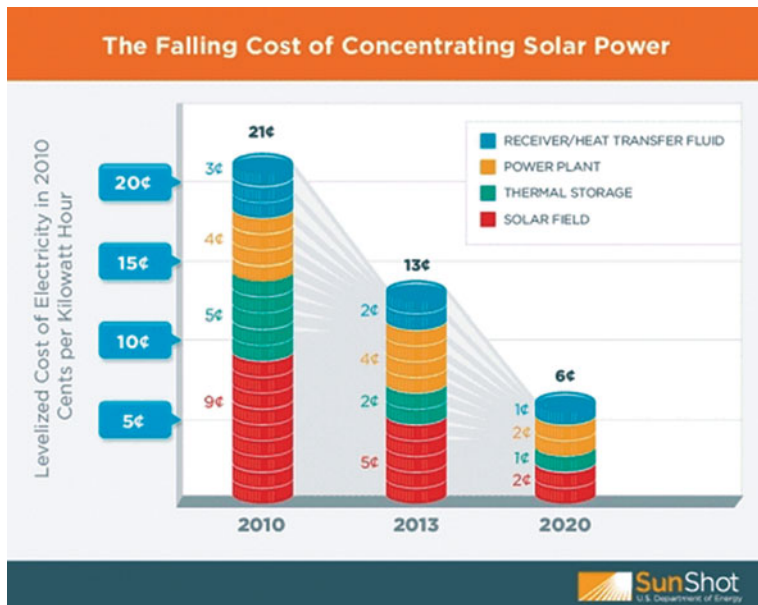


**Fig. 8.7** Falling cost of concentration solar power chart. (Courtesy of US Department of Energy)

Each of the above systems briefly was touched upon at the beginning of this section and further information with details and a description of each configuration can be found on the DOE website under SunShot Initiative Program.

The SunShot Initiative goal under the Department of Energy is to reduce the levelized cost of electricity generated by CSP to \$0.06/kWh or less, without any subsidy, by the year 2020.

Though CSP systems use different configurations to focus the sunlight, they share similar components such as collectors, receivers, power block, and thermal storage. DOE funds CSP research and development focused on developing the component technologies to achieve the technical and economic targets of the SunShot goal. The program also funds systems analysis on all of the CSP technologies to assess performance, longevity, and cost.

## 8.2 New Generation of High Temperature Solar Receivers for CSP

Power tower systems use a central receiver system, which allows for higher operating temperatures and thus greater efficiencies. Computer-controlled flat mirrors (called heliostats) track the sun along two axes and focus solar energy on a receiver at the top of a high tower. The focused energy is used to heat a transfer fluid

(over 1000 °F or 538 °C) to produce steam and run a central power generator (see Fig. 8.1).

Efficient utilization of the solar radiation resource is deemed necessary if solar electric power plants are to approach cost effectiveness relative to fossil fuel combustion plants. Systems based on cylindrical parabolic trough mirrors such as those which were built in the Mojave Desert in California in the 1980s were financially successful because of governmental subsidies in the form of tax breaks and preferential electricity tariffs, but suffer from relatively low conversion efficiencies both because of the necessity to invest significant energy in the circulation of a synthetic oil used as the working fluid for heat absorption, and because of the relatively low thermodynamic efficiency of the Rankine cycle at the moderate maximum temperatures allowed by the synthetic oil.

A solar thermal electric configuration with higher efficiency of solar-to-electric conversion has been proposed in the form of a central power tower system in which steam is generated and superheated in a central receiver by solar radiation reflected thereupon by fields of heliostats.

This system overcomes the aforementioned deficiencies of the parabolic trough technology by foregoing an intermediate working fluid and obviating the need for energy-intensive circulation, as well as by producing steam at a higher temperature which yields a higher thermal efficiency in a Rankine cycle steam turbine. It has been further proposed to construct a central solar power tower system in which the working fluid is compressed air, where the solar-heated compressed air is later used in a Brayton cycle gas turbine in place of compressed air heated by combustion of a fuel, with the possibility of further improving the overall efficiency of the system by adding, for example, a heat recovery steam generator and a Rankine cycle steam turbine in a combined-cycle configuration.

One problem encountered in the development of such a solar power tower system is the lack of availability of a solar receiver that can effectively heat a pressurized working fluid such as compressed air to the input temperature of a gas turbine, in the neighborhood of 1500 K.

Solar towers that use a combined Brayton–Rankine cycle, in which the Brayton cycle is decoupled from the Rankin cycle by means of the thermal storage system, have shown up as a cost-effective alternative due to their increased flexibility in the design and operation leading to better efficiencies and reduced costs.

The renewable resource, mainly the solar energy, can be used to produce electric energy on a large scale in solar thermal power stations, which concentrate sunlight at temperatures which range between 200 to 1200 °C and even more.

A conceptual configuration of a solar powered combined cycle power plant with a topping air Brayton cycle and a bottoming steam Rankine cycle is proposed by Mukhopadhyay and Ghosh [2]. The conventional Gas Turbine (GT) combustion chamber is replaced by a high-temperature solar thermal air heating system. During the daytime, a part of the exhaust air from the GT is bypassed to produce superheated steam in HRSG, which in turn runs a steam turbine and the remaining exhaust air from GT is utilized to charge molten salt, which acts as a storage medium. The heat energy of the molten salt is utilized to generate steam for 4 h

in another Heat Recovery Steam Generator (HRSG), when sunlight is not available. A similar innovative approach has been proposed by Zohuri [3, 4] for Next Generation Nuclear Plants (NGNP).

From the thermodynamic analysis, it is found that for the base case GT pressure ratio of 4, power obtained from the GT block is 1.75 MW, while total power obtained from the combined cycle is 2.28 MW. The overall thermal efficiency of the combined cycle at this pressure ratio is 25.39 %. The pressure ratio of the gas turbine has been varied from 2 to 20 and the optimum pressure ratio has been found where total power output of the combined cycle plant is the maximum.

The design of central receivers in solar thermal power plants in the case of Power Tower systems is critical for efficient plant operation and sufficient operational lifetimes. Power tower systems use a central receiver system, which allows for higher operating temperatures and thus greater efficiencies. Computer-controlled flat mirrors (called heliostats) track the sun along two axes and focus solar energy on a receiver at the top of a high tower. The focused energy is used to heat a transfer fluid (over 1000 °F or 538 °C) to produce steam and run a central power generator (see Fig. 8.1).

The high, non-uniform concentration ratios used in central receivers lead to high, non-uniform receiver temperatures. For the same operational conditions, small changes to the receiver design can make a big impact on the expected lifetime of the receiver. This is due to limitations of the receiver materials to high temperatures and thermal cycling.

### 8.3 Compact Heat Exchangers in High Temperature Solar Receivers of CSP

These days finding sustainable energy sources has become the subject of discussion worldwide. Renewable energy sources (solar, hydropower, wind, biomass etc.) have been found (Dincer et al.) [5] to offer cleaner and sustainable alternatives to the use of fossil fuels.

Solar energy is a promising renewable energy source, and there are two major technologies from which it can be used to generate electricity, namely;

- Photovoltaic (PV) cells: the use of PV cells to convert the sun's energy directly into electricity.
- Solar thermal system: the indirect use of solar energy for electricity generation where solar energy is converted into electricity by using the thermal energy absorbed from the sun (mostly to generate steam for electricity generation in the Rankine cycle).

Unfortunately, according to Bhargava [6] the investment cost per kilowatt for installing these two technologies happens to be the most expensive among the various means of power generation (both renewable and non-renewable). Therefore

it would be plausible if it is combined with other power plants to make it more economical.

Another study by Bhargava et al. [7] also revealed that in recent years, the use of gas turbines in the power generation market has become the preferred choice. The preference for the use of gas turbines can be traced not only to their low investment cost, but also to their high cycle efficiency coupled with small installation time, low level of CO<sub>2</sub> emissions, and single NOx emissions. It has been predicted by the United States of America's Department of Energy (DOE) in their vision-21 program, which was started in 1999–2000, that advances made in gas turbine technologies due to modifications to the Brayton cycle are expected to help achieve gas turbine based power plants efficiency of 75 % or more (Bhargava et al.) [7].

A Proposed Power Plant could be an Air-Based Gas-Turbine Bottoming-Cycles for Water-Free Solar Thermal Power (air-based bottoming-cycles for hybrid solar gas-turbine power plants) plant, which is a modification of the Brayton Cycle (as topping cycle) couple with another Brayton cycle (the bottoming cycle). The first modification is the incorporation of a solar air receiver which would heat up the air from the compressor before it enters the combustion chamber, thereby reducing the amount of gas that has to be burnt.

Bear in mind that, compared to solar Rankine Cycle systems, solar Brayton-cycle (gas turbine) systems have the following advantages. They are simple power conversion systems with higher reliability and lower operating and maintenance costs. They can be commercially attractive at smaller sizes. Their inherent low water requirements increase the sitting potential for central receivers in arid regions. They are more easily adaptable to fossil hybrid operation which increases the plant availability.

No matter if your approach to this combined cycle is gas turbine, nuclear power plant, or power tower concentrated solar power (CSP), where you have excessive heat waste that comes out of the receiver and can be put into useful work via combined cycle requires and depends on the selection of appropriate heat exchangers for waste heat recovery, recuperation, and intercooling.

In order to select the proper heat exchangers in particular when the real estate and foot print is under question or performance of these heat exchangers drive the selection toward Compact Heat Exchange (CHE), the following steps can apply:

1. Select an appropriate heat exchanger for use in the Proposed Power Plant after a literature review on available gas-to-gas heat exchangers. In the case of power tower as an approach for CSP design, gas-to-gas compact heat exchanger is recommended.
2. Build and perform 1D modeling of the selected heat exchanger using MATLAB.
3. Last but not the least; perform a 3D modeling of the designed selected heat exchanger using the COMSOL Multiphysics software.

As mentioned earlier, heat exchangers can be classified in various ways one of which is according to the surface compactness (either compact or non-compact) and choosing between traditional heat exchangers versus compact ones. Compact heat exchangers (CHEs) have in recent studies and times become the preferred choice

relative to the conventional shell and tube exchangers because of their large heat transfer area per unit volume of the exchanger. Compact heat exchangers are defined subjectively as heat exchangers with surface area densities of equal or greater than  $700 \text{ m}^2/\text{m}^3$  for gas-to-fluid heat exchangers and equal or greater than  $400 \text{ m}^2/\text{m}^3$  for liquid-liquid and phase-change heat exchangers (Shah et al.) [7]. Surface area density is the total surface area per unit volume of the heat exchanger (measured in  $\text{m}^2/\text{m}^3$ ).

Advantages of using Compact Heat Exchangers (CHEs) include:

- Improved effectiveness, CHEs give effectiveness of 90 % or more (reported by Shah et al. [8], and Jeong et al. [9])
- Its smaller volume and weight makes it easier for retrofitting
- Its lower fluid inventory improves the safety of its usage
- Lower installation cost as a result of less pipe work, reduced foundations need, etc.
- It gives multi-stream and multi-pass configurations and therefore offers the flexibility for it to be applied in a lot of applications

## 8.4 Summary

In summary we saw that generating a renewable source of energy from Concentrated Solar Power (CSP) has four different proposed designs published by the Department of Energy (DOE) as part of commercialized CSP technologies and they are summarized here:

### 1. Parabolic Trough

Parabolic trough systems use curved mirrors to focus the sun's energy onto a receiver tube that runs down the center of a trough. In the receiver tube, a high-temperature heat transfer fluid (such as a synthetic oil) absorbs the sun's energy, reaching temperatures of 750 °F or even higher, and passes through a heat exchanger to heat water and produce steam. The steam drives a conventional steam turbine power system to generate electricity. A typical solar collector field contains hundreds of parallel rows of troughs connected as a series of loops, which are placed on a north-south axis so the troughs can track the sun from east to west. Individual collector modules are typically 15–20 ft tall and 300–450 ft long (see Fig. 8.8).

### 2. Power Tower

Power tower systems use a central receiver system, which allows for higher operating temperatures and thus greater efficiencies. Computer-controlled flat mirrors (called heliostats) track the sun along two axes and focus solar energy on a receiver at the top of a high tower. The focused energy is used to heat a transfer fluid (over 1000 °F) to produce steam and run a central power generator (see Fig. 8.9).



**Fig. 8.8** Illustration of parabolic trough. (Courtesy of Department of Energy)



**Fig. 8.9** Illustration of power tower. (Courtesy of Department of Energy)

### 3. Compact Linear Fresnel Reflector (CLFR)

CLFR uses the principles of curved-mirror trough systems, but with long parallel rows of lower-cost flat mirrors. These modular reflectors focus the sun's energy onto elevated receivers, which consist of a system of tubes through which water



**Fig. 8.10** Illustration of compact linear Fresnel reflector (CLFR). (Courtesy of Department of Energy)

flows. The concentrated sunlight boils the water, generating high-pressure steam for direct use in power generation and industrial steam applications (see Fig. 8.10).

#### 4. Dish-Engine

Mirrors are distributed over a parabolic dish surface to concentrate sunlight on a receiver fixed at the focal point. In contrast to other CSP technologies that employ steam to create electricity via a turbine, a dish-engine system uses a working fluid such as hydrogen that is heated up to 1200 °F in the receiver to drive an engine such as the Stirling engine. Each dish rotates along two axes to track the sun (see Fig. 8.11).

A critical component of the Concentrated Solar Power (CSP) system is the solar receiver. This component will transfer heat to pressurized air that will generate electricity. The solar receiver will be operated at temperatures up to 900 °C and pressure in the range of 10 bars. There are major high temperature design, materials availability, and fabrication issues that need to be addressed.

It is concluded, among others in the review, that solar receivers based upon CHE technology have been rarely reported, and therefore, more work is needed in this field for a comprehensive understanding and to improve the uses of new energy sources and contribute to sustainability.

Pressurized air is usually selected as the working fluid considering the cost and environmental impacts. In an open air Brayton cycle the air heated to high temperature inside the solar receiver flows directly through the turbine or via a combustion chamber (fossil fuel back-up) where it is expanded. Closed cycles could be envisioned using supercritical carbon dioxide as the working fluid, which is a



**Fig. 8.11** Illustration of dish engine. (Courtesy of Department of Energy)

suggestion and readers of this research type can use their own intuition (Dostal et al.) [10].

Either open or closed Brayton cycle options require the use of a heat exchange device having superior performance and reliable mechanical characteristics at high pressure and high temperature to guarantee the cycle efficiency; moreover, geometric constraints are also important for such application. Thus, compact heat exchangers (CHEs) technologies are expected to be one of the solutions for this new generation of solar receiver [11].

When the use of a CHE is a possibility in a process or other applications, often, it is preferable that the principal features of CHEs largely confine the choice of type and its surface to a small selection. Plate-fin and tube-fin heat exchangers are the representatives of CHEs for gas flow on one or both fluid sides, and gasketed, brazed, welded Plated Heat Exchangers (PHEs), Fig. 8.12 and Printed Circuit Heat Exchangers (PCHEs), Fig. 8.13 are examples of CHEs for liquid flow.

Due to the high temperature requirements of the heat exchangers and the relatively high cost of the associated construction materials, CHEs are receiving attention for a new generation of solar receiver systems.

Efficient design of solar receivers is also critical for the Concentrated Solar Power (CSP) system. Advanced CSP systems use a pressurized gas solar receiver associated with a Brayton cycle.

The choice of the working fluid for the gas solar receiver and the one used in the Compact Heat Exchanger (CHE) of the electric generator utilizing this Brayton cycle is the same for the CSP taking the path to power tower design technology and the following references by Zohuri [3, 4], Heller et al. [12], and Garcia et al. [13]. As part of the selection process for the right CHE type, we can see

**Fig. 8.12** Plated heat exchanger



**Fig. 8.13** Printed circuit heat exchanger

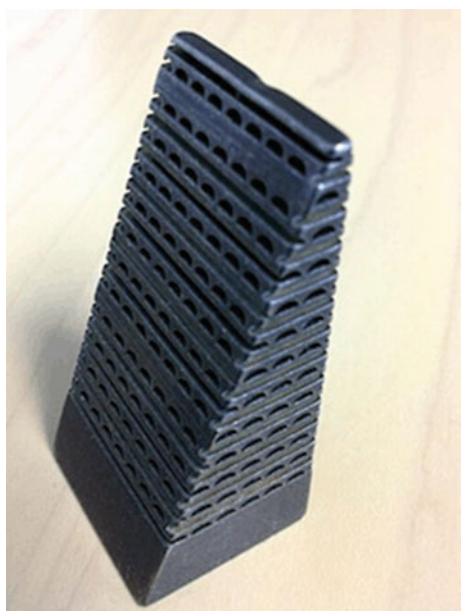


**Table 8.1** Operating conditions of compact heat exchangers

Technology	Maximum pressure (bar)	Maximum temperature (°C)
Gasketed PHE	35	200–250
Brazed PHE	45	225
AlfaReX PHE	40	350
Compabloc PHE	45	350
Shell & Plate	200	950
Hybrid PHE	80	900
PFHE	120	800
Ceramic HE	10	1300
Diffusion bonded PFHE	620	800
PCHE	500–1000	900
Marbond	400	900
SHE	25	540

that the CHE technologies depend on the operating conditions such as pressure and temperature as the number one priority, and second priority is based on the results of comparison on the thermo-hydraulic performance among the types of compact heat exchangers and their classifications.

Compact Heat Exchangers play an important role in saving and high-efficiency utilizing energy. In the coming years, increasing demand for heat exchangers to comply with the principles of ecological and economic sustainability will certainly further expand their industrial applications.

The technologies of compact heat exchangers that may fit the specifications for a new generation of solar receiver, which is a critical component of the Concentrated Solar Power (CSP) system, are proposed and discussed in Chap. 3. For more details refer to the chapter on Compact Heat Exchangers (CHEs) and their classification as well as their types in this book.

Table 8.1 summarizes the principal features of different types of CHEs. This indicates the operational temperature and pressure ranges available for each type [11].

Performance of a heat exchanger depends upon the heat transfer between the working fluids flowing through it. Heat transfer rate for turbulent flow is higher than that for laminar flow and different technologies are used to enhance heat transfer by introducing turbulence, better fluid mixing, and so on. However, any technology that enhances heat transfer is most likely to increase pressure drop also, and it is common knowledge that the ratio of pressure drop increase is often larger than the ratio of heat transfer enhancement [11].

## References

1. U.S. Energy Information Administration. <http://www.eia.gov/todayinenergy/detail.cfm?id=530>
2. Mukhopadhyay, Soumitra, and Sudip Ghosh. 2014. MW level solar powered combined cycle plant with thermal storage: Thermodynamic performance prediction. *International Journal of Renewable Energy Research-IJRER* 4(4): 832–839.
3. Zohuri, B. 2015. *Combined cycle driven efficiency for next generation nuclear power plants: An innovative design approach*. New York: Springer Publishing Company, Vol. 4, No. 4, 2014
4. Zohuri, B. 2014. *Innovative open air Brayton combined cycle systems for the next generation nuclear power plants*. Albuquerque, NM: University of New Mexico Publications.
5. Dincer, Ibrahim, and Marc A. Rosen. 1998. A worldwide perspective on energy, environment and sustainable development. *International Journal of Energy Research* 22: 1305–1321.
6. Bhargava, R. K. 2006. Global Energy Market—Past, present, and future. ASME Paper No. GT2006-91322.
7. Bhargava, R. K., M. Bianchi, A. De Pascale, G. Negri di Montenegro, and A. Peretto. 2007. Gas turbine based power cycles—A state-of-the-art review. International Conference on Power Engineering, October 23–27, 2007, Hangzhou, China.
8. Shah, R.K., and Dusan P. Sekulic. 2003. *Fundamentals of heat exchanger design*. Hoboken, NJ: Wiley.
9. Jeong, Ji Hwan, Lae Sung Kim, Jae Keun, Man Yeong Ha, Kui Soon Kim, and Young Cheol Ahn. 2007. Review of heat exchanger studies for high-efficiency gas turbines. ASME Turbo Expo 2007: Power for Land, Sea and Air, May 14–17, 2007, Montreal, Canada.
10. Dostal, V., P. Hejzlar, and M.J. Driscoll. 2006. High-performance supercritical carbon dioxide cycle for next-generation nuclear reactor. *Nuclear Technology* 154: 265–282.
11. Li, Qi, Gilles Flamant, Xigang Yuan, Pierre Neveu, and Lingai Luo. 2011. Compact heat exchangers: A review and future applications for a new generation of high temperature solar receivers. *Renewable and Sustainable Energy Reviews* 15: 4855–4875.
12. Heller, P., M. Pfänder, T. Denk, F. Tellez, A. Valverde, J. Fernandez, et al. 2006. Test and evaluation of a solar powered gas turbine system. *Solar Energy* 80: 1225–1230.
13. Garcia, P., A. Ferrière, G. Flamant, P. Costerg, R. Soler, and B. Gagnepain. 2008. Solar field efficiency and electricity generation estimations for a hybrid solar gas turbine project in France. *ASME Journal of Solar Energy Engineering* 130/1: 014502.

# **Chapter 9**

## **Compact Heat Exchangers Driven Hydrogen Production Plants**

Research is going forward to produce hydrogen based on nuclear energy. Hydrogen production processes necessitate high temperatures that can be reached in the Fourth Generation nuclear reactors. Technological studies are now underway in order to define and qualify components that in the future will enable us to retrieve and transfer heat produced by these reactors. Hydrogen combustion turbine power could be one of the solutions to our future energy needs particularly in on-peak demand for electricity, but until recently the problem with hydrogen power was its production for use as an energy source. Although hydrogen is the most common element in the known universe to human beings, actually capturing it for energy use is a process which itself usually requires some form of fuel or energy.

### **9.1 Introduction to Hydrogen Production Plants**

The aftermath of the Fukushima nuclear disaster has forced many countries such as Japan and Germany to take drastic measures to revise their nuclear energy policy that had long heralded nuclear power plants as its main source of energy. For example while Germany decided to abandon all of their atomic power plants, the new energy policy that was announced by Japan is taking steps to decrease its dependency on nuclear as much as possible, while increasing and enhancing their Research and Development (R&D) to quest for an alternative renewable energy source. Also in parallel effort the government is promoting a “Hydrogen Society” and use of hydrogen as a source of energy to pave their way to a such goal, by making for example a Fuel Cell Vehicle (FCV), where the Fuel Cell and Hydrogen Technology Group at the New Energy and Industrial Technology Development Organization (NEDO) is in charge of such R&D.

Burning hydrogen in a combustion form does not emit any carbon dioxide ( $\text{CO}_2$ ), so it is considered as a source of clean energy that can greatly help reduce the greenhouse gases effects. Although expectations are set high, it comes with the



**Fig. 9.1** A typical oil refinery plant

technical challenges and cost of ownership as well as return on investment of such research and development toward full production of such a source of energy as part of a renewable form. As an example setting up expensive hydrogen stations for FCVs, securing sufficient supplies of the gas, and coming up with ways to produce it without emitting carbon dioxide are just a few of those challenges and hurdles.

Another industrial application of hydrogen is in oil refinery, where it is used to process crude oil into refined fuel, such as gasoline and diesel, and for removing contaminants, such as sulfur, from these fuels (see Fig. 9.1).

Total hydrogen consumption in oil refineries is estimated at 12.4 billion standard cubic feet per day, which equates to an average hydrogen consumption of 100–200 standard cubic feet per barrel of oil processed. Hydrogen consumption in the oil refining industry grew at a compound annual growth rate of 4 % from 2000 to 2003, and growth in consumption is expected to increase to between 5 and 10 % through to 2010 [Oil & Gas Journal, CryoGas International] [1].

The principal drivers of this growth in refinery hydrogen demand are:

- Low sulfur in diesel fuel regulations—hydrogen is used in refineries to remove sulfur from fuels such as diesel.
- Increased consumption of low quality ‘heavy’ crude oil, which requires more hydrogen to refine.
- Increased oil consumption in developing economies such as China and India.

Approximately 75 % of hydrogen currently consumed worldwide by oil refineries is supplied by large hydrogen plants that generate hydrogen from natural gas or other hydrocarbon fuels, with the balance recovered from hydrogen-containing streams generated in the refinery process. Pressure Swing Adsorption (PSA) (see

Figs. 9.3 and 9.4) technology is used in both hydrogen generation plants and for hydrogen recovery.

### Pressure Swing Adsorption (PSA)

Pressure Swing Adsorption (PSA) technology is a technology used to separate some gas species from a mixture of gases under pressure according to the species' molecular characteristics and affinity for an adsorbent material. It operates at near-ambient temperatures and differs significantly from cryogenic distillation techniques of gas separation. Specific adsorptive materials (e.g., zeolites, activated carbon, molecular sieves, etc.) are used as a trap, preferentially adsorbing the target gas species at high pressure. The process then swings to low pressure to desorb the adsorbed material [2].

Hydrogen is used in a range of other industries, including chemical production, metal refining, food processing, and electronics manufacturing. Hydrogen is either delivered to customers in these industries as compressed or liquid hydrogen, or generated on-site from water using a process known as electrolysis or from natural gas using a process called reforming. In certain applications, there is a gradual shift toward on-site generation to replace delivered compressed or liquid hydrogen, largely based on the lower cost of new on-site hydrogen generation technologies when compared to delivered hydrogen (Fig. 9.2).

Other applications of hydrogen in industry that are worth mentioning are listed below:

1. Weather balloons in meteorology, where these balloons are fitted with equipment to record information necessary to study the climates.
2. Hydrogen is used in fertilizer and paint industries.

**Fig. 9.2** Hydrogen PSA unit—HYDROSWING.  
(Courtesy of Mahler Advanced Gas Systems) [3]



3. Food industries, where in food it is used as an element to make hydrogenated vegetable oils, while using Nickel as a catalyst, solid fat substances are produced.
4. Welding companies use the hydrogen as part of welding torch elements. These torches are utilized for steel melting.
5. Chemical industries use them for metal extraction. For example, hydrogen is needed to treat mined tungsten to make it pure.
6. In home uses, Hydrogen Peroxide can be used in non-medical ways. Other applications include a pest controller in gardens, removing stains on clothing, and functioning as a bleaching agent for cleaning homes.

As we can see Hydrogen is an important utility for numerous applications in multiple industries. Users in a wide range of industries can benefit from operating a cost-effective hydrogen plant and reduce their production costs significantly (see Figs. 9.3 and 9.4).

As we know from our knowledge of chemistry, hydrogen is the lightest and most common element in the cosmos. Its atomic number is 1. In its elemental state, hydrogen is rare, but it is one of the components of water and vital to life. Hydrogen alone does not exist as a natural resource and it needs to be produced by separating it from other elements and molecules, such as water as we have waste oceans sounding us. By far the most common method of producing hydrogen in industry currently is due to stripping hydrogen from natural gas using a process known as steam reforming.

Where, 95 % of the world's hydrogen for energy usage is produced this way. Steam reforming of natural gas requires temperatures as high as 850 degrees Celsius ( $^{\circ}\text{C}$ ) and pressures of up to 365 lb/in.<sup>2</sup> (25 bar). If we're aiming for a sustainable future, creating hydrogen this way from the world's finite resources of fossil fuels is not going to be the answer nor will it be cost effective in the long run.

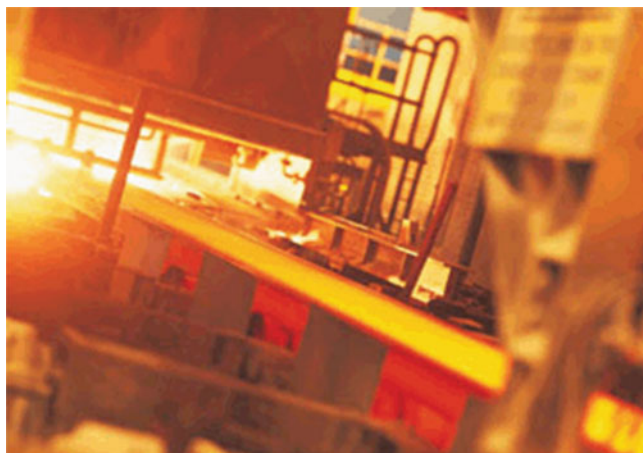


**Fig. 9.3** A typical metal refining plant

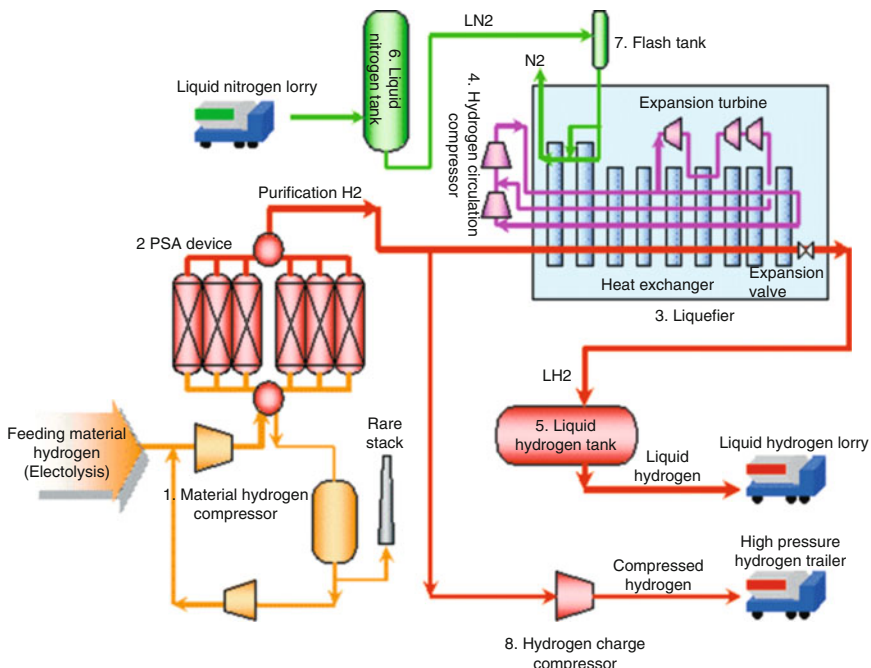


**Fig. 9.4** Flow of liquid hydrogen production facilities

Another way of producing hydrogen is through electric hydrolysis as an alternate to the steam reforming approach and both methods are mentioned below.

Currently, fossil fuels, including naphtha, natural gas, and coal, are the main sources of hydrogen, which is generated by the “steam reforming” method, in which steam is added to methane to yield hydrogen. A huge amount of hydrogen is also produced as a by-product from the production of caustic soda plants and from coke ovens.

In contrast electric hydrolysis is a relatively simple process and method in which production of hydrogen takes place. Any high school chemistry laboratory course has shown two electrodes, one with positive charge known as an anode and the other negatively charged known as a cathode, attached to a battery and placed in water. The result of such induced electric current through water splits the hydrogen ion from oxygen with the positive hydrogen ion attracted to the cathode and the negative oxygen ion to the anode. Once the ions touch the electrodes the hydrogen gains an electron while oxygen loses one and they create fully-fledged atoms of hydrogen and oxygen, which then rise in the water and they can be collected separately at the top of the water container.

The Japanese organization, NEDO published a white paper on hydrogen energy in July 2012 that states the importance of promoting hydrogen-related products, which in Japan are expected to develop into a market worth ¥1 trillion by 2030 and ¥8 trillion by 2050 [4].

## 9.2 Electrical Energy on Supply and Demand

Consumer's demand for electricity is a function of daily and seasonal changes. These variables are based on, for example, changes on demands of a manufacturing facility on line where there are starts and stops throughout the day and week, air conditions are turned off and on seasonally during early hours of the morning, and late afternoon demand for electricity changes per consumers need at home or their work offices. During the peak times, the largest amount of electricity is needed known as peak load, but a "base load" of electricity is needed year-round.

Because electricity cannot be stored easily, utilities must anticipate demand, even on the hottest summer day, and supply enough electricity as a means of renewable energy to meet the demand. Consumption depends predominantly on the time of day and on the season. Utilities meet this demand with in-state power plants where the demand and peak load takes place or/and by purchasing electricity from power plants in other neighboring states. The balancing of supply and demand is required in order to maintain a reliable electric system without a power interruption within grid to the consumers and end users.

There are three major elements that power supply companies need to encounter in order to be able to meet such a supply and demand event, and they are:

1. **Demand**, or need for electricity is the total amount of electricity that consumers use at a particular time and is measured as electrical capacity in kilowatts. 1000 kilowatts (kW) equals a megawatt (MW). 1 kW will turn on ten 100-W light bulbs. Most home air conditioners require 2 kW to operate. A power plant rated at 1 MW will supply enough energy for 500–1000 homes, simultaneously. Electricity is also needed to supply industrial, commercial, and agriculture portions of the economy. Demand or energy use can be divided into "base load," "intermediate load," and "peak load" (see Fig. 9.5). This helps to determine the type and quantity of power plants needed to produce the electricity at the right times. Different types of plants using different fuels or combination of fuels are needed to fulfill one or more of these three types of demand.
2. **Energy use**, as opposed to demand, is the total amount of measured electricity that consumers use over time. Energy use is typically measured in kilowatt-hours (kWh). A kWh is equal to the energy of 1 kW working for 1 h. 1000 kWh equals a megawatt-hour (MWh).
3. **The capacity factor** of a power plant is the actual output of a plant over a period of time compared to its potential output if it had operated at full nameplate capacity the entire time. It generally relates to how often a plant is run during a year and is expressed as a ratio or a percentage. For instance, new, more efficient coal-fired plants might have a capacity factor of 80 % because they would be producing electricity 80 % of the time, while older, less efficient coal-fired plants might have a capacity factor of 40 % because they would be operated for only 40 % of the time.

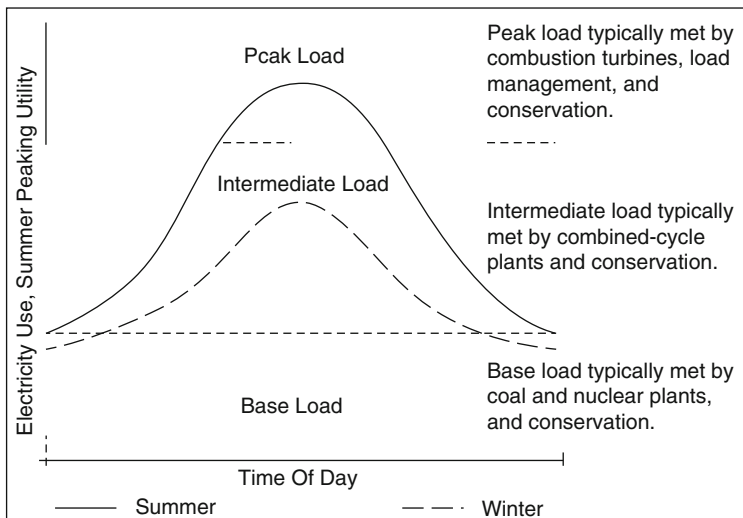


**Fig. 9.5** Typical electric load curve

Base load plants provide a base level of electricity to the system and are typically large generating units. Base load plants operate almost continuously (approximately 70–80 % of the time), except when down for scheduled preventive maintenance, repairs, or unplanned outages. They take a long time to ramp back up to full capacity and have limited to no ability to vary their output of electricity.

In contrast, plants that satisfy peak demand (peaker plants) are highly responsive to changes in electrical demand. They can be turned off and on relatively quickly. However, they typically operate less than 10 % of the time. Peaker plants are most often natural gas combustion turbines and are relatively expensive to operate but cost less to build than base load or intermediate load plants.

Per these variables mentioned above, flexibility, control, and reliability are therefore key variables in electricity supply and on this basis electricity sources can be ranked in the following categories:

**1. Class 1 Electricity:** This class is derived from energy stores, can be switched on and off, and ramped up and down with little penalty to efficiency and these include:

- Combined cycle gas turbines (CCGT)
- Coal fired power
- Hydro electric power
- Geothermal power

**2. Class 2 Electricity:** This class derived from energy stores, tends to be on all the time, providing stable base load, but not contributing much to load variance and this includes:

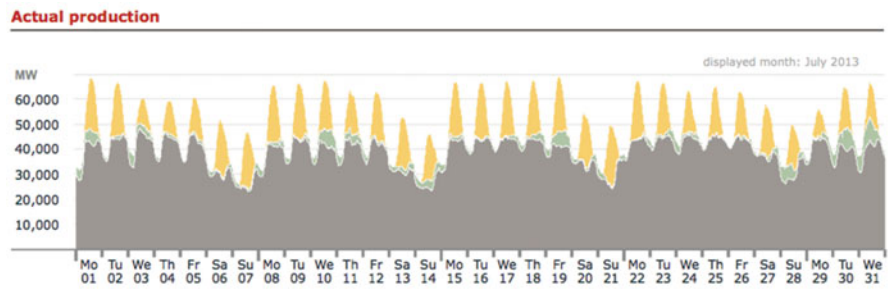
- Nuclear power

**3. Class 3 Electricity:** This class is derived from intermittent energy flow from renewable energy sources and these include:

- Solar power
- Tidal power
- Wind power
- Hydrogen power

Of these, some power providers and owners of electricity generation plants strongly believe that solar is by far superior since it is predictably intermittent and on during the day, every day, when demand is highest (Fig. 9.6, German Production Electricity). Tidal power is also predictably intermittent but supply is not as well correlated with demand as solar. Wind is worst of all and is best described as randomly intermittent. Class 3 electricity can be converted to Class 1 if large capacity storage is available, but this remains an elusive goal.

The classification given above is based upon the engineering requirements of balancing the grid. If you were to perform the same exercise from the perspective of CO<sub>2</sub> emissions then you would clearly derive a different hierarchy. Solar may actually deserve to be elevated to Class 1. On the daily cycle, solar performs very well (Fig. 9.6) but on the annual cycle it does not at the high-mid-latitude of West Europe. Solar is on during the day when it is most needed, but largely off in winter, when it is also most needed. This is one of the driving factors behind the push for hydrogen production plants as means of an innovative approach to a renewable



Graph: Bruno Burger, Fraunhofer ISE; Data: EEX Transparency Platform /

**Fig. 9.6** Electricity production in Germany: July 2013. (Courtesy of Professor Bruno Burger)

energy source for electricity. Bear in mind the part of generation power options in electricity demand, the need for low-cost continuous, reliable supply can be distinguished from peak demand occurring over a few hours daily and is able to command higher prices. Supply needs to match demand instantly and reliably over time.

This is another justification that one can argue; world demand for more energy needs nuclear power based on the following highlights:

- The world will need a greatly increased energy supply in the next 20 years, especially cleanly-generated electricity.
- Electricity demand is increasing twice as fast as overall energy use and is likely to rise by more than two-thirds between 2011–2035. In 2012, 42 % of primary energy used was converted into electricity.
- Nuclear power provides about 11 % of the world's electricity, and 21 % of electricity in Organization for Economic Co-operation and Development (OECD) countries.
- Nuclear power is the most environmentally benign way of producing electricity on a large scale.
- Renewable energy sources such as solar and wind are costly per unit of output and are intermittent but can be helpful at the margin in providing clean power.

There are number of characteristics of nuclear power which make it particularly valuable apart from its actual generation cost per unit—MWh or kWh. Fuel is a low proportion of power cost, giving power price stability, its fuel is on site (not depending on continuous delivery), it is dispatchable on demand, it has fairly quick ramp-up, it contributes to clean air and low-CO<sub>2</sub> objectives, and it gives good voltage support for grid stability. These attributes are mostly not monetized in merchant markets, but have great value which is increasingly recognized where dependence on intermittent sources has grown, and governments address long-term reliability and security of supply.

Knowing how your electric use is billed and how your demand and energy charges are calculated will help the end users to understand and manage their total energy costs. Figure 9.7 depicts a path to such understanding.

The electricity use diagram below shows the difference between energy (kWh) and demand (kW):

In order to have better understanding of the energy charges on your bill, this bill will indicate how much energy was used on-peak (between 9 a.m. and 9 p.m. Monday–Friday) and off-peak (between 9 p.m. and 9 a.m. Monday–Friday), weekends, and designated holidays (New Year's Day, Memorial Day, Independence Day, Labor Day, Thanksgiving Day, Christmas Day). Customers billed on the amount of consumption less than 10,000 kWh/month or more for example will notice that the kWh energy charge is more during on-peak hours than for energy used during off-peak hours.

With the United Nations predicting world population growth from 6.7 billion in 2011 to 8.7 billion by 2035, demand for energy must increase substantially over that period. Both population growth and increasing standards of living for many people

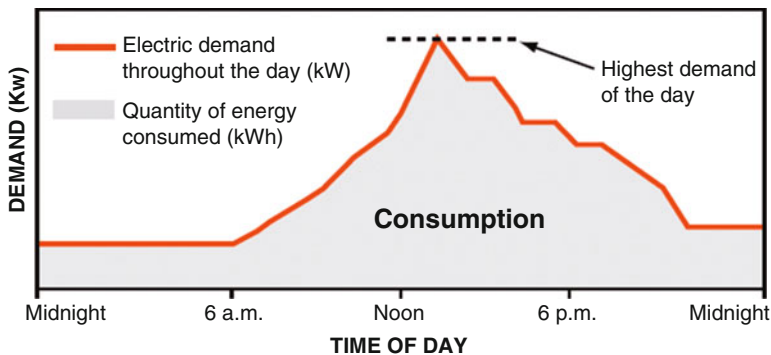
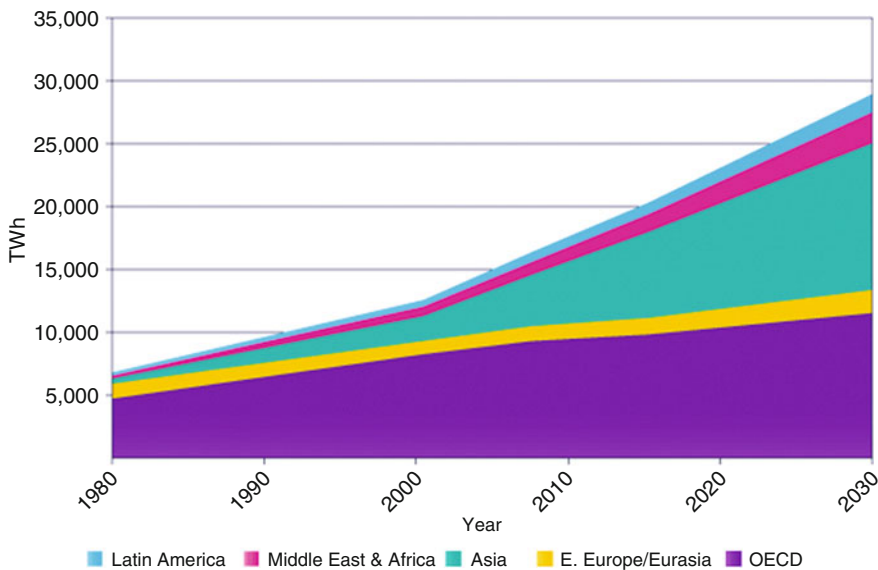


**Fig. 9.7** Sample of electricity use profile



Source: OECD/IEA World Energy Outlook 2009 - Reference Scenario

**Fig. 9.8** World electricity consumption by region

in developing countries will cause strong growth in energy demand, as outlined above. Over 70 % of the increased energy demand is from developing countries, led by China and India—China overtook the USA as the top CO<sub>2</sub> emitter in 2007. Superimposed on this, the UN Population Division projects an ongoing trend of urbanization, from 52 % in 2011 to 62 % in 2035 and reaching 70 % worldwide by 2050, enabling world population to stabilize at about nine billion with better food supply, clean water, sanitation, health, education, and communication facilities [5] (see Fig. 9.8).

The World Energy Outlook 2013 from the OECD's International Energy Agency (IEA) sets out the present situation and also presents current policies\*, new policies, and carbon reduction ('450') scenarios. From 2000 to 2010 total world primary energy demand grew by 26 %, and up to 2020 it is projected to grow less (by 20 % under current policies scenario, and less under other scenarios). Growth up to 2035 is 45 % under current policies, and 33 % under a more restrained scenario. Electricity growth is about double this in each case. Electricity demand almost doubled from 1990 to 2011, and is projected to grow 81 % from 2011 to 2035 (from 19,004 to 34,454 TWh) in the current policies scenario and 69 % (to 32,150 TWh) in the central New Policies scenario. Increased demand is most dramatic in Asia, projected to average 4.0 % or 3.6 % per year respectively up to 2035. Currently some two billion people have no access to electricity, and it is a high priority to address this lack. Electricity Information 2013 from the same source gives the latest available data on world electricity generation and its fuels.

As demonstrated above, the renewable energy sources for electricity constitute a diverse group, from wind, solar, tidal, and wave energy to hydro, geothermal, and biomass-based power generation and now Germany and Japan lead research and development by looking at the hydrogen production plant as another power generation option. Apart from hydro power in the few places where it is very plentiful, none of these is suitable, intrinsically or economically, for large-scale power generation where continuous, reliable supply is needed.

Growing use will however be made of the renewable energy sources in the years ahead, although their role is limited by their intermittent nature. Their economic attractiveness is still an issue also. Renewables will have most appeal where demand is for a small-scale, intermittent supply of electricity. In the OECD about 2 % of electricity is from renewables other than hydro and this is expected to increase to 4 % by 2015 [6]. Figure 9.9, shows that much of the electricity demand is in fact for continuous 24/7 supply (base-load), while some is for a lesser amount of predictable supply for about three quarters of the day, and less still for variable peak demand up to half of the time.

## 9.3 Hydrogen as a Source of Renewable Energy

Hydrogen is considered to be the main choice for storing renewable energy, as it is easily transported and stored in large amounts. A major advantage of hydrolysis is that it produces hydrogen in a clean way. The problem is that it needs a source of the electrical power in the first place. A new working project in Prenzlau, 75 miles North of Berlin in Germany aims to combine the advantages of wind power and hydrogen to overcome the problems of both forms of power production and to embrace the advantages [7].

The three wind turbines at the Prenzlau project can each produce 2 MW of power. Based on an estimated assumption that 1 MW can supply enough power for 240–500 households, WindUpBattery® estimates that the three turbines together

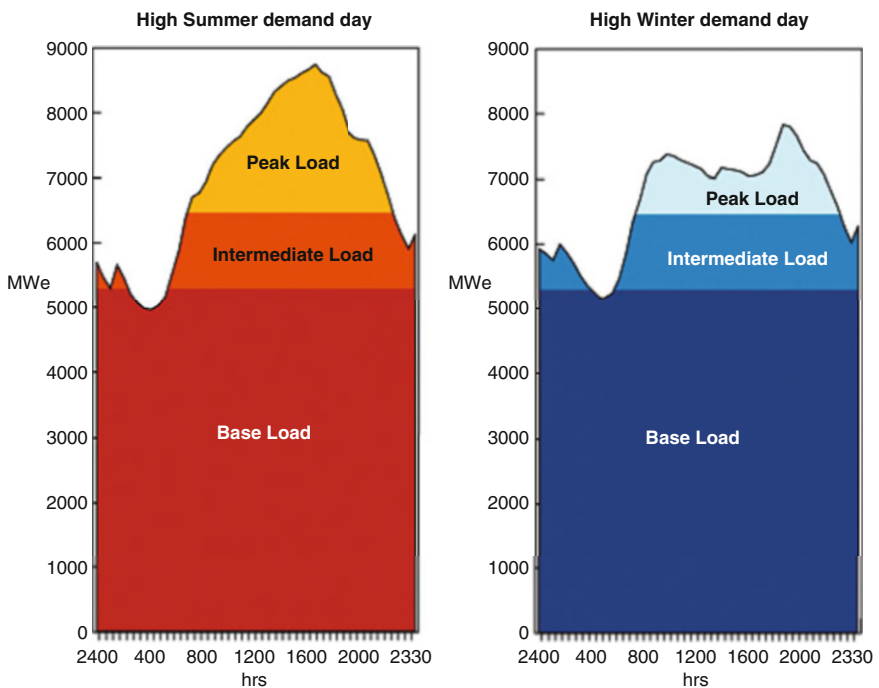


**Fig. 9.9** Load curves for typical electricity grid. (Courtesy of World Nuclear Association)

should therefore be able to supply enough energy between them to power between 720 and 1500 homes, assuming a constant wind. As we all know, the wind isn't constant and reliable though, so when it comes to the future power companies working out how many homes should be powered by a certain number of wind turbines, the calculations need to take into consideration periods of low wind. This is combined with the fact that people do not use a set amount of electricity constantly, but instead vary their demands during the day, which means that there is always the possibility of differences between supply and demand.

Interestingly, according to Vattenfall, one of the energy companies participating in the Prenzlau project, currently there is no system within the renewable energy sector which is designed to compensate for supply and demand differences. Wind farms produce energy which is fed directly into the power grid but the challenge is to develop and employ a way of storing the energy when wind power production is greater than demand. The Prenzlau project enables a balance to be found in the renewable energy production system. Operating on the 6 MW that it provides, this is the first full scale European hybrid power plant to convert the variable nature of wind power to hydrogen for a reliable long-term renewable energy source for general electrical usage and for use in hydrogen fuel cell powered cars and other transport, as well as for heat to co-fire the power plant itself [7].

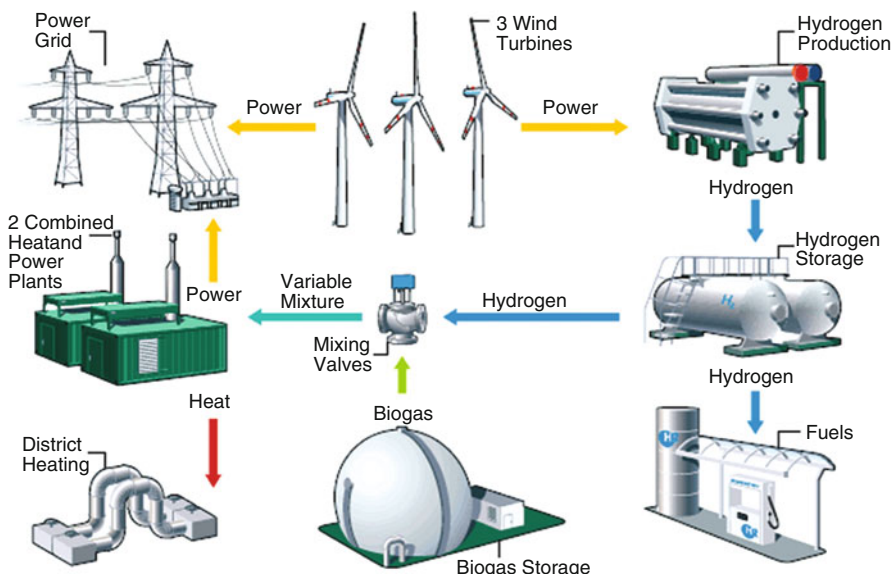


**Fig. 9.10** Hydrogen production plant based on wind energy. (Courtesy of Prenzlau Corporation)

From the three 2 MW wind turbines the electrical power can either be fed straight into the Power Grid, or to an electrolysis unit which is used to produce the hydrogen. This is stored in the plant's hydrogen storage tanks. From there the hydrogen can then be fed along the system and mixed with biogas from a separate unit at the project, and this mixture can be used to run two combined heat and power plants to produce both electricity for the Power Grid and district heating at times when high demand coincides with low wind power production (see Fig. 9.10).

Alternatively the hydrogen from the storage tanks can be used at vehicle filling stations in chosen locations and facilities which can be run by the energy related companies to supply fuel cell cars and other vehicles.

Hydrogen is a significant chemical product where about half of annual production is used to make nitrogen fertilizers and about half to convert low-grade crude oils (especially those from tar sands) into transport fuels [8]. Both uses are increasing significantly. Some is used for other chemical processes. World consumption in 2009 was about 70 million tonnes [9] per year, growing at about 7 % pa. There is a lot of experience handling hydrogen on a large scale, though it is not entirely straightforward. About 96 % of hydrogen is made from fossil fuels: half from natural gas, 30 % from liquid hydrocarbons, and 18 % from coal. This gives rise to quantities of carbon dioxide emissions—each tonne produced gives rise to 11 t of CO<sub>2</sub>. Electrolysis accounts for only 4 %.

### 9.3.1 Why Hydrogen as a Source of Renewable Energy Now?

At the rate that we are burning fossil fuels, due to increasing demand on electricity driven by growth of the world population, there exists a looming specter of the exhaustion of fossil resources, therefore a lot of industrial countries that are in quest of more electrical energy are vigorously conducting research and development on various kinds of new energies. Recent global environmental and green effect problems have imposed great importance on utilizing clean energy as a solution to this problem. Hydrogen seems an attractive source of energy since when it goes through any combustion process it results in the form of water. Up to now, almost all practical-use hydrogen has been produced by fossil fuels.

Figure 9.11 depicts all the characteristics of hydrogen, and if hydrogen could be produced by renewable energies then energy use will truly become harmonized with the environment.

As a matter of fact the Iwatani Corporation, with its headquarters in Osaka and Tokyo in Japan and capital of 20 billion yen, was the first plant to produce liquid hydrogen at the Gases Corporations Chiba facility in Ichihara, Chiba as a renewable source of energy to meet the increasing demand for liquid hydrogen nationwide and to improve the stability of the supply chain system. This plant has been in operation since July of 2009 and it is the first liquid hydrogen plant in Eastern Japan along

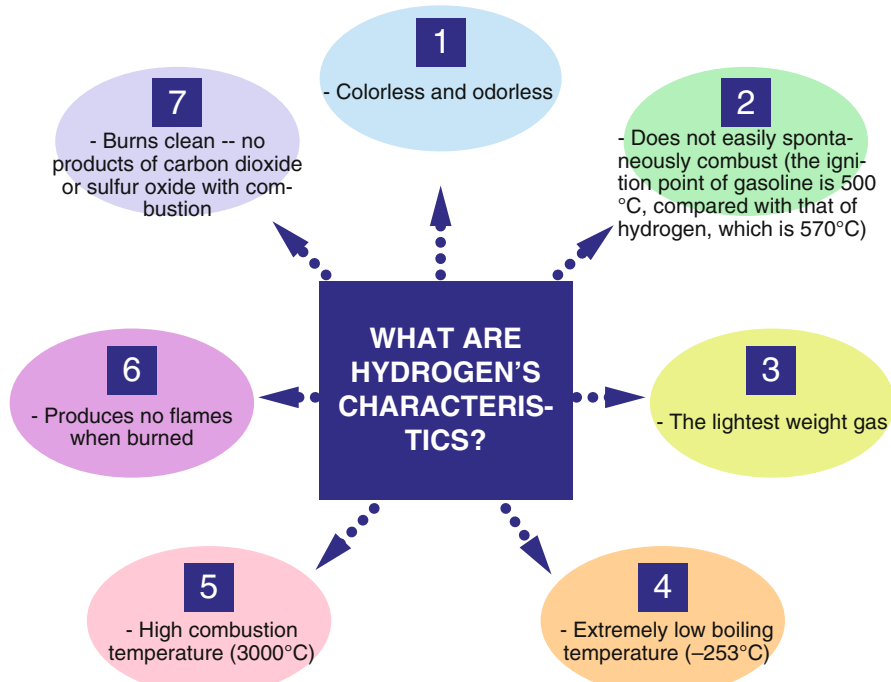


Fig. 9.11 Hydrogen characteristics



**Fig. 9.12** Liquid hydrogen facility in Japan. (Courtesy of Iwatani Corporation)

with Hydro-Edge facilities in Sakai and Osaka which started operation in April 2006. These plants establish a hydrogen supply/chain system in order to improve manufacturing efficiency and supply stability, logistic efficiency, and back-up systems with two bases located in each eastern and western front of Japan as part of their continuous research and development program to go forward with hydrogen production plants (Fig. 9.12).

Companies like Iwatani use by-product hydrogen produced by the adjacent factory in the industrial complex as material, with a liquid hydrogen manufacturing capability of 3000 Liter/Hour (l/h) and a storage capacity of 300 Kilo/Liter (k/l).

### 9.3.2 *Technical Development for Hydrogen Production*

As part of the process to produce hydrogen, in particular in the form of a liquid substance, some manufacturers use the Solid Polymer Electrolyte Membrane Water Electrolysis (SPE) approach as part of their production plan. The reason behind it is that SPE supposedly attains a higher current density and higher estimated energy efficiency, over 90 % compared to Alkaline Water Electrolysis at the current commercial market value.

Note that the SPE process is still in the premature stage of research and technology must be developed around increasing its scale and life expectancy. Figure 9.13 is a snap of the conceptual production plant for the SPE process.

As part of producing hydrogen as a new source of energy one should analyze the capital and operating costs associated with storing and transporting hydrogen if the production plant is not close to the proximity of the end user facility. The storage techniques considered by industry are centered on liquid hydrogen, compressed gas, metal hydride, and underground storage facilities and mode of transportation for liquid hydrogen in terms of delivery by truck, rail road, and barge seems very feasible. Gaseous hydrogen delivery by truck, rail, and pipeline is another transport

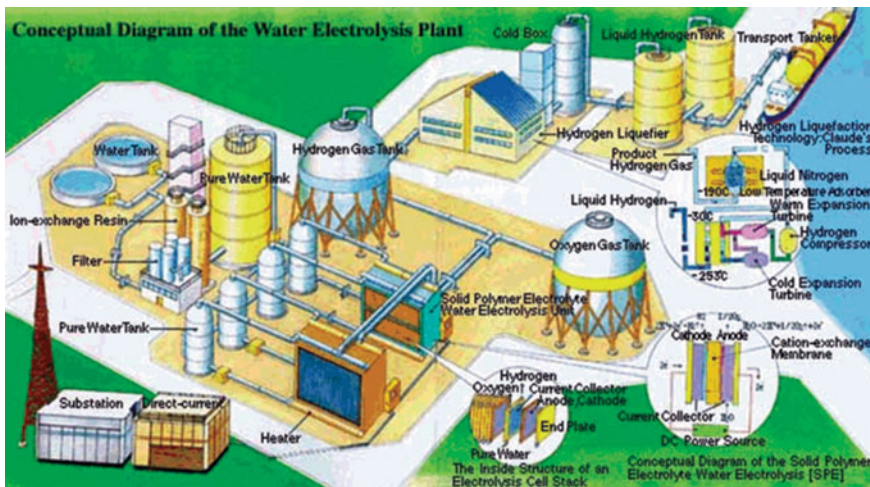


**Fig. 9.13** SPE conceptual of the water electrolysis plant. (Courtesy of World Energy Networking) [10]

mode, and for metal hydride delivery by truck and rail can be taken under consideration [11].

The optimum options for storing hydrogen are as:

1. Compressed gas.
2. As a form of liquid.
3. Combined with a metal hydride.

Underground can also be considered, although it is just a special case of compressed gas storage. Each alternative has their pros and cons. For instance, liquid hydrogen has the highest storage density of any method, but it also requires an insulated storage container and an energy-intensive liquefaction process. The liquefaction process of hydrogen can be done by cooling a gas to form a liquid, and the process uses a combination of compressors, heat exchangers (subject of this book), expansion engines, and throttle valves to achieve the desired cooling [12].

The simplest method for liquefaction is either Linde cycle or Joule-Thompson expansion cycle, where the hydrogen gas is at ambient pressure, then cooled in a heat exchanger, before passing through a nozzle valve where it undergoes an isenthalpic Joule-Thompson expansion, producing some liquid. Depictions of a flow-sheet for both Linda process and Temperature-Entropy techniques are shown in Figs. 9.14 and 9.15 respectively.

For further and more detailed information we encourage readers to look at reference (Flynn) [12].

The Linde cycle works for gases, such as nitrogen, that cool upon expansion at room temperature. Hydrogen, however, warms upon expansion at room temperature. In order for hydrogen gas to cool upon expansion, its temperature must be below its inversion temperature of 202 K (-95 °F). To reach the inversion

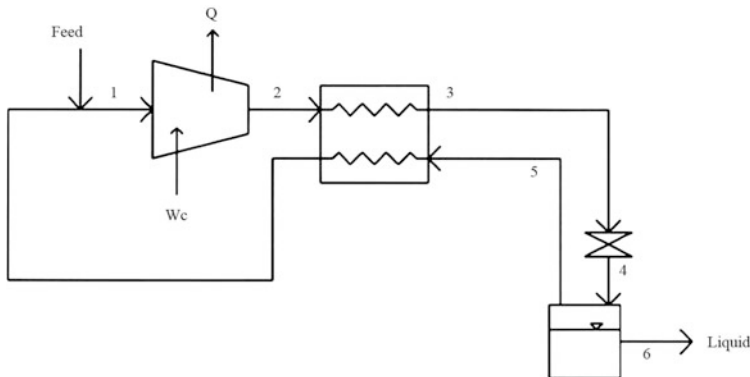


**Fig. 9.14** Linde liquefaction process flow-sheet [1]

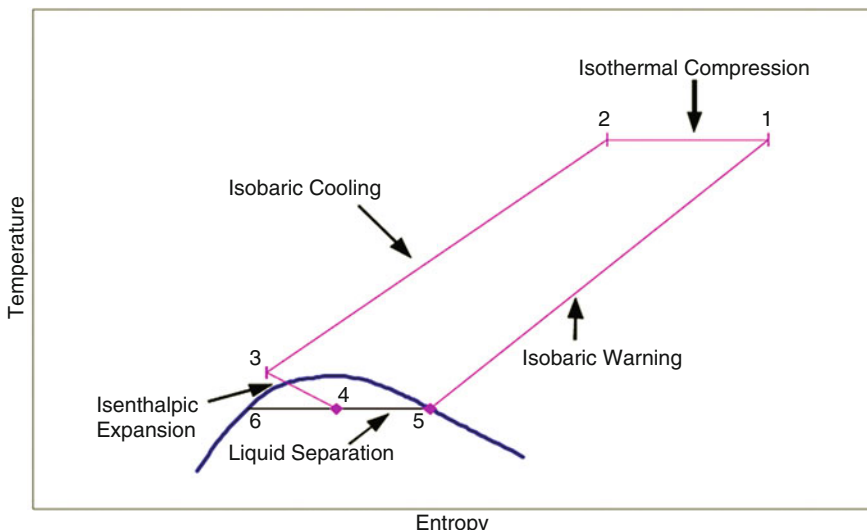


**Fig. 9.15** Linde process temperature-entropy diagram [11]

temperature, modern hydrogen liquefaction processes use liquid nitrogen pre-cooling to lower the temperature of the hydrogen gas to 78 K ( $-319^{\circ}\text{F}$ ) before the first expansion valve. The nitrogen gas is recovered and recycled in a continuous refrigeration loop (Flynn [12]; Timmerhaus and Flynn [13]).

The pre-cooled Linde process is shown in Fig. 9.16. Figure 9.17 is the associated temperature-entropy diagram for the process.

An alternative to the pre-cooled Linde process is to pass the high-pressure gas through an expansion engine. An expansion engine, or turbine, will always cool a gas, regardless of its inversion temperature (Flynn) [12]. The theoretical process, referred to as ideal liquefaction, uses a reversible expansion to reduce the energy

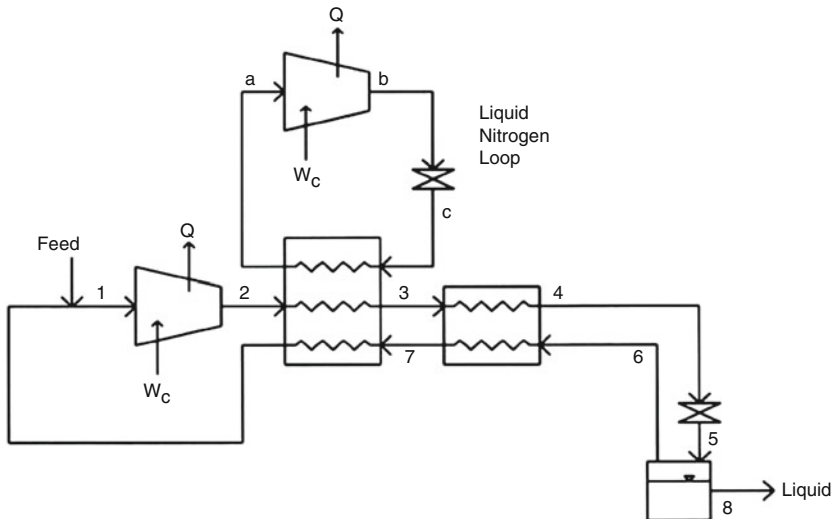


**Fig. 9.16** Pre-cooled liquefaction flow-sheet [11]

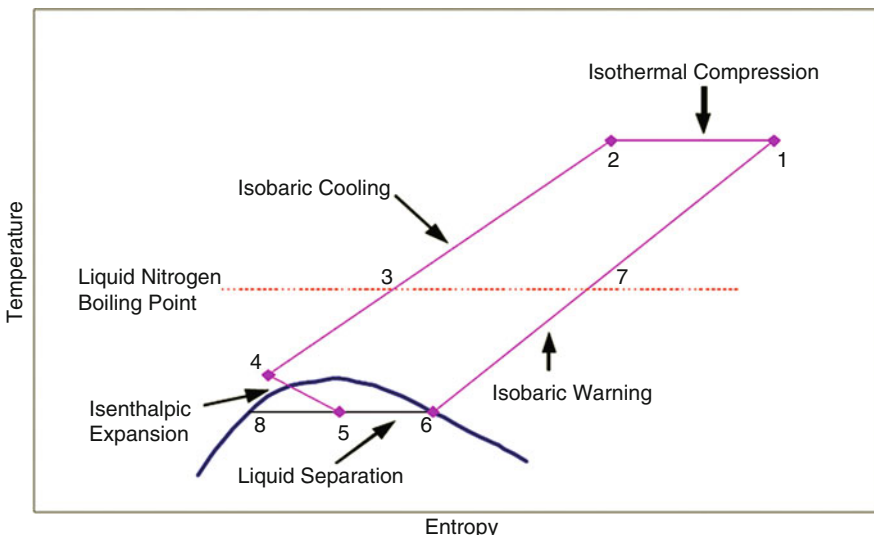


**Fig. 9.17** Pre-cooled liquefaction temperature-entropy diagram [11]

required for liquefaction. It consists of an isothermal compressor, followed by an isentropic expansion to cool the gas and produce a liquid.

Hydrogen liquefaction technology development will consist of system optimization, a large-scale compressor, and a large-scale expansion turbine.

### ***9.3.3 Technical Development for Hydrogen Production***

For the purpose of transportation of hydrogen products to the end user and to store them for further use by consumers, a hydrogen tanker for transportation, a storage system, various related machinery and equipment (pumps, piping, valves, and so on) for liquid hydrogen, and metal hydride alloys to be used in distributed storage and transportation facilities need to be researched and reviewed. Based on the above research, information concerning the transportation and storage of liquid hydrogen will be gathered. Structural material will be developed to withstand the extremely low temperature of liquid-hydrogen ( $-253^{\circ}\text{C}$ ). In the previous section we expanded upon storage options and production of hydrogen in the form of Liquefaction and briefly discussed the process of such liquefaction.

Taking the approach of compressed gas storage of hydrogen is the simplest storage solution—the only equipment required is a compressor and a pressure vessel (Schwarz and Amonkwah) [4]. The main problem with compressed gas storage is the low storage density, which depends on the storage pressure. Higher storage pressures result in higher capital and operating costs (Garrett) [14]. Compressed gas storage, liquefaction, underground storage, and pipelines all require compressors; only metal hydride storage does not, although a compressor may also be used for hydrides depending upon the hydride plateau pressure (Schwarz and Amonkwah) [15].

Looking at underground storage options depends on the geology of the area that is considered for such storage facility. Underground storage of hydrogen gas may be possible (Zittel and Wurster) [16]. Underground storage of natural gas is common and underground storage of helium, which diffuses faster than hydrogen, has been practiced successfully in Texas (Hart) [17].

The pipeline storage approach of hydrogen requires systems that are usually extended to several miles of piping and in some cases may be hundreds of miles long. Because of the great length, and therefore great volume, of these piping systems, a slight change in the operating pressure of a pipeline system can result in a large change in the amount of gas contained within the piping network. By making small changes in operating pressure, the pipeline can be used to handle fluctuations in supply and demand, avoiding the cost of onsite storage (Hart; Report to Congress 1995) [17].

Good details of the capital costs of these types of storage options are given by Wade A. Amos [1] and readers should refer to his report.

## 9.4 Development of a Hydrogen Combustion Turbine

As part of a hydrogen production plant and for consideration of hydrogen as an option for a renewable source of energy, we need to design some kind of hydrogen combustion turbine and do basic required research and development for its optimum operation and cost related issues.

The hydrogen combustion turbine is an extremely clean system for the environment. The system does not emit carbon dioxide, sulfur oxide or nitrogen oxide at all because the combustion process only uses hydrogen and oxygen. The energy efficiency of a hydrogen combustion turbine is expected to be 60 %, even with a temperature of 1200 °C at the entrance of the turbine, because there is no exhaust gas and therefore no exhaust gas loss. Concerning the hydrogen combustion turbine, as part of the overall project plan for its design one can take the following steps in Phase I:

1. System optimization,
2. Combustion control technology,
3. Major components (turbine blade, rotor),
4. Major auxiliaries and
5. Super-high temperature materials.

These research results will eventually be applied to a hydrogen combustion turbine at a pilot or prototype plant. These steps can also be considered in the case of a feasibility study of hydrogen production at existing nuclear power plants (i.e., Generation III) or to be considered as part of Next Generation Nuclear Plants (NGNP), (i.e., Generation IV), which in this case we need to consider an intermediate heat exchanger subsystem in the loop between the primary and secondary loop of the nuclear plant (subject of this book). We are also considering a cycle such as Brayton combined cycle to drive higher efficiency [18, 19] or nuclear air Brayton combined cycle (NACC) [20], taking advantage of reactors such as Very High Temperature Reactor (VHTR) where they operate at similar temperatures as part of the family of NGNP and they require super high temperature materials as well. Figure 9.18 is a sketch of a conceptual model of a hydrogen combustion turbine.

## 9.5 Feasibility Study on Utilization of Hydrogen Energy

Utilization of hydrogen as a source of renewable energy requires investigating to estimate the amount of hydrogen consumption in different sectors such as electric power, transportation, industry, and public welfare as depicted in Fig. 9.19. The utilization of liquid hydrogen for cryogenic energy will also need to be investigated and reviewed. If this source of energy can be realized and disseminated through the world by the beginning of this century and next, we will all witness hydrogen being

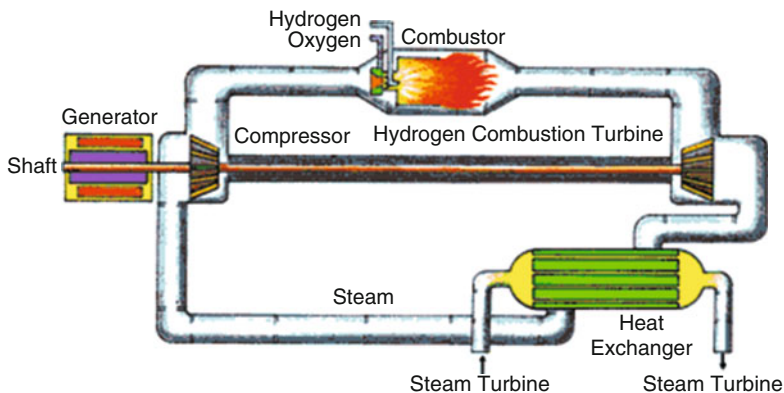


**Fig. 9.18** Conceptual model of hydrogen combustion turbine

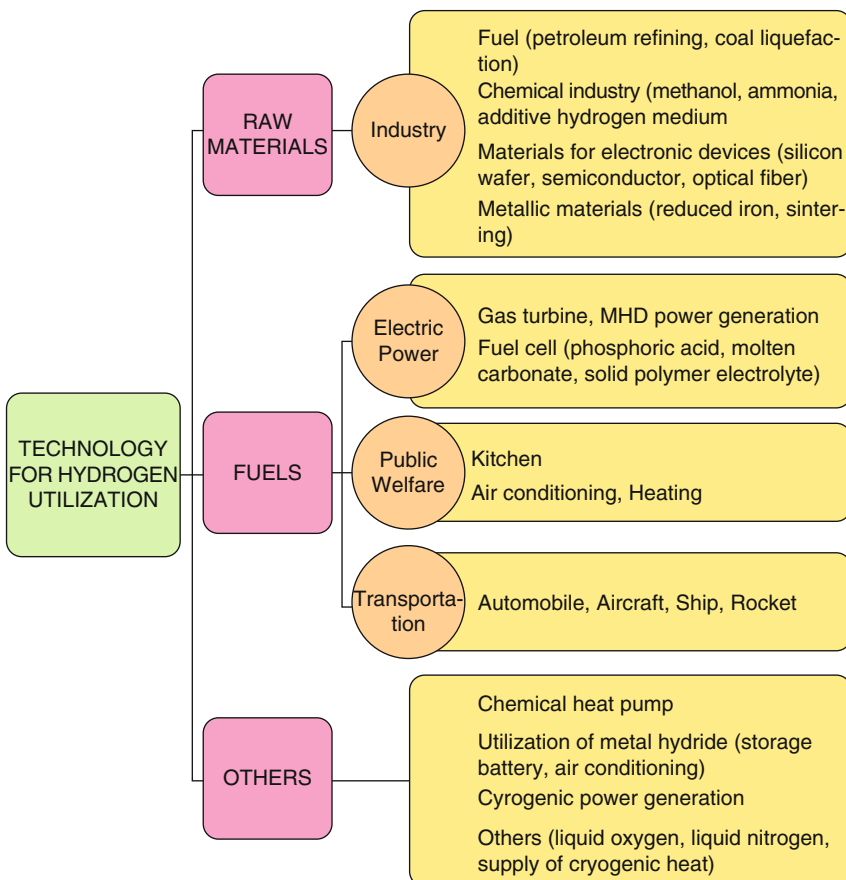


**Fig. 9.19** Forms of hydrogen utilization



- |                            |                                   |
|----------------------------|-----------------------------------|
| 1. Liquid Hydrogen Station | 5. Hydrogen Bus                   |
| 2. Hydrogen Aircraft       | 6. Hydrogen Combustion Generation |
| 3. Hydrogen Storage Tank   | 7. Hydrogen (Transport) Tanker    |
| 4. Energy Consumer Site    | 8. Hydrogen Car                   |

**Fig. 9.20** Utilization of hydrogen energy in twenty-first century and beyond



**Fig. 9.21** Honda FCX Clarity and Silverado hydrogen internal combustion engine truck

used not only to run automobiles and fly aircraft, but also to power all of the appliances necessary for our day-to-day living as well (see Fig. 9.20).

Utilizing hydrogen and burning it as fuel for transport produces only water vapor, with no carbon dioxide or carbon monoxide to deal with. However, it is far from an energy-dense fuel, and this limits its potential use for motor vehicles. By March 2014, there were 186 hydrogen refueling stations worldwide, 26 of them in Germany that mainly were used in trials of fuel cell vehicles. Japan is also pushing for migration toward Fuel Cell Vehicles (FCV) (see Fig. 9.21).

Several automotive companies have developed demonstration Hydrogen Fuel Cell Vehicles (HFCV). The Honda FCX Clarity, Chevy Equinox Fuel Cell, and others have been demonstrated. Other original equipment manufacturers (e.g., Toyota) have announced plans for fuel cell vehicles. The rarity of the platinum currently used in fuel cells may be a problem for wide-spread adoption, along with the expense of the fuel cell itself. However, incentives and political focus can push development forward and prices down.

Hydrogen can be burned in a normal internal combustion engine, and some test cars are thus equipped. Trials in aircraft have also been carried out. In the immediate future the internal combustion engine is the only affordable technology available for using hydrogen. For instance, 100 BMW Hydrogen 7s have been built, and 25 were used in test programs in the USA. The cars covered more than 2 million kilometers in test programs around the globe. BMW is the only car manufacturer to have used hydrogen stored in its liquid state. The low energy density of 10.1 MJ/L is the limiting factor (cf 3.5 times this for petrol), coupled with the need to cool the 170-l tank to minus 253 °C. BMW has abandoned this development and is collaborating with Toyota on fuel cell vehicles, with a view of marketing a joint mid-sized platform and fuel cell stack by 2020 [21].

## 9.6 Hydrogen Production Using Nuclear Energy

Nuclear generated hydrogen has important potential advantages over other sources that will be considered for a growing hydrogen share in a future world energy economy. Still, there are technical uncertainties in nuclear hydrogen processes that need to be addressed through a vigorous research and development effort. Safety issues as well as hydrogen storage and distribution are important areas of research to be undertaken to support a successful hydrogen economy in the future.

The hydrogen economy is gaining higher visibility and stronger political support in several parts of the world. In recent years, the scope of the IAEA's program has been widened to include other more promising applications such as nuclear hydrogen production and higher temperature process heat applications. The OECD (Organization for Economic Co-operation and Development) Nuclear Energy Agency, Euratom, and the Generation IV International Forum have also shown interest in the non-electric applications of nuclear power based on future generation advanced and innovative nuclear reactors.

Nuclear power already produces electricity as a major energy carrier. It is well placed, though beyond the capability of most current plants, to produce hydrogen if this also becomes a major energy carrier.

The evolution of nuclear energy's role in hydrogen production over perhaps three decades is seen to be:

1. Electrolysis of water, using off-peak capacity,
2. Use of nuclear heat to assist steam reforming of natural gas,

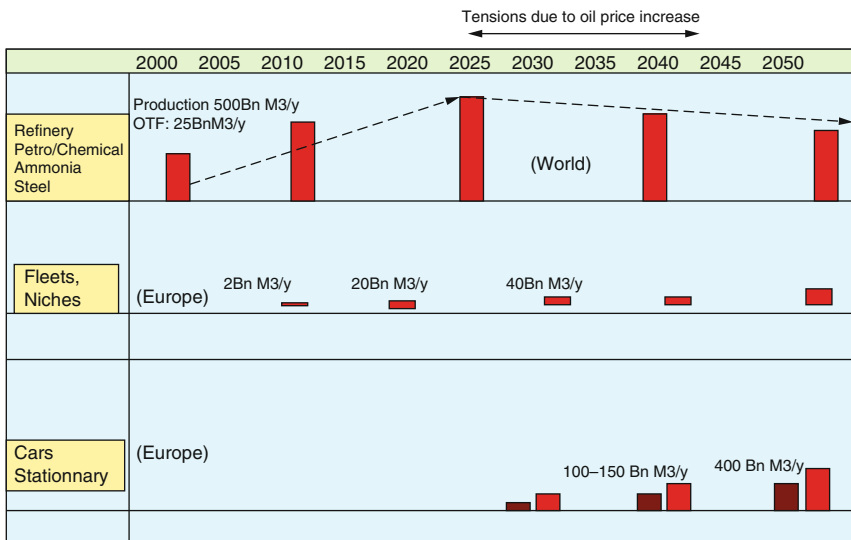


Fig. 9.22 Hydrogen production roadmap

3. High-temperature electrolysis of steam, using heat and electricity from nuclear reactors,
4. High-temperature thermo-chemical production using nuclear heat.

The first three are essentially cogeneration or known as Combined Heat and Power (CHP). The last three are described in detail in the paper in this series: Nuclear Process heat for Industry. See also 2013 I.E. technical report: Hydrogen Production Using Nuclear Energy [22].

The projection of the European Commission High Level Group shown in Fig. 9.22 offers a realistic scenario of the hydrogen market and the application areas. The figure clearly shows that the largest near term markets will be the petrochemical industries, requiring massive amounts of H<sub>2</sub> for the conversion of heavy oils, tar sands, and other low grade hydrocarbons, as well as the fertilizer and steel industries.

Per our discussion above, hydrogen's main application as a source of fuel for transportation use comes as fuel cells. Conceptually speaking, a fuel cell can be considered as a refuelable battery, making electricity as a direct product of a chemical reaction, except where the normal battery has all the active chemical ingredients built in at the factory, fuel cells are supplied with fuel from an external source and oxygen from air.

These fuel cells catalyze by converting the oxidation of hydrogen straight to electricity energy at relatively cryogenics (low temperatures) mode in a very efficient way. The claimed, as per a Japanese researcher in the field of hydrogen as a renewable energy, theoretical efficiency of converting chemical to electrical energy to drive the cars is about 60 % or more. However, in practice about half that

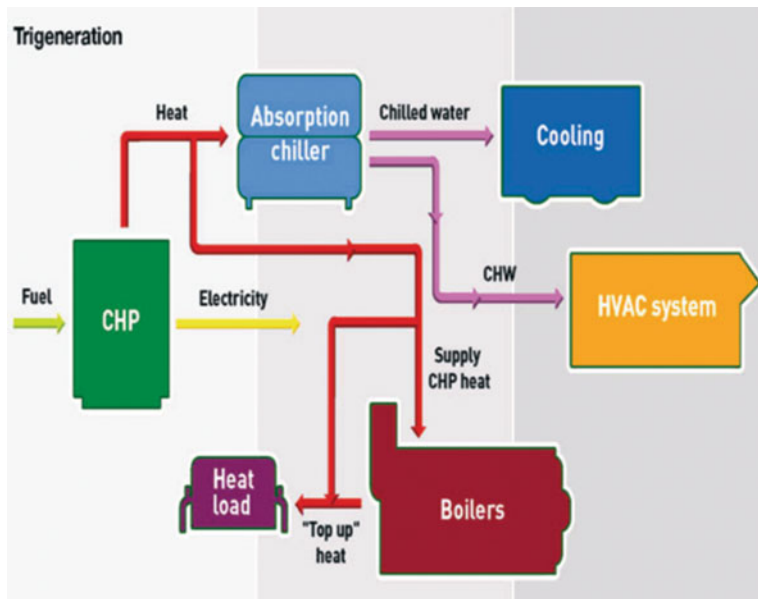


**Fig. 9.23** Diagram of typical trigeneration power plant

amount of efficiency has been demonstrated, except for the high-temperature solid oxide fuel cells that peaked at 46 %.

### Definition of Cogeneration

Cogeneration or combined heat and power (CHP) is the use of a heat engine or power station to generate electricity and useful heat at the same time. Trigeneration or combined cooling, heat, and power (CCHP) refers to the simultaneous generation of electricity and useful heating and cooling from the combustion of a fuel or a solar heat collector. See Fig. 9.23 for layout of a typical Trigeneration power plant.

As part of the advantages and disadvantages of hydrogen use for fuel cell argument, although we can say that this combustion is a carbon-free process, on-board storage for the distribution to consumers is a challenging problem for the manufacturer of such vehicles, where hydrogen is going to be used as a source of fuel. It is impossible to store hydrogen as simple as gasoline when we consider the compactness and simplicity of carrying a tank of gasoline or Liquefied Natural Gas (LNG) on-board. So to overcome this problem one technical approach is suggesting storing the hydrogen cryogenically at very high pressure, or chemically as hydrides. The latter seems a more promising and potential approach than the first

one; although, from a refueling point of view it is not as straightforward as we want for usage purpose in Fuel Cell Vehicles (FCVs).

Pressurized storage is the main technology available now and this means that at 345 times atmospheric pressure (34.5 MPa, 5000 psi), ten times the volume is required for an equivalent amount of petrol/gasoline. By 2010 however 680 atm (70 MPa) was practical, and the weight penalty of a steel tank was reduced by use of carbon fiber. Earlier, the tank had been about 50 times heavier than the hydrogen it stored, now it is about 20 times as heavy, and the new target is ten times as heavy.

Another promising potential for a storage system among researchers is utilization of sodium borohydride ( $\text{NaBO}_2$ ) as the energy carrier, with energy density. The  $\text{NaBO}_2$  is catalyzed to yield its hydrogen, leaving a borate  $\text{NaBO}_2$  to be reprocessed.

Fuel cells are currently used in electric forklift trucks and this use is expected to increase steadily. They apparently are not very cost effective, about three times as much as batteries but last twice as long (10,000 h) and have less downtime. We must produce the hydrogen at lower cost, using its production feasibilities at existing nuclear power plants or aligning with the next generation power plant (NGNP) in the near future. The first fuel cell electric cars running on hydrogen were expected to be on the free market soon after 2010, but 2015 is now the target. Fuel cell buses have clocked up over 2 million kilometers and a fleet of 20 has been used in Vancouver. Another project has three Mercedes Citaro buses in 11 cities. Japan has a goal of five million fuel cell vehicles on the road by 2020.

Current fuel cell design consists of bipolar electrode plates in a frame with an electrolyte between, and development of the most common proton exchange membrane type and Fuel cells using hydrogen can also be used for stand-alone small-scale stationary generating plants—where higher temperature operation (e.g., of solid oxide fuel cells) and hydrogen storage may be less of a problem or where it is reticulated like natural gas. Cogeneration fuel cell units for domestic power and heat are being deployed in Japan under a subsidy scheme which terminates in 2012, by which time unit costs were expected to drop from US\$ 50,000 to \$6000, and they also need to last for a decade [21].

However, at present fuel cells are much more expensive to make than internal combustion engines (burning petrol/gasoline or natural gas). In the early 2000s, PEM units cost over \$1000/kW, compared with \$100/kW for a conventional internal combustion engine. The target cost for a PEM fuel cell stack is below EUR100/kW, which will require reducing the amount of palladium catalyst.

### Proton Exchange Membrane (PEM) Unit

Proton exchange membrane (PEM) fuel cells work with a polymer electrolyte in the form of a thin, permeable sheet. This membrane is small and light, and it works at low temperatures (about 80 °C, or about 175 °F). Other electrolytes require temperatures as high as 1000 °C.

PEM technology was invented at General Electric in the early 1960s, through the work of Thomas Grubb and Leonard Niedrach. GE announced

(continued)

an initial success in the mid-1960s when the company developed a small fuel cell for a program with the U.S. Navy's Bureau of Ships (Electronics Division) and the U.S. Army Signal Corps. The unit was fueled by hydrogen generated by mixing water and lithium hydride. This fuel mixture was contained in disposable canisters that could be easily supplied to personnel in the field. The cell was compact and portable, but its platinum catalysts were expensive.

The feasibility of Hydrogen production study at existing nuclear power plants has been led by most nuclear owned countries and at the tip of this spear is the United States with the most nuclear power of GEN-III in a production line supporting a network of electricity by being in a grid system within a nation. Idaho National Laboratory is leading efforts of research and development on this matter (Idaho National Laboratory INL/EXT-09-16326) [23].

Although this report concentrates on existing nuclear power in line and current design of such plants based on GEN-III configurations and specifications, it has no recommendation for producing hydrogen based on current designs of GEN-IV or NGNP efforts. Currently, electrolysis equipment that is sized to produce 1 kg of hydrogen per second does not exist due to lack of demand for such a plant, but demand for such a plant is increasing significantly and this is due to the recent effort toward a quest for a renewable source of energy to be able to counter demand on electricity demand during the peak power upon base-load.

As we have discussed so far, the cost of electricity is an important consideration in the economic feasibility of any hydrogen production facility. Prior to the release of this report, much of the discussion on keeping electrical costs low centered on use of the production facility during utility off-peak hours when costs are generally lower. However, this study shows that off-peak only results in higher breakeven hydrogen pricing because the high capital cost plant is idle for many hours. Indeed there are times when the on-peak electrical cost is lower than some of the off-peak costs.

A need for such a feasibility study based on existing nuclear power plants should extend beyond GEN-III in transition to GEN-IV and should be included as part of an overall effort of the research and development package on next generation power plants (NGNP) as well.

Recent experiences with Combined Cycle Natural Gas Power plants have demonstrated efficiencies approaching 60 %. A Combined Cycle Molten Salt Nuclear Brayton-Rankine cycle appears to achieve efficiencies 5–10 % higher than a straight High Temperature Rankine cycle with peak coolant temperatures near 1000 K [17–19].

The key to achieving these efficiencies is a multi-turbine, multi-heat exchanger system that adds as much heat as possible near the peak output temperature of the Molten Salt Coolant.

Since the nuclear heating system does not consume the oxygen in the Brayton working fluid, it might be possible to build a hybrid system that burns the oxygen in the air after it has been heated by the nuclear heat exchangers.

This would provide a topping capability for a hybrid nuclear plant that could use natural gas to expand its power output to meet peak demand above the base-load capability of the plant. If all that is required is to initiate injection of natural gas into the flow path of the nuclear Brayton cycle, the response time for adding significant power will be very short. The details of how this might be done are intriguing. Ignition of the injected gas should not be a problem as the working fluid would be at high temperature.

In any gas turbine system that drives a rotating shaft (turboprop, turbo-shaft, etc.) the turbine load is usually split between a gas generator turbine and a power turbine. The two turbines are not on the same shaft and usually rotate at different speeds. Normally it is desirable for the power turbine (connected to the drive shaft) to maintain rpm control separate from the level of torque delivered. The simplistic hybrid approach that has often been proposed would have the natural gas injected after the gas generator turbine and before the power turbine.

This will be a problem as the pressure driving the gas through the turbine will not be strong enough to overcome the resistance of the higher temperature gas to flow through the power turbine nozzles. Some of the flow could be bled off prior to the power turbine, but that would lower the efficiency of the injected combustible mixture by about 50 %.

The combustible gas will have to be injected prior to the gas generator turbine so that it can drive the pressure up and get the hotter working fluid through the power turbine nozzles. This essentially requires the Brayton power system to be designed for two conditions. The peak power with the combustion taking place will be the “design” condition and the base-load nuclear heating will be the “off design” condition.

With support from INL under its NUEP program among universities that are involved with such efforts including the University of New Mexico where this author has association, we are currently building models to address this combination of conditions—“design” and “off-design” to quantify the tradeoffs on both the high temperature Brayton system and the bottoming Rankine cycle.

It is the classic “off-design” problem, where the machinery is designed to operate at a specific pressure temperature point and it is then asked to also operate at a different set of conditions. “Off-design” operation will affect system efficiency and performance. It is important to quantify the effects of this multiple operating point scenario.

The base-load nuclear only system will probably become the “off-design” point and if the effects of operating at this “off-design” point are severe, the concept of a hybrid system may not be viable.

The variables associated with hydrogen production, including the storage and transpiration as discussed above, as well as variation of cost of electricity due to on-peak and off-peak per season consumption and from year-to-year makes the matter of production a challenging problem using the existing technology of hydrogen production. The cost variance has an impact on total cost of production, transportation, and storage as well.

Production process such as the electrolyzing process requires a large amount of water and such water source has its own challenging issue of purification for the process, as well as availability of such water source is varying from year-to-year. There are years that drought becomes an issue for certain states and regions in the country.

Producing hydrogen via nuclear energy by combining a hydrogen production facility with a new nuclear power plant has its own sets of rules such as, regulations, safety, and licensing process as well as policy involved; and they are not well defined by regulators so far. This includes study of what would be involved to build such a facility side-by-side of a nuclear power plant facility, and the utilities must provide generation resources capable of supplying its customer base through the variations of daily and seasonal energy demands. Although there is a tremendous move toward a means for a renewable source of energy and today's political leaders and regulation are asking for clean energy and encourages the use of renewable resources such as wind or solar, the demand on electricity per population growth for the future shows that these two resources are not enough to meet such demand, therefore we need to think of alternative solutions. An assessment of the reliability of the bulk electric power system on future generation capabilities and trends according to the North American Electric Reliability Corporation (NERC) is depicted by fuel mix as a source of producing energy. To accomplish this requirement, electrical utilities owners utilize various fuels, including nuclear, hydro, coal, gas, oil, wind, and solar, as the energy source for electric generation. This diversity provides the electric utility industry independence from any single source of fuel [23].

The capability of the electric utility industry to utilize a variety of energy sources to generate electric energy, and to move quickly to the most economical fuel resource, is an important factor in the planning of future generation resources (see Fig. 9.24).

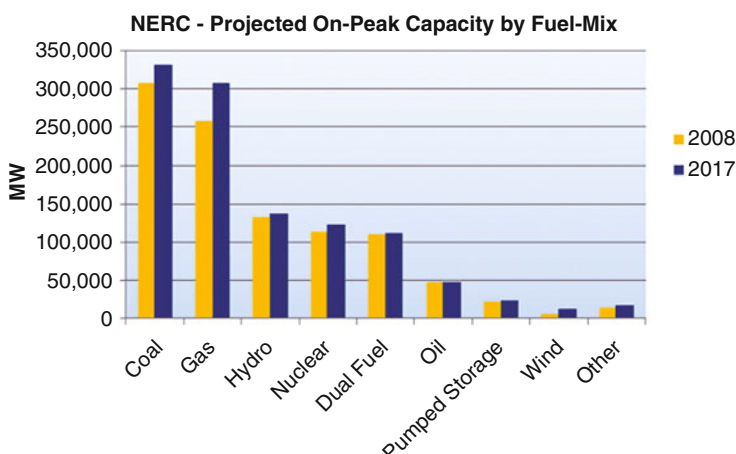


**Fig. 9.24** NERC current and projected generation capacity for electricity

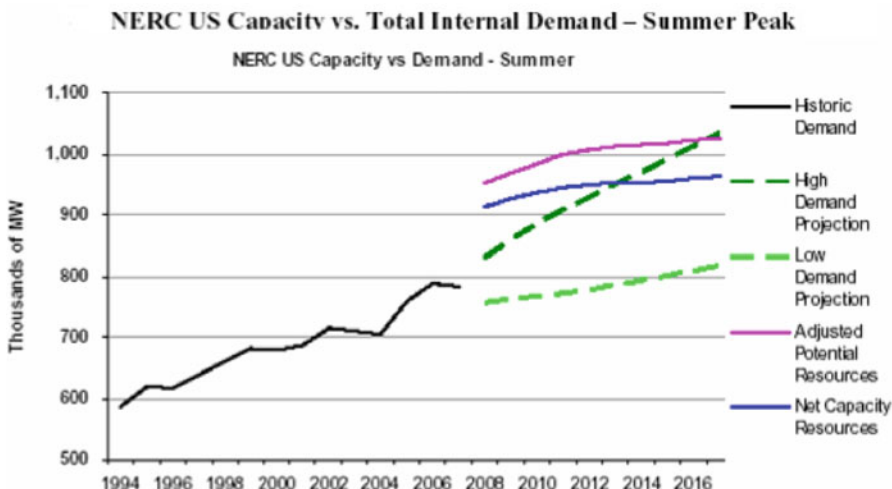


Fig. 9.25 United States capacity versus total demand

The projected growth in capacity in response to meet an increase in electricity demand per NERC is depicted in Fig. 9.25, and note that these graphs provide overall United States capacity and demand and locally they might have a different illustration.

The National Renewable Energy Laboratory (NREL) published a report in 2004 based on the subject of *Hydrogen Demand* in which several sizes of production units were classified on the number of vehicles that are expected to utilize hydrogen as a source of fuel. Their finding was structured on 12,000 miles/year for the typical distance driven by each hydrogen fueled car and each car averages 60 miles/kg of hydrogen consumption (i.e., 12,000 miles/year relates to about 32 miles/day, which is close to that projected for each Electric Vehicle (EV)). Therefore, each Hydrogen Fuel Cell Vehicle (HFCV) requires approximately 200 kg of hydrogen per year. This is calculated based on the factor that 1 kg of hydrogen contains approximately the same energy as 1 gal of gasoline and of course each vehicle depending on their type have different consumption rate per mileage that they cover, so the above assumption is just averaged out over all the vehicle types and may not be a good foundation but it is a good departure point to have an idea of what the demand would be for hydrogen as a fuel cell.

On the other hand, if the average HFCV achieves 45 miles/kg of hydrogen, then it means the hydrogen production plant designs need to serve fewer than the five size types that are identified here [12].

- The home size will serve the fuel needs of one to five cars with a hydrogen production rate of 200–1000 kg H<sup>2</sup>/year.
- The small neighborhood size will serve the fuel needs of 5–50 cars with a hydrogen production rate of 1000–10,000 kg H<sup>2</sup>/year.

- The neighborhood size will serve the fuel needs of 50–150 cars with a hydrogen production rate of 10,000–30,000 kg H<sup>2</sup>/year.
- The small forecourt (refueling station) size, which could be a single hydrogen pump at an existing station, will serve the fuel needs of 150–500 cars with a hydrogen production rate of 30,000–100,000 kg H<sup>2</sup>/year.
- A full hydrogen forecourt size will serve more than 500 cars per year with a hydrogen production rate greater than 100,000 kg H<sup>2</sup>/year.

Manufacturers of electrolytic hydrogen generators are sizing up their production equipment to meet such demand and be able to deliver the quantity of hydrogen needed above, but if the production of Hydrogen Fuel Cell Vehicles (HFCV) and Hydrogen Internal Combustion Engines (HICE) rises, then the growth for hydrogen production should be justified accordingly and that is almost up to 1 kg/s for production facilities, which is equivalent to 86,400 kg/day leading to 31,500 metric tons per year or 0.032 million metric tons of hydrogen. Thus, production facilities of this magnitude will require being able to meet such projected demand for growth. Such projection and demand is depicted in Figs. 9.26 and 9.27.

Demand for hydrogen will be driven by the local user. Figure 9.28 provides the demand increase for various market sizes based on HFCV market penetration.

The Idaho National Laboratory report (INL/EXT-09-16326) 11, based on the analysis of existing gasoline stations in four major U.S. cities, indicates they have determined general trends in station sizes and geographic distribution in each city; stations of different sizes are more or less uniformly distributed across the urban area. Although there is a slight tendency for large stations to be found away from the downtown area and city center in three of the four cities, when normalized by average station size and total number of outlets in each city, relative station size distributions are nearly identical in each city.

This result is preserved during cluster analysis, which simulates reduced station networks that might resemble early hydrogen station networks. The relative station size distributions for both existing gasoline networks and simulated early hydrogen

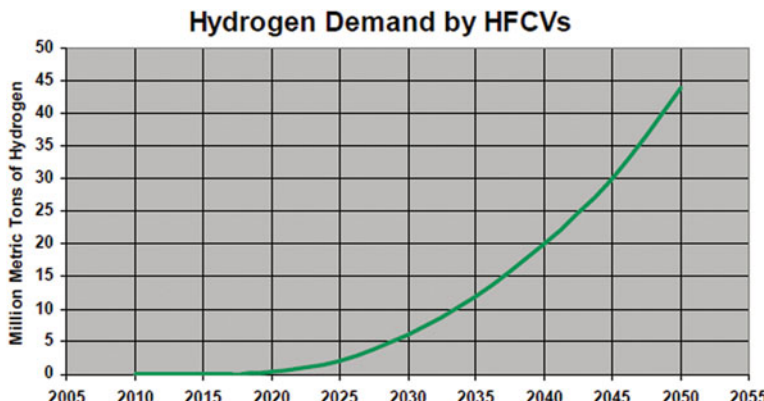


Fig. 9.26 Hydrogen demand million in metric tons per year [10]

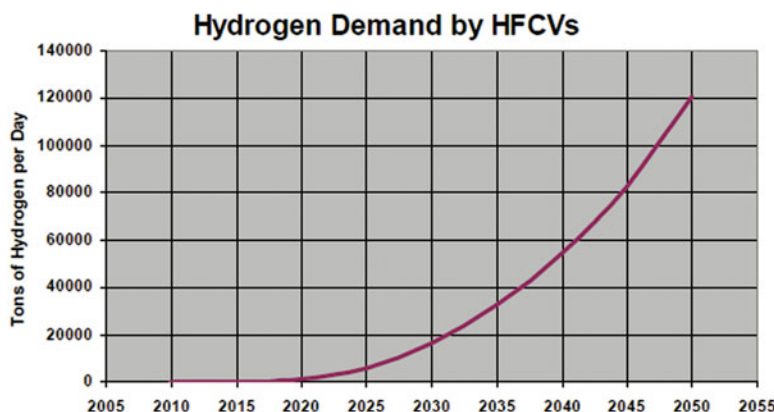


Fig. 9.27 Hydrogen demand tons per day [12]

Market \ Penetration	1%	10%	30%	70%
<b>Small Urban</b>				
Population	100,000	100,000	100,000	100,000
Vehicles	116,000	116,000	116,000	116,000
H <sub>2</sub> fueled vehicles	1,160	11,600	34,800	81,200
H <sub>2</sub> fuel stations	12 <sup>a</sup>	6 <sup>b</sup>	17 <sup>b</sup>	39 <sup>b</sup>
H <sub>2</sub> demand (tpd)	1	8.3	2.5	58
<b>Large Urban</b>				
Population	1,000,000	1,000,000	1,000,000	1,000,000
Vehicles	890,000	890,000	890,000	890,000
H <sub>2</sub> fueled vehicles	8,900	89,000	267,000	623,000
H <sub>2</sub> fuel stations	86 <sup>a</sup>	43 <sup>b</sup>	128 <sup>b</sup>	298 <sup>b</sup>
H <sub>2</sub> demand (tpd)	9	83	250	580

a. 100 kg/d station (home size)

b. 1,500 kg/d station (small neighborhood)

Fig. 9.28 Key demand assumptions by market and penetration [1]

networks suggest that some 10 % of the stations will be at least twice as large as the average station size, and some 30 % of stations will be smaller than half the average station size [24].

The mix of home, neighborhood, and forecourt sizes will evolve as the demand changes. The flexibility of a location to adapt with the demand will be important as well. Other issues potentially limiting the siting and permitting of a hydrogen production facility include the “determination of need” for hydrogen as required by state environmental reviews and water availability.

## 9.7 Constraints Involved for Hydrogen Production Using Nuclear Energy

In conjunction with producing hydrogen from a nuclear power plant operation certain constraints are associated with them that need to be addressed and overcome in order to deal with the design and construction of large-scale hydrogen production facilities. These requirements are for codes and standards and consideration of the regulatory, environmental, and licensing aspects of these facilities. The task becomes greater when considering co-locating this hydrogen facility with an existing or new nuclear reactor or even locating the hydrogen facility adjacent to a nuclear site.

### 9.7.1 Safety: Hydrogen Generation

The Department of Energy (DOE) through the Hydrogen, Fuel Cells, and Infrastructure Technologies Program, with the National Renewable Energy Laboratory (NREL), are coordinating a collaborative effort with leading standards-development organizations, code-development organizations, and other national laboratories “to prepare, review, and promulgate hydrogen codes and standards needed to expedite hydrogen infrastructure development” [25].

The development and promulgation of codes and standards are essential if hydrogen is to become a significant energy carrier and fuel because codes and standards are critical to establishing a market receptive environment for commercializing hydrogen-based products and systems. The Hydrogen, Fuel Cells, and Infrastructure Technologies (HFCIT) Program of the U.S. Department of Energy (DOE) and the National Renewable Energy Laboratory (NREL), with the help of the leading standards and model code development organizations, other national laboratories, and key stakeholders in the U.S., are coordinating a collaborative government-industry effort to prepare, review, and promulgate hydrogen codes and standards needed to expedite hydrogen infrastructure development [25].

The DOE has undertaken a comprehensive program to support and facilitate the development of hydrogen codes and standards based on research, development, and testing (RD&T) needed to establish the scientific and technical foundation for requirements embodied in the codes and standards. The overall structure of the program is shown in Fig. 9.29.

Over the past several years, a coordinated national agenda for hydrogen and fuel cell codes and standards has emerged through DOE leadership and the support and collaboration of industry and key Standards Development Organizations (SDO) and model code organizations [14].

The Research and Development (R&D) Roadmap provides a guide to the research, development, and demonstration activities needed to obtain data required

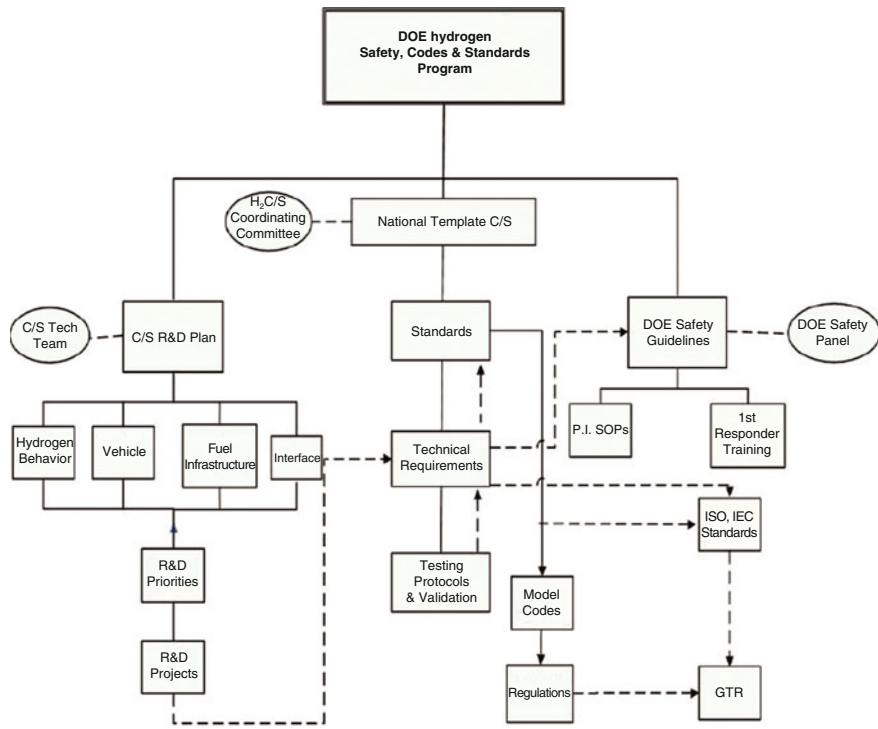


**Fig. 9.29** DOE hydrogen safety, codes and standards program [14]

for SDOs to develop performance-based codes and standards for a commercial hydrogen fueled transportation sector in the U.S.

Currently no large scale, cost-effective, environmentally attractive hydrogen production process is available for commercialization nor has such a process been identified. Our goal is to determine the potential for efficient, cost-effective, large scale production of hydrogen utilizing high temperature heat from an advanced nuclear power station. The benefits of this effort will include generation of a low-polluting transportable energy feedstock in a highly efficient method from an energy source that has little or no affect on greenhouse gas emissions and whose availability and sources are domestically controlled. This will help to ensure energy supply for a future transportation/energy infrastructure that is not influenced and controlled by foreign governments.

Conventional nuclear plants readily generate electric power but fossil fuels are firmly entrenched in the transportation sector. Hydrogen is an environmentally attractive transportation fuel that has the potential to displace fossil fuels. Hydrogen will be particularly advantageous when coupled with fuel cells. Fuel cells have higher efficiency than conventional battery/internal combustion engine combinations and do not produce nitrogen oxides during low-temperature operation. Contemporary hydrogen production is primarily based on fossil fuels and most

specifically on natural gas. When hydrogen is produced using energy derived from fossil fuels, there is little or no environmental advantage [26].

### ***9.7.2 Safety: Hydrogen Generation by Facility Location***

The public acceptance of nuclear energy is still greatly dependent on the risk of radiological consequences in case of severe accidents. Such consequences were recently emphasized with the Fukushima-Daiichi accident in 2011. The nation's nuclear power plants are among the safest and most secure industrial facilities in the United States. Multiple layers of physical security, together with high levels of operational performance, protect plant workers, the public, and the environment.

As a matter of fact, despite the highly-efficient prevention measures adopted for the current plants, some accident scenarios may, with a low probability, result in a severe accident, potentially leading to core melting, plant damage, and dispersal of radioactive materials out of the plant containment.

Even if the Japanese power station was not equipped with the newest devices for the prevention or mitigation of severe accidents, Fukushima, as well as the Three Mile Island accident in 1979, confirmed the key role of the containment barrier in the significant mitigation of radioactive releases.

The improvement of nuclear designs and the set-up of adequate accident management strategies require confinement structures and emergency systems that must be properly dimensioned (configuration, choice of materials, and cooling circuits), to guarantee the integrity of the safety barriers and avoid the release of radioactive gasses and aerosols to the outside environment.

In this chapter, schematics of typical nuclear power plants are preliminarily shown, together with the main concepts of nuclear reactions and the formation of radioactive isotopes.

The risk of radioactive release to the external environment because of accidents is then pointed out, in order to explain the reasons for safety criteria that characterize these kinds of installations. Attention is paid to the needs of maintaining the structural integrity of both cooling circuits and confinement structures. Seismic analyses are cited, as well as the risk of containment building damage due to over-pressurization in the case of a severe accident.

U.S. nuclear plants are well designed, operated by trained personnel, defended against attack, and prepared in the event of an emergency and the following measures are taken under consideration;

- 1. Emergency Preparedness:** Every nuclear power plant in the country has a detailed plan for responding in the event of an emergency. Operators test that plan regularly, with the participation of local and state emergency response organizations.

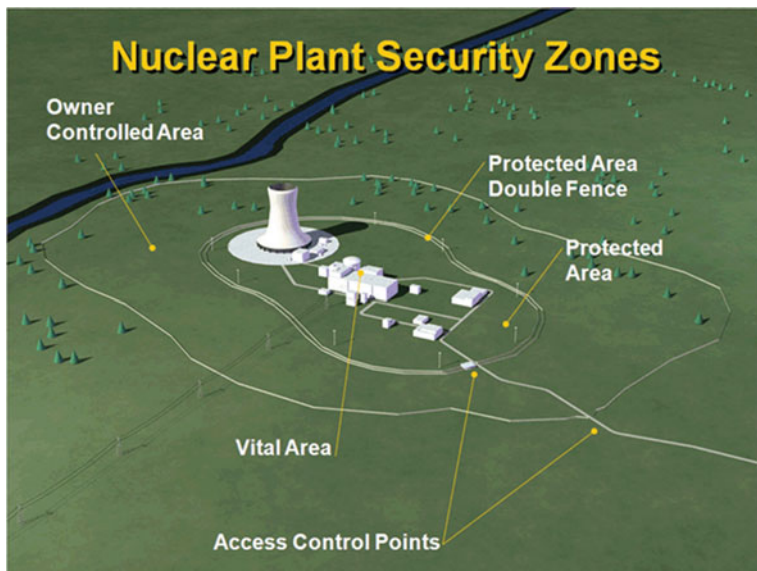


**Fig. 9.30** Nuclear plant security zones. Source NEI

2. **Operational Safety:** Stringent federal regulation, automated, redundant safety systems, and the industry's commitment to comprehensive safety procedures keep nuclear power plants and their communities safe.
3. **Personnel Training and Screening:** Operators receive rigorous training and must hold valid federal licenses. All nuclear power plant staff are subject to background and criminal history checks before they are granted access to the plant.
4. **Plant Security:** Each nuclear power plant has extensive security measures in place to protect the facility from intruders. Since Sept. 11, 2001, the nuclear energy industry has substantially enhanced security at nuclear plants.

An illustration of the area of a nuclear power plant protected by armed guards, physical barriers, and surveillance equipment from top-level point of view is depicted below (see Fig. 9.30).

5. **Nuclear Licensing:** All U.S. nuclear power plant facilities that are currently operational, are reviewed and granted operating licenses under licensing regulation 10 CFR Part 50 by the Nuclear Regulatory Commission (NRC), and by requirement each particular nuclear facility is described in its Final Safety Analysis Report (FSAR). Included in the FSAR is a description of the activities of each facility that take place at the site, “including the products and materials most likely to be processed, stored, or transported such as the above four points that are mentioned” [27]. Therefore, the licensees make changes to their facility accordingly and pursuant to 10 CFR 50.59, each facility regulates itself. This includes all the subsequent changes or modifications that the licensee wants to furthermore impose on its operations at the facility.

6. **Nuclear Liability Insurance:** The NRC requires all the owners of nuclear power plants to maintain financial protection through primary and secondary liability insurance coverage mandated by the rules.
7. **Electrical System Up-time and Stability:** Preventive maintenance of nuclear power plants require long term shutdown cooling requirements that consume power and have very restrictive voltage and frequency limitations. The stability of the electrical system associated with a nuclear power plant is not common in oil or gas and coal generating electricity. Safety related issues during their shutdown for preventive maintenance have a different set of rules than traditional power plants. Even if the hydrogen production facility is powered from the grid, a shutdown or degraded operation could cause a grid disturbance adversely impacting the nuclear plant load. The nature of hydrogen generation is that it can go very quickly from full production to zero. This type of load rejection is a feasible occurrence. Nuclear plants are currently designed and licensed for a loss of load event. However, depending on the power distribution provided to the hydrogen production facility (dedicated or off the grid) and the reliability and frequency of load disturbances, the licensee will likely need to review the electrical system stability. If it is determined that the frequency of a loss of external load event is increased, the licensee would need to evaluate the change under 10 CFR 50.59, as previously discussed above, and request a license amendment from NRC and approval, as required.
8. **Environment Review:** When issuing an amendment to a license it is necessary for NRC to make a determination as to whether an environmental review is required. An environmental review may be conducted in the form of an environmental assessment or an environmental impact statement.

## 9.8 Efficient Generation of Hydrogen Fuels Utilizing Nuclear Power

The combustion process from fossil fuel in order to provide power for transportation, electricity generation, heat for homes, and fuel for industry covers 86 % of the world's energy in today's time frame [28, 29]. The disadvantages and drawbacks of utilizing fossil fuel lie in supply limitation, pollution, and emission of carbon dioxide ( $\text{CO}_2$ ), which is considered a reason behind global warming and is now the subject of intonation treaties among the world countries [30, 31].

Hydrogen is an environmentally attractive transportation fuel that has the potential to displace fossil fuels. Hydrogen will be particularly advantageous when coupled with fuel cells. Fuel cells have higher efficiency than conventional battery/internal combustion engine combinations and do not produce nitrogen oxides during low-temperature operation. Contemporary hydrogen production is primarily based on fossil fuels and most specifically on natural gas. When hydrogen is

produced using energy derived from fossil fuels, there is little or no environmental advantage [32].

Currently no large scale, cost-effective, environmentally attractive hydrogen production process is available for commercialization nor has such a process been identified.

To overcome these combined drawbacks is the subject of the quest for a new source of renewable energy to replace fossil fuels, in particular, with a less-polluting process, primarily in parallel with nuclear energy coupled with an efficient hydrogen production plant adjacent to it. This type of combination requires a very high temperature operating nuclear power plant that is coupled with an efficient hydrogen production plant via Intermediate Heat Exchangers (IHXs) [26].

For example Japan Atomic Energy Agency (JAEA) under the concept of a Small Modular Reactor (SMR) for their High Temperature Test Reactor (HTTR) has selected the option of coupling a High Temperature Gas Reactor (HTGR) to a SMR by the employment of an intermediate heat exchanger for the steam reforming process.

This approach has been applied in the Japanese HTTR project. A flow diagram of the hydrogen production system based on SMR and its potential coupling to the HTTR is shown in Fig. 9.31. The total system is subdivided by the dotted line into the existing nuclear part on the left hand side and the—not yet existing—chemical part on the right hand side.

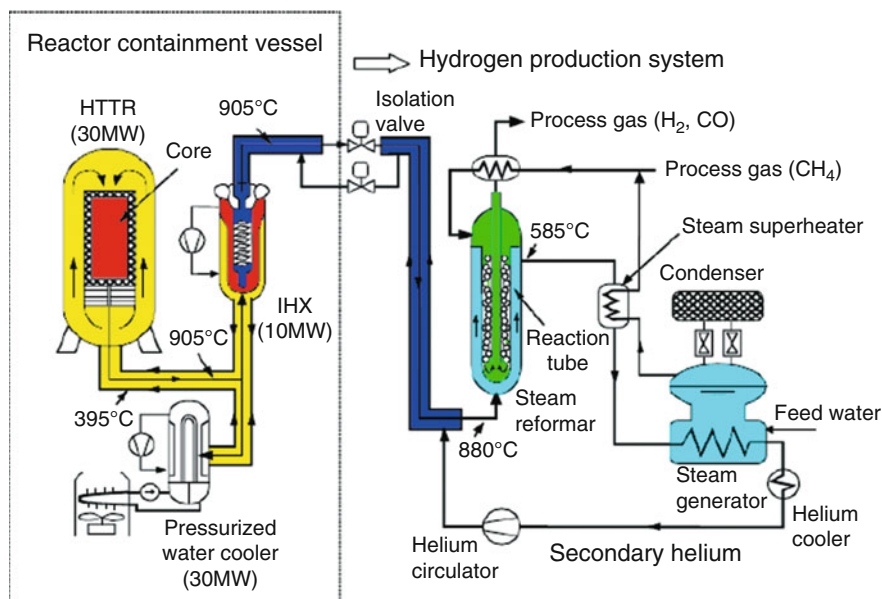


**Fig. 9.31** HTTR coupled to a hydrogen production plant based on SMR

The requirements for a system with safe operation and high hydrogen production efficiency have initiated engineering design work on key components for the nuclear steam reforming process:

- A new concept steam reformer heated by helium gas from the nuclear reactor has been designed to achieve high hydrogen production performance and competitiveness with an economical, fossil fired hydrogen production plant.
- A natural convection type of steam generator has been selected to achieve sufficient system controllability accommodating the large difference in thermal dynamics between the nuclear reactor and the steam reformer.
- An air-cooled radiator is connected to the steam generator to operate as a final heat sink during normal and anticipated operational occurrence conditions.

The separation of the primary circuit and the chemical process avoids the possibility of contamination in the steam reformer and reduces the permeation rates of hydrogen and tritium to negligible values. However, the heat fluxes in the steam reformer have values of around  $40 \text{ kW/m}^2$  if the same conditions in the reforming process are fulfilled. The fabrication of the steam reformer and steam generator requires different standards than those of components that are directly integrated into the primary helium circuit [21].

For several years, steam reforming of methane has been considered the top candidate process to be connected to the HTTR for the world's first nuclear hydrogen production. The HTTR nuclear steam reforming system will therefore be taken as an example and described in more detail.

The HTTR steam reforming system has been designed to provide about  $4200 \text{ Nm}^3/\text{h}$  of hydrogen production using a Ni-based catalyst with 10 MW of thermal energy. A heat utilization ratio (defined as the ratio of output hydrogen energy to total input thermal energy) of 73 % is expected. This value is competitive with that of the conventional system, where the heat utilization ratio is about 80 %.

The HTTR can provide high temperature helium gas of  $905^\circ\text{C}$  at the outlet of the Intermediate Heat Exchanger (IHX) and, owing to further heat loss from the hot gas duct between the IHX and the steam reformer, secondary helium of  $880^\circ\text{C}$  at the inlet of the steam reformer. The steam reformer component is shown in Fig. 9.32 [33].

With the recent worldwide increased interest in hydrogen as a clean fuel of the future, Europe has also embarked on comprehensive research, development, and demonstration activities, with the main objective of moving from a carbon-based economy toward a  $\text{CO}_2$  emission free energy structure. Due to the growing demand for hydrogen in the petrochemical, fertilizer, and refining industries, however, the near and medium terms will be characterized by coexistence between the energy carrier's hydrogen and hydrocarbons.

In Europe countries under the Framework Program (FP) and closer collaborations among them as part of their strategies are required to provide a balanced choice of energy supply technologies while achieving the principal objectives of energy supply and continue for further developments with a Network of Excellence (NOE) with long term joint planning and Integrated Project (IP).

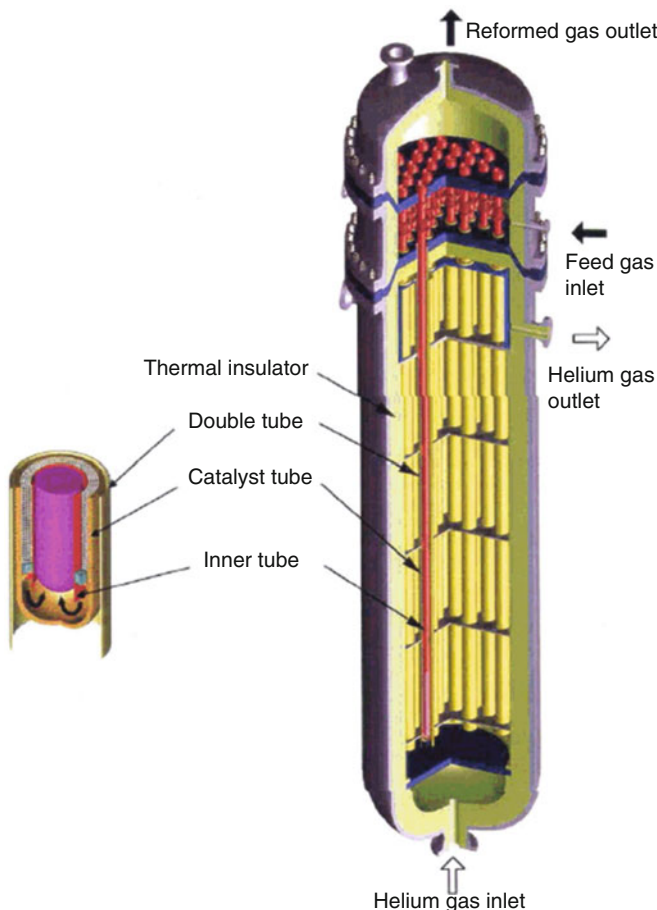


**Fig. 9.32** Steam reformer component for connection to HTTR [33]

For the demonstration, the coupling should involve a full scale proven industrial process with high reliability of the nuclear heat supply to the process. A schedule for the European demonstrator HTR/VHTR is suggested in Fig. 9.33.

Among the tasks of FP-6 and the nuclear projects with a certain relationship to hydrogen, the most important was the Integrated Project (IP) and Reactor for Process Heat, Hydrogen, and Electricity Generation (RAPHEL) which started in 2005 and was terminated in 2010. This IP consisted of 33 partners from ten European countries, with the objectives being, on the one hand, a study of advanced Gas Cooled Fast Reactor (GFR) technologies needed for industrial reference designs, but concurring with and benefiting from Japanese (HTR/VHTR) and Chimes (HTR-10) effort toward such technologies with their demonstrator projects in hand.

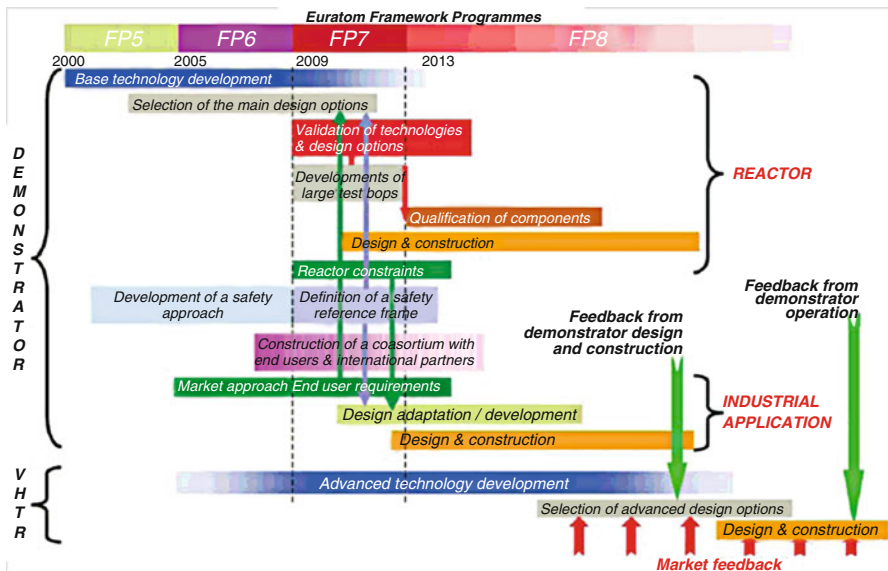


**Fig. 9.33** Suggested schedule for the development of a demonstrator HTR/VHTR for industrial process heat applications [33]

While RAPHAEL was fully concentrated on the development of a VHTR, five more activities were launched in the form of Specific Targeted Research Projects (STREPs) to deal with the other Generation IV reactor systems:

- RAPHAEL: Reactor for Process Heat, Hydrogen, and Electricity Generation (VHTR), 2005–2010;
- GCFR: Gas Cooled Fast Reactor (GFR), 2005–2009;
- HPLWR: High Performance Light Water Reactor (SCWR), 2006–2010;
- ELSY: European Lead Cooled SYstem (LFR), 2006–2010;
- EISOFAR: Road map for European Innovative Sodium Cooled Fast Reactor (SFR), 2007–2008;
- ALISIA: Assessment of liquid salts for innovative applications (MSR), 2007.

Several years' joint research among the European industries that was dedicated to High Temperature Gas Reactor (HTGR) technologies in conjunction with hydrogen production using these power plants has concluded to build such demonstration reactors with industrial process heat applications in mind and such collaboration requires strong partnership with end user industries as well. Figure 9.33 demonstrates a scheduling and timeline for demonstration of HTR/VHTR types under their Framework Program (FP). Their main objectives are pointed out as follows:

- To identify the main applications for nuclear process heat;
- To determine the viability of combining a nuclear heat source with conventional industrial processes and CHP applications;

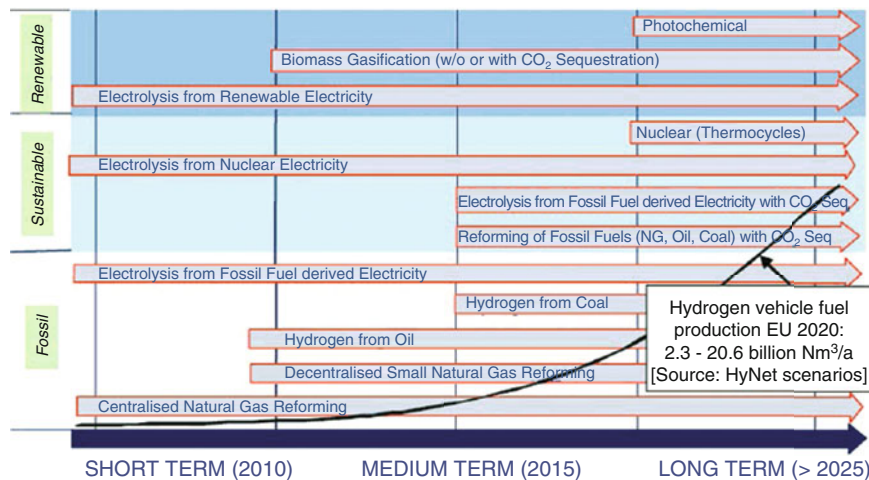


Fig. 9.34 HyNet timeline for hydrogen production technologies [21]

- To elaborate a program for the development of a coupled demonstrator between a VHTR and industrial processes that require heat supply;
- To form a strategic alliance between nuclear industry and process industries.

An essential prerequisite for the success of this project is the significant involvement of private companies in the form of industrial participation to develop and deploy innovative energy supply systems. As part of their effort on the hydrogen side of Research and Development (R&D), Hydrogen Network (HyNet) became active from 2001 to 2004 as a “thematic network” for their FP-5 with 12 European contractors and more than 70 interested partners. Figure 9.34 is a demonstration of the road map working on the development of strategies for the introduction of a European hydrogen fuel infrastructure.

Hydrogen production is deemed a crucial element for the introduction of hydrogen into the energy sector in the form of renewable energy. Research efforts were to be concentrated on the further improvement of known reforming and gasification methods, also with regard to high temperature primary energy systems such as Generation IV nuclear reactors and solar–thermal concentrating systems; on the development of CO<sub>2</sub> sequestration systems; on gas separation technologies; and on the efficiency improvement of hydrogen liquefaction technologies and system integration with hydrogen production facilities [33].

## 9.9 Thermal Characteristics for Coupling a Hydrogen Product Plant to HTR/VHTR

As part of the Department of Energy (DOE) effort in collaboration with Universities and National Laboratories under NUEP toward Research and Development (R&D) for employing the next generation high temperature nuclear reactors a huge

movement, by these universities and industries across the world along with national labs led by INL, has taken place. The use of high temperature nuclear reactors to produce hydrogen utilizing either thermochemical cycles or high temperature electrolysis is underway under the current budget of the DOE and NUEP as a renewable source of energy.

Although the production of hydrogen using these types of processes in conjunction with these next generation nuclear reactors to be coupled with hydrogen production plants is at its early stage of R&D, there is the need for study of such coupling for either of these processes to the high temperature reactor both for efficient heat transfer and adequate separation of these facilities to assure that facility safety and security during off-normal events in both plants do not impact each other.

To prevent such events the need for implementing an intermediate heat transport loop such as IHX is required to separate the operations and safety function between these two plants. The proposed investigation by DOE in order to utilize such high temperature nuclear power plants in order to produce hydrogen as a source of renewable energy could be either [34]:

1. Single Purpose or
2. Dual Purpose.

Early plants, such as the proposed Next Generation Nuclear Plant, may be dual-purpose facilities that demonstrate both hydrogen and efficient electrical generation. Later plants could be single-purpose facilities. At this stage of development, both single- and dual-purpose facilities need to be understood. Either way both purposes should be studied and understood no matter which way the plants in production are going.

Seven possible configurations for such intermediate loop have been proposed by INL and they are all reported in their INL/EXT-05-00453 report [33], while other researchers around universities have also reported new design configurations (Per Peterson) [35].

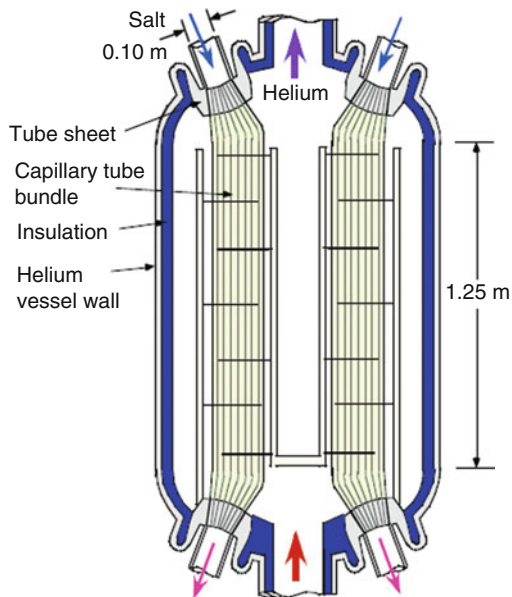
The one proposed by Peterson has been depicted here (see Fig. 9.35) and it is designed based on transportation of heat from the reactor to the chemical process plant, where the IHX needs to couple these two plans. He suggested this design based on the following configuration:

- Small Diameter Channels ( $D_0 = 3$  mm,  $D_1 = 1$  mm,  $L = 2$  m).
- Salt laminar flow regime ( $Re \sim 150$ )
- Linear Heat Rate of  $200$  °C/M

Where he proposed a capillary tube and shell heat exchanger showing the tube-bundle geometry formed by diffusion bonding of a multiple bundle of (approximately 2500) 3.0 mm diameter tubes with hexagonally tapered ends to form inlet and outlet tube sheets [21].

These types of IHXs are coupled between two production plants if they are adjacent to each other with a facility for the purpose of removing heat from the reactor side of the intermediate loop and a Process Heat Exchanger (PHX), where

**Fig. 9.35** IHX design proposed at UCB (UCBTH-07-003) [21]



the high quantity of heat then can be utilized by the hydrogen production plant in order to produce the hydrogen via processes such as either thermochemical cycles or high temperature electrolysis.

As mentioned before, to take advantage of HTR/VHTR of next generation in order to produce hydrogen as a new source of renewable energy, acquisition of such intermediate heat exchangers are required and further research studies should be conducted, both from a thermal hydraulic point of view and in order for the materials that these IHXs are built from to have the integrity to stand the high temperature that NGNPs demand for their base operational optimum designs. Another example of NGNP is the High Temperature Gas-Cooled Reactor (HTGR) being envisioned that will generate not just electricity, but also hydrogen to charge up fuel cells for cars, trucks, and other mobile energy uses. INL engineers studied various heat-transfer working fluids—including helium and liquid salts—in seven different configurations. In computer simulations, serial configurations diverted some energy from the heated fluid flowing to the electric plant and hydrogen production plant.

For these IHXs to be able to act as an intermediate loop between Liquid Salt (LS) or gas cooled loop as a safety net or buffer to separate the reactor side from the hydrogen or chemical side of the plant combined within a facility, we need these intermediate loops, because by increasing the thermal inertia in the system with liquid salt in the loop in particular, the intermediate loop mitigates for reduction of the sensitivity to temperature transients stresses.

In another purposed configuration of the Intermediate Heat Exchanger (IHX) by Peterson et al. (Report UCBTH-03-004) [35] they compare the Molten Salt and

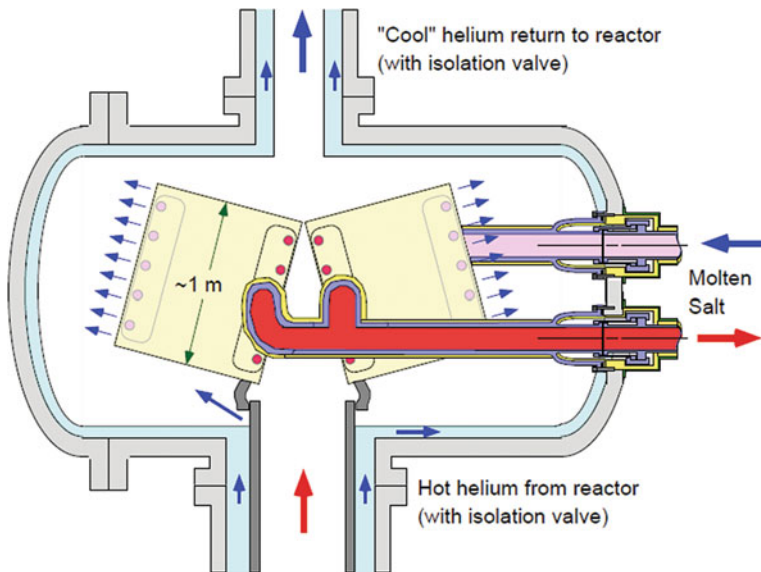


**Fig. 9.36** Pre-conceptual design for a 50 MW(t) intermediate heat exchanger in NGNP, based on a plate type, compact high-temperature composite design [35]

High-Pressure Helium for the NGNP Intermediate Heat Transfer Fluid, and it is depicted here in Fig. 9.36.

They suggest a base design of 50 MW(t) intermediate loop be implied by the Next Generation Nuclear Plant (NGNP) to transfer heat from the primary coolant to generate heat for the production plant of hydrogen using thermochemical and high-temperature electrolysis processes in order to achieve an efficiency higher than 50 % where the high temperatures are required for the baseline Sulfur-Iodine (SI) thermochemical process. The functional requirements for NGNP do include a 1000 °C core outlet temperature for this proposed design.

The high temperature imposes substantial technical challenges for the intermediate heat exchanger (IHX) and process heat exchangers, as well as intermediate heat transfer loop components. They have also considered the two candidate fluids for the NGNP intermediate loop for this approach to be the intermediate-pressure of Molten-Salt (MS) and high-pressure Helium (HE) [36].

The best suggested approach for thermal analysis of designing such heat exchangers is to use the method of NTU-Effectiveness in a one dimensional coordinate system by neglecting the longitudinal in  $x$ -direction for main flow conduction and then expand it to a more accurate two-dimensional model to include cross flow conduction of fluids as well as spatially varying both longitudinal and latitudinal constraints. A Finite Elements Method (FEM) can be employed to handle such computational analysis for each unit cell and can be built based on each region that captures the most important information of that particular region

both in steady-state to start with it and then expand to transient mode for better accuracy of results. Utilization of dimensional analysis methods [37] is also recommended in order to deal with the complex form of fluid mechanics and fluid dynamics partial differential equations for thermal hydraulic and heat transfer analysis purposes.

As we mentioned above per INL/EXT-05-00453 [38], seven possible configurations for the high-temperature reactor primary coolant system and the intermediate heat transfer loop have been proposed; and the advantages/disadvantages of each are identified and the working fluid (i.e., LiF-NaF-KF (Flinak) in the form of molar concentrations of 46.5 %, 11.5 %, and 42 %, respectively as well as NaBF<sub>4</sub>-NaF in molar concentrations of 92 % and 8 %) for each of these suggested configurations for design option has been specified as well.

However, the recommendation of a specific design requires input from a variety of disciplines related to materials, thermal-hydraulics, economics, safety, and plant operability. This report also describes each of these intermediate heat transport loop configurations and summarizes the thermal hydraulic, structural, and efficiency calculations that have been processed and computed to characterize the advantage and issues associated with each configuration. The base key issues that were taken under consideration and addressed include:

- Configuration options.
- System parameters, such as temperature and pressure.
- Structural issues.
- Working fluid options and materials issues.

In order to perform this analysis report (Davis) [34] has identified key requirements by picking two top-level high temperature reactors from NGNP that fit into this calculation and basic thermal hydraulic analysis for interfacing and coupling between the nuclear power and hydrogen production plant via the intermediate heat transport loop that is required.

Therefore for the purpose of any heat transfer and thermal hydraulic analysis one needs to consider the following conditions:

1. Identify key requirements of the high-temperature reactor and the hydrogen production plant that affect the choice of the intermediate heat transport loop;
2. Identify and justify assumptions that were used in the evaluation of such analysis;
3. Identify possible configurations of the intermediate heat transport loop along with the choice of fluids that are going to be used for heat transfer media;
4. Perform preliminary stress evaluations to determine allowable materials for the intermediate heat transport loop to deal with the high-temperature of base plants;
5. Estimate the size and thermal hydraulic performance of various components in the intermediate heat transport loop including the heat exchangers and loop piping;
6. Estimate the overall cycle efficiency of each configuration;
7. Determine the sensitivity of the cycle efficiency to various parameters; and

8. Compare and contrast the different options to help in the selection of the configuration and working fluid.

One other important key requirement is what will be the choice for nuclear reactor among the NGNP generation, based on its output of thermal power and what coolant system is going to be used in that particular reactor. For example the Small Modular Reactors (SMRs) thermal power output among SMRs varies between 20 and 100 MW, such as the ones produced by the NuScale Corporation [39]. The choice of thermal power output impacts the nominal rise in fluid temperature across the core, based on point design, and other variables such as pressure drop across the hot stream of the Intermediate Heat Exchanger (IHX) can be assumed, which also drives the dependency on the pumping power associated with this pressure drop across the IHX.

All the above constraints do play a huge role in determining the separation distance between the nuclear and hydrogen production plants which is a part of safety factors and licensing criteria too. For example for Japanese High Temperature Test Reactor (HTTR) this distance was calculated to be 300 m [40] while a similar distance for Next Generation Nuclear Plant (NGNP), based on point design and other variables that were mentioned in the above set, was calculated to be between 60 and 120 m [41].

Such separation distance has direct impact and affects the diameters and insulation requirements of the hot and cold legs in the heat transport loop as well and the nominal temperature drop between the outlet of the NGNP and the maximum temperature delivered to the hydrogen production plant assumed to be 50 °C. This temperature drop imposes requirements on the effectiveness of the heat exchangers that connect the NGNP and production plant and the amount of heat loss than can be tolerated in the intermediate loop. In order to perform preliminary calculations, heat loss was assumed to cause the fluid temperature to drop 10 °C in the hot leg of the intermediate loop at nominal conditions [34].

As part of the strategy of IHX acquisition one can select it to be a Compact Heat Exchanger rather than shell and tube design, therefore NTU-Effectiveness design should be taken under consideration (Dewson and Thonon) [42], while the Process Heat Exchanger (PHX), which is the Heat Exchanger (HX) that connects the heat transport loop to the hydrogen production plant, can be chosen as Tube-In-Shell type and possible Logarithmic Mean Temperature Difference (LMTD) analysis may be utilized to design a PHX heat exchanger.

This type of shell-and-tube type HXs consists of tubes spirally wound into bundles and fitted into a shell. Because of the tube bundle geometry, a considerable amount of surface can be accommodated inside the shell. These HXs are used for gas-liquid heat transfer applications, primarily when the operating temperature and/or pressure are very high. The challenging part of this type of configuration is in Preventive Maintenance (PM) and cleaning associated with such PM.

Sizing of these IHX as part of thermal hydraulic analysis is a function of the overall temperature difference between the outlet of the reactor core and the inlet on the cold side of the Processing Heat Exchanger (PHX) and could be assumed to be

tube-in-shell heat exchangers with the heat transport fluid flowing on the shell side. This configuration allows the tubes to contain the catalysts necessary for hydrogen production, which is judged to be the most convenient configuration. The tube side can be assumed to be at low pressure (less than 1 MPa). The hot and cold legs of the intermediate loop may be assumed to be separate pipes, as opposed to an annular configuration for the purpose of such analysis [34].

For the purpose of stress analysis a simplified approach can be taken for different components in any desired configuration based on points of design in order to determine the thickness requirement so that the circumferential stress can be allowed within optimum values and configurations as well. The creep rupture strength of materials also needs to be taken under consideration as part of stress analysis and it depends on the operating time at a given temperature.

Figure 9.37 shows that the rupture strength of Alloy 800 decreases sharply with temperature. At an operating time of  $10^5$  h (about 11 years), the rupture strength is 240 MPa at 500 °C, but decreases to 8 MPa at 900 °C. The rupture strength also depends on the time at temperature. At 900 °C, the rupture strength increases from 8 to 16 MPa when the operating time decreases from  $10^5$  to  $10^4$  h. The data presented in Fig. 9.37 suggest that the mechanical design of the heat transport loop will be a challenge because of the desired high temperature and the long lifetime, both of which act to reduce the rupture strength.

The creep rupture strengths of three candidate materials for the heat transport loop are shown in Fig. 9.38 for a temperature of 900 °C. These three materials are

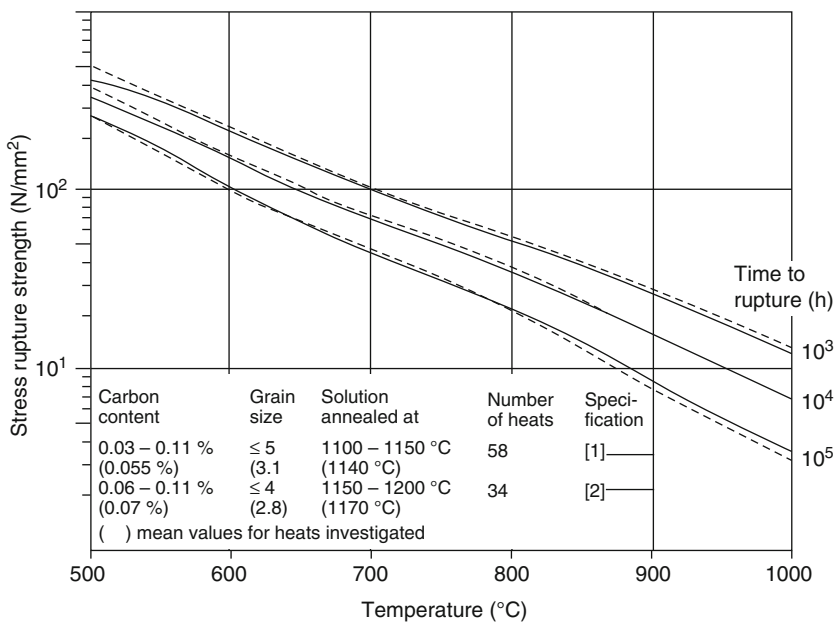


Fig. 9.37 Creep rupture strength of alloy 800 (From Diehl and Bodman 1990) [43]

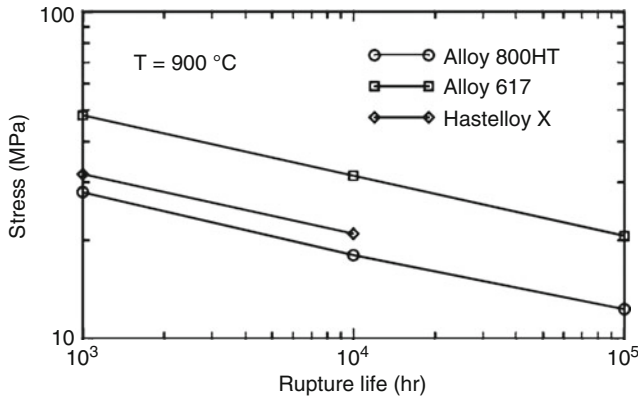


Fig. 9.38 Creep rupture strengths of candidate materials [22]

Alloy 800HT, which is a high-temperature variation of Alloy 800 (Special Metals 2004a), Alloy 617 (Special Metals 2004b), and Hastelloy X (Haynes International 2005). Alloy 617 has the highest rupture strength of these three materials at 900 °C. The allowable stress will eventually be specified by an applicable code, but will be less than the strengths shown in Fig. 9.38 to account for safety factors. For this analysis, the allowable stress was assumed to be half of the creep rupture strength.

Crandall et al. [44] suggests using the following mathematical relationship to calculate the tangential stress  $\sigma$  for a thick wall

$$\sigma = \frac{P_i \left[ (r_o/r)^2 + 1 \right] - P_o \left[ (r_o/r_i)^2 + (r_o/r)^2 \right]}{(r_o/r_i)^2 - 1} \quad (\text{Eq. 9.1})$$

Where  $r$  is radius,  $P$  is the pressure, and the subscripts i and o refer to the inner and outer surfaces respectively.

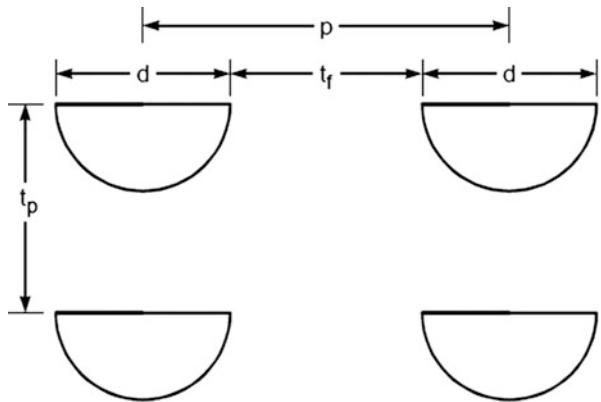
If the external pressure exceeds the internal pressure, then the stress is a negative value, but the maximum magnitude always occurs at the inner surface. The radius ratio that causes the maximum stress to be less than or equal to the allowable stress,  $\sigma_D$ , can be calculated from Eq. (9.1). For those cases where the internal pressure exceeds the external pressure, the limiting ratio is:

$$\frac{r_o}{r_i} \geq \sqrt{\frac{\sigma_D + P_i}{\sigma_D + 2P_o - P_i}} \quad (\text{Eq. 9.2})$$

For cases where the external pressure exceeds the internal pressure, the maximum, absolute value of the stress will be less than or equal to the allowable stress when the radius ratio is:

$$\frac{r_o}{r_i} \geq \sqrt{\frac{\sigma_D - P_i}{\sigma_D - 2P_o - P_i}} \quad (\text{Eq. 9.3})$$

**Fig. 9.39** Illustration of IHX channels



A simple stress analysis was also performed for the IHX assuming that it is a compact heat exchanger of the type designed by Heatic (Dewson and Thonon) [42]. The design of the heat exchanger channels is defined by the channel diameter,  $d$ , pitch,  $p$ , and plate thickness,  $t_p$ , as illustrated in Fig. 9.39. Each plate contains either hot or cold fluid, but not both. Adjacent plates contain the other fluid. Following the method used by Dostal et al. [45], the minimum wall thickness between channels,  $t_f$ , can be approximated as

$$t_f \geq \frac{p}{\frac{\sigma_D}{\Delta P} + 1} \quad (\text{Eq. 9.4})$$

where  $\sigma_D$  is the allowable stress and  $\Delta P$  is the differential pressure between the hot and cold streams. Expressing Eq. (9.4) in terms of pitch-to-diameter ration yields:

$$\frac{p}{d} \geq 1 + \frac{\Delta P}{\sigma_D} \quad (\text{Eq. 9.5})$$

The required plate thickness can also be calculated based on the method explained and reported by Dostal et al. [45]. The plate is assumed to be a thick-walled cylinder, with an inner radius of  $d/2$  and an outer radius of  $t_p$ . Equations (9.2) and (9.5) can be used to calculate the thickness-to-diameter and pitch-to-diameter ratios for the IHX as a function of allowable stress and various pressures of the hot and cold streams. The allowable stress is assumed to be 10 MPa, which is approximately half of the rupture strength of Alloy 617 at 900 °C [38].

As part of thermal hydraulics and heat analysis component sizing comes into play when we look at the nominal temperature drop between the outlet of the Next Generation Nuclear Plant (NGNP) and the maximum temperature delivered to the hydrogen production plant per design point assumption as a fixed value rather than being variable. This temperature drop has a constraint on the effectiveness of the heat exchangers that bridge between the NGNP and the hydrogen production plant

and the amount of heat loss that would be tolerable in the intermediate loop. The distribution of the temperature drop between the heat exchangers and heat loss can be taken as a variable value. For example, if the heat loss can be reduced while the temperature drop across the heat exchanger can be increased then as a result a smaller or more compact heat exchanger can be implemented. As part of analysis one can take the remaining temperature drop between the outlet of the NGNP and the maximum temperature delivered to the hydrogen production plant and divide it evenly between the Intermediate Heat Exchanger (IHX) and Process Heat Exchanger (PHX), and if present, the Secondary Heat Exchanger (SHX).

The effectiveness of a heat exchanger  $\epsilon$  can be written as Eq. (9.6) as suggested by (Kreith) [46] knowing that the temperature drop between the NGNP and the production plant drives the requirements of the heat exchanger.

$$\epsilon = \frac{(\dot{m} c_p)_{\text{hot}} [(T_{\text{hot}})_{\text{in}} - (T_{\text{hot}})_{\text{out}}]}{(\dot{m} c_p)_{\text{min}} [(T_{\text{hot}})_{\text{in}} - (T_{\text{cold}})_{\text{in}}]} \quad (\text{Eq. 9.6})$$

where  $\dot{m} = v\rho$  ( $v$  is flow rate and  $\rho$  is flow density) is the mass flow rate,  $c_p$  is the specific heat capacity at constant pressure and is assumed constant, and  $T_{\text{hot}}$  and  $T_{\text{cold}}$  are the temperatures for the hot and cold sides of the heat exchanger while the subscripts in and out refer to the inlet and outlet ends of the heat exchangers, and subscript min refers to the minimum value for the hot and cold sides.

Equation (9.6) applies when a counter-flow type heat exchanger is chosen, which requires less surface area (i.e., more compact shape and presumably more cost effective from a production point of view) than is required by parallel-flow type.

If we encounter the condition where the value of  $\dot{m} c_p$  is the same for the hot and cold flow streams, then effectiveness temperature-wise just depends on the inlet and outlet temperature. Approximation can also be imposed to analyze the required heat transfer area  $A_{\text{ht}}$  in order to size the heat exchanger, where this is given by:

$$A_{\text{ht}} = \frac{\epsilon (\dot{m} c_p)_{\text{min}} [(T_{\text{hot}})_{\text{in}} - (T_{\text{cold}})_{\text{in}}]}{U \Delta T} \quad (\text{Eq. 9.7})$$

Where  $U$  is the overall heat transfer coefficient and  $\Delta T$  is the Logarithmic Mean Temperature Difference (LMTD), which is calculated as follows:

$$\Delta T = \frac{\Delta T_a - \Delta T_b}{\ln(\Delta T_a / \Delta T_b)} \quad (\text{Eq. 9.8})$$

where  $\Delta T_a$  is the temperature difference between the hot and cold fluid streams at one end of the heat exchanger and  $\Delta T_b$  is the temperature difference at the other end.

**Example 9.1** Calculate heat transfer area for heat exchangers given the following values:

Flow Rate = 20,000 m/h
Density of Fluid = 1020 kg/m <sup>3</sup>
Specific Heat = 3.95 kJ/kg K
Overall Heat Transfer Coefficient = 5000 W/m <sup>2</sup> K
Temperature Change = 30 °C
Temperature Difference = 20.8 °C
Effectiveness = 1

**Solution** Using Eq. (9.7), we can calculate the heat transfer area as

$$A = \frac{1 \times 20,000 \times 1020 \times 3.95 \times 30}{3600 \times 20.8 \times 5000} = 6.5 \text{ m}^2$$

The overall heat transfer coefficient is calculated from the heat transfer coefficients on both sides of the exchanger and the thermal conductivity and thickness of the metal. The heat transfer coefficients and the thermal conductivity are assumed constant over the length of the heat exchanger. For turbulent flow, the heat transfer coefficients are calculated using the Dittus-Boelter correlation, with a leading coefficient of 0.021 for gases and 0.023 for liquids (INEEL) [47]. For laminar flow, the heat transfer coefficients are calculated from the exact solution for fully developed flow with constant heating rate (Kayes and Crawford) [48] or (Zohuri and Fathi) [23]. The thermal conductivity of the metal is calculated assuming Alloy 800, and varies between 18 and 26 W/m K over the temperature range of interest.

Further analysis related to the subject of sizing of heat exchangers, including estimating the pumping power, efficiency evaluation can be found in the next two chapters as well the books by Zohuri [18] and Zohuri and Fathi [37] or Zohuri and McDaniel [49].

The inner diameters of the hot and cold leg pipes in the heat transport loop are sized to produce a given pressure drop. The thickness of the piping is based on the results of the stress analysis. The heat loss is calculated using an overall heat transfer coefficient, which accounts for the thermal resistance of the heat transfer coefficient at the inner and outer surfaces, the pipe metal, and the insulation (Bird et al.) [38].

Pumping power  $Q_p$  is given below by the approximation analysis provide by Glasstone and Sesonske [50] as:

$$Q_p = \frac{\dot{m} \Delta P}{\rho} \quad (\text{Eq. 9.9})$$

Where  $\dot{m}$  is the mass flow rate,  $\Delta P$  is the pressure drop, and  $\rho$  is the fluid density, which is based on the temperature at the inlet to the reactor for the hot stream of the

IHX and based on the temperature of the cold stream entering the IHX or the SHX for the intermediate and tertiary loops.

Further research, analysis, and development are required going forward with the concept of utilizing next Generation of Nuclear Plant coupling with a Hydrogen Production Plant since NGNP are still at the conceptual stage of design and their thermal efficacies are constantly challenged (Zohuri) [17, 18].

## 9.10 Next Generation Nuclear Plant Intermediate Heat Exchanger Acquisition

As part of the acquisition strategy for the right choice of Intermediate Heat Exchanger (IHX) for Next Generation Nuclear Plant (NGNP), first we need to select the right generation of nuclear power plant for this purpose with the quality of delivering the high temperature we are looking for as a base design; and the Department of Energy (DOE) has selected the High Temperature Gas-cooled Reactor (HTGR) design for the Next Generation Nuclear Plant (NGNP) Project to be coupled with a hydrogen production plant via IHX and its sub-components that are most efficient and cost effective.

The NGNP will demonstrate the use of nuclear power for electricity and hydrogen production. The reactor design will be a graphite moderated, helium-cooled, and prismatic or pebble-bed, thermal neutron spectrum reactor. The NGNP will use very high burn-up, low-enriched uranium, Tri-Isotopic (TRISO)-coated fuel, and have a projected plant design service life of 60 years. The HTGR concept is considered to be the nearest-term reactor design among the other six choices designated as Generation-IV (GEN-IV) nuclear power plants of the future, and has the capability to efficiently produce hydrogen by being coupled to the hydrogen plant via its designated IHX set (see Fig. 9.40). The plant size, reactor thermal power, and core configuration will ensure a passive decay heat removal system without fuel damage or radioactive material releases during accidents as part of a safety net imposed on Generation-IV (GEN-IV).

Figure 9.40 is the six proposed Generation IV systems that are on the table for consideration as part of efforts by Gen-IV International Forum (GIF) initiated in 2001. As can be seen from this figure there are a total of six advanced nuclear power plant designs proposed and the main desired aspects behind all of them address: inherent safety, proliferation resistance, and last but not least, efficiency and process heat capability that they share as a common denominator.

Figure 9.41 is a conceptual illustration of a High Temperature Gas cooled Reactor (HTGR) that is coupled with a Hydrogen Production Plant along with a Power Conversion Unit (PCU). There are various iterations on this concept and the most notable is a proposed concept by IAEA which is the Very High Temperature Reactor (VHTR) as part of the Generation IV family design (see Fig. 9.41), where in the case of Pebble Bed Reactor or the HTGR in all cases they share a number of

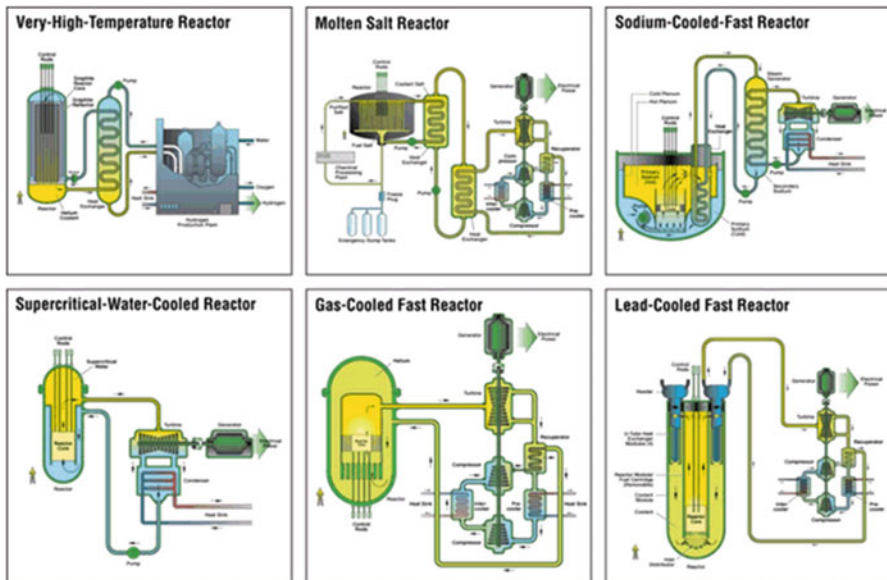


Fig. 9.40 Six proposed generation IV systems

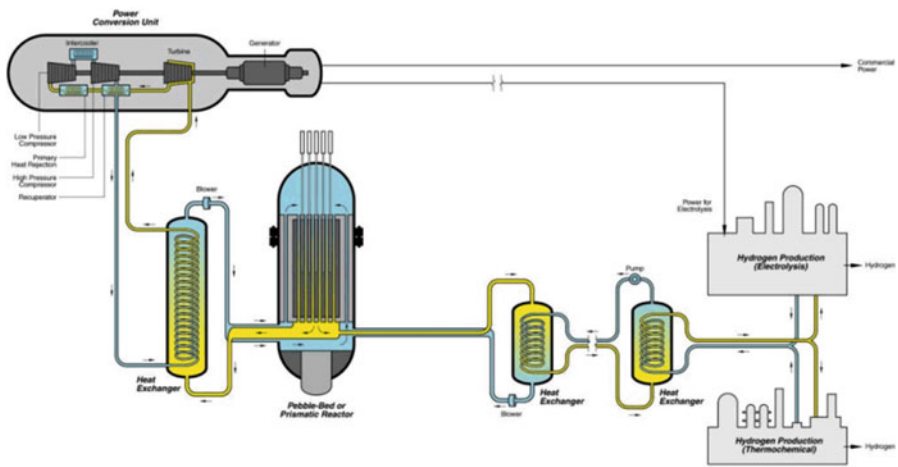
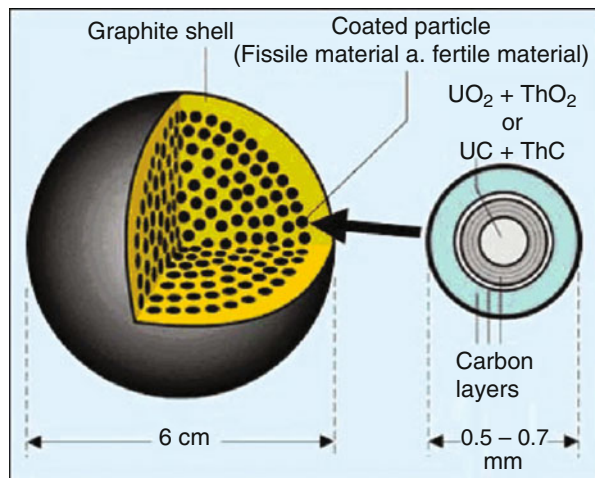


Fig. 9.41 HTGR schematic, with optional hydrogen production plant attached [51]

common characteristics. They all can be grouped under the High Temperature Gas Reactors (HTGRs) and in principle all of them have a graphite moderated reactor core using an inert gas, likely helium, as a cooling fluid moderator.

As part of the core design and fuel options for HTGR, the fuel would be either in the form of roughly 60 mm graphite spheres inside of which are suspended a matrix

**Fig. 9.42** HTGR fuel pellet

of silicon carbide and Uranium dioxide particles, or stacks of prismatic blocks of a similar composition. By including Thorium dioxide within the fuel mix, we can also partly utilize the Thorium fuel cycle. However, as Thorium has no naturally occurring fissile isotope, it must be used in a mixed mode with Uranium (see Fig. 9.42).

One of the key advantages of HTGRs is the high operating temperatures, ranging from a minimum of around 650 °C all the way up to 1000 °C. This has several useful advantages and they are as follows:

1. First, we can now utilize the Brayton cycle, which can potentially allow for thermal efficiencies of up to 65 % (although 45–55 % is more typical) compared with a maximum of 47 % for the more conventional Rankine (with a typical range of 33–40 %) (Zohuri) [17, 18].
2. Alternatively, if the operating temperature can be maintained well south of 800 °C, we can utilize the Sulfur-Iodine process to manufacture hydrogen directly using heat energy with a high level of energy efficiency (Zohuri) [17, 18].

The operating conditions for the NGNP represent a major departure from existing water-cooled reactor technologies. Few choices exist for metallic alloys for use at NGNP conditions and the design lifetime considerations for the metallic components may restrict the maximum operating temperature. Qualification of materials for successful and long-life application at the high-temperature conditions planned for the NGNP is a large portion of the effort in the NGNP Materials Research and Development (R&D) Program [51].

Selection of the technology and design configuration for the NGNP must consider both the cost and risk profiles to ensure that the demonstration plant establishes a sound foundation for future commercial deployments. The NGNP challenge is to achieve a significant advancement in nuclear technology while at the

same time setting the stage for an economically viable deployment of the new technology in the commercial sector soon after 2020 [37].

Now that we have a better understanding of the Very High Temperature Reactor (VHTR) concept and how they operate, we can go back to our original topic of this section and the strategy of selecting the right Intermediate Heat Exchanger (IHX) for this type of reactor to be used to couple the nuclear side with the hydrogen generating plant side. As we said, the major component of the Next Generation Nuclear Power Plant (NGNP) driving the Hydrogen Production Plant (HPP) is the Intermediate Heat Exchanger (IHX).

This component will transfer heat to secondary systems that will generate electricity or hydrogen. The IHX will be operated in flowing impure helium on the primary and secondary side at temperatures up to 950 °C. There are major high temperature design, materials availability, and fabrication issues that need to be addressed. The prospective materials are Alloys 617, 230, 800H, and XR with Alloy 617 being the leading candidate for use at 950 °C.

Developing an acquisition strategy policy is part of the NGNP Materials Research and Development (R&D) Program. The objective of the NGNP Materials R&D Program is to provide the essential materials studies and laboratory investigations needed to support the design and licensing of the reactor and balance of plant, excluding the hydrogen plant. The materials R&D program was initiated prior to the design effort to ensure that materials R&D activities are initiated early enough to support the design process. The thermal, environmental, and service life conditions of the NGNP will make selection and qualification of the high-temperature materials a significant challenge; thus, new materials and approaches may be required. The mission of the NGNP Materials Program must support the objectives associated with the NGNP in the Energy Policy Act of 2005 and provide any materials related support required during the development of the NGNP.

As a result of such energy policy act the selection of an Intermediate Heat Exchanger should take place based on certain assumptions that are listed below [52]:

- The NGNP will be a full-sized reactor plant capable of electricity generation with a hydrogen demonstration unit of appropriate size.
- The reactor design will be a helium-cooled, graphite moderated core design fueled with TRISO design fuel particles in carbon-based compacts or pebbles.
- The NGNP must demonstrate the capability to obtain a Nuclear Regulatory Commission (NRC) operating license. The design, materials, and construction will need to meet appropriate Quality Assurance (QA) methods and criteria and other nationally recognized codes and standards.
- The demonstration plant will be designed to operate for a nominal 60 years.
- The NGNP Program including the materials program will continue to be directed by the Idaho National Laboratory (INL) based on the guidelines given in the Energy Policy Act of 2005. The scope of work will be adjusted to reflect the level of congressional appropriations.

- Application for an NRC operating license and fabrication of the NGNP will occur with direct interaction and involvement of one or more commercial organizations.

Certain issues are arising due to the above assumptions that require some attention with respect to the design effort for the NGNP driven hydrogen generation plant and associated IHX to perform such duty. These issues are listed here as general concerns [37]:

- The last HTGR design reactor built in the US was the Fort Saint Vrain (FSV) gas-cooled reactor [39] which was constructed in the early 1970s, generated the first power sent to the grid in 1976, and was taken out of service in 1989. The fact that there has been no HTGR construction in this country since then along with the long gap in construction of Light Water Reactors (LWRs) puts the NGNP in the situation where there is a lack of current industry technical information and experience with regard to the materials of construction and fabrication practices associated with the NGNP designs currently under consideration.
- The design effort completed needs to include a final IHX design so a material acquisition list can be developed. There needs to be new information developed as regards the primary metals producers who can produce the high temperature alloys in the required product forms specified for use in the IHX. For compact IHX designs joining and inspection R&D will be necessary.
- Another issue is the identification of vessel fabrication vendors with the appropriate American Society of Mechanical Engineers (ASME) certifications to perform nuclear work. The number of these firms has declined over the last 20 years and the NGNP will be competing for these services with resurgent orders for LWRs and chemical process facility components in a world market. There is significant competition for these fabrication resources.
- To meet the NGNP startup date of 2021, these IHX must be delivered much earlier. The needed delivery date must be identified and a schedule for material acquisition and fabrication must be developed. For a given desired delivery date the following steps need to be completed with the appropriate completion dates:
  1. Place material order with primary metal producer to obtain position in the melting schedule to secure material for fabrication.
  2. Finalize material shapes and sizes (tubing, sheet, forgings, plate) and choose the appropriate specifications for the intermediate product mill.
  3. Secure fabrication vendor services and ship material to his facility.
  4. Completion date for fabrication.
  5. Shipment to Idaho.
  6. Installation of the IHX and other major equipment to meet start up schedule.

According to the Pros and Cons discussed above, two alternative IHX designs were developed based on the Printed Circuit Heat Exchanger (PCHE) concept with one design developed by the Heatic Corporation and the second design developed by the Toshiba Corporation. These designs consist of metal plates that are diffusion

bonded together with flow channels that are chemically milled into the plate. The PCHE concept allows for simultaneous high-temperature and high pressure operation with relatively thin wall thicknesses between the primary and secondary coolants. The PCHE designs are typically four to six times smaller than conventional shell-and tube heat exchangers of equivalent duty and designs have been developed with thermal effectiveness greater than 98 %. The description of PCHE is presented throughout this book in various chapters that readers can look up per pages indicated in the index at the end of the book.

An alternative design using a shell and tube, counter-flow heat exchanger using a helically coiled tube was developed by the Toshiba Corporation. For an equivalent heat duty and Long Mean Temperature Difference (LMTD), this type of heat exchanger is considerably larger than a PCHE. This design allows for In-Service Inspection (ISI) of the heat transfer tubes. This design has successfully operated in the HTTR [51, 52].

## 9.11 Applicability of Heat Exchanger to Process Heat Applications

The strategic goal of the Advanced Reactor Concept Program is to broaden the environmental and economic benefits of nuclear energy in the U.S. economy from power production to meet energy needs and also demonstrate applicability to market sectors not being served by light water reactors. The Advanced High Temperature Reactor (AHTR) offers unique advantages for a variety of markets beyond power production because of the high Reactor Outlet Temperature (ROT) and because of the superior heat transport characteristics of molten salt. Increased ROT would expand the AHTRs applicability to many other applications; readers should direct themselves to a report by Sabharwall et al. [53].

The integration of AHTR technology with conventional chemical industrial processes is presented in this section. The process heat industrial applications being considered are: hydrogen production via steam methane reforming of natural gas and high temperature steam electrolysis, substitute natural gas production, oil sands recovery via steam assisted gravity drainage, coal-to-liquid production, natural gas-to-liquids production, methanol-to-gasoline production, ammonia production, ex-situ oil shale, and in-situ oil shale. The temperature ranges of applications that could be coupled to the AHTR with the current ROT (green band) and others that could potentially be coupled if the ROT was raised (red band) are shown in Fig. 9.43. These are representative and should not be considered inclusive of all potential applications.

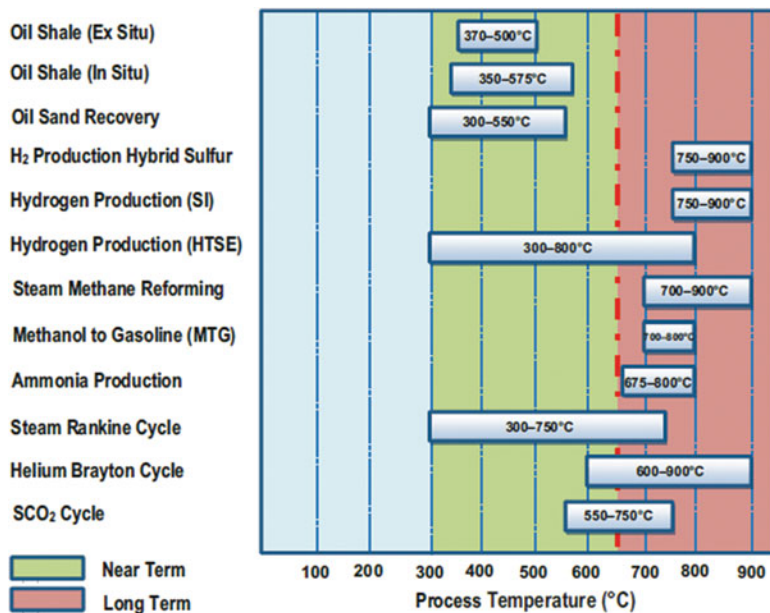


**Fig. 9.43** Process applications for AHTR versus process required temperature range [53]

### Situ Oil Definition

This relatively new method is mainly used to get bitumen in oil sand that is buried too deep below the earth's surface to be recovered with a truck and shovel. In situ technology injects steam deep beneath the earth to separate the viscous bitumen from the sand and pump it up to the surface. The bitumen then goes through the same upgrading process as it would in the mining method.

Sabharwall et al. [53], in their analyses, reported heat from an AHTR which was transferred from the reactor core by the primary liquid-salt coolant to an intermediate heat-transfer loop through an IHX. The intermediate heat-transfer loop circulates intermediate liquid-salt coolant through a Secondary Heat Exchanger (SHX) to move the heat to a power conversion system or for process industrial application as shown in Fig. 9.44.

The Reactor Outlet Temperature (ROT) is currently 704 °C and was reported by Sabharwall et al. [53], but will possibly increase to 900–1000 °C for the *n*th-of-a-kind.. The process heat application becomes an attractive option due to its ability to provide higher ROT. Even though the ROT for the AHTR is 700 °C (~704 °C), the maximum available temperature for any process application is 650 °C as shown by the dashed line in Fig. 9.44. Process heat applications are mentioned in this section,

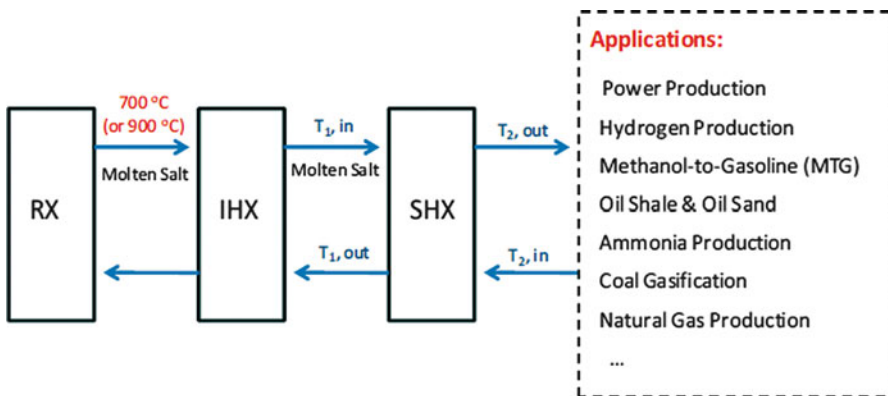


**Fig. 9.44** Thermal energy transfer in AHTR for power or process application [53]

but details are given in TEV-1160, “AHTR Technical Evaluation” (Sabharwall and Kim) [54].

Sabharwall et al. [53], for their analysis assumed the following conditions in order to carry out their calculation:

- The reactor outlet temperature for AHTR is assumed to be 700 °C.
- An AHTR ROT should be sufficiently larger (~50 °C) than the process application temperature requirement.
- Any power production/industrial application requiring greater than 650 °C is referred to as a long term objective.
- The minimum AHTR heat exchanger temperature should be maintained high enough to avoid molten salt freezing (>500 °C), which will provide about a 50 and 65 °C temperature threshold before fluoride salts such as LiF-NaF-KF (FLiNaK) and chloride salts such as KCl-MgCl<sub>2</sub> freeze.
- Heat exchanger tube material should have sufficient mechanical integrity to sustain pressure difference across the tube wall (will depend on application).

The process heat applications mentioned briefly in this section are discussed in greater detail in TEV-1160, “AHTR Technical Evaluation” (Sabharwall and Kim) [54]. With the ROT of 704 °C and the maximum available temperature of 650 °C for process heat applications, the current AHTR could provide process heat for the following applications:

- Near-term integration (<650 °C):
  - Power production cycles (Steam Rankine Cycle, Helium Brayton Cycle,  $\text{SCO}_2$  cycle)
  - Oil shale (in situ)
  - Oil shale (ex situ)
  - Oil sands.

- Long-term integration ( $>650$  °C):
  - Hydrogen production via steam methane reforming
  - Substitute natural gas production
  - Coal-to-liquid production
  - Natural gas-to-liquid production
  - Methanol-to-gasoline production
  - Ammonia production.

An AHTR, when compared to gas-cooled reactors for process heat applications, benefits from a higher reactor inlet temperature because the molten salt is a more efficient heat transport medium and can transfer all of the reactor's heat with less temperature drop. This allows smaller and more efficient heat exchange equipment and produces smaller thermal stresses on those components.

## 9.12 Applicability of Compact Heat Exchanger to Process Heat Applications

As we have explained and described in previous chapters of the book, the Compact Heat Exchangers (CHEs), based on their physical properties—namely having light weight, minimum volume due to the nature of their compact design [having surface area density above about  $700 \text{ m}^2/\text{m}^3$  ( $213 \text{ ft}^2/\text{ft}^3$ ) compactness on at least one of the fluid sides which usually has gas flow], and therefore small foot print and high effectiveness—have played a major technological role in the advancement of the transportation of nuclear energy to produce better thermal efficiencies [17, 18] for production of electricity, process industry, and now similar important roles in hydrogen generation plants not only for industrial process, but recently we can also see application of high temperature thermal devices for nuclear process heat transfer driven hydrogen production plants. At the beginning of this chapter and through the previous section we talked about the RX-Series as an air-to-air or gas-to-gas heat exchanger (see Fig. 9.45 below), Intermediate Heat Exchanger (IHX), Process Heat Exchanger (PHX) and Secondary Heat Exchanger (SHX), heat exchangers in the form of primary, intermediate, and secondary thermal devices for industrial applications; and in particular production of hydrogen using an advanced high temperature reactor (AHTR) of new generation power plants, namely GEN-IV. However, the operating environment and applications for the process industry are significantly different and the major limitations of compact heat exchangers are maximum operating pressure and temperature and minimum allowed fouling, which have prevented their widespread adoption and use in the process industry. However, significant advances and steps have taken place in manufacturing technology as well as in the design theory and our knowledge of fundamentals of flow phenomena in compact heat exchangers. These new developments together with new and improved types of CHEs, in particular fine plate or

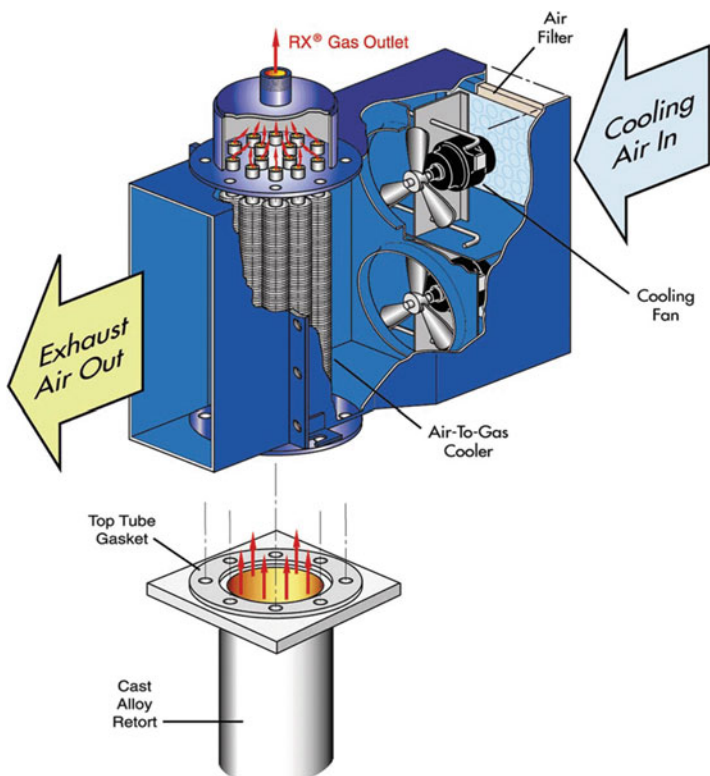


**Fig. 9.45** Diagram of Rx-series air-to-air heat exchanger

planner surfaces as part of SHX applications, present an excellent opportunity to introduce compact heat exchangers in the process industry, particularly when energy saving during off-line periods is also an important objective in terms of the quest for new sources of renewable energy such as a hydrogen production plant for fuel-cells and other applications.

In acquisition of a Secondary Heat Exchanger (SHX) in process industry such as hydrogen production, in terms of high temperature thermal devices, some concepts identified as potential options for the SHX are: shell and tube, plate, plate and fin, printed circuit, helical coil, and ceramic type compact heat exchangers; and each of these exchangers are fully described in the beginning chapters of this book.

The SHX serves as the coolant boundary and must be constructed to maintain system integrity under normal, off-normal, and accident conditions. To maintain high cycle efficiencies, it must also minimize temperature differences between the intermediate molten salt and the process working fluid while minimizing the pressure drop. The difference in pressure required in the power conversion system and process heat applications imposes stringent requirements on the heat exchanger design. Thus, the fundamental objective is to identify and evaluate heat exchanger

concepts for use as the SHX for the AHTR. The SHX provides the interface between the intermediate coolant and the power conversion system or process application. The identification of a viable SHX concept is based on the options for the power conversion scheme or the process heat application design needs.

In the case of the Advanced High Temperature Reactor (AHTR), the SHX serves as the coolant boundary and must be constructed to maintain system integrity under normal, off-normal, and accident conditions. To maintain high cycle efficiencies, it must also minimize temperature differences between the intermediate molten salt and the process working fluid while minimizing the pressure drop. The difference in pressure required in the power conversion system and process heat applications imposes stringent requirements on the heat exchanger design. In this case, candidate materials of construction include Alloys N, 800H, and 617, which exhibit (in varying degrees) high temperature tensile and creep strength and resistance to environmental degradation in molten salts. Longer-term research and development programs will evaluate ceramic and composite designs. Issues that must be addressed during the design process include material compatibility with both the intermediate salt and the working fluid used in the power conversion system, high temperature strength, creep and creep-fatigue resistance, and the fabrication processes needed to manufacture an acceptable design (Holcomb et al.) [55]. For further information readers should refer to the book by Zohuri [56].

## References

1. Amos, Wade A. 1998. Costs of storing and transporting hydrogen. National Renewable Energy Laboratory, US Department of Energy DE-AC36-83CH10093, November 1998.
2. [http://en.wikipedia.org/wiki/Pressure\\_swings\\_adsorption](http://en.wikipedia.org/wiki/Pressure_swings_adsorption)
3. <http://www.mahler-ags.com/hydrogen/index.htm>
4. <http://www.japantimes.co.jp/news/2014/10/12/national/japan-rises-challenge-becoming-hydrogen-society>
5. <http://www.nxuranium.com/primary-energy-and-electricity-outlook>
6. <http://www.world-nuclear.org/info/Current-and-Future-Generation/World-Energy-Needs-and-Nuclear-Power>
7. <http://www.windupbattery.com/wind/hydrogen-hybrid-prenzlau.htm>
8. Eg  $(CH_4)_n$  tar sands or  $(CH_{1.5})_n$  heavy crude to  $(CH_2)_n$  transport fuel. Upgrading heavy crude oil and tar sands requires 3 to 4 kilograms of hydrogen per barrel (159 liters) of product.
9. In thermal terms @ 121 MJ/kg: 8470 PJ, equivalent to all of US nuclear electricity.
10. <https://www.enaq.or.jp/WE-NET/index.html>
11. <http://www.xebecinc.com/applications-industrial-hydrogen.php>
12. Flynn, T.M. 1992. *A liquefaction of gases*, McGraw-Hill encyclopedia of science & technology, vol. 10, 7th ed, 106–109. New York: McGraw-Hill.
13. Timmerhaus, C., and T.M. Flynn. 1989. *Cryogenic engineering*. New York: Plenum Press.
14. Garret, D.E. 1989. *Chemical engineering economics*. New York: Von Nostrand Reinhold.
15. Schwarz, J.A., and K.A.G. Amonkwah. 1993. *Hydrogen storage systems*. Washington, DC: U.S. Geological Survey.
16. Hart, D. 1997. *Hydrogen power: The commercial future of the ultimate fuel*. London, UK: Financial Times Energy Publishing.

17. Zittel, W., and R. Wurster. 1996. Hydrogen in the energy sector. Ludwig-Bolkow Systemtechnik GmbH, August 7, 1996
18. Zohuri, B. 2015. *Combined cycle driven efficiency for next generation nuclear power plants: An innovative design approach*. New York: Springer Publishing Company.
19. Zohuri, B. 2014. *Innovative open air Brayton combined cycle systems for the next generation nuclear power plants*. Albuquerque, NM: University of New Mexico Publications.
20. Forsberg, Charles, Pat McDaniel, and B. Zohuri. Variable electricity and steam from salt, helium, and sodium cooled base-load reactors with gas turbines and heat storage. Proceedings of ICAPP 2015 May 03–06, 2015, Nice (France) Paper 15115.
21. <http://www.world-nuclear.org/info/Non-Power-Nuclear-Applications/Transport/Transport-and-the-Hydrogen-Economy/>
22. [http://www-pub.iaea.org/MTCD/Publications/PDF/Pub1577\\_web.pdf](http://www-pub.iaea.org/MTCD/Publications/PDF/Pub1577_web.pdf)
23. INL/EXT-09-16326 Feasibility Study of Hydrogen Production at Existing Nuclear Power Plants, Electric Transportation Applications.
24. Melaina, M.W. 2005. Estimating relative station sizes in early hydrogen station networks. Proceeding of the National Hydrogen Association (NHA) Annual Conference, Washington, DC, March 2005
25. Ohi, James M. Hydrogen codes and standards: An overview of U.S. DOE activities. WHEC 16/13-16 June 2006, Lyon, France.
26. Besenbruch, G.E., L.C. Brown, J.F. Funk\*, and S.K. Showalter. 2000. High efficiency generation of hydrogen fuels using nuclear power. \*University of Kentucky, Lexington, Kentucky, † Sandia National Laboratory, Albuquerque, New Mexico GA PROJECT 30047 September 2000.
27. NUREG-0800, 2.2.1-2.2.2, Rev. 3, March 2007.
28. International Energy Outlook 2000: DOE/EIA-0484 (2000). The Energy Information Administration of the Department of Energy. [www.eia.doe.gov](http://www.eia.doe.gov)
29. Annual Energy Outlook 2000 with projections to 2020: DOE/EIA-0383 (2000). The Energy Information Administration of the Department of Energy. [www.eia.doe.gov](http://www.eia.doe.gov)
30. Analysis of the Impacts of an Early Start for Compliance with the Kyoto Protocol: SR/OIAF/99-02. The Energy Information Administration of the Department of Energy. [www.eia.doe.gov](http://www.eia.doe.gov)
31. Impacts of the Kyoto Protocol on U.S. Energy Markets and Economic Activity: SR/OIAF/98-03. The Energy Information Administration of the Department of Energy. [www.eia.doe.gov](http://www.eia.doe.gov)
32. Davis, C.B., R.B. Barner, S.R. Sherman, and D.F. Wilson. 2005. Thermal-hydraulic analyses of heat transfer fluid requirements and characteristics for coupling a hydrogen product plant to a high-temperature nuclear reactor. The INL is a U.S. Department of Energy National Laboratory operated by Battelle Energy Alliance, June 2005.
33. Hydrogen production using nuclear energy. International Atomic Energy Agency (IAEA) Nuclear Energy Series No. NP-T-42 Report.
34. Davis, C.B., R.B. Barner, S.R. Sherman, and D.F. Wilson. Thermal-hydraulic analyses of heat transfer fluid requirements and characteristics for coupling a hydrogen product plant to a high-temperature nuclear reactor. Idaho National Laboratory, INL/EXT-05-00453, June 2005.
35. Peterson, Per F. 2007. Intermediate heat exchanger dynamic thermal response model. Eugenio Urquiza Fernández U.C. Berkeley Report UCBTH-07-006 August 31, 2007.
36. Peterson, Per F., H. Zhao, and G. Fukuda. U.C. Berkeley Report UCBTH-03-004 December 5, 2003.
37. Zohuri, B., and N. Fathi. 2015. *Thermal-hydraulic analysis of nuclear reactors*. New York: Springer Publishing Company.
38. Bird, R.B., W.E. Stewart, and E.N. Lightfoot. 1960. *Transport phenomena*. New York: Wiley.
39. [www.nuscalepower.com](http://www.nuscalepower.com)
40. Vernonern, K., and T. Nishihara. 2004. Valuation of the safety concept of the combined nuclear/chemical complex for hydrogen production with HTTR. JUEL-4135.

41. Smith, C., S. Beck, and B. Galyean. 2005. An engineering analysis for separation requirements of a hydrogen production plant and high-temperature nuclear reactor. INL/EXT-05-00137 Rev 0, March 2005.
42. Dewson, S.J., and B. Thonon. 2003. The development of high efficiency heat exchangers for helium gas cooled reactors. Paper 3213, ICAPP03.
43. Diehl, H., and E. Bodman. 1990. Alloy 800 specifications in compliance with component requirements. *Journal of Nuclear Materials* 171: 63–70.
44. Crandall, S.H., N.C. Dahl, and T.J. Lardner. 1972. *An introduction to the mechanics of solids*, 2nd ed. New York: McGraw-Hill Book Company.
45. Dostal, V., M.J. Driscoll, and P. Hejzlar. 2004. A supercritical carbon dioxide cycle for next generation nuclear reactors. MIT-ANP-TR-100, March 2004.
46. Krieth, F. 1964. Principles of heat transfer. International Textbook Company, Scranton. General Atomics, 1996, Gas Turbine-Modular Helium Reactor (GT-MHR) Conceptual Design Description Report, GA Project No. 7658, 910720 Revision 1, July 1996.
47. INEEL. 2003. RELAP5-3D Code Manual Volume 4: Models and correlations. INEEL-98-00834, Revision 2.2, October 2003.
48. Kayes, W.M., and M.E. Crawford. 1980. *Convective heat and mass transfer*, 2nd ed. New York: McGraw-Hill Book Company.
49. Zohuri, B., and Patrick J. McDaniel. 2014. *Thermodynamics in nuclear power plant systems*. New York: Springer Publishing Company.
50. Glasstone, Samuel, and Alexander Sesonske. 1967. *Nuclear reactor engineering*. New York: D. Van Nostrand Company, Inc.
51. [https://daryanenergyblog.wordpress.com/ca/part-6\\_htgr/](https://daryanenergyblog.wordpress.com/ca/part-6_htgr/)
52. Mizia, R.E. 2008. Next generation nuclear plant intermediate heat exchanger acquisition strategy. INL/EXT-08-14054, April 2008.
53. Sabharwall, Piyush, Eung Soo Kim, Michael McKellar, Nolan Anderson, and Mike Patterson. 2001. Process heat exchanger options for the advanced high temperature reactor. INL/EXT-11-21584 Revision 1, Idaho National Laboratory, June 2011.
54. Sabharwall, P., and E.S. Kim. 2011. Fluoride high temperature reactor integration with industrial process applications. Idaho National Laboratory, TEV-1160.
55. Holcomb, D.E., S.M. Cetiner, G.F. Flanagan, F.J. Pertz, and G.L. Yoder. 2009. An analysis of testing requirements for fluoride salt-cooled high temperature reactor components. ORNL/TM-2009/297, November 2009.
56. Zohuri, B. 2016. *Nuclear energy for hydrogen generation through intermediate heat exchanger. A renewable source of energy*. New York: Springer Publishing Company.

## **Appendix A**

### **Table and Graphs Compilations**

The following tables provide samples of engineering data for materials of interest to Thermodynamics. For any detailed design work, more extensive handbooks should be consulted. The thermophysical property data for water, carbon dioxide and sodium were generated for this book. They represent the best fit to the latest physical measurements. More extensive tables are available from the National Institutes of Standards and Technology (NIST).

## A.1 Physical Constants

Acceleration of Gravity	$g = 9.80665 \text{ m/sec}^2 \text{ or } 32.174 \text{ ft/sec}^2$
Sea Level Atmospheric Pressure	$p_{SL} = 101.325 \text{ kPa}$ $= 1.01325 \text{ bar}$ $= 14.696 \text{ psia}$ $= 760 \text{ mm Hg (0°C)}$ $= 29.9213 \text{ in Hg (32°F)}$ $= 10.3323 \text{ m H}_2\text{O (4°C)}$
Boltzmann's Constant	$k = 1.3806503 \times 10^{-23} \text{ joule/K}$
Avogadro's Number	$N_a = 6.02214199 \times 10^{23} \text{ 1/gm mole}$
Electronic Charge	$q_e = 1.60217646 \times 10^{-19} \text{ coulomb}$
Electron Volt	$\epsilon = 1.60217646 \times 10^{-19} \text{ joules}$
Atomic Mass Unit	$amu = 1.6605402 \times 10^{-27} \text{ kg}$ $= 931.49432 \text{ MeV/c}^2$
Plank's Constant	$h = 6.62606876 \times 10^{-34} \text{ joule-sec}$ $\hbar = h/2\pi = 1.054571596 \times 10^{-34} \text{ joule-sec}$
Stefan Boltzmann's Constant	$\sigma = 0.17123 \times 10^{-8} \text{ Btu/(h-ft}^2\text{)}\text{R}^4\text{}$ $\sigma = 5.670400 \times 10^{-8} \text{ w/(m}^2\text{-K}^4\text{)}$
Speed of Light in Vacuum	$c = 2.99792458 \times 10^8 \text{ meters/sec}$
Solar constant	$q_{solar} = 429 \text{ Btu/(h-ft}^2\text{)}$ $q_{solar} = 1,353 \text{ W/m}^2$
Universal Gas Constant	$\mathcal{R} = 8.31447 \text{ kj/(kgmol-K)}$ $= 8.31447 \text{ kPa-m}^3\text{/(kgmol-K)}$ $= 0.0831447 \text{ bar-m}^3\text{/(kgmol-K)}$ $= 82.05 \text{ L-atm/(kgmol-K)}$ $= 1.98583 \text{ Btu/(lbmol-}^\circ\text{R)}$ $= 1545.37 \text{ ft-lbf/(lbmol-}^\circ\text{R)}$ $= 10.73 \text{ psia-ft}^3\text{/(lbmol-}^\circ\text{R)}$

## A.2 Conversion Factors

Distance

<u>To Convert</u>	<u>To</u>	<u>Multiply By</u>
millimeters	meters	$10^{-3}$
centimeters	meters	$10^{-2}$
kilometers	meters	$10^3$
inches	feet	1/12
feet	yards	1/3
feet	miles	1/5,280
yards	miles	1/1,760
inches	centimeters	2.54
feet	meters	0.3048

Area

<u>To Convert</u>	<u>To</u>	<u>Multiply By</u>
millimeters <sup>2</sup>	meters <sup>2</sup>	$10^{-6}$
centimeters <sup>2</sup>	meters <sup>2</sup>	$10^{-4}$
kilometers <sup>2</sup>	meters <sup>2</sup>	$10^6$
inches <sup>2</sup>	feet <sup>2</sup>	1/144
inches <sup>2</sup>	centimeters <sup>2</sup>	6.4516
centimeters <sup>2</sup>	inches <sup>2</sup>	0.1550
feet <sup>2</sup>	meters <sup>2</sup>	0.092903
meters <sup>2</sup>	feet <sup>2</sup>	10.7639

Volume

<u>To Convert</u>	<u>To</u>	<u>Multiply By</u>
milimeters <sup>3</sup>	meters <sup>3</sup>	$10^{-9}$
centimeters <sup>3</sup>	meters <sup>3</sup>	$10^{-6}$
liters	meters <sup>3</sup>	$10^{-3}$
kilometers <sup>3</sup>	meters <sup>3</sup>	$10^9$
inches <sup>3</sup>	centimeters <sup>3</sup>	16.3871
centimeters <sup>3</sup>	inches <sup>3</sup>	0.061024
feet <sup>3</sup>	meters <sup>3</sup>	0.0283168
meters <sup>3</sup>	feet <sup>3</sup>	35.3147

Force

<u>To Convert</u>	<u>To</u>	<u>Multiply By</u>
kg-m/sec <sup>2</sup>	newtons	1.0
pound-mass-ft/sec <sup>2</sup>	pounds-force	1/32.1745
Newton's	pounds-force	4.4482
pounds-force	newtons	0.2248

Mass and Density

<u>To Convert</u>	<u>To</u>	<u>Multiply By</u>
grams	kilograms	$10^{-3}$
metric tonnes	kilograms	$10^3$
ounces	pounds-mass	1/16
tons	pounds-mass	2000
grams	ounces	1/28.35
ounces	grams	28.35
pounds-mass	kilograms	0.4536
kilograms	pounds-mass	2.2046
tons	metric tonnes	0.9072
metric tonnes	tons	1.1023
grams/cc	lbm/ft <sup>3</sup>	62.427
grams/cc	kg/m <sup>3</sup>	$10^3$
lb/ft <sup>3</sup>	kg/m <sup>3</sup>	16.0187

## Pressure

<u>To Convert</u>	<u>To</u>	<u>Multiply By</u>
psi	in Hg	2.036
psi	in H <sub>2</sub> O	27.7
atm	in Hg	29.92
atm	ft H <sub>2</sub> O	33.93
atm	Pa	101,320
atm	bar	1.0133
atm	psi	14.69
kPa	psi	0.145
psi	kPa	6.895

## Energy

<u>To Convert</u>	<u>To</u>	<u>Multiply By</u>
joules	ergs	107
lbf-ft	joules	1.356
Btu	joules	1055
Btu	ft-lbf	778
Cal	Btu	0.003968
Cal	ft-lbf	3.088
Btu	W-hr	0.2930
kW-hr	Btu	3412
Cal	joules	4.1868
kj/kg	Btu/lbm	0.4992
Btu/lbm	kj/kg	2.3260
Cal/gm	Btu/lbm	1.8000

## Power

<u>To Convert</u>	<u>To</u>	<u>Multiply By</u>
hp	ft-lbf/s	550
hp	Btu/hr	2545
hp	kW	0.7455
W	Btu/hr	3.412
kW	hp	1.341
ton	Btu/hr	12,000
ton	kW	3.517

## Heat Transfer

<u>To Convert</u>	<u>To</u>	<u>Multiply By</u>
W/m/K	Btu/hr/ft/R	0.57779
kcal/h/m/K	W/m/K	1.1630
kcal/h/m/K	Btu/h/ft/R	0.67197
Btu/h/ft/R	W/m/K	1.7307
W/m <sup>2</sup> /K	Btu/h/ft <sup>2</sup> /R	0.17611
Btu/hr/ft <sup>2</sup> /R	W/m <sup>2</sup> /K	5.6783

## Fluid Flow

<u>To Convert</u>	<u>To</u>	<u>Multiply By</u>
m <sup>3</sup> /s	ft <sup>3</sup> /s	35.3147
g/cm/sec (poise)	lbf-sec/ft <sup>2</sup>	0.002088
lbf-sec/ft <sup>2</sup>	g/cm/sec	478.96
lbf-sec/ft <sup>2</sup>	kg/m/hr	172,400
lbm/ft/sec	gm/cm/sec	14.882
m <sup>2</sup> /sec	ft <sup>2</sup> /sec	10.7639
cm <sup>2</sup> /sec	ft <sup>2</sup> /hr	3.875
ft <sup>2</sup> /sec	m <sup>2</sup> /hr	334.45

### A.3 Standard Atmosphere

Table A3.1: SI Units $p_{SL} = 101325 \text{ Pas}$  $T_{SL} = 288.2 \text{ K}$  $\rho_{SL} = 1.225 \text{ kg/m}^3$ 

<u>Altitude (km)</u>	<u>P/P<sub>SL</sub></u>	<u>T/T<sub>SL</sub></u>	<u><math>\rho/\rho_{SL}</math></u>
0	1	1	1
1	0.887	0.9774	0.9075
2	0.7846	0.9549	0.8217
3	0.692	0.9324	0.7423
4	0.6085	0.9098	0.6689
5	0.5334	0.8873	0.6012
6	0.466	0.8648	0.5389
7	0.4057	0.8423	0.4817
8	0.3519	0.8198	0.4292
9	0.304	0.7973	0.3813
10	0.2615	0.7748	0.3376
11	0.224	0.7523	0.2978
12	0.1915	0.7519	0.2546
13	0.1636	0.7519	0.2176
14	0.1399	0.7519	0.186
15	0.1195	0.7519	0.159
16	0.1022	0.7519	0.1359

Table A3.2: English Units $p_{SL} = 2116 \text{ lbf/ft}^3$  $T_{SL} = 518.7^\circ\text{R}$  $\rho_{SL} = 0.07647 \text{ lbm/ft}^3$ 

<u>Altitude (kft)</u>	<u>P/P<sub>SL</sub></u>	<u>T/T<sub>SL</sub></u>	<u><math>\rho/\rho_{SL}</math></u>
0	1.0	1.0	1.0
2	0.9298	0.9863	0.9428
4	0.8637	0.9725	0.8881
6	0.8014	0.9588	0.8359
8	0.7429	0.945	0.7861
10	0.6878	0.9313	0.7386
12	0.6362	0.9175	0.6933
14	0.5877	0.9038	0.6502
16	0.5422	0.8901	0.6092
18	0.4997	0.8763	0.5702
20	0.4599	0.8626	0.5332
22	0.4227	0.8489	0.498
24	0.388	0.8352	0.4646
26	0.3557	0.8215	0.433
28	0.3256	0.8077	0.4031
30	0.2975	0.794	0.3747
32	0.2715	0.7803	0.348
34	0.2474	0.7666	0.3227
36	0.225	0.7529	0.2988
38	0.2044	0.7519	0.2719
40	0.1858	0.7519	0.2471
42	0.1688	0.7519	0.2245
44	0.1534	0.7519	0.204
46	0.1394	0.7519	0.1854
48	0.1267	0.7519	0.1685
50	0.1151	0.7519	0.1531

## A.4 Critical State Properties of Gases

		Molar	P <sub>crit</sub>	T <sub>crit</sub>	P <sub>crit</sub>	T <sub>crit</sub>	V <sub>crit</sub>	Z <sub>crit</sub>
		Mass	MPa	K	atm	R	cm <sup>3</sup> /gm-mol	
Air		28.996	3.77	133.0	37.21	239.0	88.3	0.300
Ammonia	NH <sub>3</sub>	17.031	11.28	405.5	111.32	729.8	72.5	0.243
Argon	Ar	39.950	4.86	151.0	47.96	272.0	75.2	0.291
Carbon Dioxide	CO <sub>2</sub>	44.010	7.39	304.2	72.93	547.5	94.0	0.293
Carbon Monoxide	CO	28.010	3.50	133.0	34.54	240.0	93.1	0.294
Chlorine	Cl <sub>2</sub>	70.906	7.99	416.9	78.87	750.4	124.0	0.276
Helium	He	4.003	0.23	5.3	2.27	9.5	57.5	0.303
Hydrogen	H <sub>2</sub>	2.016	1.30	33.3	12.83	59.9	65.0	0.304
Iodine	I <sub>2</sub>	253.809	11.70	819.0	115.47	1474.2	167.0	0.287
Krypton	Kr	83.800	5.50	209.4	54.28	376.9	92.2	0.291
Lithium	Li	6.941	67.00	3223.0	661.24	5801.4	120.0	0.300
Mercury	Hg	200.590	150.97	1763.2	1490.0	3173.7	29.1	0.300
Methane	CH <sub>4</sub>	16.043	4.64	191.1	45.79	343.9	99.0	0.290
Neon	Ne	20.180	2.73	44.5	26.94	227.1	41.7	0.307
Nitrogen	N <sub>2</sub>	28.013	3.39	126.2	33.46	227.1	90.1	0.291
Oxygen	O <sub>2</sub>	31.999	5.08	154.8	50.14	278.6	73.4	0.288
Potassium	K	39.098	16.42	2105.9	162.02	3790.7	320.0	0.300
Propane	C <sub>3</sub> H <sub>8</sub>	44.097	4.26	370.0	42.04	665.9	200.0	0.277
Sodium	Na	22.990	25.60	2503.9	252.65	4507.0	244.0	0.300
Water	H <sub>2</sub> O	18.015	22.10	647.4	218.11	1165.3	56.0	0.230
Water (Heavy)	D <sub>2</sub> O	20.023	21.72	644.7	214.36	1160.4	54.9	0.222
Xenon	Xe	131.290	5.84	289.8	57.65	521.6	118.8	0.290

## A.5 Constants for Van Der Waals Equation of State

<u>Substance</u>		Molar Mass	a kPa-m <sup>6</sup> / kmol <sup>2</sup>	b m <sup>3</sup> /kmol	a atm-ft <sup>6</sup> /lbmol <sup>2</sup>	b ft <sup>3</sup> /lbmol
Air		28.996	136.83	0.03666	345.21	0.58621
Ammonia	NH <sub>3</sub>	17.031	425.09	0.03736	1075.80	0.59826
Argon	Ar	39.95	136.81	0.03229	346.85	0.51752
Carbon Dioxide	CO <sub>2</sub>	44.0098	365.16	0.04278	924.18	0.68507
Carbon Monoxide	CO	28.0104	147.38	0.03949	374.96	0.63407
Chlorine	Cl <sub>2</sub>	70.906	634.26	0.05422	1605.62	0.86835
Helium	He	4.0026		3.56	0.02395	8.94
Hydrogen	H <sub>2</sub>	2.0158		24.87	0.02662	62.88
Iodine	I <sub>2</sub>	253.809		1671.81	0.07275	4232.15
Krypton	Kr	83.8		232.51	0.03957	588.59
Lithium	Li	6.941		4521.16	0.04999	11445.24
Mercury	Hg	200.59		600.48	0.01214	1520.11
Methane	CH <sub>4</sub>	16.043		229.51	0.04280	580.74
Neon	Ne	20.1797		21.15	0.01694	430.43
Nitrogen	N <sub>2</sub>	28.0134		137.00	0.03869	346.63
Oxygen	O <sub>2</sub>	31.9988		137.56	0.03167	348.12
Potassium	K	39.0983		7877.53	0.13331	19942.70
	C <sub>3</sub> H <sub>8</sub>					2.13513
Propane		44.097		937.13	0.09026	2371.61
Sodium	Na	22.9898		7141.57	0.10165	18078.79
Water	H <sub>2</sub> O	18.0152		553.04	0.03044	1399.97
Water (Heavy)	D <sub>2</sub> O	20.023		557.95	0.03084	1412.43
Xenon	Xe	131.29		419.20	0.05156	1061.20

$$R = 8314 \text{ J/kmol/K} = 1545 \text{ ft-lbf/lbmol/R} = 0.73023 \text{ atm-ft}^3/\text{lbmol/R}$$

## A.6 Constants for Redlich-Kwong Equation of State

<u>Substance</u>		Molar	a	b	a	b
		Mass	kPa-m <sup>2</sup> /K <sup>1/2</sup> /kmol <sup>2</sup>	m <sup>3</sup> /kmol	atm-ft <sup>2</sup> R <sup>1/2</sup> /lbmol <sup>2</sup>	ft <sup>3</sup> /lbmol
Air		28.996		1598.9	0.02541	5407.8
Ammonia	NH <sub>3</sub>	17.031		8673.7	0.02589	29448.7
Argon	Ar	39.95		1703.5	0.02238	5796.3
Carbon Dioxide	CO <sub>2</sub>	44.0098		6453.4	0.02965	21912.0
Carbon Monoxide	CO	28.0104		1722.3	0.02737	5886.1
Chlorine	Cl <sub>2</sub>	70.906		13122.4	0.03758	44568.3
Helium	He	4.0026		8.3	0.01660	27.9
Hydrogen	H <sub>2</sub>	2.0158		145.4	0.01845	493.2
Iodine	I <sub>2</sub>	253.809		48479.7	0.05042	164653.6
Krypton	Kr	83.8		3409.3	0.02743	11579.2
Lithium	Li	6.941		260082.9	0.03465	883330.7
Mercury	Hg	200.59		25549.3	0.00841	86774.1
Methane	CH <sub>4</sub>	16.043		3214.9	0.02967	10912.6
Neon	Ne	20.1797		143.0	0.01174	6572.7
Nitrogen	N <sub>2</sub>	28.0134		1559.5	0.02682	5293.1
Oxygen	O <sub>2</sub>	31.9988		1734.2	0.02195	5887.8
Potassium	K	39.0983		366303.6	0.09240	1244158.2
Propane	C <sub>3</sub> H <sub>8</sub>	44.097		18265.5	0.06256	62012.5
Sodium	Na	22.9898		362104.2	0.07045	1229829.9
Water	H <sub>2</sub> O	18.0152		14258.5	0.02110	48424.8
Water (Heavy)	D <sub>2</sub> O	20.023		14354.4	0.02138	48752.6
Xenon	Xe	131.29		7230.7	0.03574	24558.0

$$R = 8314 \text{ J/kmol/K} = 1545 \text{ ft-lbf/lbmol/R} = 0.73023 \text{ atm-ft}^3/\text{lbmol/R}$$

## A.7 Constants for the Peng-Robinson Equation of State

<u>Substance</u>	Molar	a	b	a	b	$\omega$
	Mass	kPa-m <sup>6</sup> /kmol <sup>2</sup>	m <sup>3</sup> /kmol	atm-ft <sup>6</sup> /lbmol <sup>2</sup>	ft <sup>3</sup> /lbmol	
Air	28.996	148.29	0.02282	374.15	0.36484	0.032
Ammonia	NH <sub>3</sub>	17.031	460.72	0.02325	1165.97	0.37234
Argon	Ar	39.95	148.28	0.02010	375.92	0.32209
Carbon Dioxide	CO <sub>2</sub>	44.0098	395.76	0.02662	1001.65	0.42636
Carbon Monoxide	CO	28.0104	159.73	0.02458	406.39	0.39462
Chlorine	Cl <sub>2</sub>	70.906	687.42	0.03374	1740.20	0.54044
Helium	He	4.0026	3.86	0.01490	9.69	0.23770
Hydrogen	H <sub>2</sub>	2.0158	26.96	0.01657	68.16	0.26517
Iodine	I <sub>2</sub>	253.809	1811.93	0.04528	4586.88	0.72512
Krypton	Kr	83.8	252.00	0.02463	637.92	0.39441
Lithium	Li	6.941	4900.11	0.03111	12404.55	0.49831
Mercury	Hg	200.59	650.81	0.00755	1647.52	0.12098
Methane	CH <sub>4</sub>	16.043	248.75	0.02664	629.41	0.42654
Neon	Ne	20.1797	22.93	0.01054	466.51	0.47874
Nitrogen	N <sub>2</sub>	28.0134	148.48	0.02408	375.69	0.38553
Oxygen	O <sub>2</sub>	31.9988	149.09	0.01971	377.30	0.31562
Potassium	K	39.0983	8537.81	0.08297	21614.24	1.32884
Propane	C <sub>3</sub> H <sub>8</sub>	44.097	1015.67	0.05618	2570.39	0.89958
Sodium	Na	22.9898	7740.16	0.06326	19594.10	1.01318
Water	H <sub>2</sub> O	18.0152	599.40	0.01895	1517.31	0.30345
Water(Heavy)	D <sub>2</sub> O	20.023	604.71	0.01920	1530.82	0.30745
Xenon	Xe	131.29	454.34	0.03209	1150.15	0.51390

$$R = 8314 \text{ J/kmol/K} = 1545 \text{ ft-lbf/lbmol/R} = 0.73023 \text{ atm-ft}^3/\text{lbmol/R}$$

## A.8 Thermophysical Properties of Solids

Material	Melting Point (K)	Density	(Cp in J/kg/K) (k in W/m/K)								
			T(K)	200	300	400	600	800	1000	1200	1500
Aluminum(Pure)	933	2702	k	237	237	240	231	218			
			Cp	798	903	949	1033	1146			
Aluminum (2024-T6)	775	2770	k	163	177	186	186				
			Cp	787	875	925	1042				
Beryllium	1550	1850	k	301	200	161	126	106	90.8	78.7	
			Cp	1114	1825	2191	2604	2823	3018	3227	3519
Bismuth	545	9780	k	9.69	7.86	7.04					
			Cp	120	122	127					
Boron	2573	2500	k	55.5	27	16.8	10.6	9.6	9.85		
			Cp	600	1107	1463	1892	2160	2338		
Cadmium	594	8650	k	99.3	96.8	94.7					
			Cp	222	231	242					
Chromium	2118	7160	k	111	93.7	90.9	80.7	71.3	65.4	61.9	57.2
			Cp	384	449	484	542	581	616	682	779
Copper (Pure)	1358	8933	k	413	401	393	379	366	352	339	
			Cp	356	385	397	417	433	451	480	
Iron (Pure)	1810	7870	k	94	80.2	69.5	54.7	43.3	32.8	28.3	32.1
			Cp	384	447	490	574	680	975	609	654
Carbon Steel	7854	k		60.5	56.7	48	39.2	31.3			
			Cp	434	487	559	685	1169			
302 Stainless	8055	k		15.1	17.3	20	22.8	25.4			
			Cp	480	512	559	585	606			
304 Stainless	1670	7900	k	12.6	14.9	16.6	19.8	22.6	25.4	28	31.7
			Cp	402	477	515	557	582	611	640	682
316 Stainless	8238	k		13.4	15.2	18.3	21.3	24.2			
			Cp	468	504	550	576	602			
347 Stainless	7978	k		14.2	15.8	18.9	21.9	24.7			
			Cp	480	513	559	585	606			
Lead	601	11340	k	36.7	35.3	34	31.4				
			Cp	125	129	132	142				
Lithium	454	534	k		84.8						
			Cp		3580						
Magnesium	923	1740	k	159	156	153	149	146			
			Cp	934	1024	1074	1170	1267			
Molybdenum	2894	10240	k	143	138	134	126	118	112	105	98
			Cp	224	251	261	275	285	295	308	330
Nickel (Pure)	1728	8900	k	107	90.7	80.2	65.6	67.6	71.8	76.2	82.6
			Cp	383	444	485	592	530	562	594	616
Inconel X-750	1665	8510	k	10.3	11.7	13.5	17	20.5	24	27.6	33
			Cp	372	439	473	510	546	626		
Niobium	2741	8570	k	52.6	53.7	55.2	58.2	61.3	64.4	67.5	72.1
			Cp	249	265	274	283	292	301	310	324
Palladium	1827	12020	k	71.6	71.8	73.6	79.7	86.9	94.2	102	110
			Cp	227	244	251	261	271	281	291	307
Platinum (Pure)	2045	21450	k	72.6	71.6	71.8	73.2	75.6	78.7	82.6	89.5
			Cp	125	133	136	141	146	152	157	165
60%Pt-40%Rh	1800	16630	k		47	52	59	65	69	73	76
			Cp		162						
Plutonium	913	19860	k			25.1					
			Cp			104.4					
Potassium	337	862	k			102.5					
			Cp			757.1					
Rhenium	3453	21100	k	51	47.9	46.1	44.2	44.1	44.6	45.7	47.8
			Cp	127	136	139	145	151	156	162	171

Rhodium	2236	12450	k C <sub>p</sub>	154 220	150 243	146 253	136 274	127 293	121 311	116 327	110 349
Silver	1235	10500	k C <sub>p</sub>	430 225	429 235	425 239	412 250	396 2623	379 277	361 292	
Sodium	371	986	k C <sub>p</sub>		142 1084						
Tantalum	3269	16600	k C <sub>p</sub>	57.5 133	57.5 140	57.8 144	58.6 146	59.4 149	60.2 152	61 155	62.2 160
Thorium	2023	11700	k C <sub>p</sub>	54.6 112	54 118	54.5 124	55.8 134	56.9 145	56.9 156	58.7 167	
Tin	505	7310	k C <sub>p</sub>	73.3 215	66.6 227	62.2 243					
Titanium	1953	4500	k C <sub>p</sub>	24.5 465	21.9 522	20.4 551	19.4 591	19.7 633	20.7 675	22 620	24.5 686
Tungsten	3660	19300	k C <sub>p</sub>	186 122	174 132	159 137	137 142	125 145	118 148	113 152	107 157
Uranium	1406	19070	k C <sub>p</sub>	25.1 108	27.6 116	29.6 125	34 146	38.8 176	43.9 180	49 161	
Vanadium	2192	6100	k C <sub>p</sub>	31.3 430	30.7 489	31.3 515	33.3 540	35.7 563	38.2 597	40.8 645	44.6 714
Zinc	693	7140	k C <sub>p</sub>	118 367	116 389	111 402	103 436				
Zirconium	2125	6570	k C <sub>p</sub>	25.2 264	22.7 278	21.6 300	20.7 322	21.6 342	23.7 362	26 344	28.8 344
Beryllium Oxide	2725	3000	k C <sub>p</sub>		272 1030	196 1350	111 1690	70 1865	47 1975	33 2055	21.5 2145
Carbon Amorphous	1500	1950	k C <sub>p</sub>	1.18 509	1.6 509	1.89 509	2.19 509	2.37 509	2.53 509	2.84 509	3.48 509
Graphite Pyrolytic	2273	2210	k C <sub>p</sub>		5.7 411	16.8 709	9.23 992	4.09 1406	2.68 1650	2.01 1793	1.6 1890
Silicon Carbide	3100	3160	k C <sub>p</sub>		490 675	490 880	1050 1050	1135 1195	87 1195	58 1243	30 1310
Silicon Dioxide	1883	2220	k C <sub>p</sub>	1.14	1.38 745	1.51 905	1.75 1040	2.17 1105	2.87 1155	4 1195	
Silicon Nitride	2173	2400	k C <sub>p</sub>		16 578	13.9 691	11.3 778	9.88 937	8.76 1063	8 1155	7.16 1226
Thorium Dioxide	3573	9110	k C <sub>p</sub>		13 235	10.2 255	6.6 274	4.7 285	3.68 295	3.12 303	2.73 315
Uranium Dioxide	3138	10980	k C <sub>p</sub>	13.1 278	10.05 277.4	8.17 277.3	5.95 277	4.67 277	3.849 277.2	3.27 277	2.67 277
Plutonium Dioxide	2673	11460	k C <sub>p</sub>	16.3	11.17 276.1	8.489 276.1	5.73	4.33 276.1	3.477 276.1	2.91 276.1	2.33 276.1
Concrete		2300	k C <sub>p</sub>			1.4 880					
Glass		2500	k C <sub>p</sub>			1.4 750					
Ice	273	920	k C <sub>p</sub>	2.03 1945	1.88 2040						
Paraffin		900	k C <sub>p</sub>			0.24 2890					
Paper		930	k C <sub>p</sub>			0.18 1340					
Sand		1515	k C <sub>p</sub>			0.27 800					
Soil		2050	k C <sub>p</sub>			0.52 1840					

## A.9 Thermophysical Properties of Liquids

	<u>Temp</u>	<u>273</u>	<u>280</u>	<u>300</u>	<u>320</u>	<u>340</u>	<u>360</u>	<u>400</u>
Engine Oil	$\rho$ (kg/m <sup>3</sup> )	899.1	895.3	884.1	871.8	859.9	847.8	825.1
	$C_p$ (J/kg/K)	1796	1827	1909	1993	2076	2161	2337
	$\mu$ (N-s/m <sup>2</sup> )	3.85	2.17	0.486	0.141	0.00531	0.00252	0.00087
	k (W/m/K)	0.147	0.144	0.145	0.143	0.139	0.138	0.134
	<u>Temp</u>	<u>273</u>	<u>300</u>	<u>350</u>	<u>400</u>	<u>450</u>	<u>500</u>	<u>600</u>
Water (liquid)	$\rho$ (kg/m <sup>3</sup> )	1000.0	997.0	973.7	937.2	890.5	831.3	648.9
T <sub>m</sub> =273	$C_p$ (J/kg/K)	4217.0	4179.0	4195.0	4256.0	4400.0	4660.0	7000.0
T <sub>b</sub> = 373	$\mu$ (N-s/m <sup>2</sup> )	1.75E-03	8.55E-04	3.43E-04	2.17E-04	1.52E-04	1.18E-04	8.10E-05
	k (W/m/K)	0.569	0.613	0.668	0.688	0.678	0.642	0.497
	<u>Temp</u>	<u>273</u>	<u>300</u>	<u>350</u>	<u>400</u>	<u>450</u>	<u>500</u>	<u>600</u>
Water (vapor)	$\rho$ (kg/m <sup>3</sup> )	0.0048	0.0256	0.2600	1.3680	4.8077	13.05	72.99
T <sub>m</sub> =273	$C_p$ (J/kg/K)	1854	1872	1954	2158	2560	3270	8750
T <sub>b</sub> = 373	$\mu$ (N-s/m <sup>2</sup> )	8.02E-06	9.09E-06	1.11E-05	1.31E-05	1.49E-05	1.66E-05	2.27E-05
	k (W/m/K)	0.0182	0.0196	0.023	0.0272	0.0331	0.0423	0.103
Heavy	<u>Temp</u>	<u>273</u>	<u>353</u>					
Water (liquid)	$\rho$ (kg/m <sup>3</sup> )	1105.4	1078.2					
T <sub>m</sub> =277	$C_p$ (J/kg/K)	4207.7	4178.4					
T <sub>b</sub> = 376	$\mu$ (N-s/m <sup>2</sup> )							
	k (W/m/K)	0.5931	0.632					
Heavy	<u>Temp</u>	<u>313.2</u>	<u>300</u>	<u>350</u>	<u>400</u>	<u>450</u>	<u>500</u>	<u>600</u>
Water (vapor)	$\rho$ (kg/m <sup>3</sup> )	0.0058	0.0250	0.2717	1.4771	5.2966	14.75	83.96
T <sub>m</sub> =277	$C_p$ (J/kg/K)	1694.8	1712	1743.4	1779.4	1817.1	1856.4	1938.9
T <sub>b</sub> = 376	$\mu$ (N-s/m <sup>2</sup> )							
	k (W/m/K)	0.0187	0.0202	0.0237	0.02884	0.0309	0.0371	0.0482
	<u>Temp</u>	<u>473</u>	<u>673</u>	<u>873</u>	<u>1073</u>	<u>1273</u>		
Lithium	$\rho$ (kg/m <sup>3</sup> )	508.9	491.2	475.1	457.5	441.4		
T <sub>m</sub> = 452 K	$C_p$ (kJ/kg/K)	5861.5	4563.6	3810	3056.4	2302.7		
T <sub>b</sub> = 1590 K	$\mu$ (N-s/m <sup>2</sup> )	5.65E-04	4.56E-04	4.56E-04	4.56E-04	4.56E-04		
	k (W/m/K)	46.33	39.49	25.93	11.12	10.38		
	<u>Temp</u>	<u>477.8</u>	<u>588.9</u>	<u>700.0</u>	<u>811.1</u>	<u>922.2</u>	<u>1033.3</u>	<u>1154.8</u>
Sodium	$\rho$ (kg/m <sup>3</sup> )	904.4	878.1	851.6	824.9	798.1	771.1	741.6
T <sub>m</sub> =371	$C_p$ (J/kg/K)	1.338	1.300	1.274	1.259	1.255	1.263	1.284
T <sub>b</sub> = 1156 K	$\mu$ (N-s/m <sup>2</sup> )	4.52E-04	3.33E-04	2.66E-04	2.26E-04	1.97E-04	1.74E-04	1.57E-04
	k (W/m/K)	81.52	75.81	70.27	65.08	60.23	55.56	50.88

	<u>Temp</u>	<u>600</u>	<u>800</u>	<u>1000</u>	<u>1200</u>	<u>1392.6</u>	<u>1400</u>	<u>1800</u>
Potassium	$\rho$ ( $\text{kg}/\text{m}^3$ )	588.9	700.0	811.1	922.2	1029.2	1033.3	1255.6
$T_m = 337$	$C_p$ ( $\text{J}/\text{kg}/\text{K}$ )	0.783	0.791	0.804	0.825	0.854	0.854	0.934
$T_b = 1033 \text{ K}$	$\mu$ ( $\text{N}\cdot\text{s}/\text{m}^2$ )	2.54E-04	2.06E-04	1.71E-04	1.47E-04	1.31E-04	1.31E-04	1.09E-04
	$k$ ( $\text{W}/\text{m}/\text{K}$ )	43.61	39.98	36.69	33.75	30.81	30.81	25.10
	<u>Temp</u>	<u>366</u>	<u>644</u>	<u>977</u>				
NaK (45/50)	$\rho$ ( $\text{kg}/\text{m}^3$ )	887.4	821.7	740.1				
$T_m = 292 \text{ K}$	$C_p$ ( $\text{J}/\text{kg}/\text{K}$ )	1130	1055	1043				
$T_b = 1098 \text{ K}$	$\mu$ ( $\text{N}\cdot\text{s}/\text{m}^2$ )	5.79E-04	2.36E-04	1.61E-04				
	$k$ ( $\text{W}/\text{m}/\text{K}$ )	25.6	27.5	28.9				
	<u>Temp</u>	<u>366</u>	<u>672</u>	<u>1033</u>				
NaK(22/78)	$\rho$ ( $\text{kg}/\text{m}^3$ )	849	775.3	690.4				
$T_m = 262 \text{ K}$	$C_p$ ( $\text{J}/\text{kg}/\text{K}$ )	946	879	883				
$T_b = 1057 \text{ K}$	$\mu$ ( $\text{N}\cdot\text{s}/\text{m}^2$ )	4.92E-04	2.07E-04	1.46E-04				
	$k$ ( $\text{W}/\text{m}/\text{K}$ )	24.4	26.7	29.4				
	<u>Temp</u>	<u>644</u>	<u>755</u>	<u>977</u>				
Lead	$\rho$ ( $\text{kg}/\text{m}^3$ )	10540	10412	10140				
$T_m = 600 \text{ K}$	$C_p$ ( $\text{J}/\text{kg}/\text{K}$ )	159	155	151				
$T_b = 2010 \text{ K}$	$\mu$ ( $\text{N}\cdot\text{s}/\text{m}^2$ )	2.39E-03	1.93E-03	1.37E-03				
	$k$ ( $\text{W}/\text{m}/\text{K}$ )	16.1	15.6	14.9				
	<u>Temp</u>	<u>273</u>	<u>300</u>	<u>350</u>	<u>400</u>	<u>450</u>	<u>500</u>	<u>600</u>
Mercury	$\rho$ ( $\text{kg}/\text{m}^3$ )	13595	13529	13407	13287	13167	13048	12809
$T_m = 234 \text{ K}$	$C_p$ ( $\text{J}/\text{kg}/\text{K}$ )	140.4	139.3	137.7	136.5	135.7	135.3	135.5
$T_b = 630 \text{ K}$	$\mu$ ( $\text{N}\cdot\text{s}/\text{m}^2$ )	1.69E-03	1.52E-03	1.31E-03	1.17E-03	1.08E-03	1.01E-03	9.11E-04
	$k$ ( $\text{W}/\text{m}/\text{K}$ )	8.18	8.54	9.18	9.8	10.4	10.95	11.95
	<u>Temp</u>	<u>589</u>	<u>811</u>	<u>1033</u>				
Bismuth	$\rho$ ( $\text{kg}/\text{m}^3$ )		10011	9739	9467			
$T_m = 544 \text{ K}$	$C_p$ ( $\text{J}/\text{kg}/\text{K}$ )		144.4	154.5	164.5			
$T_b = 1750 \text{ K}$	$\mu$ ( $\text{N}\cdot\text{s}/\text{m}^2$ )		1.62E-03	1.10E-03	7.90E-04			
	$k$ ( $\text{W}/\text{m}/\text{K}$ )		16.4	15.6	15.6			
	<u>Temp</u>	<u>422</u>	<u>644</u>	<u>922</u>				
PbBi(44.5/55.5)	$\rho$ ( $\text{kg}/\text{m}^3$ )		10524	10236	9835			
$T_m = 398 \text{ K}$	$C_p$ ( $\text{J}/\text{kg}/\text{K}$ )		147	147	147			
$T_b = 1943 \text{ K}$	$\mu$ ( $\text{N}\cdot\text{s}/\text{m}^2$ )		1.85E-03	1.53E-03	1.15E-03			
	$k$ ( $\text{W}/\text{m}/\text{K}$ )		9.05	11.86	15.3788			

## A.10 Thermophysical Properties of Gases

Air	$\frac{\text{Temp (K)}}{\mu (\text{N}\cdot\text{s/m}^2)}$	<u>250</u>	<u>350</u>	<u>500</u>	<u>800</u>	<u>1000</u>	<u>1200</u>	<u>1400</u>	<u>1600</u>	<u>1800</u>	
	$k (\text{W/m/K})$	1.60E-05 0.0223	2.08E-05 0.0300	2.70E-05 0.0407	3.23E-05 0.0497	3.70E-05 0.0573	4.24E-05 0.0667	4.73E-05 0.0763	5.30E-05 0.0910	5.84E-05 0.1060	
Carbon Dioxide	$\frac{\text{Temp (K)}}{\mu (\text{N}\cdot\text{s/m}^2)}$	<u>280</u>	<u>300</u>	<u>350</u>	<u>400</u>	<u>450</u>	<u>500</u>	<u>550</u>	<u>600</u>	<u>650</u>	
	$k (\text{W/m/K})$	1.40E-05 0.0152	1.49E-05 0.0166	1.69E-05 0.0205	1.90E-03 0.0243	2.10E-05 0.0283	2.31E-05 0.0325	2.51E-05 0.0366	2.70E-05 0.0407	2.88E-05 0.0445	3.05E-05 0.0481
Carbon Monoxide	$\frac{\text{Temp (K)}}{\mu (\text{N}\cdot\text{s/m}^2)}$	<u>250</u>	<u>300</u>	<u>350</u>	<u>400</u>	<u>450</u>	<u>500</u>	<u>550</u>	<u>600</u>	<u>650</u>	
	$k (\text{W/m/K})$	1.52E-05 0.0214	1.75E-05 0.0250	1.98E-05 0.0285	2.18E-05 0.0318	2.37E-05 0.0350	2.54E-05 0.0381	2.71E-05 0.0411	2.86E-05 0.0440	3.01E-05 0.0470	3.15E-05 0.0500
Helium	$\frac{\text{Temp (K)}}{\mu (\text{N}\cdot\text{s/m}^2)}$	<u>250</u>	<u>300</u>	<u>350</u>	<u>400</u>	<u>450</u>	<u>500</u>	<u>600</u>	<u>700</u>	<u>800</u>	
	$k (\text{W/m/K})$	1.70E-05 0.1335	1.99E-05 0.1520	2.21E-05 0.1700	2.43E-05 0.1870	2.63E-05 0.2040	2.83E-05 0.2200	3.20E-05 0.2520	3.50E-05 0.2780	3.82E-05 0.3040	4.14E-05 0.3300
Hydrogen	$\frac{\text{Temp (K)}}{\mu (\text{N}\cdot\text{s/m}^2)}$	<u>250</u>	<u>300</u>	<u>350</u>	<u>400</u>	<u>500</u>	<u>600</u>	<u>800</u>	<u>1000</u>	<u>1200</u>	
	$k (\text{W/m/K})$	7.89E-06 0.1570	8.96E-06 0.1830	9.88E-06 0.2040	1.08E-05 0.2260	1.26E-05 0.2660	1.42E-05 0.3050	1.72E-05 0.3780	2.01E-05 0.4480	2.26E-05 0.5280	2.51E-05 0.6100
Nitrogen	$\frac{\text{Temp (K)}}{\mu (\text{N}\cdot\text{s/m}^2)}$	<u>250</u>	<u>300</u>	<u>350</u>	<u>400</u>	<u>500</u>	<u>600</u>	<u>700</u>	<u>800</u>	<u>900</u>	
	$k (\text{W/m/K})$	1.55E-05 0.0222	1.78E-05 0.0259	2.00E-05 0.0293	2.22E-05 0.0327	2.58E-05 0.0389	2.91E-05 0.0446	3.21E-05 0.0490	3.49E-05 0.0548	3.75E-05 0.0597	4.23E-05 0.0700
Oxygen	$\frac{\text{Temp (K)}}{\mu (\text{N}\cdot\text{s/m}^2)}$	<u>250</u>	<u>300</u>	<u>350</u>	<u>400</u>	<u>500</u>	<u>600</u>	<u>700</u>	<u>800</u>	<u>900</u>	
	$k (\text{W/m/K})$	1.79E-05 0.0226	2.07E-05 0.0268	2.34E-05 0.0296	2.58E-05 0.0330	3.03E-05 0.0412	3.44E-05 0.0473	3.81E-05 0.0528	4.15E-05 0.0589	4.47E-05 0.0649	5.06E-05 0.0758
Water	$\frac{\text{Temp (K)}}{\mu (\text{N}\cdot\text{s/m}^2)}$	<u>380</u>	<u>400</u>	<u>450</u>	<u>500</u>	<u>550</u>	<u>600</u>	<u>650</u>	<u>700</u>	<u>750</u>	
	$k (\text{W/m/K})$	1.27E-05 0.0246	1.34E-05 0.0261	1.53E-05 0.0299	1.70E-05 0.0339	1.88E-05 0.0379	2.07E-05 0.0422	2.25E-05 0.0464	2.43E-05 0.0505	2.60E-05 0.0549	2.79E-05 0.0592

## A.11 Ideal Gas Heat Capacities for Selected Gases

	$\tau$	$C_0^*$	$C_1$	$C_2$	$C_3$	$C_4$	Range (°R)	Range (K)	Max Error
Air	0.0140	9.0761	-3.4743	1.7804	-0.3134	0.0188	100-6200	52-3444	0.77%
100% Air + CP(CH <sub>1</sub> )	0.0400	9.5147	-3.9901	2.1908	-0.3898	0.0229	300-4000	167-2222	0.32%
100% Air + CP(CH <sub>2</sub> )	0.0400	9.7159	-4.0842	2.1394	-0.3635	0.0202	300-4000	167-2222	0.35%
100% Air + CP(CH <sub>3</sub> )	0.0400	9.8608	-4.1581	2.1088	-0.3464	0.0184	300-4000	167-2222	0.37%
Carbon Dioxide	1.0000	-5.8291	12.0893	-2.7155	0.2747	-0.0102	300-5800	167-3222	0.18%
Carbon Monoxide	0.0750	12.1297	-7.2191	3.4222	-0.6162	0.0387	300-5800	167-3222	0.36%
Hydrogen	0.5000	12.2786	-4.7650	1.4175	-0.1407	0.0037	300-5800	167-3222	0.48%
Nitrogen	0.1000	12.2568	-7.0276	3.1766	-0.5465	0.0328	300-6400	167-3556	0.38%
Oxygen	0.0005	8.5200	-3.1865	1.9424	-0.3855	0.0261	300-6400	167-3556	0.98%
Water	0.1500	15.8257	-10.0486	4.3395	-0.6669	0.0355	300-6400	167-3556	0.28%
Hydroxyl Ion	0.0025	11.4039	-4.7972	1.7247	-0.2252	0.0099	540-6300	300-3500	0.62%
Nitrous Oxide	7.5500	-21.2671	28.5044	-9.0836	1.2789	-0.0676	540-6300	300-3500	0.71%
Nitrogen Dioxide	1.5000	-16.0807	21.1941	-5.8553	0.7382	-0.0356	540-6300	300-3500	0.81%
Methane	2.8500	-21.3124	17.0304	-1.4849	-0.0505	0.0043	540-6300	300-3500	0.20%

The Ideal Gas constant pressure specific heat is given by

$$\theta = \left( \frac{T(K)}{100} \right) = \left( \frac{T(^{\circ}R)}{180} \right) \quad C_p = \sum_{i=0}^{i=4} C_i (\theta)^{i/2} = \frac{kcal}{kgmole-K} = \frac{Btu}{lbm-^{\circ}R} \quad C_0 = C_0^* \left( \frac{\theta^2}{\theta^2 + \tau} \right)$$

## A.12 Enthalpy of Formation and Enthalpy of Vaporization

25°C (77°F), 1 atm							
		h <sub>f</sub>	g <sub>f</sub>	s°	h <sub>f</sub>	g <sub>f</sub>	s°
		kJ/kmol	kJ/kmol	kJ/kmol/K	Btu/lbmol	Btu/lbmol	Btu/lbmol/R
Carbon	C(s)	0	0	5.74	0	0	1.371
Hydrogen	H <sub>2</sub> (g)	0	0	130.68	0	0	31.215
Nitrogen	N <sub>2</sub> (g)	0	0	191.61	0	0	45.768
Oxygen	O <sub>2</sub> (g)	0	0	205.04	0	0	48.976
Carbon Monoxide	CO(g)	-110,530	-137,150	197.65	-47523	-58968	47.211
Carbon Dioxide	CO <sub>2</sub> (g)	-393,520	-394,360	213.8	-169195	-169556	51.069
Steam	H <sub>2</sub> O(g)	-241,820	-228,590	188.83	-103971	-98283	45.104
Water	H <sub>2</sub> O(l)	-285,830	-237,180	69.92	-122893	-101976	16.701
Ammonia	NH <sub>3</sub> (g)	-46,190	-16,590	192.33	-19860	-7133	45.940
Methane	CH <sub>4</sub> (g)	-74,850	-50,790	186.16	-32182	-21837	44.467
Propane	C <sub>3</sub> H <sub>8</sub> (g)	-103,850	-23,490	269.91	-44651	-10100	64.471
n-Octane	C <sub>8</sub> H <sub>18</sub> (g)	-208,450	16,530	466.73	-89624	7107	111.484
n-Octane	C <sub>8</sub> H <sub>18</sub> (l)	-249,950	6,610	360.79	-107467	2842	86.179
Methyl Alcohol	CH <sub>3</sub> OH(g)	-200,670	-162,000	239.7	-86279	-69652	57.255
Methyl Alcohol	CH <sub>3</sub> OH(l)	-277,690	-166,360	126.8	-119394	-71527	30.288
Monatomic Oxygen	O(g)	249,190	231,770	161.06	107140	99650	38.471
Monatomic Hydrogen	H(g)	218,000	203,290	114.72	93730	87405	27.402
Monatomic Nitrogen	N(g)	472,650	455,510	153.3	203217	195848	36.618
Hydroxyl Ion	OH(g)	39,460	34,280	183.7	16966	14739	43.879

	h <sub>fg</sub>	C <sub>p</sub>	h <sub>fg</sub>	C <sub>p</sub>
	kJ/kmol	kJ/kmol/K	Btu/lbmol	Btu/lbmol/R
Water	44,010	35.3	18922	8.43
Propane	15,060	122.2	6475	29.18
n-Octane	41,460	254.7	17826	60.84
Methyl Alcohol	37,900	83.5	16295	19.95
Sodium	100819	29.9	43347	7.14
Potassium	83934	30.6	36088	7.31
Mercury	61303	27.9	26358	6.66

# **Appendix B**

## **Gas Property Tables for Selected Gases**

### **B.1 Air Properties (SI Units)**

Temperature K	Temperature C	h kg/kgmol	u kj/kgmol	Pr	Vr	s <sub>o</sub> kj/kgmol/K	Gamma
100	-173.1	1604.8	1142.6	0.03	6018.5	23.8878	1.400
125	-148.1	2331.0	1663.3	0.07	1916.6	30.3695	1.401
150	-123.1	3056.4	2182.4	0.12	1217.2	35.6598	1.402
175	-98.1	3781.8	2701.0	0.21	829.17	40.1327	1.401
200	-73.1	4507.5	3219.7	0.34	594.50	44.0087	1.401
225	-48.1	5233.5	3738.5	0.51	443.22	47.4293	1.401
250	-23.1	5959.9	4257.7	0.73	340.76	50.4908	1.401
275	1.9	6686.9	4777.2	1.02	268.59	53.2620	1.400
300	26.9	7414.4	5297.2	1.39	216.07	55.7943	1.400
325	51.9	8142.9	5818.2	1.84	176.81	58.1266	1.399
350	76.9	8872.6	6340.2	2.38	146.79	60.2895	1.398
375	101.9	9603.7	6863.8	3.04	123.39	62.3073	1.396
400	126.9	10336.8	7389.2	3.82	104.82	64.1997	1.395
425	151.9	11072.0	7916.7	4.73	89.874	65.9826	1.393
450	176.9	11809.8	8446.8	5.79	77.685	67.6695	1.391
475	201.9	12550.5	8979.8	7.02	67.631	69.2711	1.389
500	226.9	13294.2	9515.8	8.44	59.253	70.7971	1.387
525	251.9	14041.4	10055.3	10.06	52.205	72.2555	1.384
550	276.9	14792.3	10598.4	11.90	46.231	73.6525	1.381
575	301.9	15547.0	11145.4	13.98	41.128	74.9945	1.379
600	326.9	16305.7	11696.3	16.33	36.742	76.2859	1.376
625	351.9	17068.5	12251.4	18.97	32.948	77.5314	1.373
650	376.9	17835.5	12810.7	21.92	29.648	78.7349	1.370
675	401.9	18606.9	13374.1	25.22	26.765	79.8992	1.367
700	426.9	19382.6	13942.1	28.89	24.233	81.0276	1.365
725	451.9	20162.6	14514.4	32.95	22.002	82.1225	1.362
750	476.9	20946.8	15090.8	37.45	20.027	83.1861	1.359
775	501.9	21735.5	15671.7	42.41	18.274	84.2203	1.357
800	526.8	22528.4	16256.8	47.87	16.711	85.2274	1.354
825	551.8	23325.6	16846.1	53.87	15.315	86.2087	1.351
850	576.8	24126.8	17439.7	60.44	14.064	87.1653	1.349
875	601.8	24932.1	18037.2	67.62	12.940	88.0990	1.347
900	626.8	25741.4	18638.5	75.46	11.926	89.0111	1.344
925	651.8	26554.5	19243.9	84.00	11.012	89.9020	1.342
950	676.8	27371.3	19852.8	93.28	10.184	90.7733	1.340
975	701.8	28191.9	20465.7	103.36	9.433	91.6261	1.338
1000	726.8	29016.1	21082.2	114.27	8.751	92.4606	1.336
1025	751.8	29843.6	21701.8	126.08	8.130	93.2783	1.334
1050	776.8	30674.4	22324.6	138.83	7.563	94.0789	1.333
1075	801.8	31508.7	22951.0	152.57	7.046	94.8638	1.331
1100	826.8	32346.0	23580.6	167.37	6.572	95.6337	1.329
1125	851.8	33186.2	24212.8	183.29	6.138	96.3890	1.328
1150	876.8	34029.3	24848.2	200.39	5.739	97.1304	1.326
1175	901.8	34875.2	25486.4	218.70	5.373	97.8575	1.325
1200	926.8	35723.9	26127.4	238.35	5.035	98.5727	1.324
1225	951.8	36574.9	26770.7	259.35	4.723	99.2747	1.322
1250	976.8	37428.9	27416.6	281.80	4.436	99.9647	1.321
1275	1001.8	38285.6	28065.2	305.76	4.170	100.6433	1.320
1300	1026.8	39143.5	28715.8	331.30	3.924	101.3101	1.319
1325	1051.8	40004.7	29369.0	358.49	3.696	101.9659	1.318
1350	1076.8	40868.0	30024.6	387.42	3.485	102.6112	1.317
1375	1101.8	41733.0	30681.8	418.17	3.288	103.2462	1.316
1400	1126.8	42600.6	31341.7	450.85	3.105	103.8718	1.315
1425	1151.8	43470.4	32003.0	485.52	2.935	104.4876	1.314
1450	1176.8	44340.9	32665.9	522.22	2.777	105.0935	1.313
1475	1201.8	45214.2	33331.4	561.10	2.629	105.6904	1.312
1500	1226.8	46089.4	33999.0	602.25	2.491	106.2789	1.311
1525	1251.8	46966.6	34668.5	645.68	2.362	106.8578	1.310
1550	1276.8	47845.5	35339.7	691.69	2.241	107.4300	1.309
1575	1301.8	48726.2	36011.9	740.16	2.128	107.9931	1.309
1600	1326.8	49607.8	36685.8	791.40	2.022	108.5495	1.308
1625	1351.8	50491.7	37362.0	845.22	1.923	109.0966	1.307
1650	1376.8	51376.2	38038.9	902.11	1.829	109.6381	1.306
1675	1401.8	52262.5	38717.5	961.77	1.742	110.1705	1.306
1700	1426.8	53152.0	39397.5	1024.76	1.659	110.6979	1.305

1725	1451.8	54042.3	40080.2	1090.79	1.581	111.2171	1.304
1750	1476.8	54932.8	40763.0	1160.12	1.508	111.7294	1.304
1775	1501.8	55825.3	41449.4	1233.09	1.439	112.2365	1.303
1800	1526.8	56720.1	42134.9	1309.56	1.375	112.7367	1.303
1825	1551.8	57613.3	42820.4	1389.69	1.313	113.2305	1.302
1850	1576.8	58509.4	43508.9	1473.67	1.255	113.7182	1.302
1875	1601.8	59409.7	44201.5	1561.58	1.201	114.2000	1.301
1900	1626.8	60306.9	44891.0	1653.65	1.149	114.6762	1.300
1925	1651.8	61207.5	45582.2	1749.90	1.100	115.1466	1.300
1950	1676.8	62110.5	46279.2	1850.59	1.054	115.6117	1.299
1975	1701.8	63012.8	46972.2	1955.91	1.010	116.0718	1.299
2000	1726.8	63915.9	47669.2	2066.18	0.968	116.5278	1.298
2025	1751.8	64819.8	48365.4	2181.02	0.928	116.9775	1.298
2050	1776.8	65726.4	49062.8	2300.86	0.891	117.4222	1.298
2075	1801.8	66632.6	49762.9	2425.62	0.855	117.8612	1.297
2100	1826.8	67543.5	50464.5	2555.79	0.822	118.2958	1.297
2125	1851.8	68450.4	51165.3	2691.76	0.789	118.7267	1.296
2150	1876.8	69360.0	51865.6	2833.21	0.759	119.1525	1.296
2175	1901.8	70272.1	52568.3	2979.99	0.730	119.5725	1.295
2200	1926.8	71182.2	53272.4	3133.78	0.702	119.9908	1.295
2225	1951.8	72097.2	53978.1	3293.20	0.676	120.4033	1.295
2250	1976.8	73011.9	54686.7	3458.58	0.651	120.8107	1.294
2275	2001.8	73923.4	55388.9	3630.89	0.627	121.2149	1.294
2300	2026.8	74842.5	56098.7	3809.81	0.604	121.6148	1.294
2325	2051.9	75754.3	56804.4	3995.67	0.582	122.0108	1.293
2350	2076.9	76674.1	57518.2	4189.73	0.561	122.4051	1.293
2375	2101.9	77592.9	58227.6	4389.97	0.541	122.7932	1.293
2400	2126.9	78507.2	58935.8	4597.72	0.522	123.1776	1.292
2425	2151.9	79426.7	59646.1	4813.26	0.504	123.5585	1.292
2450	2176.9	80349.7	60363.0	5037.23	0.486	123.9366	1.292
2475	2201.9	81273.4	61077.4	5270.24	0.470	124.3125	1.291
2500	2226.9	82192.5	61790.4	5509.22	0.454	124.6812	1.291
2525	2251.9	83114.8	62506.7	5757.86	0.439	125.0482	1.291
2550	2276.9	84041.1	63223.6	6015.53	0.424	125.4122	1.290
2575	2301.9	84969.4	63942.5	6280.78	0.410	125.7709	1.290
2600	2326.9	85886.2	64650.1	6557.81	0.396	126.1298	1.290
2625	2351.9	86807.6	65368.9	6844.26	0.384	126.4852	1.289
2650	2376.9	87741.2	66093.0	7139.73	0.371	126.8366	1.289
2675	2401.9	88664.3	66806.7	7447.82	0.359	127.1878	1.289
2700	2426.9	89596.2	67529.3	7761.68	0.348	127.5310	1.289
2725	2451.9	90518.9	68249.2	8089.94	0.337	127.8753	1.288
2750	2476.9	91450.9	68965.3	8423.94	0.326	128.2117	1.288
2775	2501.9	92381.9	69687.0	8769.42	0.316	128.5458	1.288
2800	2526.9	93311.9	70414.3	9131.02	0.307	128.8818	1.288
2825	2551.9	94248.4	71141.4	9502.36	0.297	129.2132	1.287
2850	2576.9	95182.0	71865.7	9888.05	0.288	129.5439	1.287
2875	2601.9	96115.2	72589.6	10282.3	0.280	129.8690	1.287
2900	2626.9	97050.2	73321.8	10686.3	0.271	130.1894	1.286
2925	2651.9	97967.6	74029.8	11103.6	0.263	130.5078	1.286
2950	2676.9	98908.9	74761.9	11543.9	0.256	130.8311	1.286
2975	2701.9	99845.8	75489.4	11986.1	0.248	131.1437	1.286
3000	2726.9	100781.8	76216.1	12444.3	0.241	131.4555	1.285
3025	2751.9	101706.6	76944.6	12933.0	0.234	131.7758	1.285
3050	2776.9	102662.5	77678.1	13408.5	0.227	132.0760	1.285
3075	2801.9	103596.5	78402.8	13907.1	0.221	132.3795	1.285
3100	2826.9	104539.8	79149.9	14431.7	0.215	132.6873	1.284
3125	2851.9	105465.8	79866.5	14965.8	0.209	132.9895	1.284
3150	2876.9	106407.4	80611.9	15519.7	0.203	133.2916	1.284
3175	2901.9	107353.1	81348.2	16072.2	0.198	133.5824	1.284
3200	2926.9	108280.3	82053.1	16655.2	0.192	133.8786	1.284
3225	2951.9	109232.0	82808.5	17257.4	0.187	134.1739	1.283
3250	2976.9	110178.3	83545.5	17879.8	0.182	134.4685	1.283
3275	3001.9	111123.2	84267.9	18497.0	0.177	134.7506	1.283
3300	3026.9	112069.4	85004.8	19152.7	0.172	135.0402	1.283
3325	3051.9	113008.3	85747.5	19806.8	0.168	135.3194	1.283
3350	3076.9	113938.4	86468.3	20500.1	0.163	135.6055	1.283
3375	3101.9	114883.0	87203.5	21213.6	0.159	135.8899	1.282
3400	3126.9	115838.3	87949.5	21938.6	0.155	136.1693	1.283

## B.2 Air Properties (English Units)

Temperature		<i>h</i>	<i>u</i>	<i>Pr</i>	<i>Vr</i>	<i>s<sub>o</sub></i>	Gamma
R	F	Btu/lbmol	Btu/lbmol			Btu/lbmol/R	
100	-359.7	690.0	491.3	0.004	26215.8	5.7059	1.402
140	-319.7	968.4	692.7	0.012	11288.7	8.0473	1.399
180	-279.7	1246.6	892.9	0.030	6018.51	9.7953	1.400
220	-239.7	1524.1	1091.9	0.060	3648.55	11.1878	1.401
260	-199.7	1801.4	1290.4	0.108	2406.77	12.3457	1.402
300	-159.7	2078.6	1488.6	0.178	1685.34	13.3375	1.402
340	-119.7	2355.9	1686.8	0.276	1233.92	14.2051	1.401
380	-79.7	2633.3	1885.1	0.406	935.173	14.9765	1.401
420	-39.7	2910.8	2083.4	0.576	728.608	15.6709	1.401
460	0.3	3188.5	2281.8	0.792	580.625	16.3024	1.401
500	40.3	3466.4	2480.4	1.061	471.455	16.8816	1.400
540	80.3	3744.5	2679.2	1.388	388.917	17.4166	1.400
580	120.3	4022.8	2878.2	1.784	325.178	17.9140	1.399
620	160.3	4301.6	3077.7	2.254	275.068	18.3788	1.398
660	200.3	4580.9	3277.6	2.808	235.036	18.8153	1.397
700	240.3	4860.7	3478.1	3.455	202.608	19.2269	1.396
740	280.3	5141.3	3679.3	4.204	176.016	19.6167	1.394
780	320.3	5422.6	3881.3	5.066	153.972	19.9869	1.393
820	360.3	5704.9	4084.2	6.051	135.513	20.3398	1.391
860	400.3	5988.1	4288.0	7.171	119.925	20.6771	1.389
900	440.3	6272.5	4493.0	8.438	106.655	21.0003	1.387
940	480.3	6558.0	4699.1	9.866	95.277	21.3106	1.384
980	520.3	6844.7	4906.4	11.468	85.459	21.6094	1.382
1020	560.3	7132.7	5115.0	13.257	76.939	21.8974	1.380
1060	600.3	7422.1	5325.0	15.252	69.500	22.1757	1.377
1100	640.3	7712.8	5536.3	17.466	62.978	22.4449	1.375
1140	680.3	8004.9	5749.1	19.918	57.234	22.7058	1.372
1180	720.3	8298.6	5963.3	22.626	52.152	22.9589	1.370
1220	760.3	8593.7	6178.9	25.609	47.640	23.2048	1.367
1260	800.3	8890.2	6396.0	28.886	43.620	23.4439	1.365
1300	840.3	9188.2	6614.7	32.479	40.025	23.6768	1.362
1340	880.3	9487.6	6834.7	36.411	36.802	23.9037	1.360
1380	920.3	9788.6	7056.3	40.703	33.904	24.1250	1.357
1420	960.3	10091.0	7279.2	45.382	31.290	24.3410	1.355
1460	1000.3	10394.8	7503.7	50.467	28.930	24.5520	1.353
1500	1040.3	10700.1	7729.5	55.993	26.789	24.7583	1.351
1540	1080.3	11006.8	7956.8	61.980	24.847	24.9600	1.349
1580	1120.3	11314.8	8185.4	68.460	23.079	25.1575	1.346
1620	1160.3	11624.2	8415.3	75.463	21.468	25.3509	1.344
1660	1200.3	11934.8	8646.5	83.016	19.996	25.5403	1.343
1700	1240.3	12246.8	8879.1	91.154	18.650	25.7260	1.341
1740	1280.3	12560.0	9112.8	99.909	17.416	25.9082	1.339
1780	1320.3	12874.3	9347.9	109.313	16.283	26.0868	1.337
1820	1360.3	13190.1	9584.1	119.404	15.242	26.2621	1.336
1860	1400.3	13506.8	9821.5	130.218	14.284	26.4343	1.334
1900	1440.3	13824.8	10059.9	141.791	13.400	26.6034	1.332
1940	1480.3	14143.7	10299.3	154.172	12.583	26.7696	1.331
1980	1520.3	14463.8	10540.2	167.374	11.830	26.9328	1.329
2020	1560.3	14784.7	10781.6	181.464	11.132	27.0933	1.328
2060	1600.3	15106.9	11024.3	196.483	10.484	27.2512	1.327

2100	1640.3	15429.8	11267.8	212.465	9.884	27.4065	1.325
2140	1680.3	15753.9	11512.5	229.464	9.326	27.5594	1.324
2180	1720.3	16078.8	11757.9	247.495	8.808	27.7096	1.323
2220	1760.3	16404.3	12004.1	266.670	8.325	27.8578	1.322
2260	1800.3	16731.0	12251.4	286.998	7.875	28.0036	1.321
2300	1840.3	17058.3	12499.3	308.512	7.455	28.1472	1.320
2340	1880.3	17386.4	12748.0	331.296	7.063	28.2887	1.319
2380	1920.3	17715.5	12997.7	355.367	6.697	28.4280	1.318
2420	1960.3	18045.4	13247.9	380.859	6.354	28.5655	1.317
2460	2000.3	18375.8	13498.9	407.717	6.034	28.7009	1.316
2500	2040.3	18706.8	13750.4	436.076	5.733	28.8344	1.315
2540	2080.3	19038.8	14003.3	465.990	5.451	28.9661	1.314
2580	2120.3	19371.5	14256.2	497.469	5.186	29.0960	1.313
2620	2160.3	19704.9	14510.2	530.594	4.938	29.2240	1.313
2660	2200.3	20038.5	14764.7	565.557	4.703	29.3507	1.312
2700	2240.3	20372.8	15019.5	602.250	4.483	29.4755	1.311
2740	2280.3	20708.4	15275.7	640.811	4.276	29.5988	1.310
2780	2320.3	21044.0	15531.8	681.229	4.081	29.7202	1.310
2820	2360.3	21380.2	15788.6	723.753	3.896	29.8405	1.309
2860	2400.3	21716.9	16045.9	768.283	3.723	29.9591	1.308
2900	2440.3	22054.3	16303.8	814.954	3.558	30.0762	1.308
2940	2480.3	22392.2	16562.5	863.846	3.403	30.1919	1.307
2980	2520.3	22730.5	16821.4	915.164	3.256	30.3065	1.306
3020	2560.3	23069.5	17080.2	968.642	3.118	30.4192	1.306
3060	2600.3	23409.4	17340.7	1024.76	2.986	30.5311	1.305
3100	2640.3	23749.1	17601.7	1083.25	2.862	30.6413	1.305
3140	2680.3	24090.0	17863.1	1144.37	2.744	30.7503	1.304
3180	2720.3	24430.2	18123.9	1208.42	2.632	30.8585	1.303
3220	2760.3	24772.7	18386.8	1275.04	2.525	30.9650	1.303
3260	2800.3	25113.9	18647.9	1344.65	2.424	31.0706	1.302
3300	2840.3	25456.2	18911.5	1417.230	2.328	31.1750	1.302
3340	2880.3	25799.0	19174.8	1492.974	2.237	31.2784	1.301
3380	2920.3	26141.9	19438.3	1571.546	2.151	31.3802	1.301
3420	2960.3	26485.7	19702.6	1653.649	2.068	31.4814	1.300
3460	3000.3	26829.7	19967.2	1739.133	1.989	31.5814	1.300
3500	3040.3	27175.2	20233.2	1828.024	1.915	31.6804	1.300
3540	3080.3	27519.7	20498.2	1920.853	1.843	31.7788	1.299
3580	3120.3	27863.3	20762.4	2016.791	1.775	31.8756	1.299
3620	3160.3	28210.6	21030.3	2116.627	1.710	31.9715	1.298
3660	3200.3	28555.4	21295.6	2220.483	1.648	32.0667	1.298
3700	3240.3	28902.8	21563.5	2327.995	1.589	32.1606	1.297
3740	3280.3	29248.9	21830.9	2439.306	1.533	32.2533	1.297
3780	3320.3	29597.1	22098.9	2555.792	1.479	32.3459	1.297
3820	3360.3	29943.8	22366.9	2675.917	1.428	32.4371	1.296
3860	3400.3	30290.4	22633.4	2801.559	1.378	32.5283	1.296
3900	3440.3	30640.2	22904.4	2930.566	1.331	32.6177	1.295
3940	3480.3	30986.3	23170.4	3064.678	1.286	32.7065	1.295
3980	3520.3	31337.5	23442.8	3203.413	1.242	32.7944	1.295
4020	3560.3	31685.2	23710.3	3347.464	1.201	32.8818	1.295
4060	3600.3	32034.6	23981.0	3496.259	1.161	32.9682	1.294
4100	3640.3	32384.9	24251.2	3650.195	1.123	33.0537	1.294

4140	3680.3	32735.3	24521.4	3809.811	1.087	33.1387	1.294
4180	3720.3	33082.6	24791.3	3975.642	1.051	33.2233	1.293
4220	3760.3	33434.7	25063.3	4144.901	1.018	33.3061	1.293
4260	3800.3	33783.8	25333.7	4322.743	0.985	33.3895	1.293
4300	3840.3	34136.5	25606.2	4503.871	0.955	33.4711	1.292
4340	3880.3	34488.3	25877.8	4692.876	0.925	33.5527	1.292
4380	3920.3	34839.6	26150.3	4886.152	0.896	33.6328	1.292
4420	3960.3	35191.0	26421.6	5089.733	0.868	33.7139	1.291
4460	4000.3	35543.2	26695.1	5296.056	0.842	33.7928	1.291
4500	4040.3	35895.4	26968.5	5509.218	0.817	33.8712	1.291
4540	4080.3	36248.5	27241.5	5729.551	0.792	33.9491	1.291
4580	4120.3	36602.1	27513.4	5957.094	0.769	34.0264	1.290
4620	4160.3	36952.2	27787.6	6193.744	0.746	34.1038	1.290
4660	4200.3	37307.9	28061.8	6433.935	0.724	34.1793	1.290
4700	4240.3	37662.5	28337.6	6686.213	0.703	34.2557	1.290
4740	4280.3	38016.2	28612.6	6939.447	0.683	34.3295	1.289
4780	4320.3	38370.7	28885.5	7206.479	0.663	34.4045	1.289
4820	4360.3	38721.3	29157.4	7476.027	0.645	34.4774	1.289
4860	4400.3	39078.7	29436.0	7761.679	0.626	34.5519	1.289
4900	4440.3	39433.7	29712.2	8050.20	0.609	34.6244	1.288
4940	4480.3	39787.4	29987.2	8348.87	0.592	34.6967	1.288
4980	4520.3	40143.3	30264.4	8651.44	0.576	34.7674	1.288
5020	4560.3	40499.7	30539.2	8967.89	0.560	34.8387	1.288
5060	4600.3	40853.1	30813.9	9294.72	0.544	34.9098	1.287
5100	4640.3	41209.2	31091.2	9628.23	0.530	34.9798	1.287
5140	4680.3	41569.5	31369.9	9975.90	0.515	35.0503	1.287
5180	4720.3	41920.0	31641.7	10326.3	0.502	35.1188	1.287
5220	4760.3	42283.6	31926.5	10686.3	0.488	35.1869	1.286
5260	4800.3	42634.6	32198.8	11058.6	0.476	35.2549	1.286
5300	4840.3	42998.2	32480.8	11436.7	0.463	35.3216	1.286
5340	4880.3	43352.6	32753.6	11837.8	0.451	35.3901	1.286
5380	4920.3	43707.3	33029.6	12237.7	0.440	35.4561	1.285
5420	4960.3	44063.5	33307.1	12652.2	0.428	35.5222	1.285
5460	5000.3	44425.7	33590.6	13080.4	0.417	35.5883	1.285
5500	5040.3	44778.9	33864.9	13523.8	0.407	35.6545	1.285
5540	5080.3	45140.7	34148.0	13970.3	0.397	35.7190	1.285
5580	5120.3	45503.7	34432.3	14431.7	0.387	35.7835	1.284
5620	5160.3	45860.1	34704.3	14902.8	0.377	35.8473	1.284
5660	5200.3	46219.4	34984.8	15386.9	0.368	35.9108	1.284
5700	5240.3	46574.9	35261.6	15895.4	0.359	35.9754	1.284
5740	5280.3	46937.0	35550.6	16402.2	0.350	36.0377	1.284
5780	5320.3	47297.3	35826.5	16926.3	0.341	36.1002	1.283
5820	5360.3	47652.4	36102.9	17458.6	0.333	36.1617	1.283
5860	5400.3	48016.0	36387.7	18015.0	0.325	36.2240	1.283
5900	5440.3	48376.2	36669.2	18567.9	0.318	36.2840	1.283
5940	5480.3	48741.1	36949.6	19152.7	0.310	36.3456	1.283
5980	5520.3	49098.1	37233.5	19748.3	0.303	36.4064	1.283
6020	5560.3	49454.6	37511.3	20352.3	0.296	36.4662	1.282
6060	5600.3	49816.3	37794.3	20969.2	0.289	36.5255	1.283
6100	5640.3	50180.0	38073.6	21615.6	0.282	36.5858	1.282
6140	5680.3	50540.0	38354.8	22238.5	0.276	36.6422	1.282
6180	5720.3	50901.3	38637.4	22929.3	0.270	36.7030	1.282

### B.3 H<sub>2</sub>O Properties (SI Units)

Temperature K	h kj/kgmol	u kj/kgmol	Pr	Vr	S <sub>o</sub> kj/kgmol/K	Gamma
200	-73.1	5510.1	4124.4	0.290	1259.160	169.2769
225	-48.1	6344.3	4757.4	0.460	490.529	173.2069
250	-23.1	7179.1	5389.8	0.700	356.982	176.7249
275	1.9	8015.2	6022.5	1.030	267.626	179.9124
300	26.9	8853.5	6656.6	1.460	205.544	182.8300
325	51.9	9694.8	7293.2	2.020	161.051	185.5235
350	76.9	10539.8	7933.1	2.730	128.322	188.0283
375	101.9	11389.1	8576.9	3.620	103.711	190.3722
400	126.9	12243.3	9225.3	4.710	84.853	192.5772
425	151.9	13102.8	9878.8	6.060	70.166	194.6613
450	176.9	13967.9	10537.7	7.680	58.563	196.6392
475	201.9	14838.9	11202.3	9.640	49.284	198.5230
500	226.9	15716.2	11873.1	11.970	41.779	200.3229
525	251.9	16600.0	12550.2	14.730	35.649	202.0476
550	276.9	17490.4	13233.8	17.970	30.599	203.7044
575	301.9	18387.7	13924.2	21.780	26.404	205.2997
600	326.9	19291.9	14621.5	26.210	22.895	206.8390
625	351.9	20203.2	15325.8	31.340	19.941	208.3270
650	376.9	21121.8	16037.4	37.280	17.438	209.7682
675	401.9	22047.9	16756.2	44.100	15.306	211.1660
700	426.9	22981.3	17482.5	51.930	13.481	212.5239
725	451.9	23922.3	18216.3	60.870	11.911	213.8447
750	476.9	24870.9	18957.7	71.050	10.556	215.1311
775	501.9	25827.4	19706.8	82.620	9.380	216.3855
800	526.8	26791.6	20463.6	95.730	8.357	217.6099
825	551.8	27763.5	21228.2	110.550	7.463	218.8063
850	576.8	28743.5	22000.8	127.260	6.679	219.9765
875	601.8	29731.3	22781.2	146.060	5.991	221.1218
900	626.8	30727.1	23569.5	167.160	5.384	222.2440
925	651.8	31731.0	24365.9	190.810	4.848	223.3439
950	676.8	32742.7	25170.1	217.260	4.373	224.4232
975	701.8	33762.4	25982.4	246.790	3.951	225.4828
1000	726.8	34790.1	26802.5	279.710	3.575	226.5235
1025	751.8	35825.8	27630.7	316.320	3.240	227.5464
1050	776.8	36869.4	28466.6	357.010	2.941	228.5522
1075	801.8	37920.9	29310.7	402.140	2.673	229.5419
1100	826.8	38980.1	30162.4	452.140	2.433	230.5162
1125	851.8	40047.3	31022.0	507.430	2.217	231.4753
1150	876.8	41122.3	31889.3	568.520	2.023	232.4204
1175	901.8	42204.8	32764.1	635.900	1.848	233.3515
1200	926.8	43294.8	33646.7	710.130	1.690	234.2695
1225	951.8	44392.7	34536.8	791.850	1.547	235.1750
1250	976.8	45497.7	35434.4	881.630	1.418	236.0679
1275	1002	46610.2	36338.9	980.230	1.301	236.9493
1300	1027	47729.9	37251.2	1088.310	1.195	237.8188
1325	1052	48856.9	38170.4	1206.690	1.098	238.6773
1350	1077	49991.0	39096.9	1336.320	1.010	239.5256
1375	1102	51131.9	40030.1	1477.870	0.930	240.3626
1400	1127	52279.6	40969.9	1632.520	0.858	241.1900
1425	1152	53434.1	41916.8	1801.100	0.791	242.0070
1450	1177	54595.2	42870.1	1984.990	0.730	242.8153
1475	1202	55762.9	43830.1	2185.000	0.675	243.6134
1500	1227	56936.6	44796.6	2402.600	0.624	244.4027
1525	1252	58116.8	45768.6	2638.960	0.578	245.1828
1550	1277	59302.9	46747.5	2895.720	0.535	245.9547
1575	1302	60495.3	47732.2	3174.180	0.496	246.7180
1600	1327	61693.9	48722.7	3475.590	0.460	247.4722
1625	1352	62898.1	49719.2	3802.260	0.427	248.2190
						1.208

1650	1377	64107.6	50721.0	4155.830	0.397	248.9582	1.207
1675	1402	65323.3	51729.0	4537.600	0.369	249.6889	1.206
1700	1427	66543.8	52741.4	4950.400	0.343	250.4128	1.205
1725	1452	67769.7	53760.0	5395.200	0.320	251.1281	1.204
1750	1477	69000.6	54783.2	5875.270	0.298	251.8368	1.203
1775	1502	70237.3	55811.5	6392.490	0.278	252.5382	1.202
1800	1527	71478.6	56845.0	6949.430	0.259	253.2327	1.201
1825	1552	72724.0	57883.6	7548.220	0.242	253.9198	1.200
1850	1577	73975.0	58926.9	8192.660	0.226	254.6010	1.199
1875	1602	75230.7	59974.9	8884.150	0.211	255.2746	1.198
1900	1627	76490.6	61026.3	9627.270	0.197	255.9425	1.197
1925	1652	77754.6	62083.5	10424.460	0.185	256.6039	1.196
1950	1677	79024.1	63144.5	11278.480	0.173	257.2585	1.195
1975	1702	80296.8	64209.4	12194.130	0.162	257.9074	1.195
2000	1727	81574.7	65279.6	13173.870	0.152	258.5499	1.194
2025	1752	82855.8	66353.0	14222.670	0.142	259.1868	1.193
2050	1777	84140.9	67430.4	15346.000	0.134	259.8188	1.193
2075	1802	85430.3	68512.2	16540.930	0.125	260.4421	1.192
2100	1827	86723.8	69598.0	17823.400	0.118	261.0630	1.191
2125	1852	88019.4	70685.9	19185.650	0.111	261.6753	1.191
2150	1877	89320.2	71778.9	20643.450	0.104	262.2841	1.190
2175	1902	90626.4	72875.9	22198.160	0.098	262.8878	1.189
2200	1927	91933.1	73976.5	23853.41	0.092	263.4857	1.189
2225	1952	93244.3	75078.4	25619.01	0.087	264.0793	1.188
2250	1977	94559.1	76185.5	27490.67	0.082	264.6656	1.188
2275	2002	95876.4	77295.1	29486.28	0.077	265.2482	1.187
2300	2027	97196.6	78407.7	31609.24	0.073	265.8262	1.186
2325	2052	98522.0	79526.9	33860.18	0.069	266.3981	1.186
2350	2077	99849.5	80646.8	36256.23	0.065	266.9665	1.185
2375	2102	101181.8	81769.7	38795.49	0.061	267.5293	1.185
2400	2127	102514.1	82894.4	41493.24	0.058	268.0882	1.184
2425	2152	103850.5	84023.1	44350.89	0.055	268.6419	1.184
2450	2177	105189.8	85154.6	47387.27	0.052	269.1924	1.183
2475	2202	106531.3	86288.5	50591.75	0.049	269.7364	1.183
2500	2227	107878.4	87427.9	53995.10	0.046	270.2777	1.183
2525	2252	109226.4	88568.2	57590.81	0.044	270.8137	1.182
2550	2277	110576.9	89711.0	61398.02	0.042	271.3459	1.182
2575	2302	111929.5	90855.9	65430.73	0.039	271.8747	1.181
2600	2327	113285.2	92005.5	69692.74	0.037	272.3994	1.181
2625	2352	114646.5	93157.5	74183.61	0.035	272.9185	1.180
2650	2377	116004.6	94309.6	78938.94	0.034	273.4351	1.180
2675	2402	117370.5	95466.2	83955.33	0.032	273.9473	1.180
2700	2427	118734.1	96623.8	89240.35	0.030	274.4548	1.179
2725	2452	120104.6	97784.9	94835.10	0.029	274.9603	1.179
2750	2477	121475.6	98946.5	100725.1	0.027	275.4613	1.178
2775	2502	122851.6	100113.2	106929.9	0.026	275.9583	1.178
2800	2527	124226.5	101282.1	113469.0	0.025	276.4517	1.178
2825	2552	125603.7	102449.9	120392.1	0.023	276.9441	1.177
2850	2577	126984.2	103624.4	127621.4	0.022	277.4289	1.177
2875	2602	128364.0	104798.1	135249.5	0.021	277.9115	1.177
2900	2627	129749.0	105973.8	143271.5	0.020	278.3906	1.176
2925	2652	131137.9	107153.4	151752.6	0.019	278.8687	1.176
2950	2677	132529.4	108338.8	160597.6	0.018	279.3397	1.176
2975	2702	133916.9	109520.3	169925.2	0.018	279.8090	1.176
3000	2727	135309.9	110704.0	179739.8	0.017	280.2758	1.175
3025	2752	136707.7	111892.5	190023.6	0.016	280.7384	1.175
3050	2777	138101.4	113080.1	200807.2	0.015	281.1973	1.175
3075	2802	139504.2	114270.3	212141.3	0.014	281.6538	1.174
3100	2827	140902.4	115465.7	224116.0	0.014	282.1103	1.174
3125	2852	142306.1	116666.6	236620.6	0.013	282.5617	1.174
3150	2877	143714.6	117859.2	249705.6	0.013	283.0092	1.173
3175	2902	145122.6	119057.9	263395.2	0.012	283.4529	1.173
3200	2927	146534.1	120260.1	277801.660	0.012	283.8956	1.173

## B.4 H<sub>2</sub>O Properties (English Units)

Temperature R	h Btu/lbmol	u Btu/lbmol	Pr	Vr	so Btu/lbmol/R	Gamma
300	-159.7	2369.1	1773.3	0.138	2180.3	40.4340
340	-119.7	2687.7	2016.1	0.227	1495.8	41.4308
380	-79.7	3006.4	2258.2	0.355	1069.9	42.3172
420	-39.7	3325.3	2500.0	0.531	791.26	43.1150
460	0.3	3644.4	2741.7	0.765	601.31	43.8408
500	40.3	3964.1	2983.5	1.070	467.29	44.5071
540	80.3	4284.5	3226.0	1.460	369.98	45.1236
580	120.3	4606.0	3469.2	1.949	297.60	45.6979
620	160.3	4928.7	3713.5	2.555	242.62	46.2359
660	200.3	5252.8	3959.1	3.298	200.12	46.7425
700	240.3	5578.5	4206.2	4.198	166.75	47.2216
740	280.3	5905.9	4455.0	5.279	140.19	47.6765
780	320.3	6235.2	4705.5	6.566	118.80	48.1098
820	360.3	6566.5	4957.9	8.088	101.38	48.5240
860	400.3	6899.8	5212.3	9.877	87.07	48.9208
900	440.3	7235.2	5468.8	11.968	75.20	49.3020
940	480.3	7572.8	5727.4	14.397	65.29	49.6690
980	520.3	7912.7	5988.3	17.207	56.95	50.0231
1020	560.3	8254.8	6251.4	20.444	49.89	50.3653
1060	600.3	8599.4	6516.8	24.155	43.88	50.6966
1100	640.3	8946.3	6784.7	28.397	38.74	51.0179
1140	680.3	9295.7	7054.9	33.228	34.31	51.3299
1180	720.3	9647.5	7327.6	38.712	30.48	51.6332
1220	760.3	10001.9	7602.8	44.919	27.16	51.9285
1260	800.3	10358.8	7880.6	51.925	24.27	52.2164
1300	840.3	10718.3	8160.8	59.814	21.73	52.4972
1340	880.3	11080.3	8443.7	68.674	19.51	52.7716
1380	920.3	11445.0	8729.1	78.604	17.56	53.0397
1420	960.3	11812.3	9017.2	89.707	15.83	53.3021
1460	1000.3	12182.4	9308.0	102.10	14.30	53.5591
1500	1040.3	12555.0	9601.4	115.90	12.94	53.8109
1540	1080.3	12930.4	9897.5	131.25	11.73	54.0578
1580	1120.3	13308.4	10196.2	148.29	10.66	54.3002
1620	1160.3	13689.1	10497.7	167.16	9.69	54.5382
1660	1200.3	14072.6	10801.9	188.05	8.83	54.7719
1700	1240.3	14458.7	11108.7	211.13	8.05	55.0019
1740	1280.3	14847.6	11418.3	236.59	7.35	55.2280
1780	1320.3	15239.2	11730.6	264.64	6.73	55.4504
1820	1360.3	15633.5	12045.6	295.50	6.16	55.6695
1860	1400.3	16030.5	12363.2	329.42	5.65	55.8852
1900	1440.3	16430.2	12683.6	366.64	5.182	56.0979
1940	1480.3	16832.6	13006.6	407.45	4.761	56.3074
1980	1520.3	17237.5	13322.3	452.14	4.379	56.5141
2020	1560.3	17645.2	13660.6	501.01	4.032	56.7179
2060	1600.3	18055.5	13991.6	554.41	3.716	56.9190
2100	1640.3	18468.5	14325.1	612.69	3.428	57.1175
2140	1680.3	18883.9	14661.4	676.25	3.165	57.3135
2180	1720.3	19302.0	15000.1	745.49	2.924	57.5071
2220	1760.3	19722.6	15341.4	820.84	2.705	57.6983
2260	1800.3	20145.8	15685.2	902.78	2.503	57.8873
2300	1840.3	20571.4	16031.4	991.74	2.319	58.0739
2340	1880.3	20999.5	16380.1	1088.31	2.150	58.2584
2380	1920.3	21430.1	16731.3	1193.04	1.995	58.4409
2420	1960.3	21863.0	17084.8	1306.48	1.852	58.6213
2460	2000.3	22298.3	17440.8	1429.28	1.721	58.7997
2500	2040.3	22735.9	17799.0	1562.15	1.600	58.9762
2540	2080.3	23175.9	18159.7	1705.67	1.489	59.1507
2580	2120.3	23618.1	18522.4	1860.70	1.387	59.3235
2620	2160.3	24062.5	18887.5	2027.89	1.292	59.4944
2660	2200.3	24509.1	19254.7	2208.25	1.205	59.6636
2700	2240.3	24958.0	19624.3	2402.60	1.124	59.8311
2740	2280.3	25408.8	19995.7	2611.83	1.049	59.9969
2780	2320.3	25861.9	20369.3	2836.81	0.980	60.1610
2820	2360.3	26316.9	20745.1	3078.89	0.916	60.3236
2860	2400.3	26774.0	21122.7	3338.68	0.857	60.4844
2900	2440.3	27233.1	21502.4	3617.71	0.802	60.6438
2940	2480.3	27694.1	21884.1	3917.13	0.751	60.8017
2980	2520.3	28157.1	22267.6	4238.07	0.703	60.9581
3020	2560.3	28621.8	22652.9	4581.75	0.659	61.1130

3060	2600.3	29088.6	23040.2	4950.40	0.618	61.2666	1.205
3100	2640.3	29556.9	23429.2	5344.50	0.580	61.4188	1.204
3140	2680.3	30027.3	23820.2	5765.36	0.545	61.5693	1.203
3180	2720.3	30498.9	24212.7	6216.06	0.512	61.7188	1.202
3220	2760.3	30972.8	24607.1	6696.83	0.481	61.8667	1.201
3260	2800.3	31447.9	25002.8	7210.55	0.452	62.0135	1.200
3300	2840.3	31925.1	25400.5	7758.22	0.425	62.1589	1.199
3340	2880.3	32403.6	25799.5	8342.94	0.400	62.3031	1.199
3380	2920.3	32883.8	26200.3	8964.83	0.377	62.4459	1.198
3420	2960.3	33365.2	26602.3	9627.27	0.355	62.5875	1.197
3460	3000.3	33848.5	27006.1	10332.8	0.335	62.7279	1.196
3500	3040.3	34333.3	27411.5	11083.4	0.316	62.8672	1.196
3540	3080.3	34819.3	27818.0	11881.8	0.298	63.0053	1.195
3580	3120.3	35307.1	28226.7	12730.8	0.281	63.1424	1.194
3620	3160.3	35795.5	28635.7	13632.1	0.266	63.2782	1.194
3660	3200.3	36286.0	29046.7	14587.9	0.251	63.4128	1.193
3700	3240.3	36777.7	29459.3	15603.8	0.237	63.5465	1.192
3740	3280.3	37270.8	29872.9	16681.3	0.224	63.6791	1.192
3780	3320.3	37765.0	30287.7	17823.4	0.212	63.8106	1.191
3820	3360.3	38260.4	30703.7	19031.2	0.201	63.9408	1.191
3860	3400.3	38757.5	31121.3	20314.7	0.190	64.0704	1.190
3900	3440.3	39256.3	31540.6	21672.0	0.180	64.1988	1.189
3940	3480.3	39754.2	31959.8	23104.2	0.171	64.3259	1.189
3980	3520.3	40254.5	32380.6	24626.0	0.162	64.4526	1.188
4020	3560.3	40756.8	32802.8	26228.5	0.153	64.5778	1.188
4060	3600.3	41259.2	33225.7	27925.1	0.145	64.7022	1.187
4100	3640.3	41763.0	33650.8	29712.9	0.138	64.8255	1.187
4140	3680.3	42267.9	34075.5	31609.3	0.131	64.9483	1.186
4180	3720.3	42774.2	34502.4	33603.3	0.124	65.0698	1.186
4220	3760.3	43281.6	34930.3	35710.0	0.118	65.1906	1.185
4260	3800.3	43789.6	35358.9	37931.6	0.112	65.3104	1.185
4300	3840.3	44299.2	35789.0	40277.3	0.107	65.4296	1.185
4340	3880.3	44809.7	36220.1	42746.5	0.102	65.5477	1.184
4380	3920.3	45320.6	36652.2	45340.8	0.097	65.6647	1.184
4420	3960.3	45832.4	37084.5	48086.0	0.092	65.7815	1.183
4460	4000.3	46346.1	37518.8	50963.2	0.088	65.8969	1.183
4500	4040.3	46860.5	37953.7	53994.9	0.083	66.0116	1.183
4540	4080.3	47375.0	38388.8	57190.8	0.079	66.1258	1.182
4580	4120.3	47891.9	38826.2	60542.9	0.076	66.2389	1.182
4620	4160.3	48409.0	39263.8	64063.8	0.072	66.3512	1.181
4660	4200.3	48927.8	39702.5	67771.4	0.069	66.4629	1.181
4700	4240.3	49445.7	40141.6	71653.6	0.066	66.5735	1.181
4740	4280.3	49964.5	40581.7	75740.5	0.063	66.6837	1.180
4780	4320.3	50485.9	41023.0	80033.8	0.060	66.7932	1.180
4820	4360.3	51006.9	41465.2	84536.6	0.057	66.9019	1.180
4860	4400.3	51527.9	41907.5	89240.3	0.054	67.0094	1.179
4900	4440.3	52051.3	42350.8	94201.3	0.052	67.1168	1.179
4940	4480.3	52575.6	42794.9	99387.8	0.050	67.2233	1.179
4980	4520.3	53100.7	43241.2	104828	0.048	67.3291	1.178
5020	4560.3	53625.6	43687.4	110520	0.045	67.4341	1.178
5060	4600.3	54151.9	44133.5	116483	0.043	67.5385	1.178
5100	4640.3	54679.0	44581.9	122741	0.042	67.6424	1.177
5140	4680.3	55207.7	45030.4	129266	0.040	67.7452	1.177
5180	4720.3	55735.8	45478.4	136123	0.038	67.8479	1.177
5220	4760.3	56263.8	45927.6	143271	0.036	67.9495	1.176
5260	4800.3	56795.0	46378.6	150767	0.035	68.0508	1.176
5300	4840.3	57325.7	46830.5	158623	0.033	68.1516	1.176
5340	4880.3	57857.0	47281.7	166780	0.032	68.2512	1.176
5380	4920.3	58388.1	47734.1	175311	0.031	68.3503	1.175
5420	4960.3	58921.9	48189.1	184290	0.029	68.4495	1.175
5460	5000.3	59454.2	48641.3	193579	0.028	68.5471	1.175
5500	5040.3	59989.7	49098.0	203309	0.027	68.6445	1.175
5540	5080.3	60523.7	49551.9	213526	0.026	68.7419	1.174
5580	5120.3	61059.2	50008.6	224116	0.025	68.8380	1.174
5620	5160.3	61597.8	50465.0	235132	0.024	68.9333	1.174
5660	5200.3	62135.0	50924.1	246738	0.023	69.0290	1.173
5700	5240.3	62670.5	51380.8	258763	0.022	69.1235	1.173
5740	5280.3	63210.0	51838.8	271347	0.021	69.2178	1.173
5780	5320.3	63746.5	52299.4	284416	0.020	69.3112	1.173

## B.5 CO<sub>2</sub> Properties (SI Units)

Temperature		<i>h</i>	<i>u</i>	<i>Pr</i>	<i>Vr</i>	<i>s<sub>o</sub></i>	Gamma
K	C	kJ/kgmol	kJ/kgmol			kJ/kgmol/K	
200	-73.1	4898.9	3513.4	0.28	1292.15	194.0903	1.345
225	-48.1	5723.6	4168.1	0.44	506.17	197.9744	1.329
250	-23.1	6579.3	4847.3	0.69	364.53	201.5795	1.313
275	1.9	7465.7	5552.2	1.03	267.07	204.9580	1.300
300	26.9	8382.0	6283.1	1.51	198.55	208.1462	1.288
325	51.9	9326.8	7039.4	2.17	149.50	211.1705	1.277
350	76.9	10298.7	7820.2	3.07	113.86	214.0510	1.267
375	101.9	11296.2	8624.6	4.28	87.607	216.8035	1.259
400	126.9	12318.0	9451.5	5.88	68.045	219.4409	1.252
425	151.9	13362.7	10299.9	7.97	53.308	221.9741	1.245
450	176.9	14429.0	11168.8	10.69	42.099	224.4118	1.239
475	201.9	15516.0	12057.2	14.18	33.493	226.7625	1.234
500	226.9	16622.5	12964.2	18.63	26.832	229.0325	1.229
525	251.9	17747.4	13889.0	24.27	21.635	231.2279	1.224
550	276.9	18890.0	14830.6	31.34	17.551	233.3538	1.220
575	301.9	20049.4	15788.5	40.15	14.320	235.4150	1.217
600	326.9	21224.9	16762.0	51.08	11.746	237.4160	1.213
625	351.9	22415.5	17750.2	64.54	9.684	239.3600	1.210
650	376.9	23620.8	18752.7	81.02	8.023	241.2508	1.207
675	401.9	24840.1	19768.7	101.10	6.677	243.0914	1.204
700	426.9	26072.5	20797.6	125.43	5.581	244.8847	1.202
725	451.9	27317.8	21839.1	154.78	4.684	246.6325	1.199
750	476.9	28575.4	22892.7	190.02	3.947	248.3377	1.197
775	501.9	29844.5	23957.4	232.14	3.339	250.0022	1.195
800	526.8	31124.9	25033.3	282.27	2.834	251.6279	1.193
825	551.8	32415.8	26119.5	341.74	2.414	253.2172	1.191
850	576.8	33717.0	27215.8	411.95	2.063	254.7706	1.189
875	601.8	35027.9	28321.6	494.59	1.769	256.2906	1.188
900	626.8	36348.2	29436.6	591.50	1.522	257.7783	1.186
925	651.8	37677.6	30560.6	704.80	1.312	259.2352	1.185
950	676.8	39015.2	31692.8	836.76	1.135	260.6620	1.183
975	701.8	40361.3	32833.2	990.10	0.985	262.0610	1.182
1000	726.8	41715.3	33981.6	1167.6	0.856	263.4322	1.181
1025	751.8	43076.4	35137.1	1372.6	0.747	264.7767	1.180
1050	776.8	44445.2	36299.4	1608.6	0.653	266.0959	1.179
1075	801.8	45820.7	37468.8	1879.7	0.572	267.3905	1.178
1100	826.8	47202.7	38644.7	2190.0	0.502	268.6610	1.177
1125	851.8	48591.4	39827.4	2544.8	0.442	269.9092	1.176
1150	876.8	49985.1	41015.0	2949.0	0.390	271.1346	1.175
1175	901.8	51385.5	42209.0	3408.9	0.345	272.3395	1.174
1200	926.8	52791.4	43408.4	3930.4	0.305	273.5230	1.173
1225	951.8	54201.5	44612.9	4521.0	0.271	274.6868	1.172
1250	976.8	55618.1	45822.6	5188.2	0.241	275.8313	1.172
1275	1001.8	57039.4	47037.0	5940.2	0.215	276.9566	1.171
1300	1026.8	58464.9	48255.7	6786.6	0.192	278.0639	1.170
1325	1051.8	59895.8	49479.7	7737.8	0.171	279.1545	1.170
1350	1076.8	61329.7	50707.6	8803.1	0.153	280.2268	1.169
1375	1101.8	62768.5	51939.5	9994.9	0.138	281.2824	1.169
1400	1126.8	64211.8	53175.9	11326.2	0.124	282.3220	1.168
1425	1151.8	65658.4	54415.7	12812.8	0.111	283.3473	1.168
1450	1176.8	67108.3	55658.6	14466.2	0.100	284.3563	1.167
1475	1201.8	68563.2	56906.7	16304.6	0.090	285.3509	1.167
1500	1226.8	70020.9	58157.6	18344.6	0.082	286.3310	1.166
1525	1251.8	71481.7	59410.6	20600.9	0.074	287.2954	1.166
1550	1276.8	72945.4	60668.3	23101.9	0.067	288.2480	1.165
1575	1301.8	74412.2	61927.4	25868.1	0.061	289.1882	1.165
1600	1326.8	75883.0	63192.1	28916.1	0.055	290.1142	1.164
1625	1351.8	77355.4	64456.8	32270.5	0.050	291.0267	1.164
1650	1376.8	78831.3	65726.7	35969.4	0.046	291.9289	1.164
1675	1401.8	80312.5	67000.2	40024.4	0.042	292.8169	1.163

1700	1426.8	81791.3	68272.9	44496.2	0.038	293.6975	1.163
1725	1451.8	83278.7	69551.0	49369.3	0.035	294.5615	1.163
1750	1476.8	84762.2	70828.5	54730.5	0.032	295.4185	1.162
1775	1501.8	86252.2	72110.8	60579.4	0.029	296.2627	1.162
1800	1526.8	87742.6	73395.1	66965.8	0.027	297.0959	1.162
1825	1551.8	89235.2	74680.0	73954.8	0.025	297.9212	1.162
1850	1576.8	90731.9	75972.3	81574.9	0.023	298.7365	1.161
1875	1601.8	92231.5	77262.6	89849.9	0.021	299.5398	1.161
1900	1626.8	93730.0	78555.0	98864.0	0.019	300.3346	1.161
1925	1651.8	95230.1	79845.8	108640.8	0.018	301.1186	1.160
1950	1676.8	96736.7	81146.4	119300.4	0.016	301.8968	1.160
1975	1701.8	98244.5	82444.8	130839.1	0.015	302.6643	1.160
2000	1726.8	99751.9	83746.2	143305.3	0.014	303.4209	1.160
2025	1751.8	101259.1	85044.1	156882.2	0.013	304.1735	1.160
2050	1776.8	102767.9	86346.8	171483.8	0.012	304.9133	1.159
2075	1801.8	104283.4	87653.0	187278.1	0.011	305.6458	1.159
2100	1826.8	105797.3	88960.8	204390.5	0.010	306.3727	1.159
2125	1851.8	107314.4	90271.8	222790.0	0.010	307.0894	1.159
2150	1876.8	108833.1	91581.2	242630.1	0.009	307.7986	1.159
2175	1901.8	110353.8	92895.8	264062.5	0.008	308.5023	1.158
2200	1926.8	111871.4	94204.1	287095.1	0.008	309.1976	1.158
2225	1951.8	113391.6	95521.6	311872.0	0.007	309.8858	1.158
2250	1976.8	114915.7	96836.3	338455.4	0.007	310.5658	1.158
2275	2001.8	116442.1	98153.4	367187.4	0.006	311.2432	1.158
2300	2026.8	117966.3	99471.5	397703.9	0.006	311.9070	1.158
2325	2051.9	119491.0	100793.5	430530.6	0.005	312.5663	1.157
2350	2076.9	121023.1	102109.7	465834.2	0.005	313.2215	1.157
2375	2101.9	122555.9	103439.7	503490.9	0.005	313.8678	1.157
2400	2126.9	124083.5	104758.0	544061.8	0.004	314.5121	1.157
2425	2151.9	125613.1	106078.3	587250.6	0.004	315.1472	1.157
2450	2176.9	127156.1	107418.5	633421.1	0.004	315.7764	1.157
2475	2201.9	128681.3	108734.4	682687.7	0.004	316.3991	1.157
2500	2226.9	130225.1	110068.8	735216.5	0.003	317.0154	1.156
2525	2251.9	131764.7	111399.1	791136.3	0.003	317.6248	1.156
2550	2276.9	133298.1	112723.1	851306.1	0.003	318.2342	1.156
2575	2301.9	134830.4	114052.7	914842.4	0.003	318.8326	1.156
2600	2326.9	136372.1	115385.0	982925.9	0.003	319.4294	1.156
2625	2351.9	137910.9	116721.1	1054793.8	0.002	320.0161	1.156
2650	2376.9	139455.6	118056.4	1132149.1	0.002	320.6044	1.156
2675	2401.9	140996.3	119387.8	1213719.6	0.002	321.1828	1.156
2700	2426.9	142542.7	120731.5	1299797.3	0.002	321.7525	1.155
2725	2451.9	144091.2	122070.6	1393380.3	0.002	322.3305	1.155
2750	2476.9	145633.1	123403.2	1491186.5	0.002	322.8945	1.155
2775	2501.9	147180.6	124741.3	1594517.1	0.002	323.4515	1.155
2800	2526.9	148735.4	126086.8	1705346.0	0.002	324.0101	1.155
2825	2551.9	150272.8	127428.0	1821001.6	0.002	324.5557	1.155
2850	2576.9	151831.0	128776.9	1945136.3	0.001	325.1039	1.155
2875	2601.9	153381.2	130104.7	2077527.0	0.001	325.6513	1.155
2900	2626.9	154935.0	131462.2	2215282.5	0.001	326.1851	1.155
2925	2651.9	156479.4	132797.3	2363265.3	0.001	326.7227	1.155
2950	2676.9	158032.4	134141.0	2516307.0	0.001	327.2444	1.154
2975	2701.9	159594.8	135494.0	2681335.5	0.001	327.7725	1.154
3000	2726.9	161139.8	136842.8	2854293.8	0.001	328.2921	1.154
3025	2751.9	162703.6	138197.3	3035087.0	0.001	328.8027	1.154
3050	2776.9	164262.6	139533.9	3231907.8	0.001	329.3251	1.154
3075	2801.9	165809.9	140884.9	3433278.0	0.001	329.8276	1.154
3100	2826.9	167368.2	142233.9	3647235.0	0.001	330.3302	1.154
3125	2851.9	168937.7	143594.1	3874568.3	0.001	330.8329	1.154
3150	2876.9	170504.6	144951.7	4115300.8	0.001	331.3340	1.154
3175	2901.9	172053.7	146304.5	4366548.0	0.001	331.8267	1.154
3200	2926.9	173619.6	147648.0	4633662.0	0.001	332.3203	1.154

## B.6 CO<sub>2</sub> Properties (English Units)

Temperature R F	h Btu/lbmol	u Btu/lbmol	Pr	Vr	S <sub>o</sub> Btu/lbmol/R	Gamma
300 -159.7	2106.3	1510.6	0.139	2152.4	46.3610	1.369
340 -119.7	2405.9	1749.9	0.223	1521.8	47.2980	1.353
380 -79.7	2715.2	1995.7	0.345	1103.0	48.1580	1.338
420 -39.7	3035.0	2249.4	0.515	814.94	48.9579	1.323
460 0.3	3365.3	2511.7	0.752	611.48	49.7090	1.310
500 40.3	3706.0	2782.8	1.076	464.84	50.4190	1.298
540 80.3	4056.8	3062.7	1.511	357.39	51.0939	1.288
580 120.3	4417.3	3351.2	2.090	277.56	51.7378	1.278
620 160.3	4787.1	3648.1	2.850	217.53	52.3541	1.269
660 200.3	5165.6	3953.0	3.839	171.90	52.9458	1.262
700 240.3	5552.6	4265.8	5.114	136.89	53.5150	1.255
740 280.3	5947.6	4586.0	6.741	109.78	54.0636	1.249
780 320.3	6350.1	4913.3	8.802	88.62	54.5933	1.243
820 360.3	6759.9	5247.5	11.392	71.98	55.1057	1.238
860 400.3	7176.6	5588.2	14.626	58.80	55.6018	1.233
900 440.3	7599.8	5935.3	18.635	48.30	56.0828	1.229
940 480.3	8029.4	6288.3	23.574	39.87	56.5498	1.225
980 520.3	8465.0	6647.1	29.626	33.08	57.0036	1.221
1020 560.3	8906.3	7011.6	37.001	27.57	57.4450	1.218
1060 600.3	9353.2	7381.3	45.939	23.07	57.8746	1.215
1100 640.3	9805.3	7756.2	56.722	19.39	58.2933	1.212
1140 680.3	10262.6	8136.0	69.673	16.36	58.7017	1.209
1180 720.3	10724.8	8520.6	85.149	13.86	59.1001	1.206
1220 760.3	11191.6	8909.7	103.578	11.78	59.4891	1.204
1260 800.3	11662.9	9303.3	125.433	10.05	59.8693	1.202
1300 840.3	12138.6	9701.1	151.242	8.596	60.2409	1.199
1340 880.3	12618.4	10102.9	181.629	7.378	60.6045	1.197
1380 920.3	13102.2	10508.7	217.266	6.352	60.9602	1.195
1420 960.3	13589.9	10918.2	258.923	5.484	61.3086	1.194
1460 1000.3	14081.3	11331.3	307.466	4.748	61.6498	1.192
1500 1040.3	14576.3	11748.0	363.861	4.122	61.9842	1.190
1540 1080.3	15074.6	12168.0	429.178	3.588	62.3121	1.189
1580 1120.3	15576.2	12591.3	504.618	3.131	62.6336	1.187
1620 1160.3	16080.9	13017.6	591.502	2.739	62.9491	1.186
1660 1200.3	16588.8	13447.0	691.365	2.401	63.2589	1.185
1700 1240.3	17099.6	13879.2	805.734	2.110	63.5629	1.184
1740 1280.3	17613.1	14314.1	936.428	1.858	63.8614	1.182
1780 1320.3	18129.4	14751.8	1085.49	1.640	64.1548	1.181
1820 1360.3	18648.2	15192.0	1255.08	1.450	64.4430	1.180
1860 1400.3	19169.6	15634.8	1447.55	1.285	64.7264	1.179
1900 1440.3	19693.5	16079.8	1665.6	1.141	65.0049	1.178
1940 1480.3	20219.4	16527.1	1912.1	1.015	65.2791	1.177
1980 1520.3	20747.9	16976.7	2190.0	0.904	65.5486	1.177
2020 1560.3	21278.2	17428.2	2503.0	0.807	65.8138	1.176
2060 1600.3	21810.7	17882.0	2854.7	0.722	66.0749	1.175
2100 1640.3	22345.2	18337.8	3248.9	0.646	66.3318	1.174
2140 1680.3	22881.5	18795.1	3690.6	0.58	66.5849	1.173
2180 1720.3	23420.2	19254.7	4183.8	0.521	66.8340	1.173
2220 1760.3	23959.9	19715.7	4734.5	0.469	67.0796	1.172
2260 1800.3	24501.8	20178.5	5347.8	0.423	67.3215	1.172
2300 1840.3	25045.1	20643.0	6029.7	0.381	67.5598	1.171
2340 1880.3	25590.1	21108.9	6786.6	0.345	67.7946	1.170
2380 1920.3	26136.7	21576.7	7626.4	0.312	68.0263	1.170
2420 1960.3	26684.6	22045.6	8555.0	0.283	68.2545	1.169
2460 2000.3	27234.1	22515.9	9583.4	0.257	68.4799	1.169
2500 2040.3	27785.2	22988.0	10716.0	0.233	68.7017	1.168
2540 2080.3	28337.1	23461.1	11966.3	0.212	68.9209	1.168
2580 2120.3	28890.4	23935.0	13342.3	0.193	69.1370	1.167
2620 2160.3	29445.2	24411.0	14855.7	0.176	69.3504	1.167
2660 2200.3	30001.2	24887.9	16518.6	0.161	69.5611	1.166
2700 2240.3	30558.6	25366.2	18344.6	0.147	69.7693	1.166
2740 2280.3	31116.4	25845.2	20339.8	0.135	69.9743	1.166
2780 2320.3	31676.4	26325.8	22525.3	0.123	70.1770	1.165
2820 2360.3	32236.2	26806.9	24913.5	0.113	70.3771	1.165
2860 2400.3	32797.9	27289.1	27520.3	0.104	70.5747	1.165
2900 2440.3	33360.1	27772.5	30363.9	0.096	70.7700	1.164
2940 2480.3	33923.7	28256.7	33463.0	0.088	70.9630	1.164
2980 2520.3	34488.2	28742.4	36840.5	0.081	71.1540	1.164

3020	2560.3	35053.5	29228.3	40502.2	0.075	71.3421	1.163
3060	2600.3	35619.3	29715.4	44496.3	0.069	71.5289	1.163
3100	2640.3	36186.2	30202.8	48807.2	0.064	71.7125	1.163
3140	2680.3	36754.6	30691.8	53499.3	0.059	71.8948	1.162
3180	2720.3	37323.8	31182.2	58565.9	0.054	72.0745	1.162
3220	2760.3	37894.3	31673.2	64062.9	0.05	72.2526	1.162
3260	2800.3	38464.2	32163.7	70006.4	0.047	72.4288	1.162
3300	2840.3	39035.2	32655.3	76418.2	0.043	72.6029	1.161
3340	2880.3	39606.3	33147.6	83339.1	0.04	72.7750	1.161
3380	2920.3	40180.1	33642.6	90818.4	0.037	72.9457	1.161
3420	2960.3	40752.4	34136.2	98864.0	0.035	73.1143	1.161
3460	3000.3	41326.5	34630.1	107520.6	0.032	73.2809	1.161
3500	3040.3	41900.9	35125.8	116863.0	0.030	73.4464	1.160
3540	3080.3	42476.5	35622.6	126858.2	0.028	73.6094	1.160
3580	3120.3	43051.5	36117.4	137653.7	0.026	73.7716	1.160
3620	3160.3	43629.7	36616.9	149204.5	0.024	73.9316	1.160
3660	3200.3	44205.8	37112.8	161585.4	0.023	74.0899	1.160
3700	3240.3	44783.2	37611.5	174927.8	0.021	74.2474	1.159
3740	3280.3	45361.9	38111.4	189169.0	0.020	74.4029	1.159
3780	3320.3	45940.8	38610.2	204391.3	0.018	74.5565	1.159
3820	3360.3	46519.2	39109.8	220690.0	0.017	74.7089	1.159
3860	3400.3	47100.7	39611.2	238098.2	0.016	74.8597	1.159
3900	3440.3	47680.2	40112.0	256730.5	0.015	75.0093	1.158
3940	3480.3	48261.0	40614.0	276623.2	0.014	75.1575	1.158
3980	3520.3	48843.2	41117.5	297891.2	0.013	75.3046	1.158
4020	3560.3	49423.9	41617.9	320487.7	0.013	75.4498	1.158
4060	3600.3	50007.8	42123.1	344603.6	0.012	75.5939	1.158
4100	3640.3	50588.8	42624.0	370381.8	0.011	75.7371	1.158
4140	3680.3	51172.8	43129.3	397704.7	0.010	75.8785	1.158
4180	3720.3	51756.2	43633.9	426811.9	0.010	76.0187	1.157
4220	3760.3	52341.1	44140.0	457729.2	0.009	76.1576	1.157
4260	3800.3	52925.3	44642.7	490688.2	0.009	76.2957	1.157
4300	3840.3	53509.1	45150.5	525804.1	0.008	76.4329	1.157
4340	3880.3	54095.4	45655.2	562836.0	0.008	76.5681	1.157
4380	3920.3	54680.1	46161.2	602004.0	0.007	76.7017	1.157
4420	3960.3	55268.8	46668.4	644330.8	0.007	76.8366	1.157
4460	4000.3	55853.4	47174.2	688207.0	0.006	76.9675	1.157
4500	4040.3	56443.5	47685.6	735215.0	0.006	77.0987	1.156
4540	4080.3	57030.7	48194.0	785035.6	0.006	77.2289	1.156
4580	4120.3	57616.4	48700.9	837485.5	0.005	77.3573	1.156
4620	4160.3	58205.2	49208.2	893302.4	0.005	77.4854	1.156
4660	4200.3	58793.7	49717.9	952144.0	0.005	77.6121	1.156
4700	4240.3	59383.1	50228.6	1014058.7	0.005	77.7372	1.156
4740	4280.3	59971.4	50738.1	1080090.8	0.004	77.8625	1.156
4780	4320.3	60560.5	51248.5	1149724.5	0.004	77.9866	1.156
4820	4360.3	61147.8	51757.1	1223372.8	0.004	78.1099	1.156
4860	4400.3	61739.5	52270.0	1299799.6	0.004	78.2302	1.155
4900	4440.3	62331.9	52783.6	1382923.1	0.004	78.3533	1.155
4940	4480.3	62921.9	53292.1	1468143.8	0.003	78.4720	1.155
4980	4520.3	63513.1	53807.4	1559496.6	0.003	78.5919	1.155
5020	4560.3	64102.9	54312.8	1655452.1	0.003	78.7105	1.155
5060	4600.3	64698.0	54829.1	1755773.1	0.003	78.8273	1.155
5100	4640.3	65286.3	55338.7	1862446	0.003	78.9445	1.155
5140	4680.3	65878.2	55851.9	1973642	0.003	79.0596	1.155
5180	4720.3	66474.8	56369.7	2091677	0.002	79.1750	1.155
5220	4760.3	67067.6	56883.7	2215282	0.002	79.2890	1.155
5260	4800.3	67664.1	57401.5	2345174	0.002	79.4021	1.154
5300	4840.3	68253.5	57912.1	2480459	0.002	79.5135	1.154
5340	4880.3	68847.6	58427.5	2625082	0.002	79.6260	1.154
5380	4920.3	69441.6	58937.1	2776344	0.002	79.7373	1.154
5420	4960.3	70032.3	59449.0	2934292	0.002	79.8472	1.154
5460	5000.3	70626.9	59964.9	3101107	0.002	79.9570	1.154
5500	5040.3	71225.6	60490.4	3274133	0.002	80.0648	1.154
5540	5080.3	71821.0	61001.5	3457955	0.002	80.1733	1.154
5580	5120.3	72413.3	61515.0	3647232	0.002	80.2791	1.154
5620	5160.3	73007.7	62030.7	3851144	0.001	80.3871	1.154
5660	5200.3	73615.6	62554.3	4063894	0.001	80.4939	1.154
5700	5240.3	74205.5	63071.0	4279592	0.001	80.5966	1.154
5740	5280.3	74808.4	63589.5	4513548	0.001	80.7023	1.154
5780	5320.3	75401.4	64103.8	4753843	0.001	80.8053	1.153

## B.7 Nitrogen Properties (SI Units)

Temperature K	h kJ/kgmol	u kJ/kgmol	Pr	Vr	S <sub>o</sub> kJ/kgmol/K	Gamma
200	-73.1	4842.2	3456.7	0.34	1072.9	174.5226
225	-48.1	5570.4	3981.6	0.51	443.82	177.9535
250	-23.1	6298.6	4505.5	0.73	340.92	181.0223
275	1.9	7026.5	5028.6	1.02	268.58	183.7977
300	26.9	7754.4	5551.2	1.39	216.03	186.3310
325	51.9	8482.4	6073.4	1.84	176.82	188.6617
350	76.9	9210.7	6595.7	2.38	146.87	190.8208
375	101.9	9939.8	7118.5	3.04	123.53	192.8329
400	126.9	10670.1	7642.3	3.81	105.04	194.7179
425	151.9	11401.8	8167.4	4.71	90.150	196.4925
450	176.9	12135.5	8694.3	5.77	78.014	198.1698
475	201.9	12871.4	9223.4	6.99	68.000	199.7613
500	226.9	13609.9	9754.9	8.38	59.654	201.2764
525	251.9	14351.2	10289.2	9.97	52.632	202.7233
550	276.9	15095.7	10826.5	11.78	46.675	204.1086
575	301.9	15843.5	11367.2	13.83	41.584	205.4382
600	326.9	16594.9	11911.4	16.13	37.204	206.7174
625	351.9	17350.1	12459.2	18.71	33.413	207.9503
650	376.9	18109.0	13010.8	21.59	30.112	209.1411
675	401.9	18872.0	13566.4	24.79	27.225	210.2928
700	426.9	19639.0	14126.0	28.35	24.688	211.4086
725	451.9	20410.0	14689.6	32.30	22.448	212.4909
750	476.9	21185.3	15257.4	36.65	20.464	213.5421
775	501.9	21964.7	15829.3	41.44	18.700	214.5643
800	526.8	22748.2	16405.3	46.71	17.125	215.5594
825	551.8	23535.9	16985.5	52.49	15.717	216.5289
850	576.8	24327.7	17569.7	58.81	14.452	217.4743
875	601.8	25123.5	18158.0	65.72	13.314	218.3971
900	626.8	25923.4	18750.3	73.24	12.288	219.2984
925	651.8	26727.3	19346.6	81.43	11.359	220.1794
950	676.8	27534.9	19946.6	90.32	10.518	221.0410
975	701.8	28346.4	20550.5	99.96	9.754	221.8840
1000	726.8	29161.6	21158.1	110.40	9.058	222.7097
1025	751.8	29980.4	21769.3	121.68	8.424	223.5184
1050	776.8	30802.9	22384.0	133.85	7.844	224.3111
1075	801.8	31628.7	23002.2	146.97	7.314	225.0885
1100	826.8	32458.0	23623.8	161.09	6.828	225.8510
1125	851.8	33290.4	24248.6	176.26	6.383	226.5993
1150	876.8	34126.0	24876.5	192.54	5.973	227.3338
1175	901.8	34964.7	25507.5	210.00	5.595	228.0554
1200	926.8	35806.4	26141.4	228.69	5.247	228.7641
1225	951.8	36650.9	26778.3	248.67	4.926	229.4606
1250	976.8	37498.2	27417.9	270.02	4.629	230.1453
1275	1002	38348.2	28060.2	292.80	4.355	230.8186
1300	1027	39200.7	28704.9	317.08	4.100	231.4809
1325	1052	40055.8	29352.3	342.93	3.864	232.1324
1350	1077	40913.3	30002.1	370.42	3.645	232.7735
1375	1102	41773.1	30654.2	399.63	3.441	233.4045
1400	1127	42635.2	31308.5	430.64	3.251	234.0258
1425	1152	43499.3	31964.9	463.53	3.074	234.6377
1450	1177	44365.7	32623.6	498.38	2.909	235.2404
1475	1202	45234.0	33284.2	535.27	2.756	235.8341
1500	1227	46104.4	33946.7	574.30	2.612	236.4192
1525	1252	46976.4	34611.0	615.54	2.477	236.9958
1550	1277	47850.4	35277.3	659.11	2.352	237.5643
1575	1302	48726.0	35945.2	705.07	2.234	238.1247
1600	1327	49603.5	36614.8	753.54	2.123	238.6775
1625	1352	50482.5	37285.9	804.59	2.020	239.2224
1650	1377	51363.2	37958.9	858.34	1.922	239.7601
1675	1402	52245.1	38633.2	914.92	1.831	240.2907
1700	1427	53128.6	39308.8	974.39	1.745	240.8144
1725	1452	54013.4	39985.9	1036.90	1.664	241.3313
1750	1477	54899.8	40664.5	1102.50	1.587	241.8413
1775	1502	55787.6	41344.7	1171.36	1.515	242.3450
1800	1527	56676.6	42025.8	1243.57	1.447	242.8423

1825	1552	57566.8	42708.1	1319.26	1.383	243.3335	1.304
1850	1577	58458.1	43391.7	1398.50	1.323	243.8184	1.304
1875	1602	59350.7	44076.7	1481.52	1.266	244.2979	1.303
1900	1627	60244.3	44762.3	1568.34	1.211	244.7713	1.303
1925	1652	61139.2	45449.6	1659.15	1.160	245.2393	1.302
1950	1677	62035.0	46137.7	1754.00	1.112	245.7015	1.302
1975	1702	62932.4	46827.0	1853.15	1.066	246.1586	1.301
2000	1727	63830.5	47517.4	1956.68	1.022	246.6106	1.301
2025	1752	64729.4	48208.6	2064.67	0.981	247.0572	1.300
2050	1777	65629.4	48900.8	2177.38	0.942	247.4991	1.300
2075	1802	66530.4	49593.8	2294.82	0.904	247.9358	1.300
2100	1827	67432.2	50287.9	2417.25	0.869	248.3679	1.299
2125	1852	68335.2	50983.2	2544.70	0.835	248.7951	1.299
2150	1877	69238.7	51679.0	2677.57	0.803	249.2182	1.298
2175	1902	70143.8	52376.0	2815.68	0.772	249.6364	1.298
2200	1927	71049.1	53073.7	2959.36	0.743	250.0501	1.298
2225	1952	71955.4	53772.2	3108.89	0.716	250.4599	1.297
2250	1977	72862.1	54471.2	3264.18	0.689	250.8652	1.297
2275	2002	73770.2	55171.6	3425.64	0.664	251.2666	1.297
2300	2027	74679.0	55872.4	3593.33	0.640	251.6639	1.296
2325	2052	75588.3	56574.0	3767.45	0.617	252.0573	1.296
2350	2077	76498.6	57276.6	3948.23	0.595	252.4469	1.296
2375	2102	77409.8	57979.6	4135.53	0.574	252.8322	1.295
2400	2127	78321.5	58683.6	4329.93	0.554	253.2141	1.295
2425	2152	79233.6	59388.1	4531.69	0.535	253.5928	1.295
2450	2177	80147.2	60093.6	4740.30	0.517	253.9669	1.295
2475	2202	81061.3	60799.6	4956.64	0.499	254.3380	1.294
2500	2227	81974.9	61506.3	5180.90	0.483	254.7058	1.294
2525	2252	82889.7	62213.5	5412.57	0.467	255.0695	1.294
2550	2277	83806.5	62921.7	5653.13	0.451	255.4310	1.293
2575	2302	84722.2	63629.7	5901.50	0.436	255.7885	1.293
2600	2327	85639.7	64339.5	6158.56	0.422	256.1430	1.293
2625	2352	86557.4	65048.8	6424.15	0.409	256.4940	1.293
2650	2377	87474.6	65759.0	6698.76	0.396	256.8420	1.292
2675	2402	88394.1	66470.0	6982.77	0.383	257.1872	1.292
2700	2427	89313.6	67181.9	7276.13	0.371	257.5293	1.292
2725	2452	90232.9	67893.5	7579.28	0.360	257.8687	1.292
2750	2477	91153.4	68606.3	7891.81	0.348	258.2046	1.292
2775	2502	92074.3	69318.7	8214.82	0.338	258.5381	1.291
2800	2527	92995.6	70033.0	8547.82	0.328	258.8685	1.291
2825	2552	93917.5	70746.5	8891.44	0.318	259.1961	1.291
2850	2577	94840.0	71461.3	9246.23	0.308	259.5214	1.291
2875	2602	95762.3	72176.7	9612.03	0.299	259.8440	1.291
2900	2627	96685.2	72891.1	9988.31	0.290	260.1632	1.290
2925	2652	97609.5	73607.7	10376.35	0.282	260.4801	1.290
2950	2677	98533.2	74323.8	10777.49	0.274	260.7954	1.290
2975	2702	99457.2	75039.2	11188.71	0.266	261.1068	1.290
3000	2727	100382.7	75757.0	11613.83	0.258	261.4168	1.290
3025	2752	101307.1	76473.7	12049.96	0.251	261.7233	1.290
3050	2777	102233.1	77192.0	12500.42	0.244	262.0284	1.290
3075	2802	103158.5	77909.7	12963.57	0.237	262.3308	1.289
3100	2827	104084.9	78628.4	13439.74	0.231	262.6307	1.289
3125	2852	105011.0	79346.8	13930.07	0.224	262.9286	1.289
3150	2877	105937.8	80065.2	14434.00	0.218	263.2241	1.289
3175	2902	106865.5	80786.8	14951.77	0.212	263.5171	1.289
3200	2927	107793.2	81505.2	15484.30	0.207	263.8080	1.289
3225	2952	108720.8	82225.1	16030.68	0.201	264.0963	1.289
3250	2977	109649.0	82945.6	16593.23	0.196	264.3831	1.289
3275	3002	110577.2	83666.1	17171.93	0.191	264.6681	1.288
3300	3027	111504.7	84386.0	17764.55	0.186	264.9502	1.288
3325	3052	112434.6	85108.1	18374.79	0.181	265.2310	1.288
3350	3077	113363.7	85829.6	18999.02	0.176	265.5087	1.288
3375	3102	114292.6	86550.8	19643.30	0.172	265.7859	1.288
3400	3127	115224.0	87272.8	20301.83	0.167	266.0601	1.288
3425	3152	116154.8	87995.9	20979.58	0.163	266.3331	1.288
3450	3177	117084.1	88719.2	21673.51	0.159	266.6036	1.287
3475	3202	118014.7	89442.1	22386.46	0.155	266.8727	1.287
3500	3227	118947.9	90166.0	23118.61	0.151	267.1403	1.287
3525	3252	119880.8	90891.2	23867.95	0.148	267.4055	1.287
3550	3277	120813.0	91615.7	24637.25	0.144	267.6692	1.287

## B.8 Nitrogen Properties (English Units)

Temperature		<i>h</i>	<i>u</i>	<i>Pr</i>	<i>Vr</i>	<i>s<sub>o</sub></i>	Gamma
R	F	Btu/lbmol	Btu/lbmol			Btu/lbmol/R	
300	-159.7	2081.9	1486.2	0.177	1692.8	41.6870	1.400
340	-119.7	2360.0	1687.3	0.275	1237.9	42.5571	1.400
380	-79.7	2638.2	1888.1	0.406	937.06	43.3308	1.399
420	-39.7	2916.5	2088.5	0.576	729.35	44.0272	1.399
460	0.3	3194.8	2288.7	0.792	580.81	44.6601	1.400
500	40.3	3473.0	2488.5	1.061	471.43	45.2400	1.400
540	80.3	3751.2	2688.2	1.389	388.86	45.7752	1.400
580	120.3	4029.4	2887.8	1.784	325.19	46.2722	1.400
620	160.3	4307.7	3087.4	2.253	275.18	46.7363	1.399
660	200.3	4586.3	3287.2	2.805	235.26	47.1717	1.399
700	240.3	4865.2	3487.2	3.449	202.95	47.5819	1.398
740	280.3	5144.5	3687.6	4.194	176.46	47.9700	1.397
780	320.3	5424.5	3888.5	5.048	154.50	48.3384	1.396
820	360.3	5705.1	4090.1	6.024	136.12	48.6893	1.394
860	400.3	5986.5	4292.4	7.131	120.60	49.0243	1.392
900	440.3	6268.8	4495.6	8.382	107.38	49.3451	1.391
940	480.3	6552.0	4699.8	9.788	96.040	49.6531	1.389
980	520.3	6836.4	4904.9	11.362	86.252	49.9493	1.387
1020	560.3	7121.8	5111.2	13.119	77.752	50.2348	1.384
1060	600.3	7408.4	5318.6	15.072	70.330	50.5104	1.382
1100	640.3	7696.3	5527.3	17.237	63.815	50.7770	1.380
1140	680.3	7985.5	5737.2	19.631	58.073	51.0352	1.378
1180	720.3	8275.9	5948.5	22.269	52.988	51.2856	1.375
1220	760.3	8567.8	6161.0	25.171	48.469	51.5288	1.373
1260	800.3	8861.0	6375.0	28.354	44.438	51.7653	1.370
1300	840.3	9155.6	6590.3	31.839	40.831	51.9955	1.368
1340	880.3	9451.6	6807.1	35.645	37.593	52.2198	1.366
1380	920.3	9749.0	7025.2	39.795	34.677	52.4385	1.363
1420	960.3	10047.9	7244.7	44.312	32.046	52.6520	1.361
1460	1000.3	10348.1	7465.6	49.217	29.664	52.8605	1.359
1500	1040.3	10649.8	7688.0	54.537	27.504	53.0643	1.356
1540	1080.3	10952.8	7911.7	60.297	25.540	53.2637	1.354
1580	1120.3	11257.2	8136.8	66.523	23.751	53.4588	1.352
1620	1160.3	11563.0	8363.2	73.244	22.118	53.6499	1.350
1660	1200.3	11870.1	8591.0	80.487	20.624	53.8372	1.348
1700	1240.3	12178.6	8820.1	88.285	19.256	54.0208	1.346
1740	1280.3	12488.3	9050.5	96.664	18.001	54.2009	1.344
1780	1320.3	12799.3	9282.2	105.660	16.846	54.3776	1.342
1820	1360.3	13111.6	9515.1	115.308	15.784	54.5511	1.340
1860	1400.3	13425.1	9749.2	125.636	14.805	54.7215	1.339
1900	1440.3	13739.7	9984.5	136.685	13.901	54.8889	1.337
1940	1480.3	14055.5	10221.0	148.490	13.065	55.0534	1.335
1980	1520.3	14372.5	10458.6	161.090	12.291	55.2151	1.334
2020	1560.3	14690.6	10697.3	174.521	11.575	55.3741	1.332
2060	1600.3	15009.8	10937.1	188.827	10.909	55.5306	1.331
2100	1640.3	15330.0	11177.9	204.048	10.292	55.6845	1.329
2140	1680.3	15651.2	11419.8	220.229	9.717	55.8361	1.328
2180	1720.3	15973.4	11662.6	237.408	9.183	55.9852	1.327
2220	1760.3	16296.6	11906.4	255.635	8.684	56.1321	1.325
2260	1800.3	16620.7	12151.2	274.959	8.219	56.2768	1.324
2300	1840.3	16945.7	12396.7	295.426	7.785	56.4194	1.323
2340	1880.3	17271.6	12643.3	317.078	7.380	56.5599	1.322

2380	1920.3	17598.4	12890.6	339.970	7.001	56.6983	1.321
2420	1960.3	17925.9	13138.8	364.158	6.645	56.8348	1.320
2460	2000.3	18254.3	13387.8	389.695	6.313	56.9694	1.319
2500	2040.3	18583.4	13637.5	416.625	6.001	57.1021	1.318
2540	2080.3	18913.3	13888.0	445.019	5.708	57.2330	1.317
2580	2120.3	19243.9	14139.2	474.922	5.432	57.3622	1.316
2620	2160.3	19575.2	14391.1	506.397	5.174	57.4896	1.315
2660	2200.3	19907.2	14643.7	539.497	4.931	57.6153	1.314
2700	2240.3	20239.9	14897.0	574.296	4.701	57.7395	1.313
2740	2280.3	20573.1	15150.8	610.851	4.486	57.8620	1.313
2780	2320.3	20907.0	15405.4	649.229	4.282	57.9830	1.312
2820	2360.3	21241.5	15660.4	689.473	4.090	58.1024	1.311
2860	2400.3	21576.5	15916.1	731.685	3.909	58.2204	1.310
2900	2440.3	21912.2	16172.2	775.912	3.738	58.3370	1.310
2940	2480.3	22248.3	16429.0	822.200	3.576	58.4520	1.309
2980	2520.3	22585.0	16686.3	870.690	3.423	58.5658	1.308
3020	2560.3	22922.3	16944.2	921.370	3.278	58.6782	1.308
3060	2600.3	23260.0	17202.4	974.393	3.140	58.7893	1.307
3100	2640.3	23598.0	17461.2	1029.80	3.010	58.8991	1.307
3140	2680.3	23936.7	17720.4	1087.65	2.887	59.0077	1.306
3180	2720.3	24275.9	17980.2	1148.04	2.770	59.1150	1.306
3220	2760.3	24615.5	18240.3	1211.08	2.659	59.2211	1.305
3260	2800.3	24955.4	18500.9	1276.77	2.553	59.3260	1.305
3300	2840.3	25295.9	18761.9	1345.29	2.453	59.4298	1.304
3340	2880.3	25636.7	19023.3	1416.60	2.358	59.5324	1.304
3380	2920.3	25977.8	19285.1	1490.97	2.267	59.6340	1.303
3420	2960.3	26319.4	19547.2	1568.34	2.181	59.7345	1.303
3460	3000.3	26661.4	19809.7	1648.83	2.098	59.8339	1.302
3500	3040.3	27003.8	20072.7	1732.57	2.020	59.9322	1.302
3540	3080.3	27346.5	20336.0	1819.63	1.945	60.0296	1.302
3580	3120.3	27689.5	20599.7	1910.11	1.874	60.1260	1.301
3620	3160.3	28032.8	20863.5	2004.12	1.806	60.2214	1.301
3660	3200.3	28376.6	21127.9	2101.77	1.741	60.3158	1.300
3700	3240.3	28720.7	21392.7	2203.02	1.680	60.4093	1.300
3740	3280.3	29065.2	21657.7	2308.13	1.620	60.5018	1.300
3780	3320.3	29409.8	21922.9	2417.25	1.564	60.5936	1.299
3820	3360.3	29754.8	22188.4	2530.38	1.510	60.6844	1.299
3860	3400.3	30100.3	22454.5	2647.55	1.458	60.7743	1.299
3900	3440.3	30445.8	22720.7	2769.04	1.408	60.8634	1.298
3940	3480.3	30791.8	22987.2	2894.83	1.361	60.9516	1.298
3980	3520.3	31137.9	23253.9	3025.20	1.316	61.0391	1.298
4020	3560.3	31484.6	23521.1	3159.98	1.272	61.1256	1.297
4060	3600.3	31831.1	23788.4	3299.54	1.230	61.2115	1.297
4100	3640.3	32178.1	24055.9	3443.92	1.191	61.2965	1.297
4140	3680.3	32525.6	24324.0	3593.33	1.152	61.3808	1.296
4180	3720.3	32873.0	24591.9	3747.78	1.115	61.4644	1.296
4220	3760.3	33220.9	24860.3	3907.33	1.080	61.5472	1.296
4260	3800.3	33569.1	25129.1	4072.25	1.046	61.6293	1.296
4300	3840.3	33917.3	25398.0	4242.58	1.014	61.7107	1.295
4340	3880.3	34266.0	25667.3	4418.55	0.982	61.7914	1.295
4380	3920.3	34614.7	25936.5	4600.30	0.952	61.8714	1.295

4420	3960.3	34963.6	26206.0	4787.81	0.923	61.9508	1.294
4460	4000.3	35313.2	26476.1	4981.34	0.895	62.0295	1.294
4500	4040.3	35662.5	26746.3	5180.90	0.869	62.1075	1.294
4540	4080.3	36012.3	27016.7	5386.68	0.843	62.1848	1.294
4580	4120.3	36362.4	27287.3	5598.82	0.818	62.2615	1.294
4620	4160.3	36712.3	27557.7	5817.90	0.794	62.3377	1.293
4660	4200.3	37062.9	27828.8	6043.10	0.771	62.4132	1.293
4700	4240.3	37413.4	28099.9	6275.62	0.749	62.4881	1.293
4740	4280.3	37764.0	28371.1	6514.80	0.728	62.5624	1.293
4780	4320.3	38115.1	28642.7	6761.13	0.707	62.6361	1.292
4820	4360.3	38466.5	28914.7	7015.17	0.687	62.7094	1.292
4860	4400.3	38817.8	29186.5	7276.14	0.668	62.7819	1.292
4900	4440.3	39169.1	29458.4	7544.44	0.649	62.8538	1.292
4940	4480.3	39520.6	29730.4	7821.43	0.632	62.9254	1.292
4980	4520.3	39873.0	30003.4	8105.91	0.614	62.9963	1.291
5020	4560.3	40224.8	30275.7	8398.19	0.598	63.0667	1.291
5060	4600.3	40577.1	30548.5	8699.26	0.582	63.1366	1.291
5100	4640.3	40929.5	30821.5	9008.12	0.566	63.2059	1.291
5140	4680.3	41281.6	31094.5	9326.59	0.551	63.2749	1.291
5180	4720.3	41634.7	31368.2	9653.38	0.537	63.3433	1.291
5220	4760.3	41987.2	31641.2	9988.32	0.523	63.4110	1.290
5260	4800.3	42340.2	31914.7	10333.02	0.509	63.4784	1.290
5300	4840.3	42693.8	32188.9	10686.94	0.496	63.5453	1.290
5340	4880.3	43046.5	32462.5	11050.74	0.483	63.6118	1.290
5380	4920.3	43399.9	32736.1	11423.45	0.471	63.6776	1.290
5420	4960.3	43753.4	33010.2	11806.61	0.459	63.7432	1.290
5460	5000.3	44107.0	33284.6	12198.95	0.448	63.8081	1.290
5500	5040.3	44460.7	33558.8	12602.40	0.436	63.8727	1.290
5540	5080.3	44814.5	33832.9	13015.39	0.426	63.9367	1.289
5580	5120.3	45168.7	34108.0	13439.72	0.415	64.0004	1.289
5620	5160.3	45522.8	34382.3	13874.76	0.405	64.0637	1.289
5660	5200.3	45876.8	34657.2	14319.60	0.395	64.1264	1.289
5700	5240.3	46231.2	34931.8	14777.22	0.386	64.1888	1.289
5740	5280.3	46586.3	35207.4	15245.71	0.376	64.2508	1.289
5780	5320.3	46940.0	35482.3	15725.32	0.368	64.3123	1.289
5820	5360.3	47294.6	35757.5	16217.27	0.359	64.3735	1.289
5860	5400.3	47648.8	36032.3	16721.14	0.350	64.4342	1.288
5900	5440.3	48004.0	36308.0	17236.29	0.342	64.4945	1.288
5940	5480.3	48358.9	36583.4	17764.58	0.334	64.5545	1.288
5980	5520.3	48714.6	36859.7	18306.96	0.327	64.6142	1.288
6020	5560.3	49069.8	37135.4	18859.23	0.319	64.6732	1.288
6060	5600.3	49424.7	37410.9	19427.11	0.312	64.7321	1.288
6100	5640.3	49780.2	37687.0	20007.33	0.305	64.7906	1.288
6140	5680.3	50135.4	37962.7	20600.29	0.298	64.8486	1.288
6180	5720.3	50491.1	38238.9	21209.51	0.291	64.9064	1.288
6220	5760.3	50847.7	38516.1	21830.38	0.285	64.9637	1.287
6260	5800.3	51202.9	38791.8	22466.66	0.279	65.0208	1.287
6300	5840.3	51559.1	39068.6	23118.64	0.273	65.0776	1.287
6340	5880.3	51915.2	39345.2	23782.05	0.267	65.1338	1.287
6380	5920.3	52271.8	39622.4	24462.81	0.261	65.1898	1.287

## B.9 Oxygen Properties (SI Units)

Temperature K	Temperature C	h kJ/kgmol	u kJ/kgmol	Pr	Vr	$s_o$ kJ/kgmol/K	Gamma
200	-73.1	4844.7	3459.2	0.330	1074.6	188.0074	1.399
225	-48.1	5573.2	3979.9	0.510	444.49	191.4393	1.399
250	-23.1	6302.3	4501.1	0.730	341.27	194.5121	1.398
275	1.9	7032.8	5023.8	1.020	268.54	197.2970	1.397
300	26.9	7765.6	5548.8	1.390	215.56	199.8474	1.395
325	51.9	8501.6	6077.0	1.850	175.89	202.2038	1.392
350	76.9	9241.6	6609.2	2.410	145.49	204.3974	1.389
375	101.9	9986.3	7146.0	3.080	121.74	206.4524	1.385
400	126.9	10736.2	7688.1	3.890	102.89	208.3882	1.381
425	151.9	11491.8	8235.9	4.850	87.693	210.2205	1.377
450	176.9	12253.4	8789.6	5.980	75.307	211.9616	1.373
475	201.9	13021.2	9349.5	7.300	65.100	213.6220	1.369
500	226.9	13795.1	9915.7	8.830	56.611	215.2100	1.365
525	251.9	14575.5	10488.2	10.610	49.493	216.7328	1.361
550	276.9	15362.2	11067.0	12.650	43.479	218.1965	1.357
575	301.9	16155.0	11652.1	14.990	38.366	219.6063	1.353
600	326.9	16954.0	12243.2	17.650	33.992	220.9665	1.350
625	351.9	17759.0	12840.3	20.670	30.230	222.2808	1.346
650	376.9	18569.7	13443.2	24.090	26.980	223.5526	1.343
675	401.9	19386.0	14051.6	27.940	24.158	224.7849	1.340
700	426.9	20207.7	14665.5	32.260	21.697	225.9803	1.337
725	451.9	21034.5	15284.5	37.100	19.544	227.1409	1.334
750	476.9	21866.4	15908.5	42.490	17.653	228.2688	1.332
775	501.9	22702.9	16537.2	48.480	15.986	229.3661	1.329
800	526.8	23544.0	17170.5	55.130	14.512	230.4342	1.327
825	551.8	24389.3	17807.9	62.470	13.206	231.4744	1.325
850	576.8	25238.9	18449.7	70.580	12.043	232.4888	1.323
875	601.8	26092.4	19095.3	79.500	11.006	233.4786	1.321
900	626.8	26949.3	19744.4	89.300	10.079	234.4443	1.319
925	651.8	27810.0	20397.4	100.030	9.248	235.3876	1.318
950	676.8	28674.0	21053.5	111.750	8.501	236.3092	1.316
975	701.8	29541.2	21712.9	124.550	7.828	237.2105	1.314
1000	726.8	30411.7	22375.4	138.470	7.222	238.0915	1.313
1025	751.8	31284.8	23040.8	153.610	6.673	238.9542	1.312
1050	776.8	32160.9	23708.9	170.030	6.175	239.7984	1.310
1075	801.8	33039.5	24379.7	187.820	5.723	240.6257	1.309
1100	826.8	33921.0	25053.3	207.050	5.313	241.4361	1.308
1125	851.8	34804.5	25729.1	227.810	4.938	242.2303	1.307
1150	876.8	35690.4	26407.2	250.190	4.597	243.0094	1.306
1175	901.8	36578.8	27087.6	274.280	4.284	243.7737	1.305
1200	926.8	37469.3	27770.3	300.160	3.998	244.5233	1.304
1225	951.8	38362.2	28455.3	327.960	3.735	245.2596	1.303
1250	976.8	39256.8	29142.2	357.750	3.494	245.9826	1.302
1275	1002	40153.4	29830.7	389.660	3.272	246.6929	1.301
1300	1027	41051.8	30521.4	423.800	3.068	247.3910	1.300
1325	1052	41952.2	31214.1	460.240	2.879	248.0768	1.300
1350	1077	42854.5	31908.4	499.160	2.705	248.7517	1.299
1375	1102	43758.2	32604.3	540.600	2.543	249.4148	1.298
1400	1127	44664.2	33302.6	584.770	2.394	250.0678	1.297
1425	1152	45572.1	34002.5	631.780	2.256	250.7106	1.297
1450	1177	46480.9	34703.6	681.690	2.127	251.3426	1.296
1475	1202	47391.8	35406.7	734.760	2.007	251.9659	1.295
1500	1227	48304.3	36111.1	791.040	1.896	252.5795	1.295
1525	1252	49218.7	36817.5	850.640	1.793	253.1835	1.294
1550	1277	50133.9	37525.4	913.810	1.696	253.7789	1.293
1575	1302	51051.3	38234.7	980.670	1.606	254.3660	1.293
1600	1327	51970.3	38946.0	1051.430	1.522	254.9453	1.292
1625	1352	52890.2	39657.4	1126.040	1.443	255.5152	1.291
1650	1377	53811.9	40372.2	1205.050	1.369	256.0790	1.291
1675	1402	54735.2	41087.9	1288.250	1.300	256.6340	1.290
1700	1427	55660.0	41804.1	1375.960	1.236	257.1816	1.290
1725	1452	56586.7	42523.1	1468.570	1.175	257.7232	1.289
1750	1477	57513.6	43242.3	1565.810	1.118	258.2562	1.288
1775	1502	58444.0	43964.2	1668.390	1.064	258.7838	1.288
1800	1527	59374.3	44687.6	1776.380	1.013	259.3051	1.287
1825	1552	60306.7	45412.4	1889.640	0.966	259.8190	1.287
1850	1577	61239.9	46137.1	2008.650	0.921	260.3268	1.286

1875	1602	62175.3	46864.8	2133.750	0.879	260.8291	1.286
1900	1627	63111.9	47593.7	2264.990	0.839	261.3253	1.285
1925	1652	64050.0	48323.3	2402.790	0.801	261.8163	1.284
1950	1677	64989.3	49054.8	2547.020	0.766	262.3010	1.284
1975	1702	65929.9	49786.9	2697.750	0.732	262.7790	1.283
2000	1727	66870.6	50521.6	2856.260	0.700	263.2536	1.283
2025	1752	67815.3	51258.6	3021.750	0.670	263.7219	1.282
2050	1777	68759.6	51993.6	3195.660	0.641	264.1871	1.282
2075	1802	69706.0	52732.3	3376.570	0.615	264.6449	1.281
2100	1827	70653.6	53472.2	3565.950	0.589	265.0986	1.281
2125	1852	71602.0	54212.9	3763.990	0.565	265.5479	1.280
2150	1877	72552.5	54955.7	3970.630	0.541	265.9922	1.280
2175	1902	73505.1	55699.0	4186.520	0.520	266.4324	1.279
2200	1927	74456.5	56444.3	4412.320	0.499	266.8691	1.279
2225	1952	75410.8	57190.9	4646.560	0.479	267.2992	1.278
2250	1977	76366.4	57938.9	4892.130	0.460	267.7273	1.278
2275	2002	77324.9	58688.0	5147.180	0.442	268.1498	1.277
2300	2027	78282.5	59439.6	5413.640	0.425	268.5695	1.277
2325	2052	79242.9	60190.7	5690.300	0.409	268.9838	1.276
2350	2077	80202.2	60942.3	5978.470	0.393	269.3945	1.276
2375	2102	81165.1	61697.5	6278.510	0.378	269.8016	1.275
2400	2127	82128.8	62451.9	6591.310	0.364	270.2058	1.275
2425	2152	83092.6	63209.4	6915.330	0.351	270.6048	1.274
2450	2177	84060.2	63967.9	7253.860	0.338	271.0021	1.274
2475	2202	85028.5	64726.9	7605.280	0.325	271.3954	1.273
2500	2227	85997.5	65489.8	7969.600	0.314	271.7845	1.273
2525	2252	86964.4	66250.6	8348.850	0.302	272.1710	1.273
2550	2277	87935.4	67015.6	8740.540	0.292	272.5521	1.272
2575	2302	88909.4	67780.3	9149.560	0.281	272.9323	1.272
2600	2327	89883.7	68545.3	9573.050	0.272	273.3085	1.271
2625	2352	90857.1	69312.6	10011.66	0.262	273.6809	1.271
2650	2377	91831.8	70077.9	10468.70	0.253	274.0521	1.270
2675	2402	92811.6	70851.8	10942.12	0.244	274.4198	1.270
2700	2427	93788.0	71618.8	11430.69	0.236	274.7829	1.269
2725	2452	94769.9	72391.4	11939.27	0.228	275.1448	1.269
2750	2477	95754.4	73166.6	12466.23	0.221	275.5039	1.269
2775	2502	96733.4	73939.4	13008.47	0.213	275.8579	1.268
2800	2527	97720.0	74716.8	13570.96	0.206	276.2098	1.268
2825	2552	98698.0	75492.0	14159.12	0.200	276.5625	1.267
2850	2577	99688.5	76269.9	14760.84	0.193	276.9085	1.267
2875	2602	100674.1	77052.6	15385.88	0.187	277.2533	1.267
2900	2627	101660.0	77829.3	16033.14	0.181	277.5959	1.266
2925	2652	102649.4	78609.3	16702.24	0.175	277.9358	1.266
2950	2677	103642.2	79392.9	17392.24	0.170	278.2724	1.265
2975	2702	104632.1	80176.6	18109.35	0.164	278.6083	1.265
3000	2727	105629.1	80964.3	18842.33	0.159	278.9381	1.265
3025	2752	106618.5	81747.7	19605.69	0.154	279.2683	1.264
3050	2777	107617.3	82537.1	20394.44	0.150	279.5962	1.264
3075	2802	108613.8	83324.3	21208.77	0.145	279.9217	1.264
3100	2827	109604.7	84112.4	22050.11	0.141	280.2451	1.263
3125	2852	110603.4	84901.8	22912.96	0.136	280.5643	1.263
3150	2877	111600.9	85690.0	23813.95	0.132	280.8849	1.263
3175	2902	112598.4	86484.7	24740.19	0.128	281.2021	1.262
3200	2927	113599.7	87276.7	25688.12	0.125	281.5147	1.262
3225	2952	114600.5	88068.1	26669.83	0.121	281.8265	1.262
3250	2977	115604.2	88862.5	27674.83	0.117	282.1341	1.261
3275	3002	116609.5	89658.5	28729.51	0.114	282.4450	1.261
3300	3027	117612.1	90458.3	29793.74	0.111	282.7474	1.261
3325	3052	118627.2	91257.6	30908.52	0.108	283.0528	1.260
3350	3077	119629.9	92057.5	32048.53	0.105	283.3539	1.260
3375	3102	120639.1	92857.4	33222.66	0.102	283.6530	1.260
3400	3127	121644.6	93653.5	34440.44	0.099	283.9523	1.259
3425	3152	122653.0	94459.1	35676.52	0.096	284.2455	1.259
3450	3177	123666.0	95262.8	36961.71	0.093	284.5397	1.259
3475	3202	124674.9	96062.4	38297.42	0.091	284.8348	1.259
3500	3227	125690.8	96869.0	39663.05	0.088	285.1261	1.258
3525	3252	126703.0	97671.8	41036.38	0.086	285.4091	1.258
3550	3277	127718.6	98484.7	42482.84	0.084	285.6971	1.258

## B.10 Oxygen Properties (English Units)

Temperature		h	u	Pr	Vr	S <sub>o</sub>	Gamma
R	F	Btu/lbmol	Btu/lbmol			Btu/lbmol/R	
300	-159.7	2083.0	1487.3	0.177	1696.0	44.9080	1.400
340	-119.7	2361.2	1686.1	0.274	1240.0	45.7784	1.399
380	-79.7	2639.5	1885.0	0.405	938.55	46.5524	1.399
420	-39.7	2918.0	2084.0	0.575	730.37	47.2491	1.399
460	0.3	3196.7	2283.4	0.791	581.31	47.8831	1.398
500	40.3	3476.1	2483.2	1.061	471.30	48.4653	1.397
540	80.3	3756.2	2683.9	1.392	388.01	49.0043	1.395
580	120.3	4037.4	2885.7	1.792	323.61	49.5066	1.392
620	160.3	4319.9	3088.8	2.272	272.87	49.9777	1.390
660	200.3	4604.0	3293.5	2.841	232.28	50.4217	1.387
700	240.3	4889.8	3499.8	3.511	199.35	50.8421	1.383
740	280.3	5177.5	3708.1	4.294	172.33	51.2418	1.380
780	320.3	5467.1	3918.3	5.203	149.92	51.6229	1.376
820	360.3	5758.8	4130.6	6.252	131.17	51.9876	1.372
860	400.3	6052.6	4344.9	7.456	115.34	52.3375	1.369
900	440.3	6348.6	4561.5	8.832	101.90	52.6738	1.365
940	480.3	6646.7	4780.1	10.398	90.403	52.9979	1.361
980	520.3	6946.9	5001.0	12.171	80.517	53.3106	1.358
1020	560.3	7249.3	5223.9	14.174	71.965	53.6131	1.355
1060	600.3	7553.8	5448.9	16.425	64.536	53.9058	1.351
1100	640.3	7860.3	5676.0	18.949	58.052	54.1897	1.348
1140	680.3	8168.8	5905.1	21.768	52.371	54.4651	1.345
1180	720.3	8479.2	6136.0	24.909	47.372	54.7328	1.342
1220	760.3	8791.5	6368.9	28.397	42.962	54.9931	1.340
1260	800.3	9105.7	6603.7	32.262	39.055	55.2465	1.337
1300	840.3	9421.6	6840.1	36.531	35.586	55.4932	1.335
1340	880.3	9739.2	7078.3	41.237	32.495	55.7339	1.332
1380	920.3	10058.4	7318.1	46.411	29.734	55.9686	1.330
1420	960.3	10379.2	7559.4	52.088	27.262	56.1977	1.328
1460	1000.3	10701.4	7802.3	58.302	25.042	56.4216	1.326
1500	1040.3	11025.2	8046.6	65.092	23.044	56.6403	1.324
1540	1080.3	11350.2	8292.2	72.494	21.243	56.8542	1.322
1580	1120.3	11676.6	8539.1	80.549	19.615	57.0634	1.321
1620	1160.3	12004.2	8787.4	89.298	18.142	57.2682	1.319
1660	1200.3	12333.1	9036.8	98.787	16.804	57.4687	1.318
1700	1240.3	12663.1	9287.3	109.057	15.588	57.6651	1.316
1740	1280.3	12994.2	9539.1	120.159	14.481	57.8577	1.315
1780	1320.3	13326.4	9791.8	132.140	13.471	58.0464	1.314
1820	1360.3	13659.6	10045.5	145.054	12.547	58.2316	1.312
1860	1400.3	13993.7	10300.2	158.939	11.703	58.4131	1.311
1900	1440.3	14328.8	10555.9	173.867	10.928	58.5914	1.310
1940	1480.3	14664.9	10812.5	189.878	10.217	58.7663	1.309
1980	1520.3	15001.7	11069.9	207.053	9.563	58.9383	1.308
2020	1560.3	15339.4	11328.1	225.424	8.961	59.1071	1.307
2060	1600.3	15677.9	11587.3	245.068	8.406	59.2730	1.306
2100	1640.3	16017.1	11847.0	266.042	7.893	59.4361	1.305
2140	1680.3	16357.1	12107.6	288.437	7.419	59.5966	1.304
2180	1720.3	16697.9	12368.9	312.265	6.981	59.7542	1.304
2220	1760.3	17039.2	12630.9	337.650	6.575	59.9094	1.303
2260	1800.3	17381.4	12893.6	364.668	6.197	60.0623	1.302
2300	1840.3	17724.2	13157.0	393.349	5.847	60.2126	1.301
2340	1880.3	18067.6	13420.9	423.798	5.522	60.3607	1.300

2380	1920.3	18411.9	13685.7	456.060	5.219	60.5064	1.300
2420	1960.3	18756.6	13951.0	490.289	4.936	60.6501	1.299
2460	2000.3	19101.8	14216.9	526.500	4.672	60.7916	1.298
2500	2040.3	19447.6	14483.3	564.786	4.426	60.9310	1.298
2540	2080.3	19794.1	14750.4	605.319	4.196	61.0686	1.297
2580	2120.3	20141.4	15017.9	648.093	3.981	61.2042	1.296
2620	2160.3	20489.0	15286.3	693.189	3.780	61.3378	1.296
2660	2200.3	20837.0	15554.9	740.793	3.591	61.4697	1.295
2700	2240.3	21185.9	15824.3	791.037	3.413	61.6000	1.295
2740	2280.3	21535.4	16094.4	843.836	3.247	61.7283	1.294
2780	2320.3	21885.1	16364.7	899.451	3.091	61.8551	1.293
2820	2360.3	22235.5	16635.4	957.983	2.944	61.9803	1.293
2860	2400.3	22586.5	16907.2	1019.44	2.805	62.1038	1.292
2900	2440.3	22938.1	17179.4	1084.06	2.675	62.2258	1.292
2940	2480.3	23290.0	17451.8	1151.88	2.552	62.3463	1.291
2980	2520.3	23642.0	17724.4	1223.12	2.436	62.4655	1.291
3020	2560.3	23994.9	17997.9	1297.84	2.327	62.5832	1.290
3060	2600.3	24348.5	18272.0	1375.96	2.224	62.6993	1.290
3100	2640.3	24702.3	18546.3	1458.02	2.126	62.8143	1.289
3140	2680.3	25057.2	18821.8	1543.78	2.034	62.9278	1.289
3180	2720.3	25412.4	19097.5	1633.68	1.947	63.0402	1.288
3220	2760.3	25767.9	19373.6	1727.83	1.864	63.1515	1.287
3260	2800.3	26123.7	19649.9	1826.07	1.785	63.2613	1.287
3300	2840.3	26480.3	19927.1	1928.68	1.711	63.3699	1.286
3340	2880.3	26836.9	20204.6	2036.13	1.640	63.4776	1.286
3380	2920.3	27194.4	20482.6	2147.96	1.574	63.5837	1.285
3420	2960.3	27552.4	20761.2	2264.99	1.510	63.6891	1.285
3460	3000.3	27910.7	21039.7	2387.13	1.449	63.7934	1.285
3500	3040.3	28269.7	21319.2	2514.14	1.392	63.8963	1.284
3540	3080.3	28629.2	21599.6	2646.86	1.337	63.9985	1.284
3580	3120.3	28988.8	21879.8	2785.34	1.285	64.0997	1.283
3620	3160.3	29348.9	22160.4	2929.13	1.236	64.1997	1.283
3660	3200.3	29710.1	22442.2	3078.65	1.189	64.2986	1.282
3700	3240.3	30071.2	22723.8	3235.02	1.144	64.3970	1.282
3740	3280.3	30433.1	23006.3	3397.46	1.101	64.4942	1.281
3780	3320.3	30795.0	23288.7	3565.94	1.060	64.5904	1.281
3820	3360.3	31157.5	23571.8	3741.25	1.021	64.6857	1.280
3860	3400.3	31520.6	23855.4	3924.16	0.984	64.7805	1.280
3900	3440.3	31884.3	24139.6	4114.02	0.948	64.8743	1.279
3940	3480.3	32247.9	24424.7	4310.84	0.914	64.9671	1.279
3980	3520.3	32612.7	24709.1	4515.11	0.881	65.0590	1.278
4020	3560.3	32978.3	24995.2	4727.45	0.850	65.1503	1.278
4060	3600.3	33343.0	25280.5	4947.04	0.821	65.2404	1.278
4100	3640.3	33708.5	25566.6	5175.92	0.792	65.3303	1.277
4140	3680.3	34075.1	25854.4	5413.64	0.765	65.4194	1.277
4180	3720.3	34441.8	26141.0	5659.10	0.739	65.5075	1.276
4220	3760.3	34809.4	26429.1	5914.01	0.714	65.5950	1.276
4260	3800.3	35176.7	26717.0	6177.31	0.690	65.6815	1.275
4300	3840.3	35545.1	27005.9	6450.56	0.667	65.7674	1.275
4340	3880.3	35913.5	27294.8	6734.85	0.644	65.8531	1.275
4380	3920.3	36282.0	27584.6	7026.65	0.623	65.9373	1.274

4420	3960.3	36650.8	27874.7	7330.08	0.603	66.0213	1.274
4460	4000.3	37021.3	28163.6	7644.56	0.583	66.1047	1.273
4500	4040.3	37392.1	28455.7	7969.59	0.565	66.1874	1.273
4540	4080.3	37762.7	28746.1	8305.63	0.547	66.2694	1.273
4580	4120.3	38133.7	29038.3	8653.25	0.529	66.3508	1.272
4620	4160.3	38504.2	29330.1	9013.26	0.513	66.4318	1.272
4660	4200.3	38876.5	29623.7	9383.72	0.497	66.5117	1.271
4700	4240.3	39249.3	29916.3	9767.59	0.481	66.5914	1.271
4740	4280.3	39622.2	30210.4	10162.9	0.466	66.6702	1.271
4780	4320.3	39995.4	30503.5	10573.0	0.452	66.7487	1.270
4820	4360.3	40369.8	30797.7	10995.9	0.438	66.8266	1.270
4860	4400.3	40741.7	31090.9	11430.7	0.425	66.9036	1.269
4900	4440.3	41117.8	31386.8	11879.5	0.412	66.9801	1.269
4940	4480.3	41492.4	31682.7	12343.5	0.400	67.0562	1.269
4980	4520.3	41867.4	31977.5	12823.6	0.388	67.1319	1.268
5020	4560.3	42244.0	32275.3	13321.3	0.377	67.2076	1.268
5060	4600.3	42619.0	32570.2	13831.8	0.366	67.2822	1.268
5100	4640.3	42995.1	32867.5	14356.2	0.355	67.3561	1.267
5140	4680.3	43373.6	33165.5	14897.9	0.345	67.4297	1.267
5180	4720.3	43750.6	33464.1	15455.8	0.335	67.5027	1.267
5220	4760.3	44126.3	33761.1	16033.1	0.326	67.5755	1.266
5260	4800.3	44505.8	34060.4	16624.9	0.316	67.6475	1.266
5300	4840.3	44883.6	34359.5	17240.2	0.307	67.7197	1.265
5340	4880.3	45262.6	34658.3	17867.5	0.299	67.7906	1.265
5380	4920.3	45641.6	34958.6	18513.8	0.291	67.8612	1.265
5420	4960.3	46019.8	35258.0	19178.5	0.283	67.9312	1.265
5460	5000.3	46400.1	35556.8	19868.9	0.275	68.0015	1.264
5500	5040.3	46779.6	35860.3	20578.2	0.267	68.0711	1.264
5540	5080.3	47162.7	36159.1	21300.1	0.260	68.1396	1.264
5580	5120.3	47542.1	36462.5	22050.1	0.253	68.2083	1.263
5620	5160.3	47924.1	36762.9	22821.5	0.246	68.2766	1.263
5660	5200.3	48306.8	37066.9	23609.7	0.240	68.3440	1.263
5700	5240.3	48689.4	37370.7	24424.0	0.233	68.4114	1.262
5740	5280.3	49071.1	37670.9	25258.6	0.227	68.4781	1.262
5780	5320.3	49452.4	37973.4	26122.2	0.221	68.5449	1.262
5820	5360.3	49836.4	38278.6	27005.5	0.216	68.6109	1.262
5860	5400.3	50219.4	38583.0	27911.8	0.210	68.6765	1.261
5900	5440.3	50604.0	38886.0	28843.0	0.205	68.7416	1.261
5940	5480.3	50984.9	39190.9	29793.6	0.199	68.8060	1.261
5980	5520.3	51369.0	39496.3	30780.5	0.194	68.8707	1.260
6020	5560.3	51755.9	39801.7	31791.3	0.189	68.9349	1.260
6060	5600.3	52142.4	40106.5	32828.2	0.185	68.9986	1.260
6100	5640.3	52526.9	40412.4	33889.5	0.180	69.0618	1.260
6140	5680.3	52910.4	40717.1	34992.4	0.175	69.1254	1.259
6180	5720.3	53295.7	41023.6	36107.9	0.171	69.1877	1.259
6220	5760.3	53684.3	41333.4	37269.0	0.167	69.2506	1.259
6260	5800.3	54071.3	41638.9	38424.6	0.163	69.3112	1.259
6300	5840.3	54458.4	41947.2	39662.9	0.159	69.3742	1.258
6340	5880.3	54843.1	42253.2	40889.6	0.155	69.4347	1.258
6380	5920.3	55229.9	42561.3	42160.0	0.151	69.4955	1.258

## B.11 Hydrogen Properties (SI Units)

Temperature K	h kJ/kgmol	u kJ/kgmol	Pr	Vr	$s_o$ kj/kgmol/K	Gamma
200	-73.1	4805.7	3420.1	0.350	1029.2	114.446
225	-48.1	5495.8	3924.5	0.520	435.08	117.697
250	-23.1	6198.6	4437.6	0.740	338.55	120.659
275	1.9	6910.5	4956.6	1.020	268.69	123.373
300	26.9	7628.8	5479.7	1.380	216.99	125.873
325	51.9	8351.6	6005.5	1.830	177.96	128.187
350	76.9	9077.5	6532.9	2.370	147.95	130.338
375	101.9	9805.5	7061.1	3.010	124.49	132.347
400	126.9	10534.8	7589.8	3.780	105.88	134.230
425	151.9	11265.0	8118.5	4.670	90.912	136.001
450	176.9	11995.8	8647.1	5.720	78.734	137.672
475	201.9	12727.0	9175.5	6.910	68.713	139.253
500	226.9	13458.4	9703.7	8.280	60.384	140.754
525	251.9	14190.1	10231.7	9.830	53.397	142.182
550	276.9	14922.0	10759.6	11.580	47.487	143.544
575	301.9	15654.3	11287.4	13.550	42.449	144.846
600	326.9	16386.9	11815.4	15.740	38.124	146.093
625	351.9	17120.1	12343.6	18.180	34.387	147.290
650	376.9	17853.8	12872.2	20.870	31.138	148.441
675	401.9	18588.3	13401.3	23.850	28.299	149.550
700	426.9	19323.5	13931.1	27.130	25.804	150.619
725	451.9	20059.8	14461.6	30.720	23.601	151.653
750	476.9	20797.1	14993.2	34.640	21.649	152.653
775	501.9	21535.7	15525.8	38.930	19.910	153.621
800	526.8	22275.6	16059.6	43.580	18.356	154.561
825	551.8	23016.8	16594.8	48.640	16.962	155.473
850	576.8	23759.7	17131.3	54.120	15.707	156.360
875	601.8	24504.3	17669.5	60.040	14.575	157.224
900	626.8	25250.5	18209.4	66.430	13.549	158.065
925	651.8	25998.7	18751.0	73.310	12.617	158.884
950	676.8	26748.8	19294.5	80.720	11.769	159.685
975	701.8	27500.9	19840.0	88.670	10.995	160.466
1000	726.8	28255.2	20387.5	97.210	10.287	161.230
1025	751.8	29011.6	20937.1	106.340	9.638	161.977
1050	776.8	29770.2	21489.0	116.120	9.042	162.708
1075	801.8	30531.1	22043.0	126.570	8.493	163.425
1100	826.8	31294.6	22599.6	137.720	7.987	164.126
1125	851.8	32060.3	23158.3	149.620	7.519	164.815
1150	876.8	32828.6	23719.8	162.280	7.087	165.490
1175	901.8	33599.4	24283.3	175.750	6.686	166.153
1200	926.8	34372.8	24849.8	190.080	6.313	166.8049
1225	951.8	35148.7	25418.6	205.290	5.967	167.4448
1250	976.8	35927.5	25990.4	221.430	5.645	168.0741
1275	1001.8	36708.8	26564.4	238.530	5.345	168.6927
1300	1026.8	37493.0	27141.3	256.670	5.065	169.3019
1325	1051.8	38279.6	27720.8	275.850	4.803	169.9012
1350	1076.8	39068.9	28303.0	296.150	4.559	170.4915
1375	1101.8	39861.4	28888.0	317.590	4.329	171.0727
1400	1126.8	40656.2	29475.7	340.260	4.115	171.6458
1425	1151.8	41453.9	30066.2	364.180	3.913	172.2106
1450	1176.8	42254.3	30659.3	389.400	3.724	172.7673
1475	1201.8	43057.5	31254.8	415.990	3.546	173.3165
1500	1226.8	43863.2	31853.6	444.010	3.378	173.8584
1525	1251.8	44671.7	32454.5	473.490	3.221	174.3928
1550	1276.8	45483.5	33058.9	504.510	3.072	174.9204
1575	1301.8	46297.5	33665.3	537.150	2.932	175.4416
1600	1326.8	47113.8	34274.7	571.450	2.800	175.9562
1625	1351.8	47933.5	34886.7	607.450	2.675	176.4641
1650	1376.8	48755.8	35501.8	645.290	2.557	176.9665
1675	1401.8	49580.5	36118.8	684.920	2.446	177.4620
1700	1426.8	50407.3	36738.3	726.580	2.340	177.9529
1725	1451.8	51237.3	37361.0	770.150	2.240	178.4370

1750	1476.8	52069.7	37985.7	815.840	2.145	178.9162	1.332
1775	1501.8	52903.8	38612.9	863.700	2.055	179.3901	1.331
1800	1526.8	53740.8	39241.4	913.720	1.970	179.8581	1.330
1825	1551.8	54581.4	39875.1	966.120	1.889	180.3218	1.328
1850	1576.8	55424.0	40510.0	1020.85	1.812	180.7799	1.327
1875	1601.8	56267.7	41146.0	1078.02	1.739	181.2329	1.326
1900	1626.8	57114.5	41785.2	1137.85	1.670	181.6819	1.325
1925	1651.8	57963.9	42427.7	1200.31	1.604	182.1262	1.324
1950	1676.8	58816.2	43072.4	1265.35	1.541	182.5649	1.322
1975	1701.8	59669.1	43717.5	1333.32	1.481	183.0000	1.321
2000	1726.8	60524.9	44365.6	1404.24	1.424	183.4308	1.320
2025	1751.8	61382.1	45016.0	1478.15	1.370	183.8572	1.319
2050	1776.8	62242.3	45667.7	1555.15	1.318	184.2794	1.318
2075	1801.8	63105.5	46323.1	1635.33	1.269	184.6973	1.317
2100	1826.8	63969.2	46979.2	1718.79	1.222	185.1112	1.316
2125	1851.8	64836.1	47638.4	1805.64	1.177	185.5210	1.315
2150	1876.8	65704.2	48300.4	1896.32	1.134	185.9284	1.314
2175	1901.8	66575.0	48963.5	1990.34	1.093	186.3307	1.313
2200	1926.8	67446.9	49627.8	2088.08	1.054	186.729	1.312
2225	1951.8	68324.0	50295.5	2189.74	1.016	187.124	1.311
2250	1976.8	69197.7	50963.2	2295.26	0.980	187.516	1.310
2275	2001.8	70077.9	51634.0	2405.30	0.946	187.905	1.310
2300	2026.8	70956.1	52304.6	2519.14	0.913	188.290	1.309
2325	2051.9	71839.3	52980.1	2637.34	0.882	188.671	1.308
2350	2076.9	72722.6	53657.3	2759.89	0.851	189.048	1.307
2375	2101.9	73608.8	54335.9	2887.56	0.822	189.424	1.306
2400	2126.9	74496.5	55015.8	3019.41	0.795	189.795	1.305
2425	2151.9	75383.7	55697.0	3156.42	0.768	190.164	1.305
2450	2176.9	76275.0	56378.9	3298.22	0.743	190.530	1.304
2475	2201.9	77168.5	57063.2	3444.71	0.718	190.891	1.303
2500	2226.9	78065.4	57754.0	3597.46	0.695	191.252	1.302
2525	2251.9	78958.7	58441.2	3755.16	0.672	191.608	1.302
2550	2276.9	79858.3	59131.5	3918.30	0.651	191.962	1.301
2575	2301.9	80757.3	59824.4	4087.42	0.630	192.313	1.300
2600	2326.9	81660.9	60518.7	4262.98	0.610	192.663	1.299
2625	2351.9	82562.7	61211.2	4443.41	0.591	193.008	1.299
2650	2376.9	83468.5	61911.0	4630.75	0.572	193.351	1.298
2675	2401.9	84374.3	62607.4	4824.38	0.554	193.691	1.297
2700	2426.9	85280.6	63307.7	5023.60	0.537	194.028	1.297
2725	2451.9	86190.2	64007.9	5230.92	0.521	194.364	1.296
2750	2476.9	87100.1	64711.8	5444.85	0.505	194.697	1.295
2775	2501.9	88012.9	65418.5	5666.24	0.490	195.029	1.295
2800	2526.9	88928.4	66124.7	5893.76	0.475	195.356	1.294
2825	2551.9	89842.6	66829.6	6130.21	0.461	195.683	1.293
2850	2576.9	90761.3	67545.5	6370.52	0.447	196.003	1.293
2875	2601.9	91678.1	68252.9	6621.13	0.434	196.323	1.292
2900	2626.9	92599.3	68964.8	6879.94	0.422	196.642	1.291
2925	2651.9	93523.4	69679.6	7146.94	0.409	196.959	1.291
2950	2676.9	94447.0	70393.8	7424.87	0.397	197.276	1.290
2975	2701.9	95365.3	71109.4	7707.28	0.386	197.586	1.290
3000	2726.9	96299.9	71828.1	8001.78	0.375	197.898	1.289
3025	2751.9	97225.9	72551.3	8304.25	0.364	198.206	1.289
3050	2776.9	98155.4	73271.5	8614.29	0.354	198.511	1.288
3075	2801.9	99082.3	73989.1	8934.31	0.344	198.814	1.287
3100	2826.9	100015.5	74712.9	9264.16	0.335	199.116	1.287
3125	2851.9	100948.4	75443.1	9604.56	0.325	199.416	1.286
3150	2876.9	101874.6	76160.0	9951.58	0.317	199.711	1.286
3175	2901.9	102824.7	76900.7	10313.1	0.308	200.008	1.285
3200	2926.9	103754.9	77628.2	10687.4	0.299	200.3040	1.284

## B.12 Hydrogen Properties (English Units)

Temperature R	h Btu/lbmol	u Btu/lbmol	Pr	Vr	$S_o$ Btu/lbmol/R	Gamma
300	-159.7	2066.2	1470.5	0.195	1541.3	27.3370
340	-119.7	2319.9	1656.3	0.290	1171.3	28.1307
380	-79.7	2580.6	1847.0	0.418	908.85	28.8554
420	-39.7	2846.5	2041.2	0.584	718.63	29.5205
460	0.3	3116.2	2238.0	0.796	577.94	30.1338
500	40.3	3388.7	2436.7	1.060	471.90	30.7019
540	80.3	3663.4	2636.7	1.383	390.58	31.2303
580	120.3	3939.5	2837.6	1.772	327.23	31.7236
620	160.3	4216.8	3039.0	2.237	277.16	32.1859
660	200.3	4494.8	3240.8	2.784	237.05	32.6204
700	240.3	4773.4	3442.8	3.422	204.54	33.0302
740	280.3	5052.3	3644.9	4.160	177.90	33.4177
780	320.3	5331.5	3847.0	5.005	155.84	33.7851
820	360.3	5610.8	4049.0	5.968	137.41	34.1344
860	400.3	5890.3	4250.9	7.056	121.88	34.4671
900	440.3	6169.8	4452.8	8.280	108.69	34.7848
940	480.3	6449.4	4654.5	9.650	97.410	35.0888
980	520.3	6729.1	4856.3	11.175	87.693	35.3802
1020	560.3	7009.0	5058.0	12.867	79.276	35.6601
1060	600.3	7288.9	5259.8	14.734	71.940	35.9293
1100	640.3	7569.0	5461.6	16.790	65.514	36.1887
1140	680.3	7849.2	5663.5	19.045	59.857	36.4389
1180	720.3	8129.7	5865.6	21.512	54.854	36.6807
1220	760.3	8410.5	6067.8	24.202	50.410	36.9147
1260	800.3	8691.5	6270.3	27.128	46.447	37.1414
1300	840.3	8972.9	6473.1	30.303	42.899	37.3612
1340	880.3	9254.6	6676.1	33.742	39.713	37.5747
1380	920.3	9536.7	6879.6	37.457	36.842	37.7821
1420	960.3	9819.3	7083.4	41.465	34.246	37.9839
1460	1000.3	10102.3	7287.7	45.779	31.892	38.1805
1500	1040.3	10385.8	7492.4	50.417	29.752	38.3721
1540	1080.3	10669.9	7697.6	55.392	27.802	38.5590
1580	1120.3	10954.6	7903.4	60.724	26.019	38.7415
1620	1160.3	11239.8	8109.8	66.427	24.388	38.9198
1660	1200.3	11525.7	8316.7	72.521	22.890	39.0941
1700	1240.3	11812.3	8524.3	79.026	21.512	39.2647
1740	1280.3	12099.5	8732.6	85.961	20.242	39.4317
1780	1320.3	12387.4	8941.5	93.341	19.070	39.5953
1820	1360.3	12676.1	9151.2	101.193	17.985	39.7557
1860	1400.3	12965.5	9361.5	109.533	16.981	39.9129
1900	1440.3	13255.7	9572.7	118.388	16.049	40.0673
1940	1480.3	13546.7	9784.6	127.776	15.183	40.2189
1980	1520.3	13838.5	9997.4	137.723	14.377	40.3677
2020	1560.3	14131.1	10210.8	148.254	13.625	40.5141
2060	1600.3	14424.6	10425.3	159.396	12.924	40.6580
2100	1640.3	14718.8	10640.4	171.165	12.269	40.7994
2140	1680.3	15014.1	10856.5	183.598	11.656	40.9387
2180	1720.3	15310.2	11073.4	196.724	11.082	41.0758
2220	1760.3	15607.1	11291.2	210.553	10.544	41.2107
2260	1800.3	15905.1	11510.0	225.140	10.038	41.3437
2300	1840.3	16203.8	11729.5	240.496	9.564	41.4747
2340	1880.3	16503.5	11950.1	256.667	9.117	41.6040
2380	1920.3	16804.0	12171.5	273.665	8.697	41.7313
2420	1960.3	17105.6	12393.8	291.537	8.301	41.8569
2460	2000.3	17408.0	12617.1	310.317	7.927	41.9809
2500	2040.3	17711.4	12841.2	330.038	7.575	42.1033
2540	2080.3	18015.7	13066.4	350.727	7.242	42.2240
2580	2120.3	18321.1	13292.4	372.431	6.927	42.3433
2620	2160.3	18627.3	13519.5	395.188	6.630	42.4610
2660	2200.3	18934.6	13747.4	419.029	6.348	42.5774
2700	2240.3	19242.4	13976.2	444.012	6.081	42.6924
2740	2280.3	19551.5	14206.0	470.143	5.828	42.8059
2780	2320.3	19861.4	14436.7	497.506	5.588	42.9183
2820	2360.3	20172.2	14668.2	526.107	5.360	43.0293
2860	2400.3	20483.9	14900.6	555.982	5.144	43.1389
2900	2440.3	20796.5	15133.9	587.240	4.938	43.2476
2940	2480.3	21110.2	15368.3	619.862	4.743	43.3549
2980	2520.3	21424.6	15603.4	653.922	4.557	43.4611

3020	2560.3	21739.9	15839.4	689.489	4.380	43.5663	1.336
3060	2600.3	22056.0	16076.3	726.583	4.211	43.6704	1.335
3100	2640.3	22373.2	16314.2	765.241	4.051	43.7733	1.334
3140	2680.3	22690.9	16552.8	805.452	3.898	43.8750	1.332
3180	2720.3	23009.8	16792.3	847.464	3.752	43.9760	1.331
3220	2760.3	23329.4	17032.4	891.139	3.613	44.0758	1.330
3260	2800.3	23650.2	17273.7	936.736	3.480	44.1749	1.329
3300	2840.3	23971.1	17515.6	983.986	3.354	44.2726	1.328
3340	2880.3	24293.4	17758.7	1033.37	3.232	44.3698	1.327
3380	2920.3	24616.2	18002.0	1084.55	3.116	44.4658	1.326
3420	2960.3	24939.8	18246.3	1137.85	3.006	44.5611	1.325
3460	3000.3	25264.2	18491.2	1193.24	2.900	44.6555	1.324
3500	3040.3	25589.6	18737.5	1250.77	2.798	44.7490	1.323
3540	3080.3	25916.0	18984.8	1310.49	2.701	44.8416	1.322
3580	3120.3	26242.3	19231.6	1372.46	2.608	44.9334	1.321
3620	3160.3	26570.1	19479.9	1436.67	2.520	45.0242	1.320
3660	3200.3	26898.3	19729.1	1503.57	2.434	45.1146	1.319
3700	3240.3	27227.4	19978.7	1572.68	2.353	45.2038	1.318
3740	3280.3	27557.4	20229.3	1644.49	2.274	45.2925	1.317
3780	3320.3	27887.0	20479.4	1718.79	2.199	45.3802	1.316
3820	3360.3	28218.9	20731.8	1795.98	2.127	45.4675	1.315
3860	3400.3	28550.0	20983.5	1875.66	2.058	45.5537	1.314
3900	3440.3	28882.4	21237.2	1958.71	1.991	45.6397	1.314
3940	3480.3	29215.3	21490.6	2044.45	1.927	45.7248	1.313
3980	3520.3	29549.5	21745.3	2132.74	1.866	45.8087	1.312
4020	3560.3	29883.8	22000.2	2224.60	1.807	45.8925	1.311
4060	3600.3	30219.1	22256.8	2319.38	1.750	45.9753	1.310
4100	3640.3	30555.0	22513.2	2417.69	1.696	46.0578	1.310
4140	3680.3	30891.1	22769.1	2519.14	1.643	46.1394	1.309
4180	3720.3	31227.8	23027.1	2623.96	1.593	46.2204	1.308
4220	3760.3	31566.3	23286.1	2731.96	1.545	46.3005	1.307
4260	3800.3	31904.5	23544.9	2844.50	1.498	46.3806	1.307
4300	3840.3	32243.1	23804.0	2959.95	1.453	46.4596	1.306
4340	3880.3	32582.4	24064.6	3079.53	1.409	46.5383	1.305
4380	3920.3	32922.2	24325.6	3203.30	1.367	46.6165	1.304
4420	3960.3	33263.4	24586.7	3330.60	1.327	46.6939	1.304
4460	4000.3	33604.6	24849.2	3461.81	1.288	46.7706	1.303
4500	4040.3	33947.7	25112.1	3597.46	1.251	46.8470	1.302
4540	4080.3	34288.8	25374.5	3737.92	1.215	46.9230	1.302
4580	4120.3	34632.8	25638.3	3882.32	1.180	46.9983	1.301
4620	4160.3	34976.3	25901.6	4030.11	1.146	47.0725	1.300
4660	4200.3	35318.8	26166.8	4183.69	1.114	47.1468	1.300
4700	4240.3	35664.8	26432.6	4342.71	1.082	47.2208	1.299
4740	4280.3	36010.7	26698.3	4504.54	1.052	47.2935	1.298
4780	4320.3	36354.3	26963.2	4672.92	1.023	47.3664	1.298
4820	4360.3	36702.3	27231.0	4846.26	0.995	47.4387	1.297
4860	4400.3	37049.9	27499.9	5023.59	0.967	47.5101	1.297
4900	4440.3	37397.7	27767.5	5207.93	0.941	47.5816	1.296
4940	4480.3	37745.1	28036.2	5396.59	0.915	47.6523	1.295
4980	4520.3	38094.5	28305.4	5591.04	0.891	47.7226	1.295
5020	4560.3	38442.8	28575.0	5790.58	0.867	47.7922	1.294
5060	4600.3	38793.1	28846.5	5998.17	0.844	47.8622	1.294
5100	4640.3	39141.9	29116.6	6207.91	0.822	47.9304	1.293
5140	4680.3	39495.4	29388.5	6425.75	0.800	47.9989	1.293
5180	4720.3	39846.4	29660.7	6649.98	0.779	48.0670	1.292
5220	4760.3	40196.6	29932.2	6879.93	0.759	48.1345	1.291
5260	4800.3	40549.5	30203.6	7117.84	0.739	48.2021	1.291
5300	4840.3	40902.4	30477.7	7361.83	0.720	48.2690	1.290
5340	4880.3	41256.2	30752.8	7610.55	0.702	48.3350	1.290
5380	4920.3	41610.1	31027.9	7868.25	0.684	48.4011	1.289
5420	4960.3	41960.6	31299.7	8132.56	0.666	48.4667	1.289
5460	5000.3	42316.4	31576.7	8406.08	0.650	48.5324	1.288
5500	5040.3	42674.0	31852.7	8681.65	0.634	48.5965	1.288
5540	5080.3	43026.8	32129.6	8971.08	0.618	48.6616	1.287
5580	5120.3	43385.2	32403.6	9264.15	0.602	48.7254	1.287
5620	5160.3	43743.0	32685.5	9566.16	0.587	48.7891	1.286
5660	5200.3	44099.9	32960.9	9875.62	0.573	48.8523	1.286
5700	5240.3	44455.9	33238.0	10197.0	0.559	48.9160	1.285
5740	5280.3	44814.2	33517.6	10519.0	0.546	48.9777	1.285
5780	5320.3	45171.6	33796.3	10854.5	0.532	49.0400	1.284

# **Appendix C**

## **Thermodynamic Properties for Water**

## C.1 The Saturation Temperature vs. Pressure (SI Units)

Press (kPa)	Temp (K)	Specific Volume (m <sup>3</sup> /kg)	Internal Energy (kJ/kg)			Enthalpy (kJ/kg)			Entropy (kJ/kg/K)		
		vf	vg	uf	ug	hf	hg	sf	sfg	sg	
0.61	273.2	0.0001000	205.9	2364.3	2374.9	0.00	2500.9	2500.9	0.00000	9.15549	9.15549
0.80	276.9	0.001000	159.6461	15.81	2364.3	15.81	2492.0	2507.8	0.05748	8.999925	9.05672
1.00	280.1	0.001000	129.1833	29.30	2355.2	2384.5	29.30	2484.4	2513.7	0.10591	8.86902
1.20	282.8	0.001000	108.6740	40.57	2347.6	2388.2	40.57	2478.0	2518.6	0.14595	8.76236
1.40	285.1	0.001001	93.9033	50.28	2341.1	2391.4	50.28	2472.5	2522.8	0.18016	8.67199
1.60	287.2	0.001001	82.4663	58.83	2335.0	2394.2	58.84	2467.7	2526.6	0.21005	8.59355
1.80	289.0	0.001001	74.0143	66.49	2330.2	2396.7	66.49	2463.4	2529.4	0.23663	8.52424
2.00	290.6	0.001001	66.9896	73.43	2325.5	2398.9	73.43	2459.5	2532.9	0.26058	8.46214
2.50	294.2	0.001002	54.241	88.43	2315.4	2403.8	88.43	2451.0	2539.4	0.31186	8.33030
3.00	297.2	0.001003	45.6550	100.99	2306.9	2407.9	100.99	2443.9	2544.9	0.35433	8.22223
3.50	299.8	0.001003	39.4678	111.83	2299.6	2411.4	111.84	2437.7	2549.6	0.39066	8.13060
4.00	302.1	0.001004	34.7925	121.40	2293.1	2414.5	121.40	2432.3	2553.7	0.42245	8.05104
5.00	306.0	0.001005	28.1863	137.76	2282.1	2419.8	137.76	2423.0	2560.8	0.47625	7.91766
6.00	309.3	0.001006	23.7342	151.49	2272.8	2424.3	151.49	2415.2	2566.7	0.52087	7.80827
7.00	312.2	0.001007	20.5252	163.36	2264.7	2428.1	163.37	2408.4	2571.8	0.55908	7.71549
8.00	314.7	0.001008	18.0994	173.84	2257.6	2431.4	173.85	2402.4	2576.2	0.59253	7.63488
9.00	316.9	0.001009	16.2497	183.25	2251.2	2434.5	183.26	2397.0	2580.3	0.62233	7.56359
10.00	319.0	0.001010	14.6706	191.80	2245.4	2437.2	191.81	2392.1	2583.9	0.64922	7.49968
15.00	327.1	0.001014	10.0204	225.92	2222.1	2448.0	225.94	2372.4	2598.3	0.75484	7.25228
20.00	333.2	0.001017	7.6482	251.38	2204.6	2456.0	251.40	2357.5	2608.9	0.83195	7.07528
25.00	338.1	0.001020	6.2034	271.90	2190.5	2462.4	271.93	2345.5	2617.4	0.89309	6.93708
30.00	342.2	0.001022	5.2286	289.20	2178.5	2467.7	289.23	2335.3	2624.6	0.94394	6.82351
40.00	349.0	0.001026	3.9931	317.53	2158.8	2476.3	317.57	2318.5	2636.1	1.02590	6.64307
50.00	354.5	0.001030	3.2401	340.42	2142.8	2483.2	340.48	2304.7	2645.2	1.09101	6.50196
60.00	359.1	0.001033	2.7318	359.77	2129.2	2488.9	359.84	2293.0	2652.9	1.14524	6.38586
70.00	363.1	0.001036	2.3649	376.61	2117.3	2493.9	376.68	2282.7	2659.4	1.19186	6.28709
80.00	366.6	0.001038	2.0872	391.56	2106.6	2498.2	391.64	2273.5	2665.2	1.23283	6.20106
90.00	369.8	0.001041	1.8695	405.03	2097.0	2502.1	405.13	2265.2	2670.3	1.26944	6.124479
101.33	373.1	0.001043	1.6733	418.88	2087.1	2506.0	418.99	2256.5	2675.5	1.30672	6.04766
120.00	377.9	0.001047	1.4284	439.17	2072.5	2511.6	439.30	2243.8	2683.1	1.36075	5.93688
140.00	382.4	0.001051	1.2366	458.22	2058.6	2516.9	458.37	2231.6	2690.0	1.41085	5.83517
160.00	386.4	0.001054	1.0914	475.17	2046.2	2521.4	475.34	2220.7	2696.0	1.45494	5.74643
180.00	390.1	0.001058	0.9775	490.48	2035.0	2525.5	490.67	2210.7	2701.4	1.49437	5.66765
200.00	393.4	0.001061	0.8857	504.47	2024.6	2529.1	504.68	2201.6	2706.2	1.53010	5.59676

Press (kPa)	Temp (K)	Specific Volume (m <sup>3</sup> *3/kg)	Internal Energy (kJ/kg)			Enthalpy (kJ/kg)			Entropy (kJ/kg/K)		
			v <sub>f</sub>	v <sub>g</sub>	u <sub>f</sub>	u <sub>g</sub>	h <sub>f</sub>	h <sub>g</sub>	s <sub>f</sub>	s <sub>g</sub>	
300.00	406.7	0.001073	0.6058	561.13	1982.0	2543.2	561.46	2163.4	2724.9	1.67176	5.31980
400.00	416.8	0.001084	0.4624	604.29	1948.8	2553.1	604.72	2133.3	2738.1	1.77660	5.11882
500.00	425.0	0.001093	0.3748	639.64	1922.1	2560.7	640.19	2107.9	2748.1	1.86060	4.95998
600.00	432.0	0.001101	0.3156	669.84	1897.0	2566.8	670.50	2085.6	2756.1	1.93110	4.82807
700.00	438.1	0.001108	0.2728	696.37	1875.4	2571.8	697.14	2065.6	2762.7	1.99208	4.71490
800.00	443.6	0.001115	0.2403	720.13	1855.9	2576.0	721.02	2047.3	2768.3	2.04599	4.61555
900.00	448.5	0.001121	0.2149	741.72	1837.9	2579.7	742.72	2030.3	2773.0	2.09440	4.52683
1000.00	453.0	0.001127	0.1943	761.56	1821.2	2582.7	762.68	2014.4	2777.1	2.13843	4.44655
1200.00	461.1	0.001139	0.1632	797.13	1790.7	2587.9	798.50	1985.3	2783.8	2.21630	4.30539
1400.00	468.2	0.001149	0.1408	828.52	1763.3	2591.8	830.13	1958.8	2788.9	2.28388	4.18364
1600.00	474.5	0.001159	0.1237	856.76	1738.2	2594.9	858.61	1934.3	2792.9	2.34381	4.07621
1800.00	480.3	0.001168	0.1104	882.51	1714.8	2597.3	884.61	1911.4	2796.0	2.39779	3.97980
2000.00	485.5	0.001177	0.0996	906.27	1693.0	2599.2	908.62	1889.8	2798.4	2.44702	3.89914
2500.00	497.1	0.001197	0.0799	958.99	1643.2	2602.2	961.98	1840.1	2802.0	2.55443	3.70155
3000.00	507.0	0.001217	0.0667	1004.7	1598.6	2603.3	1008.37	1794.9	2803.3	2.64562	3.54017
4000.00	523.5	0.001253	0.0498	1082.42	1519.4	2601.8	1087.43	1713.5	2800.9	2.79665	3.27306
5000.00	537.1	0.001286	0.0394	1148.07	1448.9	2597.0	1154.50	1639.7	2794.2	2.92075	3.05296
6000.00	548.7	0.001319	0.0324	1205.82	1384.1	2589.9	1213.73	1570.8	2784.6	3.02744	2.86263
7000.00	559.0	0.001352	0.0274	1257.97	1322.9	2580.9	1267.44	1505.1	2772.6	3.12199	2.69264
8000.00	568.2	0.001385	0.0235	1306.0	1264.4	2570.4	1317.08	1441.5	2758.6	3.20765	2.53720
9000.00	576.5	0.001418	0.0205	1350.89	1207.6	2558.4	1363.65	1379.2	2742.9	3.28657	2.39244
10000.00	584.1	0.001453	0.0180	1393.34	1151.8	2545.1	1407.87	1317.6	2725.5	3.36029	2.25560
11000.00	591.2	0.001489	0.0160	1433.90	1096.6	2530.5	1450.28	1256.1	2706.4	3.42995	2.12458
12000.00	597.8	0.001526	0.0143	1473.01	1041.3	2514.4	1491.33	1194.3	2685.6	3.49646	1.99766
13000.00	604.0	0.001566	0.0128	1511.04	985.6	2496.7	1531.40	1131.5	2662.9	3.56058	1.87331
14000.00	609.8	0.001610	0.0115	1548.34	928.9	2477.3	1570.88	1067.2	2638.1	3.62300	1.75005
15000.00	615.3	0.001657	0.0103	1585.30	870.5	2455.8	1610.15	1000.7	2610.9	3.68445	1.62636
16000.00	620.5	0.001710	0.0093	1622.32	809.6	2431.9	1649.67	931.1	2580.8	3.74568	1.50059
17000.00	625.4	0.001769	0.0084	1659.98	745.2	2405.1	1690.05	857.4	2547.4	3.80770	1.37081
18000.00	630.1	0.001840	0.0075	1698.93	675.6	2374.6	1732.04	777.5	2509.5	3.87170	1.23384
19000.00	634.6	0.001925	0.0036	1740.32	279.6	2019.9	1776.91	310.7	2087.6	3.93967	0.48827
20000.00	638.9	0.002039	0.0034	1786.35	235.7	2022.1	1827.12	263.1	2090.2	4.01541	4.42653
21000.00	643.0	0.002212	0.0033	1842.97	180.8	2023.8	1889.43	203.0	2092.4	4.10930	0.31555
220064.00	647.1	0.003209	0.0032	2034.47	0.0	2034.5	2105.27	0.0	2105.3	4.43941	0.00000

## C.2 The Saturation Pressure vs. Temperature (SI Units)

Temp (K)	Press (kPa)	Specific Volume (m <sup>3</sup> /kg)		Internal Energy (kJ/kg)		Enthalpy (kJ/kg)		Entropy (kJ/kg/K)				
		v <sub>f</sub>	v <sub>g</sub>	u <sub>f</sub>	u <sub>fg</sub>	u <sub>g</sub>	h <sub>f</sub>	h <sub>fg</sub>	h <sub>g</sub>	s <sub>f</sub>	s <sub>fg</sub>	s <sub>g</sub>
273.1	0.61	0.001000	206.1397	0.00	2374.9	2374.9	0.00	2500.9	2500.9	0.00000	9.15591	9.15591
275.0	0.70	0.001000	181.6044	7.76	2369.7	2377.4	7.76	2496.5	2504.3	0.02831	9.107831	9.10662
280.0	0.99	0.001000	130.1941	28.79	2355.5	2384.3	28.80	2484.7	2513.5	0.10412	8.87382	8.97794
285.0	1.39	0.001001	94.6073	49.78	2341.4	2391.2	49.78	2472.8	2522.6	0.17840	8.67661	8.85501
290.0	1.92	0.001001	69.6305	70.73	2327.3	2398.1	70.73	2461.0	2531.7	0.25128	8.48623	8.73751
295.0	2.62	0.001002	51.8694	91.66	2313.2	2604.9	91.66	2449.2	2540.8	0.32229	8.30229	8.62511
300.0	3.54	0.001003	39.0821	112.57	2299.1	2411.7	112.57	2437.3	2549.9	0.39312	8.12441	8.51154
305.0	4.72	0.001005	29.7669	133.47	2285.0	2418.4	133.48	2425.4	2558.9	0.46222	7.95228	8.41451
310.0	6.23	0.001007	22.9051	154.37	2270.8	2425.2	154.38	2413.5	2567.9	0.53018	7.78559	8.31577
315.0	8.14	0.001009	17.7969	175.26	2256.6	2431.9	175.27	2401.6	2576.8	0.59104	7.62405	8.22110
320.0	10.55	0.001011	13.9557	196.16	2242.4	2438.6	196.17	2389.6	2585.7	0.66285	7.46741	8.13026
325.0	13.53	0.001013	11.0396	217.06	2228.1	2445.2	217.07	2377.5	2594.6	0.72765	7.31540	8.04305
330.0	17.21	0.001015	8.8056	237.96	2213.8	2451.8	237.98	2365.4	2603.3	0.79148	7.16779	7.95928
335.0	21.72	0.001018	5.0792	258.87	2189.4	2458.3	258.89	2353.2	2612.1	0.85438	7.02436	7.87875
340.0	27.19	0.001021	5.7341	279.80	2185.0	2464.8	279.82	2340.9	2620.7	0.91638	6.88491	7.80128
345.0	33.78	0.001024	4.6778	300.73	2170.5	2471.2	300.77	2328.5	2629.3	0.97751	6.74921	7.72673
350.0	41.68	0.001027	3.8420	321.69	2155.9	2477.6	321.73	2316.0	2637.7	1.03781	6.61710	7.65492
355.0	51.08	0.001030	3.1760	342.66	2141.2	2483.9	342.71	2303.4	2646.1	1.09731	6.48839	7.58570
360.0	62.19	0.001034	2.6409	363.66	2126.4	2490.1	363.72	2290.7	2654.4	1.16504	6.36289	7.51894
365.0	75.26	0.001037	2.0299	384.68	2111.5	2496.2	384.75	2277.8	2662.5	1.21403	6.24046	7.45449
370.0	90.54	0.001041	1.8591	405.12	2096.5	2502.3	405.81	2264.8	2670.6	1.27129	6.12094	7.39223
375.0	108.30	0.001045	1.5723	426.79	2081.4	2508.2	426.91	2251.6	2678.5	1.32787	6.00417	7.33204
380.0	128.85	0.001049	1.3365	447.90	2066.1	2514.0	448.03	2238.2	2686.3	1.38378	5.89001	7.27379
385.0	152.52	0.001053	1.1415	469.04	2050.7	2519.8	469.20	2224.7	2693.9	1.43904	5.77834	7.21738
390.0	179.64	0.001058	0.9794	490.21	2035.2	2525.4	490.40	2210.9	2701.3	1.49369	5.66901	7.16270
395.0	210.59	0.001062	0.8440	511.43	2019.5	2530.9	511.65	2197.0	2708.6	1.54775	5.56190	7.10964
400.0	245.75	0.001067	0.7303	532.68	2003.5	2536.2	532.95	2182.8	2715.7	1.60122	5.45690	7.05812
405.0	285.55	0.001072	0.6345	553.99	1987.5	2541.4	554.29	2168.3	2722.6	1.65415	5.35389	7.00804
410.0	330.42	0.001077	0.5533	575.33	1971.2	2546.5	575.69	2153.6	2729.3	1.70654	5.25277	6.95931
415.0	380.82	0.001082	0.4842	596.73	1954.7	2551.4	597.15	2138.7	2735.8	1.75843	5.15343	6.91186
420.0	437.24	0.001087	0.4253	618.19	1938.0	2556.1	618.66	2123.4	2742.1	1.80982	5.05578	6.86560
425.0	500.18	0.001093	0.3747	639.70	1921.0	2560.7	640.24	2107.9	2748.1	1.86074	4.95972	6.82046
430.0	570.18	0.001098	0.3311	661.27	1903.8	2565.3	661.90	2092.0	2753.9	1.91121	4.86516	6.77637
435.0	647.77	0.001104	0.2935	682.91	1886.4	2569.3	683.62	2075.8	2759.4	1.96124	4.77202	6.73327
440.0	733.55	0.001110	0.2609	704.61	1868.7	2573.3	705.43	2059.3	2764.7	2.01086	4.68022	6.69108
445.0	828.10	0.001117	0.2326	726.39	1850.7	2577.1	727.32	2042.4	2769.7	2.06009	4.58966	6.64975

Temp (K)	Press (kPa)	Specific Volume (m <sup>3</sup> /kg)	Internal Energy (kJ/kg)				Enthalpy (kJ/kg)				Entropy (kJ/kg/K)			
			v <sub>f</sub>	v <sub>g</sub>	u <sub>f</sub>	u <sub>g</sub>	h <sub>f</sub>	h <sub>g</sub>	s <sub>f</sub>	s <sub>g</sub>	h <sub>f,g</sub>	h <sub>g,f</sub>	s <sub>f,g</sub>	s <sub>g,f</sub>
455.0	1046.02	0.001130	0.1862	770.18	1813.9	2584.1	771.37	2007.4	277.8	8	2.15744	4.41199	6.56943	
460.0	1170.68	0.001137	0.1672	792.21	1795.0	2587.2	793.54	1989.4	278.2	9	2.20560	4.32472	6.53032	
465.0	1306.72	0.001144	0.1504	814.33	1775.8	2590.1	815.82	1970.8	278.6	7	2.25345	4.23839	6.49183	
470.0	1454.84	0.001152	0.1356	836.55	1756.2	2592.7	838.22	1951.5	279.0	1	2.30099	4.15929	6.45392	
475.0	1615.75	0.001159	0.1226	858.87	1736.3	2595.7	860.74	1932.4	279.3	2	2.34826	4.06826	6.41652	
480.0	1790.19	0.001167	0.1110	881.30	1715.9	2597.2	883.39	1912.5	279.5	9	2.39527	3.98331	6.37958	
485.0	1978.94	0.001176	0.1006	903.85	1695.2	2599.0	906.18	1892.0	279.8	2	2.44204	3.90101	6.34305	
490.0	2182.77	0.001185	0.0914	926.53	1674.0	2600.6	929.11	1871.0	280.0	1	2.48859	3.81829	6.30688	
495.0	2402.48	0.001194	0.0832	949.34	1652.4	2601.8	952.20	1849.3	280.5	1	2.53495	3.73606	6.27101	
500.0	2638.90	0.001203	0.0758	972.29	1630.0	2602.6	975.46	1827.1	280.2	6	2.58113	3.55426	6.23539	
505.0	2892.85	0.001213	0.0691	995.40	1607.8	2603.2	998.90	1804.3	280.3	2	2.62717	3.57281	6.19997	
510.0	3165.22	0.001223	0.0632	1018.66	1584.7	2603.3	1022.53	1780.2	280.3	3	2.67307	3.59163	6.16470	
515.0	3456.86	0.001233	0.0578	1042.10	1561.0	2603.1	1046.37	1756.5	280.2	8	2.71888	3.41064	6.12952	
520.0	3768.70	0.001245	0.0529	1065.73	1536.8	2602.5	1070.42	1731.5	280.1	9	2.76461	3.32979	6.09437	
525.0	4101.65	0.001256	0.0485	1089.55	1511.9	2601.4	1094.70	1705.7	280.0	4	2.81029	3.24892	6.05921	
530.0	4456.65	0.001268	0.0445	1113.58	1486.4	2599.9	1119.23	1679.1	279.8	3	2.85595	3.16802	6.02396	
535.0	4834.69	0.001281	0.0409	1137.84	1460.1	2598.0	1144.0	1651.5	279.5	6	2.90162	3.08696	5.98857	
540.0	5236.75	0.001294	0.0376	1162.35	1433.1	2595.5	1169.13	1623.1	279.2	2	2.94734	3.00554	5.95298	
545.0	5663.85	0.001308	0.0345	1187.12	1405.4	2592.5	1194.53	1593.6	278.8	1	2.99314	2.92397	5.91711	
550.0	6117.05	0.001323	0.0318	1212.18	1376.7	2588.9	1220.27	1563.0	278.3	3	3.03906	2.84182	5.88087	
555.0	6597.43	0.001339	0.0292	1237.54	1347.2	2584.7	1246.37	1531.3	277.7	6	3.0815	2.75905	5.84420	
560.0	7106.12	0.001355	0.0269	1263.25	1316.6	2579.7	1272.88	1498.3	277.7	3	3.13146	2.67553	5.80700	
565.0	7644.26	0.001373	0.0248	1289.32	1285.0	2574.3	1299.82	1464.0	276.3	8	3.17805	2.59110	5.76915	
570.0	8213.06	0.001392	0.0228	1315.80	1252.2	2568.0	1327.23	1428.2	275.5	4	3.22497	2.50557	5.73054	
575.0	8813.76	0.001412	0.0210	1342.73	1218.0	2560.8	1355.17	1390.8	274.5	9	3.27187	2.41873	5.69103	
580.0	9447.69	0.001433	0.0193	1370.16	1182.5	2552.7	1383.70	1351.6	273.5	3	3.32014	2.33033	5.65048	
585.0	10116.21	0.001457	0.0178	1398.14	1145.4	2543.5	1412.88	1310.5	272.3	3	3.36858	2.24011	5.60849	
590.0	10820.77	0.001482	0.0163	1426.75	1106.4	2533.2	1442.79	1267.1	270.9	9	3.41772	2.14771	5.56544	
595.0	11562.92	0.001510	0.0150	1456.07	1065.5	2521.6	1473.53	1221.4	269.4	9	3.46773	2.05273	5.52046	
600.0	12344.30	0.001540	0.0137	1486.21	1022.2	2508.5	1505.22	1172.8	267.8	0	3.51877	1.95463	5.47340	
605.0	13166.69	0.001573	0.0126	1517.30	976.3	2493.6	1538.01	1120.9	265.8	9	3.57108	1.85272	5.42380	
610.0	14032.02	0.001611	0.0114	1549.53	927.1	2476.6	1572.14	1065.1	263.7	3	3.62498	1.74610	5.37108	
615.0	14942.40	0.001654	0.0104	1583.17	873.9	2457.1	1607.89	1004.6	261.2	5	3.68092	1.63352	5.31444	
620.0	15900.20	0.001704	0.0094	1618.61	815.8	2434.4	1645.70	938.2	258.3	9	3.73955	1.51329	5.25284	
630.0	17969.08	0.001837	0.0075	1697.70	677.9	2375.6	1730.71	780.1	250.8	8	3.86968	1.23822	5.10789	
640.0	20265.91	0.002076	0.0034	1799.92	222.7	2022.7	1842.00	248.9	209.0	9	4.03783	0.38844	4.42627	
647.1	22063.97	0.003209	0.0032	2034.52	0.0	2034.5	2105.33	0.0	2105.3	3	4.43950	0.00000	4.43950	

### C.3 Superheated Steam Table (SI Units)

Press =	0.010 MPa	Tsat=	319.0 K										
T (K) =	325.	350.	400.	450.	500.	550.	600.	650.	700.	800.	900.	1000.	
v-m3/kg	14.9541	16.1208	18.4417	20.7557	23.0669	25.3768	27.6860	29.9947	32.3032	36.177.9	41.5356	46.1514	
u-kj/kg	2446.0	2482.1	2554.3	2627.2	2701.3	2776.8	2853.8	2932.4	3012.6	3177.9	3350.3	3529.6	
h-kj/kg	2595.6	2643.3	2738.7	2834.7	2932.0	3030.6	3130.7	3232.3	3335.6	3547.1	3765.6	3991.2	
s-kj/kg/K	8.18513	8.32676	8.58137	8.80763	9.01251	9.20046	9.37463	9.53734	9.69038	9.977710.2300210.46758			
Press =	0.015 MPa	Tsat=	327.1 K										
T (K) =	350.	400.	450.	500.	550.	600.	650.	700.	800.	900.	1000.	1100.	
v-m3/kg	10.7362	12.2880	13.8328	15.3748	16.9155	18.4555	19.9950	21.5343	24.6123	27.6899	30.7672	33.8444	
u-kj/kg	2481.4	2553.9	2627.0	2701.2	2776.7	2853.7	2932.3	3012.5	3177.9	3350.2	3529.6	3716.1	
h-kj/kg	2642.5	2738.2	2834.5	2931.8	3030.4	3130.6	3232.2	3335.5	3547.1	3765.6	3991.1	4223.8	
s-kj/kg/K	8.13764	8.39336	8.62004	8.82509	9.01314	9.18737	9.35011	9.50318	9.7855910.0428610.2804310.50212				
Press =	0.025 MPa	Tsat=	338.1 K										
T (K) =	350.	400.	450.	500.	550.	600.	650.	700.	800.	900.	1000.	1100.	
v-m3/kg	6.4284	7.3650	8.2944	9.2211	10.1464	11.0710	11.9952	12.9191	14.7664	16.6132	18.4599	20.3063	
u-kj/kg	2480.0	2553.2	2626.6	2700.9	2776.5	2853.6	2932.2	3012.4	3177.8	3350.2	3529.6	3716.1	
h-kj/kg	2640.7	2737.3	2833.9	2931.4	3030.2	3130.4	3232.1	3335.4	3547.0	3765.5	3991.1	4223.7	
s-kj/kg/K	7.89785	8.15585	8.38335	8.58878	8.77701	8.95134	9.11416	9.26727	9.54974	9.8070410.0446310.26633			
Press =	0.040 MPa	Tsat=	349.0 K										
T (K) =	350.	400.	450.	500.	550.	600.	650.	700.	800.	900.	1000.	1100.	
v-m3/kg	4.0050	4.5957	5.1791	5.7596	6.3388	6.9173	7.4953	8.0731	9.2281	10.3826	11.5370	12.6912	
u-kj/kg	2477.8	2552.1	2625.9	2700.5	2776.2	2853.3	2932.0	3012.3	3177.7	3350.1	3529.5	3716.0	
h-kj/kg	2638.0	2736.0	2833.1	2930.8	3029.8	3130.0	3231.8	3335.2	3546.9	3765.4	3991.0	4223.7	
s-kj/kg/K	7.67465	7.93627	8.16504	8.37102	8.55954	8.73403	8.89695	9.05013	9.33269	9.59003	9.8276410.04936		
Press =	0.060 MPa	Tsat=	359.1 K										
T (K) =	400.	450.	500.	550.	600.	650.	700.	800.	900.	1000.	1100.	1200.	
v-m3/kg	3.05719	3.44835	3.83661	4.22350	4.60967	4.99541	5.38086	6.15124	6.92120	7.69092	8.46050	9.22998	
u-kj/kg	2550.7	2625.1	2699.9	2775.8	2853.0	2931.8	3012.0	3177.6	3350.0	3529.4	3716.0	3909.4	
h-kj/kg	2734.1	2832.0	2930.1	3029.2	3129.6	3231.5	3334.9	3546.7	3765.3	3990.9	4223.6	4463.2	
s-kj/kg/K	7.74553	7.97603	8.18276	8.37166	8.54637	8.70943	8.86270	9.14537	9.40277	9.64043	9.8621710.07059		

Press =	0.101	MPa	Tsat=	373.1	K							
T (K) =	400.	450.		500.	550.	600.	650.	700.	800.	900.	1000.	1100.
v-m3/kg	1.80206	2.03654	2.26798	2.49803	2.72735	2.95623	3.18482	3.64148	4.09772	4.55372	5.00959	5.46535
u-kj/kg	2547.7	2623.3	2698.7	2774.9	2852.4	2931.2	3011.6	3177.3	3349.8	3522.3	3715.8	3909.3
h-kj/kg	2730.3	2829.7	2928.5	3028.1	3128.7	3230.8	3334.3	3546.3	3765.0	3990.7	4223.4	4463.0
s-kj/kg/K	7.49608	7.73027	7.93859	8.12828	8.30345	8.46679	8.62025	8.90315	9.16068	9.39942	9.62020	9.82866
Press =	0.200	MPa	Tsat=	393.4	K							
T (K) =	400.	450.		500.	550.	600.	650.	700.	800.	900.	1000.	1100.
v-m3/kg	0.90251	1.02507	1.14427	1.26200	1.37897	1.49549	1.61172	1.84366	2.07517	2.30945	2.53758	2.76862
u-kj/kg	2540.0	2619.0	2695.9	2772.9	2850.8	2930.0	3010.6	3176.6	3349.2	3528.8	3715.5	3909.0
h-kj/kg	2720.5	2824.0	2924.8	3025.3	3126.6	3229.1	3332.9	3545.3	3764.3	3990.1	4223.0	4462.7
s-kj/kg/K	7.16292	7.40676	7.61907	7.81074	7.98701	8.15104	8.30496	8.58842	8.84625	9.08417	9.30606	9.51459
Press =	0.300	MPa	Tsat=	406.7	K							
T (K) =	450.	500.		550.	600.	650.	700.	800.	900.	1000.	1100.	1200.
v-m3/kg	0.67872	0.75960	0.83891	0.91743	0.99550	1.07327	1.22829	1.38288	1.53724	1.69145	1.84557	1.99962
u-kj/kg	2614.4	2693.0	2770.8	2849.2	2928.7	3009.6	3175.8	3348.7	3528.4	3715.1	3908.7	4108.8
h-kj/kg	2818.1	2920.8	3022.5	3124.5	3227.4	3331.5	3544.3	3763.5	3989.6	4222.6	4462.4	4708.7
s-kj/kg/K	7.20939	7.42604	7.61979	7.79722	7.96195	8.11634	8.40036	8.65851	8.89861	9.11862	9.32722	9.52438
Press =	0.400	MPa	Tsat=	416.8	K							
T (K) =	450.	500.		550.	600.	650.	700.	800.	900.	1000.	1100.	1200.
v-m3/kg	0.50545	0.56722	0.62735	0.68666	0.74550	0.80405	0.92061	1.03674	1.15263	1.26838	1.38404	1.49963
u-kj/kg	2609.7	2690.0	2768.7	2847.6	2927.4	3008.5	3175.1	3348.1	3528.0	3714.8	3908.4	4108.6
h-kj/kg	2811.9	2916.9	3019.6	3122.3	3225.6	3330.1	3543.3	3762.8	3989.0	4222.2	4462.0	4708.5
s-kj/kg/K	7.06594	7.28723	7.48316	7.66177	7.82722	7.98208	8.26667	8.52513	8.76341	8.98553	9.19421	9.39142
Press =	0.500	MPa	Tsat=	425.0	K							
T (K) =	450.	500.		550.	600.	650.	700.	800.	900.	1000.	1100.	1200.
v-m3/kg	0.40140	0.45177	0.50040	0.54819	0.59550	0.64251	0.73599	0.82905	0.92187	1.01455	1.10712	1.19964
u-kj/kg	2604.8	2686.9	2766.6	2846.0	2926.2	3007.5	3174.3	3347.6	3527.6	3714.5	3908.1	4108.4
h-kj/kg	2805.5	2912.8	3016.8	3120.1	3223.9	3328.7	3542.3	3762.1	3988.5	4221.7	4461.7	4708.2
s-kj/kg/K	6.95182	7.17807	7.37626	7.55608	7.72226	7.87760	8.16276	8.42153	8.66000	8.88223	9.09098	9.28825

Press =	0.600	MPa	Tsat=	432.0	K							
T (K) =	450.	500.	550.	600.	650.	700.	800.	900.	1000.	1100.	1200.	1300.
v-m3/kg	0.33195	0.37477	0.41576	0.45587	0.49549	0.53482	0.61292	0.69059	0.76803	0.84532	0.92251	0.99965
u-kj/kg	259.7	2683.8	2764.4	2844.4	2924.9	3006.4	3173.6	3347.0	3527.1	3714.1	3907.8	4108.1
h-kj/kg	2798.8	2908.7	3013.9	3117.9	3222.2	3327.3	3541.4	3761.4	3988.0	4221.3	4461.3	4707.9
s-kj/kg/K	6.85603	7.08760	7.28815	7.46921	7.63613	7.79195	8.07769	8.33677	8.57542	8.79777	9.00659	9.20392
Press =	0.700	MPa	Tsat=	438.1	K							
T (K) =	450.	500.	550.	600.	650.	700.	800.	900.	1000.	1100.	1200.	1300.
v-m3/kg	0.28228	0.31976	0.35529	0.38992	0.42406	0.45789	0.52501	0.59170	0.65814	0.72444	0.79065	0.85679
u-kj/kg	2594.3	2680.6	2762.2	2842.7	2923.6	3005.4	3172.9	3346.5	3526.7	3713.8	3907.5	4107.9
h-kj/kg	2791.9	2904.4	3010.9	3115.7	3220.4	3325.9	3540.4	3760.7	3987.4	4220.9	4461.0	4707.6
s-kj/kg/K	6.77268	7.00998	7.21299	7.39533	7.56300	7.71931	8.00562	8.26502	8.50385	8.72631	8.93521	9.13258
Press =	0.800	MPa	Tsat=	443.6	K							
T (K) =	450.	500.	550.	600.	650.	700.	800.	900.	1000.	1100.	1200.	1300.
v-m3/kg	0.24496	0.27847	0.30993	0.34046	0.37049	0.40020	0.45908	0.51752	0.57572	0.63339	0.69175	0.74965
u-kj/kg	2588.7	2677.4	2760.0	2841.1	2922.3	3004.3	3172.1	3345.9	3526.3	3713.4	3907.3	4107.6
h-kj/kg	2784.7	2900.1	3007.9	3113.5	3218.7	3324.5	3539.4	3759.9	3986.9	4220.4	4460.7	4707.4
s-kj/kg/K	6.69816	6.94173	7.14729	7.33094	7.49938	7.65617	7.94306	8.20278	8.44180	8.66437	8.87334	9.07077
Press =	0.900	MPa	Tsat=	448.5	K							
T (K) =	450.	500.	550.	600.	650.	700.	800.	900.	1000.	1100.	1200.	1300.
v-m3/kg	0.21586	0.24634	0.27465	0.30199	0.32881	0.35533	0.40779	0.45983	0.51162	0.56327	0.61483	0.66632
u-kj/kg	2582.7	2674.0	2757.8	2839.4	2921.0	3003.3	3171.4	3345.4	3525.9	3713.1	3907.0	4107.4
h-kj/kg	2777.0	2895.7	3004.9	3111.2	3216.9	3323.1	3538.4	3759.2	3986.3	4220.0	4460.3	4707.1
s-kj/kg/K	6.63002	6.88060	7.08881	7.27380	7.44301	7.60031	7.88778	8.14781	8.38701	8.60970	8.81874	9.01622
Press =	1.000	MPa	Tsat=	453.0	K							
T (K) =	500.	550.	600.	650.	700.	800.	900.	1000.	1100.	1200.	1300.	1400.
v-m3/kg	0.22063	0.24641	0.27121	0.29547	0.31943	0.36677	0.41368	0.46034	0.50687	0.55329	0.59966	0.64598
u-kj/kg	2670.6	2755.5	2837.8	2919.7	3002.2	3170.6	3344.8	3525.4	3712.7	3906.7	4107.1	4313.9
h-kj/kg	2891.3	3001.9	3109.0	3215.2	3321.6	3537.4	3758.5	3985.8	4219.6	4460.0	4706.8	4959.9
s-kj/kg/K	6.82505	7.03601	7.22237	7.39237	7.55017	7.83822	8.09857	8.33796	8.56076	8.76988	8.96741	9.15493

Press =	1.200	MPa	Tsat=	461.1	K
T (K) =	500.	550.	600.	650.	700.
v-m3/kg	0.18201	0.20405	0.22503	0.24546	0.26557
u-kj/kg	2663.7	2750.9	2834.4	2917.1	3000.1
h-kj/kg	2882.1	2995.7	3104.4	3211.6	3318.8
s-kj/kg/K	6.72659	6.94336	7.13256	7.30417	7.46298
Press =	1.400	MPa	Tsat=	468.2	K
T (K) =	500.	550.	600.	650.	700.
v-m3/kg	0.15437	0.17376	0.19203	0.20974	0.22711
u-kj/kg	2656.4	2746.2	2831.0	2914.4	2998.0
h-kj/kg	2872.5	2989.4	3099.8	3208.1	3315.9
s-kj/kg/K	6.64047	6.86348	7.05567	7.22894	7.38878
Press =	1.600	MPa	Tsat=	474.5	K
T (K) =	500.	550.	600.	650.	700.
v-m3/kg	0.13360	0.15103	0.16728	0.18294	0.19825
u-kj/kg	2648.8	2741.3	2827.5	2911.8	2995.8
h-kj/kg	2862.6	2983.0	3095.2	3204.5	3313.0
s-kj/kg/K	6.56317	6.79289	6.98820	7.16319	7.32408
Press =	1.800	MPa	Tsat=	480.3	K
T (K) =	500.	550.	600.	650.	700.
v-m3/kg	0.11740	0.13334	0.14802	0.16209	0.17581
u-kj/kg	2640.9	2736.4	2824.0	2909.1	2993.7
h-kj/kg	2852.2	2976.4	3090.5	3200.9	3310.1
s-kj/kg/K	6.49238	6.72934	6.92792	7.10466	7.26663
Press =	2.000	MPa	Tsat=	485.5	K
T (K) =	500.	550.	600.	650.	700.
v-m3/kg	0.10439	0.11917	0.13261	0.14541	0.15786
u-kj/kg	2632.6	2731.3	2820.5	2906.4	2991.5
h-kj/kg	2841.4	2969.7	3085.7	3197.2	3307.2
s-kj/kg/K	6.42645	6.67128	6.87328	7.05184	7.21490

Press =	2.500	MPa	Tsat=	497.1	K							
T (K) =	500.	550.	600.	650.	700.	800.	900.	1000.	1100.	1200.	1300.	1400.
v-m3/kg	0.08080	0.09361	0.10484	0.11538	0.12553	0.14522	0.16445	0.18342	0.20226	0.22099	0.23967	0.25830
u-kj/kg	2609.7	2718.1	2811.4	2899.5	2986.1	3159.4	3336.5	3519.0	3707.5	3902.4	4103.5	4310.8
h-kj/kg	2811.7	2952.2	3073.5	3188.0	3299.9	3522.5	3747.6	3977.6	4213.2	4454.8	4702.7	4956.5
s-kj/kg/K	6.27535	6.54361	6.75484	6.93818	7.10407	7.40126	7.66643	7.90864	8.13314	8.34338	8.54170	8.72980
Press =	3.000	MPa	Tsat=	507.0	K							
T (K) =	550.	600.	650.	700.	800.	900.	1000.	1100.	1200.	1300.	1400.	1500.
v-m3/kg	0.07650	0.08631	0.09534	0.10397	0.12060	0.13675	0.15265	0.16841	0.18407	0.19967	0.21522	0.23074
u-kj/kg	2704.1	2801.9	2892.5	2980.5	3155.6	3333.7	3516.8	3705.8	3900.9	4102.3	4309.7	4523.0
h-kj/kg	2933.7	3060.9	3178.5	3292.5	3517.4	3744.0	3974.8	4211.0	4453.1	4701.3	4955.4	5215.2
s-kj/kg/K	6.43310	6.65462	6.84310	7.01196	7.31236	7.57918	7.82233	8.04742	8.25802	8.45662	8.64491	8.82414
Press =	3.500	MPa	Tsat=	515.7	K							
T (K) =	550.	600.	650.	700.	800.	900.	1000.	1100.	1200.	1300.	1400.	1500.
v-m3/kg	0.06422	0.07304	0.08102	0.08857	0.10301	0.11697	0.13068	0.14424	0.15770	0.17110	0.18445	0.19777
u-kj/kg	2689.3	2792.2	2885.4	2974.9	3151.8	3330.9	3514.7	3704.1	3899.5	4101.0	4308.7	4522.1
h-kj/kg	2914.0	3047.8	3168.9	3284.9	3512.4	3740.3	3972.1	4208.9	4451.4	4699.9	4954.3	5214.3
s-kj/kg/K	6.33371	6.56677	6.76677	6.93274	7.23644	7.50492	7.74903	7.97469	8.18567	8.38453	8.57302	8.75240
Press =	4.000	MPa	Tsat=	523.5	K							
T (K) =	550.	600.	650.	700.	800.	900.	1000.	1100.	1200.	1300.	1400.	1500.
v-m3/kg	0.05494	0.06306	0.07027	0.07701	0.08982	0.10213	0.11419	0.12610	0.13792	0.14967	0.16138	0.17305
u-kj/kg	2673.4	2782.0	2878.1	2969.3	3148.0	3328.1	3512.5	3702.3	3898.0	4099.8	4307.6	4521.2
h-kj/kg	2893.1	3034.3	3159.1	3277.3	3507.3	3736.7	3969.3	4206.7	4449.7	4698.5	4953.1	5213.4
s-kj/kg/K	6.24171	6.48774	6.68676	6.86621	7.17000	7.44017	7.68524	7.91147	8.12284	8.32196	8.51064	8.69017
Press =	4.500	MPa	Tsat=	530.6	K							
T (K) =	550.	600.	650.	700.	800.	900.	1000.	1100.	1200.	1300.	1400.	1500.
v-m3/kg	0.04765	0.05528	0.06189	0.06802	0.07955	0.09059	0.10137	0.11200	0.12254	0.13300	0.14343	0.15382
u-kj/kg	2656.3	2771.5	2870.6	2963.5	3144.1	3325.3	3510.4	3700.6	3896.6	4098.6	4306.6	4520.3
h-kj/kg	2870.7	3020.3	3149.1	3269.6	3502.1	3733.0	3966.5	4204.6	4448.0	4697.1	4952.0	5212.5
s-kj/kg/K	6.15444	6.41525	6.62155	6.80022	7.11079	7.38267	7.62871	7.85553	8.06727	8.26666	8.45554	8.63521

Press =	5.000	MPa	Tsat=	537.1	K
T (K) =	550.	600.	700.	800.	900.
v-m3/kg	0.04175	0.04904	0.05519	0.06082	0.07134
u-kj/kg	2637.7	2760.6	2862.9	2957.7	3140.3
h-kj/kg	2846.5	3005.8	3138.9	3261.8	3497.0
s-kj/kg/K	6.06984	6.34772	6.56087	6.74313	7.05728
Press =	6.000	MPa	Tsat=	548.7	K
T (K) =	550.	600.	700.	800.	900.
v-m3/kg	0.03267	0.03961	0.04510	0.05001	0.05902
u-kj/kg	2594.6	2737.5	2847.1	2945.8	3132.5
h-kj/kg	2790.6	2975.2	3117.7	3245.9	3486.6
s-kj/kg/K	5.90115	6.22319	6.45166	6.64164	6.96328
Press =	7.000	MPa	Tsat=	559.0	K
T (K) =	600.	650.	700.	800.	900.
v-m3/kg	0.03280	0.03787	0.04227	0.05022	0.05762
u-kj/kg	2712.3	2830.5	2933.5	3124.5	3311.1
h-kj/kg	2941.9	3095.6	3229.5	3476.1	3714.4
s-kj/kg/K	6.10772	6.35409	6.55258	6.88213	7.16288
Press =	8.000	MPa	Tsat=	568.2	K
T (K) =	600.	650.	700.	800.	900.
v-m3/kg	0.02761	0.03241	0.03646	0.04361	0.05020
u-kj/kg	2684.6	2813.1	2920.9	3116.5	3305.3
h-kj/kg	2905.5	3072.4	3212.6	3465.4	3706.9
s-kj/kg/K	5.99692	6.26455	6.47242	6.81035	7.09482
Press =	9.000	MPa	Tsat=	576.5	K
T (K) =	600.	650.	700.	800.	900.
v-m3/kg	0.02349	0.02815	0.03193	0.03847	0.04442
u-kj/kg	2653.8	2794.8	2907.9	3108.4	3299.5
h-kj/kg	2865.2	3048.1	3195.2	3454.6	3699.3
s-kj/kg/K	5.88729	6.18066	6.39887	6.74568	7.03398

Press = 10.000 MPa Tsat= 584.1 K  
 $T(K) = 600.$  650. 700. 800. 900. 1000. 1100. 1200. 1300. 1400. 1500. 1600.  
 $v-m3/kg = 0.02009$  0.02471 0.02829 0.03436 0.03980 0.04496 0.04995 0.05485 0.05968 0.06446 0.06921 0.07393  
 $u-kj/kg = 261.9$  2775.4 2894.4 3100.1 3293.7 3486.2 3681.2 3880.5 4085.1 4295.1 4510.4 4730.7  
 $h-kj/kg = 281.9$  281.8 3022.5 3177.3 3443.7 3691.7 3935.8 4180.7 4429.0 4681.9 4939.7 5202.5 5470.0  
 $s-kj/kg/K = 5.77538$  6.10069 6.33038 6.68660 6.97883 7.23595 7.46938 7.68539 7.88777 8.07881 8.26009 8.43276

Press = 12.000 MPa Tsat= 597.8 K  
 $T(K) = 600.$  650. 700. 750. 800. 850. 900. 950. 1000. 1050.  
 $v-m3/kg = 0.01459$  0.01947 0.02280 0.02562 0.02818 0.03058 0.03287 0.03510 0.03727 0.03940  
 $u-kj/kg = 2528.8$  2733.1 2866.2 2979.0 3083.3 3183.5 3281.9 3379.6 3477.2 3575.3  
 $h-kj/kg = 2703.9$  2966.8 3139.8 3286.5 3421.4 3550.4 3676.4 3800.7 3924.4 4048.1  
 $s-kj/kg/K = 5.52472$  5.94753 6.20430 6.40683 6.58105 6.73752 6.88148 7.01595 7.14285 7.26349

Press = 14.000 MPa Tsat= 609.8 K  
 $T(K) = 650.$  700. 750. 800. 850. 900. 950. 1000. 1050.  
 $v-m3/kg = 0.01563$  0.01885 0.02145 0.02376 0.02589 0.02792 0.02987 0.03177 0.03363  
 $u-kj/kg = 2684.9$  2835.9 2957.0 3066.0 3169.3 3269.9 3369.2 3468.2 3567.3  
 $h-kj/kg = 2903.7$  3099.8 3257.3 3398.6 3531.8 3660.8 3787.5 3913.0 4038.1  
 $s-kj/kg/K = 5.79671$  6.08799 6.30540 6.48786 6.64947 6.79693 6.933391 7.06267 7.18475

Press = 16.000 MPa Tsat= 620.5 K  
 $T(K) = 650.$  700. 750. 800. 850. 900. 950. 1000. 1050.  
 $v-m3/kg = 0.01263$  0.01586 0.01831 0.02044 0.02238 0.02421 0.02596 0.02765 0.02930  
 $u-kj/kg = 2628.3$  2803.4 2933.9 3048.2 3154.8 3257.8 3358.8 3459.1 3559.3  
 $h-kj/kg = 2830.4$  3057.1 3226.9 3375.1 3512.9 3645.1 3774.1 3901.5 4028.1  
 $s-kj/kg/K = 5.64059$  5.97752 6.21205 6.40350 6.57059 6.72171 6.86128 6.99195 7.11548

Press = 18.000 MPa Tsat= 630.1 K  
 $T(K) = 650.$  700. 750. 800. 850. 900. 950. 1000. 1050.  
 $v-m3/kg = 0.01014$  0.01350 0.01586 0.01785 0.01964 0.02132 0.02291 0.02445 0.02594  
 $u-kj/kg = 2559.0$  2768.3 2909.9 3029.8 3140.1 3245.4 3348.3 3449.9 3551.2  
 $h-kj/kg = 2741.5$  3011.2 3195.3 3351.1 3493.7 3629.2 3760.7 3890.0 4018.1  
 $s-kj/kg/K = 5.46893$  5.87012 6.12446 6.32572 6.49863 6.65356 6.79580 6.92843 7.05344

Press = 20.000 MPa Tsat= 638.9 K  
 $T(K) = 650.$  700. 750. 800. 850. 900. 950. 1000. 1050.  
 $v-m3/kg = 0.00790$  0.01158 0.01388 0.01577 0.01745 0.01901 0.02047 0.02188 0.02325  
 $u-kj/kg = 2466.8$  2730.1 2884.7 3011.0 3125.0 3232.9 3337.6 3440.7 3543.0  
 $h-kj/kg = 2624.9$  2961.6 3162.4 3326.5 3474.1 3613.1 3747.1 3878.4 4008.0  
 $s-kj/kg/K = 5.26183$  5.76355 6.04101 6.25298 6.43206 6.59096 6.73595 6.87059 6.99709

Press = 22.000 MPa Tsat= 646.9 K  
 $T(K) = 650.$  700. 750. 800. 850. 900. 950. 1000. 1050.  
 $v-m3/kg = 0.00147$  0.00997 0.01226 0.01407 0.01566 0.01711 0.01848 0.01979 0.02105  
 $u-kj/kg = 1596.4$  2688.3 2858.4 2991.6 3109.7 3220.3 3326.9 3431.4 3534.9  
 $h-kj/kg = 1698.6$  2907.8 3128.1 3301.2 3454.2 3596.8 3733.5 3866.7 3997.9  
 $s-kj/kg/K = 3.69088$  5.65591 5.96051 6.18419 6.36978 6.53282 6.68065 6.81732 6.94536

Press = 24.000 MPa  
 $T(K) = 650.$  700. 750. 800. 850. 900. 950. 1000. 1050.  
 $v-m3/kg = 0.00146$  0.00861 0.01090 0.01265 0.01416 0.01554 0.01682 0.01804 0.01921  
 $u-kj/kg = 1590.2$  2642.3 2830.8 2971.7 3094.1 3207.5 3316.1 3422.0 3526.6  
 $h-kj/kg = 1695.8$  2848.9 3092.4 3275.4 3434.0 3580.4 3719.7 3855.0 3987.8  
 $s-kj/kg/K = 3.68017$  5.54534 5.888208 6.11853 6.31101 6.47834 6.62908 6.76784 6.89743

Press = 26.000 MPa  
 $T(K) = 650.$  700. 750. 800. 850. 900. 950. 1000. 1050.  
 $v-m3/kg = 0.00145$  0.00742 0.00974 0.01145 0.01290 0.01420 0.01542 0.01656 0.01766  
 $u-kj/kg = 1584.4$  2591.2 2801.9 2951.2 3078.2 3194.5 3305.1 3412.6 3518.4  
 $h-kj/kg = 1693.3$  2784.1 3055.2 3248.9 3413.6 3563.8 3705.9 3843.2 3977.7  
 $s-kj/kg/K = 3.67008$  5.42987 5.80500 6.05541 6.25513 6.42692 6.58065 6.72153 6.85270

#### C.4 H<sub>2</sub>O Compressed Liquid Table (SI Units)

Press = 28.000 MPa							
T (K) =	650.	700.	750.	800.	850.	900.	950.
v-m3/kg	0.00144	0.00637	0.00874	0.01042	0.01182	0.01306	0.01421
u-kj/kg	1578.9	2533.7	2771.6	2930.2	3062.0	3181.4	3294.1
h-kj/kg	1691.1	2712.0	3016.4	3221.9	3392.8	3547.1	3692.0
s-kj/kg/K	3.66050	5.30724	5.72875	5.99434	6.20169	6.37808	6.53487
Press = 30.000 MPa							
T (K) =	650.	700.	750.	800.	850.	900.	950.
v-m3/kg	0.00143	0.00543	0.00787	0.00952	0.01088	0.01207	0.01317
u-kj/kg	1573.7	2468.6	2739.9	2908.7	3045.6	3168.1	3283.0
h-kj/kg	1689.1	2631.5	2976.2	3194.4	3371.8	3530.2	3678.1
s-kj/kg/K	3.65138	5.17540	5.65290	5.93499	6.15032	6.33146	6.49139
Press = 35.000 MPa							
T (K) =	650.	700.	750.	800.	850.	900.	950.
v-m3/kg	0.00141	0.00141	0.00613	0.00773	0.00900	0.01010	0.01109
u-kj/kg	1561.7	1701.7	2654.4	2852.5	3003.4	3134.3	3254.9
h-kj/kg	1685.0	1899.7	2868.9	3123.2	3318.4	3487.6	3643.0
s-kj/kg/K	3.63027	3.833785	5.46347	5.79237	6.02927	6.22286	6.39089
Press = 40.000 MPa							
T (K) =	650.	700.	750.	800.	850.	900.	950.
v-m3/kg	0.00139	0.00139	0.00483	0.00640	0.00760	0.00862	0.00953
u-kj/kg	1550.8	1691.1	2560.8	2793.3	2959.9	3099.8	3226.4
h-kj/kg	1681.8	1897.7	2754.1	3049.3	3263.9	3444.6	3607.7
s-kj/kg/K	3.61114	3.81901	5.27412	5.65605	5.91650	6.12322	6.29967

Temperature=	273.1 K	P <sub>sat</sub> =	0.001 MPa						
Press(MPa)=	1	2	5	8	10	15	20	25	30
v-m3/kg	0.001	0.001	0.001	0.001	0.001	0.00099	0.00099	0.00099	0.00098
u-kj/kg	0	0	0	0.1	0.1	0.2	0.2	0.3	0.3
h-kj/kg	1	2	5	8.1	10.1	15.1	20	25	29.1
s-kJ/kg/K	0	0	0.00014	0.00027	0.00034	0.00045	0.00047	0.00041	0.00028
Temperature=	280.0 K	P <sub>sat</sub> =	0.001 MPa						
Press(MPa)=	1	2	5	8	10	15	20	25	30
v-m3/kg	0.001	0.001	0.001	0.001	0.001	0.00099	0.00099	0.00099	0.00098
u-kj/kg	28.8	28.8	28.7	28.7	28.6	28.5	28.4	28.3	27.9
h-kj/kg	29.8	30.8	33.7	36.7	38.6	43.5	48.3	53.1	57.9
s-kJ/kg/K	0.10407	0.10402	0.10386	0.10368	0.10354	0.10315	0.1027	0.10219	0.10162
Temperature=	300.0 K	P <sub>sat</sub> =	0.004 MPa						
Press(MPa)=	1	2	5	8	10	15	20	25	30
v-m3/kg	0.001	0.001	0.001	0.001	0.001	0.00099	0.00099	0.00099	0.00098
u-kj/kg	112.5	112.4	112.2	111.9	111.8	111.4	111	110.6	110.2
h-kj/kg	113.5	114.4	117.2	119.9	121.7	126.3	130.8	135.4	139.9
s-kJ/kg/K	0.39285	0.39257	0.39174	0.39089	0.39033	0.3889	0.38744	0.38597	0.38448
Temperature=	320.0 K	P <sub>sat</sub> =	0.011 MPa						
Press(MPa)=	1	2	5	8	10	15	20	25	30
v-m3/kg	0.00101	0.00101	0.00101	0.00101	0.00101	0.001	0.001	0.001	0.00099
u-kj/kg	196	195.9	195.5	195	194.8	194.1	193.4	192.8	192.1
h-kj/kg	197	197.9	200.5	203.1	204.8	209.2	213.5	217.8	222.1
s-kJ/kg/K	0.66242	0.66198	0.66066	0.65934	0.65847	0.65628	0.65409	0.65191	0.64973

Temperature=		340.0 K		Psat= 0.027 MPa									
Press(MPa)=		1		2		5		8		10		15	
v-m3/kg	0.00102	0.00102	0.00102	0.00102	0.00102	0.00102	0.00102	0.00101	0.00101	0.00101	0.00101	0.00101	0.00101
u-kj/kg	279.6	279.4	278.8	278.3	277.9	276.9	276.9	276	275.1	274.2	274.2	274.2	274.2
h-kj/kg	280.6	281.5	283.9	286.4	288	292.2	292.2	296.3	300.4	304.5	304.5	304.5	304.5
s-kj/kg/K	0.91582	0.91524	0.91352	0.91181	0.91067	0.90785	0.90785	0.90504	0.90226	0.89949	0.89949	0.89949	0.89949
Temperature=		360.0 K		Psat= 0.062 MPa									
Press(MPa)=		1		2		5		8		10		15	
v-m3/kg	0.00103	0.00103	0.00103	0.00103	0.00103	0.00103	0.00103	0.00103	0.00102	0.00102	0.00102	0.00102	0.00102
u-kj/kg	363.4	363.2	362.4	361.7	361.2	361.2	361.2	360	358.8	357.7	356.5	356.5	356.5
h-kj/kg	364.5	365.2	367.6	369.9	371.5	375.4	375.4	379.3	383.2	387.1	387.1	387.1	387.1
s-kj/kg/K	1.15538	1.15468	1.15259	1.15052	1.14914	1.14573	1.14573	1.14236	1.13902	1.13572	1.12283	1.12283	1.12283
Temperature=		380.0 K		Psat= 0.129 MPa									
Press(MPa)=		1		2		5		8		10		15	
v-m3/kg	0.00105	0.00105	0.00105	0.00105	0.00104	0.00104	0.00104	0.00104	0.00104	0.00104	0.00104	0.00104	0.00104
u-kj/kg	447.6	447.3	446.4	445.5	444.9	443.4	443.4	441.9	441.9	440.5	439.1	439.1	439.1
h-kj/kg	448.7	449.4	451.6	453.8	455.3	459	459	462.7	466.4	470.1	470.1	470.1	470.1
s-kj/kg/K	1.38306	1.38224	1.37978	1.37735	1.37574	1.37175	1.37175	1.36782	1.36394	1.36011	1.34526	1.34526	1.34526
Temperature=		400.0 K		Psat= 0.246 MPa									
Press(MPa)=		1		2		5		8		10		15	
v-m3/kg	0.00107	0.00107	0.00107	0.00106	0.00106	0.00106	0.00106	0.00106	0.00106	0.00106	0.00106	0.00106	0.00106
u-kj/kg	532.4	532	530.9	529.8	529	527.3	527.3	525.5	523.8	522.1	522.1	522.1	522.1
h-kj/kg	533.5	534.1	536.2	538.3	539.7	543.1	543.1	546.6	550.1	553.6	553.6	553.6	553.6
s-kj/kg/K	1.60051	1.59955	1.59672	1.59392	1.59207	1.58749	1.58749	1.58298	1.57854	1.57417	1.57417	1.57417	1.57417

Temperature=	420.0	K	P <sub>sat</sub> =	0.437	MPa						
Press(MPa)=	1		2	5		8	10	15	20	25	30
v-m3/kg	0.00109		0.00109	0.000108		0.000108	0.000108	0.000108	0.000107	0.000107	0.000106
u-kj/kg	617.9		617.5	616.1		614.8	613.9	611.7	609.6	607.6	605.6
h-kj/kg	619		619.6	621.5		623.4	624.7	627.9	631.1	634.4	637.7
s-kj/kg/K	1.8092		1.80811	1.80487		1.80166	1.79954	1.79432	1.78919	1.78415	1.7792
Temperature=	440.0	K	P <sub>sat</sub> =	0.734	MPa						
Press(MPa)=	1		2	5		8	10	15	20	25	30
v-m3/kg	0.00111		0.00111	0.000111		0.00011	0.00011	0.00011	0.000109	0.000109	0.000108
u-kj/kg	704.5		703.9	702.3		700.7	699.6	697.1	694.6	692.1	689.8
h-kj/kg	705.6		706.1	707.8		709.5	710.7	713.6	716.5	719.5	722.4
s-kj/kg/K	2.01053		2.00928	2.00556		2.00189	1.99947	1.99352	1.9877	1.98199	1.9764
Temperature=	460.0	K	P <sub>sat</sub> =	1.171	MPa						
Press(MPa)=	1		2	5		8	10	15	20	25	30
v-m3/kg	0.19849		0.00114	0.000113		0.000113	0.000113	0.000113	0.000112	0.000112	0.000111
u-kj/kg	2597		791.7	789.7		787.8	786.5	783.4	780.5	777.6	774.8
h-kj/kg	2795.5		793.9	795.4		796.8	797.8	800.3	802.9	805.5	808.2
s-kj/kg/K	6.62522		2.20441	2.20012		2.19591	2.19314	2.18633	2.1797	2.17322	2.16689
Temperature=	480.0	K	P <sub>sat</sub> =	1.790	MPa						
Press(MPa)=	1		2	5		8	10	15	20	25	30
v-m3/kg	0.20981		0.00117	0.000116		0.000116	0.000116	0.000116	0.000115	0.000114	0.000114
u-kj/kg	2634.9		881.1	878.7		876.4	874.9	871.2	867.6	864.2	860.9
h-kj/kg	2844.7		883.5	884.6		885.7	886.5	888.5	890.6	892.8	895.1
s-kj/kg/K	6.73004		2.39491	2.38993		2.38504	2.38184	2.374	2.36639	2.35899	2.35179

Temperature=	500.0	K	P <sub>sat</sub> =	2.639	MPa						
Press(MPa)=	1		2	5		8	10	15	20	25	30
v·m3/kg	0.22063	0.10439	0.0012	0.0012	0.00119	0.00119	0.00118	0.00118	0.00117	0.00115	
u·kj/kg	2670.6	2632.6	970	967.1	965.3	960.8	956.5	952.3	948.4	933.8	
h·kj/kg	2891.3	2841.4	976	976.7	977.2	978.6	980.1	981.7	983.5	991.3	
s·kj/kg/K	6.82505	6.42645	2.57651	2.57075	2.56699	2.55784	2.54901	2.54049	2.53223	2.50153	
Temperature=	520.0	K	P <sub>sat</sub> =	3.769	MPa						
Press(MPa)=	1		2	5		8	10	15	20	25	30
v·m3/kg	0.23111	0.11055	0.00124	0.00124	0.00123	0.00123	0.00122	0.00122	0.00121	0.00121	0.00118
u·kj/kg	2705.1	2674	1064.2	1060.7	1058.3	1052.8	1047.5	1042.5	1037.7	1037.7	1020.3
h·kj/kg	2936.2	2895.1	1070.4	1070.6	1070.7	1071.2	1071.9	1072.8	1073.8	1073.8	1079.4
s·kj/kg/K	6.91324	6.53188	2.7617	2.75477	2.75027	2.73938	2.72897	2.719	2.70941	2.67426	
Temperature=	540.0	K	P <sub>sat</sub> =	5.237	MPa						
Press(MPa)=	1		2	5		8	10	15	20	25	30
v·m3/kg					0.00129	0.00128	0.00127	0.00126	0.00125	0.00125	0.00122
u·kj/kg					1158.1	1155.1	1148.1	1141.5	1135.2	1129.3	1108.5
h·kj/kg					1168.4	1168	1167.2	1166.7	1166.6	1166.7	1169.3
s·kj/kg/K					2.93939	2.93382	2.9205	2.90793	2.89602	2.88469	2.84393
Temperature=	560.0	K	P <sub>sat</sub> =	7.106	MPa						
Press(MPa)=	1		2	5		8	10	15	20	25	30
v·m3/kg					0.00135	0.00135	0.00133	0.00132	0.00131	0.00129	0.00126
u·kj/kg					1261.4	1257.4	1248	1239.4	1231.5	1224.1	1198.7
h·kj/kg					1272.2	1270.8	1268	1265.8	1264.2	1263	1261.6
s·kj/kg/K					3.12812	3.12086	3.1038	3.08808	3.07344	3.0597	3.01163



## C.5 The Saturation Temperature vs. Pressure (English Units)

Press (psi)	Temp (R)	Specific Volume (ft <sup>3</sup> /lbm)	Internal Energy (Btu/lbm)				Enthalpy (Btu/lbm)				Entropy (Btu/1bm·R)			
		v <sub>f</sub>	v <sub>g</sub>	u <sub>f</sub>	u <sub>fg</sub>	u <sub>g</sub>	h <sub>f</sub>	h <sub>fg</sub>	h <sub>g</sub>	s <sub>f</sub>	s <sub>fg</sub>	s <sub>g</sub>		
0.1	494.7	0.0161	2951.1577	3.01	1021.2	1024.2	3.02	1075.8	1078.8	0.00611	2.1747	2.18090		
0.2	512.8	0.0161	1529.1317	21.25	1008.9	1030.2	21.25	1065.5	1086.8	0.04231	2.07785	2.12017		
0.3	524.1	0.0161	1041.6294	32.60	1001.3	1033.9	32.60	1059.1	1091.7	0.06421	2.02075	2.08496		
0.4	532.5	0.0161	793.5160	41.00	995.6	1036.6	41.00	1054.4	1095.4	0.08010	1.98002	2.06013		
0.6	544.8	0.0161	541.0339	53.35	987.3	1040.6	53.36	1047.4	1100.7	0.10305	1.92229	2.02534		
0.8	554.0	0.0161	412.4360	62.52	981.1	1043.6	62.52	1042.1	1104.7	0.11973	1.88108	2.00081		
1.0	561.4	0.0162	334.2068	69.88	976.1	1046.0	69.88	1037.9	1107.8	0.13292	1.84897	1.98188		
1.5	575.3	0.0162	228.1557	83.83	966.6	1050.4	83.83	1029.9	1113.8	0.17902	1.79023	1.94769		
2.5	594.1	0.0163	141.1594	102.58	953.8	1056.4	102.59	1019.1	1121.7	0.18954	1.71547	1.90501		
3.0	601.1	0.0163	118.9527	109.62	949.0	1058.6	109.63	1015.0	1124.6	0.20132	1.68857	1.88989		
3.5	607.2	0.0164	102.9342	115.73	944.7	1060.5	115.74	1011.4	1127.1	0.21143	1.66571	1.87715		
4.0	612.6	0.0164	90.8181	121.13	941.0	1062.1	121.15	1008.2	1129.4	0.22030	1.64584	1.86614		
5.0	621.9	0.0164	73.6775	130.43	934.6	1065.0	130.44	1002.9	1133.2	0.23536	1.61246	1.84781		
6.0	629.7	0.0165	62.1094	138.27	929.1	1067.4	138.29	998.0	1136.3	0.24789	1.58501	1.83290		
7.0	636.5	0.0165	53.7612	145.08	924.3	1069.4	145.11	994.0	1139.1	0.25865	1.56168	1.82033		
8.0	642.5	0.0166	47.4442	151.13	920.1	1071.2	151.15	990.3	1141.5	0.26811	1.54137	1.80947		
10.0	652.8	0.0166	38.5033	161.54	912.7	1074.3	161.57	984.0	1145.5	0.28418	1.50721	1.79139		
12.5	663.6	0.0167	31.2495	172.36	905.0	1077.4	172.40	977.3	1149.7	0.30062	1.47276	1.77337		
14.7	671.6	0.0167	26.8597	180.48	899.2	1079.7	180.52	972.2	1152.8	0.31278	1.44757	1.76035		
20.0	687.6	0.0169	20.1340	196.61	887.6	1084.2	196.67	962.0	1158.7	0.33651	1.39911	1.73562		
25.0	699.7	0.0170	16.3406	208.88	878.6	1087.5	208.96	954.1	1163.1	0.35421	1.36356	1.71777		
30.0	710.0	0.0170	13.7771	219.30	870.9	1090.2	219.40	954.1	1166.6	0.36900	1.33420	1.70320		
35.0	718.9	0.0171	11.9251	228.41	864.1	1092.5	228.52	941.2	1169.7	0.38175	1.30914	1.69089		
40.0	726.9	0.0172	10.5224	236.53	857.9	1094.5	236.66	935.7	1172.4	0.39298	1.28724	1.68022		
45.0	734.1	0.0172	9.4220	243.88	852.3	1096.2	244.02	930.7	1174.7	0.40304	1.26777	1.67081		
50.0	740.7	0.0173	8.5350	250.61	847.2	1097.8	250.77	926.0	1176.8	0.41217	1.25022	1.66239		
55.0	746.7	0.0174	7.8041	256.82	842.4	1099.2	257.00	921.6	1178.6	0.42052	1.23424	1.65476		
60.0	752.4	0.0174	7.1912	262.61	837.9	1100.5	262.80	917.5	1180.3	0.42824	1.21955	1.64779		
65.0	757.6	0.0175	6.6696	268.02	833.7	1101.7	268.24	913.7	1181.9	0.43542	1.20595	1.6137		
70.0	762.6	0.0175	6.2201	273.13	829.6	1102.8	273.35	910.0	1183.3	0.44213	1.19329	1.63542		
75.0	767.3	0.0176	5.8286	277.95	825.8	1103.8	278.19	906.5	1184.7	0.44844	1.18143	1.62987		
80.0	771.7	0.0176	5.4844	282.53	822.2	1104.7	282.79	903.1	1185.9	0.45439	1.17028	1.62467		
85.0	775.9	0.0176	5.1794	286.89	818.7	1105.6	287.79	899.9	1188.1	0.46003	1.15975	1.61977		
90.0	779.9	0.0177	4.9071	291.06	815.3	1106.4	291.36	896.8	1188.1	0.46539	1.14977	1.61515		
95.0	783.8	0.0177	4.6626	295.05	812.1	1107.1	295.37	893.7	1189.1	0.47049	1.14028	1.61078		
100.0	787.5	0.0178	4.4417	298.89	809.0	1107.9	299.22	890.8	1190.1	0.47538	1.13124	1.60661		

Press (psi)	Temp (R)	Specific Volume (ft <sup>3</sup> /lbm)	Internal Energy (Btu/lbm)				Enthalpy (Btu/lbm)				Entropy (Btu/lbm/R)			
			v <sub>f</sub>	v <sub>g</sub>	u <sub>f</sub>	u <sub>g</sub>	h <sub>f</sub>	h <sub>g</sub>	s <sub>f,g</sub>	s <sub>g</sub>	h <sub>f,g</sub>	h <sub>g</sub>	s <sub>f,g</sub>	s <sub>g</sub>
110.0	794.5	0.0178	4.0581	306.14	803.0	1109.2	306.50	885.3	1191.8	0.48454	1.11432	1.59886		
120.0	800.9	0.0179	3.7365	312.90	797.4	1110.3	313.29	880.0	1193.3	0.49302	1.09874	1.59176		
130.0	807.0	0.0180	3.4626	319.24	792.1	1111.4	319.67	875.0	1194.7	0.50091	1.08429	1.58520		
140.0	812.7	0.0181	3.2267	325.22	787.1	1112.3	325.69	870.2	1195.9	0.50830	1.07080	1.57910		
150.0	818.1	0.0181	3.0211	330.89	782.3	1113.2	331.40	865.7	1197.1	0.51525	1.05814	1.57340		
160.0	823.2	0.0182	2.8404	336.28	777.7	1114.0	336.82	861.3	1198.1	0.52183	1.04622	1.56805		
170.0	828.1	0.0183	2.6802	341.43	773.3	1114.7	342.00	857.0	1199.0	0.52806	1.03494	1.56300		
180.0	832.8	0.0183	2.5373	346.35	769.0	1115.4	346.96	852.9	1199.9	0.53399	1.02423	1.55822		
190.0	837.2	0.0184	2.4088	351.07	764.9	1116.0	351.70	849.0	1200.7	0.53965	1.01403	1.55367		
200.0	841.5	0.0184	2.2928	355.62	760.9	1116.5	356.30	845.1	1201.4	0.54506	1.00429	1.54935		
250.0	860.7	0.0187	1.8478	376.11	742.6	1118.7	376.97	827.2	1204.2	0.56915	0.96114	1.53029		
300.0	877.0	0.0189	1.5467	393.80	726.3	1120.1	394.85	811.1	1206.0	0.58953	0.92485	1.51438		
350.0	891.4	0.0192	1.3290	409.48	711.5	1121.0	410.72	796.3	1207.1	0.60728	0.89335	1.50063		
400.0	904.3	0.0194	1.1640	423.66	697.8	1121.5	425.09	782.6	1207.6	0.62308	0.86537	1.48845		
450.0	916.0	0.0196	1.0345	436.64	685.0	1121.6	438.27	769.5	1207.8	0.63730	0.84010	1.47747		
500.0	926.7	0.0198	0.9301	448.67	672.9	1121.6	450.50	757.1	1207.6	0.65045	0.81698	1.46743		
600.0	945.9	0.0202	0.7718	470.48	650.3	1120.8	472.72	733.7	1206.5	0.67378	0.77569	1.44947		
700.0	962.8	0.0206	0.6572	490.01	629.3	1119.4	492.68	711.8	1204.5	0.69430	0.73931	1.43361		
800.0	977.9	0.0209	0.5704	507.83	609.6	1117.4	510.93	691.0	1201.9	0.71271	0.70654	1.41925		
900.0	991.7	0.0213	0.5021	524.31	590.8	1115.1	527.86	670.9	1198.7	0.72950	0.67650	1.40600		
1000.0	1004.3	0.0216	0.4470	539.73	572.7	1112.4	543.75	651.4	1195.1	0.74501	0.64861	1.39362		
1100.0	1016.0	0.0220	0.4015	554.27	555.1	1109.4	558.75	632.4	1191.1	0.75948	0.62242	1.38190		
1200.0	1026.9	0.0224	0.3632	568.10	538.0	1106.1	573.07	613.7	1186.8	0.77310	0.59760	1.37069		
1300.0	1037.2	0.0227	0.3306	581.34	521.2	1102.5	586.81	595.2	1182.0	0.78600	0.57389	1.35990		
1400.0	1046.8	0.0231	0.3023	594.07	504.6	1098.6	600.06	576.9	1177.0	0.79831	0.55110	1.34941		
1500.0	1055.9	0.0235	0.2776	606.38	488.1	1094.5	612.91	558.6	1171.5	0.81012	0.52904	1.33916		
1600.0	1064.6	0.0239	0.2558	618.34	471.7	1090.0	625.42	540.4	1165.8	0.82151	0.50751	1.32907		
1800.0	1080.7	0.0248	0.2189	641.42	438.9	1080.3	649.67	503.5	1153.2	0.84327	0.46589	1.30916		
2000.0	1095.5	0.0257	0.1886	663.74	405.4	1069.2	673.25	465.7	1139.0	0.86408	0.42510	1.28918		
2250.0	1112.4	0.0270	0.1573	691.19	361.7	1052.9	702.44	416.0	1118.4	0.88942	0.37393	1.26335		
2500.0	1127.8	0.0287	0.1309	719.11	314.2	1033.3	732.37	361.5	1093.9	0.91498	0.32054	1.23552		
2750.0	1142.0	0.0308	0.0573	749.09	121.2	870.3	764.78	134.6	899.4	0.94233	0.11756	1.05990		
3000.0	1155.1	0.0345	0.0531	785.51	86.3	871.8	804.64	96.7	901.3	0.97571	0.08362	1.05933		
3200.0	1164.8	0.0517	0.0517	877.11	0.0	877.1	907.70	0.0	907.7	1.06317	0.00000	1.06317		

## C.6 The Saturation Pressure vs. Temperature (English Units)

Temp (R)	Press (psi)	Specific Volume (ft <sup>3</sup> *3/lbm)	Internal Energy (Btu/lbm)			Enthalpy (Btu/lbm)			Entropy (Btu/lbm/R)		
			v <sub>f</sub>	v <sub>g</sub>	u <sub>f</sub>	u <sub>fg</sub>	u <sub>g</sub>	h <sub>f</sub>	h <sub>fg</sub>	h <sub>g</sub>	s <sub>f</sub>
491.7	0.09	0.0161	3308.9548	0.00	1023.2	1023.2	0.00	1077.5	1077.5	0.00000	2.19152
500.0	0.12	0.0161	2418.8743	8.38	1017.6	1026.0	8.38	1072.8	1081.2	0.01690	2.14557
510.0	0.18	0.0161	1686.7268	18.44	1010.8	1029.3	18.44	1067.1	1085.6	0.03681	2.12920
520.0	0.26	0.0161	1195.2240	28.47	1004.1	1032.5	28.47	1089.9	1094.3	0.05630	2.04126
530.0	0.37	0.0161	859.8069	38.49	997.3	1035.8	38.49	1055.8	1094.3	0.07538	2.06744
540.0	0.51	0.0161	627.3451	48.50	990.6	1039.1	48.50	1050.1	1098.6	0.09410	1.94466
550.0	0.71	0.0161	463.8765	58.51	983.8	1042.3	58.51	1044.4	1102.9	0.11246	1.89896
560.0	0.96	0.0162	347.3375	68.51	977.0	1045.7	68.51	1038.7	1107.2	0.13048	1.98535
570.0	1.29	0.0162	263.1730	78.51	970.2	1048.7	78.52	1033.0	1111.5	0.14819	1.81227
580.0	1.71	0.0162	201.6415	88.52	963.4	1051.9	88.52	1027.2	1115.8	0.16558	1.77109
590.0	2.25	0.0163	156.1334	98.52	956.6	1055.1	98.53	1021.4	1120.0	0.18269	1.73126
600.0	2.92	0.0163	122.1055	108.53	949.7	1058.2	108.54	1015.6	1124.2	0.19951	1.69269
610.0	3.75	0.0164	96.3962	118.55	942.2	1061.3	118.56	1018.7	1128.3	0.21606	1.65531
620.0	4.78	0.0164	76.7798	128.57	935.9	1064.4	128.58	1003.8	1132.4	0.23236	1.61906
630.0	6.05	0.0165	61.6720	138.60	928.9	1067.5	138.62	997.8	1136.5	0.24841	1.58387
640.0	7.57	0.0165	49.9327	148.64	921.8	1070.5	148.66	991.8	1140.5	0.26422	1.54969
650.0	9.42	0.0166	40.7337	158.69	914.8	1073.4	158.72	985.7	1144.4	0.27981	1.51645
660.0	11.62	0.0167	33.4671	168.76	907.6	1076.4	168.79	979.5	1148.3	0.29518	1.48411
670.0	14.23	0.0167	27.6832	178.84	900.4	1079.2	178.88	973.3	1152.1	0.31034	1.45261
680.0	17.31	0.0168	23.0457	188.93	893.1	1082.1	188.99	966.9	1155.9	0.32529	1.42190
690.0	20.92	0.0169	19.3017	199.05	885.8	1084.8	199.11	960.5	1159.6	0.34006	1.39195
700.0	25.13	0.0170	16.2589	209.18	878.4	1087.5	209.26	953.9	1163.2	0.35464	1.36270
710.0	30.02	0.0170	13.7705	219.33	870.8	1090.2	219.43	947.2	1166.7	0.36904	1.33412
720.0	35.64	0.0171	11.7232	229.51	863.2	1092.7	229.62	940.4	1170.1	0.38327	1.30616
730.0	42.10	0.0172	10.0291	239.71	855.5	1095.2	239.84	933.5	1173.4	0.39734	1.27880
740.0	49.48	0.0173	8.6197	249.93	847.7	1097.6	250.09	926.5	1176.6	0.41125	1.25198
750.0	57.86	0.0174	7.4409	260.18	839.8	1100.0	260.37	919.3	1179.6	0.42501	1.222569
760.0	67.35	0.0175	6.4501	270.46	831.7	1102.2	270.68	911.9	1182.6	0.43863	1.19989
770.0	78.05	0.0176	5.6133	280.77	823.6	1104.3	281.03	904.4	1185.4	0.45211	1.17454
780.0	90.07	0.0177	4.9034	291.12	815.3	1106.4	291.41	896.7	1188.1	0.46546	1.14963
790.0	103.52	0.0178	4.2985	301.50	806.8	1108.3	301.84	888.8	1190.7	0.47869	1.12511
800.0	118.52	0.0179	3.7809	311.92	798.2	1110.2	312.31	880.8	1193.1	0.49180	1.10098
810.0	135.18	0.0180	3.3362	322.38	789.5	1111.9	322.83	872.5	1195.4	0.50480	1.07719
820.0	153.64	0.0181	2.9527	332.89	780.6	1113.5	333.40	864.1	1197.5	0.51769	1.05372
830.0	174.03	0.0183	2.6207	343.44	771.5	1115.0	344.03	855.4	1199.4	0.53048	1.03055
840.0	196.49	0.0184	2.3323	354.04	762.3	1116.3	354.71	846.4	1201.1	0.54319	1.00766

Temp (R)	Press (psi)	Specific Volume (ft <sup>3</sup> *3/lbm)	Internal Energy				Enthalpy				Entropy			
			uf	ug	hf	hg	sf	fg	sg	fg	sg	Btu/lbm/R)		
850.0	221.14	0.0185	2.0809	364.69	752.9	1117.6	365.45	837.3	1204.7	0.55580	0.98501	1.54082		
860.0	248.15	0.0187	1.8611	375.41	743.2	1118.6	376.26	827.8	1204.1	0.56834	0.96259	1.53093		
870.0	277.66	0.0188	1.6683	386.18	733.4	1119.6	387.15	818.1	1205.3	0.58080	0.94038	1.52118		
880.0	309.82	0.0190	1.4986	397.02	723.3	1120.3	398.11	808.1	1206.2	0.59320	0.91833	1.51153		
890.0	344.79	0.0191	1.3488	407.93	713.0	1120.9	409.15	797.8	1207.0	0.60553	0.89644	1.50198		
900.0	382.74	0.0193	1.2163	418.91	702.4	1121.3	420.28	787.2	1207.5	0.61782	0.87668	1.49250		
910.0	423.83	0.0195	0.986	429.98	691.6	1121.6	431.50	776.3	1207.8	0.63006	0.85302	1.48309		
920.0	468.23	0.0197	0.9940	441.13	680.5	1121.6	442.83	764.9	1207.8	0.64227	0.83144	1.47371		
930.0	516.12	0.0199	0.9006	452.37	669.1	1121.5	454.27	753.2	1207.5	0.65444	0.80992	1.46436		
940.0	567.68	0.0201	0.8171	463.72	657.4	1121.1	465.83	741.1	1206.9	0.66660	0.78841	1.45501		
950.0	623.10	0.0203	0.7122	475.17	645.3	1120.5	477.51	728.6	1206.1	0.67874	0.76691	1.44565		
960.0	682.56	0.0205	0.6749	486.74	632.9	1119.6	489.33	715.6	1204.9	0.69089	0.74537	1.43625		
970.0	746.26	0.0207	0.6143	498.44	620.5	1118.5	501.30	702.1	1203.4	0.70304	0.72376	1.42680		
980.0	814.41	0.0210	0.5595	510.28	606.9	1117.1	513.44	688.0	1201.5	0.71522	0.70206	1.41728		
990.0	887.21	0.0212	0.5100	522.27	593.2	1115.4	525.75	673.4	1199.2	0.72743	0.68022	1.40765		
1000.0	964.87	0.0215	0.4651	534.42	579.0	1113.4	538.26	658.2	1196.5	0.73969	0.65819	1.39789		
1010.0	1047.63	0.0218	0.4243	546.75	564.3	1092.5	550.98	642.3	1193.3	0.75202	0.63951	1.38796		
1020.0	1135.71	0.0221	0.3871	559.29	549.0	1108.3	563.94	625.7	1189.6	0.76443	0.61341	1.37784		
1030.0	1229.35	0.0225	0.3531	572.04	533.0	1105.1	577.16	608.3	1185.4	0.77695	0.59054	1.36749		
1040.0	1328.81	0.0229	0.3220	585.05	516.4	1101.4	590.67	589.9	1180.6	0.78960	0.56724	1.35685		
1050.0	1434.35	0.0233	0.2935	598.34	498.9	1097.2	604.52	570.6	1175.1	0.80242	0.54344	1.34587		
1060.0	1546.25	0.0237	0.2672	611.95	480.5	1092.5	618.73	550.2	1168.9	0.81544	0.51904	1.33448		
1070.0	1664.83	0.0242	0.2429	625.93	461.1	1087.0	633.38	528.5	1161.9	0.82869	0.49390	1.32260		
1080.0	1790.40	0.0247	0.2205	640.33	440.4	1080.8	648.52	505.3	1153.8	0.84225	0.46786	1.31011		
1090.0	1923.31	0.0253	0.1995	655.24	418.3	1073.6	664.26	480.4	1144.6	0.85619	0.44069	1.29688		
1100.0	2063.95	0.0260	0.1800	670.78	394.5	1065.3	680.71	453.3	1134.0	0.87060	0.41209	1.28270		
1110.0	2212.74	0.0268	0.1616	687.10	368.4	1055.5	698.08	423.6	1121.7	0.88566	0.38163	1.26730		
1120.0	2370.19	0.0278	0.1411	704.47	339.5	1044.0	716.64	390.6	1107.2	0.90160	0.34870	1.25030		
1130.0	2536.83	0.0289	0.1274	723.34	306.7	1030.0	736.92	352.9	1089.8	0.91885	0.31230	1.23114		
1140.0	2713.33	0.0305	0.0580	744.45	125.6	870.1	759.76	139.4	899.2	0.93811	0.12195	1.06006		
1150.0	2900.52	0.0327	0.0547	769.61	101.6	871.2	787.17	113.4	900.5	0.96110	0.09844	1.05953		
1160.0	3099.69	0.0371	0.0517	805.97	65.9	871.9	827.28	74.2	901.5	0.99470	0.06398	1.05868		
1164.8	3200.12	0.0515	0.0515	876.57	0.0	876.6	907.08	0.0	907.1	1.06264	0.00000	1.06264		

## C.7 Superheated Steam Table (English Units)

Press = 1.0 psi, Tsat = 561.4 R	T (R) = 600.	v-ft3/lbm	357.745	387.798	417.779	447.720	477.638	507.541	537.435	597.207	656.965	716.715	776.461	836.203
u-Btu/lbm	1059.3	1076.5	1093.7	1111.0	1128.5	1145.1	1163.9	1200.1	1237.0	1274.9	1313.6	1353.1		
h-Btu/lbm	1125.5	1148.2	1170.9	1193.8	1216.8	1240.0	1263.3	1310.5	1358.6	1407.4	1457.2	1507.8		
s-Btu/lbm/R	2.011229	2.04866	2.08238	2.11392	2.14360	2.17168	2.19835	2.24811	2.29388	2.33640	2.37620	2.41372		
Press = 2.5 psi, Tsat = 594.1 R	T (R) = 600.	v-ft3/lbm	142.701	154.841	166.904	178.926	190.924	202.909	214.883	238.816	262.735	286.646	310.553	334.456
u-Btu/lbm	1058.5	1076.0	1093.3	1110.7	1128.3	1145.9	1163.8	1200.0	1237.0	1274.8	1313.5	1353.1		
h-Btu/lbm	1124.5	1147.5	1170.5	1193.5	1216.5	1239.8	1263.1	1310.4	1358.5	1407.4	1457.1	1507.7		
s-Btu/lbm/R	1.90967	1.94663	1.98065	2.01236	2.04214	2.07028	2.09699	2.14680	2.19260	2.23513	2.27495	2.31247		
Press = 5.0 psi, Tsat = 621.9 R	T (R) = 650.	v-ft3/lbm	77.185	83.277	89.327	95.353	101.364	107.366	119.352	131.325	143.290	155.250	167.206	179.161
u-Btu/lbm	1075.1	1092.7	1110.3	1127.9	1145.7	1163.6	1199.8	1236.9	1274.7	1313.4	1353.0	1393.6		
h-Btu/lbm	1146.4	1169.7	1192.9	1216.1	1239.4	1262.8	1310.2	1358.3	1407.2	1457.0	1507.7	1559.2		
s-Btu/lbm/R	1.86870	1.90322	1.93521	1.96516	1.99340	2.02019	2.07008	2.11592	2.15848	2.19832	2.23586	2.27143		
Press = 7.5 psi, Tsat = 639.6 R	T (R) = 650.	v-ft3/lbm	51.297	55.400	59.460	63.495	67.516	71.527	79.531	87.521	95.504	103.482	111.457	119.429
u-Btu/lbm	1074.2	1092.1	1109.9	1127.6	1145.4	1163.4	1199.7	1236.8	1274.6	1313.4	1353.0	1393.5		
h-Btu/lbm	1145.3	1169.0	1192.4	1215.7	1239.1	1262.6	1310.0	1358.2	1407.1	1456.9	1507.6	1559.2		
s-Btu/lbm/R	1.82250	1.85755	1.88983	1.91995	1.94831	1.97516	2.02514	2.07103	2.11362	2.15347	2.19103	2.22661		
Press = 10.0 psi, Tsat = 652.8 R	T (R) = 700.	v-ft3/lbm	41.4602	44.5258	47.5662	50.5914	53.6069	59.6202	65.6198	71.6115	77.5984	83.5819	89.5631	95.5426
u-Btu/lbm	1091.5	1109.4	1127.3	1145.2	1163.1	1199.5	1236.7	1274.6	1313.3	1352.9	1393.5	1434.9		
h-Btu/lbm	1168.2	1191.8	1215.3	1238.7	1262.3	1309.8	1358.0	1407.0	1456.8	1507.5	1559.1	1611.6		
s-Btu/lbm/R	1.82489	1.85746	1.88776	1.91622	1.94315	1.99321	2.03915	2.08177	2.12164	2.15920	2.19480	2.22869		

Press = 12.5 psi, Tsat = 663.6 R  
 $T(R) = 700.$     750.    800.    850.    900.    1000.    1100.    1200.    1300.    1400.    1500.    1600.  
 $v-ft^3/lbm = 33.0955.$     35.5648.    38.0085.    40.4367.    42.8550.    47.9737.    52.4787.    57.2759.    62.0681.    66.8570.    71.6435.    76.4284.  
 $u-Btu/lbm = 109.9.$     1109.0.    1126.9.    1144.9.    1162.9.    1199.4.    1236.5.    1274.5.    1313.2.    1352.9.    1393.4.    1434.9.  
 $h-Btu/lbm = 1167.4.$     1191.2.    1214.8.    1238.4.    1262.0.    1309.6.    1357.9.    1406.9.    1456.7.    1507.4.    1559.0.    1611.6.  
 $s-Btu/lbm/R = 1.79933.$     1.83221.    1.89126.    1.91827.    1.96841.    2.01440.    2.05704.    2.09693.    2.13451.    2.17011.    2.20401

Press = 14.7 psi, Tsat = 671.6 R  
 $T(R) = 700.$     750.    800.    850.    900.    1000.    1100.    1200.    1300.    1400.    1500.    1600.  
 $v-ft^3/lbm = 28.0952.$     30.2085.    32.2956.    34.3669.    36.4283.    40.5332.    44.6241.    48.7072.    52.7854.    56.8603.    60.9328.    65.0036.  
 $u-Btu/lbm = 109.3.$     1108.6.    1126.7.    1144.7.    1162.7.    1199.3.    1236.4.    1274.4.    1313.2.    1352.8.    1393.4.    1434.8.  
 $h-Btu/lbm = 1166.7.$     1190.7.    1214.4.    1238.1.    1261.8.    1309.4.    1357.7.    1406.8.    1456.6.    1507.4.    1559.0.    1611.5.  
 $s-Btu/lbm/R = 1.78065.$     1.81380.    1.84444.    1.87311.    1.90018.    1.95040.    1.99643.    2.03910.    2.07901.    2.11659.    2.15220.    2.18611

Press = 20.0 psi, Tsat = 687.6 R  
 $T(R) = 700.$     750.    800.    850.    900.    1000.    1100.    1200.    1300.    1400.    1500.    1600.  
 $v-ft^3/lbm = 20.5449.$     22.1217.    23.6710.    25.2040.    26.7268.    29.7540.    32.7671.    35.7724.    38.7726.    41.7696.    44.7642.    47.7572.  
 $u-Btu/lbm = 1088.9.$     1107.6.    1125.9.    1144.1.    1162.3.    1198.9.    1236.2.    1274.2.    1313.0.    1352.7.    1393.3.    1434.8.  
 $h-Btu/lbm = 1164.9.$     1189.4.    1213.5.    1237.3.    1261.2.    1309.0.    1357.4.    1406.5.    1456.4.    1507.2.    1558.8.    1611.4.  
 $s-Btu/lbm/R = 1.74461.$     1.77846.    1.80949.    1.83841.    1.86564.    1.91605.    1.96217.    2.00490.    2.04485.    2.08246.    2.11809.    2.15201

Press = 40.0 psi, Tsat = 726.9 R  
 $T(R) = 750.$     800.    850.    900.    1000.    1100.    1200.    1300.    1400.    1500.    1600.    1700.  
 $v-ft^3/lbm = 10.9125.$     11.7197.    12.5083.    13.2855.    14.8204.    16.3406.    17.8527.    19.3597.    20.8634.    22.3648.    23.8644.    25.3628.  
 $u-Btu/lbm = 1103.8.$     1123.1.    1142.0.    1160.6.    1197.8.    1235.3.    1273.5.    1312.4.    1352.2.    1392.9.    1434.4.    1476.9.  
 $h-Btu/lbm = 1184.5.$     1209.8.    1234.5.    1258.9.    1307.4.    1356.2.    1405.6.    1455.7.    1506.6.    1558.3.    1611.0.    1664.5.  
 $s-Btu/lbm/R = 1.69668.$     1.72936.    1.75928.    1.78714.    1.83827.    1.88478.    1.92774.    1.96784.    2.00555.    2.04126.    2.07523.    2.10768

Press = 60.0 psi, Tsat = 752.4 R  
 $T(R) = 800.$     850.    900.    1000.    1100.    1200.    1300.    1400.    1500.    1600.    1700.    1800.  
 $v-ft^3/lbm = 7.7325.$     8.2745.    8.8041.    9.8422.    10.8650.    11.8794.    12.8887.    13.8947.    14.8983.    15.9002.    16.9008.    17.9005.  
 $u-Btu/lbm = 1120.1.$     1139.7.    1158.8.    1196.5.    1234.4.    1272.8.    1311.9.    1351.8.    1392.5.    1434.1.    1476.6.    1520.0.  
 $h-Btu/lbm = 1205.9.$     1231.5.    1256.5.    1305.8.    1355.0.    1404.6.    1454.9.    1505.9.    1557.8.    1610.5.    1664.1.    1718.6.  
 $s-Btu/lbm/R = 1.68079.$     1.71180.    1.74036.    1.79226.    1.83917.    1.88236.    1.92261.    1.96043.    1.99620.    2.03022.    2.06272.    2.09388

Press = 80.0 psi, Tsat = 771.7 R  
 $T(R) = 800.$   
 $v-ft^3/lbm = 5.7361$   
 $u-Btu/lbm = 1117.0$   
 $h-Btu/lbm = 1201.8$   
 $s-Btu/lbm/R = 1.64497$   
 1.67722 1.70652 1.75924 1.80656 1.84999 1.89039 1.92831 1.96416 1.99923 2.03077 2.06196

Press = 100.0 psi, Tsat = 787.5 R  
 $T(R) = 800.$   
 $v-ft^3/lbm = 4.5358$   
 $u-Btu/lbm = 1113.6$   
 $h-Btu/lbm = 1197.5$   
 $s-Btu/lbm/R = 1.61596$   
 1.64965 1.67975 1.73333 1.78107 1.82474 1.86529 1.90332 1.93924 1.97337 2.00595 2.03717

Press = 120.0 psi, Tsat = 800.9 R  
 $T(R) = 850.$   
 $v-ft^3/lbm = 4.0347$   
 $u-Btu/lbm = 1132.4$   
 $h-Btu/lbm = 1221.9$   
 $s-Btu/lbm/R = 1.62645$   
 1.65742 1.71191 1.76009 1.80401 1.84471 1.88284 1.91884 1.95302 1.98564 2.01689 2.04692

Press = 140.0 psi, Tsat = 812.7 R  
 $T(R) = 850.$   
 $v-ft^3/lbm = 3.4272$   
 $u-Btu/lbm = 1129.7$   
 $h-Btu/lbm = 1218.5$   
 $s-Btu/lbm/R = 1.60622$   
 1.63813 1.69358 1.74221 1.78638 1.82724 1.86547 1.90154 1.93578 1.96844 1.99972 2.02977

Press = 160.0 psi, Tsat = 823.2 R  
 $T(R) = 850.$   
 $v-ft^3/lbm = 2.9707$   
 $u-Btu/lbm = 1127.0$   
 $h-Btu/lbm = 1214.9$   
 $s-Btu/lbm/R = 1.58812$   
 1.62105 1.67750 1.72659 1.77102 1.81204 1.85038 1.88653 1.92082 1.95351 1.98482 2.01490

Press =	180.0	psi,	Tsat =	832.8	R								
T (R) =	850.		1000.	1100.		1200.		1400.		1600.		1700.	1800.
v-ft3/lbm	2.6148	2.8207	3.2017	3.5630	3.9145	4.2605	4.6029	4.9428	5.2811	5.6181	5.9541	6.2895	
u-Btu/lbm	1124.1	1147.0	1188.9	1228.8	1268.5	1308.4	1348.9	1389.1	1432.1	1474.8	1518.5	1563.0	
h-Btu/lbm	1211.1	1240.9	1295.4	1347.5	1398.8	1450.3	1502.1	1554.6	1607.9	1661.9	1716.7	1772.4	
s-Btu/lbm/R	1.57158	1.60564	1.66314	1.71272	1.75740	1.79858	1.83703	1.87325	1.90759	1.94033	1.97167	2.00177	
Press =	200.0	psi,	Tsat =	841.5	R								
T (R) =	850.	900.	1000.	1100.	1200.	1300.	1400.	1500.	1600.	1700.	1800.	1900.	
v-ft3/lbm	2.3291	2.5202	2.8693	3.1977	3.5162	3.8290	4.1382	4.4451	4.7501	5.0540	5.3568	5.6590	
u-Btu/lbm	1121.0	1144.8	1187.5	1227.9	1267.8	1307.8	1348.4	1389.7	1431.7	1474.6	1518.2	1562.8	
h-Btu/lbm	1207.2	1238.1	1293.6	1346.2	1397.8	1449.5	1501.5	1554.1	1607.4	1661.5	1716.4	1772.1	
s-Btu/lbm/R	1.55619	1.59152	1.65013	1.70020	1.74515	1.78649	1.82505	1.86134	1.89574	1.92832	1.95989	1.99002	
Press =	250.0	psi,	Tsat =	860.7	R								
T (R) =	900.	1000.	1100.	1200.	1300.	1400.	1500.	1600.	1700.	1800.	1900.	2000.	
v-ft3/lbm	1.9779	2.2703	2.5400	2.7991	3.0523	3.3019	3.5490	3.7944	4.0385	4.2816	4.5241	4.7660	
u-Btu/lbm	1139.1	1184.1	1225.5	1265.9	1306.4	1347.2	1388.7	1430.9	1473.8	1511.6	1562.2	1607.7	
h-Btu/lbm	1230.6	1289.0	1342.9	1395.4	1447.5	1499.9	1552.8	1606.3	1660.5	1715.6	1771.4	1828.1	
s-Btu/lbm/R	1.56033	1.62195	1.67333	1.71896	1.76072	1.79954	1.83603	1.87056	1.90344	1.93489	1.96507	1.99414	
Press =	300.0	psi,	Tsat =	877.0	R								
T (R) =	900.	1000.	1100.	1200.	1300.	1400.	1500.	1600.	1700.	1800.	1900.	2000.	
v-ft3/lbm	1.6144	1.8704	2.1013	2.3209	2.5345	2.7443	2.9517	3.1572	3.3615	3.5649	3.7675	3.9696	
u-Btu/lbm	1133.0	1180.5	1223.0	1264.1	1304.9	1346.0	1387.7	1430.0	1473.1	1517.0	1561.7	1607.2	
h-Btu/lbm	1222.6	1284.2	1339.6	1392.9	1445.5	1498.3	1551.5	1605.2	1659.6	1714.8	1770.7	1827.5	
s-Btu/lbm/R	1.53305	1.59813	1.65091	1.69726	1.73944	1.77854	1.81522	1.84989	1.88287	1.91439	1.94463	1.97375	
Press =	350.0	psi,	Tsat =	891.4	R								
T (R) =	900.	1000.	1100.	1200.	1300.	1400.	1500.	1600.	1700.	1800.	1900.	2000.	
v-ft3/lbm	1.3527	1.5842	1.7877	1.9793	2.1646	2.3460	2.5250	2.7021	2.8780	3.0529	3.2270	3.4007	
u-Btu/lbm	1126.2	1176.7	1220.5	1262.2	1303.4	1344.8	1386.7	1429.2	1472.4	1516.3	1561.1	1606.7	
h-Btu/lbm	1213.8	1279.3	1336.2	1390.3	1443.6	1496.7	1550.1	1604.1	1658.7	1713.9	1770.0	1826.8	
s-Btu/lbm/R	1.50812	1.57726	1.63155	1.67865	1.72127	1.76065	1.79752	1.83233	1.86541	1.89701	1.92731	1.95647	

Press = 400.0 psi, Tsat = 904.3 R  
 $T(R) = 1000.$  1100. 1200. 1300. 1400. 1500. 1600. 1700. 1800. 1900. 2000.  
 v-ft3/lbm 1.3691 1.5523 1.7230 1.8871 2.0473 2.2049 2.3608 2.5153 2.6689 2.8217 2.9741 3.1259  
 u-Btu/lbm 1172.8 1217.9 1260.3 1302.0 1343.6 1385.7 1428.3 1471.6 1515.7 1560.5 1606.2 1652.7  
 h-Btu/lbm 1274.1 1332.7 1387.8 1441.6 1495.1 1548.8 1603.0 1657.7 1713.1 1769.3 1826.2 1884.0  
 s-Btu/lbm/R 1.55851 1.61441 1.66230 1.70536 1.74503 1.78209 1.81704 1.85022 1.88190 1.91226 1.94146 1.96963

Press = 450.0 psi, Tsat = 916.0 R  
 $T(R) = 1000.$  1100. 1200. 1300. 1400. 1500. 1600. 1700. 1800. 1900. 2000.  
 v-ft3/lbm 1.2012 1.3691 1.5236 1.6712 1.8149 1.9560 2.0953 2.2332 2.3702 2.5065 2.6422 2.7775  
 u-Btu/lbm 1168.8 1215.3 1258.4 1300.5 1342.4 1384.7 1427.5 1470.9 1515.0 1560.0 1605.7 1652.3  
 h-Btu/lbm 1268.8 1329.2 1385.2 1439.5 1493.5 1547.5 1601.8 1656.8 1712.3 1768.6 1825.6 1883.4  
 s-Btu/lbm/R 1.54131 1.59895 1.64671 1.69119 1.73115 1.76840 1.80349 1.83678 1.86853 1.89895 1.92820 1.95640

Press = 500.0 psi, Tsat = 926.7 R  
 $T(R) = 1000.$  1100. 1200. 1300. 1400. 1500. 1600. 1700. 1800. 1900. 2000.  
 v-ft3/lbm 1.0665 1.2223 1.3640 1.4985 1.6290 1.7568 1.8828 2.0075 2.1313 2.2543 2.3767 2.4987  
 u-Btu/lbm 1164.6 1212.6 1256.4 1298.9 1341.2 1383.7 1426.6 1470.2 1514.4 1559.4 1605.2 1651.8  
 h-Btu/lbm 1263.2 1325.6 1382.6 1437.5 1491.8 1546.1 1600.7 1655.8 1711.5 1767.9 1825.0 1882.9  
 s-Btu/lbm/R 1.52530 1.58481 1.63438 1.67838 1.71863 1.75608 1.79132 1.82471 1.85654 1.88702 1.91631 1.94454

Press = 550.0 psi, Tsat = 936.7 R  
 $T(R) = 1000.$  1100. 1200. 1300. 1400. 1500. 1600. 1700. 1800. 1900. 2000.  
 v-ft3/lbm 0.9559 1.1021 1.2333 1.3572 1.4769 1.5939 1.7091 1.8229 1.9358 2.0479 2.1595 2.2707  
 u-Btu/lbm 1160.2 1209.8 1254.5 1297.4 1340.0 1382.6 1425.7 1469.4 1513.8 1558.8 1604.7 1651.3  
 h-Btu/lbm 1257.5 1321.9 1379.9 1435.5 1490.2 1544.8 1599.6 1654.8 1710.7 1767.2 1824.4 1882.3  
 s-Btu/lbm/R 1.51020 1.57171 1.62218 1.66666 1.70722 1.74487 1.78025 1.81374 1.84565 1.88719 1.90552 1.93380

Press = 600.0 psi, Tsat = 945.9 R  
 $T(R) = 1000.$  1100. 1200. 1300. 1400. 1500. 1600. 1700. 1800. 1900. 2000.  
 v-ft3/lbm 0.8632 1.0017 1.1243 1.2394 1.3501 1.4581 1.5642 1.6690 1.7729 1.8760 1.9785 2.0806  
 u-Btu/lbm 1155.7 1207.0 1252.5 1295.9 1338.7 1381.6 1424.9 1468.7 1513.1 1558.3 1604.2 1650.9  
 h-Btu/lbm 1251.5 1318.2 1377.2 1433.4 1488.5 1543.4 1598.5 1653.9 1709.8 1766.4 1823.7 1881.8  
 s-Btu/lbm/R 1.49578 1.55946 1.61087 1.65586 1.69672 1.73458 1.77010 1.80369 1.83568 1.86628 1.89566 1.92397

Press = 700.0 psi, Tsat = 962.8 R  
 $T(R) = 1000.$  1100. 1200. 1300. 1400. 1500. 1600. 1700. 1800. 1900.  
 $v-ft^3/lbm = 0.7162$  0.8437 0.9530 1.0541 1.1508 1.2447 1.3366 1.4272 1.5169 1.6057  
 $u-Btu/lbm = 1145.9$  1201.2 1248.4 1292.8 1336.2 1379.6 1423.2 1467.2 1511.8 1557.1  
 $h-Btu/lbm = 1238.6$  1310.4 1371.8 1429.3 1485.2 1540.7 1596.2 1652.0 1708.2 1765.0  
 $s-Btu/lbm/R = 1.46837$  1.53696 1.59037 1.63641 1.67790 1.71617 1.75198 1.78579 1.81793 1.84865  
 $\quad \quad \quad 1.87812$  1.90650

Press = 800.0 psi, Tsat = 977.9 R  
 $T(R) = 1000.$  1100. 1200. 1300. 1400. 1500. 1600. 1700. 1800. 1900.  
 $v-ft^3/lbm = 0.6041$  0.7246 0.8243 0.9151 1.0013 1.0846 1.1659 1.2459 1.3249 1.4031  
 $u-Btu/lbm = 1134.9$  1195.1 1244.2 1289.6 1333.7 1377.5 1421.4 1465.7 1510.5 1556.0  
 $h-Btu/lbm = 1224.3$  1302.3 1366.2 1425.0 1481.9 1538.0 1593.9 1650.0 1706.6 1763.6  
 $s-Btu/lbm/R = 1.44194$  1.51644 1.57205 1.61919 1.66134 1.70004 1.73614 1.77016 1.80246 1.83330  
 $\quad \quad \quad 1.86286$  1.89131

Press = 900.0 psi, Tsat = 991.7 R  
 $T(R) = 1000.$  1100. 1200. 1300. 1400. 1500. 1600. 1700. 1800. 1900.  
 $v-ft^3/lbm = 0.5148$  0.6315 0.7239 0.8069 0.8850 0.9600 1.0331 1.1048 1.1755 1.2454  
 $u-Btu/lbm = 1122.5$  1188.7 1239.9 1286.4 1331.2 1375.4 1419.7 1464.2 1509.2 1554.9  
 $h-Btu/lbm = 1208.2$  1293.8 1360.4 1420.7 1478.5 1535.2 1591.6 1648.1 1704.9 1762.2  
 $s-Btu/lbm/R = 1.41552$  1.49735 1.55536 1.60367 1.64649 1.68563 1.72203 1.75627 1.78873 1.81969  
 $\quad \quad \quad 1.84934$  1.87787

Press = 1000.0 psi, Tsat = 1004.3 R  
 $T(R) = 1100.$  1200. 1300. 1400. 1500. 1600. 1700. 1800. 1900. 2000.  
 $v-ft^3/lbm = 0.5565$  0.6435 0.7203 0.7919 0.8604 0.9269 0.9920 1.0560 1.1193 1.1821  
 $u-Btu/lbm = 1181.9$  1235.5 1283.2 1328.6 1373.3 1417.9 1462.7 1507.9 1553.7 1600.1  
 $h-Btu/lbm = 1284.9$  1354.5 1416.4 1475.1 1532.5 1589.3 1646.2 1703.2 1760.7 1818.7  
 $s-Btu/lbm/R = 1.47927$  1.53992 1.58948 1.63300 1.67258 1.70929 1.74374 1.77636 1.80744 1.83719  
 $\quad \quad \quad 1.86579$  1.89338

Press = 1100.0 psi, Tsat = 1016.0 R  
 $T(R) = 1100.$  1200. 1300. 1400. 1500. 1600. 1700. 1800. 1900. 2000.  
 $v-ft^3/lbm = 0.4947$  0.5776 0.6493 0.7157 0.7788 0.8399 0.8996 0.9583 1.0162 1.0735  
 $u-Btu/lbm = 1174.8$  1230.9 1279.8 1326.1 1371.2 1416.1 1461.2 1506.6 1552.6 1599.1  
 $h-Btu/lbm = 1275.5$  1348.4 1411.9 1471.6 1529.7 1587.0 1644.2 1701.6 1759.3 1817.5  
 $s-Btu/lbm/R = 1.46191$  1.52547 1.57634 1.62060 1.66064 1.69765 1.73233 1.76511 1.79631 1.82615  
 $\quad \quad \quad 1.85482$  1.88247

Press = 1200.0 psi, Tsat = 1026.9 R	T(R) = 1100.	1200.	1300.	1400.	1500.	1600.	1700.	1800.	1900.	2000.	2100.	2200.
v-ft3/lbm	0.4428	0.5224	0.5901	0.6522	0.7109	0.7675	0.8227	0.8768	0.9302	0.9830	1.0353	1.0873
u-Btu/lbm	1167.3	1226.2	1276.5	1323.4	1369.1	1414.4	1459.7	1505.3	1551.4	1598.1	1645.4	1693.4
h-Btu/lbm	1265.6	1342.2	1407.4	1468.2	1526.9	1584.7	1642.3	1699.9	1757.9	1816.2	1875.1	1934.7
s-Btu/lbm/R	1.44502	1.51180	1.56408	1.60909	1.64959	1.68692	1.72182	1.75477	1.78609	1.81602	1.84477	1.87248
Press = 1300.0 psi, Tsat = 1037.2 R	T(R) = 1100.	1200.	1300.	1400.	1500.	1600.	1700.	1800.	1900.	2000.	2100.	2200.
v-ft3/lbm	0.3983	0.4756	0.5400	0.5983	0.6533	0.7062	0.7576	0.8079	0.8575	0.9064	0.9549	1.0031
u-Btu/lbm	1159.3	1221.4	1273.0	1320.8	1367.0	1412.6	1458.2	1504.0	1550.3	1597.0	1644.4	1692.6
h-Btu/lbm	1255.0	1335.8	1402.9	1464.6	1524.0	1582.4	1640.3	1698.2	1756.4	1815.0	1874.0	1933.7
s-Btu/lbm/R	1.42838	1.49877	1.55252	1.59832	1.63931	1.67696	1.71208	1.74519	1.77664	1.80667	1.83549	1.86326
Press = 1400.0 psi, Tsat = 1046.8 R	T(R) = 1100.	1200.	1300.	1400.	1500.	1600.	1700.	1800.	1900.	2000.	2100.	2200.
v-ft3/lbm	0.3596	0.4354	0.4969	0.5522	0.6040	0.6536	0.7017	0.7488	0.7951	0.8408	0.8860	0.9309
u-Btu/lbm	1150.7	1216.4	1265.5	1318.1	1364.8	1410.8	1456.6	1502.7	1549.1	1596.0	1643.5	1691.7
h-Btu/lbm	1243.8	1329.2	1398.2	1461.1	1521.2	1580.0	1638.3	1696.6	1755.0	1813.7	1872.9	1932.8
s-Btu/lbm/R	1.41181	1.48626	1.54158	1.58819	1.62967	1.66764	1.70300	1.73627	1.76785	1.79796	1.82686	1.85470
Press = 1500.0 psi, Tsat = 1055.9 R	T(R) = 1100.	1200.	1300.	1400.	1500.	1600.	1700.	1800.	1900.	2000.	2100.	2200.
v-ft3/lbm	0.3255	0.4003	0.4596	0.5122	0.5613	0.6081	0.6534	0.6976	0.7411			
u-Btu/lbm	1141.5	1211.3	1266.0	1315.4	1362.6	1409.0	1455.1	1501.4	1547.9			
h-Btu/lbm	1231.7	1322.4	1393.5	1457.5	1518.3	1577.7	1636.4	1694.9	1753.5			
s-Btu/lbm/R	1.39510	1.47415	1.53114	1.57860	1.62058	1.65889	1.69447	1.72792	1.75962			
Press = 1600.0 psi, Tsat = 1064.6 R	T(R) = 1100.	1200.	1300.	1400.	1500.	1600.	1700.	1800.	1900.			
v-ft3/lbm	0.2950	0.3695	0.4268	0.4772	0.5238	0.5682	0.6110	0.6528	0.6938			
u-Btu/lbm	1131.4	1206.0	1262.4	1312.7	1360.4	1407.2	1453.6	1500.0	1546.8			
h-Btu/lbm	1218.7	1315.3	1388.7	1453.9	1515.5	1575.3	1634.4	1693.2	1752.1			
s-Btu/lbm/R	1.37804	1.46238	1.52113	1.56948	1.61198	1.65062	1.68643	1.72005	1.75187			

Press = 1700.0 psi, Tsat = 1072.9 R  
 $T(R) = 1100.$  1200. 1300. 1400. 1500. 1600. 1700. 1800. 1900.  
 $v-ft^3/lbm = 0.2673$  0.3422 0.3979 0.4462 0.4908 0.5330 0.5737 0.6133 0.6521  
 $u-Btu/lbm = 1120.4$  1200.5 1258.7 1309.9 1358.2 1405.4 1452.0 1498.7 1545.6  
 $h-Btu/lbm = 1204.5$  1308.1 1383.8 1450.2 1512.6 1572.9 1632.4 1691.5 1750.6  
 $s-Btu/lbm/R = 1.36037$  1.45087 1.51150 1.56076 1.60379 1.64277 1.67883 1.71261 1.74456

Press = 1800.0 psi, Tsat = 1080.7 R  
 $T(R) = 1100.$  1200. 1300. 1400. 1500. 1600. 1700. 1800. 1900.  
 $v-ft^3/lbm = 0.2418$  0.3178 0.3721 0.4187 0.4614 0.5017 0.5405 0.5781 0.6150  
 $u-Btu/lbm = 1108.2$  1194.8 1254.9 1307.1 1356.0 1403.5 1450.5 1497.4 1544.4  
 $h-Btu/lbm = 1188.7$  1300.6 1378.8 1446.5 1509.6 1570.6 1630.4 1689.8 1749.2  
 $s-Btu/lbm/R = 1.34174$  1.43955 1.50219 1.55240 1.59598 1.63531 1.67160 1.70555 1.73764

Press = 1900.0 psi, Tsat = 1088.3 R  
 $T(R) = 1100.$  1200. 1300. 1400. 1500. 1600. 1700. 1800. 1900.  
 $v-ft^3/lbm = 0.2179$  0.2958 0.3490 0.3941 0.4351 0.4738 0.5108 0.5467 0.5818  
 $u-Btu/lbm = 1094.2$  1189.0 1251.1 1304.3 1353.8 1401.7 1448.9 1496.0 1543.3  
 $h-Btu/lbm = 1170.8$  1292.9 1373.7 1442.7 1506.7 1568.2 1628.4 1688.1 1747.7  
 $s-Btu/lbm/R = 1.32165$  1.422838 1.49317 1.544346 1.58849 1.62817 1.66471 1.69884 1.73105

Press = 2000.0 psi, Tsat = 1095.5 R  
 $T(R) = 1100.$  1200. 1300. 1400. 1500. 1600. 1700. 1800. 1900.  
 $v-ft^3/lbm = 0.1949$  0.2758 0.3281 0.3719 0.4115 0.4486 0.4840 0.5184 0.5519  
 $u-Btu/lbm = 1077.8$  1182.8 1247.2 1301.4 1351.5 1399.8 1447.4 1494.7 1542.1  
 $h-Btu/lbm = 1149.9$  1284.9 1368.5 1439.0 1503.7 1565.8 1626.4 1686.4 1746.2  
 $s-Btu/lbm/R = 1.29918$  1.41730 1.48438 1.53660 1.58130 1.62134 1.65812 1.69242 1.72476

Press = 2500.0 psi, Tsat = 1127.8 R  
 $T(R) = 1200.$  1300. 1400. 1500. 1600. 1700. 1800. 1900.  
 $v-ft^3/lbm = 0.1980$  0.2483 0.2873 0.3214 0.3528 0.3824 0.4109 0.4385  
 $u-Btu/lbm = 1148.2$  1226.4 1286.5 1340.0 1390.4 1439.5 1487.9 1536.2  
 $h-Btu/lbm = 1239.7$  1341.3 1419.4 1488.6 1553.6 1616.3 1677.9 1738.9  
 $s-Btu/lbm/R = 1.36160$  1.44310 1.50107 1.54884 1.59077 1.62881 1.66401 1.69701

**Press = 3000.0 psi, Tsat = 1155.1 R**

T(R) =	1200.	1300	1400.	1500.	1600.	1700.	1800.	1900.
v-ft3/lbm	0.1421	0.1943	0.2307	0.2613	0.2889	0.3147	0.3392	0.3629
u-Btu/lbm	1103.1	1203.5	1270.8	1328.0	1380.8	1431.5	1481.1	1530.2
h-Btu/lbm	1181.9	1311.3	1398.8	1473.0	1541.1	1606.1	1669.3	1731.6
s-Btu/lbm/R	1.30046	1.40439	1.46935	1.52058	1.56455	1.60393	1.64007	1.67375

**Press = 3500.0 psi**

T(R) =	1200.	1300	1400.	1500.	1600.	1700.	1800.	1900.
v-ft3/lbm	0.0244	0.1550	0.1900	0.2183	0.2433	0.2663	0.2881	0.3089
u-Btu/lbm	720.0	1177.7	1254.1	1315.6	1370.9	1423.3	1474.1	1524.2
h-Btu/lbm	768.0	1278.1	1377.1	1456.9	1528.4	1595.7	1660.6	1724.2
s-Btu/lbm/R	0.91193	1.36649	1.44004	1.49513	1.54131	1.58210	1.61920	1.65358

**Press = 4000.0 psi**

T(R) =	1200.	1300	1400.	1500.	1600.	1700.	1800.	1900.
v-ft3/lbm	0.0240	0.1249	0.1594	0.1860	0.2091	0.2301	0.2497	0.2685
u-Btu/lbm	714.7	1148.8	1236.4	1302.7	1360.8	1415.0	1467.1	1518.2
h-Btu/lbm	765.3	1241.1	1354.3	1440.3	1515.5	1585.2	1651.9	1716.8
s-Btu/lbm/R	0.90685	1.32818	1.41226	1.47167	1.52020	1.56247	1.60058	1.63567

**Press = 4500.0 psi**

T(R) =	1200.	1300	1400.	1500.	1600.	1700.	1800.	1900.
v-ft3/lbm	0.0237	0.1009	0.1355	0.1609	0.1825	0.2019	0.2200	0.2370
u-Btu/lbm	709.9	1116.0	1217.7	1289.4	1350.5	1406.6	1460.0	1512.1
h-Btu/lbm	763.2	1200.0	1330.4	1423.4	1502.4	1574.6	1643.1	1709.3
s-Btu/lbm/R	0.90232	1.28852	1.38550	1.44969	1.50072	1.54453	1.58367	1.61949

**Press = 5000.0 psi**

T(R) =	1200.	1300	1400.	1500.	1600.	1700.	1800.	1900.
v-ft3/lbm	0.0234	0.0815	0.1163	0.1409	0.1613	0.1794	0.1962	0.2119
u-Btu/lbm	705.6	1079.1	1198.0	1275.8	1340.0	1398.1	1452.9	1505.9
h-Btu/lbm	761.3	1154.4	1305.5	1406.0	1489.1	1564.0	1634.3	1701.9
s-Btu/lbm/R	0.89820	1.24703	1.35941	1.42885	1.48232	1.52792	1.56811	1.60468

## C.8 H<sub>2</sub>O Compressed Liquid Tables (English Units)

Temperature=	500.0 R	Psat=	0.1 psi				
Press[psi]=	250	500	1000	1500	2000	2500	3000
v-ft3/lbm	0.016	0.016	0.016	0.016	0.016	0.0159	0.0159
u-Btu/lbm	8.4	8.4	8.4	8.4	8.4	8.3	8.3
h-Btu/lbm	9.1	9.9	11.3	12.8	14.3	15.7	17.1
s-Btu/lbm/R	0.0169	0.01689	0.01687	0.01684	0.01682	0.01675	0.01664
Temperature=	550.0 R	Psat=	0.7 psi				
Press[psi]=	250	500	1000	1500	2000	2500	3000
v-ft3/lbm	0.0161	0.0161	0.0161	0.0161	0.016	0.016	0.016
u-Btu/lbm	58.4	58.4	58.4	58.1	57.9	57.8	57.6
h-Btu/lbm	59.2	59.9	61.2	62.5	63.9	65.2	66.5
s-Btu/lbm/R	0.11232	0.11219	0.11192	0.11165	0.11137	0.11111	0.11082
Temperature=	600.0 R	Psat=	2.9 psi				
Press[psi]=	250	500	1000	1500	2000	2500	3000
v-ft3/lbm	0.0163	0.0163	0.0163	0.0163	0.0162	0.0162	0.0162
u-Btu/lbm	108.4	108.3	108	107.8	107.5	107.3	107
h-Btu/lbm	109.2	109.8	111	112.3	113.5	114.8	116
s-Btu/lbm/R	0.19929	0.19907	0.19884	0.19864	0.19842	0.19777	0.19734
Temperature=	650.0 R	Psat=	9.4 psi				
Press[psi]=	250	500	1000	1500	2000	2500	3000
v-ft3/lbm	0.0166	0.0166	0.0166	0.0165	0.0165	0.0165	0.0165
u-Btu/lbm	158.5	158.3	158	157.6	157.2	156.9	156.5
h-Btu/lbm	159.3	159.9	161	162.2	163.3	164.5	165.6
s-Btu/lbm/R	0.27953	0.27924	0.27896	0.27866	0.27839	0.27795	0.27759

Temperature=	700.0 R	Psat=	25.1 psi					
Press(psi)=	250	500	1000	1500	2000	2500	3000	3500
v-ft3/lbm	0.017	0.0169	0.0169	0.0169	0.0169	0.0168	0.0168	0.0167
u-Btu/lbm	209	208.7	208.2	207.7	207.2	206.8	205.8	205.4
h-Btu/lbm	209.7	210.3	211.3	212.4	213.5	214.5	215.6	216.7
s-Btu/lbm/R	0.35431	0.35395	0.35323	0.35252	0.35182	0.35113	0.35044	0.34976
Temperature=	750.0 R	Psat=	57.9 psi					
Press(psi)=	250	500	1000	1500	2000	2500	3000	3500
v-ft3/lbm	0.0174	0.0174	0.0173	0.0173	0.0173	0.0172	0.0172	0.0171
u-Btu/lbm	259.9	259.6	259	258.3	257.7	257.1	256.5	255.9
h-Btu/lbm	260.7	261.2	262.2	263.1	264.1	265.1	266	267
s-Btu/lbm/R	0.42467	0.42423	0.42337	0.42251	0.42167	0.42083	0.42001	0.41919
Temperature=	800.0 R	Psat=	118.5 psi					
Press(psi)=	250	500	1000	1500	2000	2500	3000	3500
v-ft3/lbm	0.0179	0.0179	0.0178	0.0178	0.0178	0.0177	0.0177	0.0176
u-Btu/lbm	311.7	311.3	310.4	309.6	308.8	308.1	307.3	306.5
h-Btu/lbm	312.5	312.9	313.7	314.6	315.4	316.2	317.1	318
s-Btu/lbm/R	0.49152	0.49099	0.48994	0.48891	0.4879	0.4869	0.48592	0.48495
Temperature=	850.0 R	Psat=	221.1 psi					
Press(psi)=	250	500	1000	1500	2000	2500	3000	3500
v-ft3/lbm	0.0185	0.0185	0.0185	0.0184	0.0184	0.0183	0.0183	0.0182
u-Btu/lbm	364.6	364.1	363	362	360.9	359.9	358.9	358
h-Btu/lbm	365.5	365.8	366.4	367.1	367.7	368.4	369.1	369.8
s-Btu/lbm/R	0.55573	0.55508	0.5538	0.55255	0.55132	0.55012	0.54894	0.54778
Temperature=	900.0 R	Psat=	382.7 psi					
Press(psi)=	250	500	1000	1500	2000	2500	3000	3500
v-ft3/lbm	0.0193	0.0192	0.0192	0.0192	0.0191	0.019	0.019	0.0189
u-Btu/lbm	418.6	417.1	415.8	414.4	413.1	411.8	410.6	409.4
h-Btu/lbm	420.4	420.7	421.1	421.5	421.9	422.4	422.9	423.4
s-Btu/lbm/R	0.61744	0.61584	0.61428	0.61277	0.61129	0.60985	0.60844	0.60706

Temperature=	950.0	R	Psat=	623.1	psi						
Press(psi)=	250		500	1000		1500	2000	2500	3000	3500	4000
v-ft3/lbm			0.0202	0.0201	0.02	0.0199	0.0198	0.0197	0.0197	0.0197	5000
u-Btu/lbm			473.7	471.8	470	468.2	466.6	464.9	463.4	462.4	0.0195
h-Btu/lbm			477.4	477.4	477.4	477.4	477.6	477.7	477.9	478.4	
s-Btu/lbm/R			0.67717	0.67515	0.67321	0.67133	0.66951	0.66775	0.66604	0.66277	
Temperature=	1000.0	R	Psat=	964.9	psi						
Press(psi)=	250		500	1000		1500	2000	2500	3000	3500	4000
v-ft3/lbm			0.0215	0.0214	0.0212	0.0211	0.0209	0.0208	0.0207	0.0207	5000
u-Btu/lbm			534.2	531.4	528.8	526.3	524	521.8	519.6	517.5	0.0205
h-Btu/lbm			538.2	537.4	536.7	536.1	535.6	535.2	534.9	534.6	
s-Btu/lbm/R			0.73949	0.73666	0.73399	0.73146	0.72905	0.72675	0.72454	0.72038	
Temperature=	1050.0	R	Psat=	1434.3	psi						
Press(psi)=	250		500	1000		1500	2000	2500	3000	3500	4000
v-ft3/lbm			0.0232	0.0229	0.0227	0.0224	0.0222	0.0222	0.0221	0.0221	5000
u-Btu/lbm			597.7	593.4	589.5	585.9	582.6	579.5	573.9	573.9	0.0217
h-Btu/lbm			604.2	601.9	599.9	598.3	597	595.8	594	594	
s-Btu/lbm/R			0.80183	0.7976	0.79376	0.79024	0.78696	0.7839	0.7783	0.7783	
Temperature=	1100.0	R	Psat=	2063.9	psi						
Press(psi)=	250		500	1000		1500	2000	2500	3000	3500	4000
v-ft3/lbm							0.0254	0.0249	0.0244	0.024	5000
u-Btu/lbm							663.3	656.4	650.6	645.4	0.0234
h-Btu/lbm							675.1	670.2	666.4	663.2	636.7
s-Btu/lbm/R							0.86361	0.85706	0.85149	0.8466	0.83821

# **Appendix D**

## **Thermodynamic Property Tables**

### **for Carbon Dioxide**

### D.1 CO<sub>2</sub>Saturation Temperature Table (SI Units)

T (K)	P (MPa)	Volume (m <sup>3</sup> /kg)	Energy (kJ/kg)	Enthalpy (kJ/kg)	Entropy (kJ/kg/K)
		v <sub>f</sub>	u <sub>f</sub>	h <sub>f</sub>	s <sub>f</sub>
		v <sub>fg</sub>	u <sub>fg</sub>	h <sub>fg</sub>	s <sub>fg</sub>
216.5	0.5173	0.000847	0.071931	0.072778	0.00
220.0	0.6000	0.000857	0.062281	0.063137	6.49
225.0	0.7365	0.000871	0.050940	0.051811	16.88
230.0	0.8949	0.000885	0.041984	0.042869	27.28
235.0	1.0769	0.000901	0.034828	0.035729	37.55
240.0	1.2849	0.000918	0.029049	0.029967	47.72
245.0	1.5211	0.000936	0.024333	0.025269	57.89
250.0	1.7875	0.000956	0.020449	0.021405	68.15
255.0	2.0866	0.000977	0.017222	0.018199	78.52
260.0	2.4208	0.001001	0.014516	0.015516	89.06
265.0	2.7924	0.001027	0.012227	0.013254	99.79
270.0	3.2043	0.001056	0.010272	0.011328	110.77
275.0	3.6592	0.001090	0.008586	0.009676	122.13
280.0	4.1602	0.001129	0.007113	0.008242	134.02
285.0	4.7106	0.001177	0.005805	0.006982	146.67
290.0	5.3143	0.001239	0.004616	0.005854	160.36
295.0	5.9765	0.001324	0.003484	0.004808	175.75
300.0	6.7058	0.001471	0.002278	0.003749	195.40
304.2	7.3834	0.002155	0.000000	0.002155	241.37

## D.2 CO<sub>2</sub> Saturation Pressure Table (SI Units)

P (MPa)	T (K)	Volume (m <sup>3</sup> /kg)			Energy (kJ/kg)			Enthalpy (kJ/kg)			Entropy (kJ/kg/K)		
		v <sub>f</sub>	v <sub>fg</sub>	v <sub>g</sub>	u <sub>f</sub>	u <sub>fg</sub>	u <sub>g</sub>	h <sub>f</sub>	h <sub>fg</sub>	h <sub>g</sub>	s <sub>f</sub>	s <sub>fg</sub>	s <sub>g</sub>
0.5173	216.5	0.000847	0.071926	0.072774	0.00	314.66	314.23	0.00	351.87	351.87	0.00001	1.62495	1.62496
0.6000	220.0	0.000857	0.062281	0.063137	6.49	308.75	315.24	7.00	346.12	351.12	0.03175	1.57326	1.60301
0.7000	223.7	0.000867	0.053559	0.054425	14.23	302.01	316.24	14.84	339.50	354.34	0.06669	1.51745	1.58143
0.8000	227.1	0.000877	0.046942	0.047819	21.24	295.84	317.08	21.94	333.39	355.33	0.09780	1.46610	1.56590
0.9000	230.2	0.000886	0.041744	0.042630	27.59	290.18	317.77	28.38	327.75	356.13	0.12561	1.42406	1.54967
1.0000	233.0	0.000895	0.037547	0.038442	33.39	284.95	318.34	34.29	322.50	356.78	0.15071	1.38428	1.53499
1.5000	244.6	0.000935	0.024695	0.025630	57.04	262.97	320.00	58.44	300.01	358.45	0.24998	1.22664	1.47662
2.0000	253.6	0.000971	0.018062	0.019033	75.62	244.73	320.36	77.56	280.86	359.42	0.3248	1.10744	1.43229
2.5000	261.1	0.001006	0.013974	0.014981	91.43	228.41	319.84	93.94	263.35	357.29	0.38657	1.0857	1.39514
3.0000	267.6	0.001041	0.011180	0.012221	105.43	213.22	318.65	108.55	246.76	355.32	0.43989	0.92220	1.36208
3.5000	273.3	0.001078	0.009131	0.010209	118.23	198.63	316.86	122.00	230.59	352.59	0.48766	0.84371	1.33137
4.0000	278.5	0.001116	0.007549	0.008665	130.27	184.22	314.48	134.73	214.41	349.15	0.53182	0.77001	1.30183
4.5000	283.1	0.001158	0.006275	0.007433	141.86	169.62	311.48	147.07	197.86	344.93	0.57374	0.69880	1.27254
5.0000	287.5	0.001205	0.005210	0.006415	153.23	154.53	307.77	159.56	180.58	339.84	0.61437	0.62821	1.24258
5.5000	291.5	0.001260	0.004285	0.005545	164.60	138.54	303.14	171.53	162.11	333.64	0.65445	0.55620	1.21085
6.0000	295.2	0.001328	0.003445	0.004773	176.32	120.92	297.23	184.28	141.59	325.87	0.69592	0.47968	1.17560
6.5000	298.6	0.001420	0.002199	0.003619	189.34	77.22	266.56	198.56	90.42	288.95	0.74169	0.30631	1.04800
7.0000	301.9	0.001571	0.000955	0.002526	205.65	14.70	220.35	216.64	39.24	255.88	0.79940	0.13294	0.93234
7.3834	304.2	0.002155	0.000000	0.002155	241.37	0.00	241.37	257.31	0.00	257.31	0.93116	0.00000	0.93116

### D.3 Superheated CO<sub>2</sub> Table (SI Units)

$P = 0.5173 \text{ MPa } T(K) 216.5$	220.	250.	300.	350.	400.	500.	600.	700.	800.	900.	1000.
$v, m^3/kg$	0.07277	0.07429	0.08591	0.10672	0.12556	0.14469	0.18190	0.21881	0.25559	0.29229	0.32955
$u, kJ/kg$	314.23	316.52	336.19	369.47	404.41	441.28	520.67	606.76	698.42	794.67	894.67
$h, kJ/kg$	351.87	354.95	381.15	424.68	469.32	516.13	614.77	719.95	830.64	945.88	1064.84
$s, kJ/kg/K$	1.62496	1.63907	1.75074	1.90943	2.04760	2.17203	2.39184	2.58344	2.75397	2.90778	3.04786
$P = 0.6000 \text{ MPa } T(K) 220.0$	220.	250.	300.	350.	400.	500.	600.	700.	800.	900.	1000.
$v, m^3/kg$	0.06314	0.06000	0.07429	0.09161	0.10824	0.12456	0.15673	0.18861	0.22036	0.25202	0.28365
$u, kJ/kg$	315.24	0.0	335.31	368.92	404.01	440.97	520.47	606.50	698.30	794.57	894.58
$h, kJ/kg$	353.12	0.0	379.89	423.89	468.96	515.71	614.50	719.77	830.51	945.78	1064.77
$s, kJ/kg/K$	1.60501	0.00000	1.71914	1.87954	2.01844	2.14324	2.36341	2.55516	2.72578	2.87964	3.01975
$P = 0.7000 \text{ MPa } T(K) 223.7$	250.	300.	350.	400.	500.	600.	700.	800.	900.	1000.	1200.
$v, m^3/kg$	0.05443	0.06301	0.07811	0.09250	0.10656	0.13424	0.16162	0.18887	0.21604	0.24316	0.27026
$u, kJ/kg$	316.24	334.23	368.24	403.52	440.60	520.21	606.41	698.15	794.44	894.48	997.60
$h, kJ/kg$	354.34	378.34	422.91	466.27	515.19	614.18	719.55	830.36	945.67	1064.69	1186.78
$s, kJ/kg/K$	1.58413	1.68559	1.84813	1.98793	2.111318	2.333378	2.52573	2.69644	2.85036	2.99051	3.11911
$P = 0.8000 \text{ MPa } T(K) 227.1$	250.	300.	350.	400.	500.	600.	700.	800.	900.	1000.	1200.
$v, m^3/kg$	0.04752	0.05454	0.06798	0.08069	0.09367	0.11737	0.14138	0.16526	0.18905	0.21280	0.23652
$u, kJ/kg$	317.08	333.12	367.55	403.04	440.22	519.96	606.23	698.10	794.32	894.37	997.50
$h, kJ/kg$	355.33	376.75	421.94	467.59	514.68	613.86	719.33	830.21	945.56	1064.61	1186.72
$s, kJ/kg/K$	1.55650	1.65582	1.82060	1.96130	2.08702	2.30805	2.50019	2.67100	2.82498	2.96516	3.09379
$P = 0.9000 \text{ MPa } T(K) 230.2$	250.	300.	350.	400.	500.	600.	700.	800.	900.	1000.	1200.
$v, m^3/kg$	0.04263	0.04794	0.06010	0.07150	0.08258	0.10425	0.12564	0.14689	0.16806	0.18919	0.21028
$u, kJ/kg$	317.77	331.99	366.86	402.55	439.85	519.71	606.04	697.85	794.20	894.27	997.41
$h, kJ/kg$	356.13	375.13	420.95	466.90	514.17	613.54	719.11	830.05	945.45	1064.54	1186.67
$s, kJ/kg/K$	1.54967	1.62888	1.79601	1.93764	2.06383	2.28530	2.47762	2.64854	2.820257	2.94280	3.07145
$P = 1.0000 \text{ MPa } T(K) 233.0$	250.	300.	350.	400.	500.	600.	700.	800.	900.	1000.	1200.
$v, m^3/kg$	0.03844	0.04265	0.05379	0.06416	0.07418	0.09376	0.11305	0.13220	0.15127	0.17030	0.18929
$u, kJ/kg$	318.34	330.83	366.16	402.05	439.47	519.46	605.85	697.70	794.07	894.16	997.32
$h, kJ/kg$	356.78	373.47	419.95	466.21	513.55	613.22	718.90	829.90	945.34	1064.46	1186.61
$s, kJ/kg/K$	1.53499	1.60415	1.77374	1.91632	2.04298	2.26489	2.45741	2.62942	2.79227	3.05145	3.30066
$P = 1.5000 \text{ MPa } T(K) 244.6$	250.	300.	350.	400.	500.	600.	700.	800.	900.	1000.	1200.
$v, m^3/kg$	0.02563	0.02665	0.03485	0.04211	0.04889	0.06228	0.07527	0.08812	0.10090	0.11362	0.12632
$u, kJ/kg$	320.00	324.48	362.54	395.55	437.58	518.19	604.91	696.95	793.45	893.63	996.86

$h, \text{kJ/kg}$	358.45	364.46	414.82	462.71	511.06	611.61	717.81	829.13	944.80	1064.07	1186.34	1438.11
$s, \text{kJ/kg/K}$	1.47662	1.50091	1.68488	1.83254	1.96164	2.18577	2.37925	2.55076	2.70515	2.84559	2.97439	3.20379
$P = 2.0000 \text{ MPa } T(\text{K})$	253.6	300.	350.	400.	500.	600.	700.	800.	900.	1000.	1200.	1400.
$v, \text{m}^3/\text{kg}$	0.01903	0.013107	0.03640	0.04654	0.05638	0.06608	0.07571	0.08549	0.09484	0.11388	0.13287	
$u, \text{kJ/kg}$	320.36	358.72	396.99	435.65	516.92	603.97	636.21	792.83	893.10	996.40	1210.25	1431.83
$h, \text{kJ/kg}$	358.42	409.41	459.13	508.45	610.01	716.73	828.37	944.25	1063.68	1186.07	1438.01	1697.57
$s, \text{kJ/kg/K}$	1.43229	1.61745	1.77081	1.90250	2.12891	2.32355	2.49535	2.65003	2.79066	2.91959	3.14914	3.34913
$P = 2.5000 \text{ MPa } T(\text{K})$	261.1	300.	350.	400.	500.	600.	700.	800.	900.	1000.	1200.	1400.
$v, \text{m}^3/\text{kg}$	0.01498	0.02445	0.02884	0.03710	0.04505	0.05286	0.06060	0.06829	0.07595	0.09121	0.10642	
$u, \text{kJ/kg}$	319.84	354.65	394.35	433.71	515.65	603.03	695.46	792.22	892.58	995.94	1209.89	1431.53
$h, \text{kJ/kg}$	357.29	403.69	455.48	505.81	608.40	715.66	827.62	943.71	1063.30	1185.81	1437.91	1697.58
$s, \text{kJ/kg/K}$	1.39514	1.56125	1.72105	1.85548	2.08423	2.27964	2.45215	2.60711	2.74793	2.87698	3.10668	3.30675
$P = 3.0000 \text{ MPa } T(\text{K})$	267.6	300.	350.	400.	500.	600.	700.	800.	900.	1000.	1200.	1400.
$v, \text{m}^3/\text{kg}$	0.01222	0.01577	0.02003	0.02381	0.03081	0.03750	0.04405	0.05050	0.05695	0.06335	0.07609	0.08879
$u, \text{kJ/kg}$	318.65	350.28	391.64	431.73	514.38	602.09	694.72	791.60	892.06	995.49	1209.53	1431.22
$h, \text{kJ/kg}$	355.32	397.58	451.73	503.15	606.80	714.59	826.87	943.18	1062.92	1185.55	1437.81	1697.60
$s, \text{kJ/kg/K}$	1.36208	1.51160	1.67877	1.81611	2.04727	2.24365	2.41666	2.57182	2.71291	2.84208	3.07193	3.27210
$P = 3.5000 \text{ MPa } T(\text{K})$	273.3	300.	350.	400.	500.	600.	700.	800.	900.	1000.	1200.	1400.
$v, \text{m}^3/\text{kg}$	0.01021	0.01299	0.01687	0.02021	0.02632	0.03211	0.03776	0.04333	0.04886	0.05436	0.06530	0.07620
$u, \text{kJ/kg}$	316.86	345.55	388.85	429.73	513.10	601.15	693.98	790.99	891.53	995.03	1209.17	1430.92
$h, \text{kJ/kg}$	352.59	391.01	447.90	500.47	605.21	713.52	826.13	942.65	1062.55	1185.29	1437.72	1697.61
$s, \text{kJ/kg/K}$	1.33137	1.46584	1.64157	1.78201	2.01563	2.21299	2.38650	2.54204	2.68321	2.81251	3.04251	3.24276
$P = 4.0000 \text{ MPa } T(\text{K})$	278.5	300.	350.	400.	500.	600.	700.	800.	900.	1000.	1200.	1400.
$v, \text{m}^3/\text{kg}$	0.00867	0.01087	0.01450	0.01751	0.02295	0.02806	0.03304	0.03794	0.04279	0.04761	0.05720	0.06675
$u, \text{kJ/kg}$	311.48	340.37	385.38	427.71	511.82	600.21	693.24	790.38	891.02	994.58	1208.81	1430.62
$h, \text{kJ/kg}$	344.93	383.86	443.96	497.76	603.61	712.47	825.39	941.13	1062.18	1185.03	1437.62	1697.63
$s, \text{kJ/kg/K}$	1.30183	1.42218	1.60799	1.75173	1.975173	2.18624	2.36023	2.51606	2.65742	2.78684	3.01699	3.21732
$P = 4.5000 \text{ MPa } T(\text{K})$	283.1	300.	350.	400.	500.	600.	700.	800.	900.	1000.	1200.	1400.
$v, \text{m}^3/\text{kg}$	0.00743	0.00919	0.01265	0.01541	0.02033	0.02492	0.02937	0.03374	0.03807	0.04237	0.05091	0.05940
$u, \text{kJ/kg}$	307.77	328.03	379.95	423.57	509.24	598.34	694.77	789.17	889.50	994.13	1208.45	1430.33
$h, \text{kJ/kg}$	339.84	366.98	435.76	492.26	600.43	710.37	823.93	941.10	1061.45	1184.53	1437.45	1697.67
$s, \text{kJ/kg/K}$	1.24258	1.33514	1.54826	1.69927	1.94068	2.14103	2.31602	2.47242	2.61414	2.74380	2.97424	3.17474
$P = 5.0000 \text{ MPa } T(\text{K})$	287.5	300.	350.	400.	500.	600.	700.	800.	900.	1000.	1200.	1400.
$v, \text{m}^3/\text{kg}$	0.00641	0.00779	0.01116	0.01374	0.01824	0.02241	0.02643	0.03039	0.03429	0.03817	0.04587	0.05353
$u, \text{kJ/kg}$	301.48	334.61	383.01	425.66	510.53	599.47	692.50	789.77	889.98	993.68	1208.09	1430.03
$h, \text{kJ/kg}$	344.93	375.94	439.92	495.02	602.02	711.41	824.66	941.61	1061.81	1184.78	1437.53	1697.65
$s, \text{kJ/kg/K}$	1.27254	1.37913	1.577711	1.72436	1.96311	2.116246	2.333695	2.49307	2.63460	2.76414	2.99444	3.19486

$P = 5.5000 \text{ MPa } T(K) 291.5$	300.	350.	400.	500.	600.	700.	800.	900.	1000.	1200.	1400.
$v, \text{m}^3/\text{kg}$	0.00659	0.00995	0.01236	0.01653	0.02035	0.02403	0.02764	0.03120	0.03475	0.04175	0.04872
$u, \text{kJ/kg}$	303.14	320.24	376.78	421.47	507.95	597.40	691.03	788.56	889.47	993.23	1207.73
$h, \text{kJ/kg}$	333.64	356.46	431.48	489.47	598.84	709.33	823.21	940.59	1061.09	1184.29	1437.36
$s, \text{kJ/kg/K}$	1.21085	1.28813	1.52098	1.67602	1.92015	2.12151	2.29699	2.45368	2.59557	2.72535	2.95594
$P = 6.0000 \text{ MPa } T(K) 295.2$	300.	350.	400.	500.	600.	700.	800.	900.	1000.	1200.	1400.
$v, \text{m}^3/\text{kg}$	0.00477	0.00548	0.00893	0.01122	0.01510	0.01864	0.02203	0.02535	0.02863	0.03188	0.03832
$u, \text{kJ/kg}$	297.23	325.87	373.50	419.33	506.66	596.47	690.30	787.96	888.95	992.78	1207.38
$h, \text{kJ/kg}$	325.87	343.29	427.06	486.66	597.26	708.29	822.50	940.08	1060.73	1184.04	1437.28
$s, \text{kJ/kg/K}$	1.17560	1.22416	1.49490	1.65226	1.90119	2.10356	2.27954	2.43650	2.57858	2.70848	2.93921
$P = 6.5000 \text{ MPa } T(K) 298.6$	300.	350.	400.	500.	600.	700.	800.	900.	1000.	1200.	1400.
$v, \text{m}^3/\text{kg}$	0.00142	0.00435	0.00806	0.01025	0.01389	0.01719	0.02034	0.02342	0.02645	0.02946	0.03541
$u, \text{kJ/kg}$	189.33	295.63	370.09	417.16	505.36	595.54	689.57	787.36	888.44	992.34	1207.02
$h, \text{kJ/kg}$	198.55	323.90	422.95	483.81	593.68	707.26	821.79	939.58	1060.38	1183.38	1437.19
$s, \text{kJ/kg/K}$	0.74165	1.16131	1.46975	1.63375	1.88354	2.08694	2.26341	2.42026	2.56290	2.69292	2.92380
$P = 7.0000 \text{ MPa } T(K) 301.9$	350.	400.	500.	600.	700.	800.	900.	1000.	1200.	1400.	1600.
$v, \text{m}^3/\text{kg}$	0.00152	0.00732	0.00943	0.01286	0.01595	0.01889	0.02176	0.02459	0.02738	0.03292	0.03842
$u, \text{kJ/kg}$	205.74	366.55	414.96	504.06	594.61	688.84	786.76	887.93	991.90	1206.67	1428.85
$h, \text{kJ/kg}$	216.75	417.79	480.95	594.10	706.24	821.08	939.09	1050.03	1183.57	1437.11	1697.76
$s, \text{kJ/kg/K}$	0.79975	1.44529	1.61429	1.86703	2.07144	2.24840	2.40993	2.54835	2.67849	2.90951	3.11034
$P = 7.3834 \text{ MPa } T(K) 304.2$	350.	400.	500.	600.	700.	800.	900.	1000.	1200.	1400.	1600.
$v, \text{m}^3/\text{kg}$	0.00221	0.00682	0.00887	0.01217	0.01510	0.01791	0.02064	0.02333	0.02598	0.03124	0.03645
$u, \text{kJ/kg}$	243.72	363.73	413.26	503.07	593.89	688.29	786.30	887.55	991.56	1206.40	1428.62
$h, \text{kJ/kg}$	260.02	414.06	478.73	592.89	705.46	820.55	938.71	1059.77	1183.39	1437.05	1697.78
$s, \text{kJ/kg/K}$	0.94013	1.42690	1.59999	1.85503	2.06022	2.23756	2.39530	2.53786	2.66808	2.89922	3.10011
$P = 7.500 \text{ MPa }$	350.	400.	500.	600.	700.	800.	900.	1000.	1200.	1400.	1600.
$v, \text{m}^3/\text{kg}$	0.00166	0.00667	0.00871	0.01197	0.01487	0.01764	0.02032	0.02297	0.02558	0.03076	0.03590
$u, \text{kJ/kg}$	214.30	362.86	412.74	502.76	593.68	688.12	786.16	887.43	991.46	1206.32	1428.56
$h, \text{kJ/kg}$	226.75	412.90	478.05	592.53	705.23	820.38	938.59	1059.69	1183.33	1437.03	1697.79
$s, \text{kJ/kg/K}$	0.83007	1.42135	1.59573	1.85148	2.05691	2.23437	2.39217	2.53477	2.66502	2.89919	3.09710
$P = 8.000 \text{ MPa }$	350.	400.	500.	600.	700.	800.	900.	1000.	1200.	1400.	1600.
$v, \text{m}^3/\text{kg}$	0.00148	0.00610	0.00808	0.01119	0.01393	0.01654	0.01907	0.02155	0.02401	0.02887	0.03369
$u, \text{kJ/kg}$	200.44	359.01	410.48	501.46	592.75	687.39	785.57	886.92	991.02	1205.97	1428.27
$h, \text{kJ/kg}$	212.29	407.83	475.13	590.96	704.22	819.69	938.11	1059.35	1183.10	1436.96	1697.81
$s, \text{kJ/kg/K}$	0.78001	1.39775	1.57794	1.83678	2.04324	2.22118	2.37926	2.52203	2.65240	2.88371	3.08470

$P = 9.000 \text{ MPa}$	350.	400.	500.	600.	700.	800.	900.	1000.	1200.	1400.	1600.
$v, \text{m}^3/\text{kg}$	0.00137	0.00515	0.01074	0.01989	0.02127	0.01471	0.01697	0.01920	0.02139	0.02573	0.03429
$u, \text{kJ/kg}$	189.73	350.78	405.88	498.85	590.90	685.95	784.39	885.92	990.14	1205.27	1427.69
$h, \text{kJ/kg}$	202.07	397.10	469.21	587.83	702.21	818.32	937.15	1058.68	1182.65	1436.81	1697.87
$s, \text{kJ/kg/K}$	0.74177	1.35107	1.54429	1.80950	2.01803	2.19696	2.35559	2.49870	2.62930	2.86089	3.06204
$P = 10.000 \text{ MPa}$	350.	400.	500.	600.	700.	800.	900.	1000.	1200.	1400.	1600.
$v, \text{m}^3/\text{kg}$	0.00132	0.00437	0.00620	0.00885	0.01112	0.01325	0.01530	0.01731	0.01929	0.02321	0.02708
$u, \text{kJ/kg}$	183.35	341.76	401.15	496.24	589.05	684.52	783.21	884.92	989.27	1204.58	1427.11
$h, \text{kJ/kg}$	196.51	385.51	463.19	584.73	700.24	816.97	936.20	1058.02	1182.21	1436.67	1697.94
$s, \text{kJ/kg/K}$	0.71907	1.30438	1.51273	1.78460	1.99520	2.17510	2.33428	2.47773	2.60855	2.84042	3.04173
$P = 12.500 \text{ MPa}$	350.	400.	500.	600.	700.	800.	900.	1000.	1200.	1400.	1600.
$v, \text{m}^3/\text{kg}$	0.00124	0.00300	0.00472	0.00699	0.00888	0.01062	0.01229	0.01392	0.01552	0.01868	0.02180
$u, \text{kJ/kg}$	173.03	315.84	388.84	489.68	584.47	680.97	780.30	882.45	987.12	1202.87	1425.69
$h, \text{kJ/kg}$	188.49	353.29	447.78	577.07	695.41	813.69	933.93	1056.45	1181.16	1436.36	1698.12
$s, \text{kJ/kg/K}$	0.68224	1.18642	1.44045	1.73002	1.94585	2.12816	2.28867	2.43295	2.56433	2.79668	2.99857
$P = 15.000 \text{ MPa}$	350.	400.	500.	600.	700.	800.	900.	1000.	1200.	1400.	1600.
$v, \text{m}^3/\text{kg}$	0.00119	0.00222	0.00374	0.00576	0.00739	0.00887	0.01029	0.01166	0.01301	0.01566	0.01827
$u, \text{kJ/kg}$	165.95	289.68	376.00	483.13	579.93	677.47	777.44	880.02	985.01	1201.19	1424.28
$h, \text{kJ/kg}$	183.79	322.92	432.17	569.58	690.74	810.55	931.75	1054.96	1180.18	1436.10	1698.34
$s, \text{kJ/kg/K}$	0.65685	1.08136	1.37520	1.68334	1.90438	2.08905	2.25087	2.39596	2.52788	2.776108	3.14185
$P = 20.000 \text{ MPa}$	350.	400.	500.	600.	700.	800.	900.	1000.	1200.	1400.	1600.
$v, \text{m}^3/\text{kg}$	0.00113	0.00163	0.00262	0.00426	0.00554	0.00670	0.00779	0.00885	0.00988	0.01189	0.01387
$u, \text{kJ/kg}$	155.78	255.86	350.57	470.16	571.04	670.64	771.86	875.29	980.90	1197.91	1421.54
$h, \text{kJ/kg}$	178.36	288.43	403.03	555.30	681.94	804.67	927.13	1052.23	1178.42	1435.70	1698.87
$s, \text{kJ/kg/K}$	0.61997	0.95621	1.26338	1.60545	1.83658	2.02578	2.19003	2.33671	2.46965	2.70411	3.08604

# **Appendix E**

## **Thermodynamic Property Tables for Sodium**

## E.1 Sodium Temperature Saturation Table—SI Units

T(K)	P(MPa)	Volume (m <sup>3</sup> /kg) vf vg	Energy (kJ/kg) uf urg	Enthalpy (kJ/kg) hf hfg	Entropy (kJ/kg) sf sg
800.0	0.001	0.001211	298.0341	298.0353	0.0
850.0	0.002	0.001229	127.4088	127.4100	66.4
900.0	0.005	0.001247	60.0689	60.0702	132.7
950.0	0.011	0.001266	30.7359	30.7372	200.2
1000.0	0.020	0.001286	16.8587	16.8587	266.5
1050.0	0.036	0.001306	9.8135	9.8148	336.6
1100.0	0.060	0.001327	6.1137	6.0150	405.1
1154.6	0.101	0.001351	3.7069	3.7083	479.9
1200.0	0.150	0.001372	2.5685	2.5699	542.4
1250.0	0.224	0.001395	1.7722	1.7736	611.0
1300.0	0.325	0.001419	1.2599	1.2613	682.9
1400.0	0.625	0.001469	0.6885	0.6899	831.8
1500.0	1.101	0.001523	0.4091	0.4106	998.1
1600.0	1.802	0.001581	0.2590	0.2606	1194.0
1700.0	2.776	0.001642	0.1713	0.1729	1440.8
					2804.2
					1445.0
					4245.0
					1445.4
					3279.7
					4725.1
					1.0487
					1.9292
					2.9780

## E.2 Sodium Pressure Saturation Table—SI Units

P (MPa)	T (K)	Volume v <sub>f</sub>	Volume v <sub>fg</sub>	Volume v <sub>g</sub>	Energy (kJ/kg)				Enthalpy (kJ/kg)				Entropy (kJ/kg)			
					u <sub>f</sub>	u <sub>fg</sub>	u <sub>g</sub>	h <sub>f</sub>	h <sub>fg</sub>	h <sub>g</sub>	s <sub>f</sub>	s <sub>fg</sub>	s <sub>g</sub>			
0.009	941.1	0.001263	34.4471	34.4483	188.2	3848.4	4036.6	188.2	4170.3	4358.5	0.2165	4.4313	4.6479			
0.020	999.9	0.001286	16.8773	268.2	3765.5	4033.7	268.2	4103.1	4371.3	0.2988	4.1035	4.4023				
0.040	1060.5	0.001311	8.8223	8.8236	351.0	3679.4	4030.3	351.0	4032.3	4383.3	0.3788	3.8024	4.1811			
0.060	1099.5	0.001327	6.0411	6.0425	404.3	3624.2	4028.6	404.4	3986.7	4391.1	0.4278	3.6228	4.0536			
0.080	1129.1	0.001340	4.6196	4.6209	444.9	3582.8	4027.7	445.0	3952.4	4397.4	0.4637	3.5006	3.9643			
0.100	1153.1	0.001351	3.7528	3.7541	477.9	3549.6	4027.5	478.0	3924.9	4402.9	0.4921	3.4036	3.8958			
0.101	1154.6	0.001351	3.7070	3.7084	480.0	3547.5	4027.5	480.1	3923.1	4403.2	0.4939	3.3978	3.8917			
0.200	1235.2	0.001388	1.9714	1.9728	591.3	3439.4	4030.7	591.5	3833.7	4425.3	0.5844	3.1038	3.6882			
0.300	1289.0	0.001413	1.3548	1.3562	667.1	3370.0	4037.2	667.6	3776.5	4444.0	0.6414	2.9298	3.5712			
0.400	1330.2	0.001434	1.0390	1.0404	726.6	3318.3	4044.9	727.2	3733.9	4461.1	0.6836	2.8070	3.4905			
0.500	1364.1	0.001451	0.8459	0.8474	777.0	3276.3	4053.2	777.7	3699.2	4476.9	0.7175	2.7118	3.4293			
0.750	1430.6	0.001485	0.5826	0.5841	880.3	3194.6	4074.9	881.4	3631.6	4513.0	0.7825	2.5385	3.3210			
1.000	1481.9	0.001513	0.4471	0.4486	966.2	3130.5	4096.8	967.7	3577.6	4545.3	0.8320	2.4142	3.2461			
2.000	1623.0	0.001594	0.2348	0.2364	1245.1	2936.1	4181.1	1248.3	3405.6	4653.8	0.9691	2.0983	3.0675			
3.000	1719.4	0.001655	0.1586	0.1603	1497.8	2766.0	4263.7	1502.7	3241.9	4744.6	1.0698	1.8855	2.9553			

### E.3 Superheated Sodium Table—SI Units

$P = 0.0093 \text{ MPa } T(K) 941.1$	950.	1000.	1050.	1100.	1150.	1200.	1250.	1300.	1350.	1400.	1450.
$v, m^3/kg$	34.44834	34.3420	37.4751	39.7787	41.9451	44.0527	46.0856	48.0955	50.0854	52.0603	54.0195
$u, kJ/kg$	4036.59	4053.95	4131.43	4187.49	4231.91	4269.71	4303.53	4334.91	4364.73	4393.52	4421.62
$h, kJ/kg$	4356.54	4389.48	4481.67	4559.26	4623.98	4681.33	4734.23	4784.41	4823.83	4880.08	4926.55
$s, kJ/kg/K$	4.64786	4.6711	4.7751	4.8509	4.9111	4.9622	5.0072	5.0481	5.0861	5.1218	5.1555
$P = 0.0500 \text{ MPa } T(K) 1081.6$	1100.	1150.	1200.	1250.	1300.	1350.	1400.	1450.	1500.	1550.	1600.
$v, m^3/kg$	7.16339	7.3656	7.8738	8.3370	8.7728	9.1880	9.5989	9.9813	10.3661	10.7461	11.1220
$u, kJ/kg$	4029.30	4067.50	4152.25	4217.57	4270.57	4315.56	4355.23	4391.29	4424.85	4456.64	4487.15
$h, kJ/kg$	4387.47	4435.77	4545.94	4624.47	4709.21	4774.96	4834.71	4890.36	4943.17	4993.95	5043.27
$s, kJ/kg/K$	4.11076	4.1553	4.2536	4.3291	4.3902	4.4418	4.4870	4.5275	4.5645	4.5990	4.6313
$P = 0.1000 \text{ MPa } T(K) 1153.1$	1200.	1250.	1300.	1350.	1400.	1450.	1500.	1550.	1600.	1700.	1800.
$v, m^3/kg$	3.75411	4.0095	4.2583	4.4909	4.7099	4.9198	5.1238	5.3224	5.5175	5.7113	6.0886
$u, kJ/kg$	4027.47	4118.13	4194.78	4257.01	4309.31	4354.73	4395.35	4432.52	4467.19	4500.04	4551.93
$h, kJ/kg$	4402.87	4510.07	4620.66	4706.08	4780.30	4846.74	4907.72	4964.76	5018.94	5071.02	5170.79
$s, kJ/kg/K$	3.89575	3.9956	4.0790	4.1462	4.2023	4.2507	4.2932	4.3372	4.3678	4.4009	4.4614
$P = 0.1013 \text{ MPa } T(K) 1154.6$	1200.	1250.	1300.	1350.	1400.	1450.	1500.	1550.	1600.	1700.	1800.
$v, m^3/kg$	3.70836	3.9531	4.2086	4.4293	4.6460	4.8546	5.0551	5.2515	5.4449	5.6342	6.0083
$u, kJ/kg$	4027.46	4115.61	4193.14	4255.49	4308.11	4353.79	4394.57	4431.88	4466.67	4499.59	4551.62
$h, kJ/kg$	4403.21	4516.16	4618.74	4704.29	4778.88	4845.62	4906.79	4963.99	5018.31	5070.48	5170.40
$s, kJ/kg/K$	3.89173	3.9887	4.0736	4.1403	4.1967	4.2453	4.2883	4.3271	4.3627	4.3958	4.4564
$P = 0.2000 \text{ MPa } T(K) 1235.2$	1250.	1300.	1350.	1400.	1450.	1500.	1550.	1600.	1700.	1800.	1800.
$v, m^3/kg$	1.97278	2.0149	2.1492	2.2746	2.3923	2.5043	2.6118	2.7161	2.8176	2.9153	3.2077
$u, kJ/kg$	4030.70	4060.32	4148.92	4222.58	4284.70	4338.27	4385.53	4428.13	4467.23	4538.19	4602.85
$h, kJ/kg$	4425.26	4463.26	4578.76	4677.48	4763.15	4839.12	4907.90	4971.33	5030.76	5141.23	5244.38
$s, kJ/kg/K$	3.68816	3.7197	3.8120	3.8874	3.9501	4.0036	4.0503	4.0920	4.1297	4.1968	4.2557
$P = 0.3000 \text{ MPa } T(K) 1289.0$	1300.	1350.	1400.	1450.	1500.	1550.	1600.	1700.	1800.	1800.	1800.
$v, m^3/kg$	1.35620	1.3768	1.4673	1.5524	1.6330	1.7094	1.7830	1.8541	1.9910	2.1230	
$u, kJ/kg$	4037.18	4057.97	4145.04	4219.93	4284.39	4340.57	4390.39	4435.34	4514.89	4585.34	
$h, kJ/kg$	4444.04	4471.01	4585.23	4685.67	4774.27	4853.41	4925.30	4991.58	5112.20	5222.25	
$s, kJ/kg/K$	3.57121	3.5931	3.6823	3.7568	3.8197	3.8736	3.9210	3.9632	4.0364	4.0994	
$P = 0.4000 \text{ MPa } T(K) 1330.2$	1350.	1400.	1450.	1500.	1550.	1600.	1700.	1800.	1800.	1800.	1800.
$v, m^3/kg$	1.04040	1.0678	1.1349	1.1987	1.2593	1.3172	1.3729	1.4792	1.5807		
$u, kJ/kg$	4044.92	4079.76	4161.92	4224.45	4298.05	4354.22	4404.49	4492.10	4568.10		
$h, kJ/kg$	4461.08	4506.88	4615.92	4713.95	4801.77	4881.10	4953.64	5083.78	5200.44		
$s, kJ/kg/K$	3.49055	3.5271	3.6100	3.6806	3.7410	3.7935	3.8398	3.9190	3.9858		

## E.4 Superheated Sodium Table—SI Units

$P = 0.5000 \text{ MPa } T(K) 1364.1$	1400.	1450.	1500.	1550.	1600.	1700.	1800.
$v, m^* \text{ m}^3/\text{kg}$	0.84736	0.88677	0.9396	0.9901	1.0382	1.0845	1.1723
$u, \text{kJ/kg}$	4053.23	4112.29	4189.33	4258.40	4319.85	4374.83	4469.86
$h, \text{kJ/kg}$	4476.92	4555.62	4659.12	4753.43	4838.98	4917.08	5056.02
$s, \text{kJ/kg/K}$	3.42932	3.4912	3.5674	3.6332	3.6903	3.7404	3.8957
$P = 0.6000 \text{ MPa } T(K) 1393.2$	1400.	1450.	1500.	1550.	1600.	1700.	1800.
$v, m^* \text{ m}^3/\text{kg}$	0.71675	0.7229	0.7679	0.8113	0.8529	0.8926	0.9679
$u, \text{kJ/kg}$	4061.83	4072.44	4149.78	4222.09	4287.59	4346.48	4448.24
$h, \text{kJ/kg}$	4491.87	4506.21	4610.55	4708.87	4799.27	4882.03	5028.97
$s, \text{kJ/kg/K}$	3.38018	3.3918	3.4718	3.5419	3.6030	3.6564	3.8205
$P = 0.7000 \text{ MPa } T(K) 1419.8$	1450.	1500.	1550.	1600.	1700.	1700.	1800.
$v, m^* \text{ m}^3/\text{kg}$	0.62230	0.6464	0.6843	0.7208	0.7558	0.8220	0.8842
$u, \text{kJ/kg}$	4070.56	4116.64	4189.55	4257.59	4319.61	4427.27	4534.51
$h, \text{kJ/kg}$	4506.11	4569.10	4668.54	4762.13	4848.67	5002.68	5137.18
$s, \text{kJ/kg/K}$	3.33927	3.3893	3.4624	3.5268	3.5833	3.6782	3.7556
$P = 0.8000 \text{ MPa } T(K) 1441.8$	1450.	1500.	1550.	1600.	1700.	1700.	1800.
$v, m^* \text{ m}^3/\text{kg}$	0.55049	0.5561	0.5895	0.6221	0.6535	0.7128	0.7683
$u, \text{kJ/kg}$	4079.29	4090.60	4161.22	4230.19	4294.39	4407.05	4502.25
$h, \text{kJ/kg}$	4519.68	4535.45	4632.88	4727.89	4817.18	4977.26	5116.91
$s, \text{kJ/kg/K}$	3.3049	3.3172	3.3922	3.4592	3.5184	3.6178	3.6984
$P = 0.9000 \text{ MPa } T(K) 1462.7$	1500.	1550.	1600.	1700.	1700.	1800.	1800.
$v, m^* \text{ m}^3/\text{kg}$	0.49413	0.5164	0.5458	0.5741	0.6280	0.6782	
$u, \text{kJ/kg}$	4088.04	4137.55	4205.62	4270.94	4387.58	4486.67	
$h, \text{kJ/kg}$	4532.75	4602.32	4696.79	4787.66	4952.69	5097.06	
$s, \text{kJ/kg/K}$	3.27341	3.3295	3.3985	3.4599	3.5633	3.6470	
$P = 1.0000 \text{ MPa } T(K) 1481.9$	1500.	1550.	1600.	1700.	1700.	1800.	1800.
$v, m^* \text{ m}^3/\text{kg}$	0.44859	0.4583	0.4849	0.5109	0.5601	0.6062	
$u, \text{kJ/kg}$	4096.75	4118.89	4184.13	4249.42	4368.93	4471.50	
$h, \text{kJ/kg}$	4545.34	4577.20	4669.06	4760.28	4929.03	5077.67	
$s, \text{kJ/kg/K}$	3.24613	3.2730	3.3433	3.4066	3.5136	3.6002	
$P = 2.0000 \text{ MPa } T(K) 1623.0$	1700.	1800.					
$v, m^* \text{ m}^3/\text{kg}$	0.23636	0.2574	0.2834				
$u, \text{kJ/kg}$	4181.14	4241.43	4347.27				
$h, \text{kJ/kg}$	4653.85	4756.31	4914.13				
$s, \text{kJ/kg/K}$	3.06745	3.1640	3.2716				

## E.5 Sodium Temperature Saturation Table—English Units

T (R)	P (psi)	Volume (ft <sup>3</sup> *3/lbm)	Energy (Btu/lbm)				Enthalpy (Btu/lbm)				Entropy (Btu/lbm)			
			vf	vfg	ug	hf	hfg	hg	sf	sfg	sg			
1440.0	0.1	0.01944	4784.0732	4784.0928	-0.1	8412.9	8412.8	-0.1	8999.3	8999.2	2.77752	3.47195	6.24947	
1500.0	0.3	0.01963	2683.4402	2683.4597	91.3	8326.1	8417.4	91.3	8933.5	9024.8	2.70908	3.30871	6.01779	
1600.0	0.6	0.01996	1131.0094	1131.0293	245.7	8174.2	8419.9	245.7	8815.3	9061.0	2.61041	3.06085	5.67126	
1700.0	1.4	0.02029	527.3803	527.4006	436.5	7979.5	8416.0	436.6	8652.6	9089.1	2.53727	2.82764	5.36491	
1800.0	2.9	0.02065	270.5976	270.6182	559.9	7851.7	8411.6	559.9	8555.6	9115.5	2.45895	2.64062	5.09957	
1900.0	5.5	0.02101	148.8262	148.8472	717.8	7687.2	8405.0	717.9	8420.5	9138.5	2.40120	2.46215	4.86335	
2000.0	9.8	0.02139	87.1279	87.1493	876.3	7523.6	8400.0	876.5	8285.3	9161.8	2.35325	2.30148	4.65473	
2100.0	16.4	0.02178	53.8157	53.8375	1035.4	7363.3	8398.6	1035.7	8152.4	9188.1	2.31376	2.15673	4.47049	
2200.0	26.2	0.02218	34.8169	34.8391	1195.4	7207.8	8403.2	1195.9	8023.8	9219.7	2.28164	2.02621	4.30784	
2300.0	40.1	0.02260	23.4509	23.4735	1357.7	7057.5	8415.3	1358.6	7899.8	9258.4	2.25603	1.90818	4.16421	
2400.0	59.2	0.02304	16.3607	16.3838	1523.8	6912.6	8436.4	1525.0	7780.7	9305.7	2.23610	1.80108	4.03717	
2500.0	84.7	0.02349	11.7652	11.7887	1698.8	6768.5	8467.3	1700.6	7661.5	9362.1	2.22161	1.70256	3.92417	
2600.0	117.8	0.02396	8.6896	8.7136	1882.8	6626.0	8508.8	1885.3	7543.0	9428.3	2.21143	1.61176	3.82319	
2800.0	211.7	0.02495	5.0603	5.0833	2298.4	6326.7	8625.1	2303.1	7286.1	9589.2	2.20253	1.44566	3.64818	
3000.0	350.7	0.02602	3.1440	3.1700	2819.0	5971.7	8790.7	2827.1	6959.5	9786.6	2.20581	1.28880	3.49461	

## E.6 Sodium Pressure Saturation Table—English Units

P (psi)	T (R)	Volume (ft <sup>3</sup> *3/lbm)	Energy (Btu/lbm)				Enthalpy (Btu/lbm)				Entropy (Btu/lbm)			
			vf	vfg	vg	uf	ufg	ug	hf	hfg	hg	sf	sfg	sg
1.4	1694.0	0.02027	552.9115	552.9318	392.7	8024.8	8417.5	392.7	8696.2	9088.9	0.25091	5.13362	5.38454	
2.5	1778.1	0.02057	311.3963	311.4169	525.6	7887.4	8412.9	525.6	8584.7	9110.3	0.32730	4.82810	5.15540	
5.0	1884.3	0.02095	162.7399	162.7609	693.0	7713.0	8406.0	693.0	8441.9	9134.9	0.41842	4.48007	4.89849	
7.5	1952.7	0.02121	111.4133	111.4345	801.4	7600.7	8402.0	801.4	8349.2	9150.6	0.47446	4.27565	4.75011	
10.0	2004.5	0.02140	85.1776	85.1990	883.8	7516.0	8399.8	883.8	8279.1	9162.9	0.51564	4.13034	4.64598	
12.5	2046.6	0.02157	69.1843	69.2059	950.6	7448.2	8398.7	950.6	8223.0	9173.6	0.54812	4.01794	4.56606	
14.7	2078.3	0.02169	59.5053	59.5270	1001.2	7397.3	8398.5	1001.2	8180.9	9182.1	0.57219	3.93639	4.50858	
15.0	2082.4	0.02171	58.3823	58.4040	1007.5	7391.0	8398.5	1007.5	8175.6	9183.2	0.57520	3.92615	4.50135	
17.5	2113.6	0.02183	50.5836	50.6055	1057.4	7341.4	8398.9	1057.4	8134.7	9192.1	0.59845	3.84866	4.44711	
20.0	2141.5	0.02194	44.6815	44.7034	1101.8	7297.9	8399.7	1101.8	8098.7	9200.5	0.61875	3.78177	4.40052	
25.0	2189.8	0.02214	36.3213	36.3435	1179.6	7222.8	8402.4	1179.6	8036.6	9216.2	0.65350	3.66995	4.32345	
30.0	2231.0	0.02231	30.6741	30.6964	1246.1	7160.0	8406.0	1246.1	7984.8	9230.9	0.68238	3.57897	4.26135	
45.0	2328.6	0.02272	21.0823	21.1030	1405.9	7014.4	8420.3	1405.9	7865.1	9271.0	0.74868	3.37755	4.12623	
60.0	2403.4	0.02305	16.1681	16.1911	1531.9	6905.3	8437.2	1531.9	7775.5	9307.4	0.79783	3.23519	4.03302	
75.0	2464.9	0.02333	13.1648	13.1881	1638.8	6816.4	8455.2	1638.8	7702.3	9341.2	0.83749	3.12481	3.96230	
100.0	2549.2	0.02372	10.1038	10.1275	1790.1	6696.3	8486.4	1790.1	7603.4	9393.5	0.89046	2.98265	3.87311	
200.0	2779.2	0.02485	5.3337	5.3586	2256.0	6354.9	8610.9	2256.0	7314.8	9570.8	1.03310	2.63194	3.66503	
300.0	2935.0	0.02567	3.6502	3.6758	2640.2	6090.6	8730.7	2640.2	7078.3	9718.5	1.13168	2.41166	3.54334	

## E.7 Superheated Sodium Table—English Units

P= 1.4 Psi	T(R) 1694.0	1700.	1800.	1900.	2000.	2100.	2200.	2300.	2400.	2500.	2600.	2700.
v, ft <sup>3</sup> /lbm	552.9318	555.9260	601.5211	642.4615	680.8931	717.9449	754.1944	789.7718	825.1837	860.1784	895.1399	929.9736
u, Btu/lbm	8417.5	8431.5	8615.3	8743.4	8843.3	8927.9	9003.8	9074.5	9142.0	9207.5	9271.7	9334.9
h, Btu/lbm	9088.9	9106.5	9345.6	9523.5	9670.0	9799.6	9919.4	10033.4	10143.8	10252.0	10358.5	10464.1
s, Btu/lbm/R	5.3845	5.3949	5.5319	5.6282	5.7034	5.7667	5.8224	5.8731	5.9201	5.9642	6.0060	6.0459
P= 2.5 Psi	T(R) 1778.1	1800.	1900.	2000.	2100.	2200.	2300.	2400.	2500.	2600.	2700.	2800.
v, ft <sup>3</sup> /lbm	311.4169	317.4174	342.4559	365.0533	386.2528	406.6337	426.4664	446.0121	465.3169	484.4529	503.5057	522.4739
u, Btu/lbm	8412.9	8464.1	8647.7	8780.0	8884.3	8972.8	9051.9	9125.1	9194.5	9261.5	9326.9	9391.0
h, Btu/lbm	9110.3	9174.9	9414.5	9597.4	9749.3	9883.4	10006.9	10123.8	10236.5	10346.3	10454.3	10561.0
s, Btu/lbm/R	5.11554	5.1916	5.3214	5.4153	5.4895	5.5519	5.6068	5.6566	5.7026	5.7457	5.7864	5.8252
P= 5.0 Psi	T(R) 1884.3	1900.	2000.	2100.	2200.	2300.	2400.	2500.	2600.	2700.	2800.	2900.
v, ft <sup>3</sup> /lbm	162.7609	164.9819	178.0859	189.8740	200.8656	211.3520	221.5073	231.4532	241.2410	250.9281	260.5435	270.0991
u, Btu/lbm	8406.0	8444.5	8644.1	8790.5	8905.9	9002.9	9088.3	9166.3	9239.4	9309.2	9376.8	9442.7
h, Btu/lbm	9134.9	9183.3	9441.7	9640.8	9805.5	9949.4	10080.3	10202.8	10319.8	10433.0	10543.6	10652.3
s, Btu/lbm/R	4.8985	4.9242	5.0571	5.1545	5.2312	5.2952	5.3509	5.4009	5.4468	5.4895	5.5298	5.5679
P= 7.5 Psi	T(R) 1952.7	2000.	2100.	2200.	2300.	2400.	2500.	2600.	2700.	2800.	2900.	3000.
v, ft <sup>3</sup> /lbm	111.4345	115.8719	124.4683	132.3047	139.6536	146.6837	153.5009	160.1333	166.7368	173.2347	179.6686	186.0625
u, Btu/lbm	8402.0	8513.1	8698.8	8840.1	8954.4	9051.8	9138.2	9217.4	9291.7	9362.6	9431.1	9497.8
h, Btu/lbm	9150.6	9291.4	9534.9	9728.9	9892.6	10037.2	10169.4	10293.4	10411.8	10526.3	10638.1	10747.8
s, Btu/lbm/R	4.7501	4.8217	4.9410	5.0314	5.1043	5.1658	5.2198	5.2684	5.3132	5.3548	5.3940	5.4312
P= 10.0 Psi	T(R) 2004.5	2100.	2200.	2300.	2400.	2500.	2600.	2700.	2800.	2900.	3000.	
v, ft <sup>3</sup> /lbm	85.1990	91.8104	98.0478	103.8186	109.2796	114.5324	119.6472	124.6441	129.5703	134.5207	139.2899	
u, Btu/lbm	8399.8	8609.7	8775.6	8906.7	9015.7	9110.4	9195.6	9274.3	9348.5	9419.5	9488.2	
h, Btu/lbm	9162.9	9432.0	9653.8	9836.6	9994.5	10136.3	10267.2	10390.7	10509.1	10623.8	10735.8	
s, Btu/lbm/R	4.6460	4.7781	4.8816	4.9630	5.0303	5.0882	5.1396	5.1862	5.2293	5.2697	5.3075	
P= 12.5 Psi	T(R) 2046.6	2100.	2200.	2300.	2400.	2500.	2600.	2700.	2800.	2900.	3000.	
v, ft <sup>3</sup> /lbm	69.2059	72.2589	77.5131	82.3293	86.8434	91.1549	95.3236	99.3923	103.3869	107.3276	111.2298	
u, Btu/lbm	8398.7	8523.8	8712.5	8859.6	8980.0	9082.8	9173.9	9257.0	9334.5	9408.0	9487.6	
h, Btu/lbm	9173.6	9323.9	9580.3	9781.4	9952.3	10103.4	10241.2	10369.8	10492.0	10609.6	10723.9	
s, Btu/lbm/R	4.5661	4.6436	4.7594	4.8491	4.9220	4.9837	5.0378	5.0863	5.1308	5.1721	5.2108	

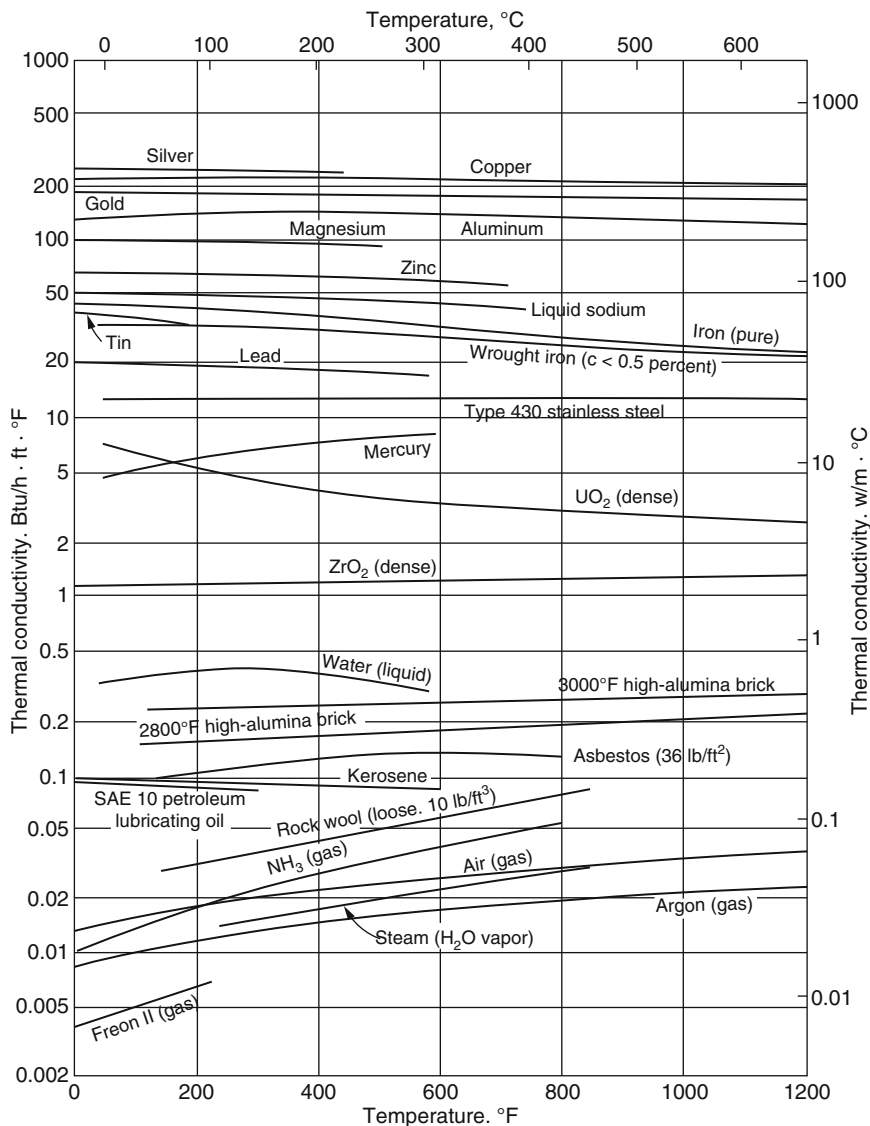
P= 14.7 psi	T(R)2078.3	2100.	2200.	2300.	2400.	2500.	2600.	2700.	2800.	2900.	3000.
v,ft**3/lbm	57.52270	60.6072	65.2546	69.4941	73.4376	77.1835	80.7923	84.2977	87.7346	91.1159	94.4552
u,Btu/lbm	8398.5	8451.6	8658.4	8819.0	8949.0	9058.8	9155.0	9241.8	9322.2	9397.9	9470.2
h,Btu/lbm	9182.1	9249.3	9517.4	9733.7	9915.7	10074.8	10238.4	10351.5	10477.0	10597.2	10713.5
s,Btu/lbm/R	4.5086	4.5412	4.6670	4.7637	4.8413	4.9063	4.9627	5.0129	5.0586	5.1008	5.1402
P= 15.0 psi	T(R)2082.4	2100.	2200.	2300.	2400.	2500.	2600.	2700.	2800.	2900.	3000.
v,ft**3/lbm	58.4040	59.2735	63.8431	68.0124	71.8927	75.5716	79.1147	82.5565	85.9165	89.2437	92.5195
u,Btu/lbm	8398.5	8441.9	8651.0	8813.4	8944.8	9055.5	9152.4	9239.7	9320.5	9396.5	9469.0
h,Btu/lbm	9183.2	9238.1	9508.8	9727.2	9910.7	10070.9	10225.3	10348.9	10474.9	10595.5	10712.1
s,Btu/lbm/R	4.5013	4.5280	4.6551	4.7526	4.8309	4.8964	4.9531	5.0036	5.0494	5.0917	5.1312
P= 20.0 psi	T(R)2141.5	2200.	2300.	2400.	2500.	2600.	2700.	2800.	2900.	3000.	3000.
v,ft**3/lbm	44.7034	46.8068	50.1409	53.2172	56.1055	58.8591	61.5165	64.1042	66.6435	69.1359	72.7000
u,Btu/lbm	8399.7	8534.1	8723.8	8875.9	9001.7	9109.8	9205.6	9292.7	9373.6	9450.0	9537.7
h,Btu/lbm	9200.5	9372.6	9622.1	9829.1	10006.7	10164.2	10307.6	10441.0	10567.4	10688.4	10810.5
s,Btu/lbm/R	4.4005	4.4811	4.5931	4.6817	4.7544	4.8162	4.8704	4.9190	4.9633	5.0044	5.0444
P= 25.0 psi	T(R)2189.8	2200.	2300.	2400.	2500.	2600.	2700.	2800.	2900.	3000.	3000.
v,ft**3/lbm	36.3435	36.6427	39.4482	42.0280	44.4280	46.7121	48.8968	51.0140	53.0731	55.1066	57.7000
u,Btu/lbm	8402.4	8426.7	8638.6	8808.9	8949.0	9067.9	9171.9	9265.2	9350.9	9431.1	9512.3
h,Btu/lbm	9216.2	9247.2	9521.9	9750.0	9944.0	10113.9	10266.8	10407.5	10539.5	10665.0	10810.5
s,Btu/lbm/R	4.3235	4.3379	4.4623	4.5603	4.6398	4.7067	4.7645	4.8157	4.8620	4.9046	4.9444
P= 30.0 psi	T(R)2231.0	2300.	2400.	2500.	2600.	2700.	2800.	2900.	3000.	3000.	3000.
v,ft**3/lbm	30.6964	32.3466	34.5823	36.6599	38.6262	40.4872	42.2885	44.0402	45.7548	47.4681	49.1819
u,Btu/lbm	8406.0	8558.4	8744.6	8897.8	9026.9	9138.6	9238.4	9328.4	9412.3	9496.0	9581.7
h,Btu/lbm	9230.9	9427.6	9673.9	9882.9	10064.6	10226.5	10374.3	10511.8	10641.7	10777.9	10914.7
s,Btu/lbm/R	4.2614	4.3505	4.4569	4.5429	4.6146	4.6758	4.7296	4.7832	4.8360	4.8822	4.9220
P= 45.0 psi	T(R)2328.6	2400.	2500.	2600.	2700.	2800.	2900.	3000.	3000.	3000.	3000.
v,ft**3/lbm	21.1050	22.2378	23.7421	25.1384	26.4846	27.7569	28.9821	30.1735	31.3860	32.5987	33.8000
u,Btu/lbm	8420.3	8570.1	8753.6	8908.8	9042.1	9158.4	9262.3	9366.8	9470.2	9574.0	9677.7
h,Btu/lbm	9271.0	9466.5	9710.6	9922.5	10109.5	10277.2	10440.4	10572.9	10705.8	10838.5	10972.2
s,Btu/lbm/R	4.1262	4.2126	4.3147	4.3988	4.4701	4.5313	4.5852	4.6336	4.6865	4.7398	4.7820
P= 60.0 psi	T(R)2403.4	2500.	2600.	2700.	2800.	2900.	3000.	3000.	3000.	3000.	3000.
v,ft**3/lbm	16.1911	17.3290	18.4446	19.4989	20.5009	21.4601	22.3860	23.3027	24.2287	25.1548	26.0808
u,Btu/lbm	8437.2	8627.0	8800.6	8951.1	9082.2	9198.3	9302.7	9419.0	9536.8	9654.5	9772.2
h,Btu/lbm	9307.4	9558.3	9791.9	9999.0	10184.0	10351.6	10505.8	10661.7	10818.4	10974.5	11121.2
s,Btu/lbm/R	4.0330	4.1415	4.2360	4.3155	4.3834	4.4426	4.4951	4.5578	4.6196	4.6818	4.7437

P= 75.0 psi T(R)2464.9  
 v, ft\*\*3/lbm 13.1881  
 u,Btu/lbm 8455.2  
 h,Btu/lbm 9341.2  
 s,Btu/lbm/R 3.9623

P= 100.0 psi T(R)2549.2  
 v, ft\*\*3/lbm 10.1275  
 u,Btu/lbm 8486.4  
 h,Btu/lbm 9393.5  
 s,Btu/lbm/R 3.8731

P= 200.0 psi T(R)2779.2  
 v, ft\*\*3/lbm 5.3386  
 u,Btu/lbm 8610.9  
 h,Btu/lbm 9570.8  
 s,Btu/lbm/R 3.6650

P= 300.0 psi T(R)2935.0  
 v, ft\*\*3/lbm 3.6758  
 u,Btu/lbm 8730.7  
 h,Btu/lbm 9718.5  
 s,Btu/lbm/R 3.5433



# **Appendix F**

## **Practical Design Steps for Compact Heat Exchangers**

A heat exchanger is an instrument or device that is used for the transfer of thermal energy in terms of enthalpy between two or more fluids, between a solid surface and a fluid, between a solid surface and a fluid, or between solid particulates and a fluid. This process takes place at different temperatures and in thermal contact, usually without external heat and work interaction. The fluids may be presented as a single compounds or mixture, where the choice of such fluid depends on typical applications of the heat exchanger. Generally speaking, typical applications involve heating or cooling of a fluid stream of concern, evaporation, or condensation of a single or multi-component fluid stream, and heat recovery or heat rejection from a system. In most heat exchangers, the fluids are separated by a heat transfer surface, and ideally they do not mix. Such heat exchangers are referred to as the *direct transfer type*, or namely *recuperators*. In contrast, heat exchangers in which there is an intermittent exchanger between the hot and cold fluids via thermal energy storage and rejection through the exchanger surface or matrix are referred to as the *indirect transfer type* or *storage type*, or simply *regenerators*. Note that such exchangers usually have leakage and fluid carryover from one fluid stream to the other. The work presented here is based on analysis carried out by Akash Pandey [2] thesis work on performance analysis of a compact heat exchanger.

### **F.1 Compact Heat Exchangers Design Rating Procedure**

Design of heat exchanger involves two types of problem;

(a) **Sizing**

Sizing involves the determination or we can say selection of the type of heat exchanger, flow arrangement, material of heat exchanger, and physical dimensions of the heat exchanger to meet the specified heat transfer and pressure drop requirements.

(b) Rating

Rating of the heat exchanger consists of finding the thermal performance parameters like; effectiveness heat transfer coefficient and pressure drop of an already designed heat exchanger whose dimensions are known to us.

In this appendix, we work on the rating problem based on analysis which is presented by Pandy [1]. Since the outlet temperatures are not known for the rating problem, the average fluids mean temperatures have to be projected first.

The heat transfer coefficient and the effectiveness of the plate fin heat exchanger are found based on different correlations existing in literature. The outlet temperatures and the average fluid temperatures are calculated from the effectiveness value and then compared with the values assumed earlier. The above procedure is carried out until the calculated values of the mean fluid temperatures match with the assumed values. The following steps show the detailed rating procedure:

1. The first step in the rating procedure is to calculate the various surface geometrical properties of the heat exchanger. We use a plate fin heat exchanger with offset strip fin geometry, and geometry of the offset strip fin surface is described by the following parameters:
  - (a) Fin spacing ( $s$ ), excluding the fin thickness,
  - (b) Fin height ( $h$ ), excluding the fin thickness,
  - (c) Fin thickness ( $\delta$  or  $t$ ) as it can be seen in Fig. F.1 and,
  - (d) Fin strip length or length of a plate as mentioned in Table 5.2 ( $l$  or  $L_f$ )

**Fig. F.1** Geometry of typical offset strip fin surface

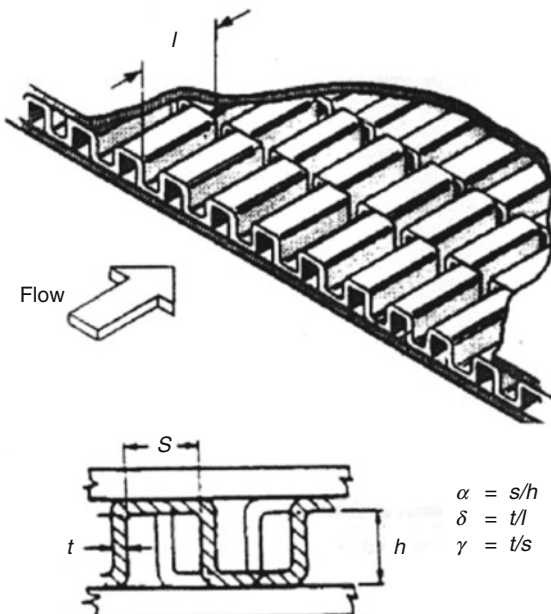


**Table F.1** Core data (fin specifications)

Parameters	Hot fluid	Cold fluid
Number of passes ( $N$ )	4	5
Fin thickness ( $\delta$ or $t$ )	0.2 mm	0.2 mm
Fin frequency ( $f$ )	588	714
Fin length ( $l$ )	5 mm	3 mm
Fin height ( $h$ )	9.3 mm	9.3 mm
Pate thickness ( $t$ )	0.8 mm	0.8 mm

The lateral fin offset is generally the same and equal to half the fin spacing (including fin thickness). Figure F.1 shows a schematic view of the rectangular offset strip fin surface and defines the basic geometric parameters. But the present heat exchanger has different fin geometries for the hot and cold side fluids. Table F.1 shows the fin specifications for hot and cold side of the heat exchanger.

There are some secondary geometrical parameters which are derived from the above basic fin geometries, which are calculated as follows. The calculation is done for the hot side fluid and by following the same steps the results can be obtained for the cold side.

### 1. Basic Fin Geometries

There are some secondary geometrical parameters which are derived from the above basic fin geometries, which are calculated as follows. The calculation is done for the hot side fluid and by following the same steps the results can be obtained for cold side. The following calculation will be applied as well;

(a) Fin spacing or gaps

$$s = \frac{(1 - f \times \delta)}{f} = \frac{1 - 588 \times 0.0002 \text{ (meter)}}{588} = \frac{1 - 0.1176}{588} \approx 0.001501 \text{ meter}$$

(b) Free flow area ( $a_{ff}$ ) to Frontal area ( $a_{fr}$ )

$$\sigma = \frac{a_{ff}}{a_{fr}} = \frac{(s - t)h}{(h + t)(s + t)} = \frac{(0.001501 - 0.0002) \times 0.0093}{(0.0093 + 0.0002)(0.001501 + 0.0002)} = 0.00001615$$

(c) Heat transfer area per fin,  $a_s$

$$a_s = 2hl + 2ht + 2sl = 2(0.0093)(0.005) \\ 2(0.001501)(0.05) + \\ 2(0.0093)(0.0002) = 0.0001117$$

(d) Ratio of fin area to heat transfer area of fin

$$\frac{2h(l + t)}{2(hl + sl + ht)} = \frac{2(0.0093)(0.005 + 0.0002)}{2(0.0093)(0.005) + (0.005)(0.001501) + (0.0093)(0.0002)} \\ = 0.86565$$

(e) Equivalent diameter,  $D_e$

$$\begin{aligned}
 D_e &= \frac{4(\text{Free Flow Area})(\text{Length})}{\text{Heat Transfer Area}} \\
 &= \frac{2(s-t)hl}{hl + sl + ht} \\
 &= \frac{2(0.001501 - 0.0002)(0.0093)(0.005)}{(0.0093)(0.005) + (0.001501)(0.005) + (0.0093)(0.0002)} \\
 &= 0.002165810 \text{ meter}
 \end{aligned}$$

(f) Distance between plates

$$b = h + t = 0.0093 + 0.0002 = 0.0095 \text{ meter}$$

## 2. Heat Transfer Area $A$

The various heat transfer area for hot side are calculated as follows

- (a) Total area between plates,  $A_{frh} = b \times N_h \times W = 0.0095 \times 4 \times 0.073 = 0.0028$
- (b) Total free flow area,  $A_{ffh} = \sigma \times A_{frh} = (0.748742226)(0.0028) = 0.0021 \text{ m}^2$
- (c) Wall conduction area,  $a_{wh} = A_{frh} - A_{ffh} = 0.0028 - 0.0021 = 0.001213 \text{ m}^2$
- (d) Total heat transfer area,  $A_h = \frac{4 \times A_{ffh} \times L}{D_e} = \frac{4 \times 0.0021 \times 0.9}{0.002165810} = 3.4524 \text{ m}^2$
- (e) Total wall conduction area =  $a_{wh} + a_{wc} = 0.0007 + 0.001 = 0.0017 \text{ m}^2$

## 3. Heat Exchanger Input Data

- (a) Temperature of hot gas at inlet = 368.81 K
- (b) Temperature of cold gas at inlet = 311.93 K
- (c) Pressure at inlet of cold gas = 1.21 bar
- (d) Pressure of gas at hot inlet = 1.17 bar
- (e) Mass flow rate of cold gas = 0.0095 kg/s
- (f) Mass flow rate of hot gas = 0.0095 kg/s

## 4. Estimation of Average Temperature

Since the fluid outlet temperatures are not known for the rating problem, the average fluids mean temperatures have to be predicted first. The fluid properties at the predicted mean temperatures of 342.02 and 338.71 K for hot and cold fluid are obtained from property package, Gaspak.

The properties of hot gas at the mean temperature are;

- (a) Specific heat,  $c_p = 1.04086 \text{ kJ/kg.K}$
- (b) Viscosity,  $\mu = 0.0000198 \text{ Pa.s}$
- (c) Prandtl number,  $\text{Pr} = 0.7169882$
- (d) Density,  $\rho = 1.14249 \text{ kg/m}^3$

The properties of cold gas at the mean temperature are;

- (a) Specific heat,  $c_p = 1040.67 \text{ kJ/kg.K}$
- (b) Viscosity,  $\mu = 0.0000192 \text{ Pa.s}$
- (c) Prandtl number,  $\text{Pr} = 0.7167$
- (d) Density,  $\rho = 1.32 \text{ kg/m}^3$

## 5. Heat Transfer Coefficient and Surface Effectiveness of Fins

The calculations for the heat transfer coefficients for the hot and cold gas are analogous. So the calculations are presented for the hot fluid and can be obtained for cold gas by following the same procedure.

- (a) Core mass velocity,  $G = \frac{m}{A_{\text{effh}}} = \frac{0.0095}{0.0021} = 4.5739 \text{ kg/s.m}^2$
- (b) The Reynolds number,  $\text{Re} = \frac{GD_e}{\mu} = \frac{4.5739 \times 0.002165810}{0.0000198} = 500.31$
- (c) The critical Reynolds number proposed by Joshi and Webb is

$$\begin{aligned} \text{Re}^* &= 257 \left( \frac{l}{s} \right)^{1.23} \left( \frac{l}{D_h} \right)^{0.58} D_h \left[ t + 1.328 \left( \frac{\text{Re}}{ID_h} \right)^{-0.5} \right]^{-1} \\ &= 257 \times \left( \frac{0.005}{0.001501} \right)^{1.23} \times \left( \frac{0.0002}{0.005} \right)^{0.58} \\ &\quad \times 0.002165 \left[ 0.0002 + 1.328 \left( \frac{500.310}{0.005 \times 0.002165} \right)^{-0.5} \right]^{-1} \\ &= 9561.1409069 \end{aligned}$$

- (d) The Colburn factor  $j$  for ( $\text{Re}^* > \text{Re}$ ) is given by correlation proposed by Joshi and Webb [3] is

$$\begin{aligned} j &= 0.53 \text{Re}^{-0.5} (1/D_h)^{-0.15} \alpha^{-0.14} \\ &= 0.53 \times (500.31)^{-0.5} \times (2.30860462)^{-0.15} \times (0.161397849)^{-0.14} \\ &= 0.02698 \end{aligned}$$

- (e) The convective heat transfer coefficient is given by

$$h_h = \frac{(j_h * c_p * G_h)}{(\text{Pr})^{0.667}} = \frac{(0.02698 \times 1040.86 \times 4.5739)}{(0.7169882)} = 160.3 \text{ W/m}^2$$

- (f) The fin parameter is given by

$$M = \sqrt{\frac{(2 * h_h)}{(K_f * t)}} = \sqrt{\frac{(2 \times 160.3430)}{(165 \times 0.0002)}}$$

- (g)  $l_h$  = Height of fins for hot side =  $b$  and for cold side passages which are the outer layers  $l_h = b/2$   
 (h) The fin effectiveness is given by

$$n_f = \tanh(Ml_h)/(Ml_h) = 0.93280$$

- (i) Overall surface effectiveness is given by

$$\eta_{oh} = 1 - (a_f/a_s)*(1 - n_f) = 1 - (0.86565)(1 - 0.93280) = 0.94183$$

Similarly, convective heat transfer coefficient and overall surface effectiveness for cold fluid are

$$h_c = 179.948 \text{ W/m}^2\text{.K} \quad \text{and} \quad \eta_{oc} = 0.87593 \quad \text{and} \quad j_c = 0.03536$$

## 6. Overall Heat Transfer Coefficient and NTU

The overall heat transfer coefficient is given by;

$$\frac{1}{(U_o A_o)_h} = \frac{1}{(\eta_{oh} h_h A_h)} + \frac{a}{K_w A_w} + \frac{1}{(\eta_{oc} h_c A_c)}$$

Where;

$$A_w = \text{Lateral conduction area} = W \times L \times (2N_p + 2) = 2.073 \times 0.886 \\ (2 \times 4 + 2) = 0.657 \text{ m}^2$$

Therefore,

$$\begin{aligned} \frac{1}{(U_o A_o)_h} &= \frac{1}{(0.941 \times 160.34 \times 304524)} \\ &+ \frac{1}{165 \times 0.657} \\ &+ \frac{1}{(0.87593 \times 179.948 \times 5.2152)} \\ &= 0.0031419 \end{aligned}$$

And finally, we can write

$$(U_o A_o)_h = 318.27751 \text{ W/K}$$

Overall heat transfer coefficient,

$$U_{\text{oh}} = \frac{(U_o A_o)_h}{A_{\text{oh}}} = \frac{318.27751}{3.4524} = 92.19027 \text{ W/m}^2 \text{ K}$$

And similarly for the cold side we can write the following result;

$$U_{\text{oc}} = \frac{(U_o A_o)}{A_{\text{oc}}} = \frac{318.27751}{9.8876} = 32.18956 \text{ W/m}^2 \text{ K}$$

$$\text{Number of Transfer Units (NTU), } NTU = N_{\text{tu}} = \frac{U_o A_o}{C_{\min}} = \frac{318.27751}{9.8876} = 32.18956$$

## 7. Effectiveness of Heat Exchanger without Considering the Effect of Longitudinal Conduction

$$\epsilon = \frac{1 - e^{-N_{\text{tu}}(t-C_r)}}{1 - C_r e^{-N_{\text{tu}}(1-C_r)}} = \frac{1 - e^{-32.18956(1-0.9999)}}{1 - 0.9999 e^{-32.18956(1-0.9999)}} = 0.96989$$

## 8. Effect of Wall Longitudinal Heat Conduction

The consequence of longitudinal heat conduction is to decrease the effectiveness of heat exchanger. The decrease in the effectiveness of heat exchanger is found out by using the Kroeger's equation.

- (a) Wall conduction area,  $a_w = 0.0017 \text{ m}^2$
- (b) Conductivity of fin,  $K_w = 165 \text{ W/m}^2 \cdot \text{K}$
- (c) Wall conduction parameter,  $\lambda = \frac{K_w a_w}{LC_{\min}} = \frac{165 \times 0.0017}{0.9 \times 9.8876} = 0.03225$
- (d)  $y = \lambda N_{\text{tu}} C_r = 0.03225 \times 32.18956 \times 0.9999 = 1.03795$
- (e)  $\gamma = \frac{(1-C_r)}{(1-C_r)(1+y)} = \frac{(1-0.9999)}{(1-0.9999)(1+1.037955)} = 0.0000141432$
- (f)  $\phi = \gamma \left[ \frac{y}{(1+y)^{1/2}} \right] \left\{ \frac{(1+\gamma)y}{1-\gamma(1+\gamma)y} \right\} = 1.047 \times 10^{-5}$
- (g)  $\varphi = \frac{(1+\phi)}{(1-\phi)} = \frac{(1+1.04768 \times 10^{-5})}{(1-1.04768 \times 10^{-5})} = 1.00002$
- (h)  $r_1 = \frac{(1-C_r)N_{\text{tu}}}{1+\lambda N_{\text{tu}} C_r} = \frac{(1-0.9999) \times 32.18956}{1+0.032247 \times 32.18956 \times 0.9999} = 0.000910499$
- (i)  $(1 - \epsilon) = \frac{(1-C_r)}{\varphi \exp(r_1) - C_r} = \frac{(1-0.9999)}{1.0002 \times \exp(0.000910499) - 0.9999} = 0.0582595$
- (j)  $\epsilon [1 - (1 - \epsilon)] = 1 - 0.058254 = 0.94174$

This is the value of the actual effectiveness of heat exchanger subsequently considering wall longitudinal heat conduction effect. Outlet temperatures of fluids based on this value of effectiveness are found as follows.

The outlet temperature of hot fluid is given by

$$T_{\text{ho}} = T_{\text{hi}} - \frac{\epsilon C_{\min} (T_{\text{hi}} - T_{\text{ci}})}{C_h} = 368.81 - \frac{0.94174 \times 9.8876 (368.81 - 311.93)}{9.88817} \\ = 315.24$$

Mean temperature of hot and cold fluid is given as follows:

$$(k) \text{ Mean temperature of hot fluid is, } (T_h)_{\text{Mean}} = T_{\text{hm}} = \frac{T_{\text{hi}} + T_{\text{ho}}}{2} = \frac{368.81 + 315.246}{2} = 342.028 \text{ K}$$

$$(l) \text{ Mean temperature of cold fluid is, } (T_c)_{\text{Mean}} = T_{\text{hm}} = \frac{T_{\text{ci}} + T_{\text{co}}}{2} = \frac{311.93 + 365.4964}{2} = 338.713 \text{ K}$$

Since our calculated mean temperatures match with the assumed values of mean temperature we can stop the iteration here, otherwise we would have taken the values of mean temperature obtained in the above step and carried out the iteration once again, till the assumed and found values are identical.

## 9. Pressure Drop

Since the pressure drop of cold fluid is more critical , the calculation is shown for cold fluid

(a) The friction factor ( $f$ ) for  $\text{Re}^* > \text{Re}$  is given by

$$f = 8.12 \text{Re}^{-0.74} \left( \frac{1}{D_h} \right)^{-0.41} \alpha^{-0.02} = 0.05999$$

(b) The pressure drop is given by

$$\Delta p = \frac{4fLG^2}{2D_e \rho_b} = \frac{4 \times 0.05999 \times 0.9 \times (3.9169)^2}{2 \times 0.00167 \times 1.18351} = 836.0924 \text{ Pa}$$

## F.2 Compact Heat Exchanger Performance Analysis

The main aim of the present work is to calculate the performance parameters like, effectiveness, overall heat transfer coefficient of the plate fin heat exchanger. In order to find the performance of the present heat exchanger a number of experiments were carried out at different mass flow rates and at different hot fluid inlet temperature under balanced flow. Table F.2 shows the experimentally observed data.

### F.2.1 Calculations

The temperatures values which are obtained experimentally by Ref. 2 are first of all corrected using the calibration chart, and also the pressure values are converted in units of Pa or bar, and then used for further calculations.

**Table F.2** Experimental data observed and reported by Pandey [2]

Flow rate (l/min)	$P_1$ (kg/cm <sup>2</sup> )	$P_2$ (kg/cm <sup>2</sup> )	$\Delta h_c$ (mm of Hg)	$\Delta h_h$ (mm of Hg)	$T_1$ (°C)	$T_2$ (°C)	$T_3$ (°C)	$T_4$ (°C)
300	0.08	0.06	9	6	42.24	87.34	96.20	47.15
400	0.14	0.12	15	12	38.35	87.02	95.12	43.01
500	0.20	0.17	25	22	38.93	88.49	96.12	43.11
550	0.24	0.20	30	26	39.82	88.83	96.66	43.48
588	0.28	0.24	31	27	40.41	88.45	96.20	43.99
650	0.32	0.26	40	35	41.16	87.86	95.95	44.17
300	0.08	0.06	8	6	40.92	62.06	66.48	43.06
400	0.135	0.10	16	14	42.77	62.90	66.43	44.56
500	0.20	0.16	24	22	39.57	62.52	66.02	41.69
600	0.28	0.23	31	30	39.94	62.44	65.98	41.73
650	0.34	0.28	37	34	42.72	62.77	66.34	44.06

$T_1 = 38.93$  °C,  $T_2 = 87.23$  °C,  $T_3 = 95.96$  °C,  $T_4 = 48.10$  °C,  $P_1 = 1.21$  bar,  $P_2 = 1.18$  bar, Flow rate = 500 l/min.

1. Mass flow rate = Volume flow rate  $\times \frac{P_4}{RT_4} = \frac{500 \times 10^{-3}}{60} \times \frac{1.01325 \times 10^5}{287 \times 316.98} = 0.01$  kg/s
2. Heat capacity of hot and cold fluids are given as follows;

For cold fluid  $C_c = m_c c_{pc} = 0.010087$  KW/K

For hot fluid  $C_h = m_h c_{ph} = 0.010093$  KW/K

3. Capacity rate ratio,  $C_r = C_{\min}/C_{\max} = 0.9994$
4. Effectiveness for hot and cold fluids are give as;

$$\text{For cold fluid } \varepsilon_c = \frac{C_c(T_{c,\text{inlet}} - T_{c,\text{exit}})}{C_{\min}(T_{h,\text{inlet}} - T_{c,\text{inlet}})} = 86.920$$

$$\text{For hot fluid } \varepsilon_h = \frac{C_h(T_{h,\text{inlet}} - T_{h,\text{exit}})}{C_{\min}(T_{h,\text{inlet}} - T_{c,\text{inlet}})} = 91.134$$

5. Number of transfer units, NTU = 15.009,

After considering the effect of longitudinal heat conduction, then, the same steps as described in Sect. F.1 here are followed, but here the NTU value is assumed in such a way that the effectiveness obtained from Kroger's equation matches with the experimental value of effectiveness.

6. Overall heat transfer conductance, UA<sub>o</sub>

$$UA_o = NTU \times C_{\min} = N_{tu} \times C_{\min} = 15.009 \times 0.010087 = 160.898 \text{ W/K}$$

Here the surface geometrical properties are also calculated by following the procedure as mentioned in Sect. F.1. Table F.3 shows the performance parameters of heat exchanger obtained after calculation.

**Table F.3** Performance analysis of heat exchanger of choice [2]

Flow rate (l/min)	Mass flow rate (kg/s)	$\varepsilon_h$	$\varepsilon_c$	NTU	$UA_o$ (W/K)	$Re_h$	$Re_c$	$\Delta T_{HOT END}$	$\Delta T_{COLD END}$
300	0.0057	89.902	83.749	13.64	80.95	298.67	199.72	8.73	5.87
400	0.0074	90.236	85.90	15.24	117.37	416.04	278.22	7.97	5.53
500	0.0103	91.134	86.920	15.00	160.89	542.44	362.75	7.44	5.05
550	0.0116	92.08	86.365	16.24	196.09	610.9	406.46	7.72	4.53
588	0.0127	92.001	86.247	15.70	207.64	668.83	445	7.64	4.45
650	0.0142	92.786	85.371	17.49	258.57	747.83	497.56	7.98	3.94
300	0.0057	88.108	83.064	11.76	69.74	280.24	186.48	4.3	3.02
400	0.0078	89.937	85.480	13.25	107.60	419.28	277.56	3.36	2.33
500	0.0101	88.48	86.814	9.79	102.89	491.54	399.77	3.48	3.04
600	0.011	90.004	86.597	11.28	135.41	702.63	465.13	3.46	2.58
650	0.014	90.572	85.114	12.00	174.87	789.66	525.48	3.49	2.21

Reference 2 also reports certain excel plots in his presentation, in order to compare his experiment results with the values that are obtained from theoretical correlations, presented in Sect. F.1. Some are plotted graphs in his report for which the experiment is conducted at room temperature and different mass flow rates and at two different hot inlet temperatures of 66 °C and 96 °C. For further information readers should refer to this reference (Pandey) [2].

## Conclusions

Conclusion of Ref. 2 is reported as follow;

“The hot test is conducted to determine the thermal performance parameters of the available plate fin heat exchanger at different mass flow rates and two different hot inlet temperatures of 96 and 66 °C. An average effectiveness of 91 % is obtained. It is found in both cases that the effectiveness and overall thermal conductance increases with increasing mass flow rate. It is also found that hot fluid effectiveness increases with flow rate of the fluid and agrees within 4 % with the effectiveness value calculated by different correlations and that obtained by using the simulation software, Aspen. Also the pressure drop increases with increasing mass flow rate and experimental values are more as compared to theoretical results because the losses in pipes and manufacturing irregularities have not been taken into account.

For a particular hot inlet temperature there is an optimum mass flow rate at which the difference between the hot and cold effectiveness of the heat exchanger is minimum and at this point the imbalance is also minimum. We found that the insulation which is provided in the heat exchanger has a significant effect on its

performance. It is expected that the imbalance, i.e., difference between the hot and cold end temperature can be brought to a minimum level if a perfect insulation like vacuum is provided.”

## References

1. F. Settle web Site <http://www.chemcases.com/nuclear/index.html>.
2. Pandey, Akash. 2011. Performance analysis of a compact heat exchanger, a thesis submitted in partial fulfillment of the requirements for the degree of Master of Technology in Mechanical Engineering. Department of Mechanical Engineering, National Institute of Technology Rourkela.
3. Joshi, H.M., and R.L. Webb. 1987. Heat transfer and friction in offset strip fin HeatExchanger. *International Journal of Heat and Mass Transfer* 30(1): 69–80.

# **Appendix G**

## **Cross-Flow Compact Heat Exchanger**

### **Design by Comsol**

This application simulates the fluid flow and heat transfer in a micro-heat exchanger of cross-flow type made of stainless steel. Compact heat exchangers of single element plate fin type are found in lab-on-chip devices in biotechnology and micro-reactors, for example for micro-fuel cells. With attention growth toward combined cycle driven efficiency high temperature advanced reactors, more interest has grown toward this type of compact heat exchangers as well. The application takes into account heat transferred through both convection and conduction.

## **G.1 Introduction**

With an average household occupation of 2.6 persons this means that the typical worldwide household uses about 14.2 KWh of electrical energy per day. Comparable domestic consumption figures for the USA are 4387 kWh per capita per year or 12 kWh per person per day or 30 kWh per household per day. The world will need greatly increased energy supply in the next 20 years, especially cleanly-generated electricity.

Electricity demand is increasing twice as fast as overall energy use and is likely to rise by more than two-thirds 2011 to 2035. In 2012, 42 % of primary energy used was converted into electricity; for meeting such demand new generation of nuclear technology is becoming more and more appealing to electricity generating companies. Nuclear power provides about 11 % of the world's electricity, and 21 % of electricity in OECD countries. See Fig. G.1.

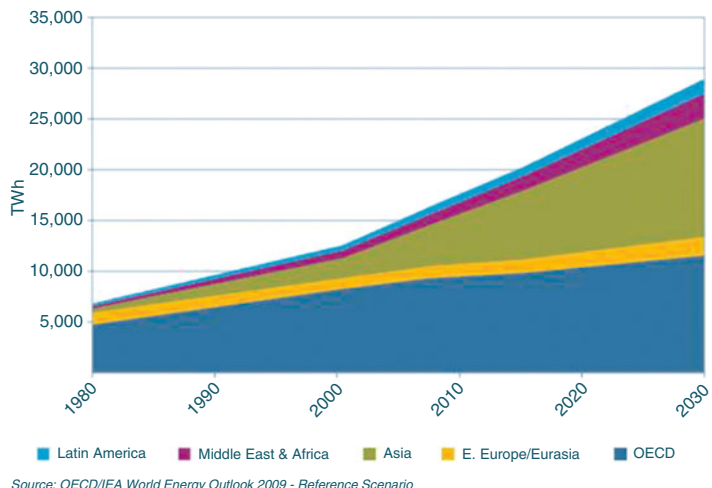


**Fig. G.1** OECD/IEA World Energy Outlook 2009 [1]

### What is OECD

The Organization for Economic Cooperation and Development (OECD) is a unique forum where the governments of 34 democracies with market economies work with each other, as well as with more than 70 non-member economies to promote economic growth, prosperity, and sustainable development.

The mission of the OECD is to promote policies that will improve the economic and social well-being of people around the world.

The OECD provides a forum in which governments can work together to share experiences and seek solutions to common problems. We work with governments to understand what drives economic, social and environmental change. We measure productivity and global flows of trade and investment. The OECD analyzes and compares data to predict future trends. We set international standards on a wide range of things, from agriculture and tax to the safety of chemicals.

The annual World Energy Outlook from the OECD's International Energy Agency (IEA) sets out the present situation and also presents current policies, new policies, and carbon reduction ('450') scenarios. In World Energy Outlook 2013, from 2000 to 2010 total world primary energy demand grew by 26 %, and to 2020 it was projected to grow less (by 20 % under the Current Policies scenario, and less under other scenarios). Growth to 2035 is 45 % under Current Policies, and 33 % under a more restrained scenario. Electricity growth is about double this in

each case. Electricity demand almost doubled from 1990 to 2011, and is projected to grow 81 % from 2011 to 2035 (from 19,004 TWh to 34,454 TWh) in the Current Policies scenario, and 69 % (to 32,150 TWh) in the central New Policies scenario. Increased electricity demand is most dramatic in Asia, projected to average 4.0 % or 3.6 % per year respectively to 2035. Currently some two billion people have no access to electricity, and it is a high priority to address this lack.

Electricity Information annually from the same source gives the latest available data on world electricity generation and its fuels [1].

With the United Nations predicting world population growth from 6.7 billion in 2011 to 8.7 billion by 2035, demand for energy must increase substantially over that period. Both population growth and increasing standards of living for many people in developing countries will cause strong growth in energy demand, as outlined above. Over 70 % of the increased energy demand is from developing countries, led by China and India—China overtook the USA as top CO<sub>2</sub> emitter in 2007. Superimposed on this, the UN Population Division projects an ongoing trend of urbanization, from 52 % in 2011 to 62 % in 2035 and reaching 70 % worldwide by 2050, enabling world population to stabilize at about nine billion with better food supply, clean water, sanitation, health, education, and communication facilities [1].

Coal is not limited globally, but large amounts need to be moved from where it is plentiful to where it is needed, mainly for power generation. This has both economic and carbon emission implications (apart from actually burning it). Natural gas is abundant and increasingly traded over long distances, with supplies in several countries increasing due to technology enabling access to gas in shale beds. Oil is more limited, in 2012 global production increased to almost 76 million barrels per day (27 billion barrels/year), and known reserves increased 8 % to 1600 billion barrels. In the World Energy Outlook 2013 New Policies scenario, coal demand increases 0.7 % per year from 2011 to 2035, gas increases 1.6 % pa, and oil increases 1.1 % pa to 2020 then 0.4 % pa. For electricity, coal use increases 35 % to 2035 thus reducing its share of generation from 41 % to 33 %, gas increases 72 % so that its share remains at 22 %, nuclear increases 66 % pa to hold its 12 % share, and renewable sources other than hydro increase nearly fivefold [1].

A question of

### How much electricity does an American home use?

This question is answered per one statistic as below.

In 2014, the average annual electricity consumption for a U.S. residential utility customer was 10,932 kilowatt-hours (kWh), an average of 911 kWh per month. Louisiana had the highest annual consumption at 15,497 kWh per residential customer, and Hawaii had the lowest at 6,077 kWh per residential customer.

Nuclear power is the most environmentally benign way of producing electricity on a large scale and its production cost of \$7 KWh will be more demandable if one can reduce this cost. Renewable energy sources such as solar and wind are costly per unit of output and are intermittent but can be helpful at the margin in providing clean power.

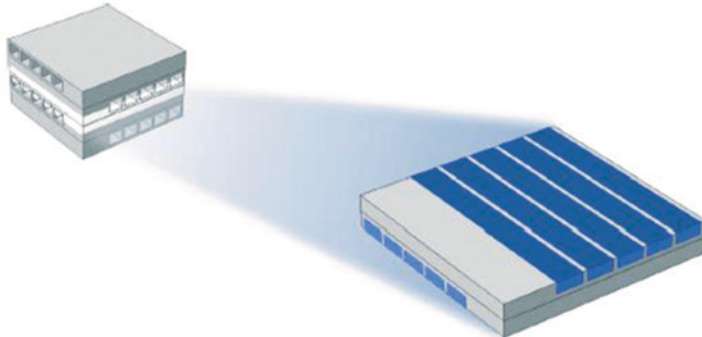


**Fig. G.2** Depiction of the modeled part of the micro-heat exchanger in COMSOL™

One solution to this cost reduction of electricity generating via nuclear power plants is suggested combined cycle driven efficiency of these plants by this author and others [2–4] as a possible solution. In order to achieve such thermal efficiency one requires combination of compact heat exchanger and recuperator as part of the turbine system where it produces electricity as a result of steam produced by heat energy induced by the nuclear plant.

As part of suggested combined cycle (CC) solution, the design of compact heat exchangers and recuperators for their applications in CC becomes very important and critical in order to push the efficiency of the new generation of nuclear plant (NGNP). One of the favorite types of compact heat exchangers (CHXs) is fine plate exchanger as shown in Fig. G.2.

Accurate design of this particular heat exchanger in cross-flow configuration form demonstrating very promising possibility in order to increase the thermal efficiency of Advanced High Temperature Reactors as part of GEN-IV families. In this appendix we utilize COMSOL Multiphysics® to demonstrate the steps for designing these particular compact heat exchangers along with basic required conditions and assumptions for such micro-heat exchanger as part of design process. Results of solution along with produced picture as part of COMSOL run are plotted.

## G.2 Model Definition

Figure G.2 shows the heat exchanger's geometry. Notice that the fluid channels have a square cross section rather than the circular cross section more commonly used in micro-heat exchangers. A cross-flow heat exchanger can typically consist of about 20 unit cells. However, because the unit cells are identical except for edge effects in the outer cells, you can restrict the model to a single unit cell. The geometry and material properties are taken from (Hessel and Löwe) [5].

Because heat is transferred by convection and conduction, the model uses a Conjugate Heat Transfer interface in the laminar flow regime. The boundary conditions are insulating for all outer surfaces except for the inlet and outlet boundaries. At the inlets for both cold and hot streams, the temperatures are constant and a laminar inflow profile with an average velocity of 2.5 mm/s is defined.

At the outlet, the heat transport is dominated by convection, which makes the outflow boundary condition suitable. For the flow field, the model applies the outlet boundary condition with a constant pressure.

As shown in Fig. G.2, you can take advantage of the model's symmetries to model only half of the channel height. Therefore, the symmetry boundary condition applies to the channels.

### G.3 COMSOL Run for Cross Flow Model

The geometry and materials for this example solves the fluid flow and heat transfer in a microscale heat exchanger made of stainless steel. Such heat exchangers are found in lab-on-chip devices and microreactors for fuel cells. The model accounts for heat transferred through both convection and conduction. Figure G.3 shows the temperature at the channel walls as well as temperature isosurfaces in the device, which clearly reveal the influence of the convective term.

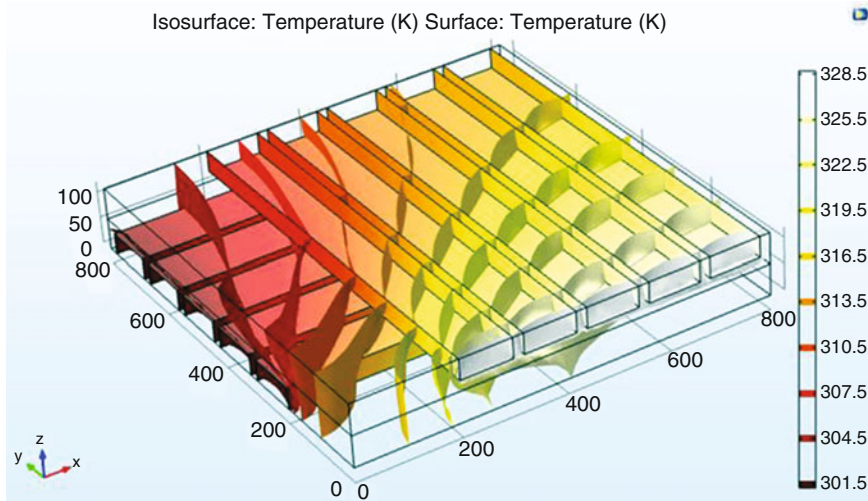


**Fig. G.3** Channel wall temperature and isotherms through the cell geometry

### G.3 Summary and Model Parameters

This example solves the fluid flow and heat transfer in a microscale heat exchanger made of stainless steel. Such heat exchangers are found in lab-on-chip devices and microreactors for fuel cells. The model accounts for heat transferred through both convection and conduction.

As can be seen in Fig. G.4, the temperature differs significantly between the different outlets in both hot and cold streams. This implies that the hot stream is not cooled uniformly.

Parameters set up for this example are shown in Table G.1 here as:

The flow field in the channels is a typical laminar velocity profile as show in Fig. G.5 here;

There are several quantities that describe the characteristics and effectiveness of a compact heat exchanger (CHX). According to Nag [6] in his book under the title of “*Heat and Mass Transfer*” in Sect. 1.4, the mixing-cup temperature of the fluid leaving the heat exchanger is calculated as per Eq. G.1 here as:

$$\langle T \rangle = \frac{\int_{\text{outlet}} \rho c_p T u ds}{\int_{\text{outlet}} \rho c_p u ds} \quad (\text{Eq. G.1})$$

**Table G.1** Example parameters and data

Name	Expression	Value	Description
T_cold	300[K]	300 K	Temperature, cold stream
T_hot	330[K]	330 K	Temperature, hot stream
u_avg	2.5[mm/s]	0.0025 m/s	Average inlet velocity

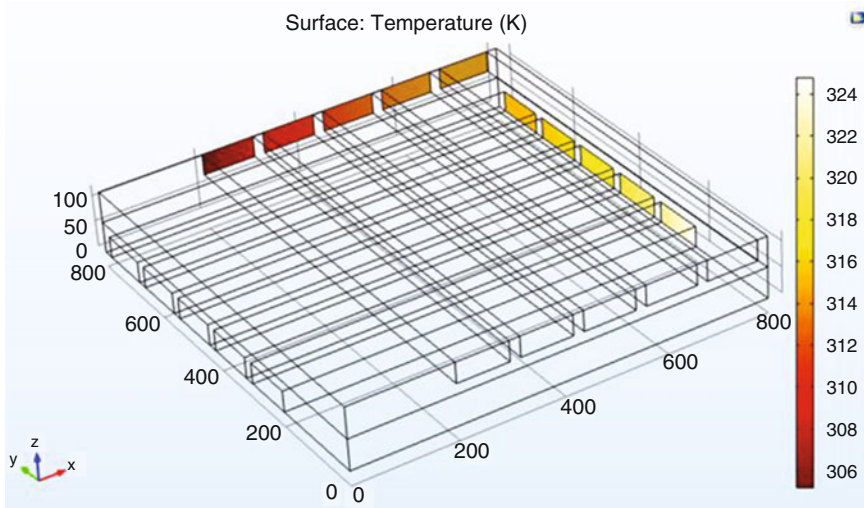


**Fig. G.4** Temperature field at the outlet temperature boundaries

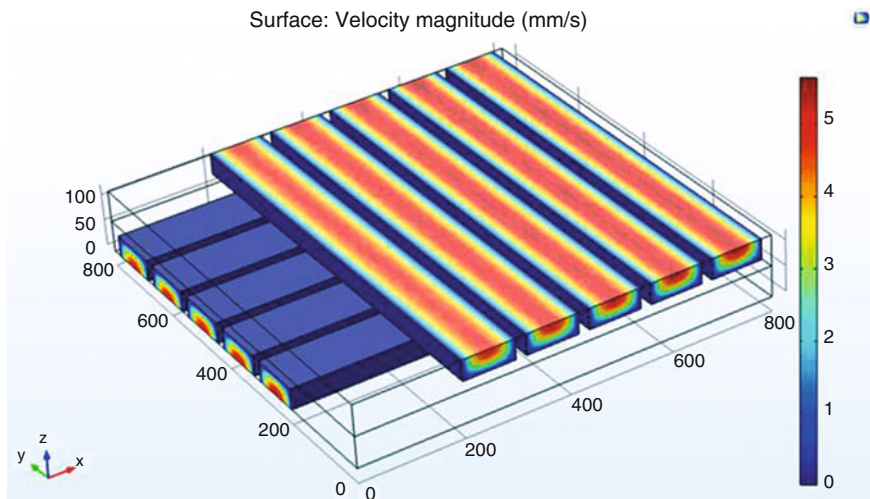


**Fig. G.5** Velocity profile in the channels

COMSOL Multiphysics provides built-in variables to easily calculate  $\langle T \rangle$ . At the upper channels, the outlet mixing-cup temperature is 45 °C. At the lower channels, despite a hotter inlet temperature, a lower value of 38.6 °C is found for the outlet mixing-cup temperature. The maximum pressure drop in the heat exchanger is 5 Pa.

The overall heat transfer coefficient is another interesting quantity. It is a measure of the performance of a heat exchanger design defined as:

$$h_{\text{eq}} = \frac{P}{A(T_{\text{hot}} - T_{\text{cold}})} \quad (\text{Eq. G.2})$$

## G.4 COMSOL Modeling Instructions Steps

The following steps in application of COMSOL Multiphysics software tools are required, and they are presented here step-by-step so users of this tool can repeat the process as it is shown in this appendix.

From the File menu, choose New.

### NEW

1. In the New window, click **Model Wizard**.

### MODEL WIZARD

1. In the **Model Wizard** window, click **3D**.
2. In the Select physics tree, select **Heat Transfer>Conjugate Heat Transfer>Laminar Flow**.

3. Click **Add**.
4. Click **Study**.
5. In the **Select study** tree, select **Preset Studies for Selected Physics Interfaces>Stationary**.
6. Click **Done**.

## GLOBAL DEFINITIONS

### *Parameters*

1. On the Home toolbar, click **Parameters**.
2. In the **Settings** window for Parameters, locate the **Parameters** section.
3. In the table, enter the following settings:

Name	Expression	Value	Description
T_cold	300[K]	300 K	Temperature, cold stream
T-hot	300[K]	330 K	Temperature, hot stream
U_avg	2.5[mm/s]	0.0025 m/s	Average inlet velocity

## GEOMETRY I

1. In the **Model Builder** window, under **Component I (compI)** click **Geometry I**.
2. In the **Settings** window for Geometry, locate the **Units** section.
3. From the **Length unit** list, choose **μm**.

First, create the cross-section of one unit cell and extrude it.

### *Block 1 (blk 1)*

1. On the **Geometry** toolbar, click **Block**.
2. In the **Settings** window for Block, locate the **Size and Shape** section.
3. In the **Width** text field, type 800.
4. In the **Depth** text field, type 800.
5. In the **Height** text field, type 60.

### *Block 2 (blk 2)*

1. Right-click **Block 1 (blk1)** and choose **Build Selected**.
2. On the **Geometry** toolbar, click **Block**.
3. In the **Settings** window for Block, locate the **Size and Shape** section.
4. In the **Width** text field, type 800.
5. In the **Depth** text field, type 100.
6. In the **Height** text field, type 40.
7. Locate the **Position** section. In the **y** text field, type 200.

### *Array 1 (arr1)*

1. Right-click **Block 2 (blk2)** and choose **Build Selected**.
2. On the **Geometry** toolbar, click **Transforms** and choose **Array**.
3. Select the object **blk2** only.

4. In the **Settings** window for Array, locate the **Size** section.
5. From the **Array type** list, choose **Linear**.
6. In the **Size** text field, type **5**.
7. Locate the **Displacement** section. In the **y** text field, type **120**.
8. Locate the Selections of Resulting Entities section. Click **New**.
9. In the New Cumulative Selection dialog box, type **Channels** in the Name text field.
10. Click **OK**.

#### *Rotate 1 (rot1)*

1. On the **Geometry** toolbar, click **Transforms** and choose **Rotate**.
2. Click in the **Graphics** window and then press **Ctrl+A** to select all objects.
3. In the **Settings** window for Rotate, locate the **Rotation Angle** section.
4. In the **Rotation** text field, type **180**.
5. Locate the **Point on Axis of Rotation** section. In the **z** text field, type **60**.
6. Locate the **Axis of Rotation** section. From the **Axis type** list, choose **Cartesian**.
7. In the **x** text field, type **1**.
8. In the **y** text field, type **1**.
9. In the **z** text field, type **0**.

Keep the existing unit cell by the following step.

1. Locate the **Input** section. Select the **Keep input objects** check box.
2. Click the **Build All Objects** button.
3. Click the **Zoom Extents** button on the **Graphics** toolbar.

Define several selections that help you throughout the model set-up.

## **DEFINITIONS**

### *Explicit 1*

1. On the Definitions toolbar, click **Explicit**.
2. In the Settings window for Explicit, type **Upper Inlets** in the **Label** text field.
3. Locate the Input Entities section. From the Geometric entity level list, choose **Boundary**.
4. Select Boundaries 41, 48, 55, 62, and 69 only.

### *Explicit 2*

1. On the Definitions toolbar, click **Explicit**.
2. In the Settings window for Explicit, type **Lower Inlets** in the **Label** text field.
3. Locate the Input Entities section. From the Geometric entity level list, choose **Boundary**.
4. Select Boundaries 8, 14, 20, 26, and 32 only.

### *Explicit 3*

1. On the Definitions toolbar, click **Explicit**.
2. In the Settings window for Explicit, type **Upper Outlets** in the **Label** text field.

3. Locate the **Input Entities** section. From the **Geometric entity level** list, choose **Boundary**.
4. Select Boundaries 44, 51, 58, 65, and 72 only.

#### *Explicit 4*

1. On the **Definitions** toolbar, click **Explicit**.
2. In the **Settings** window for Explicit, type Lower Outlets in the **Label** text field.
3. Locate the **Input Entities** section. From the **Geometric entity level** list, choose **Boundary**.
4. Select Boundaries 77–81 only.

#### *Explicit 5*

1. On the **Definitions** toolbar, click **Explicit**.
2. In the **Settings** window for Explicit, type Symmetry in the **Label** text field.
3. Locate the **Input Entities** section. From the **Geometric entity level** list, choose **Boundary**.
4. Select the **Group by continuous tangent** check box.
5. Select one of the uppermost and lowermost boundaries, which now automatically will select all uppermost and lowermost boundaries thanks to the continuous tangency.

#### *Union 1*

1. On the **Definitions** toolbar, click **Union**.
2. In the *Settings* window for Union, type Outlets in the **Label** text field.
3. Locate the **Geometric Entity Level** section. From the **Level** list, choose Boundary.
4. Locate the **Input Entities** section. Under Selections to add, click **Add**.
5. In the **Add** dialog box, In the Selections to add list, choose **Upper Outlets** and **Lower Outlets**.
6. Click **OK**.

## MATERIALS

Define the material properties.

#### *Material 1 (mat1)*

1. In the **Model Builder** window, under **Component 1 (comp1)** right-click **Materials** and choose **Blank Material**.
2. In the **Settings** window for Material, type Stainless Steel in the **Label** text field.
3. Locate the **Material Contents** section. In the table, enter the following settings:

Property	Name	Value	Units	Property group
Thermal conductivity	$k$	15	W/(m.K)	Basic
Density	$\rho$	7800	Kg/m <sup>3</sup>	Basic
Heat capacity at constant pressure	$C_p$	420	J/(kg.K)	Basic

## ADD MATERIAL

1. On the **Home** toolbar, click **Add Material** to open the **Add Material** window.
2. Go to the **Add Material** window.
3. In the tree, select **Built-In>Water, liquid**.
4. Click **Add to Component** in the window toolbar.

## MATERIALS

*Water, liquid (mat2)*

1. On the Home toolbar, click Add Material to close the Add Material window.
2. In the **Model Builder** window, under **Component 1 (comp1)>Materials** click **Water, liquid (mat2)**.
3. In the **Settings** window for Material, locate the **Geometric Entity Selection** section.
4. From the **Selection** list, choose **Channels**.

## HEAT TRANSFER (HT)

*Heat Transfer in Fluids 1*

1. In the **Model Builder** window, under **Component 1 (comp1)>Heat Transfer (ht)** click **Heat Transfer in Fluids 1**.
2. In the **Settings** window for Heat Transfer in Fluids, locate the **Domain Selection** section.
3. From the Selection list, choose Channels.

*Temperature 1*

1. On the **Physics** toolbar, click **Boundaries** and choose **Temperature**.
2. In the **Settings** window for Temperature, locate the **Boundary Selection** section.
3. From the Selection list, choose **Upper Inlets**.
4. Locate the **Temperature** section. In the  $T_0$  text field, type  $T_{\text{hot}}$ .

*Temperature 2*

1. On the **Physics** toolbar, click **Boundaries** and choose **Temperature**.
2. In the Settings window for Temperature, locate the Boundary Selection section.
3. From the Selection list, choose **Lower Inlets**.
4. Locate the **Temperature** section. In the  $T_0$  text field, type  $T_{\text{cold}}$ .

*Outflow 1*

1. On the **Physics** toolbar, click Boundaries and choose **Outflow**.
2. In the Settings window for Outflow, locate the **Boundary Selection** section.

From the **Selection** list, choose **Upper Outlets**.

*Outflow 2*

1. On the **Physics** toolbar, click **Boundaries** and choose Outflow.
2. In the **Settings** window for Outflow, locate the **Boundary Selection** section.
3. From the Selection list, choose Lower Outlets.

### *Symmetry 1*

1. On the Physics toolbar, click Boundaries and choose Symmetry.
2. In the **Settings** window for Symmetry, locate the **Boundary Selection** section.
3. From the **Selection** list, choose **Symmetry**.

So far, the boundary conditions for heat transfer have been specified. Continue with the set up of the flow equation.

### LAMINAR FLOW (SPF)

1. In the **Model Builder** window, under **Component 1 (comp1)** click **Laminar Flow (spf)**.
2. In the **Settings** window for Laminar Flow, locate the **Domain Selection** section.
3. From the **Selection** list, choose **Channels**.

Because of the different inlet temperatures, the densities for the hot and cold stream vary and produce different velocities when the laminar inflow boundary condition is used. In order to have the same velocity profile on each inlet, define the laminar inflow boundary condition for the hot and cold inlet boundaries separately.

#### *Inlet 1*

1. On the **Physics** toolbar, click **Boundaries** and choose **Inlet**.
2. In the **Settings** window for Inlet, locate the **Boundary Selection** section.
3. From the **Selection** list, choose **Upper Inlets**.
4. Locate the **Boundary Condition** section. From the list, choose **Laminar inflow**.
5. Locate the **Laminar Inflow** section. In the  $U_{av}$  text field, type  $u\_avg$ . The Entrance length value must be large enough so that the flow can reach a laminar profile. For a laminar flow,  $L_{entr}$  should be significantly greater than  $0.06ReD$ , where  $Re$  is the Reynolds number and  $D$  is the inlet length scale. In this case 1 mm is a good value.
6. In the  $L_{entr}$  text field, type 1[mm].

#### *Inlet 2*

1. On the **Physics** toolbar, click **Boundaries** and choose **Inlet**.
2. In the **Settings** window for Inlet, locate the **Boundary Selection** section.
3. From the **Selection** list, choose **Lower Inlets**.
4. Locate the **Boundary Condition** section. From the list, choose **Laminar inflow**.
5. Locate the **Laminar Inflow** section. In the  $U_{av}$  text field, type  $u\_avg$ .
6. In the  $L_{entr}$  text field, type 1[mm].

#### *Outlet 1*

1. On the **Physics** toolbar, click Boundaries and choose Outlet.
2. In the **Settings** window for Outlet, locate the **Boundary Selection** section.
3. From the **Selection** list, choose **Upper Outlets**.

### Outlet 2

1. On the **Physics** toolbar, click **Boundaries** and choose **Outlet**.
2. In the **Settings** window for Outlet, locate the **Boundary Selection** section.
3. From the **Selection** list, choose Lower Outlets.

### Symmetry 1

1. On the **Physics** toolbar, click **Boundaries** and choose **Symmetry**.
2. In the **Settings** window for **Symmetry**, locate the **Boundary Selection** section.
3. From the **Selection** list, choose **Symmetry**.

After solving the model, the equivalent heat transfer coefficient is evaluated according to Eq. (G.2). To do so, define the following coupling operator.

## DEFINITIONS

### Average 1 (aveop1)

1. On the **Definitions** toolbar, click **Component Couplings** and choose **Average**.
2. In the Settings window for Average, type Average on Upper Channel Walls in the Label text field.
3. Locate the **Source Selection** section. From the **Geometric entity level** list, choose **Boundary**.
4. Select Boundaries 40, 42, 45, 47, 49, 52, 54, 56, 59, 61, 63, 66, 68, 70, and 73 only.

To more easily select these boundaries use the **Paste** button and insert the list of numbers above in the **Paste Selection** dialog box.

## STUDY 1

On the Home toolbar, click **Compute**.

## RESULTS

### Temperature (ht)

COMSOL Multiphysics automatically creates four default plots: a temperature plot, an isothermal contour plot, a slice plot for the velocity field, and a contour plot for the pressure field. The isothermal contours will be modified, to create the plot shown in Fig. G.2.

### Isothermal Contours (ht)

1. In the **Model Builder** window, under **Results** right-click **Isothermal Contours (ht)** and choose Surface.
2. In the **Settings** window for Surface, locate the **Data** section.
3. From the **Data** set list, choose **Exterior Walls**.
4. Click Replace Expression in the upper-right corner of the Expression section. From the menu, choose **Component 1>Heat Transfer>Temperature>T - Temperature**.
5. Click to expand the **Inherit style** section. Locate the Inherit Style section. From the **Plot** list, choose **Isosurface 1**.
6. On the **Isothermal Contours (ht)** toolbar, click **Plot**.

To visualize the velocity field as in Fig. G.4, follow the steps below: Velocity (spf)

1. In the **Model Builder** window, expand the **Velocity (spf)** node.
2. Right-click **Slice 1** and choose **Delete**.
3. Right-click **Velocity (spf)** and choose **Surface**.
4. In the **Settings** window for Surface, click **Replace Expression** in the upper-right corner of the **Expression** section. From the menu, choose **Component 1>Laminar**
5. **Flow>Velocity and pressure>spf.U - Velocity magnitude**.
6. Locate the **Expression** section. From the **Unit** list, choose mm/s.
7. On the **Velocity (spf)** toolbar, click **Plot**.

#### *Data Sets*

To show the temperature on the outlet boundaries only, as in Fig. G.3, first produce a new data set for the selection built before. Then use this data set for a surface plot of the temperature.

#### *Surface 2*

On the Results toolbar, click More Data Sets and choose Surface.

#### *Data Sets*

1. In the **Settings** window for Surface, type Outlets in the **Label** text field.
2. Locate the **Selection** section. From the **Selection** list, choose **Outlets**.

#### *3D Plot Group 5*

1. On the **Results** toolbar, click **3D Plot Group**.
2. In the Settings window for 3D Plot Group, type Outlet Temperature in the **Label** text field.

#### *Outlet Temperature*

1. Right-click **Outlet Temperature** and choose **Surface**.
2. In the **Settings** window for Surface, locate the **Data** section.
3. From the **Data** set list, choose **Outlets**.
4. Locate the **Coloring and Style** section. From the **Color table** list, choose **ThermalLight**.
5. On the **Outlet Temperature** toolbar, click **Plot**.

#### *Global Evaluation 1*

On the **Results** toolbar, click **Global Evaluation**.

#### *Derived Values*

1. In the **Settings** window for Global Evaluation, type Mixing-CupTemperature (Upper Outlets) in the **Label** text field.
2. Click Replace Expression in the upper-right corner of the Expression section. From the menu, choose **Component 1>Heat Transfer>Global>Weighted average temperature>ht.ofl1.Tave - Weighted average temperature**.

3. Locate the **Expression** section. From the Unit list, choose **degC**.
4. Select the **Description** check box.
5. In the associated text field, type Mixing-cup temperature (upper outlets).
6. Click the **Evaluate** button.

## TABLE

1. Go to the **Table** window.

The mixing-cup temperature at upper outlets is about 38.5 °C.

2. Right-click **Mixing-Cup Temperature (Upper Outlets)** and choose **Duplicate**.

## RESULTS

### *Derived Values*

1. In the Settings window for Global Evaluation, click Replace Expression in the upper-right corner of the **Expression** section. From the menu, choose **Component 1>Heat Transfer>Global>Weighted average temperature>ht.ofl2. Tave - Weighted average temperature**.
2. In the **Label** text field, type Mixing-Cup Temperature (Lower Outlets).
3. Locate the **Expression** section. Select the **Description** check box.
4. In the associated text field, type Mixing-cup temperature (lower outlets).
5. Click the **Evaluate** button.

## TABLE

1. Go to the Table window.

The mixing-cup temperature at lower outlets is about 45 °C.

## RESULTS

### *Derived Values*

To calculate the maximum pressure drop proceed as follows:

#### *Surface Maximum 1*

On the **Results** toolbar, click **More Derived Values** and choose **Maximum>Surface Maximum**.

### *Derived Values*

1. In the **Settings** window for Surface Maximum, locate the **Selection** section.
2. From the **Selection** list, choose **All boundaries**.
3. Click Replace Expression in the upper-right corner of the Expression section. From the menu, choose **Component 1>Laminar Flow>Velocity and pressure>p - Pressure**.
4. In the **Label** text field, type Maximum Pressure Drop.
5. Locate the **Expression** section. Select the **Description** check box.
6. In the associated text field, type Maximum pressure drop.
7. Click the **Evaluate** button.

**TABLE**

1. Go to the Table window.

The maximum pressure is 5 Pa. The minimum pressure is defined by the outlet boundary conditions and is zero. Thus, the maximum pressure drop is also 5 Pa.

Now, evaluate the equivalent heat transfer coefficient as defined in Eq. (G.2). You can use the integration operators defined previously in **Component 1>Definitions**.

**RESULTS***Global Evaluation 3*

On the Results toolbar, click Global Evaluation.

*Derived Values*

1. In the **Settings** window for Global Evaluation, locate the **Expression** section.
2. In the Expression text field, type  $\text{aveop1(ht.nflux)/(T_hot-T_cold)}$ .
3. In the **Label** text field, type Heat Transfer Coefficient.
4. Locate the **Expression** section. Select the **Description** check box.
5. In the associated text field, type Heat transfer coefficient.
6. Click the **Evaluate** button.

**TABLE**

1. Go to the Table window.

The equivalent heat transfer coefficient is about  $1500 \text{ W}/(\text{m}^2 \cdot \text{K})$ .

**Note:** that there are other aspects of Fig. G.6 for cases such as follow for Multiphysics analysis of COMSOL<sup>®</sup> for Controlled Mesh (Fig. G.7), Laminar

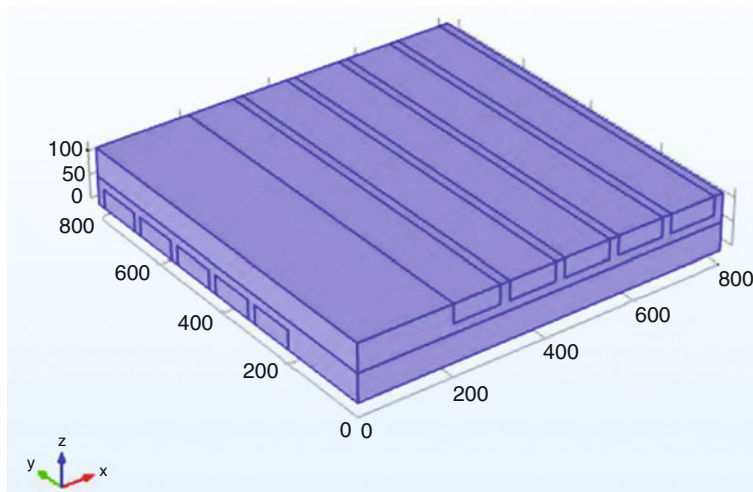


**Fig. G.6** Next selections are needed to evaluate the equivalent heat transfer coefficient for maximum pressure drop

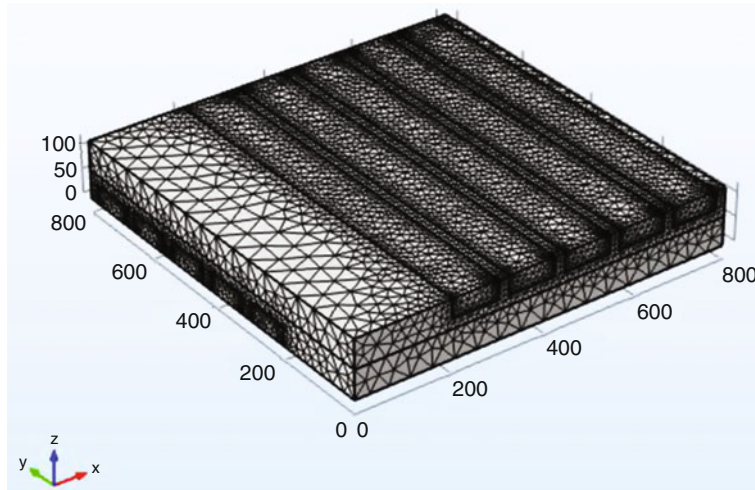


**Fig. G.7** Sketch of controlled mesh

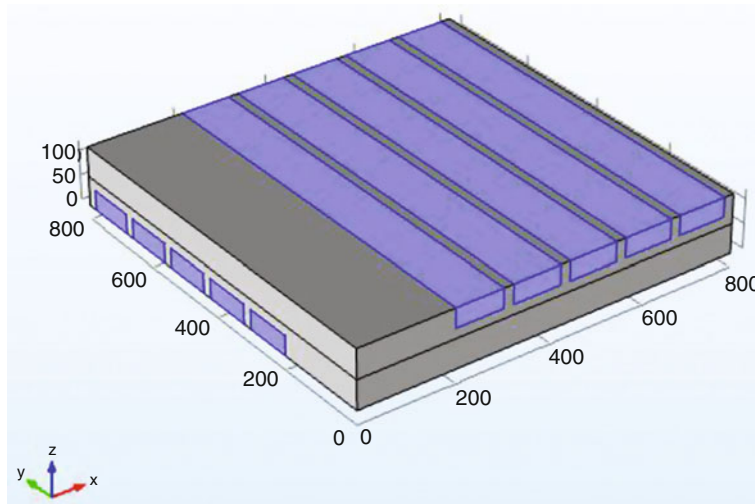


**Fig. G.8** Sketch of laminar flow within compact heat exchanger

Flow spf (Fig. G.8), General Multi Physics for Mixing Temperature approach (Fig. G.9) General Multiphysics for Heat Transfer Coefficient of flow within exchanger for Component 1 (Fig. G.10), and finally for Surface Temperature (Fig. G.11) respectively. Note also that Fig. G.6 was plotted by COMSOL Multiphysics® for Maximum Pressure Drop.

Figure G.12 plotted also using COMSOL Multiphysics for our modeled Fin Plate Compact Exchanger to draw pressure contour.

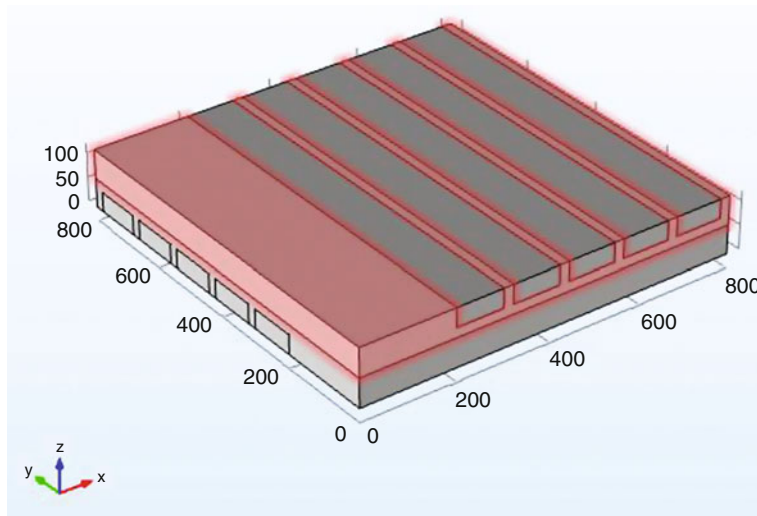


**Fig. G.9** Sketch of general multiphysics for mixing temperature

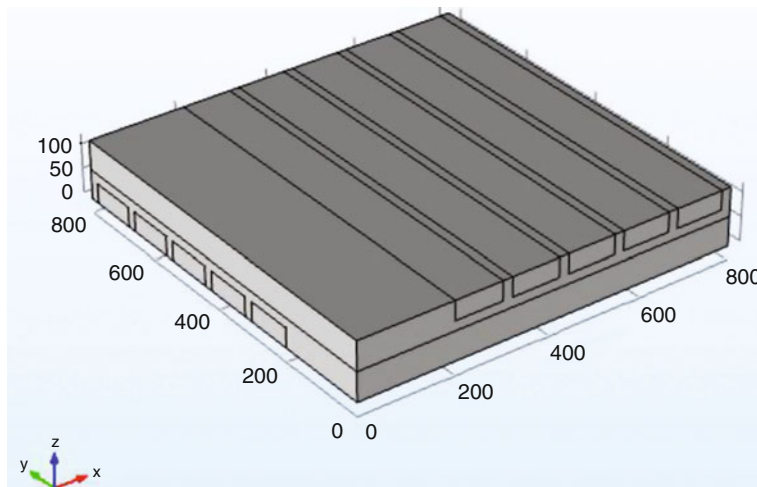


**Fig. G.10** Presentation of compact heat exchanger for heat transfer coefficient analysis purpose

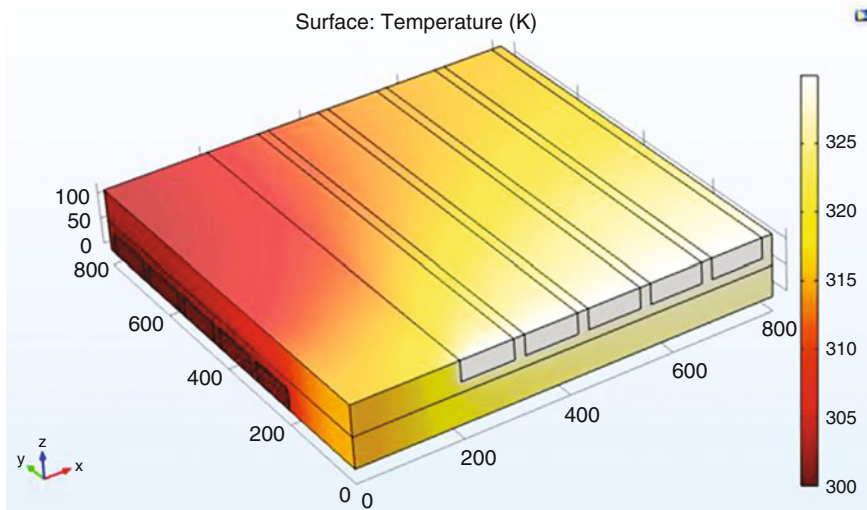


Fig. G.11 Presentation of surface temperature

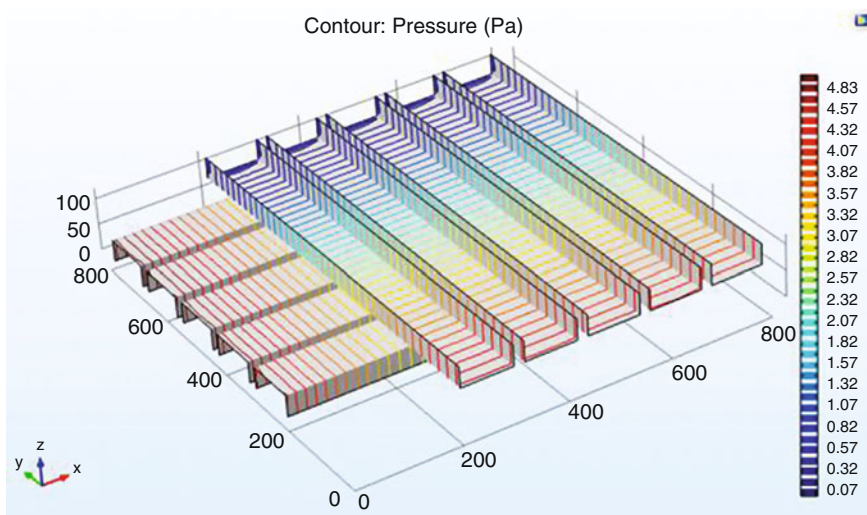


Fig. G.12 Sketch of pressure contour

## References

1. <http://www.world-nuclear.org/info/Current-and-Future-Generation/world-Energy-Needs-and-nuclear-power/>.
2. Zohuri, B. 2015. *Combined cycle driven efficiency for next generation nuclear power plants: an innovative design approach*. Springer Publishing Company.

3. Zohuri, B. 2014. *Innovative open air Brayton combined cycle systems for the next generation nuclear power plants*. University of New Mexico Publications, June 2014.
4. Forsberg, Charles, Pat McDaniel, and B. Zohuri. 2015. Variable electricity and steam from salt, helium, and sodium cooled base-load reactors with gas turbines and heat storage. In *Proceedings of ICAPP*, 2015 May 03-06, 2015—Nice (France) Paper 15115.
5. Ehrfeld, W., V. Hessel, and H. Löwe. 2000. *Microreactors*. John Wiley & Sons.
6. Nag, P.K. 2007. *Heat and mass transfer*, 2nd ed. Tata McGraw-Hill.

# Nuclear Systems Acronyms: Glossary of Nuclear Terms (US NRC)

<b>AHTR</b>	Advanced High Temperature Reactor
<b>AECL</b>	Atomic Energy of Canada Ltd.
<b>AECB</b>	Atomic Energy Control Board
<b>AESOP</b>	Atomic Energy Simulation of Optimization (computer code)
<b>ASDV</b>	Atmospheric Steam Discharge Valve
<b>ASSERT</b>	Advanced Solution of Sub-channel Equations in Reactor Thermal hydraulics (computer code)
<b>ASTM</b>	American Society for Testing Materials
<b>BLC</b>	Boiler Level Control
<b>BLW</b>	Boiling Light Water
<b>BPC</b>	Boiler Pressure Controller
<b>CBA</b>	Core Barrel Assembly
<b>CCP</b>	Critical Channel Power
<b>CHF</b>	Critical Heat Flux
<b>CHP</b>	Combined Heat and Power
<b>CPR</b>	Critical Power Ratio
<b>CRL</b>	Chalk River Laboratories
<b>CRT</b>	Cathode Ray Tube
<b>CSA</b>	Canadian Standards Association
<b>CSDV</b>	Condenser Steam Discharge Valve
<b>CSNI</b>	Canadian Standards for the Nuclear Industry
<b>DBE</b>	Design Base Earthquake
<b>DCC</b>	Digital Control Computer
<b>DF-ET</b>	Drift Flux-Equal Temperature
<b>DF-UT</b>	Drift Flux-Unequal Temperature
<b>DNB</b>	Departure from Nucleate Boiling
<b>ECC</b>	Emergency Core Cooling
<b>ECI</b>	Emergency Core Injection
<b>EFPH</b>	Effective Full Power Hours
<b>EVET</b>	Equal Velocity Equal Temperature

<b>EVUT</b>	Equal Velocity-Unequal Temperature
<b>EWS</b>	Emergency Water Supply
<b>FBR</b>	Feed, Bleed and Relief
<b>FP</b>	Full Power
<b>FP</b>	Fission Product
<b>HEM</b>	Homogeneous Equilibrium Model
<b>HTS</b>	Heat Transport System
<b>HWP</b>	Heavy Water Plant
<b>HYDNA</b>	Hydraulic Network Analysis (extinct computer code)
<b>HX</b>	Heat Exchanger
<b>IGCC</b>	Integrated Gasification Combined Cycle
<b>I&amp;C</b>	Instrumentation and Control
<b>IBIF</b>	Intermittent Buoyancy Induced Flow
<b>ICRP</b>	International Commission on Radiological Protection
<b>IHX</b>	Intermediate Heat Exchanger
<b>LOC</b>	Loss of Coolant
<b>LOCA</b>	Loss of Coolant Accident
<b>LOC/LOECC</b>	Loss of Coolant with Coincident Loss of Emergency Core Cooling
<b>LOP</b>	Loss of Pumping
<b>LOR</b>	Loss of Regulation
<b>GT-MHR</b>	Gas Turbine-Modular Helium Reactor
<b>GTHTR</b>	Gas Turbine High Temperature Reactor
<b>MCCR</b>	Ministry of Corporate and Consumer Relations
<b>MCS</b>	Maintenance Cooling System
<b>MHD</b>	Magneto hydrodynamics
<b>milli-k</b>	Unit of reactivity for reactor physics
<b>NGNP</b>	Next Generation Nuclear Plant
<b>NPD</b>	Nuclear Power Demonstration
<b>NPSH</b>	Net Positive Suction Head
<b>NUCIRC</b>	Nuclear Circuits (computer code)
<b>OECD</b>	Organization for Economic Co-operation & Development
<b>OH</b>	Ontario Hydro
<b>PBMR</b>	Pebble Bed Modular Reactor
<b>PCS</b>	Power Conversion System
<b>PGSA</b>	Pickering Generating Station A
<b>PHTS</b>	Primary Heat Transport System
<b>PHW</b>	Pressurized Heavy Water
<b>PHWR</b>	Pressurized Heavy Water Reactor
<b>PRESCON2</b>	Pressure Containment (computer code)
<b>QA</b>	Quality Assurance
<b>RAMA</b>	Reactor Analysis Implicit Algorithm
<b>R&amp;M</b>	Reliability and Maintainability
<b>RB</b>	Reactor Building

<b>RCS</b>	Reactivity Control System
<b>RIH</b>	Reactor Inlet Header
<b>ROH</b>	Reactor Outlet Header
<b>RSS</b>	Reserve Shutdown System
<b>RTD</b>	Resistance Temperature Detectors
<b>RU</b>	Reactor Unit
<b>SDM</b>	Safety Design Matrices
<b>SG</b>	Steam Generator
<b>SOPHT</b>	Simulation of Primary Heat Transport (computer code)
<b>SOX</b>	Sarbanes Oxley
<b>SRV</b>	Safety Relief Valve
<b>TMI</b>	Three Mile Island
<b>TOFFEA</b>	Two Fluid Flow Equation Analysis (computer code)
<b>TRIS</b>	Triple-Coated Isotropic
<b>UVUT</b>	Unequal Velocity Unequal Temperature
<b>VB</b>	Vacuum Building
<b>VC</b>	Vacuum Chamber
<b>VHTR</b>	Very High Temperature Reactor
<b>WRE</b>	White-shell Research Establishment
<b>LEU-TRISO</b>	Low Enriched Uranium Triple-Coated Isotropic
<b>PBMR</b>	Pebble Bed Modular Reactor
<b>HTR</b>	High Temperature Reactor
<b>CSC</b>	Core Structure Ceramics
<b>CBA</b>	Core Barrel Assembly
<b>CS</b>	Core Structures
<b>THTR</b>	Thorium High Temperature Reactor
<b>HTGR</b>	High Temperature Gas-Cooled Reactor
<b>FHSS</b>	Fuel Handling and Storage System
<b>HRSG</b>	Heat Recovery Steam Generators
<b>CHP</b>	Combined Heat and Power
<b>NGNP</b>	Next Generation Nuclear Power Plant
<b>NTU</b>	Number of Transfer Units
<b>LMTD</b>	Logarithmic Mean Temperature Difference
<b>NERI</b>	Nuclear Energy Research Initiative
<b>LFR</b>	Lead-Alloy Cooled Fast Reactor
<b>GFR</b>	Gas-Cooled Fast Reactor
<b>AFCI</b>	Advanced Fuel Cycle Initiative
<b>EBR-II</b>	Experimental Breeder Reactor
<b>LWR</b>	Light Water Reactor
<b>TRISO</b>	Tristructural-Isotropic
<b>DRACS</b>	Direct Reactor Auxiliary Cooling System
<b>DHX</b>	Dump Heat Exchanger
<b>IHX</b>	Intermediate Heat Exchanger

# Index

## A

Absolute pressure, 13  
Absolute zero, 17  
Advanced High Temperature Reactor (AHTR), 412  
Alkaline Water Electrolysis, 369  
Anode, 359

## B

Base load, 360  
Blasius friction factor, 134  
Brayton Combined Cycle (BCC), 317  
Brayton Cycle, 301, 304, 345, 347

## C

Cathode, 359  
Chilton-Colburn analogy, 217  
Classical thermodynamics, 2, 8, 9  
Clean-In-Place (CIP), 100  
Closed systems, 9  
Cogeneration, 378  
Colburn heat transfer factor, 135, 138, 158, 160, 163, 212, 214, 232  
Colburn number, 218  
Colebrook–White equation, 135  
Combined Heat and Power (CHP), 310, 378  
Compact Heat Exchangers (CHEs), 57, 66, 74, 82, 89, 101, 140, 153, 161, 188, 322, 336, 339, 347, 348, 353  
Compact heat exchangers with precision formed surfaces, 98  
Computational Fluid Dynamics (CFD), 58, 119  
COMSOL Multiphysics, 347

Concentrated Solar Power (CSP), 85, 132, 232, 234, 339–342, 347, 348, 350, 353  
Contraction Loss, 140  
Control volume, 10  
Cooling towers, 31  
Coriolis body forces, 189, 192  
Coriolis effects, 197  
Counter Flow, 46  
Critical Reynolds number, 214  
Cross Flow, 46

## D

Darcy friction factor, 133, 178, 217  
Darcy-Weisbach equation, 217  
Darcy-Weisbach Friction Factor, 133  
Density, 12  
Department of Energy (DOE), 387  
Dittus-Boelter correlation, 221  
Dynamic Pressure, 178

## E

Electric hydrolysis, 359  
Electromagnetic forces, 197  
Energy and Industrial Technology Development Organization (NEDO), 355  
Energy Technology List, 322  
English (E) system, 6  
Enhanced Capital Allowance (ECA), 322  
Entrance Loss, 140  
Entrance Pressure Drop, 142  
Entropy, 301  
Exit Loss, 140

Exit Pressure Rise, 143  
 Expansion Loss, 140  
 Extensive security measures, 390

**F**

Fanning friction factor, 133, 158, 160, 178, 232  
 Final Safety Analysis Report (FSAR), 390  
 Finite Elements Analysis (FEA), 58, 267  
 Finite Elements Method (FEM), 399  
 First Law of Thermodynamics, 17  
 Flow coefficient, 133  
 Forced convection, 189, 193  
 Free convection, 189, 192  
 Friction factor, 163  
 Fuel Cell Vehicle (FCV), 355, 376, 380  
 Fuel Cells, and Infrastructure Technologies (HFCIT), 387  
 Fukushima, 389

**G**

Gage pressure, 13  
 Gas Turbine (GT), 345  
 Goodness Factors, 162

**H**

Head loss, 179  
 Heat Exchanger (HX), 19, 22, 31, 316, 401  
 Heat Recovery Steam Generator (HRSG), 335, 346  
 High Pressure Compressor (HPC), 308  
 High Temperature Gas-Cooled Reactor (HTGR), 398  
 High Temperature Test Reactor (HTTR), 401  
 Housing and Urban Development (HUD), 343  
 Hydraulic diameter, 86, 112, 220  
 Hydrodynamically developing, 192  
 Hydrodynamically fully developed, 191  
 Hydrogen Fuel Cell Vehicle (HFCV), 377, 384  
 Hydrogen Network (HyNet), 396

**I**

Idaho National Laboratory (INL), 339  
 Incompressible liquid, 201  
 In-Service Inspection (ISI), 412  
 Intensive variables, 10  
 Intermediate Heat Exchanger (IHX), 317, 336, 392, 393, 401, 407, 410  
 Internal friction, 201

**J**

Joule-Thompson expansion cycle, 370

**K**

Kelvin degree, 15  
 Kinematic viscosity, 213

**L**

Laminar flow, 191  
 Laws of Thermodynamics, 17  
 Linde cycle, 370  
 Liquefied Natural Gas (LNG), 379  
 Liquid Salt (LS), 398  
 Local Nusselt number, 215  
 Logarithmic Mean Temperature Difference (LMTD), 38, 73, 122, 126, 132, 210, 319, 321, 401, 412  
 Low Pressure Compressor (LPC), 308

**M**

Macroscopic systems, 8  
 Manning's Friction Factor, 134  
 MATLAB, 347  
 Minimum Fluid Capacity Rate, 45  
 Mixtures of pure substances, 10  
 Momentum equation, 193  
 Moody diagrams, 133  
 Moody friction, 216  
 Moody friction factor, 133

**N**

National Renewable Energy Laboratory (NREL), 384, 387  
 Newtonian fluids, 193  
 Newtonian mechanics, 4  
 Next Generation Nuclear Plant (NGNP), 85, 132, 180, 232, 234, 315, 316, 323, 327, 335, 374, 380, 381, 401  
 Nonnewtonian fluids, 193  
 North American Electric Reliability Corporation (NERC), 383  
 Nuclear air-Brayton Combined Cycle (NACC), 317  
 Nuclear Power Plants, 35, 389, 390  
 Number of Transfer Units (NTU), 45–47, 73, 86, 127, 132, 151, 164, 210, 231, 236, 244, 287  
 Nusselt number, 212, 214, 218

**O**

- Open systems, 9
- Organization for Economic Co-operation and Development (OECD), 363
- Overall core pressure drop, 140
- Overall heat exchanger conductance, 161

**P**

- Parabolic Law, 197
- Parallel Flow, 21, 46
- Partial Differential Equations (PDEs), 268
- Peak load, 360
- Photo-Voltaic (PV), 340
- Plate Fin Compact Heat Exchanger (PFCHE), 76, 78, 151
- Plate Fin Heat Exchanger (PFHE), 62, 64, 226, 227
- Plate Frame Compact Heat Exchanger (PFCHE), 77
- Plate Heat Exchangers (PHEs), 62, 65, 69, 93, 98, 99, 109, 351
- Plate-Fin Compact Heat Exchangers (PFCHEs), 150
- Plate-Fin Heat Exchanger (PFHE), 238
- Plate-fin heat exchangers, 98
- Poiseuille's law, 134
- Power-Law Model, 193
- Pressure Swing Adsorption (PSA), 356
- Preventive Maintenance (PM), 401
- Printed Circuit Heat Exchanger (PCHE), 27, 28, 69, 70, 75, 226, 227, 233, 243, 351, 411
- Process Heat Exchanger (PHX), 397
- Proof stress (PS), 180
- Pure substances, 10, 11

**Q**

- Quasi-equilibrium process, 9

**R**

- Rankine Cycle, 345, 347
- Rankine degree, 15
- Ratio of stream capacity rates, 127
- Reactor Outlet Temperature (ROT), 412
- Research and Development (R&D), 355
- Return On Investment (ROI), 317
- Reynolds number, 44, 54, 191, 232, 240
- Risk of Radioactive Release, 389

**S**

- Second Law of Thermodynamics, 17
- Skin Friction, 133
- Solar Gas Power Plant (SGPP), 227
- Solid Polymer Electrolyte Membrane Water Electrolysis (SPE), 369
- Specific volume, 12
- Spiral Heat Exchanger (SHE), 66, 79
- Standards Development Organizations (SDO), 387
- Stanton number, 212, 218
- State emergency response, 389
- Static head, 152
- Steam reforming, 358
- Stream flow, 191
- Surroundings, 2
- System International (SI), 6

**T**

- T-Boundary Condition, 171
- Temperature, 14
- Thermal energy, 4, 7, 9, 17, 296
- Thermosyphon, 323
- Third Law of Thermodynamics, 17
- Total Cost of Ownership (TCO), 317
- Tri-Isotopic (TRISO), 407

**U**

- U.S. Department of Agriculture (USDA), 343
- U.S. Department of Energy (DOE), 343
- Ultimate tensile stress (UTS), 180

**V**

- Vacuum pressure, 13
- Vena Contracta, 142
- Verification and Validation (V&V), 188
- Very High Temperature Gas-Cooled Reactor (VHTR), 335
- Very High Temperature Reactor (VHTR), 374, 410
- Viscous dissipation, 201
- Viscous fluid flow, 191

**Z**

- Zeroth Law of Thermodynamics, 17